LATE QUATERNARY LANDSCAPE EVOLUTION

OF

WESTERN HAWKE'S BAY, NORTH ISLAND, NEW ZEALAND

A thesis presented in partial fulfilment of the requirements

for the degree of

Doctor of Philosophy in Earth Science at

Massey University, Palmerston North, New Zealand

Andrew Peter Hammond

1997

ACKNOWLEDGEMENTS

I wish to thank Drs Vince Neall, Alan Palmer and Bob Stewart for supervising my thesis studies. Dr Alan Palmer is especially thanked for his role as chief supervisor. I am most grateful to Massey University for supporting my doctorate studies by providing me with a Vice Chancellor's stipend and a Helen Acker's Scholarship.

Many people from Massey University, other universities and the Crown Research Institutes advised me on laboratory techniques, computing problems and provided technical support. My thanks to Drs Bolan, Eden, Kirkman, Loganathan, Manning, Shane, Scotter and Wallace; Harley Betts, Malcom Boag, Mike Bretherton, Lance Curry, Brian Daly, Keitha Giddens, Terry Martin, Heather Murphy, Bob Toes, Ross Wallace, Anne West and Joe Whitton. Denise Brunskill, Nicola Collins, Anne Rouse and Marion Trembath are thanked for their advice on word processing, poster presentation and their cheerful assistance in the administration of my project.

I would like to thank past and present fellow postgraduate students who willingly gave up their precious time to advise and instruct me on a number of techniques and how to overcome a myriad of technical problems. Space does not allow me to mention you all. I know who you are and will always be grateful.

Dr Rodney Grapes and Ken Palmer of the Analytical Facility, Geology Department, Victoria University of Wellington are thanked for instructing me in the operation of the electron microprobe and Doug Hopcroft of Hort Research for electron microscopy and energy dispersive x-ray analyses.

My thanks to the many farmers and landowners within the Hawke's Bay district who provided access to their properties as well as advice on the "the best places to look." Special thanks to the Renton family of Glenmore Station who provided me with accommodation and great hospitality.

Finally, I would like to thank my parents who supported me in many ways through the "ups and downs" of doing a Ph.D. There are many others friends and associates, too numerous to list, to them also I say "thanks".

ABSTRACT

Western Hawke's Bay, North Island, New Zealand, lies landward of an obliquely convergent offshore plate boundary, the Hikurangi Trough. Landscape elements exhibit classical island arc terrains. From east to west these are: an accretionary wedge, forearc basin, frontal-ridge, and a volcanic backarc basin.

The forearc was subdivided into four land systems: ranges, inland basins, hill-country, and plains. Soil patterns and geomorphological processes within each land system are detailed. The architecture and subsequent sculpturing of land systems have been subject to a complex interplay between: tectonic, climatic, fluvial, aeolian and volcanic regimes. These regimes have had a marked bearing upon the stability/instability of the landscape and its evolution.

The timing of stability/instability cycles within the district's coverbeds and aggradational/degradational terraces is facilitated by interbedded rhyolitic and andesitic tephra chronohorizons and ignimbrites (Taupo, Oruanui, Rabbit Gully and Potaka) derived from the Taupo Volcanic Zone. The glass chemistries of unknown rhyolitic tephras and ignimbrites were matched with those from the well-dated master sections around the volcanic centres. During this study the geographic distribution of many andesitic and rhyolitic tephra layers have been significantly expanded into a district not previously studied in detail. Andesitic tephras identified include members of the Tufa Trig, Ngauruhoe, Papakai, Mangamate and Bullott Formations. Rhyolitic tephras found, but not previously recorded in Hawke's Bay sequences, include Rerewhakaaitu and Rangitawa Tephras and four previously unidentified rhyolitic tephras termed A, B, C and D within Loess 4 and Loess 5.

Major cycles of landscape stability/instability are associated with Quaternary climate changes. During glacial and stadial times intense physical weathering prevailed within the ranges resulting in the transfer of material (aggradation products) through the fluvial and aeolian systems to the downlands and coastal plains. Interglacial and

interstadial times were marked by a predominance of chemical weathering (paleosols) and river degradation. The net result was landsurface stabilisation before the next episode of instability. Loess-paleosol layers recognised in Hawke's Bay are correlated to the Rangitikei River Valley sequences. Unlike the Rangitikei sequences, where the best loess-paleosol record overlies terraces, those in Hawke's Bay are found on footslopes.

Pre- and early-Ohakean loessial sequences overlying aggradational terraces are absent. Consequently, studies were focussed on colluvial foot- and toe-slopes (depositional sites) within the inland basins and hill-country land systems. Coverbeds from these slope positions have a fuller record and are more useful for stratigraphic studies.

Earthquakes, fires (both natural and man-induced), periodic cyclonic storms and ignimbrite sheets punctuate and complicate the climatically induced Quaternary cycles. The record for these non-climatic variables is often local and may mask or even destroy the imprint of older, more poorly preserved climatically-induced Pleistocene stability and instability episodes.

Field, morphological, mineralogical and chemical properties of loess and tephra layers were undertaken at four reference sections. These sections are arranged in a west (foothills of the ranges) to east (coast) transect reflecting differences in climate (1800-900mm rainfall/annum, lower rainfalls in the east), soil types (Pumice, Allophanic, Brown and Pallic Soils) and distance from volcanic source areas. The most distant site lies over 100km east of Lake Taupo.

Three aggradational terraces associated with the last stadial (Ohakean) are commonly found along Hawke's Bay rivers. Ohakean terraces along the Mohaka River have tread ages of *c.* 16-14 ka, 14-11 ka and 11-10 ka, respectively.

Field and laboratory characterisation of duripan horizons within Pallic Soils were undertaken to elucidate the nature and origin of the cementing medium. Soil chemistry and mineralogy show the cement to be highly siliceous and most likely derived from the weathering products of volcanic ash.

TABLE OF CONTENTS

CHAPTER ONE: INTRODUCTION TO STUDY

CHAPTER TWO: REVIEW OF GEOLOGICAL AND ENVIRONMENTAL SETTINGS

CHAPTER THREE:
REVIEW OF LATE QUATERNARY COVERBED STRATIGRAPHY IN LOWER NORTH ISLAND, NEW ZEALAND

CHAPTER FOUR:
SOIL STRATIGRAPHIC PRINCIPLES AND SOIL-GEOMORPHIC MODELS USED IN THE NEW ZEALAND HILL-COUNTRY

CHAPTER FIVE:
LATE QUATERNARY RECORD IN WESTERN HAWKE'S BAY

CHAPTER SIX: IDENTIFICATION AND DATING OF THE WESTERN HAWKE'S BAY TEPHRA RECORD

CHAPTER SEVEN:
CHEMICAL AND ELEMENTAL CHARACTERISTICS OF COVERBEDS AT TYPE SECTIONS

CHAPTER EIGHT:
DATING OF OHAKEAN TERRACES:
MOHAKA RIVER, WESTERN HAWKE'S BAY

CHAPTER NINE:
DURIPAN STUDY

CHAPTER TEN:
LATE QUATERNARY LANDSCAPE EVOLUTION OF WESTERN HAWKE'S BAY

LIST OF FIGURES

LIST OF TABLES

LIST OF PLATES

CHAPTER ONE:
INTRODUCTION TO STUDY

1.1 INTRODUCTION

Extensive areas of hill-country developed on "soft" Neogene rock sequences occur throughout New Zealand, and in total these comprise an important part of the nation's pastoral and forestry estates. The revenues earned from these enterprises form a valuable part of the New Zealand economy. In the "soft rock" hill-country of the eastern North Island airfall deposits such as loess and volcanic ash veneer this landscape, influencing soil development and distribution.

Despite the significance of hill-country farming to the national economy, no detailed and few semi-detailed pedological and soil resource studies have been undertaken. Published surveys by the former New Zealand Soil Bureau are at a scale of 1:253 440 (4 miles to 1 inch) and were produced in 1954 (New Zealand Soil Bureau, 1954). Little information exists on the surficial deposits and soils developed on these soft Neogene rocks and their associated loess and tephra coverbeds.

The Department of Soil Science at Massey University has a program of research, investigating soil development and distribution in the hill-country of the eastern North Island. The focus of these studies has been the development of soilscape models as a basis for land resource assessment and soil fertility studies. Models of landscape evolution are essential forerunners of soil mapping and characterisation studies. This thesis is an extension of this program.

1.2 OBJECTIVES

The principal aim of this thesis was to investigate the late Quaternary surficial landscape evolution of western Hawke's Bay.

To accomplish this the following specific objectives were established:

1. to examine the coverbed stratigraphy of western Hawke's Bay, using the principles and concepts of soil stratigraphy and tephrochronology, in order to elucidate the late Quaternary landscape history in the area
2. to trace late Pleistocene tephras from the central North Island into loess, colluvium and soils of the area
3. to assess the relative contribution of ash and quartzo-feldspathic loess to the main soils of the district, and
4. to examine selected properties of the dominant soil parent materials.

1.3 STUDY AREA

The Hawke's Bay district lies on the east coast of the North Island of New Zealand (Fig. 1.1). Field studies have been focussed on the hill-country and alluvial terrace-lands in the western part of the district. The field area (Fig. 1.1) is bounded to the north by the Napier-Taupo highway (State Highway 5), State Highway 2 to the east, the Waipawa-Tukituki Rivers to the south, and the foothills of the Ruahine and Kaweka Ranges to the west. The reader is referred to Figure 1.1 for localities mentioned in the text of this thesis.

1.4 HYPOTHESIS

The major hypothesis central to this thesis is that Quaternary climatic changes have had a profound influence upon the landforms of Hawke's Bay by inducing periods of landscape stability and instability. Periods of instability are equated to cold phases

LOCATION OF REFERENCE SECTIONS DISCUSSED IN TEXT

1. Pakaututu Road
2. Manaroa
3. Apley Road
4. Poraiti

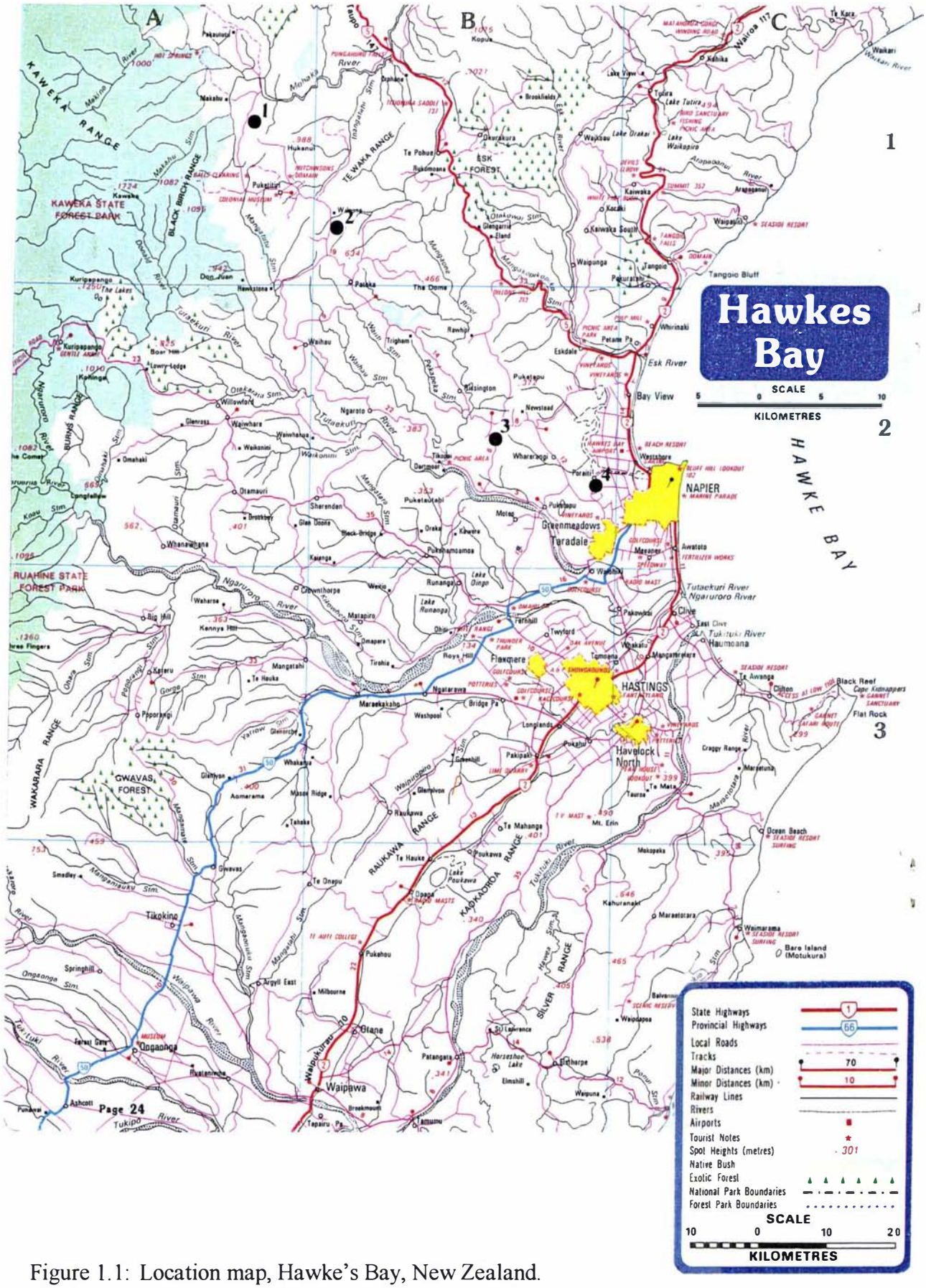

Figure 1.1: Location map, Hawke's Bay, New Zealand.

Reproduced from Shell Road Maps of New Zealand (1985).

(glacials, stadials) within the Pleistocene when intense physical weathering within the mountains led to widespread erosion. Consequently, rivers leading from the mountains carried high sediment loads and began to aggrade. Periods of stability are equated with warmer phases (interglacials, interstadials) when physical weathering and subsequent erosion were reduced. Rivers consequently had more competency and were able to incise (degrade) into and excavate the aggradation products originating during the unstable periods.

Loess and tephra stratigraphy are used to gain some age control on these periods within western Hawke's Bay. Results will be related to New Zealand late Quaternary palaeoclimate models. These are discussed in Chapter Three.

1.5 ORGANISATION OF THESIS

Chapter One, the introduction, outlines the research objectives of this thesis. In Chapter Two the reader is acquainted with the physical environment emphasising the tectonic and environmental regimes. Current loess and tephra stratigraphies are outlined in Chapter Three. In Chapter Four soil stratigraphic and geomorphic principles used to decipher the New Zealand hill-country record are reviewed.

Chapters Five, Six and Seven detail the field, morphological, soil chemical and mineralogical properties of the coverbeds sampled. The next two chapters concentrate on two problems that arose in the early phases of this research. The first, Chapter Eight, was to establish whether it is possible to gain some age control on the three substages (periods of aggradation) within the last stadial (Ohakean). The second, Chapter Nine, investigates the genesis and composition of the cemented hard pans overlying fragipans within the more eastern parts of the Hawke's Bay district.

In Chapter Ten the late Quaternary landscape evolution of western Hawke's Bay is detailed and recommends further avenues of research. The final chapter, Chapter Eleven, summarises the research findings presented in this thesis.

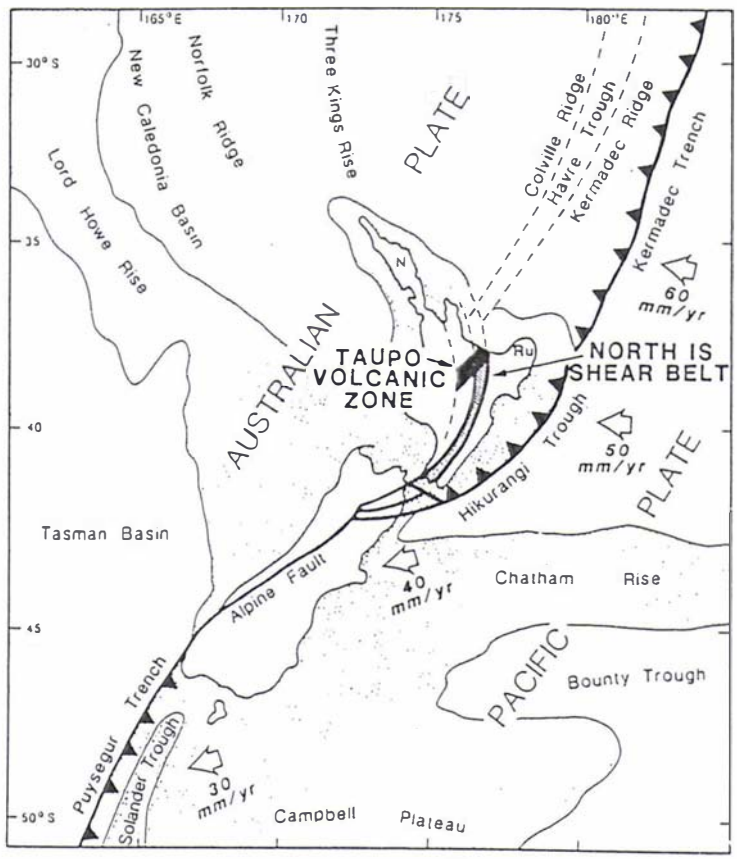

Figure 2.1: The Australian-Pacific Plate boundary in the New Zealand region. Stippling represents the continental crust above 2000m isobath and arrows show vectors of plate motion.

Reproduced from Cole and Lewis (1981).

CHAPTER TWO:
REVIEW OF GEOLOGICAL AND ENVIRONMENTAL SETTINGS

2.1 INTRODUCTION

This chapter aims to provide a selective review of the geological and environmental factors operative in the evolution of the western Hawke's Bay landscape. The approach is via the plate tectonic setting of Hawke's Bay which is later modified in Chapter Ten due to new information obtained during the conduct of this thesis.

2.2 GENERAL GEOLOGY AND TECTONIC SETTING

2.2.1 Plate tectonic setting of Hawke's Bay

Hawke's Bay lies immediately to the west of an active, obliquely convergent plate boundary, the Hikurangi Trough (Fig. 2.1). The Trough forms the southern extension into New Zealand of the Tonga-Kermadec Trench subduction system (Lewis, 1980; Cole and Lewis, 1981). Detailed geological mapping both onshore and offshore have shown that the oceanic Pacific Plate is being obliquely subducted at *c.*50mm a^{-1} beneath the leading edge of the continental Australian Plate since Miocene times (Pettinga, 1982; Kamp, 1988; De Mets *et al.*, 1990; Rait *et al.*, 1991). West of the Hikurangi Trough the upper surface of the Pacific Plate forms a shallowly dipping (5-15°) thrust for some 200-270km, westwards before it abruptly descends into the asthenosphere with a dip of 50° at a depth of 80km (Adams and Ware, 1977; Walcott, 1978a;b; Reyners, 1980; 1983). The line of marked change in the dip of the subducted Pacific Plate corresponds to the position of the Taupo Volcanic Zone (TVZ), a calc-alkaline province of Quaternary volcanics, at the surface of the Australian Plate. Geodetic studies (Walcott, 1978a; 1984; 1987), microseismicity surveys (Reyners, 1980; Bannister, 1988) and studies of coastal neo-tectonics (Hull, 1985; 1986; 1987; 1990; Berryman, 1988; Berryman *et al.*, 1989) document active crustal deformation in Hawke's Bay consistent with this model of the plate boundary zone.

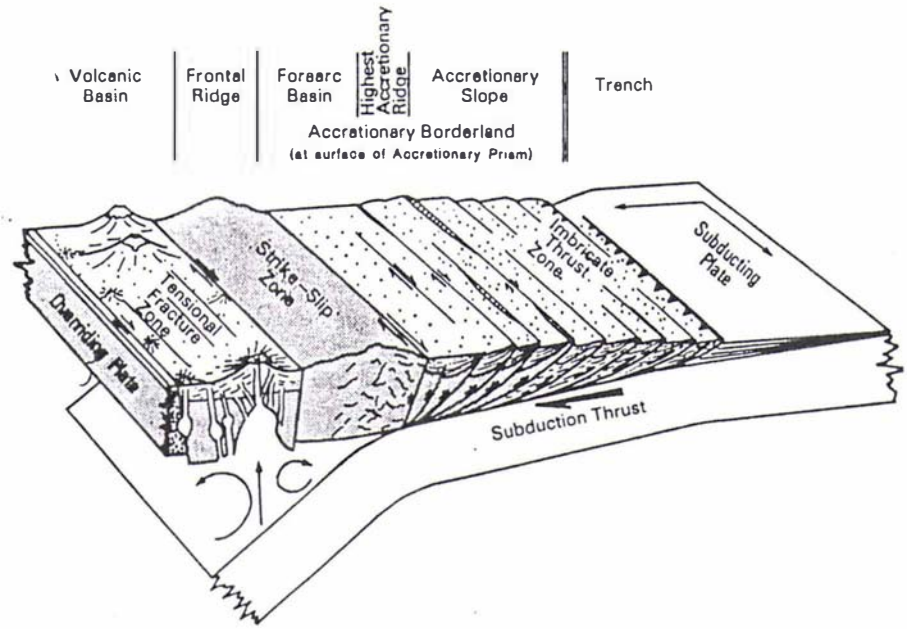

Figure 2.2: Tectonic model of the study area developed by Cole and Lewis (1981).

Four major structural and tectonic regions characterise the tectonic setting (Cashman and Kelsey, 1990; Cashman *et al.*, 1992; Erdman and Kelsey, 1992; Kelsey *et al.*, 1993). These are, in order from the Hikurangi Trench westwards:

1. an accretionary slope which extends from the Trench to the coastal hills. This is made up of Cretaceous and Tertiary aged landward dipping turbidite and basinal hemi-pelagic sequences and Plio-Pleistocene limestone units, respectively;
2. the forearc basin comprising Neogene strata within the coastal plains and adjoining inland hill country;
3. high, fault bounded mountains of the frontal ridge comprising uplifted Mesozoic greywacke sandstones and argillite rocks; and
4. a volcanic backarc basin extending from White Island to Mount Ruapehu (Fig.2.2).

The plate boundary is unusual in that the Pacific Plate is being subducted at such a shallow angle beneath the East Coast of the North Island that much of the forearc region is above sea-level and thereby is readily accessible to study. Geologic mapping and structural analysis between the trench and the backarc region, indicate that considerable strain, manifest over long periods of time (1×10^6 yr), is being partitioned into domains of extension, contraction and transcurrent displacement within each of the tectonic regions (Cashman and Kelsey, 1990; Cashman *et al.*, 1992). Boundaries between some of these domains are marked by major faults. Deformational structures resulting from strain partitioning at the plate margin, have manifested themselves within each of the landscape elements found within different parts of the study area. Table 2.1 outlines the occurrence of tectonic and geomorphic features within each of the tectonic regions. Further consideration of the broader features of the tectonic geology and geomorphology of the region are discussed elsewhere (e.g. Cole and Lewis, 1981; Walcott, 1987; Berryman, 1988; Cashman and Kelsey, 1990; Cashman *et al.*, 1992; Erdman and Kelsey, 1992; Kamp, 1992a; Ballance, 1993; Cole *et al.*, 1995).

Table 2.1: Occurrence of tectonic and geomorphic features within each of the tectonic domains.

Tectonic Domain	Tectonic Features	Geomorphic Features
Accretionary Slope	• growing anticlines and synclines • reverse faults • angular unconformities within sedimentary sequences are common • slope basins	• uplifted and generally landward tilted marine terraces • stream capture common • tilting and reverse gradient of fluvial terraces common • cliffed coastlines • superficial mass movement common • mud diapirs and mud volcanoes
Forearc Basin	• normal faults • tectonic subsidence during Holocene • moderate, regional uplift during Pleistocene • broad synclinal structure • strong uplift and formation of asymmetric syncline adjacent to western boundary faults	• low lying coastline • estuaries • barrier bars • low gradient rivers in coastal areas • fluvial terrace sequences caused by aggradation and downcutting in inland areas • large landslides, perhaps triggered by large earthquakes • landslide dammed lakes • abundant superficial mass movement • sparse hot springs
Frontal Ridge	• oblique slip faults bounding region with horizontal to vertical slip ratio commonly 5:1 • intra-mountain oblique faults • infaulted Neogene rocks along intra-mountain faults • down-stepped, faulted western margin	• horizontally offset topography including streams and ridges and formation of shutter ridges • remnants of late Tertiary marine erosion surface • general summit accordance • ignimbrite plateau onlapped at western margin • landforms and deposits of periglacial conditions including solifluction lobes, rock glaciers and shaved surfaces
Backarc Basin	• normal faults • grabens • volcanoes, calderas, domes • scoria cones • ring faults • geothermal fields	• ignimbrite plateaux • rapid fluvial sedimentation consequent on volcanic eruptions • lahars • crater and caldera lakes • rapid fluvial incision in pumice deposits • many hot springs

Reproduced from Berryman (1988).

2.2.2 Physiography

The physiography of Hawke's Bay is determined largely by rock type and structural trends which in turn reflect the tectonic setting of the district (see 2.2.1). Many of the landforms within the district have pronounced north-east/south-west structural alignment. The area has been, and still is, subject to tilting and uplift with subsequent downcutting by fluvial processes.

A major structural feature within the forearc basin is the Hawke's Bay Syncline (Grindley, 1960). The resultant inland depression is faulted and folded into minor NE-SW striking anticlines and synclines with dips ranging from 5° to 20° (Lillie, 1953).

Within the study area four major physiographic zones are identifiable and can be related to the tectonic domains identified in section 2.2.1. These are from west to east:

1. *Mountain Ranges*

   The Ruahine and Kaweka Ranges, aligned NNE-SSW, form part of the main axial divide of the North Island. They are rugged with a very close drainage pattern, mostly bush-clad, and have many peaks over 1500m a.s.l. The Ranges are composed largely of unfossiliferous, alternating greywacke sandstones and argillite strata of Triassic and Jurassic age (Kingma, 1959). Intense physical weathering of these greywackes provides the source of the gravels to most main rivers flowing eastward into the Pacific Ocean.

   The axial ranges are crossed by two broad saddles, one of which, the Kuripapango Saddle, lies within the field area. It marks the boundary between the Ruahine and Kaweka Ranges.

   The Wakarara Range (highest point 1013m a.s.l.), in the south-west of the area, is separated from the northern Ruahines by the Ohara Depression which is about 20km long and 3km wide.

2. *Western Hill-Country and Rolling Downland*

The hill-country and rolling downlands extend eastwards from the axial ranges to the plains. The hills are moderately steep to steep nearer the ranges but become more rolling towards the plains. Many of the eastward-flowing rivers have left their imprint of deeply incised valleys flanked by a series of high terraces. These are presumed to have formed during late Pleistocene climate changes and/or after uplift.

The NE-SW alignment of landforms is particularly apparent within this zone. The most prominent features are the Maungaharuru and Te Waka Ranges. These have a series of steep north-west-facing scarp slopes and long gentle south-east-facing dipslopes. Rock types within the hill country are soft sedimentary rocks, namely Neogene mudstone, siltstone, sandstone, limestone and conglomerate.

Several faults are seen within this zone, the two most prominent being the Ruahine and Mohaka Faults. These are described more fully in section 5.7. The Ruahine Fault trace is a range-bounding fault separating Mesozoic rocks of the mountainlands from the Neogene sedimentary strata of the forearc basin. The Mohaka Fault trace is seen farther to the east at the base of the Maniaroa and Te Waka Ranges. Both these faults are classified as active and strike NE-SW. Crushed zones, associated with these faults, are highly susceptible to mass movement (Lillie, 1953). Less pronounced NW-SE fault lineations are also thought to be present within the study area (Kamp, 1992a). These are thought by Kamp (1992a) to have played a major role influencing river courses and thereby determining the areas of net sedimentation.

3. *Plains and Terrace Lands*

A large inland depression, formerly occupied by a seaway during the late Neogene to the early Pleistocene, occupies this zone and runs south to Cook Strait via the Wairarapa.

River terraces decrease in height in an eastwards (downstream) direction before they merge with the Heretaunga Plains, north of the Ngaruroro River, and the Takapau-Ruataniwha Plains to the south. The hills between Maraekakaho and Gwavas form the dividing line between the Heretaunga Plains and Takapau-Ruataniwha Plains to the south. River courses within the Plains are being infilled with sediments from the ranges and hill-country, brought down by the major river systems which traverse the region.

Neogene and early Pleistocene strata dip eastwards and westwards respectively into the inland depression. In the north, the inland depression swings north-eastward to become drowned in Hawke Bay (Beu *et al.*, 1980). In northern Hawke's Bay the depression is absent and the foothills of the axial ranges extend eastwards to merge with the coastal hill-country.

4. Coastal Hill-Country

Immediately to the east of the inland depression, from Cape Kidnappers southwards, a 30-40km wide belt of coastal ranges and hills with some ridges over 500m high, separate it from the Pacific Ocean. The coastal hill-country comprises a complex pattern of softer marine sandstone, siltstone and mudstone and bands of harder, upstanding limestone and conglomerate rocks of late Cretaceous and Tertiary age (Pettinga, 1982). Parallel NE-SW striking ridges and valleys emphasise the extensive folding and faulting parallel to the plate boundary.

This zone lies immediately to the east of the study. Erosion products from this zone have contributed to the formation of the plains.

A number of major rivers, sourced within the axial ranges, flow into Hawke Bay. These are from north to south, the Mohaka, Esk, Tutaekuri, Ngaruroro and Waipawa-Tukituki Rivers. All these rivers have a number of major tributaries which have all played a significant role in the construction of the present landscape.

Several small lakes occur within the region. Some of these have formed within drowned tributary channels (e.g. Lakes Runanga and Oinga), others as cut-off meander scrolls and some result from landslides that have blocked river or stream courses.

In February 1931, a magnitude 7.8 (Richter scale) earthquake (Napier Earthquake) struck the region causing a sudden uplift of about 2m in areas surrounding Napier city. Some 13km^2 of the shallow, tidal Ahuriri Lagoon was uplifted and drained. The Tutaekuri River also changed its course and discharged into Hawke Bay near Awatoto (Henderson, 1933; Marshall, 1933). Southeast of Napier downwarping rather than uplift occurred (Hull, 1990).

2.2.3 Palaeogeographic setting and origin of the Hawke's Bay Paleogene-Neogene succession

Within Hawke's Bay the interaction of the atmosphere and lithosphere have created a unique present landscape. This is principally caused by the subduction of the Pacific Plate beneath the eastern North Island (Australian Plate), and the effects of global climatic change during the Quaternary.

The Mesozoic rock types of the Ruahine and Kaweka Ranges originally formed part of the palaeofrontal accretion at the edge of the Gondwana landmass, prior to the breakaway of New Zealand (Spörli and Ballance, 1989). Major uplift of the ranges began approximately 1Ma ago and is associated with modern orogenic (Kaikoura Orogeny) processes resulting from subduction (Walcott, 1978a; Beu *et al.*, 1981; Shane, 1996a). Consequently, many of the physiographic features parallel the plate boundary.

West of the Ranges is the back-arc basin of the Taupo Volcanic Zone (TVZ). The basement of the TVZ has traditionally been considered to be Mesozoic greywacke, from which the voluminous rhyolites of the TVZ were probably derived (Reid, 1983).

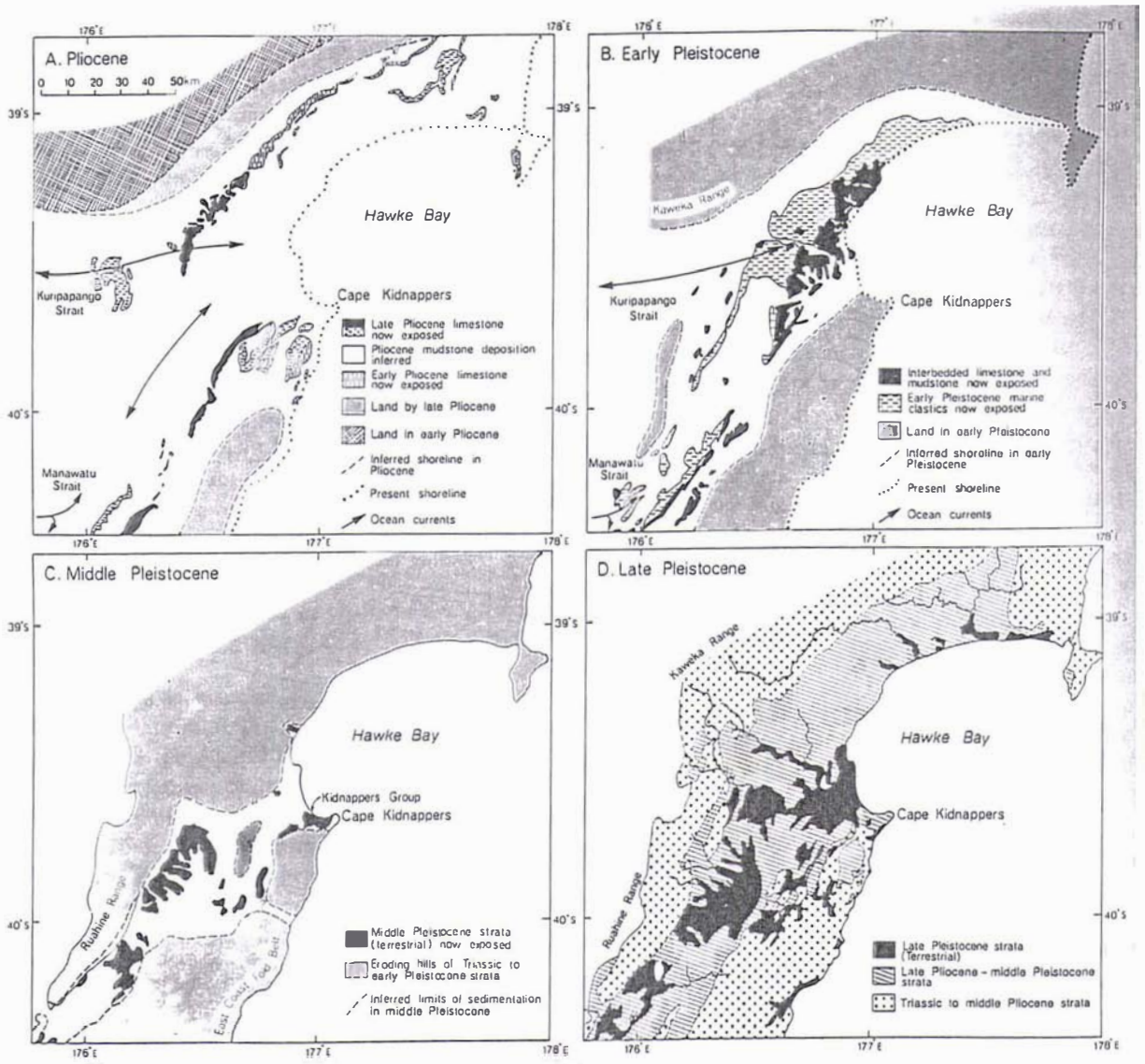

Figure 2.3: A sequence of Pliocene and Pleistocene paleogeographic maps showing the development of Hawke' Bay landforms.
Reproduced from Kamp (1992a).

During the late Cretaceous-early Tertiary a major marine basin, termed the "Eastern Basin" by Kingma (1960), extended from North Canterbury, through Wairarapa and Hawke's Bay, to the Ruakumara Peninsula. From the early Miocene onwards, the Eastern Basin was disrupted (intra-basin folding and faulting) into numerous smaller basins and adjacent basement highs. This is attributed to the development and propagation of a structurally complex accretionary prism, in response to subduction at the Hikurangi margin. By the late Miocene Hawke's Bay had been structurally differentiated into a western basement high, a central depression and an eastern high.

Changes in the Pliocene to Pleistocene palaeogeography, summarised in Figure 2.3, trace the accentuation and modification of this pattern to the evolution of the present landscape. In the early Pleistocene a major seaway 450km long and averaging 40km wide, trended NE-SW and extended southwards into modern-day Cook Strait and westwards via the Kuripapango Saddle and Manawatu Gorge into the Wanganui Basin. Within this seaway (Petane Trough) marine strata of the Petane Group were deposited as forearc basin sediments (Lillie, 1953; Beu *et al.*, 1981; Kamp and Nelson, 1988; Kamp *et al.*, 1988) underlain by Pliocene shallow marine to fluvial sedimentary strata, and Miocene outer shelf and bathyal mudstones (Grindley, 1960; Beu *et al.* 1980; Kamp *et al.*, 1988). The Petane Group preserves an exceptional record of shoreline-neritic sedimentary responses to glacio-eustatic sea-level changes and subordinate pumiceous sediment derived from the TVZ (Beu *et al.*, 1980; Beu and Edwards, 1984; Kamp and Nelson, 1987; Haywick, 1990; Haywick and Henderson, 1991; Haywick *et al.*, 1991; 1992). In the early Pleistocene the seaway became constricted in the vicinity of Mount Bruce (Wairarapa district) due to tectonic uplift of Mesozoic strata across the regional trend of the marine trough (Kamp *et al.*, 1988). Subsequently, the shoreline retreated progressively south towards Cook Strait and northwards into Hawke Bay (Vella, 1963a; Ghani, 1978; Kamp *et al.*, 1988; Kamp, 1992b). Consequently, throughflow of currents ceased and two independent basins developed, Hawke's Bay to the north and Wairarapa to the south (Kamp, 1992a;b). Sea continued to enter the Hawke's Bay basin as far as Dannevirke until *c.*700ka (Krieger, 1992; Ballance, 1993).

The northern exit of the seaway, inland from Gisborne, also became restricted by uplift. This contributed to the formation of the Wairoa Syncline, an enlarged equivalent of the present Hawke Bay, at the northern end of the strait. This general succession had superimposed glacio-eustatically induced transgressions and regressions (Haywick, 1990; Haywick and Henderson, 1991; Haywick *et al.*, 1991; 1992). These sea-level changes produced alternations of limestone and terrigenous facies, the latter during glacial times of low sea level.

Uplift of the Hawke's Bay Basin (forearc basin) was initiated on its eastern margin, near the present day coastline. Evidence for this may be seen within the early to late Miocene sediments in the coastal hills of southern Hawke's Bay (van der Lingen and Pettinga, 1980; Pettinga, 1982; Kamp, 1992a; Ballance, 1993; Lewis and Pettinga, 1993;). Imbricate thrust faulting and deformation on the leading edge of the inboard margin of the accretionary slope caused small inner slope turbidite basins (e.g. Makara Basin) to be inverted. Uplift became more regional during the mid- or late-Pliocene to mid-Pleistocene as the subduction accretionary complex grew outwards (eastwards) and upwards (Kamp *et al.*, 1988). This led to the eventual emergence of the forearc ridge and infilling of the marine trough within the forearc basin. Plio-Pleistocene limestone units within the forearc are diachronous in age from east to west and exhibit features such as interbedded terrigenous units which are indicative of active synsedimentary deformation resulting from differential uplift of the basin margins (Beu *et al.*, 1980; Kamp *et al.*, 1988).

The middle-late Pleistocene was characterised by accelerated uplift, especially of the axial ranges, and terrestrial infilling of the inland basins together with continued folding and faulting. Sediments derived mainly from the ranges, and the inland and coastal hill country indicate sea-level had withdrawn to about the present coastline by the middle Pleistocene (1.0-0.1Ma)(Kamp, 1992a).

Large alluvial fans (Salisbury and Wahora Terraces), along the eastern margin of the ranges, resulted from substantial uplift and subsequent subaerial erosion of the axial ranges (Raub, 1985; Erdman and Kelsey, 1992). Although land was emergent over

most of the southern half of the North Island by *c.*1Ma ago, measured uplift rates in the region suggest that uplift accelerated during the middle-late Pleistocene (Williams, 1988; Kamp, 1992a). Uplift induced stream incision and the subsequent erosion of material from slopes by mass movement processes.

During the Pleistocene and Holocene a number of tephras, sourced within the Taupo Volcanic Zone (Okataina, Taupo and Tongariro Volcanic Centres) and Egmont Volcano, have blanketed parts of the district (Howorth *et al.*, 1980; Eden *et al.*, 1993; Eden and Froggatt, 1996). These tephras have been carried into Hawke's Bay by the prevailing westerly winds and reworked by rivers and streams that drain ash-covered hills. The thickest and most numerous tephra layers are found in the west of the study area, closer to the volcanic centres.

During past eruptions from the TVZ, pyroclastic flows swept across the landscape incinerating the forest and flowing into valleys and depressions, filling them to a considerable depth with ignimbrite. At least three ignimbrites, the Taupo Ignimbrite (Lake Taupo source), the Potaka Ignimbrite (Mangakino source) and another unit in the Rabbit Gully beds of the Cape Kidnappers sequence (Mangakino source) have made their way into the region via low points in the ranges (e.g. Kuripapango Saddle) and the major rivers (e.g. Mohaka and Ngaruroro Rivers) sourced within the main divide (Kingma, 1971; Wilson, 1985; Wilson and Walker, 1985; Shane, 1994; Shane *et al.*, 1996a;b; Wilmhurst and McGlone, 1996). Nearer to source these form extensive sheets which have characteristically subdued the pre-existing topography. A common feature of the ignimbrites is the presence of charred logs and pieces of charcoal.

Much of the hill country and plains has been mantled by loess, a wind blown deposit, derived from the adjacent flood plains. The time of greatest loess accumulation occurred during glacial periods when cooler temperatures and a sparse vegetative cover forced rivers to aggrade as a result of increased physical weathering within their source catchments. Loess forms the dominant parent material of many Hawke's Bay soils (see section 2.3.3).

Table 2.2: Temperature Normals (°C) 1951-1980 for Hawke's Bay.
a. Mean daily maximum temperatures
b. Mean daily minimum temperatures

Location		Jan	Feb	Mar	Apr	May	Jun	Jul	Aug	Sep	Oct	Nov	Dec	Year
Esk	a	21.6	21.5	19.7	16.9	13.8	11.3	10.4	11.4	13.7	16.2	18.5	19.9	16.2
	b	11.6	12.1	10.7	8.5	6.1	4.1	3.2	4.0	5.4	6.9	8.4	10.3	7.6
Kaweka	a	22.5	22.3	20.3	17.2	14.1	11.8	10.9	11.9	14.2	16.8	19.2	20.6	16.8
	b	12.0	12.2	11.3	8.7	6.6	4.7	4.0	4.6	6.0	7.2	8.8	10.7	8.1
Napier	a	24.0	23.8	22.4	19.9	16.8	14.3	13.6	14.4	16.5	18.8	21.2	22.4	19.0
	b	14.4	14.5	12.8	10.1	7.3	4.7	4.2	5.4	7.2	9.0	11.1	13.1	9.5
Hastings	a	24.5	24.3	22.7	19.9	16.8	14.1	13.4	14.5	16.6	19.0	21.2	22.8	19.2
	b	13.5	13.6	11.8	8.8	6.1	3.3	3.1	4.4	6.2	7.9	9.9	12.3	8.4
Havelock N	a	23.9	23.8	22.2	19.6	16.6	14.1	13.4	14.3	16.4	18.7	20.7	22.1	18.8
	b	12.0	12.0	10.3	7.2	4.4	2.1	1.8	3.2	4.8	6.4	8.3	10.7	6.9
Gwavas	a	22.5	22.5	20.4	17.4	14.2	11.6	10.8	11.9	14.3	16.8	19.2	20.5	16.8
	b	9.7	9.8	8.6	6.3	4.0	1.8	1.0	2.0	3.3	4.7	6.5	8.5	5.5
Kopua	a	21.6	22.0	20.0	17.0	13.8	11.1	10.5	11.5	13.7	16.0	18.2	19.8	16.3
	b	11.3	11.4	10.2	8.0	5.6	3.4	2.8	3.7	5.3	6.5	8.3	10.0	7.2
Waipukurau	a	23.8	23.9	21.7	18.6	15.1	12.5	11.8	12.9	15.1	17.4	20.0	21.9	17.9
	b	11.5	11.7	10.2	7.5	5.0	2.7	2.2	3.6	5.1	6.3	8.0	10.3	7.0

Reproduced from Thompson (1987a)

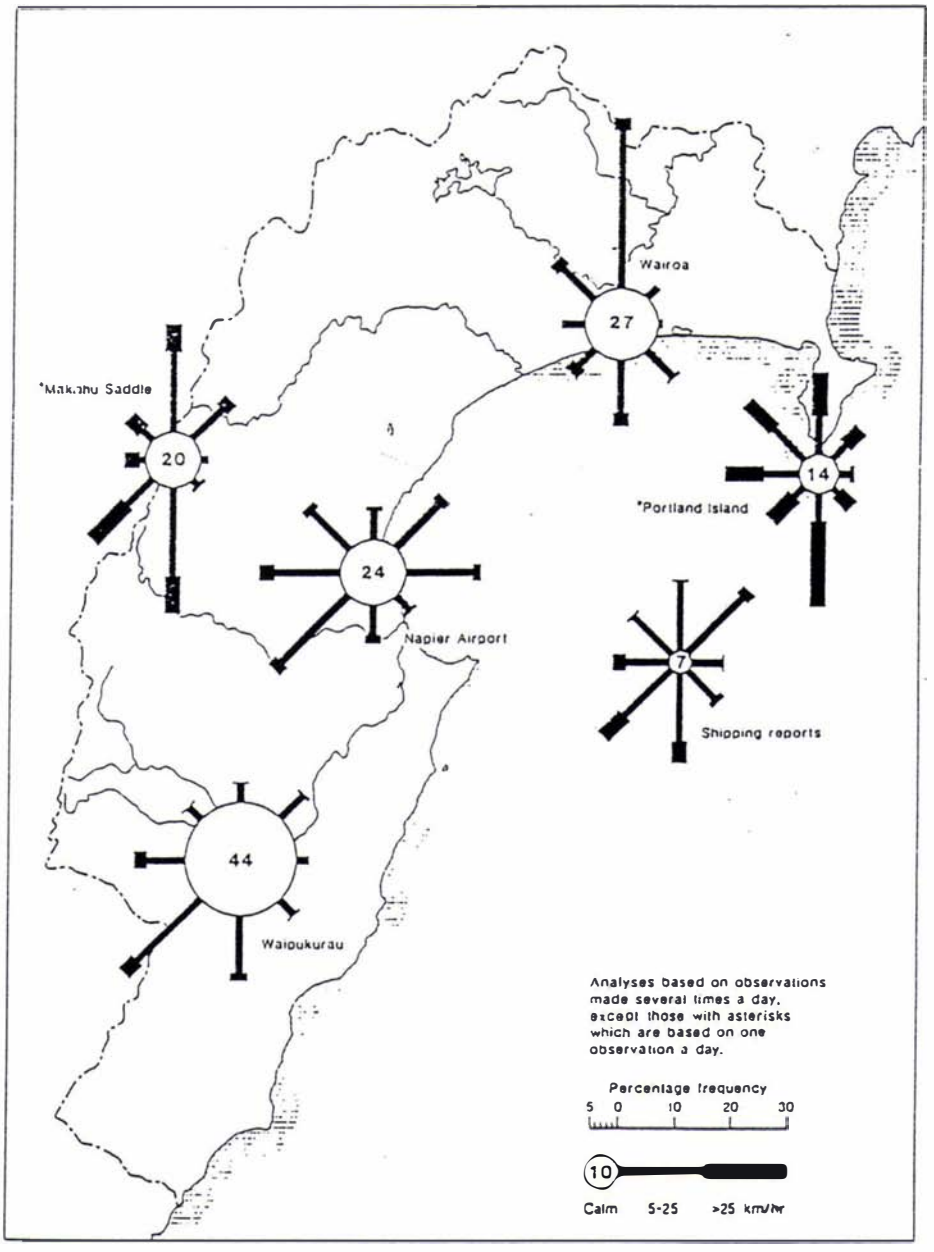

Figure 2.4: Mean annual percentage frequency of wind direction in Hawke's Bay. Reproduced from Thompson (1987).

A combination of tectonic processes and soft rock lithologies has led many of the rock types within the ranges and hill country to be susceptible to erosional processes. Intense rainstorms and earthquakes have acted as major triggering mechanisms initiating erosion (Grant, 1965; 1966; 1985; 1991; 1996; Hubbard *et al.*, 1979; Hubbard and Neall, 1980; Page *et al.*, 1994a;b). Products of this erosion have then made their way into the fluvial system, as evidenced by the aggradation of stream and river beds within upper catchments, either via mass movement along failure planes within the bedrock or by wasting processes of the regolith.

2.3 CONTEMPORARY CLIMATE, VEGETATION AND SOILS

2.3.1 Climate

The climate of Hawke's Bay is influenced largely by orography and the airstreams crossing New Zealand. The latter usually show an eastward-moving sequence of anticyclones and depressions, with their associated cold and warm fronts, dominating the weather pattern in New Zealand. Situated in the lee of the main axial ranges of the North Island, Hawke's Bay has warm summers and a sunny climate of 2100-2200 sunshine hours/annum in Napier (Thompson, 1987a), and is less windy than west coast districts (Table 2.2).

Over central and southern Hawke's Bay the predominant wind directions (Fig. 2.4) are from west to south-west across the Heretaunga and Takapau-Ruataniwha Plains. In the north the wind tends to blow most frequently from the north. Throughout the region there is a tendency for the wind to be channelled along river valleys (Thompson, 1987a). During periods of strong, west to north-west flow over the North Island, ahead of a cold front moving across the country, the winds descending across the lowlands are warm, dry föhn winds. Hawke's Bay's eastward-facing aspect makes it vulnerable to weather systems accompanied by easterly[+] winds. Nearly all of the rain is associated with cold fronts and falls as rain showers of relatively short duration.

[+] Easterly refers to those wind directions from south-east through east to north-east, and westerly to those winds which blow from between north-west to south-west.

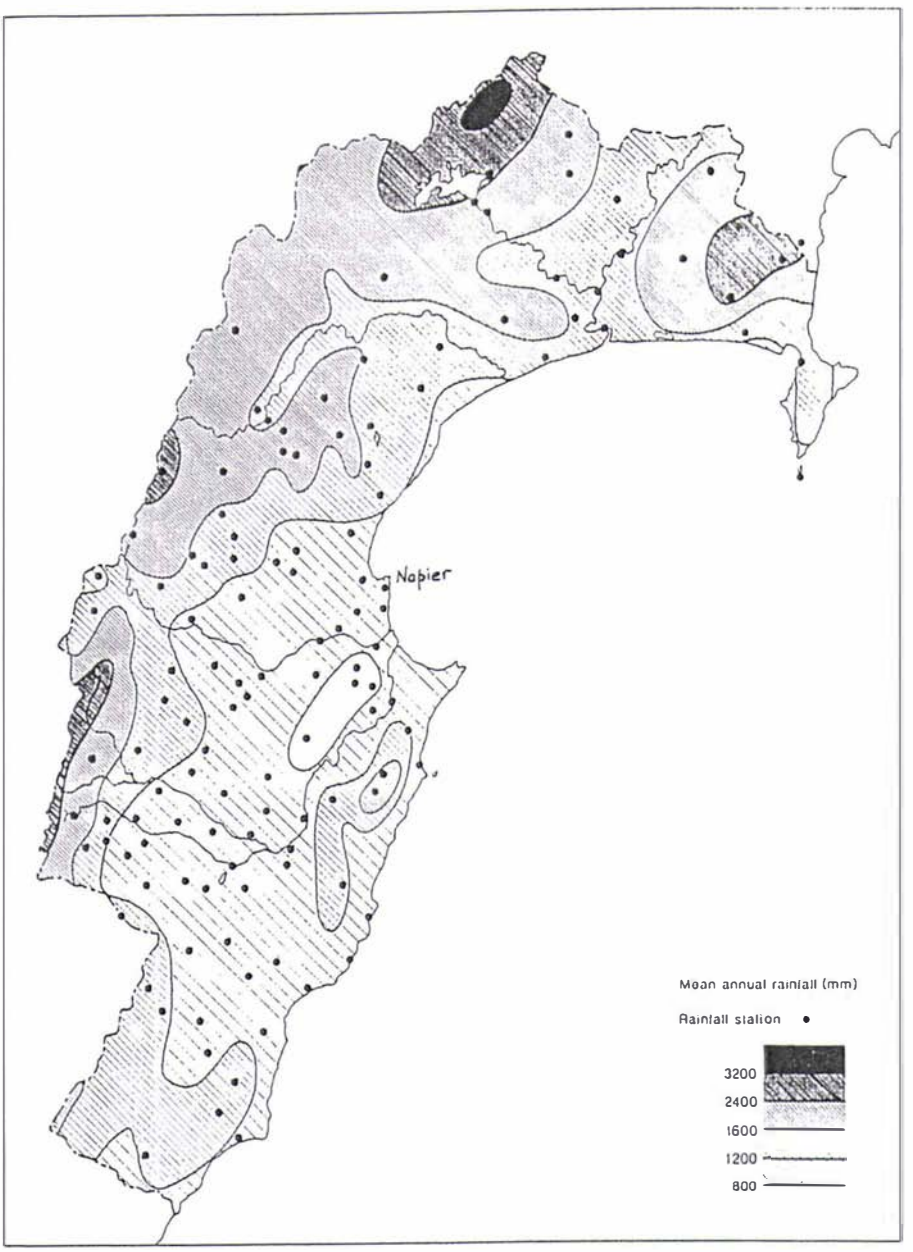

Figure 2.5: Mean annual rainfall for the Hawke's Bay region. Reproduced from Thompson (1987a).

Although westerly weather systems give Hawke's Bay less rain than most other districts, the mean annual rainfall over most of the region is not too different from that of the Manawatu and Taranaki. Rainfall increases regularly from the plains (800-1200mm mean annual rainfall) to the ranges where amounts greater than 2400mm (mean annual rainfall) can be expected (Fig. 2.5). Throughout Hawke's Bay there is a seasonal variation with a winter maximum and a spring or early summer minimum (de Lisle and Patterson, 1971). Coulter (1962) established that much of the rainfall on the plains and coastal districts of Hawke's Bay is derived from systems accompanied by winds from an easterly quarter or from the south, rather than from a westerly direction. The proportion of rainfall associated with both westerly and easterly conditions does, however, increase towards the hill-country and the ranges where it is orographically enhanced (Thompson, 1987a).

Tropical cyclones, although rare, sometimes pass near Hawke's Bay, giving winds from an easterly quarter and occasionally extremely heavy rainfall within short periods (Revell, 1981; Thompson, 1987b). A recent example, Cyclone Bola, caused massive damage to the East Coast in March 1988. The erratic appearance of cyclonic storms makes the rainfall more variable than that of most other districts in New Zealand (de Lisle and Patterson, 1971). Some of the greatest rainfall intensities recorded in New Zealand (e.g. 753mm of rain was recorded over a four-day period in the Tutira watershed during Cyclone Bola) have occurred here when these deep cyclonic depressions have passed over or near the region (de Lisle and Patterson, 1971; Thompson, 1987a; Page *et al.*, 1994a;b). These storms account for most of the slope failures on steep soft-rock hill-country areas and are the main agents of sediment generation, movement and discharge from steep watersheds (Grant, 1966; Page *et al.*, 1994a;b).

The variability in rainfall during the spring to autumn growing seasons gives periods in most years when the rainfall is insufficient to supply plant needs. At this stage the growth of crops and pasture is seriously retarded unless irrigated. Furthermore, desiccation of these soils during these seasons may result in the soils cracking making them more vulnerable to high intensity storms.

At any time of the year cold southerly airstreams can result in snow showers but snow to low levels (<500m) is extremely rare (Thompson, 1987a).

2.3.2 Vegetation

Prior to human occupation of Hawke's Bay, the evidence from soils, charcoal and wood remains show few areas below the climatic tree-line were without some form of forest or tall shrubland (McGlone, 1978). Tussock and sub-alpine scrub were present at higher altitudes in the western ranges.

Early Polynesian settlement of the lowlands had a profound effect upon the vegetation. Clearance of the lowland forest (podocarp and hardwood species) was well underway by the time the first European settlers arrived in the district during the 1840's and 1850's (Cameron, 1964). Besides the areas cleared near Maori settlements for cultivation, vast areas were set alight regularly to encourage the growth of bracken (*Pteridium esculentum*). The bracken root (aruhe) was a staple in the diet of the Maori (Shawcross, 1967). It cannot, however, be assumed that all firing of the forest by Polynesian settlers was deliberate. Some forests, especially beech and podocarp, are susceptible to fire if growing in dry areas. Some natural fires may have been initiated by lightening strikes. Whether a given area retained forest or not was principally determined by rainfall. Areas with low rainfall were almost totally denuded; wetter areas retained forest, except for minor clearance on especially fertile alluvial soils or near the coast. Fire, deliberately or accidentally lit, was the major agent in this transformation of the New Zealand landscape; climatic change played an extremely minor part (McGlone, 1983; 1989).

Much of the low-lying (plains) country, at the time of European occupation, was occupied by extensive swamps, mostly dominated by raupo (*Typha orientalis*), flax (*Phormium tenax*) and toe-toe (*Cortaderia* spp.). The hills were mainly covered by bracken (*Pteridium esculentum*) and varied scrub including tutu (*Coriaria* spp.). The gravel plains around Napier and the extensive swamp and tidal estuaries south of

Napier probably never supported forest species. In the foothills of the ranges and to the south, large areas of dense forest remained. These forests had dense stands of matai (*Prumnopitys taxiflora*), totara (*Podocarpus totara*), and on poorly drained ground and swamps, kahikatea (*Dacrycarpus dacrydioides*). Beech forest (*Nothofagus* spp.) and rimu (*Dacrydium cupressinum*) occurred inland towards the ranges and south towards Dannevirke (McGlone, 1978).

A new era of forest removal began when large numbers of European settlers arrived in the area during the 1840's and 1850's. They harvested the naturally occurring species, introduced species from elsewhere and transformed the natural vegetation into pasture-land by fire, logging and drainage.

Agriculture is the predominant economic activity of the region today. Much of the western hill-country is under pastoral species and exotic forest plantations. The plains support market gardening, orcharding and horticultural cash crops.

The foothills of the ranges still support podocarp-mixed hardwood forests in various combinations of species and some areas of mixed podocarp-beech forest. This vegetation has, however, been modified to a great extent by animals, namely: deer, opossums, goats and sheep, introduced by the European settlers. Reduction of these noxious animals has been encouraged to improve the condition of catchment forests so as to control runoff and erosion.

2.3.3 Soils

The Hawke's Bay landscape has been affected by a complex interplay of geological and environmental factors. These have had a profound influence upon the soil environment and consequently in determining the kind of soil present. Soil surveyors working in Hawke's Bay, have shown how age and composition of the deposits, dynamic processes, local climate, vegetation and relief, which together constitute the soil forming factors, are responsible for the unusually wide range of soils present within the region (Pohlen

et al., 1947; New Zealand Soil Bureau, 1968; Ministry of Works, 1971; Rijkse, 1980; Noble, 1985; Page, 1988). The following is a review of these factors.

Soil parent materials

Soil parent materials, within Hawke's Bay, are of very mixed origins and combinations. These are subdivided for convenience, into five main groups:

1. Volcanic materials. Present in the north and west of the region. These include rhyolitic tephra and ignimbrite from Taupo and underlying this, andesitic tephra from the Tongariro Volcanic Centre and Egmont Volcano. Potentially there is 5-10cm of post-Taupo andesitic ash from Ruapehu and Ngauruhoe volcanoes in the topsoil.
2. Greywacke sandstone and argillite from the axial ranges.
3. Younger sedimentary rocks such as sandstone, conglomerate, siltstone, mudstone, limestone and bentonitic mudstone from the Neogene hill-country sequences.
4. Gravelly alluvium. This includes greywacke sandstones and argillite derived from the ranges; water-sorted Taupo Ignimbrite (Taupo Pumice Alluvium); tephra and local sedimentary rocks. These form the flood plains (Heretaunga and Takapau-Ruataniwha Plains) of the major rivers and local streams. Soils of the plains are a mosaic varying in their topographic position, susceptibility to flooding, drainage characteristics, depth and fineness of alluvium over gravels. Estuarine materials of the Ahuriri Lagoon are included in this grouping.
5. Loess, derived from the flood plains of the major rivers. The loess is thicker on the more stable landforms and thin or absent on steep lands. Hawke's Bay loess contains an appreciable volcanic ash component.

Dynamic processes

The soil pattern within the steep lands is affected firstly by erosion and secondly the subsequent redistribution of erosion products onto the lower slopes and flood plains. Less stable sites have lost their younger tephra cover and other easily eroded material. Thus in the hill-country sedimentary rocks are soil-forming on the upper slopes whereas at lower levels soils are formed from admixtures of tephra, loess and bedrock brought down the slope.

Some of the eruptions from Taupo, for example the Taupo Ignimbrite, have been of the paroxysmal type in which a large volume of pumiceous material was ejected over a short period, burying the previous soil and vegetation. Consequently, soil formation and plant growth had to begin afresh on raw mineral materials. Eruptions from the Tongariro Volcanic Centre and Egmont Volcano have ejected small amounts of material on numerous occasions over long time periods. The original vegetation and soils have thus been gradually buried, their growth and development interrupted continually by fresh accretions of ash. Similar effects on soil formation are produced on the outer edges of deposits from paroxysmal eruptions, the important difference being the rate and thickness of the accumulation.

Both erosional and depositional processes are recognised within the Hawke's Bay landscape. During periods of stability soil profile differentiation has progressed on the more "stable" land surfaces. Evidence to support the cyclic nature of these events is shown by the presence of buried soils within fans and flood plains and the presence of tephra layers of known age within these deposits. Periods of instability are interspersed within these stable periods. These episodes are marked by erosion in upper slope positions and the deposition of colluvial deposits in lower slope positions.

Relief

Relief is an important factor in determining the soil patterns seen in the Hawke's Bay landscape. It determines the erosion pattern, controls soil stability, erosion and down-slope sedimentation, and indirectly by modifying the climate or distribution of native vegetation. Soils on steeper slopes are generally relatively youthful as the soil tends to be renewed regularly by mass movement or other forms of erosion.

Age

At the maximum of the Last Glaciation both erosional and depositional processes were heightened. Consequently, many of the soils seen today, even those on the more stable landsurfaces (e.g. river terraces), post-date this time. The dating of these soils will be discussed in Chapters Five and Six.

Palaeosols, or soils of an environment of the past, are intercalated within loess, tephra, colluvium and alluvium. These have been differentiated in New Zealand, into buried, relict and exhumed palaeosols (Gibbs, 1971; 1980) and will be used in this thesis to date the western Hawke's Bay soil-landscape.

Climate

This region has a wide variety of climatic conditions (see section 2.3.1). Variables which profoundly affect the soil environment include: variation in rainfall gradient as one goes from west to east; dry summer and autumns (droughts); dry westerly (föhn) winds and occasional high intensity rains which result in erosion and flooding.

Vegetation

After Europeans settled in the area the native vegetation of the region was replaced by exotic pastures and later partially by exotic forests. In the weakly to moderately leached soils the decline in chemical fertility after clearance was not great whereas in the more strongly leached soils the natural fertility declined rapidly. Present chemical fertility is maintained by humans and their animals and no longer is controlled chiefly by vegetation.

Within the New Zealand Soil Classification nine major soil groups (Hewitt, 1992) are recognised within the Hawke's Bay district. Brief notes on each of these follow and should be used in conjunction with the soil map, Figure 2.6.

Steep land soils

These soils occur within the ranges and on the steeper slopes within the western and coastal hill-countries. Here the soil pattern is often complex with weakly developed soils on unstable slopes and more strongly developed soils on stable slopes. When weakly developed the soils are usually shallow, being periodically rejuvenated by erosion, and reflect the influence of parent rocks more strongly than soils on more stable slopes, being less modified by the influences of climate and vegetation (Ministry of Works, 1971). Such soils are generally composed of a debris mantle consisting of a mixture of tephra, loess and underlying bedrock from upslope, in varying proportions.

LEGEND TO SOIL MAP


Brown Soils


Composite Allophanic over Brown Soils


Pallic Soils


Pumice Soils


Composite Pumice over Allophanic Soils


Organic Soils


Melanic Soils


Recent, Saline and Gley Recent Soils

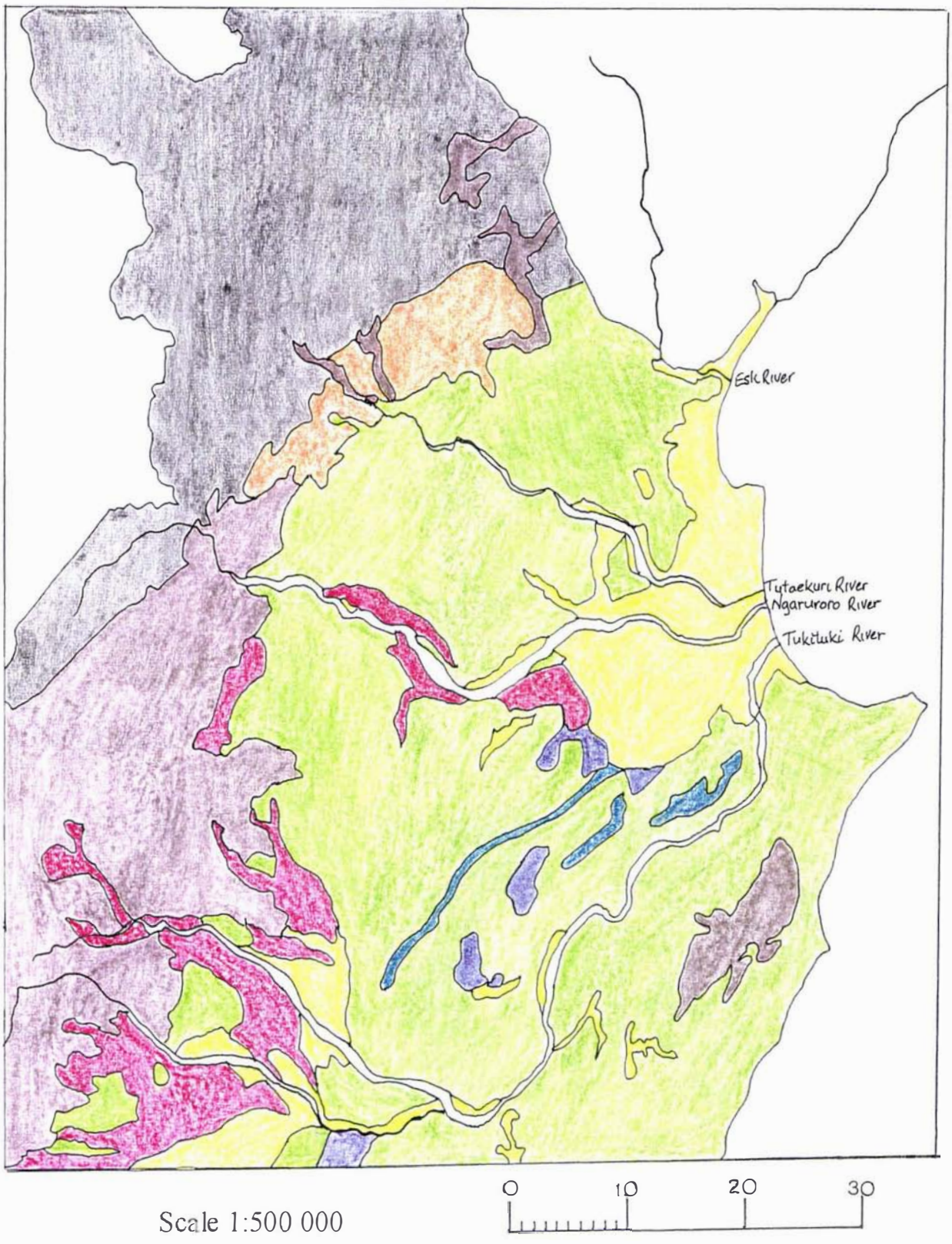

Figure 2.6: Soil distibution map for western Hawke's Bay.
Soil groups are from Hewitt (1992) and the map is adapted from Ministry of Works (1971).

The underlying rocks may be soil-forming where recent landslides have removed the debris and tephra mantle which previously blanketed the more westerly parts of the region.

Steep land soils are classified (see Fig. 2.6) according to whether they are related to Pallic Soils, Brown Soils, Melanic Soils, Allophanic Soils or to Pumice Soils.

Pumice Soils

These are widespread in the more western districts (closer to the ranges and hence volcanic sources) and are associated with airfall rhyolitic tephras (e.g. Kaharoa, Taupo and Waimihia Tephras) and ignimbrite (e.g. Taupo Ignimbrite) from paroxysmal eruptions.

Pumice Soils are very friable and are found on dissected plateaus, terrace lands and topographic lows where ignimbrite has been able to flow into the region. Topsoils are black to brown sands to sandy loams. The clay fraction consists almost entirely of allophane, produced by weak weathering of pumice. Pumice Soils are very friable and susceptible to wind erosion if the vegetative cover is destroyed by burning or cultivation. During the development of western Hawke's Bay, severe wind erosion removed the pumice to expose bedrock (Page, 1988). Many of these areas have remained bare. The combined depth of the rhyolitic tephra and/or ignimbrite usually exceeds 50cm. It may, however, be less in the case of steep land intergrades.

Composite Pumice Soils on Allophanic Soils

Composite soils occur in areas where Taupo Tephra, Taupo Ignimbrite and Waimihia Tephra are less than 50cm in depth and overlie older, more weathered, tephras (usually andesitic tephras). Here the upper part of the profiles have the characteristics of a Pumice Soil and the lower parts an Allophanic Soil.

Allophanic Soils

These are soils developed from fine-textured andesitic tephra derived from the Tongariro Volcanic Centre and Egmont Volcano. Allophanic Soils have grey or brown loamy friable topsoils overlying yellowish brown to brown friable subsoils.

Intergrades, between Allophanic and Brown Soils may be formed from alluvium of silt loam texture containing varying proportions of andesitic ash.

Brown Soils

These soils occur in hill-country, under a forest cover, and are developed on mudstones, siltstones and sandstones, where annual rainfall is in excess of 1200mm. Topsoils are loamy, brown to greyish-brown with slightly finer textured (firm clay loams) brownish-yellow subsoils. Subsoils have moderately developed nutty structures and rarely show mottling.

On dissected older terraces and also on lower terrace lands where the silt mantle is shallow these soils can include 5-50% gravel and stones.

These soils are often shallow and possess a brown topsoil overlying a shallow yellowish-brown subsoil on weathering rock.

Pallic Soils

These soils occur in the east of the study area on a wide range of terrains, from terraces and rolling hill-country to bluffs and gorges. They are developed within loess which overlies Neogene sandstones, siltstones, mudstones and limestones. Mean annual rainfall is generally less than 1000mm per annum (Hewitt, 1992).

Soils are weakly to moderately leached and experience a marked dry season when rainfall is inadequate for optimum plant growth. They are characterised by greyish-brown, weakly structured, loamy topsoils and pale brown to pale yellow, nutty subsoils that are flecked brown and grey. In these Pallic Soils hard, tabular duripans and

compact prismatic or columnar fragipans, with widely spaced cracks, are present. These horizons impede percolation during wet spells.

Intergrades between Pallic and Brown Soils are more leached, experience a higher more uniform rainfall (1000-1200mm/yr), have less well developed pans and are less mottled than their Pallic Soil counterparts. Topsoils are more strongly developed with granular and nutty structures. Subsoils are slightly darker and yellower in colour.

Steep land soils, associated with the Pallic Soils and intergrades with Brown Soils, are divided principally on the type of parent material present.

Recent, Saline and Gley Recent Soils

These groups includes soils of river flats, swamps, lagoons and sand dunes where the dominant process is recent accumulation. Soils are formed within alluvium derived from sedimentary rocks and ignimbrite and often contain minor quantities of volcanic ash. Recent Soils from alluvium are deep, brown to yellow loams with scarcely any top-soil differentiation where accumulation is rapid or with a deep, dark granular topsoil where accumulation is slow.

Gley Recent Soils are soils where drainage is poor or ground water is near the surface for prolonged periods during the year. This leads to the formation of a grey subsoil which is commonly mottled with rust colours. These soils are often confined to small, narrow seepage areas on the margins of terraces and hill-slopes. Although these soils are numerous they often cannot be shown on maps due to scale limitations.

Saline Soils are formed on sediments that have been submerged by sea water or subjected to salty ground water contamination. The most extensive saline area is the former Ahuriri Lagoon which was raised above sea level during the 1931 earthquake.

Organic Soils

These soils are formed in hollows and on low flats where the water table is permanently high and conditions lead to the accumulation of organic matter. Organic Soils have

peaty loam textures, possess at least 35% organic matter and may have up to 50% mineral constituents.

Peat (>50% organic matter) often forms in areas receiving water from limestone regions. In places peat may contain fresh-water shells and other calcareous deposits (Ministry of Works, 1971).

2.4 SUMMARY

From the above discussion it can be seen that climatic and geologic factors have predisposed the Hawke's Bay uplands (hill-country and ranges) to widespread erosion. Forest removal has been a significant triggering factor in historic times. There is, however, bountiful evidence of erosion on a large scale long before human habitation caused by a landscape of shattered hills associated with deep-seated weaknesses in the material underlying the soils, the rapid uplift of the land and the impact of infrequent, severe cyclonic storms (Molloy, 1988).

CHAPTER THREE:
REVIEW OF LATE QUATERNARY COVERBED STRATIGRAPHY IN LOWER NORTH ISLAND, NEW ZEALAND

3.1 INTRODUCTION

Dating events in the evolution the late Quaternary landscape within the central and southern North Island has been by a number of approaches because the terrestrial record is fragmentary and far from complete. The three approaches reviewed in this chapter form the basis for dating Hawke's Bay sequences. These entail the use of fluvial aggradation/degradation surfaces, loess stratigraphy and tephrostratigraphy.

The pre-existing Hawke's Bay record will then be related to the most complete and well dated late Quaternary terrestrial sequence within New Zealand, that of the interfingering marine and terrestrial sequences in the Wanganui Basin (Pillans, 1991; 1994a;b). The Wanganui Basin sequences are, in turn, correlated directly to the oxygen isotope, magnetic stratigraphy and palynology of deep sea cores (e.g. Deep Sea Drilling Program (DSDP) site 594 from east of New Zealand, Nelson *et al.*, 1985; Heusser and van de Geer, 1994; and DSDP site 593 from west of New Zealand, Head and Nelson, 1994), enabling correlation with the astronomical (Milankovitch) model for global climatic change (Pillans, 1994a).

3.2 DATING THE LATE QUATERNARY RECORD

3.2.1 Fluvial aggradational and degradational surfaces

Extensive suites of aggradational and degradational alluvial surfaces are a common feature of the southern North Island landscape and are particularly prominent in areas of rapid tectonic uplift (Cotton, 1942). Consequently, much work has been undertaken to examine the time-stratigraphic significance of these landforms.

Table 3.1: Major alluvial terraces and coeval loess sheets in Rangitikei Valley, Wanganui Basin

Terrace	Coeval loess	Age (Milne, 1973a) in ka	Age (Pillans, 1994a) in ka	$\delta^{18}O$ stages
Ohakea III		12 - 13*	10*	
Ohakea II		13 - 15*	12*	
Ohakea I	Ohakean	15*	18*	2
Rata	Ratan	30 - 40	30 - 50	3
Porewa	Porewan	70 - 80	70 - 80	4
Cliff	Cliff	100	90 - 100	5b
Greatford	Greatford	120 - 125	110 - 120	5d
Marton	Marton	130 - 140	140 - 170	6
Burnand	Burnand	170 - 180	240 - 280	8
Aldworth	Aldworth	230 - 240	340 - 350	10
Waituna	Waituna	> 245	360 - 370	10

*Tread ages after Pillans *et al.* (1993); all other ages refer to aggradation periods.

Note the Ohakean I, II and III terraces are in the order as first described by Milne (1973a) and not Pillans (1994a).

Table modified from Pillans (1994a).

Evidence for late Pleistocene glaciation, within the North Island, is very localised and restricted to Mount Ruapehu (McArthur and Shepherd, 1990) and some equivocal landforms in the Tararua Range (Shepherd, 1987; Pillans, 1991). Vella (1963b) put forward the proposition that a sequence of uplifted alluvial terraces, within the Wairarapa Valley, formed under alternating periglacial and temperate conditions. River aggradation, he stated, resulted from accelerated erosion in the high country where cooling caused a lowering of the forest-line and an increase in mechanical breakdown of rock at the surface. River aggradation, he stated, indicated cooling and an aggradation surface a culmination of cooling during glacials and stadials. Conversely, degradation indicated warming, and an erosion surface the culmination of warming during interglacials and interstadials. Vella (1963b) distinguished formations mainly on: the position of the gravels within the terraces; the microtopographic features of the aggradational surfaces; and the presence or absence of loess cover on the aggradation surfaces. He then correlated the terrace sequence with the main divisions of the South Island's late Pleistocene glacial succession model of the time.

Later studies, at other localities within the lower North Island, supported and expanded on the premise of Vella (1963b) that successive alluvial aggradation and degradation phases are attributed to climatically controlled variation in the vegetation cover of a catchment (tree-line presently *c.*1000m a.s.l.) and could therefore be equated to the cold and warm periods of the Quaternary, respectively (Cowie, 1964b; Milne, 1973a; Kaewyana, 1980; Palmer, 1982a; Warnes, 1992; Vucetich *et al.*, 1996). Palynological studies have shown that conifer and broadleaf forest taxa were the usual interglacial and interstadial cover that was replaced by shrubland/herbland taxa and grass in glacial and stadial phases (Palmer *et al.*, 1989; Heusser and van de Geer, 1994).

The most complete sequence of alluvial aggradational and degradational terraces, together with their associated coverbeds, is that described in the Rangitikei Valley, Wanganui Basin, by Te Punga (1952) and Milne (1973a;b;c). This sequence extends back *c.*350ka and serves as the bench-mark to which other North Island terrestrial sequences are correlated (Table 3.1). Aggradation terraces are given individual names

as geomorphic forms. Individual terrace gravel deposits take the same name as the terrace it forms.

Milne (1973a), following the lead of Vella (1963b), subdivided the Rangitikei River terraces into 2 broad categories: aggradational and degradational. River aggradation was seen as a response to increased sediment yields from deforested upland areas during glacial and stadial times. This is supported by the radiocarbon dating of Ohakean terrace alluvium (Milne, 1973a; Marden and Neall, 1990; Pillans *et al.*, 1993) and the presence of subalpine pollen assemblages in Marton terrace alluvium near present sea level at Otaki (Palmer *et al.*, 1988).

Terraces with greater than 3m of alluvial gravels were termed aggradational, whilst those with less than 3m of gravels were termed degradational (Milne, 1973a). The choice of 3m as the critical thickness was guided by the maximum thickness of alluvium on clearly degradational terraces younger than the Ohakean terraces.

Dating the terrace chronology of Milne was highly dependent upon the age of the Mount Curl Tephra, fission-track age of 230±30 ka and potassium-argon age of 250±120 ka (Milne, 1973c). Recent redating of Mount Curl Tephra (Kohn *et al.*, 1992; Pillans *et al.*, 1996) yielded a zircon date of 340±30 ka, suggesting that earlier fission-track ages (Milne 1973c; Pillans and Kohn, 1981) may have suffered from undetected annealing of tracks in the glass samples and under etching of zircon samples during laboratory preparation (Alloway *et al.*, 1993). Kohn *et al.* (1992) consider the Mount Curl Tephra to be a correlative of the Rangitawa Pumice and have suggested the former name now be dropped from the literature. Pillans (1994a) has revised Milne's (1973a;b;c) Rangitikei terrace ages, in accordance with the revised fission-track age (Table 3.1).

Pillans (1994a) has also raised some problems about some of the earlier fluvial terrace chronologies. The Cliff terrace, a degradational terrace, may correlate with marine oxygen isotope (MOI) stage 5b *(c.* 90 ka) and could therefore be the same age as the younger part of Loess 4, recognised to the west of Wanganui. Likewise, the Greatford

terrace was also believed to be degradational by Milne (1973a) as its' gravels are typically <2m thick. The Greatford terrace, however, is a source of loess (Greatford loess) which implies a cool (aggradation) period. Milne (1973a) gave this terrace and loess an age of >120 ka because it is overlain by Mount Stewart dunesand, a Last Interglacial age (MOI stage 5e, 120 ka) deposit. Unfortunately, he confused the issue somewhat by correlating the Mount Stewart dunesand with the Rapanui dunesand (80-100 ka, equivalent to MOI stages 5a and 5c) and correlated Greatford deposits with MOI stage 5d. Furthermore, in a later publication (Milne and Smalley, 1979), the Greatford loess was deleted from the loess stratigraphy of the southern North Island for some inexplicable reason (Pillans, 1994a). Pillans (1994a) favours the retention of Greatford loess since the stratigraphic sequence in Milne (1973a) clearly indicates a loess layer younger than Marton alluvium and older than Porewan loess. Another error appears to be that some parts of the Burnand terrace, as mapped by Milne (1973a) have been shown by Pillans (1994a) to have a marine origin and are now mapped as part of the Brunswick marine terrace

The next logical step is to establish the stratigraphic relationships between the Rangitikei River terraces and the well documented and dated Wanganui marine terraces (Pillans, 1991; 1994a;b). This still has to be realised because the stratigraphic relationships of the Ngarino and Rapanui marine terraces with the Rangitikei River terrace sequence has not been unequivocally established (Pillans, 1994a). Palmer *et al.* (1988), however, have shown that the Tokomaru marine terrace (presumed to represent MOI stage 5e) truncates Marton terrace alluvium, containing subalpine pollen taxa at Otaki.

During the climatic amelioration of the Holocene, vegetation reinvaded upper catchment areas, thereby increasing the density of forest cover and decreasing the sediment yields from hill slopes. A number of Holocene aggradation fill terraces, however, may be seen along the reaches of most river systems with little or no loess cover. These surfaces clearly do not result from Pleistocene freeze/thaw erosion cycles within upper catchments and the subsequent transfer of material downstream. Studies

Table 3.2: Holocene alluvial aggradation periods in Hawke's Bay

Name of event	Age
Taupo	1764 years B.P.
Post-Taupo	1600 - 1500 years B.P.
Pre-Kaharoa 1	1250 - 1200 years B.P.
Pre-Kaharoa 2	1000 - 950 years B.P.
Waihirere	680 - 600 years B.P.
Matawhero	450 - 330 years B.P.
Wakarara	180 - 150 years B.P.
Tamaki	1870 - 1900 years A.D. (80 - 50 years B.P.)
Waipawa	1950 A.D. - Present

Reproduced from Grant (1990).

have consequently been undertaken to contrast the Pleistocene and Holocene controls on terrace formation in non-glaciated river catchments (Bull and Knuepfer, 1987).

Grant (1985; 1990; 1994; 1996), using radiocarbon, tephra and dendrochronological dates from 51 North Island basins, identified 8 periods of "synchronous" erosion and alluvial sedimentation throughout New Zealand within the last 1800 years B.P. (Table 3.2). The Taupo erosion period, identified only in the North Island, resulted from heavy rainfalls induced by the Taupo eruption. Each subsequent erosion period, Grant states, relates to periods of increased storminess or cyclonic storm tracks passing over central New Zealand. Factors such as earthquakes, burning and wild animal impact on vegetation, he believes, have not contributed substantially to these erosion periods (Grant, 1963; 1965; 1966; 1991; 1994; 1996). During cool, tranquil years the forests recover and soil erosion is exceeded by soil development. The total amount of sediment deposited in successive erosion periods has generally decreased towards the present day despite the human population increase since *c.*1000 years B.P.

Other studies in the west Tamaki River catchment, southern Ruahine Range (Hubbard *et al.* 1979; Hubbard and Neall, 1980), are more cautious in their appraisal of the causative factors forming Holocene depositional surfaces. These workers concur with Grant's views that natural cyclic processes of erosion are operative but add that these are coupled with important triggering mechanisms such as: intense rainstorms and windthrows; earthquakes along range-bounding faults; or vegetation destruction by fire. Slope instability has also been accentuated by burning and grazing during settlement of the land.

Stewart and Neall (1984) noted that an ameliorating climate at the end of the last stadial (16 200-14 700 years B.P.) may have led to increased fluvial erosion out of the mountain ranges and increased aeolian dust transport prior to the decline of the polar westerlies and the establishment of a forest cover at higher elevations. Milne's (1973a) work concurs with this view by inferring a time lag of some 2000-3000 years between the onset of the major retreat of South Island valley glaciers and the onset of revegetation of the North Island mountains.

Bull and Kneupfer (1987), in their study of the Charwell River in southern Marlborough, dated 11 Holocene terraces by weathering rind analyses. These Holocene terraces represent brief still-stands during a general phase of river downcutting. They concluded that this flight of Holocene terraces was formed by episodes of self-arresting internal feedback mechanisms (complex-response systems, Schumm, 1977) within the catchment area itself rather than having to invoke external environmental changes (climate, tectonics) for Holocene terrace formation as proposed by others working on soil-landscape interrelations (Grant, 1985; 1991; Bull, 1990).

Investigations in the southwestern United States reveal that during the last 10 000 years B.P. the number, magnitude and duration of erosional and depositional events in river valleys not only varied from valley to valley but also varied within the same valley (Kottlowski *et al.*, 1965). This indicates that deposition was not in phase everywhere and that apparently at least some depositional episodes did not occur in response to a single external control.

Basher and Tonkin's (1985) study in the Southern Alps indicates both soil nutrient status and climate strongly influence rates of revegetation on bare ground. Soils of sufficiently high natural fertility are rapidly recolonised by plants, thereby leading to less downslope erosion. Even dense plant cover cannot, however, prevent runoff during extreme storm events (Costa and Baker, 1981) but it can reduce sediment yields during such events.

Landscape instability may also be caused by external events. Pumice-rich alluvium, forming broad, low river terraces, may be seen along many of the rivers draining the central North Island Volcanic Plateau. This alluvium is thought to have been deposited rapidly in response to high sediment inputs into rivers after the Taupo Volcano erupted *c.*180 A.D.

3.2.2 Loess stratigraphy

In the southern North Island a "silt-like" deposit of supposed marine or alluvial origin was recognised on a variety of pre-Holocene aged surfaces. Despite some earlier workers noting the similarity of these "silty" deposits with loess (e.g. Birrell and Packard, 1953; Fleming, 1953) it was Cowie (1964a;b) who confirmed its aeolian (loessial) origin. Cowie (1964a;b) identified a widespread rhyolitic tephra, the *c.*22 600 year B.P. Kawakawa Tephra (Aokautere Ash Member) within these deposits. As the Kawakawa Tephra mantles aggradation surfaces of differing heights and thereby ages, both it and the enclosing material are presumed to have been deposited subaerially. Measurements on the amount of material overlying the tephra show it to thicken towards the eastern (downwind) banks of the Rangitikei and Manawatu Rivers. Cowie (1964b) thereby concluded that this "silty" material was loess blown up from the riverbeds onto the upper terraces and downlands by the prevailing westerly winds at times of alluvial aggradation during the Late Quaternary. A similar relationship between loess thickness, texture and distance from rivers was then established in the South Island (Raeside, 1964; Young, 1967) and overseas (Ruhe, 1975).

Once the aeolian nature of the silty deposits was confirmed it was suggested that North Island loess deposits may have a high potential stratigraphic value, both for correlation and dating, because loess production was probably climatically controlled. Coupled with this is the fact that the southern North Island lies within a zone of tectonic uplift, hence fluvial aggradation surfaces, if formed during each climatic cycle, are preserved in the geological record above present base levels of erosion and subsequent deposition. North Island loessial coverbeds could therefore be correlated with loess sequences, of obvious glacial affinity, within the South Island.

Milne's (1973a) thesis on the Rangitikei River terraces and their associated coverbeds set out to test this hypothesis. Critical to the establishment of any chronology is the recognition that each phase of alluvial aggradation, caused by climate deterioration, was accompanied by deposition of loess, blown up from the floodplain to mantle all pre-existing terraces. Consequently, each successively lower terrace has one less loess layer

than the previous one until on the terrace set of the last stadial there is little or no blanket loess cover.

Implicit to the glacial origin for loess is that each loess layer and corresponding aggradation gravels represent a period that coincided with maximum ice advances in the South Island and periglacial conditions in the North Island ranges. During interstadial and interglacial times loess production was drastically reduced, resulting from general landscape stability and soil development, with consequent river degradation. Strongly developed paleosols within loessial sequences represent interglacial stages whereas weakly developed paleosols or loess contacts without detectable paleosols represent interstadial intervals. A potential problem faced by loess stratigraphers is that loess sequences predating the Last Interglacial may have been deeply weathered during this event making interstadial paleosols difficult to identify.

Milne's study (Cowie and Milne, 1973; Milne, 1973a;b;c; Milne and Smalley, 1979) established the climatic model for loess production and deposition within the North Island to be directly related to glacial advances and outwash aggradation surfaces in Westland (Suggate, 1965). Consequently, his study, spanning a *c.*350ka sequence (Table 3.1), served as a blue-print for paleoclimate and loess chronologies throughout New Zealand. Of critical importance to this chronology was the recognition and dating of two interbedded rhyolitic tephra, the Kawakawa Tephra radiocarbon dated then at *c.*21 ka and the Mount Curl Tephra then fission-track dated at *c.*230 ka (Milne, 1973a;b;c). Both tephras have widespread distributions allowing direct correlation with loess sequences containing the same tephras in the Wairarapa (Ghani, 1974; Kaewyana, 1980; Palmer, 1982a, Vella *et al.*, 1988; Palmer *et al.*, 1989; Warnes, 1992; Vucetich *et al.*, 1996), Wellington (Milne and Smalley, 1979; Te Punga, 1984), Wanganui (Pillans, 1988a; Wilde and Vucetich, 1988), Marlborough (Eden, 1987; 1989), Manawatu (Cowie, 1978) and Southland (McIntosh *et al.*, 1988; Eden *et al.*, 1992) districts.

Kawakawa Tephra occurs commonly within the youngest loess layer (Loess 1 or Ohakean loess) identified within North Island coverbed sequences. It is usually found in a position two thirds the way down from the surface of the uppermost loess (Milne

and Smalley, 1979; Palmer, 1982b; Pillans *et al.*, 1993). Radiocarbon dating of tephras, especially the widespread Kawakawa Tephra, were critical to proving loess accumulated in step with river aggradation. These dates indicate the Ohakean loess begun accumulating at 25ka and ceased accumulating in the period 10-14ka (Pillans *et al.*, 1993). Ohakean loess is therefore broadly coeval with the Last Glacial maxima and is found on all stable surfaces predating the Ohakean terrace.

Since Milne's original work both tephra dates have been revised. The Kawakawa Tephra has been redated to 22 590±230 years B.P. (Wilson *et al.*, 1988). A revised stratigraphy and new fission-track dates on the Mount Curl Tephra show it to now be 0.35±0.04Ma (see section 3.2.1) and a correlative of the Rangitawa Pumice and the Whakamaru Ignimbrite. Since most of the loess chronologies from other regions of New Zealand are tied to the original ages of the Kawakawa and Mount Curl Tephras, a revision is needed. A revised loess chronology will require concomitant adjustments to the estimated ages of underlying landforms, particularly river terraces (Kohn *et al.*, 1992; 1996; Pillans *et al.*, 1996).

Milne's method of naming each loess after its coeval aggradation gravel (lateral facies equivalent) has proved to be satisfactory in New Zealand. The lithostratigraphic and chronostratigraphic terminology used for the Rangitikei River terraces their respective loesses and their inferred climatic substages are in widespread use in the southern North Island yet were never formally defined at type or reference sections by Milne.

Pillans (1983; 1988a) sought to rectify this by describing and dating a much older sequence extending back to *c.*700 000 years B.P. containing at least 11 loesses, with intercalated tephra beds, overlying uplifted interglacial marine terraces in the Wanganui Basin. The marine terraces, by virtue of their non-marine coverbeds (loess and tephra), provide direct links between the marine and terrestrial records. Dating control has been facilitated by establishing stratigraphic relationships to: dated marine terraces (Pillans, 1988a); ages of intercalated tephras (e.g. Kohn *et al.*, 1992); thermoluminescence dates (Berger *et al.*, 1992; 1994); palaeobotanical sequences (McGlone *et al.*, 1984a; Bussell, 1988; Childs, 1992b); and a paleomagnetic stratigraphy (Pillans and Wright, 1990).

Attempts are presently being made to match the main loess accumulation episodes with the marine oxygen isotope record stages 3-17 (Pillans, 1994a). Loess stratigraphy thus provides a powerful tool for correlating and dating of terrestrial landforms such as river terraces, marine terraces and landslides.

3.2.3 Tephrostratigraphy

Much of the study area lies downwind (east) of the active volcanoes of the Taupo Volcanic Zone. Within the last *c.*50 ka there have been around 50 pyroclastic eruptions from the Taupo and Okataina calderas alone, whose airfall volumes have exceeded $1 km^3$ (Lowe, 1994). Hence, most of the region has been blanketed in andesitic and rhyolitic tephras of varying thicknesses, during the Quaternary period.

It was soon noted, within the North Island, that discrete tephra layers, intercalated within other deposits (e.g. loess columns), could be traced away from their source vent and used as time planes for dating geomorphological features and soil processes (tephrochronology). The most valuable time marker beds are those having widespread distribution over various surfaces and thick enough to be recognisable as distinct units. Rhyolitic tephra units best fit this category as their eruption style is usually violent and of quite short duration (days to a week). A tephra unit from such a source is thus virtually the same age from the top to the bottom of the unit and for stratigraphic purposes is taken to denote isochronous deposition. Andesitic eruptions, on the other hand, are commonly less violent and of an intermittent nature. Some andesitic tephra units may be short lived but others may be formed over tens of years. Differences in age between the top and bottom of the unit may be indistinguishable using current geological methods. Consequently, each andesitic tephra unit is regarded as being a single stratigraphic unit with either a single age or an age range.

Much of the early work, tracing rhyolitic tephras both towards and away from their sources areas, was undertaken by Pullar and Vucetich (Vucetich and Pullar, 1969; 1973; Pullar *et al.*, 1973; Vucetich and Howorth, 1976a). These "field" methods rely on the

Table 3.3: Late Quaternary rhyolitic tephras from the Taupo Volcanic Zone

Tephra	Symbol	Source	Volume (km3)	Age (ka)	Wilson's (1993) chronology
Kaharoa Tephra	Ka	Okataina	[6]	770±20	
Kaharoa Ignimbrite			<1		
Kaharoa Ash			5		
Taupo Tephra	Tp	Taupo	[87.5]	1850±10	Unit Y
Taupo Ignimbrite	Tpi		70		
Taupo Lapilli	Tl		12		
Rotongaio Ash	Ra		1		
Hatepe Ash	Hta		2.5		
Hatepe Lapilli	Htl		2		
Mapara Tephra	Mp	Taupo	2	2160±25	Unit X
Whakaipo Tephra	Wo	Taupo	2	2685±20	Unit V
Waimihia Tephra	Wm	Taupo	[19]	3280±20	Unit S
Waimihia Ignimbrite	Wmi		14		
Waimihia Lapilli	Wml		5		
Stent Tephra	St	Taupo ?	?	*c. 4000*	
Unnamed tephra*	-	Taupo ?	?	*c. 4300*	
Hinemaiaia Tephra	Hm	Taupo	3	4510±20	Units R-I
Whakatane Tephra	Wk	Okataina	10	4830±20	
Motutere Tephra	Mt	Taupo	1	5430±60	Units H-G
Tuhua Tephra	Tu	Tuhua	1	6130±30	
Mamaku Tephra	Ma	Okataina	6	7250±20	
Rotoma Tephra	Rm	Okataina	12	8530±10	
Opepe Tephra	Op	Taupo	4	9050±40	Unit E
Poronui Tephra	Po	Taupo	3	9810±50	Units D-C
Karapiti Tephra	Kp	Taupo	2	9820±80	Unit B
Waiohau Tephra	Wh	Okataina	18	11 850±60	
Rotorua Tephra	Rr	Okataina	7	13 080±50	
Puketerata Tephra	Pk	Maroa	1	*c. 14 000*	
Unnamed Tephra	-	Tuhua	-	*c. 14 500*	
Rerewhakaaitu Tephra	Rk	Okataina	7	14 700±110	
Okareka Tephra	Ok	Okataina	8	*c. 18 000*	
Te Rere Tephra	Te	Okataina	6	21 100±320	
Kawakawa Tephra	Kk	Taupo	[220]	22 590±230	
Oruanui Ignimbrite	Ou		150		
Aokautere Ash	Ao		70		
Poihipi Tephra	P	Taupo	1	*c. 23 000*	
Okaia Tephra	O	Taupo	7	*c. 23 500*	
Omataroa Tephra	Om	Okataina	[21]	28 220±630	
Omataroa Ignimbrite	-		5		
Omataroa Lapilli	-		16		
Awakeri Tephra	Aw	Okataina	2	*c. 29 000*	
Mangaone Tephra	Mn	Okataina	[22]	*c. 30 000*	
Mangaone Ignimbrite	-		6	35 3500±2200	
Mangaone Lapilli	-		16	*c. 33 000*	
Hauparu Tephra	Hu	Okataina	10	35 870±1270; 39 000±5600	
Te Mahoe Tephra	Tm	Okataina	0.3	*c. 39 000*	
Maketu Tephra	Mk	Okataina	15	*c. 41 000*	
Tahuna Tephra	Ta	Okataina	2	*c. 43000*	
Ngamotu Tephra	Nt	Okataina	2	*c. 45 000*	
Tihoi Tephra	Ti	Taupo	5	*c. 46 000*	
Waihora Tephra	W	Taupo	1	*c. 47 000*	
Otake Tephra	Oe	Taupo	2	*c. 48 000*	
Earthquake Flat Tephra	-	Kapenga	[7]	64 000±4000#	
Rifle Range Ash	Ra		2		
Earthquake Flat Ignimbrite	Ea		5		
Rotoiti Tephra	-	Okataina	[241]	64 000±4000#	
Rotoehu Ash	Re		90		
Rotoiti Ignimbrite	Rb		150		
Matahi Scoria	Mb		1		

* Eden *et al.* (1992)

Wilson *et al.* (1992)

Adapted from Manning (1996a)

recognition of an individual tephra unit based purely on field characteristics, namely: colour, texture, composition and consistence. Isopach maps, compiled after detailed "hand-over-hand" mapping were published, detailing the areal distribution of a particular tephra or eruptive sequence (Pullar and Birrell, 1973a;b). These maps serve as an aid in working out the likelihood of a particular tephra unit being present within an area. Table 3.3 outlines the principal rhyolite tephras within the North Island. Some of the more widespread tephras extend to the South Island and are also found in deep sea cores both west and east of New Zealand (Nelson *et al.*, 1985; Pillans and Wright, 1992; Pillans, 1994a). These facilitate regional correlation, particularly in the North Island and allow land-sea correlations to be made (e.g. Pillans, 1994a).

New Zealand stratigraphers date the enclosing deposits or associated geomorphic features by prefixing the tephra identified with pre- and post-. The tephra's age is thus used to bracket the age of a geomorphological feature or an event. In using the pre- and post- prefixes it must be recognised that the tephra deposition was probably a brief episode in what was otherwise a slow and gradual sequence of landform development (Pillans *et al.*, 1992). It does not necessarily imply sudden or catastrophic changes to the land surface.

The identification of a tephra often needs laboratory identification, especially in the case of microscopic and composite tephra layers. This entails detailed analysis of a sample's mineralogical composition (Ewart, 1963; Topping and Kohn, 1973; Kohn and Glasby, 1978; Howorth *et al.*, 1980) and glass chemistry (Froggatt, 1983; 1992), termed "tephra finger-printing." Laboratory methods are particularly useful in identifying a distal tephra unit where the full sequence of tephra units is not present. Simple count back procedures, in this situation, can be fraught with danger. Whilst many of the rhyolitic tephras can be mineralogically and chemically fingerprinted, this is rarely so with individual andesitic tephra, although major eruptive centres, such as Egmont and Tongariro, are distinguishable on their titanomagnetite chemistry (Kohn and Neall, 1973; Cronin *et al.*, 1996c). As the recognition and correlation of andesitic tephras close to source proceeds (Alloway, 1989; Alloway *et al.*, 1995; Donoghue, 1991;

Donoghue *et al.*, 1991; 1995; Donoghue and Neall, 1996; Cronin *et al.*, 1996a;b;c; 1997) so correlation into the Hawke's Bay loess column will be facilitated.

The sequence, age and distribution of many of the post-64 000 year B.P. rhyolitic tephras are now well documented and known with reasonable certainty (Froggatt and Lowe, 1990; Lowe, 1990; Lowe and Hogg, 1992; Wilson, 1993). These have been radiocarbon dated and are summarised in Table 3.3. Table 3.3 serves as the master chronology for this time period. Recent work by Wilson (1993) indicates that this chronology may have underestimated the number of eruptions from the rhyolitic centres of the Taupo Volcanic Zone. Alloway *et al.* (1994) have demonstrated this by identifying the Stent Tephra, a widespread and previously unidentified tephra from Taupo Volcano. Wilson (1993) states that some of the tephra formations identified by earlier workers in New Zealand as denoting an isochronous event may not always be true, as short time breaks (<10-20 years) within volcanic deposits may not produce a recognisable paleosol in macroscopic section. A further factor to consider is that erosion during the Last Glacial may also have deleted part of the record. Micromorphological investigations, currently underway at various sites within the central North Island, should clarify this (Bakker *et al.*, 1996).

The Kawakawa Tephra, comprising Aokautere Ash and Oruanui Ignimbrite members (Vucetich and Howorth, 1976b; Froggatt and Lowe, 1990), is one of the most widespread and important of the post-64 000 year B.P. tephra marker beds within New Zealand. Radiocarbon dates indicate ages in the range 20 000-23 000 years B.P. with ages on charcoal from Oruanui Ignimbrite averaging 22 600 years B.P. (Wilson *et al.*, 1988). This eruption occurred during the Last Glacial maximum (Ohakean) and so is particularly useful for correlating and dating deposits relating to this climatic episode (Pillans *et al.*, 1993). The consistent position of the tephra within the youngest loess bed (Ohakean loess) suggests synchronous loess deposition over a wide area of New Zealand during Ohakean time.

The sequence of older tephra beds (pre-64 000 years B.P.) is still poorly known with poor dating control in the 40-200 ka age range. Much work, most of it still ongoing, is

currently being undertaken to unravel this. Major advances and refinements in dating, especially in the areas of fission-track dating (Kohn *et al*., 1992; 1996; Alloway *et al*., 1993; Shane, 1994; Shane *et al.*, 1994a; 1995; 1996a;b; Pillans *et al.*, 1996); $^{40}Ar/^{39}Ar$ dating (Pringle *et al.*, 1992) and palaeomagnetism (Pillans and Wright, 1990, 1992) have offered new possibilities of dating materials beyond the range of the radiocarbon method (>40 000 years B.P.).

Of the pre-40 000 year B.P. tephras, the most stratigraphically important tephras are:

1. Rotoehu Ash which erupted from Okataina Volcanic Centre. It is found as a glass concentration at the base of the Ratan loess (Loess 2) with an age between 40 and 70 ka (Grant-Taylor and Rafter, 1971; Pullar and Heine, 1971; Ota *et al.*, 1989; Berryman, 1992; Buhay *et al.*, 1992; Wilson *et al.*, 1992; Whitehead and Ditchburn, 1994).
2. Rangitawa Tephra (=Mount Curl Tephra) which has a mean fission-track age of 340±40 ka (Kohn *et al.*, 1992; 1996; Pillans *et al.*, 1996) and is found within the upper part of oxygen isotope stage 10 in two deep sea cores. Rangitawa Tephra was probably associated with the eruption of the Whakamaru Ignimbrite (Froggatt *et al.*, 1986; Kohn *et al.*, 1992) from the vicinity of the Taupo-Maroa caldera (Wilson *et al.*, 1984; Lamarche and Froggatt, 1993), and
3. Potaka Pumice which is given an age of 1Ma based on fission-track, $^{40}Ar/^{39}Ar$ and magnetostratigraphic dating (Black, 1992; Shane, 1994; Shane *et al.*, 1996a). This tephra is important because it occurs close to a paleomagnetic transition from normal to reversed polarity, thus enabling substantial temporal control on early Pleistocene sequences within New Zealand.

Much of the tephrochronological work within New Zealand has been with proximal volcanic deposits. As the master chronologies are gaining more temporal resolution, distal deposits with thin or incomplete sequences of tephra can now be identified. Once identified, the relationship to the tephra's position within the master tephra chronology can be established and dates, if available, used to bracket events within distal areas. Statistical techniques on glass chemistries, such as coefficients of variation, similarity coefficients and discriminant function analyses, are proving to be increasingly useful

when used, in conjunction with stratigraphic principles, to identify an unknown tephra in distal areas, especially where the tephra is thin and the sequence incomplete (Stokes and Lowe, 1988; Stokes *et al.*, 1992; Shane and Froggatt, 1994).

Pyroclastic flow deposits (ignimbrites) are present in the west of the field area. These moved away from their eruptive centres, overtopping low points in the axial ranges and flowing downstream guided along major river valleys. Isopach maps show the Taupo, Oruanui, Rabbit Gully and Potaka Ignimbrites to be the most likely pyroclastic flow deposits to have entered Hawke's Bay (Wilson, 1993; Shane, 1994; Shane *et al.*, 1996a;b). These deposits have more local stratigraphic significance than airfall tephra but are important and useful because they are of known age and may provide information on rates of landform change.

The study area covered by this thesis is bounded by sites where drill-cores have been obtained and tephras, both rhyolitic and andesitic, identified. As these cores have been taken from lakes (Eden *et al.*, 1993; Eden and Froggatt, 1996), swamps (Howorth *et al.*, 1980; McGlone *et al.*, 1984b; Froggatt and Rogers, 1990) and offshore (Stewart and Neall, 1984; Fenner *et al.*, 1992) and not from coverbed sequences, only very broad generalisations about geomorphic processes can be made. One of the main reasons why little work has been undertaken on coverbed sequences is because thin tephra units are better preserved and clearly separated in lake and peat deposits. Tephras within these deposits are distinguished by their sharp contrasts in: continuity; colour; mineralogy and texture. Thin tephras within well drained soils e.g. loess can suffer from mixing processes by organisms which destroy the continuity of the tephra (Hogg and McCraw, 1983). Tephras present within a thick paleosol may, however, enable a maximum age for burial to be obtained. The A horizon of a paleosol may, if buried quickly by a sufficient thickness of material, be isolated from mixing processes within the overlying loess layer, enabling a maximum age for the paleosol to be obtained. Few previous studies have been undertaken on tephra units encapsulated within the Hawke's Bay coverbed sequences (Rhea, 1968; Roxburgh, 1974; Robertson, 1978; Griffiths, 1982; Hull, 1985; Raub, 1985). The object of this study is to identify the diversity of tephra

units present within these sequences and use them to elucidate the timing and rates of late Quaternary processes within the area.

3.3 SUMMARY

Correlations between on-land coverbed stratigraphy in Hawke's Bay and the marine oxygen isotope marine record are at present speculative and based on simplistic assumptions of synchronous climatic control. However, with rapidly improving methods of dating, such correlations are now becoming more soundly based, allowing for broad inter-regional correlations of increasingly finer temporal resolution.

Direct links have already been established between Chinese loess and the marine oxygen isotope record of the North Pacific (Hovan *et al.*, 1989; Ding *et al.*, 1994). Similar links can be expected in the future for the late Quaternary terrestrial record in New Zealand (e.g. Pillans, 1994a;b).

CHAPTER FOUR:
SOIL STRATIGRAPHIC PRINCIPLES AND SOIL-GEOMORPHIC MODELS USED IN THE NEW ZEALAND HILL-COUNTRY

4.1 INTRODUCTION

Surficial coverbeds mainly loess and tephra underlie a significant part of New Zealand's hill-country soilscape. In this chapter a review of soil stratigraphic principles is presented as applicable to deciphering the soilscape history within Hawke's Bay hill-country. These concepts are then applied in Chapter Five.

The second part of the review emphasises the spatial implications of paleosols to Quaternary research. New Zealand studies over the past two decades have documented the geographic distribution and stratigraphy of loess and tephra coverbeds in many regions, often as an adjunct to soil surveys, yet the integration of this knowledge into soil-geomorphic models is yet to be fully achieved. The conceptual framework of one such integrated landscape model, the fluvial system model of Schumm (1977), is reviewed. This model is then applied to the western Hawke's Bay landscape in Chapter Five and evaluated in Chapter Ten.

4.2 SOIL STRATIGRAPHY

4.2.1 Introduction

The concepts of modern soil stratigraphy, developed in the mid-western United States of America a century ago, were initially based on the premise that weathered bands in layered Quaternary successions were soils formed in past landscapes and could be used as marker horizons to denote landscape history (Finkl, 1980; 1984). Similar observations detailing the stratigraphy of loess, buried soils and the evidence of former land surfaces were made by Hardcastle (1889; 1890) in New Zealand but these remained unnoticed until the overseas work gained prominence.

Modern soil stratigraphy is now a branch of geology that entails the chronological ordering of pedological episodes, as expressed in surficial and buried soils, to facilitate the timing of Quaternary successions (Finkl, 1980). Once established, short- and long-range correlations of these layers can be made. Any assessment of the stratigraphic values of soils requires a thorough understanding of soil genesis, namely the environmental processes and factors responsible for soil development and how these change through time (Jenny, 1941; Birkeland, 1984).

4.2.2 Stratigraphic principles

Soil stratigraphers commonly employ the geological law of superposition and pedo-geomorphic concepts referred to as the principles of separate identity (Morrison, 1967) or random association (Butler, 1959), lateral continuity (Ruhe, 1959), ascendancy and descendancy (Ruhe, 1969a;b) and pedogenic persistence (Bryan and Teakle, 1946) to establish the relative age and distribution of multiple soil mantles or layers (e.g. loess) within a landscape.

The law of superposition states that in any undisturbed sequence younger surfaces overlie older surfaces. In a sequence of soil mantles there will be a relative chronology of regolith emplacement through time. A corollary to this law is that the soil can be no older than the parent material in which it is developed, and may be much younger. The independent nature or separateness of a soil mantle may be established by showing that changes in chemical and physical properties of the substrate are not reflected in the overlay, and vice versa, and by demonstrating that chemical and mineralogical trends within superimposed layers are independent of each other.

Lateral continuity in soil mantles involves the tracing of subsurface soil units from one locality to another. Soil development may take place in more than one parent material as reflected in stone-lines (Ruhe, 1959; Finkl, 1980) or different composition tephras. Leamy (1975) has shown, however, that soil development can mask the lateral

continuity of soil layers by transgressing both lithological and pedological boundaries. This needs to be taken into account when establishing lateral continuity (Finkl, 1980). According to the principle of ascendancy, a hillslope may be the same age or younger than the higher surface to which it ascends, whereas according to the principle of descendancy a hillslope deposit is the same age as the alluvial fill to which it descends (Finkl, 1984).

The concept of pedogenic persistence is based on the fact that many contemporary soils contain relict features (e.g. soil nodules) derived from a previous soil environment. The recognition of these features is critical to paleopedological studies and soil stratigraphy.

Since soil stratigraphy differs from conventional pedology, special terms have been invoked to describe the stratigraphic features of soil profiles and soil mantles.

4.2.3 The paleosol concept

Following the recommendations of the Working Group on the Origin and Nature of Paleosols (1971), a paleosol is now generally defined as "a soil formed on a landscape of the past or in environmental conditions different from those of the present day which can be either a buried or non-buried surface."

There are three basic kinds of paleosols (Morrison, 1967; 1978). These are:

1. relict soils which have remained exposed at the landsurface through at least two distinct soil-forming environments. These soils may also be termed polygenetic because climatic and biotic factors have changed during their development.
2. buried soils which formed on pre-existing landsurfaces and have subsequently been buried by younger sediment and/or rock. The depth of burial for consideration as a paleosol is a matter of contention (Hall, 1983). Buried soils may be subdivided into:

- simple buried soils where only a single buried soil is present
- compound buried soils where two or more buried soils are present that do not, or only slightly overlap in vertical succession, and

- composite buried soils where two or more buried soils are present that overlap one another to the extent that the original horizons of the individual soils are difficult to distinguish separately.

3. exhumed soils. These are soils or remnants of soils that were buried but have been exposed once more by the erosion of the covering material. The old landsurface may, in some instances, also be reexposed, appearing alongside and amongst contemporary soils and landforms giving rise to anomalous relationships to the present landsurface.

As paleosols are members of a continuum any stratigraphic succession may contain one or more of the above paleosol types.

A number of authors have criticised the definition of the term "paleosol" due to the emphasis it places on present environmental conditions (Catt, 1979; Fenwick, 1981; 1985). Climate, vegetation and anthropogenic influences have not been constant in New Zealand, even during the present post-glacial period. The term paleosol was initially restricted to buried soils of obvious antiquity (Morrison, 1967). Subsequent definitions have expanded the concept leading to increased confusion over the term (e.g. Ruellan, 1971; Bos and Sevink, 1975; Catt, 1979; Kemp, 1984; 1985). Kemp (1984; 1985) argued that the use of the term "paleosol" should be discontinued because when qualified by an adjective (e.g. buried) it implies no more than the term soil qualified by the same adjective. Hence, there is no difference between buried soil and buried paleosol, and this terminology is followed in the present work and where appropriate subdivided into simple, compound or composite types (Morrison, 1967; 1978).

From a stratigraphic viewpoint, simple and compound buried soils are of more value than relict or exhumed soils as both upper and lower soil boundaries may be defined by datable deposits. Inferences, derived from pedological properties within these soils, can then be related to a specific period of time. The value of the interpretation will depend, however, on the length of the time interval and the history of environmental changes, if known. The recognition of relict and exhumed soils is more difficult and needs to be verified by geomorphic and stratigraphic means.

Simple and compound buried soils are commonly used to separate deposits of different ages within vertical sections and to correlate deposits of the same age from one section to another. The most exhaustive stratigraphical applications of buried soils has been in the loess regions of central and eastern Europe (e.g. Kukla, 1977), the United States (e.g. Ruhe, 1969a; Follmer, 1978; 1982; 1983; Busacca, 1989; McDonald and Busacca, 1992) and China (e.g. Kukla, 1987; Hovan *et* al, 1989; Ding *et al.*, 1994).

The Working Group On the Origin and Nature of Paleosols (1971) concluded that buried soils should be studied by the same methods as used for surface soils. They particularly emphasised the complementary roles which field morphological descriptions and quantitative laboratory analyses should play in the overall identification of buried soils. Furthermore, they stated that emphasis should be placed on properties that are not subject to diagenetic change. Constituents measured should be those that persist and are relatively immobile, particularly with respect to their solubility in aqueous solutions and interactions with other soil components after burial. As no mineral is completely stable under all conditions, the objective is to choose the most stable constituent that yields the least possible room for alternative interpretations in a particular soil environment, at a particular stage of soil evolution. Less stable constituents (e.g. K, P) are also, by their absence or translocation, diagnostic of paleosols (Runge *et al.*, 1974).

Field criteria used in the identification of buried soils in New Zealand include: colour; structure; the occurrence of clay skins, roots or charcoal fragments. Buried soils are often identified by a chemical, elemental or mineralogical discontinuity within a soil-depth profile. Laboratory techniques used in New Zealand include:

1. determining levels of amino-acid nitrogen as an indication of biological activity which, when linked to stratigraphic evidence, provides confirmation of the occurrence of buried soils (Goh, 1972; Limmer and Wilson, 1980);
2. measuring the vertical variations and redistribution of:

- major and trace elements (Childs, 1973; 1975; Runge *et al.*, 1974; Childs and Searle, 1975);

- dry bulk densities (Palmer, 1982a; Palmer and Barker, 1984; Palmer and Pillans, 1996);
- quartz (Stewart and Neall, 1984; Alloway, 1989; Alloway *et al*, 1992a; Palmer and Pillans, 1996); and
- magnetic susceptibility (Pillans and Wright, 1990) by soil processes.

3. detecting the amounts of elements such as iron, aluminium and silica present in an extractable form as a measure of soil development (Birrell and Pullar, 1973; Webb *et al.*, 1986), and
4. assessing the relative proportions of primary, residual and organic phosphorus (Leamy and Burke, 1973; Runge *et al.*, 1974; McIntyre, 1975).

Many other laboratory techniques are also currently available to verify the existence of buried soils.

The affirmation that a layer represents a buried soil is rarely simple and irrefutable. Before proposing a buried soil stratigraphic unit, it is important to identify features which can be unequivocally attributed to soil development on a previous landsurface. These include: typical micromorphological soil features; characteristic depth-element functions; and a pattern of lateral variations that is logically linked to the geomorphological and geological features of that land surface (Catt, 1986). Difficulties arise when processes such as slope-wash or aeolian deposition have produced thinly layered soils not separated or isolated from subsequent pedogenic processes. If these superimposed soils are not recognised, soil properties may be incorrectly ascribed to only one set of pedogenic processes operating. In this situation, later pedogenic processes may mask or overprint those from earlier episodes, especially if they are more intense. Ruhe and Olson (1980) have proposed the term "soil welding" for such occurrences and suggested that physical and mineralogical properties could be used to identify welded soils. Other terms encountered in the literature to describe soils containing evidence of two or more different pedogenic episodes superimposed upon the same parent material (or the same vertical sequence of parent material) are composite (Morrison, 1967; 1978), layered (Valentine and Dalrymple, 1975), cumulic (Riecken and Poetsch, 1960) or polycyclic (Duchaufour, 1982) soils. If composite soils

are traced laterally to sites where the two or more component soils are separated they are known as subdivided (Morrison, 1978) or compound (Duchaufour, 1982) soils.

The value of a paleosol in reconstructing past environments depends on one's ability to recognise it in the first instance, and subsequently on one's knowledge of its properties (including those which may be ascribed to past environments), its variation over the paleo-landsurface, its stratigraphic relationship to other soils and sediments, and its relative or radiometric age (Valentine and Dalrymple, 1976).

4.2.4 Soil stratigraphic units

The comparison and correlation of soil sequences within widely separated, yet time-equivalent sites, has resulted in the need for a formal nomenclature to recognise and rank these units. Ruhe (1975) defines a soil-stratigraphic unit as a soil with features and stratigraphic relations that permit its consistent recognition and mapping as a stratigraphic unit and is distinct from rock-stratigraphic and pedologic units. The soil-stratigraphic unit is defined at a type locality by its features and relations to overlying and underlying rock-stratigraphic units and is correlated by its lateral variations and stratigraphic relationships. The unit may parallel or transgress time (Richmond and Frye, 1957; American Commission on Stratigraphic Nomenclature, 1961).

The establishment of criteria for recognising a soil-stratigraphic unit depends on detailed field and laboratory analyses on samples from type or reference sections. Reference sections must be carefully selected, bearing in mind that soil characteristics vary with physiographic position, parent material and climate. The technique consists of interpreting discontinuities or irregularities in a vertical section of materials to identify periods of soil formation and stratigraphic unconformities.

Several terms and concepts have been proposed for soil stratigraphy for inclusion into stratigraphic codes:

1. geomorphic surfaces (Ruhe, 1956; 1969a;b; Daniels *et al.*, 1971; Tonkin *et al.*, 1981);
2. pedo-morpholiths (van Dijk *et al.*, 1968);
3. ground surfaces (Butler, 1959);
4. pedoliths (Crook and Coventry, 1967);
5. pedoderms (Brewer *et al.*, 1970; Butler, 1982; Beckmann, 1984; Walker, *et al.*, 1984);
6. pedomorphic surfaces and forms (Dan and Yaalon, 1968), and
7. geosols (Morrison, 1967; 1978).

It is not the purpose of this review to define each of these proposed soil-stratigraphic units but to show that despite each of these terms differing from each other in detail they have the same central concept, that of a laterally extensive body formed by the pedological alteration of a rock-stratigraphic unit or a sequence of superimposed rock units (Brewer, 1972).

Soil-stratigraphic units in New Zealand have been defined as paleosols which by their intrinsic pedological properties and stratigraphic position can be consistently recognised and mapped. Leamy *et al.* (1973) state that a paleosol is distinct from a time-stratigraphic unit, a rock-stratigraphic unit and a pedologic unit and conforms to the following specifications:

1. it is defined on the basis of properties and stratigraphic relations described at a type locality
2. it occurs regionally, and
3. it represents only one period of time.

Implicit in the definition of a soil stratigraphic unit is the recognition that some pedological features will vary laterally in response to variations in one or more of the soil forming factors. This aspect is analogous to the "facies" concept used by geologists in lithostratigraphic and biostratigraphic units and is particularly important in the initial establishment of a soil stratigraphic unit. If this is not recognised inconsistencies will

arise by the failure to identify genetically different soils at different levels or genetically different soils at similar stratigraphic levels (Kemp, 1984). The current New Zealand Soil Classification (Hewitt, 1992) does not deal with soil-stratigraphic units. Soil stratigraphic units are time parallel where loess and tephra layers are thick. Conversely, where airfall deposits are thin soil stratigraphic units are not currently recognised because soil formation may persist on them through more than one time period (Leamy *et al.*, 1973).

Relict soils within New Zealand have not been regarded as soil-stratigraphic units because they are not buried and thus may vary in age laterally. These soils may, however, represent a specific period of time and this, it is suggested, should be indicated by using the relevant stage names. For example, soils that commenced forming in the present Interglacial and are still forming at present are termed Oturian-Aranuian soils (Leamy *et al.*, 1973).

4.3 SOILSCAPE TERMINOLOGY

4.3.1 Introduction

Models are essential tools in scientific research as they provide a conceptual framework within which to ponder facts and ask questions. Since models simplify reality, they invariably emphasise certain factors at the expense of others. Thus, different models permit the same facts to be viewed in different ways which often leads to different and sometimes new insights into the evolution of natural bodies and their inter-relationships. Beyond this, the value of any model is whether it aids in generating testable hypotheses, separates cause from effect, and advances an understanding of the system being studied.

Models of soil evolution are based on the observation that all natural bodies are complex open process and response systems. As such, they continuously adjust by varying degrees, scales and rates to constantly changing energy and mass fluxes, thermodynamic and environmental gradients and to internally evolved accessions and

threshold conditions (Johnson and Watson-Stegner, 1987). Consistent with these facts is the notion, embodied in the model, that disturbance and change are natural consequences of all soil and slope evolving processes.

The role and type of models that have been used in previous pedological studies are discussed in Dijkerman (1974), Huggett (1975), Smeck *et al.* (1983) and Tonkin (1984). In the following sections, conceptual models considered relevant to an understanding of soil development and distribution within accretionary (loessial and tephric) soils are reviewed.

4.3.2 Catena concept

The soil catena concept was developed in East Africa in the 1930's (Milne, 1935a;b; 1936) and is widely used in hilly terrain overseas to map and classify soil patterns observed on hillslopes. In New Zealand, however, the soil catena concept has been little used as a method of studying soil variability on sloping topography, except for a few studies in the South Island hill country (Tonkin *et al.*, 1977; Young *et al.*, 1977; Tonkin, 1984; 1985; Basher and Tonkin, 1985; Tonkin and Basher, 1990). A major reason for the lack of detailed investigations into these hill-country soils has been their seemingly complex erosional and depositional histories (Campbell, 1973; 1975).

A soil catena, as enunciated by Ruhe (1975), is "a physiographic complex of soils or a sequence of soils between the crests of hills and the floors of adjacent depressions or drainage ways whose profiles change from point to point in the traverse depending on the conditions of drainage and past history of the landsurface." The significance of the catena concept to soil-landform studies on slopes lies in the fact that it integrates the geomorphic processes of erosion, transport and deposition; and the hydrological processes of throughflow and solute transport with pedological processes (Ruhe, 1975; Tonkin, 1984).

Two variants of Milne's (1936) catena are recognised. In the first, physiography is shaped by denudation or other processes from a formation with a single, uniform lithological character. Soil differences then resulted from drainage conditions, the differential transport and deposition of the eroded material, and the leaching, translocation and redeposition of mobile chemical constituents. In the second, physiography is carved out of two or more formations which differ lithologically. Many workers restrict the term catena to slope sequences derived from a single type of bedrock or Quaternary sediment.

Soil catenas are subdivided into open and closed systems. Open systems are those where the drainage is such that sediments and solutes can leave the area. Closed systems are common in closed depressions whereby all of the sediment and solute is entrapped.

The catena concept fails, however, to give full prominence to the three-dimensional character of soil processes. To overcome this, the valley basin or erosional drainage basin, which accommodates catenary relations as well as the three dimensional character of soil and soil processes may be adopted as a basic functional unit of the soil system, as suggested by Huggett (1975) and Vreeken (1973; 1975a;b).

Another potential problem of the catena concept is that various parts of the hillslope are assumed to be approximately the same age and soil differences are attributed to the physiographic factor. This has been shown not to be always true as some of the material in depressions on a hillslope could be derived from the erosion of the landscape that slopes into the depression (Birkeland, 1984; Page *et al.*, 1994a;b; DeRose, 1996). It is therefore unlikely that the soil parent material of soils on slopes is the same as that in the depressions.

Milne's catena model subsequently evolved into the toposequence model. A toposequence is defined as a hydrosequence whereby soil profile colours are used as indicators of water table elevation. A major limitation of the model is that water movement, particularly lateral movement and the properties related to the movement of

materials in solution and suspension, are usually not addressed (Hall and Olson, 1991). Further criticism of the toposequence concept is that it is a two dimensional model and commonly ignores the concentrations and species of materials translocated through the landscape (Hall, 1983; Hall and Olson, 1991).

4.3.3 K-cycle model

One of the most widely quoted soil-geomorphic models for hilly terrain is the K-cycle model developed by Butler (1959) for the Riverine Plain of south-eastern Australia. In this model the development of soil-landforms were shown to be episodic and related to environmental conditions. Periods of erosion and deposition, which modified all or part of the landsurface, alternated with periods of geomorphic stability during which pedogenesis took place. Documentation of the periodic nature of landscapes and soil evolution has been undertaken in many parts of the world (Butler, 1959; Churchward, 1961; Ruhe, 1975; Leamy, 1975; Laffan and Cutler, 1977a).

Butler (1959) termed a complete erosion-deposition cycle, along with the soils which subsequently formed, one K-cycle. Subsequent periods of instability and soil formation would result in the initiation of a second K-cycle. K-cycles are designated K1 from the uppermost or most recent geomorphic surface. Older geomorphic surfaces are termed K2, K3, K4 etcetera at each locality.

Each K-cycle is initiated by an unstable period of erosion and deposition resulting in the destruction and/or burial of old surfaces. This is followed by a stable period whereby soils form on the new geomorphic surface. In this discussion the term geomorphic surface is used in preference to groundsurface, the term used by Butler; both terms describe similar concepts (see section 4.2.4). Unstable and stable phases within a K-cycle are suffixed by the letters u and s, respectively.

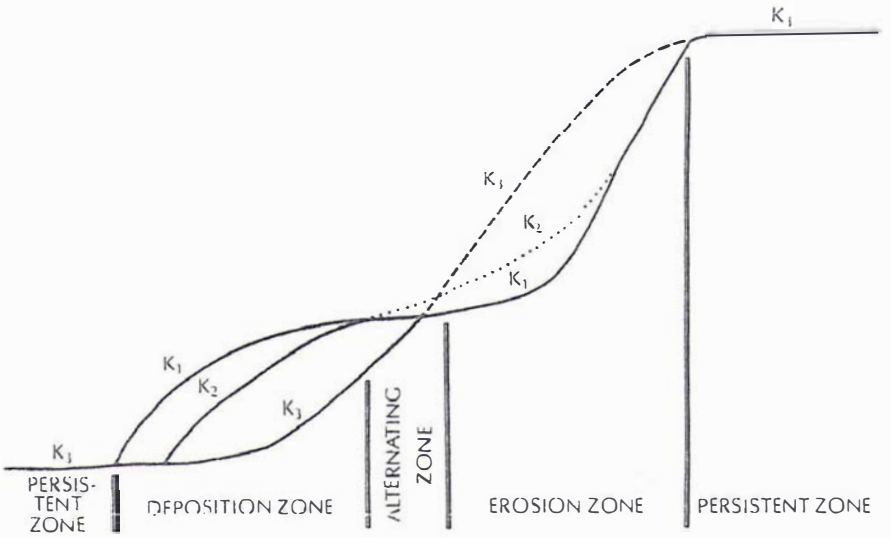

Figure 4.1: An illustration of hillslope zones and K1, K2 and K3 cycles (geomorphic surfaces) within the K-cycle model of Butler (1959) as modified by Burns and Tonkin (1982).

Hillslopes comprise four zones within the K-cycle model (Fig. 4.1). Each zone is distinguished by the spatial arrangement of its soils and the occurrence of relict, exhumed or buried soils. These are:

1. a persistent zone

   Occurs on those parts of a slope which are not affected by erosional or depositional slope processes. Relict soils are a common feature.

2. sloughing or erosion zone

   Found on the steeper part of the slope where the soil mantle is stripped away during each erosive or unstable phase.

3. an alternating zone

   Erosion has been less effective in this zone resulting in exhumed, truncated, cumulative and polygenetic profiles, and

4. an accreting or depositional zone

   Where erosion is effectively nil and below each mantle conformable superimposed geomorphic surfaces and their associated soils occur. Buried soils are common, each denoting previous K-cycles.

The depositional zone is a key area to decipher the record of K-cycles because each sedimentary deposit, along with its associated soil, is buried by colluvium from upslope. It should be noted, however, that the position and extent of both the erosion and depositional zones changes with time. Sloughing zones may become stable and accretionary zones unstable. The net result is that erosion maintains rudimentary soil development in the upper parts of slopes. A criticism of the concept is that even in quite small areas the stable and unstable phases overlap in time. This makes interregional correlations of cycles very difficult.

In summary, the K-cycle model shows a complex sequence of buried, exhumed and relict soils occurring within a landscape. To enable correlations to be established, detailed sampling strategies coupled with the application of precise stratigraphic principles need to be undertaken.

4.3.4 Chronosequence concept

The chronosequence concept is used to establish an *a priori* model of soil development with time. Land surfaces of unknown age may then be related empirically to those within reference sections. Jenny (1941) defined a chronosequence as an "array of related soils in a geographic area that differ, one from the other, in certain properties primarily as a result of time as a soil forming factor." This concept, along with examples from a variety of landforms, has been extensively reviewed (Jenny, 1941; 1980; Stevens and Walker, 1970; Vreeken, 1975a; 1984; Birkeland, 1984; Gerrard, 1992).

In the majority of chronosequence studies the comparative geographical technique is used, whereby soils of different age and location are arranged into a time sequence. This model makes the assumption that consecutive members of a sequence have at one time passed through and been identified with, the developmental stages represented by all preceding members. Daniels *et al.* (1971) questioned this by making the point that older soils in a chronosequence may not have gone through the same developmental history as the younger soils. Climate change (glacial-interglacial cycles) or differing water-table histories were cited as examples to prove this.

Studies have shown that the developmental direction is not the only pathway for pedogenesis. Interruptions to pedogenesis may occur, often as a result of landform instability or geomorphic processes. Johnston and Watson-Stegner (1987) have shown soil development may be either progressive or regressive with time. Under progressive development with time soils exhibit better horizon differentiation and stronger horizon contrasts. Regressive pedogenesis may result, for example, from the suppression of pedogenesis by subsurface erosion. It is often difficult to detect and even if detected may result in poor or no time correlations being made (Johnston and Watson-Stegner, 1987).

The construction of a chronosequence thus requires extreme care in making certain that the other soil forming factors (climate, topographic setting, vegetation and parent

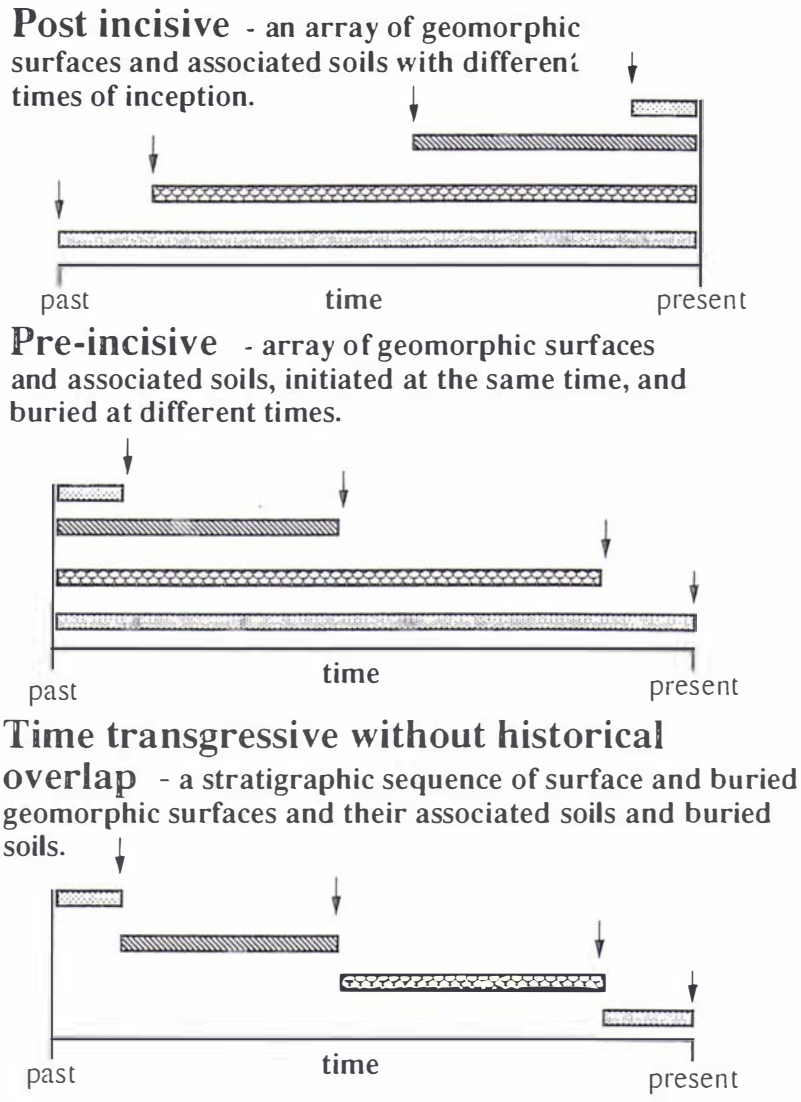

Figure 4.2: Categories of Vreeken's (1975a) soil chronosequences.

Reproduced from Tonkin (1994).

material) vary to a minimum. This restriction confines investigators to monogenetic soils (Nikiforoff, 1942). In practice, this is a major stumbling block in the quantitative interpretations of soil sequences as chronofunctions. As many soils have experienced changes in both climate and vegetation accompanying glacial-interglacial cycles those soils older than *c.*10 ka are thus a product of changing climatic conditions. Most workers recognise this within their interpretations.

Vreeken (1975a) recognised three kinds of chronosequences. He distinguished these in terms of the moments of initiation and termination of their soil development and on the degree of overlap in their soil history (Fig. 4.2). These are:

1. Post-incisive chronosequences

   A sequence of deposits of different age where the soils related to each deposit began to form in sequence at successively later times. Soils within these chronosequences are either still exposed or were buried simultaneously. Stepped river terrace sequences without coverbeds are an example of this type of chronosequence.

2. Pre-incisive chronosequences

   A sequence where soils began to form simultaneously but were buried at successively more recent times. The most recent soil is present at the surface. An example of this type of chronosequence may be seen on soils developed on a fresh glacial surface that has subsequently been buried by glacial ice.

3. Time-transgressive chronosequences

   These are soils that both began forming and ceased forming at different moments in time. Vreeken (1975a) subdivided these into: sequences with and sequences without historical overlap. In time, chronosequences with historical overlap are subject to erosion and deposition processes resulting in both buried and relict soils being present. These are often the most complicated sequences to resolve as each soil within the sequence began to form and then ceased to form at different times. Chronosequences without historical overlap are represented by a vertical stacking of sediments and buried soils, as found between successive depositional units.

Each type of chronosequence has its own particular attributes for the study of soil development with time. Vreeken (1975a) suggested that time-transgressive

chronosequences with historical overlap are the most useful chronosequences to study as they allow inferences about possible pathways of soil development to be made. Birkeland (1984) cautions that the properties of some of these chronosequences may be as much related to post-burial diagenesis or to slope position as they are to time. Few of the chronosequence studies within the literature fall into this category, most are post-incisive (e.g. Stevens and Walker, 1970; Bockheim, 1980; Birkeland, 1984). The major criticism of post incisive chronosequences, as pointed out by Vreeken (1984), is that many of them do not reflect monogenesis and until it can be proved that soil history repeats itself, they do not provide unambiguous information on rate variations of pedogenetic processes through time.

The dating of post-incisive chronosequences is often difficult as numerical dates are often lacking. Most dates obtained are age estimates based on chemical, biological, geomorphological and correlation dating methods (Colman *et al.*, 1987; Birkeland, 1990). Indices measuring the degree of soil development are sometimes used for relative age determinations in the absence of suitable reference chronosequences (Harden, 1982; 1983; Birkeland, 1984). Vreeken (1984) cautions that results obtained by this approach should be interpreted in a qualitative manner only and should not be used to the exclusion of other relative dating methods.

4.3.5 Geomorphic surface concept

The geomorphic surface concept of Ruhe (1956) has been widely used overseas (Ruhe, 1969a; 1975; Daniels *et al.*, 1971; Burns and Tonkin, 1982) and is gaining increasing use in New Zealand (Tonkin *et al.*, 1981; Tonkin, 1984; Eggleston, 1989) as a means of analysing the late Quaternary erosional and depositional soil-landscape histories of an area.

Ruhe (1969a) defined a geomorphic surface as "a portion of the landsurface comprising both erosional and depositional elements, having continuity in space and a common time of origin; it may occupy an appreciable part of the landscape and include many

landforms." A geomorphic surface may have formed in a short time (e.g. a volcanic ash fall) or have taken a long time to develop. It may be uplifted, lowered, faulted or warped by tectonic movements, and it may be buried without being destroyed. Once a geomorphic surface is eroded it is destroyed (Daniels *et al.*, 1971).

Tonkin *et al.* (1981) found a need to recognise spatial continuity within the erosional and depositional elements of a geomorphic surface. They defined:

1. buried geomorphic surfaces

   These are former geomorphic surfaces that are now buried and underlies the present geomorphic surface. Buried soils are common.
2. exhumed geomorphic surfaces

   These are buried geomorphic surfaces that have been exhumed by erosion.

The destruction or burial of existing geomorphic surfaces by erosional and depositional processes respectively results in the formation of intergrade elements prior to a new geomorphic surface being formed. These are:

1. degradational phases of a geomorphic surface. Recognised by the erosion and exposure of soil B horizons, and
2. aggradational phases of a geomorphic surface. These are recognised by the thickening of soil surface horizons (O or A horizons) as is commonly found in cumulic soils.

The establishment of a chronology of geomorphic surfaces is dependent upon the use of geomorphic and stratigraphic criteria. These are discussed in some detail in a number of publications (e.g. Ruhe, 1969a;b, 1975; Daniels *et al.*, 1971; Birkeland, 1984; Daniels and Hammer, 1992; Gerrard, 1992). The seven key points, as summarised by Tonkin *et al.* (1981), are as follows:

1. to resolve the stratigraphic relationships between geomorphic and buried geomorphic surfaces by applying the law of superposition (see section 4.2.2)
2. depositional geomorphic surfaces are the same age as the immediately underlying strata and younger than any underlying geomorphic surface. In fluvial landscapes

geomorphic surfaces commonly occur in successively lower topographic positions. In aeolian and glacial landscapes they may occur over a wider altitudinal range.

3. erosional geomorphic surfaces are more complex in their distribution and in their relationships to other geomorphic surfaces. An erosional geomorphic surface is younger than the youngest geological material it cuts and any depositional geomorphic surface that it may grade to.
4. buried geomorphic surfaces are identified by the presence of buried soils. Dating of materials associated with buried soils can provide a maximum age for sediments that underlie a depositional geomorphic surface.
5. the age of a geomorphic surface, its associated soils and surface weathering of exposed clasts are the same. These relationships are only maintained if the geomorphic surface is stable and there is minimal surface addition or removal of material.
6. the relationship between soils and geomorphic surfaces, and between buried soils and buried geomorphic surfaces, is the basis of soil stratigraphy (Morrison, 1978). Soils associated with erosional and depositional geomorphic surfaces may differ, because of contrasts in soil catenary relationships (Ruhe, 1975; Tonkin *et al.*, 1977), which may vary from exposure of bedrock to redeposited soil material.
7. maps showing the distribution and relative ages of geomorphic surfaces, depict the mappable erosional and depositional history of a drainage basin. Areas of present major surface instability can be identified because they lack the diagnostic soil, or surficial weathering features of a geomorphic surface.

The dating of geomorphic surfaces and their associated soils should ideally be undertaken by a variety of dating methods with overlapping time spans. These include:

1. radiocarbon dating
2. dendrochronology
3. rock surface dating
4. vegetation succession
5. soil profile development and soil developmental indices
6. tephrochronology
7. comparative changes in landform morphology

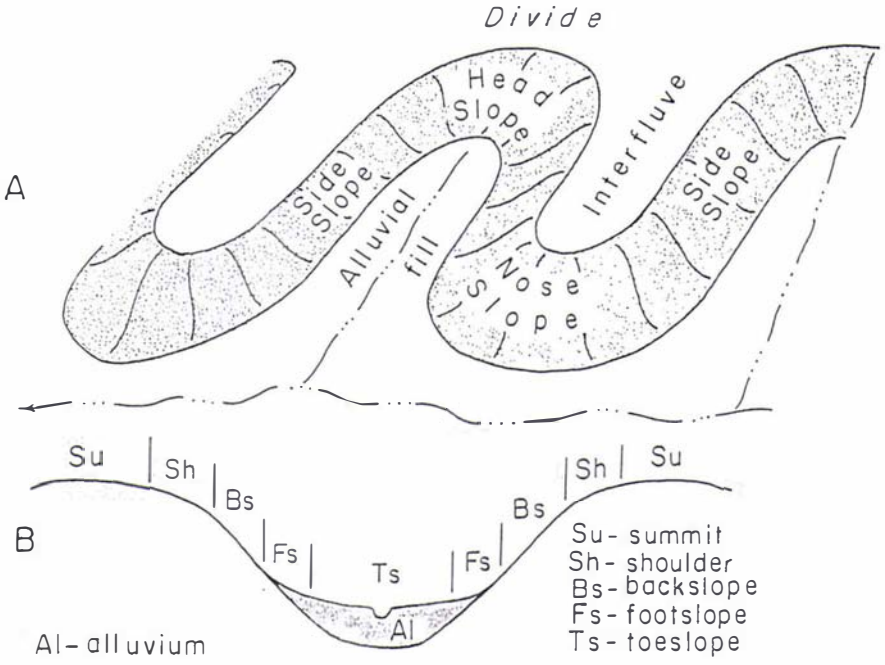

Fig. 1.—Geomorphic components of hillslope. (A) Slopes in an open system: *Headslope* is at the head of the valley, and slope lengths converge downward. *Sideslope* bounds the valley along the sides, and slope lengths generally are parallel. *Noseslope* is at the valleyward end of interfluve and slope lengths diverge downward. (B) On slope profile *summit* is upland surface and descent downslope successively crosses *shoulder*, *backslope*, *footslope*, and *toeslope*.

Figure 4.3: Geomorphic components of an open hillslope system.

Reproduced from Ruhe and Walker (1968).

The spatial relationships of the geomorphic surface concept may be integrated and used to complement Butler's (1959) K-cycle model.

4.3.6 Components of the hillslope

Ruhe (1960; 1969a;b; 1975) modified and renamed the hillslope components of Wood (1942), King (1953) and Frye (1959) by identifying elements in a fully developed hillslope (Fig. 4.3). These elements are now widely used to describe hillslope positions as they allow one to locate oneself within a landscape and help predict soil and sediment properties downslope.

Following the introduction of hillslope elements, Ruhe and Walker (1968) and Walker and Ruhe (1968) developed two models for hillslope landscape systems and formalised terms for geomorphic slope components. The two hillslope models recognised are:

1. open systems in which drainage basins are part of a more extensive drainage network and
2. closed systems in which drainage is trapped in a closed basin.

Within low order open drainage basins Ruhe and Walker (1968) distinguished a number of geomorphic hillslope components: divide; interfluve; side-slope; head-slope and nose-slope (Fig. 4.3). The head and side-slopes were further subdivided into Ruhe's (1960) slope profile components of: summit; shoulder; backslope; footslope and toeslope. In the closed landscape system Walker and Ruhe (1968) defined peripheral slopes which link divides with a central depository (Fig. 4.4).

The landscape components of a hillslope may develop in the following manner: summits and shoulders remain relatively unmodified by erosion; hillslopes (head- and side-slopes) become progressively truncated upslope by erosion and the debris eroded from the slopes may then be temporarily stored as valley fill before being removed by a stream. Sedimentologic and erosion records from these systems are often incomplete. If the basin is closed the eroded debris or fill remains in toe-slope positions. The record

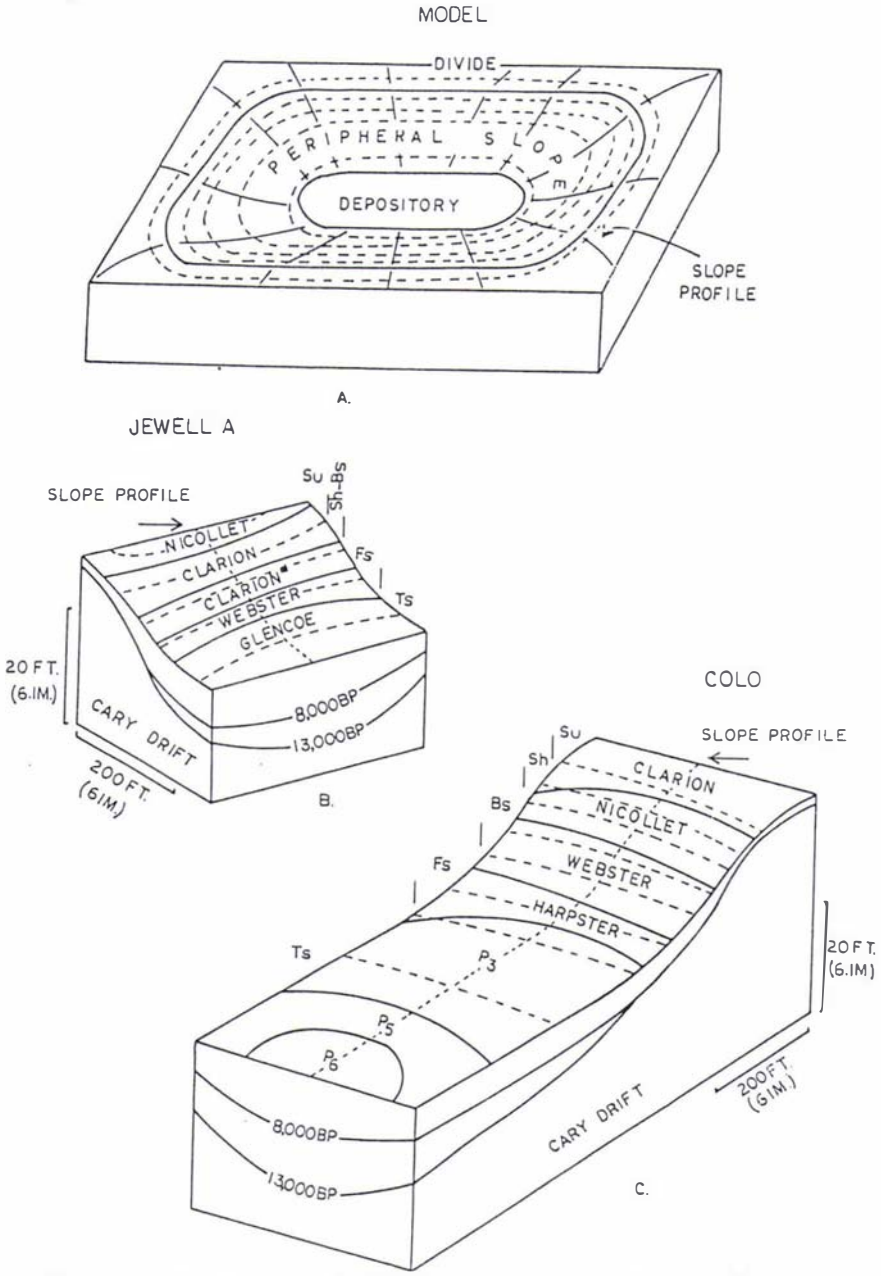

Fig. 1.—An illustration of the hillslopes of a closed system: A with concentric contours and radial slope profiles; B and C show topographic and soil data for type sites Jewell A and Colo. Contours, shown in broken lines, are at 2-foot vertical spacing. The soil unit Clarion* is a shallow-carbonate phase of the Clarion series. Slope-profile segments are as follows: Su = summit; Sh = shoulder; Bs = backslope; Fs = footslope; Ts = toeslope.

Figure 4.4: Geomorphic components of a closed hillslope system.

Reproduced from Walker and Ruhe (1968)

obtained from these positions is often complete. From this it can be seen that different landscape elements have different histories and are of different ages.

Daniels and Hammer (1992) warn that the term summit should not be used where coalescing backslopes have narrowed the interfluve or finger-ridges to the point that they are downwearing. Under these conditions the summit disappears and only a shoulder remains. They also noted that in dunal landscapes a slope may have a different genesis, depending upon whether it is on the windward or leeward side.

4.4 SOIL-GEOMORPHIC MODELS IN NEW ZEALAND

4.4.1 Introduction

It has long been realised that soil and geomorphological processes share a close relationship in the formation of a soil-landscape (Dijkerrnan, 1974). The study of soil-landscape relationships in New Zealand has often been undertaken as an adjunct to soil survey work. Webb (1994) reviewed a number of these soil-landscape studies undertaken in New Zealand.

The aim of soil-landscape studies is to produce a model whereby the ideas and experiences of the investigator, concerning the workings of the soil-landscape of interest, can be viewed at varying scales. One problem with the design of many of these models is that they simplify reality by being reductionistic in their focus. For a study to fit into the overall architecture of the soil-landscape system it needs to be holistic in its approach, integrated and capable of expressing recurring themes that govern soil-landform relationships. Tonkin (1994) feels that we are now at the stage where we can link or integrate existing models of climate, vegetation change and tectonic events with landform evolution.

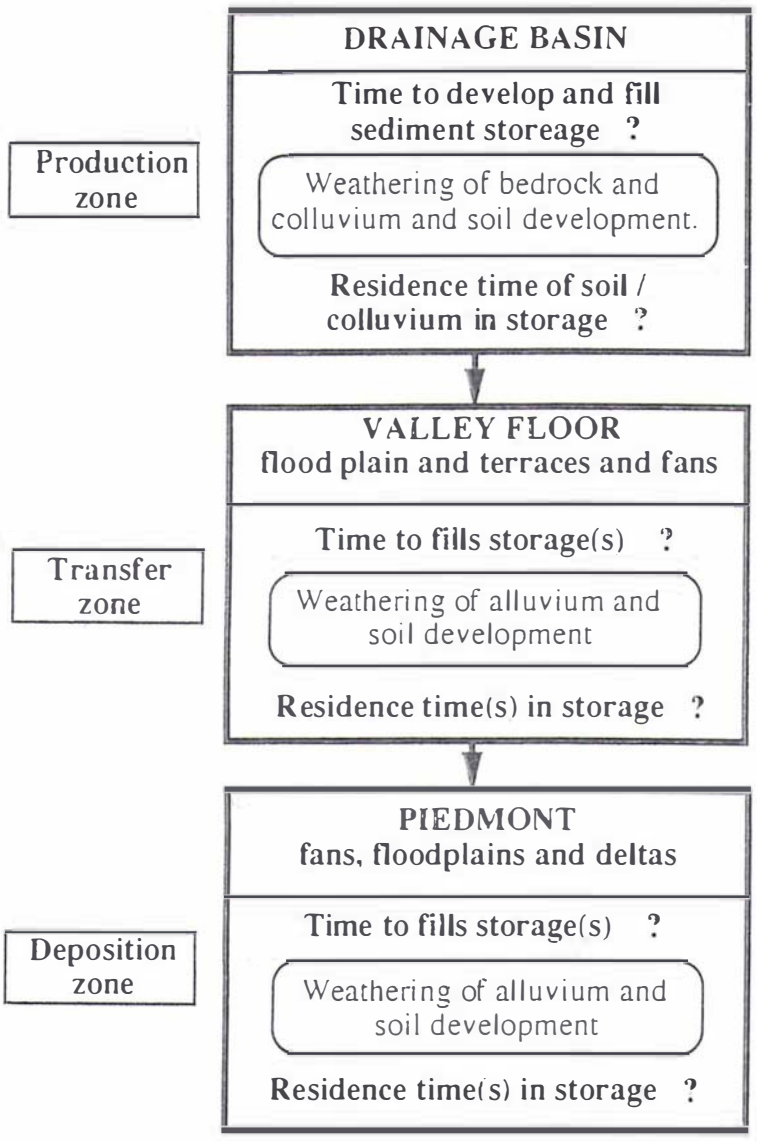

Figure 4.5: The fluvial system model of Schumm (1977), as modified by Tonkin (1994).

4.4.2 The fluvial system model

During the Quaternary there have been phases of intense erosion within drainage basins resulting in aggradation in lowlands to form valley fills, fans and piedmont plains. Many of these valley fills have subsequently been tectonically elevated and dissected to form spectacular valley terraces seen within many parts of the New Zealand landscape. Documentation and dating of landforms and their associated soil mantles within the lower North Island to date have been by loess stratigraphy and the use of tephra marker beds from the Taupo Volcanic Zone and Egmont Volcano.

Tonkin and his students (Tonkin *et al.*, 1977; Young *et al.*, 1977; Tonkin, 1984; 1985; 1994; Basher and Tonkin, 1985; Tonkin and Basher, 1990) have used Schumm's (1977) fluvial system model (Fig. 4.5) to view the interrelationships of soils to landforms within the drainage basins, valley floors, terraces and fans of the South Island of New Zealand. The utility of using this model is that it:

1. describes the movement or transfer of material through the various reaches of the fluvial system and relates these to the landforms seen
2. recognises a number of spatially linked, cascading subsystems, each of which may impact on the evolution of another linked subsystem (see Tonkin, 1994), and
3. recognises landforms as providing the foundation from which the regolith, soils and soil patterns evolve from.

The temporal and spatial organisation of landforms and their associated soils within the fluvial system model make use of the principles of soil stratigraphy, the K-cycle, soil chronosequence and soil geomorphic surface concepts described earlier on in this chapter. Further details pertaining to the principles of soil-landscape modelling and their applications in the study of soil-landform relationships within drainage basins are available in Tonkin (1994).

4.5 SUMMARY

Few New Zealand studies have attempted to describe the soil-landscape models used to unravel the late-Quaternary landscape evolution of a region or district. Most studies have been preoccupied with either late Quaternary stratigraphy, the relationships between landform elements (e.g. slopes and regolith types) or land-use aspects of soil science.

In this chapter a literature review of selected soil stratigraphic techniques and soil-geomorphic models has been made. These techniques and models are applicable to elucidating the landscape history of western Hawke's Bay and are utilised in subsequent chapters, Chapters Five to Nine.

In Chapter Ten the stratigraphic, soil-geomorphic and tectonic models used (Chapters Two to Four), along with the information obtained during the conduct of this thesis, are incorporated into an integrated landscape evolution model for western Hawke's Bay.

CHAPTER FIVE:
LATE QUATERNARY RECORD IN WESTERN HAWKE'S BAY

5.1 INTRODUCTION

Soil, land-use capability and geological surveys undertaken in the Hawke's Bay district have shown the surficial landscape comprises Quaternary aged fluvial gravels; ignimbrites; and layered loess-paleosol sequences which are intercalated with andesitic and rhyolitic tephras (e.g. Hughes *et al.*, 1939; Pohlen *et al.*, 1947; Grindley, 1960; Kingma, 1971; Rijkse, 1972; 1980; Griffiths, 1982; 1984; Noble, 1985; Page, 1988; Kamp, 1992a). Little research has been undertaken in Hawke's Bay to: characterise these deposits and record their distributions; describe the processes operative in their genesis, both during and after initial emplacement; and date these landscape-forming events. This chapter presents the research methods used to characterise these deposits and records their distributions. No attempt was made within this chapter to outline the landscape evolution of the district. This is undertaken in Chapter Ten once the analytical aspects (Chapters Six to Nine) have been interpreted and incorporated into the overall soilscape setting.

Quaternary studies undertaken within the lower North Island (e.g. Rangitikei: Te Punga, 1952; Milne, 1973a;b;c; Milne and Smalley, 1979; Wanganui: Pillans, 1988a; 1991; 1994a;b; Wilde and Vucetich, 1988; Manawatu: Cowie, 1964a;b; Wairarapa: Vella, 1963b; Palmer, 1982a;b; Kaewyana, 1980; Palmer *et al.*, 1989; Stevens, 1989; Warnes, 1992; Vucetich *et al.*, 1996; and southern Hawke's Bay: Rhea, 1968; Speden, 1978; Raub, 1985) have identified Quaternary climatic cycles (glacial-interglacial and stadial-interstadial cycles) as a major driving force behind the evolution of many of the soilscapes seen within these districts. The fluvial, loess and tephra stratigraphies and chronologies derived from these districts (see Chapter Three) were applied to the western Hawke's Bay landscape as a first approach to deciphering its late Quaternary history. The suitability of this approach, along with any insights made during the field work, is discussed.

5.2 FIELD STUDIES

5.2.1 Approach to field studies

It was realised in planning the project that the entire area designated for study (see Fig. 1.1) could not be studied in detail within the time and monetary constraints of a doctoral thesis. A general reconnaissance of the study area was undertaken. This involved driving along many of the roads within the district. The various landscape elements present were identified and their geomorphic surfaces recorded. Published information on the regional geology, soils and environmental setting (see Chapter Two) were evaluated in light of current chronologies and soilscape concepts (see Chapters Three and Four, respectively).

Representative windows were used to characterise typical landscape elements. These were then related to other landscape elements, of presumed similar origin, within the wider Hawke's Bay landscape. Landscape elements identified were: alluvial fans and terraces; loess and tephra mantled hillslopes; ignimbrites; eroded hills and terraces; and fault traces. Each of these is discussed in this chapter.

To decipher the pre-conditions and processes involved in the evolution of these landscape elements the following steps were undertaken:

1. surficial deposits and soil parent materials were characterised by established geomorphic, pedologic and stratigraphic techniques
2. soil properties were associated with their position in the landscape
3. the chronological ordering of geomorphic events and conditions, and
4. the construction of a time-stratigraphic framework within which to constrain geomorphic events. The relationships and variability both within and between individual stratigraphic units were emphasised.

Laboratory characterisation of deposits is undertaken in Chapters Six to Nine.

5.2.2 Dating the landscape

To determine the ages of surficial deposits the litho- and chronostratigraphic terminology established by Te Punga (1952) and Milne (1973a;b;c) for the Rangitikei River Valley within the Wanganui Basin (Table 3.1) were applied to aggradational terraces and loess-paleosol coverbed sequences within the district. This terminology is widely used within the lower North Island to date landscape evolution and correlate geomorphic events despite never having been formally defined, in accordance with established stratigraphic procedures, at type or reference sections.

The dating and correlation of surficial deposits were made possible by utilising andesitic and rhyolitic tephra layers found within loess-paleosol layers as time-lines. Tephra layers identified within the landscape were then correlated with the master tephra stratigraphies from the Taupo Volcanic Zone (see Table 3.3). Unknown tephra layers were identified using published data and isopach maps of andesitic and rhyolitic tephra distributions (e.g. Pullar and Birrell, 1973a;b; Donoghue, 1991; Donoghue *et al.*, 1991; 1995) coupled with distinctive field properties and known field relations, and chemical and physical properties of tephra components (Chapters Six and Seven). Once a match had been made with an eruptive event the dates obtained for tephra emplacement at the master sections could be used to correlate deposits within western Hawke's Bay and constrain the timing of landscape forming events.

5.3 ALLUVIAL FANS AND TERRACES

5.3.1 Introduction

During earlier geological surveys of the district (e.g. Grindley, 1960; Lillie, 1953; Kingma, 1971; Speden, 1978) extensive aggradational surfaces of presumed late Quaternary climatic origin and age were identified adjacent to the Mohaka, Esk, Tutaekuri, Ngaruroro and Tukituki-Waipawa Rivers. Little mention was made of their age and origin. The correlation and dating of these surfaces to Quaternary events was rudimentary, in terms of current knowledge, and required revision.

Plate 5.1: A view of the alluvial fan aggradational and degradational terraces along the true right bank of the Ngaruroro River. The prominent terrace with pine trees (arrowed) is the Ohakean terrace set. The coverbed stratigraphy on all higher terraces is fragmentary. (V21/153 748)

Plate 5.2: The current flood-plain of the Ngaruroro River is the source of present-day loess, particularly following floods where the silts are stranded on point-bars and in channels. After drying, north-west winds funnelling down the gorge lift the silt and transport it eastwards. However, there has been little long-term preservation on terraces older than the Ohakean. (U21/075 775).

A study was undertaken to find the most extensive fluvial aggradational and degradational terrace sequences in the district and to record the number of loess-paleosol layers blanketing each major terrace. Tephra layers were used as time-lines or chronohorizons. It was envisaged that a master chronosequence could be constructed to estimate the ages and sequences of aggradation and degradation events within the Hawke's Bay landscape, modelled along similar lines to that of Te Punga (1952) and Milne's (1973a;b;c) Rangitikei River Valley sequences within the Wanganui Basin (see Table 3.1). The next step was to establish whether the events recognised were induced by Quaternary climatic events (glacial-interglacial and stadial-interstadial cycles) and in-phase with sequences recognised elsewhere within the lower North Island, particularly those within the well dated Wanganui Basin marine and river terrace sequences.

5.3.2 The Ngaruroro River study: terrace-coverbed stratigraphy

5.3.2.1 *Introduction*

The Ngaruroro River has its headwaters in the Ngamatea Plateau and flows eastward incising deeply into the greywacke-argillite Kaweka Ranges. It cuts through the softer Neogene sequences of the western hill-country before crossing the Heretaunga Plains and debouching into Hawke Bay, north of Clive township (see Fig. 1.1). Details about the hydrology, former channels and man-made realignments of the lower reaches of the Ngaruroro River are available elsewhere (e.g. Hughes *et al.*, 1939; Kingma, 1971; Griffiths, 1982).

Field work was centred within the mid to upper reaches of the Ngaruroro River where exists a spectacular flight of fluvial aggradational and degradational terraces (Plate 5.1). The youngest terrace surfaces are at low elevations adjacent to the Ngaruroro River whilst older surfaces are found at successively higher elevations along the valley borders. Terraces are progressively higher above the present flood-plain with increasing distance upstream. Many of the older terraces have a partial loess and tephra cover. During the course of field work dust was observed blowing up from point-bars

on the current floodplain, indicating these to be the source of present-day loess (Plate 5.2). Former flood-plains are postulated to be the most probable loess-sources within the past. The accretion of loess on all older treads occurred whilst the river occupied a floodplain at a lower elevation.

Kingma (1971) subdivided late Pleistocene (Haweran) terraces along the Ngaruroro River into older H1 (e.g. Salisbury and Waharoa) and younger H2 (e.g. Pigsty) terraces. Holocene terrace deposits were distinguished from H1 and H2 terraces on their lower elevations and lack of dissection. H1 terraces were distinguished from H2 terraces by being more eroded and containing a greater proportion of pumice grains. Pumice in H1 terraces, unlike that in Castlecliffian deposits, are not present in bands but scattered throughout the deposit. Kingma (1971) described the greywacke gravels in both the H1 and H2 terraces as being fresh and not showing the same degree of weathering as Castlecliffian gravels. Rhea (1968) subdivided river terraces within the Dannevirke district of southern Hawke's Bay using the loess and tephra stratigraphies developed by Cowie (1962; 1964a;b) for the Manawatu district.

5.3.2.2 *Methods*

Surficial deposits were examined within both natural (e.g. terrace riser outcrops, stream cuts and gullies traversing the terraces and landslide scars) and man-made (e.g. silage pits and road cuts) exposures and by hand-augering. Heights of terrace surfaces were determined from contour intervals off 1:50 000 scale topographic maps (NZMS 260 U21 Kereru and NZMS 260 V21 Napier). Aerial photographs (1:25 000 scale) of the Ngaruroro River terraces were examined under a stereoscope. These photographs aided the preliminary mapping of these terraces and helped delineate the various geomorphic surfaces present.

Surfaces were distinguished on three main criteria:

1. their relative elevations
2. their geomorphological forms (degree of dissection), and

3. their coverbed stratigraphy (loess and tephra layers and buried soils).

5.3.2.3 *Results and discussion*

The Ngaruroro River terraces are inset within a number of low-angle alluvial fans. These alluvial fans emanate from a gorge at the range-front near Big Hill Station (Fig. 1.1), debouching eastwards into and onto the western hill-country and finally onto the Heretaunga Plains. Terrace surfaces bordering the Ngaruroro River decrease in height above the river's floodplain in a downstream (eastward) direction and merge with the late Holocene levees and floodplains of the Heretaunga Plains in the vicinity of the settlement of Maraekakaho.

In this study terraces along the Ngaruroro River were subdivided into three major groups: Holocene terraces, Ohakean terraces and pre-Ohakean terraces. The Ohakean terraces correlate with Kingma's H2 terraces and the pre-Ohakean terraces with Kingma's Hl terraces. Age control for these terraces is largely based on the correlation of late Quaternary airfall tephras from the Taupo Volcanic Zone.

Holocene terraces

Holocene aged terraces along the mid-upper reaches of the Ngaruroro River are found as point-bar deposits close to the present river level. These terraces are often localised, discontinuous and often unpaired. Some of these terraces are degradational, representing temporary still-stands in river incision whereas others are aggradational representing the temporary storage of material moving downstream. In the vicinity of Maraekakaho Holocene surfaces have prograded over Ohakean terraces to form the current surface of the Heretaunga Plains. Ohakean terraces at this location dip below the present day surface towards the axis of the NE/SW trending Hawke's Bay Syncline.

Holocene terraces comprise alluvial gravels and sediments derived from: the Mesozoic greywacke sandstone-argillite ranges; limestone, sandstone and mudstone from the softer Neogene hill-country sequences; and volcanic alluvium, principally Taupo Ignimbrite alluvium. Blanketing the terrace gravels are rhyolitic and andesitic tephras

and overbank sediments. Coverbeds are generally thin (<0.5m) hence the soils developed therein are often stony in character. They range from poorly developed (A/C) stony soil profiles to better developed (Ah/Bw/C) profiles where the tephra and sediment (loess and overbank silts) cover is thicker. Pedological differentiation within these soils are not as pronounced as in the soils of the higher Ohakean and pre-Ohakean terraces because of their younger age and thinner cover which does nor permit deep soil development.

The sequence and thickness of coverbeds overlying Holocene terraces were used to obtain minimum dates for terrace treads. Older (higher) terraces generally have thicker coverbeds than those nearer to the present floodplain. Topsoils comprise thin, often diffuse layers of andesitic ash and rhyolitic lapilli. The andesitic ashes correlate to the Tufa Trig (dated *c.*1850 years B.P.-present) and Ngauruhoe (dated *c.*1850 years B.P.-present) Formations (Donoghue, 1991; Donoghue *et al.*, 1995). Rhyolitic lapilli identified were from the Taupo-sourced Taupo (1850±10 years B.P.) and Waimihia (3280±20 years B.P.) eruptions (Froggatt and Lowe, 1990). Taupo lapilli are distinguished from Waimihia lapilli in that their vesicles (gas release channels) are long and continuous. Andesitic ashes seen beneath the Waimihia lapilli are correlated to the Papakai Formation, dated *c.*9700-3400 years B.P. (Donoghue, 1991; Donoghue *et al.*, 1995). Overbank silts are found either beneath the Papakai Formation or interspersed within the tephra coverbeds.

Closer to the ranges soils developed in Holocene terrace coverbeds have: a higher allophane content due to thicker volcanic ash accessions; dark, friable topsoil structures, greasy consistences (due to allophane) and higher organic matter concentrations due to higher mean annual rainfall. Rhyolitic tephras (e.g. Taupo and Waimihia tephras) in these regions are macroscopic and identified as discrete layers within the coverbeds.

Ohakean terraces

Kingma (1971) referred to the next set of closely spaced terrace treads above the Holocene terraces along the Ngaruroro River as H2 terraces or the Pigsty Flats. These

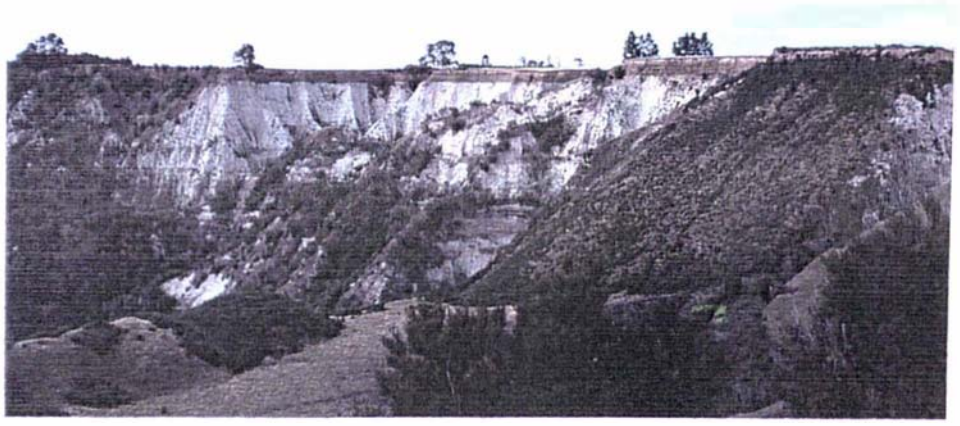

Plate 5.3: Ohakean aggradation gravels (brown) overlie a Nukumaruan mudstone strath along the Ngaruroro River. (U21/090 756).

terraces have treads up to 60m above the present river level and are referred to as Ohakean terraces using Te Punga (1952) and Milne's (1973a;b) terminology and criteria.

These are the broadest and some of the most laterally extensive surfaces in the district. Frequently, they are found at similar heights on both sides (paired terraces) of the Ngaruroro River. Typically, these terraces comprise a Nukumaruan mudstone or sandstone strath which is overlain by greywacke sandstone aggradation gravels with sand, silt and clay lenses (Plate 5.3). Blanketing the aggradation gravels are loess and tephra coverbeds.

In this study Ohakean terraces were subdivided into three subsets: Ohakean 1 (Oh_1), Ohakean 2 (Oh_2) and Ohakean 3 (Oh_3) from highest (oldest) to lowest (youngest), respectively. Risers separating each of these terraces are generally <3m in height, decreasing in a downstream direction. The greatest height difference is between the Oh_1 and Oh_2 terraces. The Oh_2 terrace has the broadest tread followed by the Oh_1 and Oh_3 treads, respectively.

In Chapter Eight a study was undertaken on a sequence of Ohakean terraces along the Mohaka River. The aim was to see whether Ohakean terrace treads could be dated by identifying the tephra/s at the base of the coverbeds using tephra fingerprinting techniques. In this chapter Oh_1, Oh_2 and Oh_3 terraces along the Ngaruroro River were separated primarily on their relative heights. Coverbeds on Ohakean terrace treads did not show a consistent increase in thickness nor in the number of loess-paleosol and tephra layers as one progresses up the sequence. No macroscopic tephra layers were present at the base of these coverbeds, consequently a minimum date could not be obtained for their respective treads. Terrace treads on all three Ohakean terraces are, however, younger than the 22 590±230 years B.P. Kawakawa Tephra (Wilson *et al.*, 1988). Kawakawa Tephra, a widespread macroscopic tephra layer within the lower North Island, was absent from their overlying coverbeds.

Plate 5.4: Coverbeds of up to a metre thick overlie Ohakean terrace gravels along the Ngaruroro River. From the current surface these comprise: rhyolitic lapilli of Taupo (1.8 ka) and Waimihia (3.3 ka) Tephras (in black topsoil); reddish brown andesitic ashes of the Papakai Formation (9.7-3.3 ka); and alluvial sands and silts on Ohakean terrace gravels. In many sections grey balls (≤3cm diameter) of fine andesitic ash may be seen near the base of the Papakai Formation ashes (not visible in this section). These correlate to the Mangamate Tephras (10-9.7 ka). (U21/088 764).

Blanketing Ohakean terrace treads are loess and tephra (rhyolitic and andesitic) coverbeds. Coverbeds rarely exceed 1.5m in depth, usually they are less than 1m in depth and thin towards the east. A sample from the topsoil was tested with Na-F to indicate the presence of reactive hydroxy-aluminium in short-range-order minerals such as allophane or ferrihydrite (Fieldes and Perrott, 1966). A high allophane content was indicated. The most likely source of allophane is from the weathering of volcanic ash. Fine layers of andesitic ash (<1mm each) from Mounts Ruapehu and Ngauruhoe have blanketed these terraces in 1946, 1974/5 (Mr Paul Renton, pers. comm. 1990) and in 1995 (Cronin *et al.*, 1996d). Andesitic ash accessions from the Tufa Trig (dated *c.*1850 years B.P.-present), Ngauruhoe (dated *c.*1850 years B.P.-present), and Papakai (dated *c.*9700-3400 years B.P.) Formations (Donoghue, 1991; Donoghue *et al.*, 1995) have also contributed to these coverbeds. Taupo (1850±10 years B.P.) and Waimihia (3280±20 years B.P.) lapilli (Froggatt and Lowe, 1990) were identified within the topsoil. Often these were not discrete layers. Beneath the Papakai Formation a quartzo-feldspathic silty layer of variable thickness (≤0.5m) and tephric content, probably tephric loess, is encountered. This silty layer exhibits a highly cemented, tabular structured horizon (duripan) which is underlain by a prismatic or columnar structured fragipan in the more eastern (downstream) sequences. Where the topsoil and Papakai Formation tephras have been removed, for example by an ephemeral stream, the duripan extends to the surface.

The thickness and preservation of loess and tephras relate to undulations within the underlying surface. Where there are hollows within the underlying landscape the tephra cover is thicker and better preserved (Plate 5.4). A soil developed within terrace tread gravels, overbank sands and silts, and tephric loess is commonly seen on the Oh_1 terrace tread. This buried soil is not evident on Oh_2 and Oh_3 terrace treads.

As one progresses eastwards the tephric component within coverbeds decreases as does the mean annual rainfall (see Fig. 2.5). Concomitant with these decreases in rainfall and tephric component is the appearance of highly indurated and cemented subsoil horizons within the coverbeds. The cemented horizons were identified as duripans and the non-cemented indurated layers as fragipans. The occurrence, distribution and

Plate 5.5: Coverbeds sequences on pre-Ohakean terraces along the Ngaruroro River are thin (≤1.5m) and lack the expected multiple loess-paleosol layers seen on similar terraces along the Rangitikei River. The absence of Kawakawa Tephra (22.6 ka), a widespread tephra commonly found within eastern North Island sequences, suggests stripping (see text). The tabular and blocky structures seen in these coverbeds are duripans and fragipans, respectively. (U21/097 704).

genesis of duripans within the soils of Hawke's Bay are discussed in Chapter Nine. Digging and hand-augering into some of the Ohakean and all of the pre-Ohakean coverbeds proved difficult due to the highly cemented and indurated nature of their subsoil horizons and was subsequently abandoned.

The owner of Glenmore station, Mr Paul Renton, informed the author that the Pigsty Flats (=Ohakean terraces) had been cleared of indigenous forest by early European settlers in the 1850's and then intensively cultivated. Severe wind erosion of the surficial soils resulted, both from deforestation and early cultivation practices. A cemented horizon is observed in many places either at or near the present-day soil surface. It is likely that the upper tephric part of the coverbeds has been stripped exposing the cemented horizon beneath.

Taupo Ignimbrite was absent from coverbeds overlying Ohakean terraces in the mid-upper reaches of the Ngaruroro River. Scattered blocks of reworked Taupo Ignimbrite are however, found overlying an Ohakean terrace which dipped beneath the Holocene floodplain near Maraekakaho.

Pre-Ohakean terraces

Above the Ohakean terraces three further sets of terraces are present. The highest and therefore oldest terrace-coverbed remnant is at 350m a.s.l., 150m above the Ohakean surface and 210m above present river level. Coverbeds on this (Plate 5.5) and other pre-Ohakean surfaces along the Ngaruroro River are thin (<1.5m) and lack the thick, multiple loess-paleosol layers recorded by Milne (1973a;b) for coverbeds overlying pre-Ohakean aged terraces along the Rangitikei River in the Wanganui Basin. Kawakawa Tephra was not found within any of the pre-Ohakean coverbeds on the Ngaruroro River terraces. This is despite the fact that *c.*1m of this tephra is known to have fallen on the Hawke's Bay district *c.*22 600 years B.P. (Berry, 1928; Pullar and Birrell, 1973a;b). These terraces could not therefore be confidently correlated to Milne's (1973a;b) pre-Ohakean sequences (i.e. Ratan, Porewan, etc; refer to Table 3.1) along the Rangitikei River. Likewise, coverbeds on what were clearly pre-Ohakean surfaces along the

Waipawa and Tutaekuri Rivers also lacked Kawakawa Tephra. These terraces are hence referred to as pre-Ohakean surfaces.

One proposition for the poor coverbed preservation on pre-Ohakean surfaces is that they had been stripped by the ensuing stadial (e.g. Ohakean). The stripping of loessial coverbeds from pre-Ohakean terraces has been observed elsewhere in Hawke's Bay (e.g. Speden, 1978; Marden, 1984; Raub, 1985; Marden *et al.*, 1986). These workers have, however, correlated their stripped pre-Ohakean sequences with the Rangitikei River sequences by simply counting back from the readily identifiable Ohakean surfaces. A further proposition is that pre-Ohakean terraces never had very thick loess coverbeds as rapid downcutting, combined with uplift and a funnelling of wind within the river valleys, meant they became increasingly isolated from the flood-plain loess source at that time. The absence of Kawakawa Tephra (22 590±230 years B.P.) on pre-Ohakean terraces indicates stripping to be the more likely explanation.

Clast sizes and sorting within terrace alluvium are variable. Many exposures revealed a considerable degree of clast segregation. Lenses within gravels can be traced for 2-3m. This variability is consistent with the constantly shifting nature of braided river channels.

Within Ohakean and pre-Ohakean terraces deeply incised gullies may be seen. Incision is often by a small ephemeral stream. As degradation of the terrace surface begins gullies become integrated and the relative relief increases. The enlargement and development of these gullies is by headward incision and bank collapse.

Surficial erosion, including sheetwash and rill erosion, has modified the terrace-coverbed edges of most pre-Ohakean surfaces. Colluvial aprons are common along many terrace risers. Overall this results in the morphology of pre-Ohakean surfaces becoming more rounded than that of Ohakean and Holocene surfaces.

The observation that many treads can be matched across the Ngaruroro River suggests that most were not simply part of the floodplain that were abandoned as the river swung

from one side of the floodplain to the other during downcutting (degradation treads). It is postulated that they have formed from base-level changes during long term uplift and climatic control. This hypothesis is supported by the fact that a major fault, the Mohaka Fault, crosses the Ngaruroro River in the vicinity of Big Hill Station and Poporangi Stream (see Fig. 1.1) resulting in fault displaced terraces. These are currently being investigated in another Ph.D thesis by Ms. Jude Hanson. Hanson's study details the periodicity of earth deformation along the Mohaka and Ruahine fault systems within western Hawke's Bay (Hanson, 1994; Neall *et al.*, 1994).

5.4 LOESS AND TEPHRA COVERED HILLSLOPES

5.4.1 Introduction

Much of the western hill-country (see section 2.2.2) between the Ruahine and Kaweka axial ranges and the Heretaunga and Takapau-Ruataniwha Plains is blanketed by layers, of varying thicknesses, of andesitic and rhyolitic tephras and quartzo-feldspathic loess. As the pre-Ohakean coverbed record on alluvial fan terraces was found to be incomplete, field studies were then focussed on the western hill-country. Coverbeds within numerous road cuttings, farm tracks and soil slips were looked at and described. Field studies showed coverbeds on the toe-slopes of hills offered the most extensive, uninterrupted records of late Quaternary landscape history.

5.4.2 Loess and tephra distribution within the western hill-country

The western Hawke's Bay hill-country comprises a series of Pliocene limestone capped NE/SW trending asymmetrical ridges or cuestas (e.g. Maniaroa, Te Waka and Maungaharuru Ranges) which alternate with gently to heavily dissected basins and downlands. Underlying the ridge-forming limestones are beds of massive siltstone, sandstone and conglomerate (Beu, 1995). These cuestas have long inclined dip slopes which dip as much as 20° SE towards Hawke Bay and shorter, steeper northwest-facing scarp slopes. The strata within these sedimentary sequences vary markedly in their

resistance to erosion. Pliocene aged limestone frequently outcrops on ridge crests and valley sides, buttressing and preserving more erodible material on the slopes above and below, respectively. Bounding some of these scarp slopes are Holocene fault traces e.g. Mohaka Fault.

The volcanic ash layers within the loess-paleosol layers that mantle the landscape thins rapidly eastwards, away from the central North Island volcanic centres. Macroscopic andesitic ash layers (e.g. Tufa Trig, Ngauruhoe, Papakai, Mangamate and Bullott Formations of Donoghue, 1991; Donoghue *et al.*, 1991; 1995) are seen only within the more western parts of the hill-country. Soils on scarp slopes are thin (<0.5m) and have developed on volcanic ash (andesitic and rhyolitic) and skeletal colluvium from the Neogene strata upslope. In contrast, dipslopes are mantled with thicker deposits (>0.5m), especially of volcanic ash, loess and colluvium.

Coverbeds seen on hillslopes comprise:

1. a topsoil of andesitic ash (Tufa Trig and Ngauruhoe Formations), rhyolitic pumice (Taupo Ignimbrite) and rhyolitic lapilli (Taupo and Waimihia Tephras)
2. a red-brown zone comprising andesitic tephras (Papakai and Mangamate Formations) which accumulated during the Holocene
3. Bullott Formation tephras, tephric loess and colluvial material which accumulated during the upper part of the last stadial, and
4. Kawakawa Tephra.

Most of the hill-country had been cleared of its original broad-leaved conifer forest *c.*100-150 years ago and replaced by exotic grass and clover species for pastoral land-use, mainly sheep farming (see section 2.3.2). The immediate effect of deforestation on hillslopes has been the loss of the reinforcing root strength of trees (O'Loughlin and Ziemer, 1982) and the reduced water-storage capacities of hillslopes under pasture species. Both these factors have substantially contributed to increases in the landslide frequency and land productivity losses on the steeper slopes, as demonstrated in the Taranaki hill-country (Trustrum and DeRose, 1988; DeRose, 1996).

In many parts of Hawke's Bay, Kawakawa Tephra occurs either as a primary deposit infilling fossil gullies or as colluvium in bedrock depressions. Often, the upper part of the deposit shows reworking. This indicates that landscape instability both predated and postdated the deposition of Kawakawa Tephra.

The greatest soil differences seen on the various hillslope elements relate to horizon thicknesses. Topsoil horizons (e.g. Ah) increase in thickness downslope from the point of slope inflection, between planar midslopes and concave lower slopes, towards the base of the slope. Soils on these positions (the foot- and toe-slope positions) and on interfluves are often poorly drained as these are also sites of water accumulation.

Soil depths to the top of the duripan and fragipan horizons are thinnest on ridges, shoulder-slopes and nose-slopes and thickest in hollows, especially in foot- and toe-slope positions. Pliocene limestone outcrops are commonly seen on nose-slopes and interfluves. This is related to the erosion of coverbed material from shoulder-slopes and its temporary storage as colluvium in interspur hollows or in toe-slope positions on the valley floor or basin. Material in these positions is subsequently remobilised, firstly by ephemeral streams and later into permanent waterways. Consequently, soils are thinnest on ridges and spurs and thickest in swales and foot-slopes.

5.4.3 Use of reference stratigraphical columns

5.4.3.1 *Site selection and criteria for reference stratigraphical columns*

After an extensive field reconnaissance, and examination of many sections, four road cuttings in a west to east transect, roughly parallel to the prevailing north-westerly winds, were selected as reference stratigraphical columns on which to undertake more detailed studies. The intention was: to follow the direction of the Pleistocene loess-bearing winds and the thinning direction of andesitic and rhyolitic tephra beds; to study a suite of related soils and document their lateral variability across the landscape, and to evaluate the parent material and pedogenetic history of coverbeds at these sites. Study sites were informally named after nearby geographic localities, a common practice in

these studies. Sites are from west to east: Pakaututu Road, Manaroa, Apley Road and Poraiti (see Fig. 1.1). The most westerly site, Pakaututu Road, lies *c.*60km east of Lake Taupo and *c.*50km west of Napier city.

Reference sites were selected on the following criteria:

1. they had the greatest number of loess-paleosol layers;
2. no evident unconformities, visible erosion breaks or hiatuses;
3. all sites had Kawakawa Tephra in their uppermost loess layer, a widespread easily identified macroscopic marker bed. The recognition of Kawakawa Tephra in the uppermost loess layer enables a confident correlation of this loess layer with Ohakean loess in the Wanganui Basin.
4. they traversed an area of varying climate (1800-900mm rainfall per annum, lower rainfalls in the east), soil types (Pumice, Allophanic, Brown and Pallic Soils), and;
5. distance from tephra source areas so that proximal-distal relationships could be described.

5.4.3.2 *Methods used to describe and sample reference stratigraphical columns*

Exposures at the reference sites were cut back *c.*0.25-0.5m to reach fresh material. Stratigraphic units within the coverbeds were described and correlated with loess-paleosol units from the Rangitikei River coverbed sequences. Soil descriptions were based largely on Hodgson *et al.* (1976). These included: horizon depth, soil colour, texture, structure, consistence, Na-F reaction, size and distribution of roots and clay films (see Appendix I). Soil colours were identified in the field and based on the Oyama and Takehara (1967) colour book.

Bulk samples for chemical, elemental and mineralogical analyses were channel sampled (±1.5cm) every 10 cm from the present soil surface (see Chapters Six to Nine). Samples were also taken from within zones of interest. Sampling in this manner ensures that the results of chemical, mineralogical and elemental analyses are

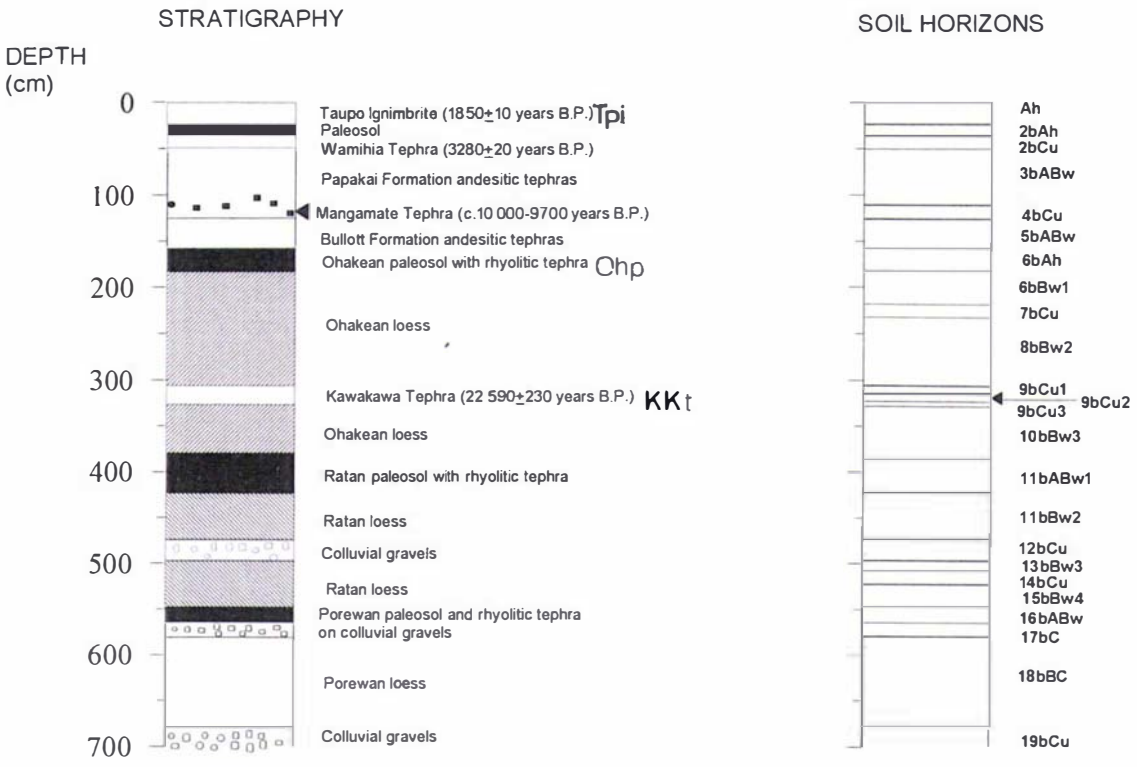

Figure 5.1: Soil and stratigraphic units recognised at the Pakaututu Road reference section

Plate 5.6: Coverbeds at the Pakaututu Road reference section.
Units in brackets refer to selected units in Fig. 5.1

independent of and not predetermined by the morphological descriptions made in the field.

Samples were air-dried, gently crushed and then sieved to separate coarse fragments from the fine earth (<2mm diameter) fraction. None of the loessial or tephric material was >2mm diameter, except for the ignimbrite pumice clasts. The fine earth fractions (<2mm diameter) were retained for chemical, elemental and mineralogical analyses which are conducted in Chapters Six to Nine

5.4.3.3 *Results from reference stratigraphical columns*

In the following subsections the stratigraphic and pedological units recognised at each of the reference sections are described, along with accompanying photographs. A summary of the major stratigraphic and pedological units recognised at each of these sections follows. Detailed pedological descriptions, along with a key to the terms used, are available in Appendix I.

Loess units are provisionally correlated to the Rangitikei River coverbed sequences (see Table 3.1). The rhyolitic and andesitic units recognised are correlated to their more proximal correlatives (see Table 3.3; Donoghue, 1991; Donoghue *et al.*, 1991; 1995).

Stratigraphic sequence at Pakaututu Road reference section (V20/117 125)

The stratigraphic and pedological units recognised are depicted in Fig. 5.1 and Plate 5.6. The following units are identified from the top to the bottom of the section:

0-22cm: a brownish black (7.YR3/2) Ah horizon. It comprises a highly allophanic topsoil of fine (<1mm thick) andesitic tephra accessions from the Tufa Trig (dated *c.*1850 years B.P.-present) and Ngauruhoe (dated *c.*1850 years B.P.-present) Formations, scattered rhyolitic lapilli, and Taupo Ignimbrite (dated at 1850±10 years B.P.) (Froggatt and Lowe, 1990; Donoghue, 1991; Donoghue *et al.*, 1995). The rhyolitic lapilli are likely to have been derived from the airfall component of the

Taupo eruption 1850±50 years B.P. but derivation from the upslope erosion of coverbeds cannot be excluded. The andesitic ashes and rhyolitic lapilli merge with the weathered surface of the underlying Taupo Ignimbrite. These layers are thin and cannot easily be separated consequently they are included with the Taupo Ignimbrite unit. At the base of the Taupo Ignimbrite a discontinuous, thin (≤10mm) pale grey layer of Hatepe Ash is present. Both the Taupo Ignimbrite and Hatepe Ash are primary deposits. Charcoal is present within the topsoil and may relate to the use of fire last century for land clearance. Charcoal fragments were also recovered from within the Taupo Ignimbrite (*c.* 15cm depth). As these fragments are from within the ignimbrite flow they may have been derived from elsewhere and brought to the site by the eastward flowing ignimbrite.

22-36cm: a dark brown (7.5YR-10YR3/4) paleosol (2bAh horizon) developed on Waimihia Tephra lapilli.

36-50cm: tightly packed, grain supported lapilli of Waimihia Tephra (3280±20 years B.P.). This comprises the 2bCu horizon.

50-110cm: a brown (7.5YR4/6), highly allophanic layer (3bABw horizon) of andesitic ashes representing the Papakai Formation (dated *c.*9700-3400 years B.P.). Fine lapilli denoting microscopic rhyolitic tephra accumulations and charcoal fragments, are common throughout the Papakai Formation. Overseas studies (e.g. Mount St. Helens) have shown ash clouds associated with volcanic eruptions can produce lightening discharges which create local forest fires (Christiansen, 1980).

110-125cm: a discontinuous layer (4bCu horizon) of yellowish grey (2.5Y4/1) to dark greyish yellow (2.5Y4/2) spheroidal balls (≤30mm diameter) composed of fine ash are seen near the base of the Papakai Formation. These are correlated with the Mangamate Tephras, a series of six eruptions from Tama Lakes and Mount Tongariro, *c.*10 000-9700 years B.P. (Donoghue, 1991; Donoghue *et al.*, 1991; 1995). Mineralogical studies are undertaken in Chapter Six to confirm the presence of

skeletal olivines, a diagnostic mineral from units within this Formation (Donoghue, 1991; Donoghue *et al.*, 1991; 1995).

125-158cm: a yellowish brown (10YR5/8), highly allophanic unit (5bABw horizon) comprising andesitic ashes from the Bullott Formation (dated *c.*22 600-10 000 years B.P. by Donoghue *et al.*, 1995) and scattered rhyolitic tephra lapilli. Volcanic glass counts are undertaken in Chapter Six to indicate the presence of microscopic rhyolitic tephra layers within the Papakai and Bullott Formations.

158-182cm: a yellowish brown (10YR5/6) to brown (10YR4/6) paleosol developed on a mixture of quartzo-feldspathic loess and Bullott Formation andesitic ash (6bAh horizon). Fine root channels and rhyolitic tephra lapilli are common.

182-380cm: a yellowish brown (10YR5/6-5/8) quartzo-feldspathic loess unit (6bBw1, 8bBw2 and 10bBw3 horizons) with a variable tephric component. The andesitic ash component (i.e. andesitic Bullott Formation of Donoghue, *et al.*, 1995) often is not discernible as it is diluted by quartzo-feldspathic loess. This loess unit is a correlative of the Ohakean loess, first described within the Rangitikei River Valley sequences and subsequently found to be widespread within the lower North Island. Rhyolitic lapilli are encountered at 218-231cm (7bCu horizon), 247-250cm , 287-291cm and 305-326cm (9bCu1 to 9bCu3 horizons) depths within the Ohakean loess.

305-326cm: a shower-bedded rhyolitic tephra comprising two lapilli layers and a fine white basal ash layer (9bCu1 to 9bCu3 horizons). This tephra is identified as Kawakawa Tephra because of: its characteristic fine, white basal ash layer; the presence of chalazoidites (accretionary lapilli) near the top of the unit (Berry, 1928), and its position at two thirds depth within the Ohakean loess (Palmer, 1982b).

380-423cm: at road level a yellowish brown (10YR5/8) paleosol within a second loess unit is encountered (11bABw1 horizon). This loess unit is correlated to the Ratan loess. Fine charcoal fragments are present at 410-430cm and scattered rhyolitic tephra lapilli at 380-408cm depth.

The identity of the microscopic rhyolitic tephra/s is investigated in Chapter Six.

423-547cm: the Ratan loess continues below road level (11bBw2, 13bBw3 and 15Bw4 horizons). It is intercalated with colluvial gravels at 474-496cm (12bCu horizon). Scattered rhyolitic lapilli are present at 450cm and 508-521cm (14bCu horizon) depths.

547-563cm: a yellowish brown (10YR5/6) paleosol developed on colluvial gravels and silts (16bABw horizon). Fine humate-coated root channels are present within the paleosol.

563-580: colluvial gravels which are intercalated by a macroscopic rhyolitic ash (17bCu horizon). The identity of this ash layer will be resolved by microprobing its glass shards in Chapter Six.

580-680cm: a third loess unit is found beneath the colluvial gravels (18bBC horizon). This is correlated to the Porewan loess unit, first described within the Rangitikei River Valley sequences.

680cm+: at the base of the section a colluvial gravel unit is encountered (19bCu horizon). This unit was not penetrated. The colluvial gravels are derived from the erosion of a presumed pre-Porewan terrace remnant at a higher level.

Kawakawa Tephra is not laterally continuous across the entire section. It varies in thickness (10-44cm) which is indicative of both erosion and local thickening. Published isopach maps indicate that the Kawakawa Tephra should be greater than 60cm thick at this site (Pullar and Birrell, 1973a;b). Close interval sampling of the Ohakean loess above the Kawakawa Tephra with a knife indicates a grittiness commonly associated with tephric material. It is highly likely that the upper portion of the Kawakawa Tephra has suffered erosion (during the last stadial) and subsequent dilution with incoming loess since emplacement. Electron microprobe analyses of glass shards obtained from within the upper parts of the Ohakea loess unit, above the readily defined layer of Kawakawa Tephra, are undertaken in Chapter Six. If reworking of Kawakawa Tephra has occurred extraneous glass shards of Kawakawa Tephra chemistry would be present within the upper parts of the Ohakean loess unit.

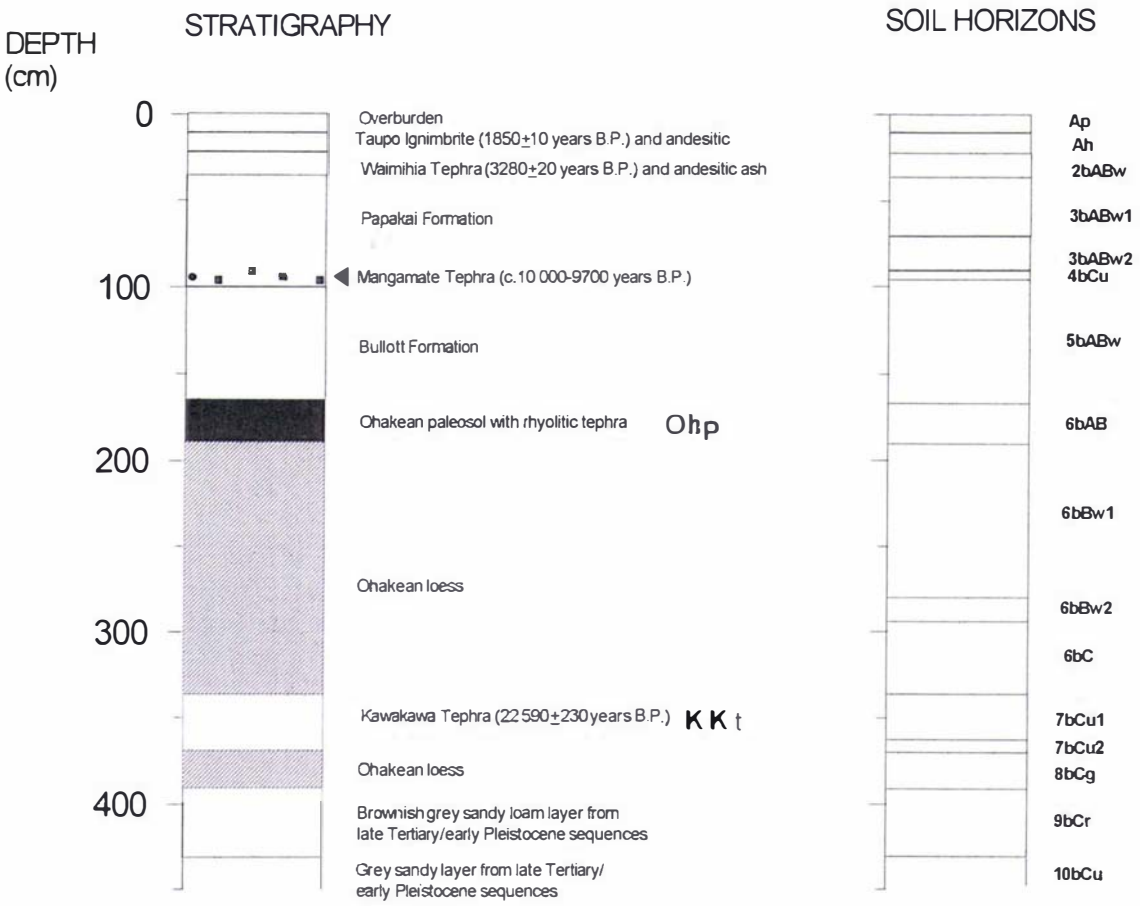

Figure 5.2: Soil and stratigraphic units recognised at the Manaroa reference section

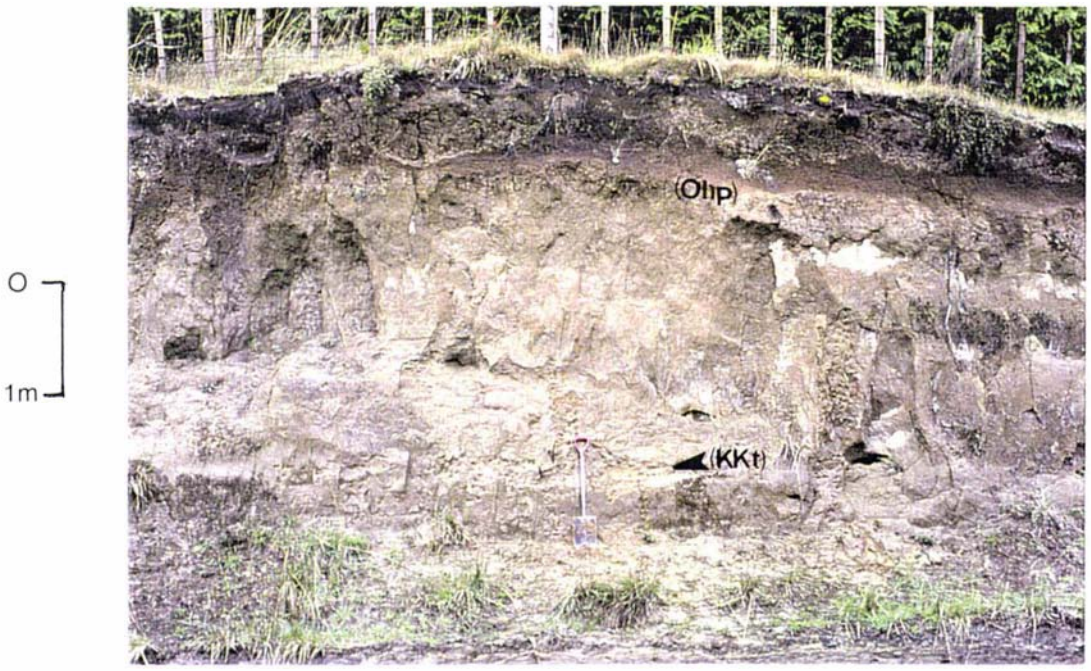

Plate 5.7: Coverbeds at the Manaroa reference section

Letters in brackets refer to selected units in Fig. 5.2

Stratigraphic sequence at Manaroa reference section (V20/186 036)

The stratigraphic and pedological units recognised are depicted in Fig. 5.2 and Plate 5.7. The Manaroa section comprises:

0-10cm: a topsoil which is disturbed (Ap horizon). This was only recognised later.

10-21cm: a brownish black (7.5YR2/2), highly allophanic topsoil comprising fine (<1 mm thick) andesitic accessions from the Tufa Trig and Ngauruhoe Formations, scattered pumice blocks (≤ 30mm in length) and fine rhyolitic lapilli (Ah horizon). The pumice blocks have been derived from Taupo Ignimbrite as they are too large to have been ejected this distance from Lake Taupo (>70km) as an airfall component (Dr Alan Palmer, pers. comm. 1990). At this site primary Taupo Ignimbrite is near its most distant or easterly limit in Hawke's Bay (see section 5.5.2). The fine rhyolitic lapilli are likely to be derived from Taupo Ignimbrite and Tephra (1850±50 years B.P) and also from the erosion of older tephras from gullies upslope.

21-36cm: rhyolitic lapilli occupy up to 10% of this unit (2bABw horizon). These lapilli are from the Waimihia Tephra (3280±20 years B.P.) as they do not have the long vesicles seen in Taupo Tephra lapilli. The Manaroa site differs from the Pakaututu Road site in that Taupo Tephra and Ignimbrite are not separated by a dark paleosol from Waimihia Tephra. At this site both these tephra units are composite.

36-95: dark brown (10YR3/4) to brown (10YR4/6) andesitic ashes of the Papakai Formation (3bABw1 and 3bABw2 horizons). Fine charcoal fragments (at 50±2cm depth) and scattered rhyolitic tephra lapilli are present. An attempt is made in Chapter Six to resolve the identities of these microscopic rhyolitic tephras by electron microprobing their glass shards.

90-95cm: a discontinuous layer comprising greyish yellow brown (10YR4/2) to dull yellowish brown (10YR4/3) balls (≤10mm diameter) of fine andesitic ash (4bCu horizon). These are correlated to the Mangamate Tephra (*c.*9700-10 000 years B.P.) described at the Pakaututu Road

section.

95-165cm: yellowish brown (10YR5/6 and 2.5Y5/6) highly allophanic andesitic ashes of the Bullott Formation underlies the Mangamate Tephra (5bABw horizon). Fine rhyolitic tephra lapilli are common within this unit. In Chapter Six an attempt is made to identify these microscopic rhyolitic tephras.

165-190cm: an olive brown (2.5Y4/6) paleosol (6bAB horizon) developed within quartzo-feldspathic loess (predominantly) and andesitic ashes of the Bullott Formation. Fine rhyolitic lapilli (microprobed in Chapter Six) are found within the upper part of this paleosol (165-180cm) as well as fine root channels.

190-390cm: a dull yellowish brown (10YR5/4) to yellowish brown (10YR5/6) quartzo-feldspathic loess unit, considered to be of Ohakean age (6bBw1, 6bBw2, 6bC and 8bCg horizons). Within the Ohakean loess fine rhyolitic lapilli are present at 230-240cm and 315-325cm. The lower lapilli zone may comprise reworked Kawakawa Tephra. This will be investigated in Chapter Six. Ohakean loess (368-390cm) beneath the Kawakawa Tephra is highly mottled denoting a perched water.

335-368cm: a macroscopic, shower-bedded tephra unit identified as Kawakawa Tephra (7bCu1 and 7bCu2 horizons). Features used to identify this tephra are similar to those used to identify Kawakawa Tephra at the Pakaututu Road section. A close examination of the Kawakawa Tephra shows it to vary laterally in thickness. This is indicative of local erosion and subsequent reworking.

390-430cm: a brownish grey (10YR5/1) sandy loam unit (9bCr horizon) belonging to the underlying late Tertiary/early Pleistocene marine sequences.

430cm+: a massive sandy sequence (10bCu horizon) belonging to the underlying late Tertiary/early Pleistocene marine sequences.

Plate 5.8: At the Apley Road reference site three loess layers are draped over two highly weathered coversand units. The site was subdivided from left to right into AR1 (not visible), AR2, AR3 and AR4 sections (marked). Refer to text for details.
(NZMS 260 V21/316 877).

Stratigraphic sequence at Apley Road reference sections (V21/316 877)

The Apley Road reference section was subdivided into four overlapping profiles taken at increasing depths through three loess layers (Plate 5.8). These profiles, from left to right, are termed Apley Road #1 (AR1), Apley Road #2 (AR2), Apley Road #3 (AR3) and Apley Road #4 (AR4) sections. It was not possible to get a continuous section through the deepest part of the section as the upper part of the section is too steep to examine and sample.

The three loess layers are draped over two highly weathered coversand sequences, separated by a paleosol. The coversand sequences have undergone intense weathering and are consequently clay rich. These two highly weathered units abut unconformably against a fossiliferous late Tertiary/early Pleistocene-aged sandy marine deposit.

The Apley Road site differs from the previous two reference sites in that the macroscopic Papakai and Bullott Formations are not present above the Ohakean loess. Loess units at this site differ morphologically to those at the Pakaututu and Manaroa sites. The subsoil of each loess unit or loess sheet comprises a cemented (duripan) horizon which is underlain by a prismatic or columnar structured fragipan horizon (see soil profile data in Appendix I).

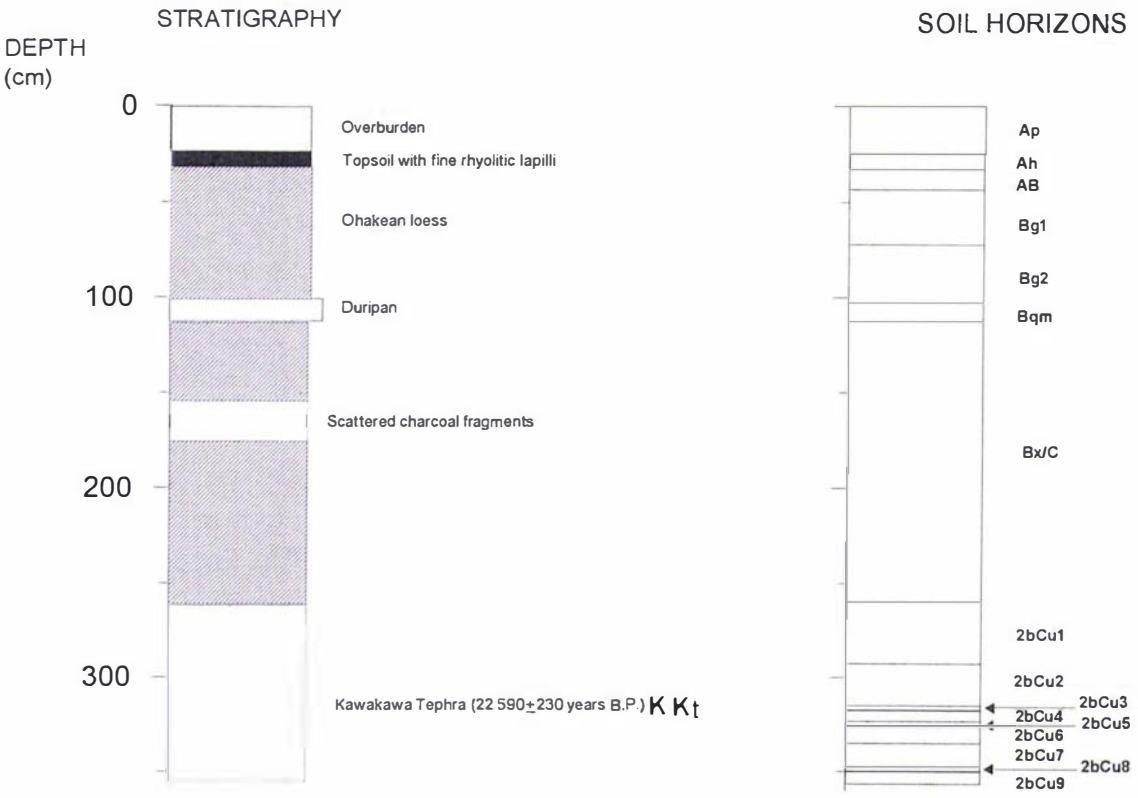

Figure 5.3: Soil and stratigraphic units recognised at Apley Road #1 section

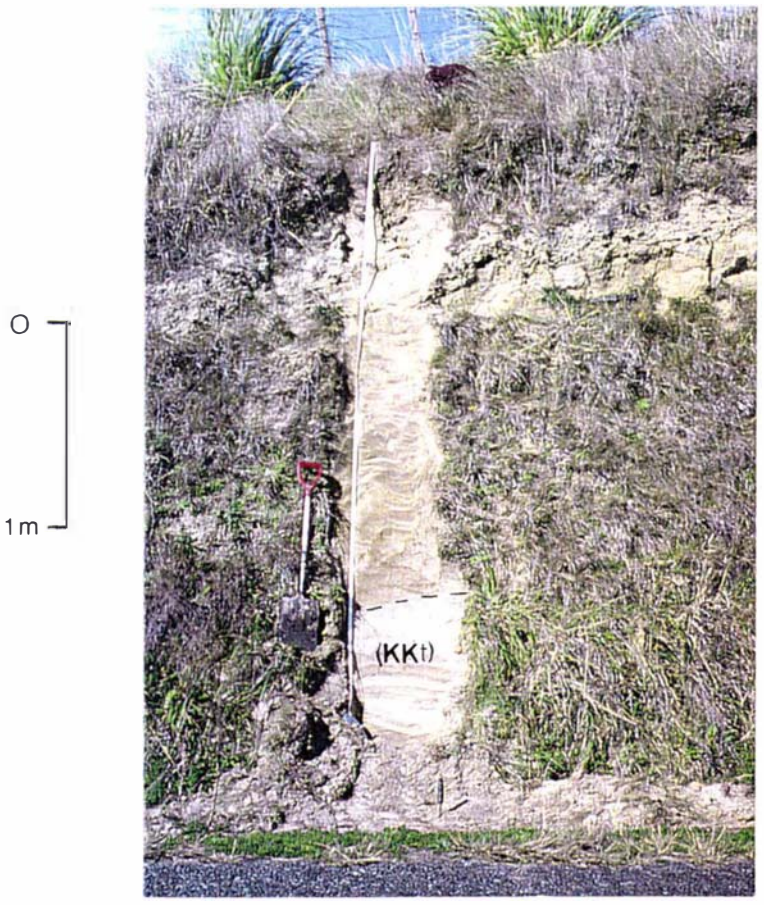

Plate 5.9: Coverbeds at the Apley Road #1 section.
Letters in brackets refer to selected units in Fig. 5.3.

The AR1 section is depicted in Fig 5.3 and Plate 5.9. It comprises:

0-22cm: overburden from road-making activities (Ap horizon)

22-260cm: a quartzo-feldspathic loess unit which extends to the top of the Kawakawa Tephra. This loess layer is correlated to the Ohakean loess unit recognised at the Pakaututu Road and Manaroa sections. The Ohakean loess unit comprises:

- a brownish black (10YR2/3) topsoil with fine pumice lapilli (Ah horizon, 22-31cm). This site may have received very fine andesitic tephra inputs from the Tufa Trig and Ngauruhoe Formations as it is downwind of the Tongariro Volcanic Centre. A Na-F test conducted on the topsoil to test for the presence of allophane failed to yield a response.
- a unit which becomes more mottled with depth (31-101cm). This unit has been subdivided into a Bg1 and a Bg2 horizon.
- a thin (101-101.3cm) iron pan (Bf horizon)
- a highly cemented, tabular structured duripan (Bqm) horizon (101.3-112cm). Fine rhyolitic lapilli along with clay and humate coated fine root channels are present within the duripan.
- scattered charcoal fragments, up to 7mm in length, are present at 156-176cm depth.
- fine rhyolitic lapilli layers are recorded at: 70cm, 121-130cm, 180cm and 210cm.
- a dull yellowish brown (10YR5/4) massive to moderately developed columnar unit (Bx/C horizon, 112-260cm)

260-352cm: shower-bedded tephra layers (2bCu1to 2bBu9 horizons) with a fine white basal ash layer (see Appendix I). This tephra is identified as Kawakawa Tephra. Erosion of Kawakawa Tephra from upslope has resulted in its overthickening at this site.

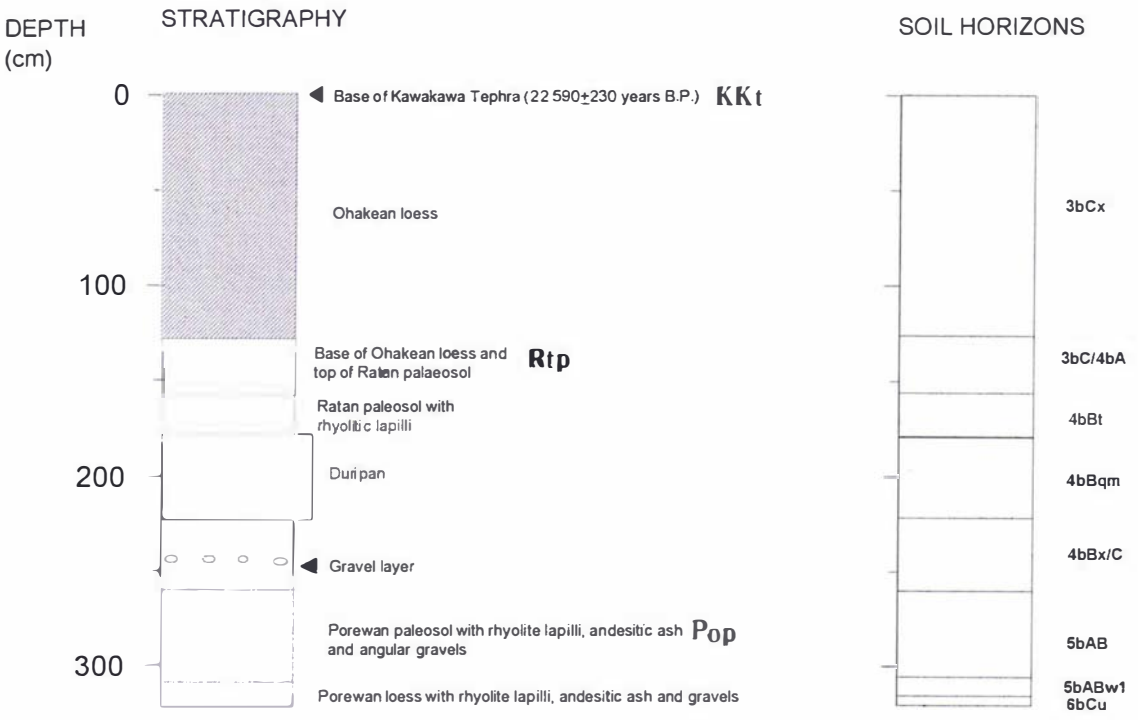

Figure 5.4: Soil and stratigraphic units recognised at the Apley Road #2 section

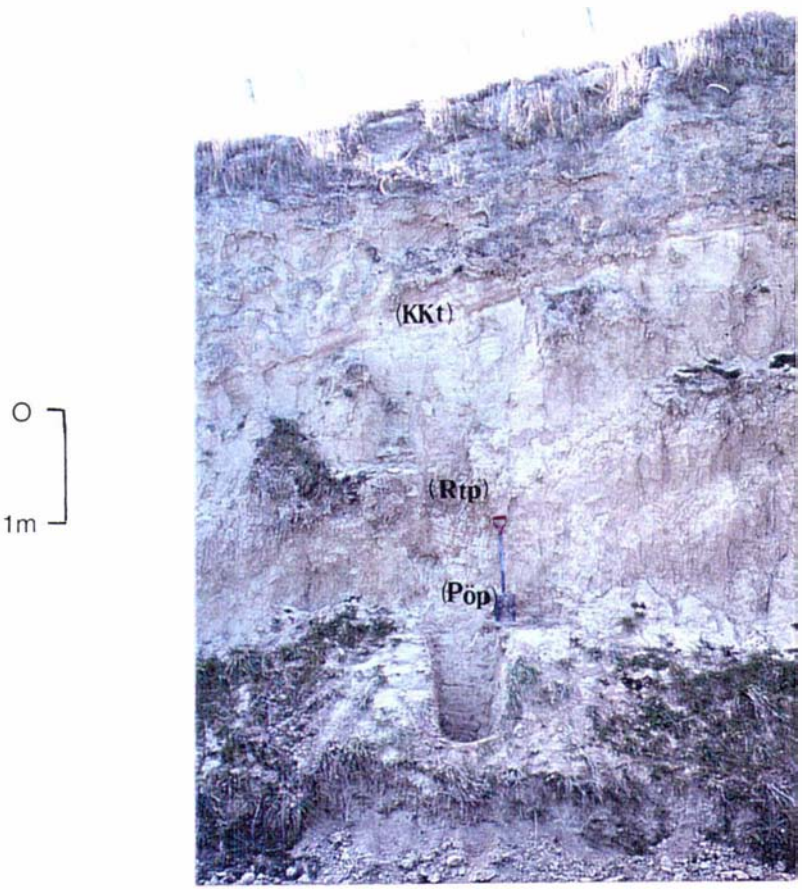

Plate 5.10: Coverbeds at the Apley Road #2 section.

Letters in brackets refer to selected units in Fig. 5.4

The AR2 section is depicted in Fig. 5.4 and Plate 5.10. It starts at the base of the Kawakawa Tephra. The following units are identified:

0-125cm: a dull yellow orange (10YR6/4), columnar structured quartzo-feldspathic Ohakean loess (3bCx horizon). Occasional root channels are present throughout this unit.

125-155cm: a darker accretionary layer within the lower part of the Ohakean loess (3bC/4bA). After a soil formed on the underlying Ratan soil Ohakean loess came in at an increasing rate before it overwhelmed the Ratan soil. Occasional (<2%) rounded gravels (≤30mm diameter) are present at 130-140cm depth which probably mark the boundary.

155-260cm: a second loess sheet correlated to the Ratan loess. Within the Ratan loess sheet the following horizons are present:

- a brown (10YR4/4), highly weathered clay loam textured layer (4bBt horizon, 155-178cm). Scattered lapilli are present at 165-175cm. Root channels and voids are clay and humate coated. This horizon exhibits bioturbation i.e. infilled worm tubules (castes).
- a tabular structured, highly cemented duripan (4bBqm) horizon (178-222cm).
- a massive to columnar structured fragipan (4bBx/C horizon, 222-260cm) with a few, subrounded gravels (2-20mm diameter) at *c.*240cm depth.

260-320cm: beneath the Ratan loess a third loess unit is encountered. It is provisionally correlated to the Porewan loess. It is made up of:

- a brown (10YR4/4), highly organic coated paleosol (5bAB horizon, 260-308cm) with rhyolitic lapilli, root channels and occasional gravels.
- a dull yellow orange (10YR6/4) quartzo-feldspathic layer (5bABw1 horizon, 308-318cm) with rhyolitic lapilli and rounded quartz gravels (≤15mm diameter).
- a mixed gravel and stone (<10%), matrix supported layer (6bCu horizon, 318-320cm) with rhyolitic lapilli.

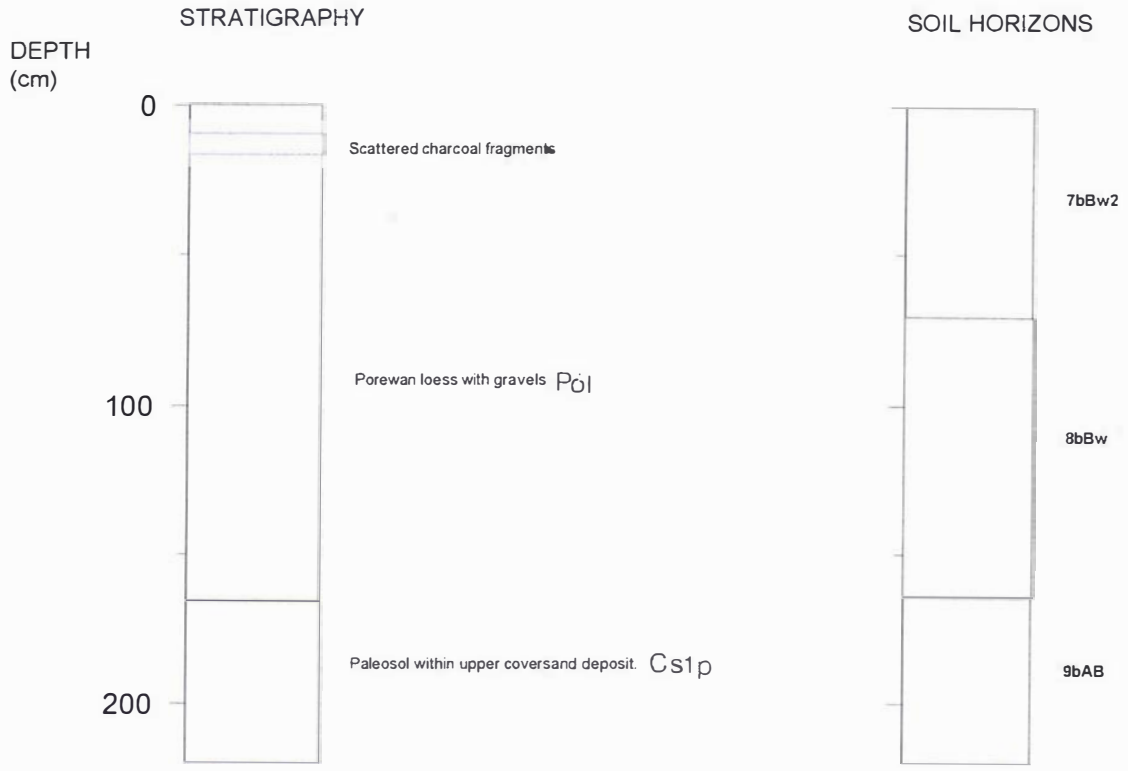

Figure 5.5: Soil and stratigraphic units recognised at the Apley Road #3 section

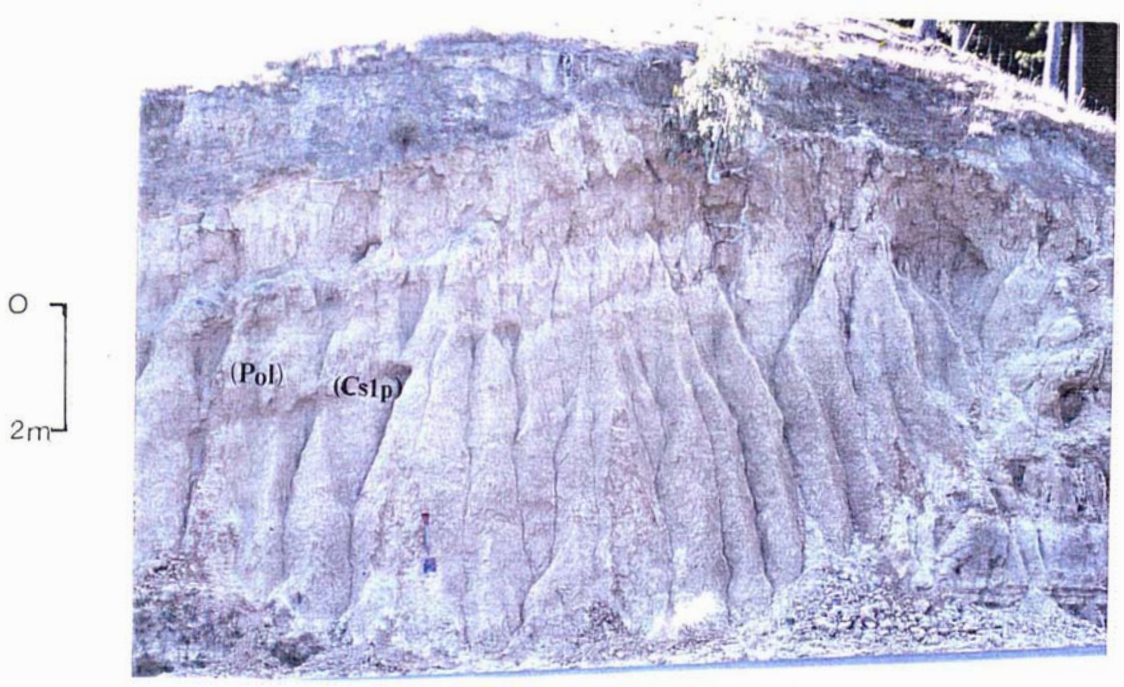

Plate 5.11: Coverbeds at the Apley Road #3 section
Letters in brackets refer to selected units in Fig. 5.5

The AR3 profile is depicted in Fig. 5.5 and Plate 5.11. This profile starts at the base of the stony layer described at the bottom of the AR2 profile. It comprises:

0-165cm: two clay-rich layers within the Porewan loess unit. These are:

- a yellowish brown (10YR5/6) layer (7bBw2 horizon, 0-70cm) characterised by clay and organic coatings. Rhyolitic lapilli are present near the top. Scattered charcoal fragments are present at 10-15cm.
- a bright yellowish brown (10YR6/6) layer (8bBw horizon, 70-165cm). It is slightly darker, has more gravels and is more structured (medium to coarse blocky) than the overlying 7bBw2 horizon.

165-223cm: a brown (10YR4/4) paleosol (9bAB horizon) developed on the surface of the upper coversand deposit. It is highly weathered and clay-rich (clay loam texture) with few scattered gravels. Root channels are abundant within this zone.

The AR4 profile is depicted in Fig. 5.6 and Plate 5.12. This profile starts at the base of the paleosol (9bAB horizon) developed on the upper coversand deposit. It comprises:

0-150cm: a yellowish brown (2.5Y5/4), highly weathered clay-coated upper coversand deposit (9bBt horizon).

150-178cm: a slightly darker (2.5Y5/6) paleosol (10bABt horizon) developed on the lower coversand unit. This horizon is identified by its strongly developed blocky structure and an increase in root channel abundances.

178-338cm: a yellowish brown (2.5Y5/4), highly weathered clay-coated lower coversand deposit (10bBt horizon). The high degree of weathering within both coversands units is indicative of them having undergone intense weathering during the Last Interglacial. Fine root channels, along with occasional stones and gravels, are seen throughout the coversands.

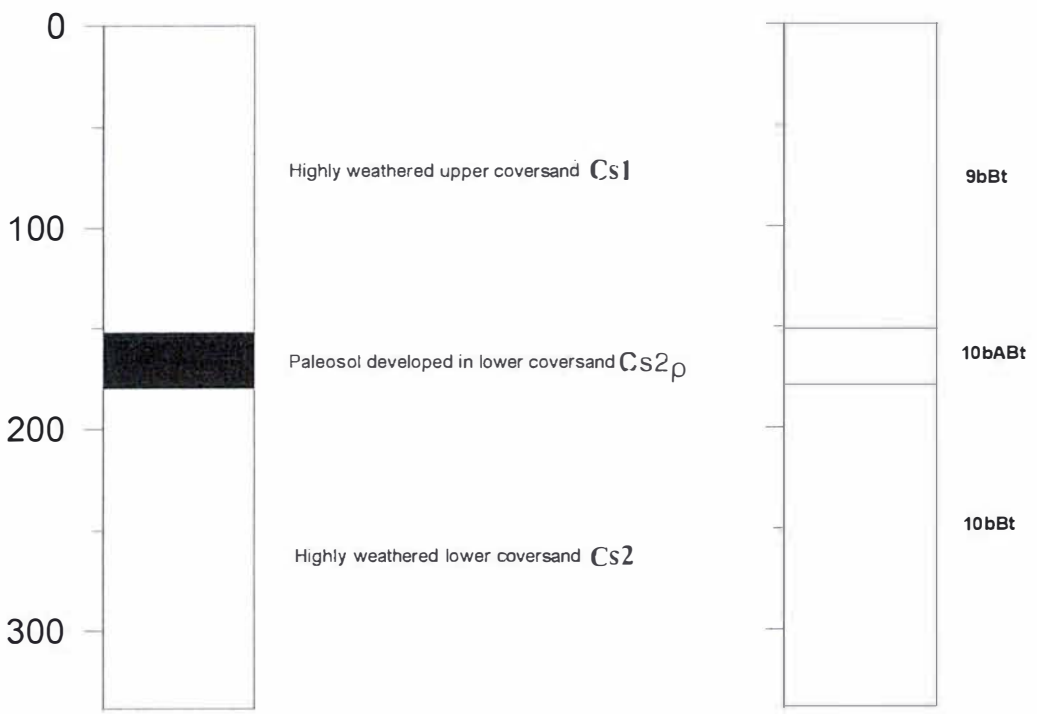

Figure 5.6: Soil and stratigraphic units recognised at the Apley Road #4 section

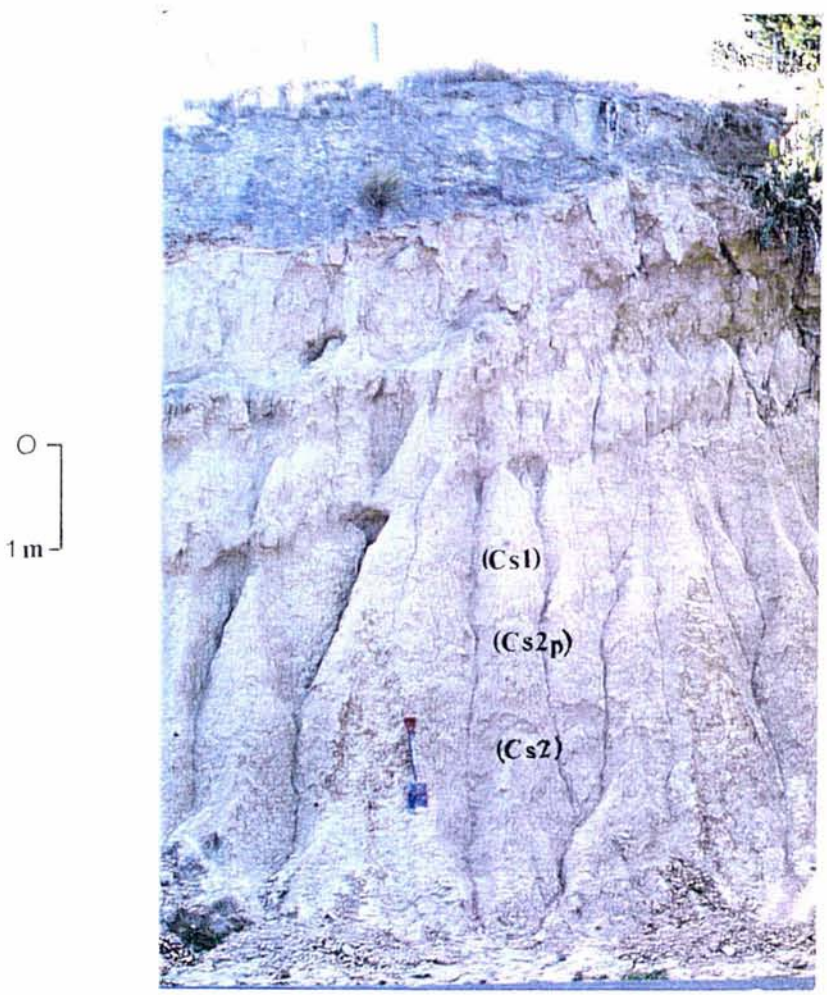

Plate 5.12: Coverbeds at the Apley Road #4 section.
Letters in brackets refer to selected units in Fig. 5.6.

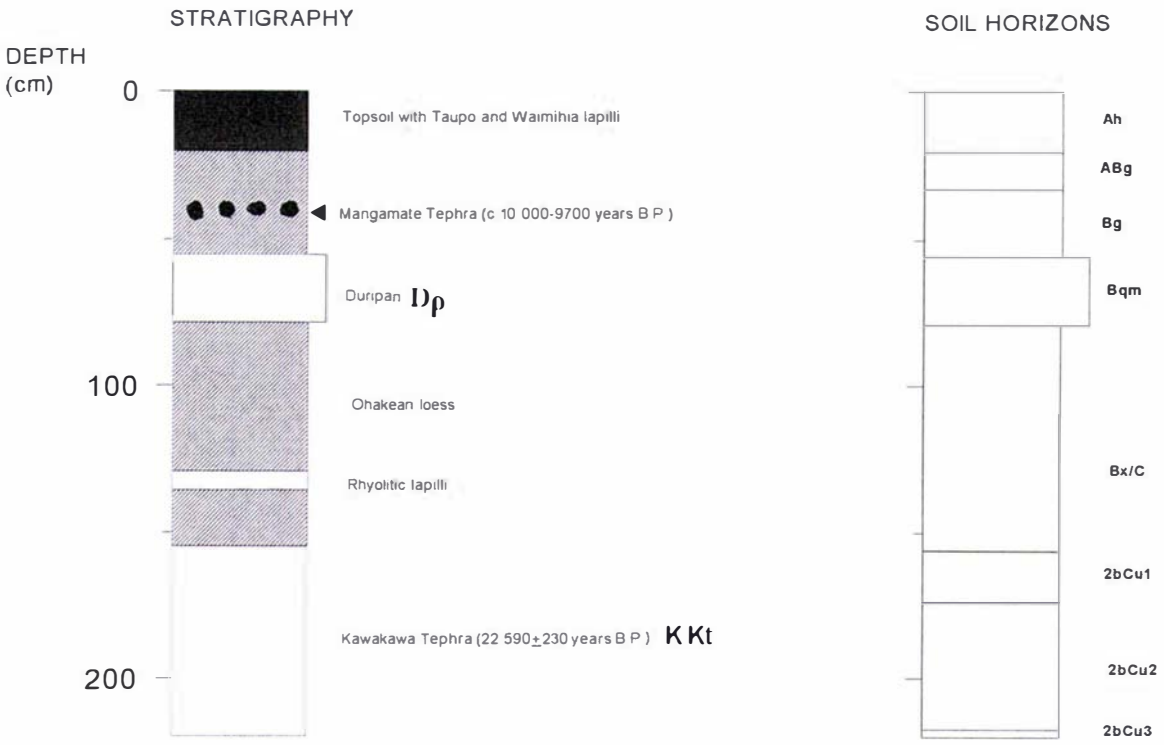

Figure 5.7: Soil and stratigraphic units recognised at the Poraiti # 1 section.

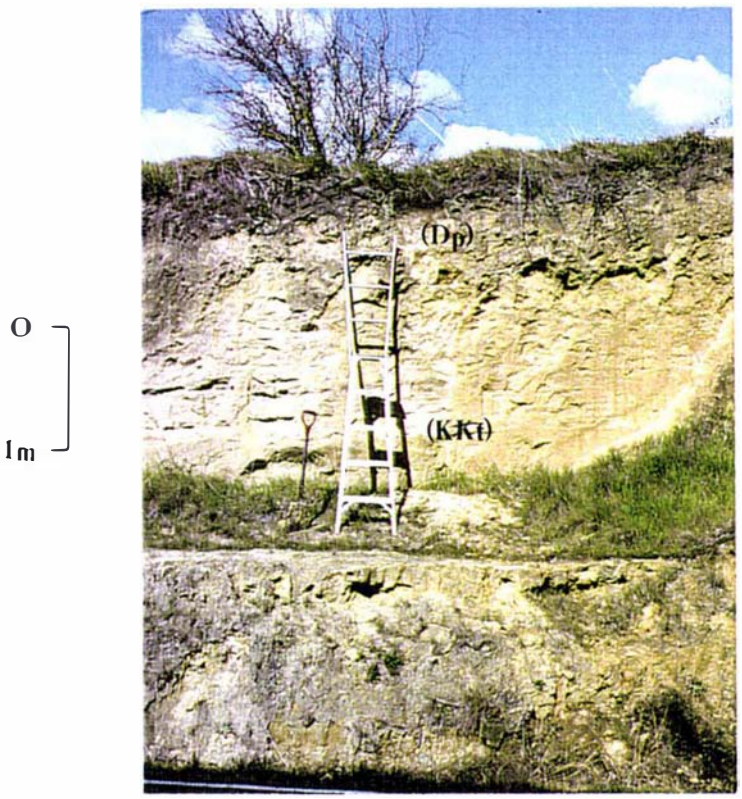

Plate 5.13: Coverbeds at the Poraiti #1 section.
Letters in brackets refer to selected units in Fig. 5.6.

Stratigraphic sequence at Poraiti reference sections (V21/398 837)

This section comprises a deep road cutting (>5m) through a loess and tephra mantled hill-slope. Coverbeds were sampled from the banks on either side of the road as the steepness of the deeper cutting precluded detailed examination and subsequent sampling from the upper part of this section. The section on the downslope side of the hill was termed Poraiti #1 (Por1). Pedological and stratigraphic observations at this section were conducted from the present-day surface to the fine white ash layer at the base of the Kawakawa Tephra. The other section, Poraiti #2 (Por2), was taken from the opposite (upslope) side of the road. This section comprises five loess-paleosol layers. Pedological and stratigraphic descriptions of the loess-paleosol layers were made from the base of the Kawakawa Tephra.

The Poraiti #1 section is depicted in Fig. 5.7 and Plate 5.13. It comprises:

0-155cm: Ohakean quartzo-feldspathic loess. Within the Ohakean loess the following layers are present:

- a dark brown (7.5YR3/1) topsoil (Ah horizon, 0-20cm) with diffuse, fine rhyolitic lapilli. These are correlated with the Taupo and Waimihia Tephras. It was not possible to separate the Taupo and Waimihia Tephras into two distinct units as they are both in a distal location and hence very thin.
- a mottled layer (ABg and Bg horizons, 20-55cm) above a duripan. At 40cm depth tiny grey balls ($\leq$4mm diameter) of fine andesitic ash were detected. These are correlated to the *c.*10 000-9700 years B.P. Mangamate Tephra.
- a protruding, cemented layer (duripan) is seen at 55-75/80cm (Bqm horizon). It has a coarse, tabular structure. Duripans are identified by their high mechanical strength and lack of porosity. They can only be broken apart with great difficulty (e.g. with a geological hammer), even when wet (see Appendix I). The Ohakean duripan has a diffuse lower boundary with the underlying fragipan. Fine rhyolitic lapilli are seen at 75$\pm$2cm.
- a columnar structured fragipan (Bx/C) horizon (75-155cm). Fine

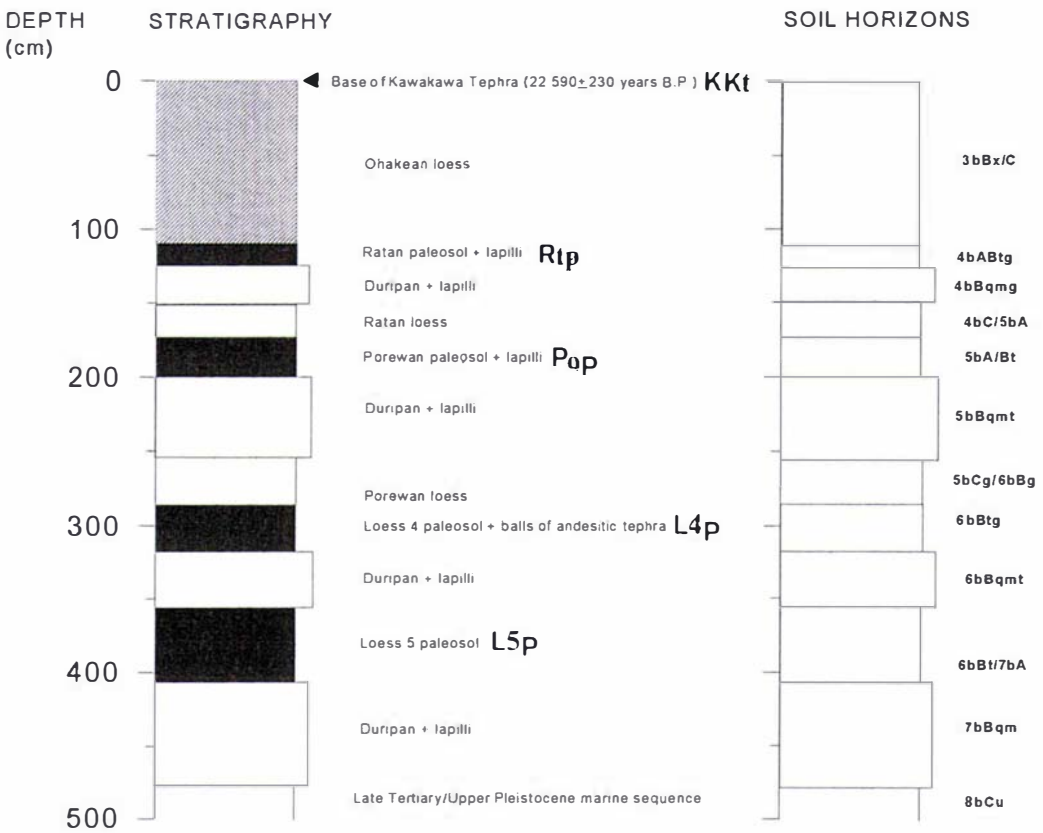

Figure 5.8: Soil and stratigraphic units recognised at the Poraiti #2 section

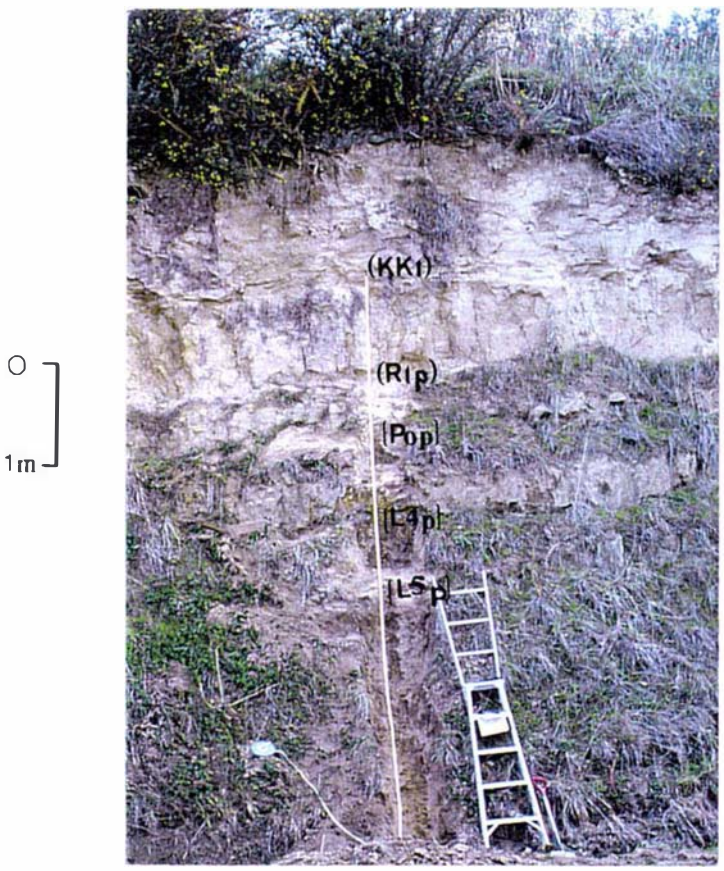

Plate 5.14: Coverbeds at the Poraiti #2 section
Letters in brackets refer to selected units in Fig. 5.8.

rhyolitic lapilli are present within the fragipan (129-135cm).

155-223cm: a shower-bedded tephric unit (2bCu1-2bCu3 horizons) identified as Kawakawa Tephra because of its prominent white basal ash layer, its thickness, its position at 2/3 depth within the Ohakean loess and the presence of chalazoidites (accretionary lapilli) within its upper part.

The Poraiti #2 (Por2) profile is depicted in Fig. 5.8 and Plate 5.14. It comprises:

0-110cm: light yellow (2.5Y7/4) quartzo-feldspathic Ohakean loess with occasional root channels and rhyolitic lapilli (3bBx/C horizon)

110-173cm: a second loess unit which is correlated to the Ratan loess. Within the Ratan loess the following layers are recognised:

- a mottled, yellowish brown (10YR5/6) paleosol (4bABtg horizon, 110-125cm) with fine to medium root channels coated with organic and clay cutans and rhyolitic lapilli
- a cemented, tabular duripan (4bBqmg horizon, 125-150cm) with rhyolitic lapilli
- a yellowish brown (10YR5/6) layer with few fine root channels (4bC/5bA horizon, 150-173cm). This layer comprises the base of the Ratan loess and the top of the underlying loess unit.

173-285cm: a third loess unit which is correlated to the Porewan loess. It comprises:

- a dull reddish brown (2.5YR5/4) paleosol (5bA/Bt horizon, 173-200cm) with rhyolitic lapilli
- a cemented, tabular structured duripan (5bBqmt horizon, 200-255cm) with dispersed rhyolitic lapilli at 225cm
- a mottled layer (5bCg/6bBg horizon, 255-285cm) which comprises the base of the Porewan loess and the top of Loess 4.

285-408cm: a fourth loess unit termed Loess 4. It comprises:

- a dull yellowish brown (10YR5/4) clay-rich layer (6bBt horizon, 285-318cm). Within this a discontinuous layer of andesitic ash balls ($\leq$20mm diameter) are found.
- a cemented, tabular duripan horizon (6bBqmt, 318-355cm) with scattered rhyolitic lapilli

- a yellowish brown (10YR5/8), highly weathered layer with common root channels (6bBt/7bA horizon, 355-408cm). This comprises the base of Loess 4 and the top of Loess 5.

408-478cm: a fifth loess unit termed Loess 5. This comprises:

- a cemented, tabular duripan horizon (7bBqmt, 408-478cm) with scattered rhyolitic lapilli

478cm+: a sequence comprising late Tertiary/early Pleistocene marine silts and sands (7bCu horizon, 478cm+).

The lower horizons within the Ohakean, Ratan, Porewan, Loess 4 and Loess 5 units are strongly jointed by well-defined vertical joints which outline the columns. The upper horizons of these loess units show traces of an original blocky structure and contain many fine root traces.

The advanced degree of weathering within the upper horizons of Loess 4 and Loess 5 argues either for a period of intense weathering (higher rainfall and/or higher temperature), or a period of weathering of comparable intensity but of longer duration than for the alteration of all the overlying layers. It is proposed that Loess units 4 and 5 either predated or occurred within a cold stage (marine oxygen isotope stages 5b or 5d) during the Last Interglacial. Subsequently these loess units have undergone intense weathering during the warmest stages within the Last Interglacial (marine oxygen isotope stages 5a, 5c and/or5e).

5.5 IGNIMBRITES

5.5.1 Introduction

Two mid-Quaternary ignimbrites (Potaka and Rabbit Gully) and one late-Quaternary ignimbrite (Taupo), emanating from the Taupo Volcanic Zone, have been recorded within the Hawke's Bay landscape (e.g. Kingma, 1971; Kamp, 1984; 1992a; Black, 1992; Erdman and Kelsey, 1992; Shane, 1994; Shane *et al.*, 1996a;b). None of these studies have, however, attempted to describe the spatial distribution and contribution

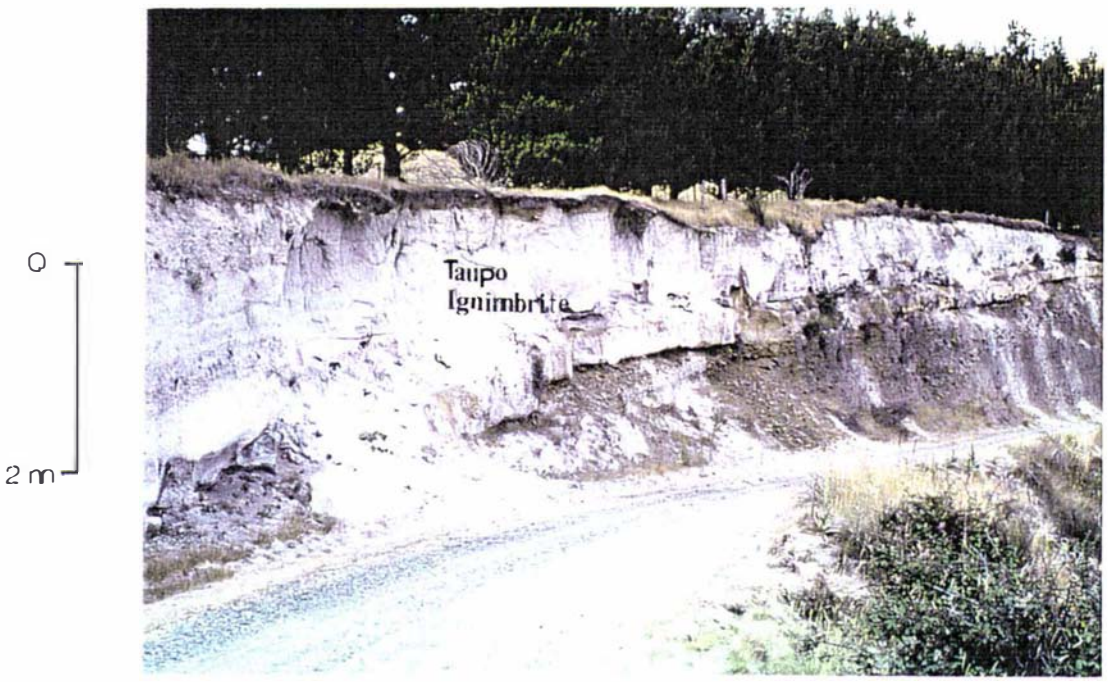

Plate 5.15: Taupo Ignimbrite, both primary and fluvially reworked, overlies Holocene coverbeds on an Ohakean aged aggradation surface along the Mohaka River. Ignimbrite flows overtopped low points (<1500m) in the ranges and flowed eastwards along rivers sourced in close proximity to Taupo (see text).
(V20/216 167).

these ignimbrites have had in terms of constructing or mantling the Hawke's Bay landscape.

During the field reconnaissance both Potaka and Taupo ignimbrites were identified at a number of new localities. The Oruanui Ignimbrite, previously not recorded in Hawke's Bay, was also identified. In this section the presence and distribution of these ignimbrites are outlined.

5.5.2 Taupo Ignimbrite

Taupo Ignimbrite, both primary and reworked, is present over parts of western Hawke's Bay. It is found either at or in close proximity to the present soil surface spanning a range of elevations from present-day flood-plains to hill and mountain summits and on slopes up to 30° (Walker *et al.*, 1980a). The best exposures are adjacent to the Mohaka and Ngaruroro Rivers (Plate 5.15). Both these rivers have their headwaters in close proximity to the volcanic centres of the Taupo Volcanic Zone and have acted as conduits for the transfer of large volumes of volcanic material to Hawke's Bay in the east. Figure 5.9 shows the distribution of primary Taupo Ignimbrite deposits within Hawke's Bay, mapped during the course of this study.

Deposits of primary Taupo Ignimbrite and Taupo Ignimbrite alluvium may be seen in numerous sections adjacent to the Mohaka and Ngaruroro River valleys. Flow structures and cross bedding are common features within Taupo Pumice alluvial deposits (Wilson, 1985; Wilson and Walker, 1985). These latter deposits have been eroded from primary Taupo Ignimbrite outcrops and reworked by water. Reworked Taupo Ignimbrite pumice clasts are found as far east as the Heretaunga Plains, within the soils of the Pakipaki series (Hughes *et al.*, 1939).

Taupo Ignimbrite was distinguished from airfall Taupo Tephra on the following field criteria:

1. it lacked shower bedding

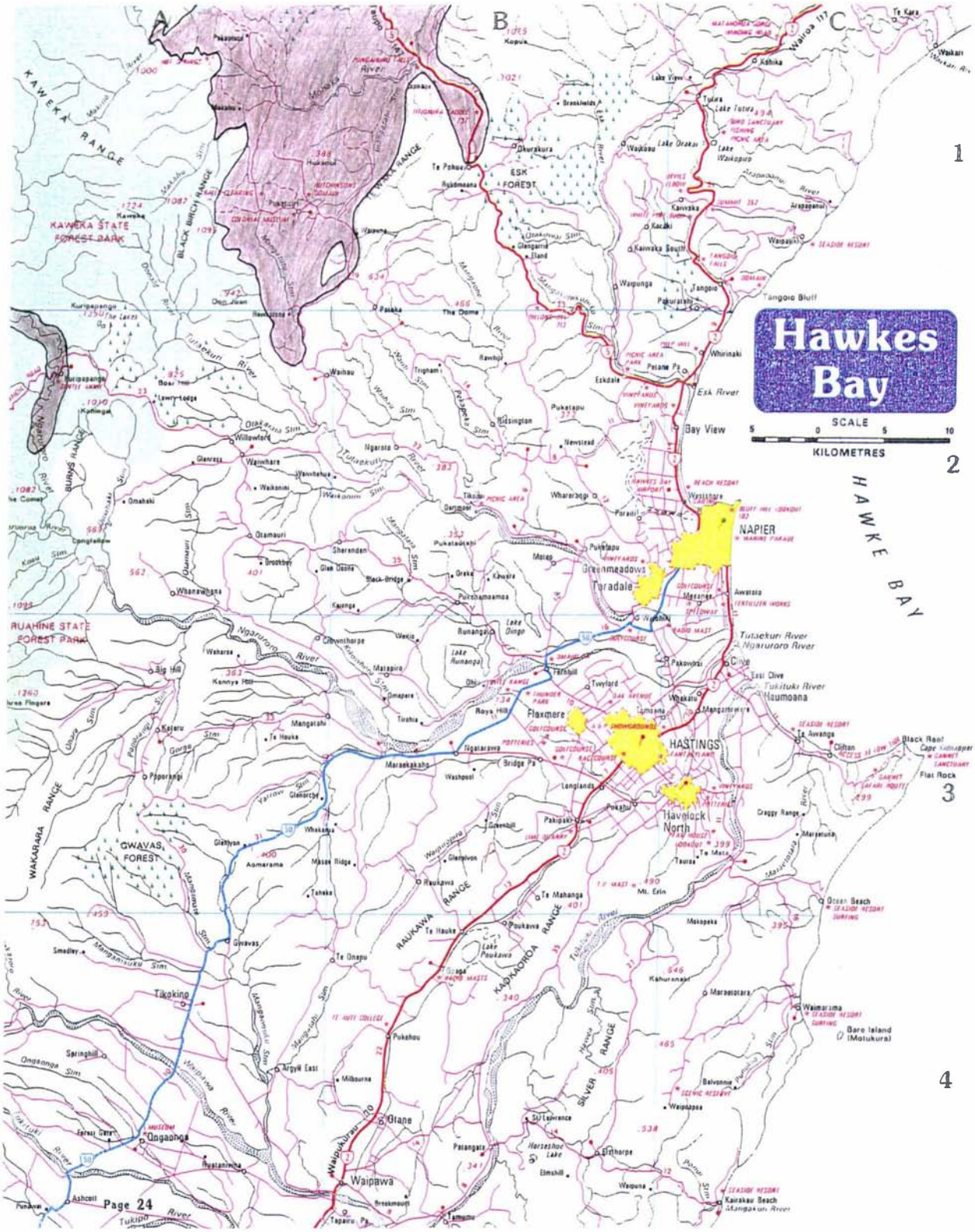

Figure 5.9: Distribution of Taupo Ignimbrite (shaded brown) in western Hawke's Bay, New Zealand. Base map reproduced from Shell Road Maps of New Zealand (1985).

2. it lacks particle sorting, clast sizes range from boulders to ash
3. charred logs and charcoal are common, especially near the base of the deposit, and
4. in some locations ripped-up soil clasts may be seen.

A reconnaissance of the area to the west of Kuripapango shows Taupo Ignimbrite within road cuttings on the Napier-Taihape Road that traverses the Gentle Annie Saddle (*c.* 720m a.s.l.) (Fig. 5.9). This low point within the Ranges coincides with the course of the Ngaruroro River through the mountains. Another low point in the Ranges coincides with the course of the Mohaka River farther to the north. Taupo Ignimbrite was thus able to overtop many of the low points within the main divide. In many localities within the ranges the ignimbrite has been removed by erosion but its former existence is revealed by residual pumice clasts within the surficial regolith or soils. Taupo Ignimbrite is unlikely to have completely overtopped the Ruahine and Kaweka Ranges as Froggatt and Rogers (1990) did not record it within any of the cores they obtained from their study of high altitude peat bogs within these ranges. Taupo Ignimbrite was also not found along the upper reaches of the Tutaekuri or Waipawa Rivers. The headwaters of both these rivers are not sourced within close proximity to Lake Taupo.

Taupo Ignimbrite deposits are present in road cuttings within the saddle (Titiokura Summit, 762m a.s.l.) separating the Te Waka (Te Waka No. 2 Summit at 1021m a.s.l.) from the Maungaharuru (Wakaateo No. 2 summit at 1095m a.s.l.) Ranges (Fig. 5.9). Ignimbrite has not been found on the summits of either range. An investigation of road cuttings along State Highway 5 from Titiokura Summit towards Napier showed a lobe of Taupo ignimbrite overtopped Titiokura Summit flowing down-hill to just beyond Te Pohue settlement. The main ignimbrite lobe flowed down the Mohaka River breaching low points in the Maungaharuru Range farther to the northeast. Ongoing research is being conducted towards defining the maximum extent of this ignimbrite in Hawke's Bay, in areas to the north of the study area.

Farther to the south the eastward progress of the Taupo Ignimbrite was impeded by the Maniaroa Range (Dunmore summit at 702m a.s.l.) (Fig. 5.9). It did, however, manage

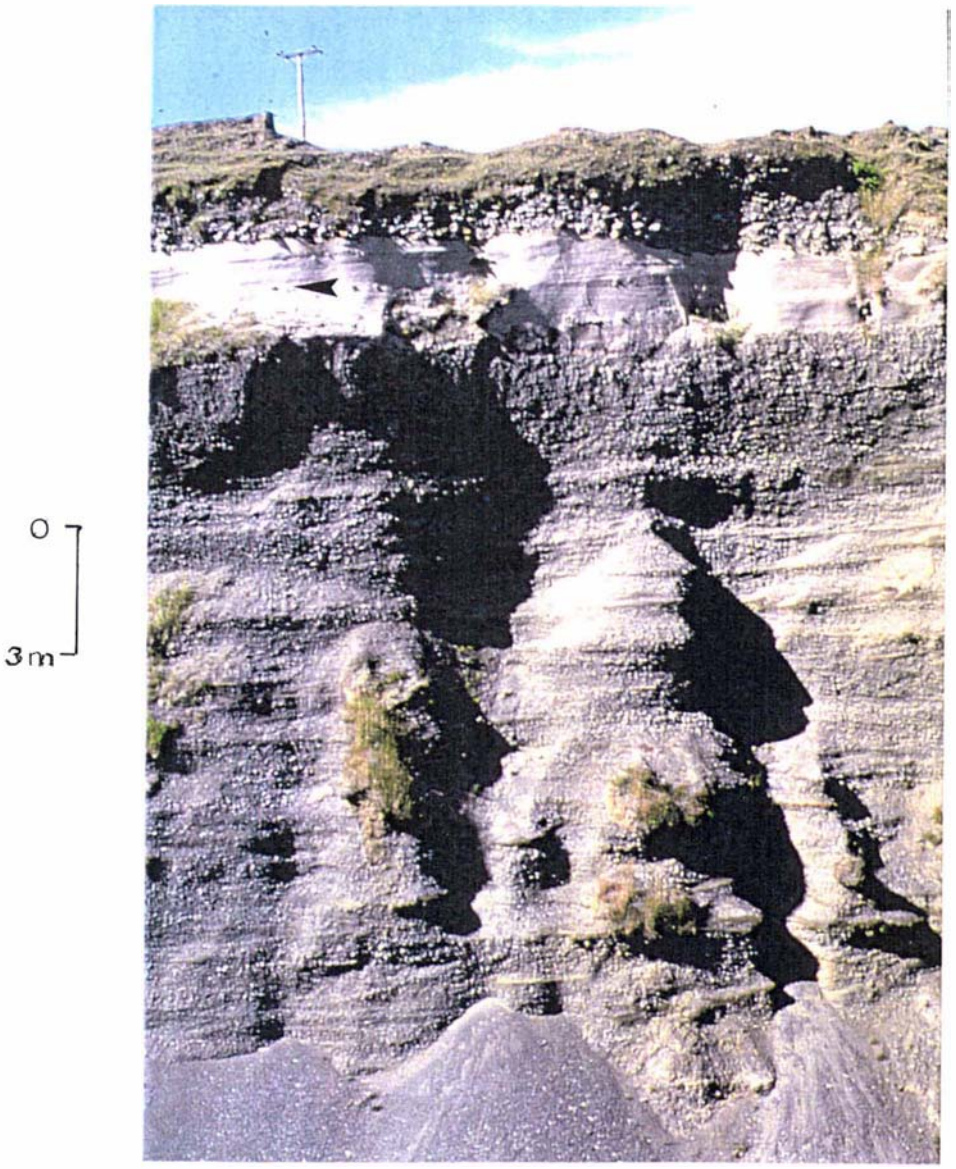

Plate 5.16: Proximally reworked Oruanui Ignimbrite (22 590±230 years B.P) is found within an Ohakean alluvial fan sequence at Tarawera Farm, west of the Mohaka Bridge. (V20/235 197)

to overtop low points within this range as seen by ignimbrite deposits within road cuttings on the Puketitiri Road (V20/183 065). Taupo Ignimbrite deposits from this flow are also seen within the valley where the William Hartree Scenic Reserve is located (V20/190 154). This flow terminated just beyond the junction of Puketitiri and Hawkston Roads (V20/190 024). Another lobe of ignimbrite flowed via the Mangatutu Stream overtopping the southern part of the Maniaroa Range, which is at lower elevations, reaching Hawkstone Station (V20/147 998). Taupo Ignimbrite, present in a number of road cuttings along Hawkston Road, forms the most easterly extent in this area.

Along reaches of the Mohaka and Ngaruroro Rivers and their tributaries there has been river incision into the readily erodible Taupo Ignimbrite. This has resulted in the exhumation of surfaces that existed prior to being inundated by Taupo Ignimbrite and the reoccupation of pre-eruption river courses. Exhumed surfaces may be seen in the banks of fluvial terraces near the confluence of the Mohaka and the Ripia Rivers (e.g. V20/135 165). Today, these rivers have the appearance of a mature meandering river system.

Ohakean terraces in the vicinity of the bridge across the Mohaka River (Fig. 5.9) have also been overridden by Taupo Ignimbrite. Ignimbrite has not, however, overtopped Ohakean terraces along the Ngaruroro River. Taupo Ignimbrite alluvium is present on some Holocene age terraces within the area known as the Pigsty (U21/085 768), below the Pigsty Flats (Pigsty Flats=Ohakean terraces).

5.5.3 Oruanui Ignimbrite

A reworked ignimbrite deposit *c.*3m thick is preserved within a gravel quarry (V20/235 197) on Tarawera Station, bordering the Mohaka River on the Taupo side of the Mohaka Bridge (Plate 5.16). The ignimbrite rests on a channelled surface within an Ohakean age alluvial fan *c.*5-6m below the fan surface and 20-25m above the quarry floor. An Ohakean age for the alluvial fan gravels is indicated by the presence of

Holocene age coverbeds. These include andesitic ashes of the Tufa Trig, Ngauruhoe, Papakai and Bullott Formations, Taupo Ignimbrite, Waimihia Tephra and microscopic rhyolitic tephras.

The reworked ignimbrite exhibits hyperconcentrated and stream flow (cross-bedding) characteristics within a distinctly erosional upper contact. Greywacke gravels immediately above the ignimbrite are coarser (pebble-boulder sized, maximum diameter of 50cm) than those immediately beneath it (pebble-cobble sized). Fluvial gravels beneath the ignimbrite commonly show bedding with sandy interlayers and channelled cross-beds.

The Ohakean age of the gravels, combined with a knowledge of the volcanic history from Taupo Volcano during this period, indicates this ignimbrite can only be the Oruanui Ignimbrite of the Kawakawa Tephra Formation, a *c.*22 600 years B.P. eruptive (Wilson *et al.*, 1988). If this is true, the most easterly occurrence of primary Oruanui Ignimbrite must have been close by. The identity of this ignimbrite will be verified in section 6.3.5 by matching its glass chemistry with that of known Oruanui Ignimbrite deposits found in more westerly locations nearer to Lake Taupo.

5.5.4 Potaka and Rabbit Gully Ignimbrites

Two primary, mid-Pleistocene ignimbrites (New Zealand Castlecliffian Stage) have been documented as far east as Cape Kidnappers within the Hawke's Bay landscape (Kingma, 1971; Seward, 1975; 1979; Kamp, 1978; 1990; 1992a; Black, 1992; Shane *et al.*, 1996a;b). The older Potaka Ignimbrite, previously referred to as Kidnappers Tuff (Kingma, 1971; Kamp, 1978; 1990; 1992a) or Kidnappers A (Black, 1992) overlies a dunal paleosol within the Maraetotara Sands of the Kidnappers Group. Charred logs are visible both at the base and top of this ignimbrite. A series of fluvially emplaced tuffs are present above the Potaka Ignimbrite in the Cape Kidnappers sequence. These have been referred to as Kidnappers B, C, D, E and F by Black (1992).

Plate 5.17: On the true-right bank of Mangaonuku Stream (U22/097 592) 1 Ma Potaka Ignimbrite (pointed at by figure) rests on Salisbury gravels.

Potaka Ignimbrite has also been documented west of Cape Kidnappers. Localities described include: Mangaonuka Stream (Kamp, 1992a; Shane, 1993; 1994); Makaroro River (Raub, 1985; Shane, 1993; 1994); underlying Salisbury gravels within the Ohara depression (Erdman and Kelsey, 1992); and is reworked within the predominantly fluvial and lacustrine Castlecliffian Mangatarata Formation in the Dannevirke and Norsewood areas (Lillie, 1953; Shane, 1991; 1993; 1994; Krieger, 1992).

During the general reconnaissance of the western hill-country, south of the Ngaruroro River, both primary and fluvially reworked ignimbrites were recognised at a number of localities along State Highway 50 between the settlements of Tikokino and Maraekakaho. A sample for electron microprobe analyses and subsequent tephra fingerprinting was obtained from the true right bank of Mangaonuku Stream (Plate 5.17) at the site of the Mangaonuku No. 1 Bridge (U22/097 592). The ignimbrite unit (3-5m) rests on fluvial gravels and sands. Electron microprobe analyses of the glass chemistry and subsequent ignimbrite correlation are undertaken in section 6.3.5. Shane (1994) correlated the ignimbrite at this site with the Kidnappers A Ignimbrite (=Potaka Ignimbrite) at Cape Kidnappers and other localities within the central and lower North Island.

Potaka Ignimbrite is also seen along State Highway 50 as prominent 5-10m cliff faces in the Maraekakaho River Valley (e.g. V21/165 642), within numerous road cuttings along Salisbury (e.g. U21/051 636) and Keruru (e.g. U21/065 630) Roads, and in Gwavas State Forest. No attempt was made to map the areal extent of this subsurface ignimbrite as it was beyond the age of deposits being looked at in detail.

Magnetostratigraphy, $^{40}Ar/^{39}Ar$ and isothermal plateau fission-track (ITPFT) ages, obtained by Shane (1994) from several exposures of Potaka tephra and ignimbrite in the East Coast region and elsewhere, indicate significantly older age estimates, 0.99-1.07 Ma, than previous age estimates of 0.60-1.0 Ma (Seward, 1974; 1975; 1976; 1979; Boellstorff and Te Punga, 1977; Seward *et al.*, 1986; Shane and Froggatt, 1991). At Cape Kidnappers the Kidnappers A Ignimbrite (Potaka Ignimbrite) is dated at 0.99 ± 0.09

Ma by the ITPFT method (Shane *et al.*, 1996b) and lies within the upper part of the Jaramillo subchron (Black, 1992).

The precise correlation of Potaka Tephra to its source vent and proximal ignimbrite sheet is still uncertain. It is likely, however, to be an eruptive from the Mangakino Volcanic Centre, in the SW part of the Taupo Volcanic Zone, which is known to have been active during this interval (Wilson *et al.*, 1984; Wilson, 1986; Pringle *et al.*, 1992). The unequivocal correlation of a number of distal tephras in early-mid Pleistocene deposits in Hawke's Bay with those in the Mangakino area is difficult as unwelded ignimbrites and tephra have been poorly preserved near source and often suffer from geochemical alteration (Wilson, 1986).

The younger ignimbrite known as the Rabbit Gully Tuff (Kingma, 1971) or Kidnappers D (Black, 1992) within the Kidnappers Group has a glass fission track date of 0.32±0.07 Ma and an $^{40}Ar/^{39}Ar$ date of 0.88±0.04 Ma (Shane *et al.*, 1996a;b). The $^{40}Ar/^{39}Ar$ date is considered a more realistic estimate of the true age of the ignimbrite than the fission track date which does not account for the underetching and annealing of volcanic glass.

A number of ignimbrites are present within early to mid-Pleistocene East Coast strata. (Shane *et al.*, 1996a). Many ignimbrites and tephras are reworked and emplaced as catastrophic flood deposits in overbank settings on former braided plains (e.g. Krieger, 1992).

5.6 ERODED HILLS AND TERRACES

5.6.1 Introduction

Erosion processes are common within the hill-country and terrace-lands on the East Coast of the North Island where a combination of soft rock lithologies, active tectonism, short and long term climatic events (cyclonic storms and Quaternary climate change) and recent deforestation by man has predisposed much of this region to erosion. This has been well documented (e.g. Eyles, 1971; Crozier *et al.*, 1980;

Plate 5.18: A view looking north-east towards the Te Waka-Maungaharuru Ranges and the associated landslide complex on its colluvial and tephra-mantled dip-slope. The sequence of moderately indurated, thick bedded limestone, massive siltstone and banded conglomerate dip gently (*c.*15°) towards the south-east. The combination of impermeable siltstone and pervious limestone gives rise to distinctive geological control on the landform and outcrop patterns of resistant rock. (V20/257 131).

Hubbard and Neall, 1980; Lambert *et al.*, 1984; Grant, 1985; Pettinga, 1987a;b; Black, 1991; Marden *et al.*, 1991; Pettinga and Bell, 1991; Trustrum and Page, 1991; Marden and Rowan, 1993; Page *et al.*, 1994a;b).

5.6.2 Hillslope erosion

For much of the Hawke's Bay hill-country factors such as geology, topography, vegetation and climate appear to be the primary influences on erosion (Plate 5.18). Soil patterns observed on these hillslopes are variable and hence complex. Not only do they reflect a complex interplay between tectonic, lithological, climatic and anthropogenic factors but also intermittent accessions of loess and tephras.

Pettinga and Bell (1991) recognise three landslide associations within Hawke's Bay:

1. deep-seated block and wedge slides on moderately deformed Upper Tertiary and early Quaternary sandstone-mudstone lithologies
2. surficial creeping earthflows, rotational slide-earth flows, debris flow slides and debris slides on complexly deformed Upper Cretaceous-Lower Tertiary mudstone and sandstone dominated lithologies, and
3. shallow regolith failures (landslides) which are independent of bedrock controls. These are normally triggered by high-intensity rainstorms.

High-intensity rainstorms (e.g. tropical cyclones) are known to be one of the main causes of sediment generation, movement and discharge within this landslide-prone hill-country (Marden and Rowan, 1993; Page *et al.*, 1994a;b), the most recent example being Tropical Cyclone Bola in March 1988. This event caused widespread slippage and removal of regolith in the hill-country, rejuvenation of old slumps, gully erosion and subsequent aggradation in many basins and valleys. Not all of this material is removed from the area during each storm event, much accumulates in colluvial foot- and toe-slope positions, in hollows and in valley bottoms. The excavation of material from these positions requires another triggering event.

Numerous deflation hollows and pedestalled grasses in the Blowhard-Kuripapango area provide clear evidence of often extreme soil erosion by wind. Much of the erosion and loss of soil in this area has resulted from the reduction in plant cover which accompanied the use of the area for pastoral farming.

The triggering of landslides by earthquake shaking is well documented within the Hawke's Bay region (Henderson, 1933; Hull, 1986; 1990). Pettinga (1987a) outlines evidence for the reactivation of the Ponui Landslide by the 1931 Napier earthquake.

Landslide-triggering earthquakes destroy complete interfluves, changing valley dimensions and create new topographic features. These events constitute a major factor in terrain development.

5.6.3 Erosion of terraces

There are four kinds of terrace erosion observed along Hawke's Bay waterways:

1. bank erosion
2. headward extension of stream channel and down-cutting of the stream bed, and
3. gully erosion, and
4. wind erosion of surficial coverbeds

The primary cause of terrace erosion is by lateral corrasion. This results in the undercutting of river banks and the collapse of terrace materials into the river or stream channel.

5.7 FAULT TRACES

5.7.1 Introduction

Hawke's Bay lies within the Main Seismic Region of Eiby (1971). The occurrence of large, destructive earthquakes in Hawke's Bay this century e.g. 1931 Napier Earthquake

are well known and documented (Henderson, 1933; Hull, 1986; 1990). Correlation of an earthquake event to a particular surface rupture is less well known, as is the distribution of fault traces relating to earthquakes prior to this century.

This section briefly looks at some of the fault-related landforms observed in Hawke's Bay, particularly those associated with the range-bounding Ruahine and Mohaka faults in western Hawke's Bay. No attempt is made to date the history of fault movements along these faults as this forms a complimentary Ph.D. study by Ms. Jude Hanson of the Soil Science Department, Massey University. Detailed mapping has already been undertaken in the Ohara depression (e.g. Raub, 1985; Raub *et al.*, 1987; Erdman and Kelsey, 1992) to the south of the field area studied in this thesis, and to the north of the field area at the confluence of the Mohaka and Te Hoe rivers, a proposed hydroelectric dam-site (Hancox and Berryman, 1986). The Mohaka and Ruahine fault traces between these two sites is currently being investigated by Hanson. Studies prior to this had only been at a reconnaissance level (e.g. Beanland and Berryman, 1987).

Detailed geological mapping, in a transect across the onland Hawke's Bay portion of the Hikurangi forearc basin, has shown six distinct north-east/south-west trending structural domains of extensional and contractional faulting within Neogene sediments related to the subduction of the Pacific Plate beneath the Australian Plate (Cashman and Kelsey, 1990; Cashman *et al.*, 1992; Erdman and Kelsey, 1992; Kelsey *et al.*, 1993). These domains from the coastal margin westwards are:

1. an uplifted zone of extensional faulting at the coast in the Cape Kidnappers/Te Mata Peak/Maraetotara Plateau areas
2. a zone of thrust faulting and folding in the Tukituki River/Middle Road areas
3. a complex zone of dextral strike-slip faulting in the Waipawa/Lake Poukawa areas
4. a relatively undeformed zone comprising the present-day Takapau-Ruataniwha Plains and the Heretaunga Plains
5. a zone of contractional folding and faulting along the eastern front of the Wakarara Range, and
6. a zone of dextral strike-slip faulting in the foothills of the axial ranges.

Plate 5.19: The NE-SW trending Ruahine Fault runs along the eastern flank of the Black Birch Range. (U20/092 077).

Plate 5.20: The Ruahine Fault trace along Lotkow Road has a prominent fault trench with an upthrown southeastern scarp. (U20/087 072).

5.7.2 The Ruahine and Mohaka Faults

Trending NE/SW through western Hawke's Bay are two dominantly dextral strike-slip faults with a small vertical component, the Ruahine and Mohaka faults. These faults are the two main northern strands of the Wellington Fault system and accommodate the dextral component of oblique convergence along the plate margin. The Wellington Fault system can be traced from Wellington City to the Bay of Plenty in the North, a distance of over 300km. Both these faults have distinct traces and exhibit offsets in late Quaternary times (Raub, 1985; Beanland and Berryman, 1987; Raub *et al.*, 1987). No surface ruptures have been reported along either the Ruahine or Mohaka Faults since European settlement (*c.*150 years ago). Many minor fault traces also exist (see Grindley, 1960).

Separating the Ruahine Fault trace from the Mohaka Fault trace are three basins or depressions, none of which are connected. From south to north these are the Ohara, Koharau and Puketitiri depressions (Kingma, 1971). These inland depressions are infilled with Neogene sediments, marine mudstones, limestones, ignimbrites, loess and tephras.

The Ruahine Fault is a major range-bounding fault on the hilly eastern flanks of the Ruahine, Black Birch and Kaweka Ranges. It is generally located within greywacke basement but slivers of Neogene sediments of the forearc basin are sometimes infaulted against it (Grindley, 1960). Near the confluence of the Mohaka and Ripia Rivers the Ruahine Fault crosses Holocene alluvial surfaces. The fault trace is hard to discern farther to the north within the Awahohonu State Forest because it has been obscured by logging operations. To the south of the Black Birch Range many of the geomorphic features associated with fault activity along the Ruahine Fault are masked by native vegetation. It is only where areas have been cleared (deforested) for pastoral landuse that major lineations, recognised as fault traces, can be easily identified.

West of the Puketitiri settlement the NE-SW trending Ruahine Fault is seen along the eastern flank of Black Birch Range (Plate 5.19). Several spurs are offset right laterally

as is the deflection of stream channels along and then eventually across upthrown southeastern fault segments. The Ruahine fault-trace is marked by a prominent fault trench in this district which is *c.*2-3m deep and *c.*3m wide at the bottom with an upthrown southeastern scarp (Plate 5.20). Near Whittle Road greywacke is seen on the northwest, now downthrown, and Tertiary mudstone upthrown on the southeastern side (U20/092 077). Greywacke sandstone and argillite beds are steeply dipping and highly crushed close to the fault zone and hence are highly susceptible to erosion.

The location of the Ruahine and Kaweka axial ranges within a tectonic zone, which is presently being uplifted (Kaikoura Orogeny), means they are prone to considerable erosion. Triggers such as earthquake shaking has facilitated the downslope movement of material which eventually makes its way into the fluvial system. Most of the slope failures are confined to loosened surficial colluvium and bedrock.

Tectonic landforms seen along the Black Birch Range include shutter ridges, offset streams, sag ponds, scarps and small folds. These are all clear evidence of recent oblique dextral movement along the Ruahine Fault. Late Holocene slip rates along the Ruahine Fault are estimated by Beanland and Berryman (1987) to be 1-2mm/year. Neall *et al.* (1994), however, believe these rates to be underestimates. A Ph.D. study, currently being undertaken by Ms Jude Hanson, aims to present revised slip rates for the Ruahine Fault in western Hawke's Bay.

The Mohaka Fault is found 3-7km east of the Ruahine Fault and forms the northern continuation of the Wellington Fault. South of the study area, between the upper reaches of the Tukituki and Waipawa Rivers, the Mohaka Fault forms the boundary between Mesozoic and Neogene rocks. North of the Waipawa River it forms the contact between Neogene rocks of the Ohara depression and the greywackes of the Wakarara Range to the east. The eastern boundary of the Wakarara Range is marked by the Wakarara Fault.

North of the Ohara depression the Mohaka Fault trace is within Neogene sediments. In the Puketitiri depression the Mohaka Fault is seen as a break in slope along the western

Plate 5.21: At Waitara Road (V20/249/178) a prominent fault scarp (seen running across the centre of the photograph from right to left) results from displacement/s along the Mohaka Fault. Raub *et al.* (1987) estimated a Holocene slip rate of 3-4mm/year at this location.

foot of the Maniaroa Range, following the Inangatahi Stream. It continues through Awahohonu State Forest and then along Waitara Road (Plate 5.21; V20/249 178), north of the Napier-Taupo highway (State Highway 5). Vertical displacement to the east is obvious all along the fault trace. No evidence of late Quaternary lateral movement was observed in the field. A major splinter fault, the Te Waka Fault, leaves the Mohaka Fault at Puketitiri and trends northeast through the summit of the Te Waka Ranges (Ms Jude Hanson, pers. comm. 1994).

Evidence of local mass movement may be seen along the western escarpment slopes of the Maniaroa Range. Large blocks of Pliocene limestone are scattered over the escarpment slope on the upthrown (eastern) side of the Mohaka Fault trace. The downslope movement of these limestone blocks may have been triggered by earth movement along the Mohaka, Te Waka or on the nearby Ruahine Fault. Limestone blocks, seen *c.*2km north along Potter's Road (V20/184 077) from the Puketitiri Road turnoff, have caused temporary blockage/s of Inangatahi Stream in the past. This resulted in the formation of a temporary lake which extended as far as Carswell Road (V20/168 081). Landowners within the district stated that this lake still existed during early European settlement (1850s) of the area. This lake was subsequently drained and the land farmed. Holocene movement along the Mohaka Fault is estimated to be 3-4mm/year (Raub, 1985; Raub *et al.*, 1987). Hanson (1994), however, has measured higher offset rates, 10-15mm/year between the Manawatu Gorge and Dannevirke and 3-6mm/year between the Ohara Depression and the Mohaka River.

Tectonic uplift on the Mohaka Fault has resulted in the preservation of flights of aggradation and degradation terraces along many of the major river systems within Hawke's Bay e.g. Ngaruroro River. These eastward draining rivers and streams have been required to incise into the steepening western limb of the Hawke's Bay Syncline forming gorges through the Neogene sequences.

Tectonic landforms seen along the Ruahine and Mohaka fault traces include fault scarps, sag ponds, tectonic bulges, pressure ridges and ponded drainage. Geomorphic

features which are offset include streams, ridges or spurs and river terraces. These features are presently being investigated by Hanson.

5.8 CONCLUSIONS

The late Quaternary landscape of Hawke's Bay has been subjected to both constructional and erosional processes. It has been constructed principally of alluvial gravels and ignimbrites which, in turn, have been blanketed by layered loess-paleosol sequences. Loess-paleosol sequences are intercalated by macroscopic and microscopic rhyolitic and andesitic tephra chronohorizons.

Tectonic forces have substantially influenced landform development in Hawke's Bay. They have produced relief features by uplift, active folding and faulting. These relief features are in turn modified by erosion and deposition, especially by drainage processes, as well as by the continued growth of active structures.

Coverbeds on alluvial fan terraces are subdivided into Holocene, Ohakean and pre-Ohakean surfaces. As the pre-Ohakean coverbed record on alluvial fan terraces was incomplete, field studies were focussed on the western hill-country. The most stratigraphically useful coverbed exposures are those from road and track cuttings through colluvial toe-slope positions.

Five loess-paleosol layers were identified. Macroscopic tephra units identified in Hawke's Bay include: Taupo Tephra (1850±10 years B.P.); Waimihia Tephra (3280±20 years B.P.); andesitic tephras of the Papakai (*c.*9700-3400 years B.P.), Mangamate (*c.*10 000-9700 years B.P.) and Bullott (22 600-10 000 years B.P) Formations; and Kawakawa Tephra (22 590±230 years B.P.). Three ignimbrite units were also identified within western Hawke's Bay, Taupo Ignimbrite (1850±10 years B.P.), proximally reworked Oruanui Ignimbrite (22 590±230 years B.P.) and Potaka Ignimbrite (1 Ma). These chronohorizons enable a detailed subdivision of last stadial (Ohakean) and older events to be made. Microscopic tephra chronohorizons within Ohakean and older (pre-Ohakean) sequences needed to be identified to refine the chronologies. This is

undertaken in Chapter Six using a number of tephra fingerprinting techniques. Once this has been completed coverbed sequences in western Hawke's Bay can be correlated with those in the Rangitikei Valley and offshore cores.

CHAPTER SIX:
IDENTIFICATION AND DATING OF THE WESTERN HAWKE'S BAY TEPHRA RECORD

6.1 INTRODUCTION

In Chapter Five surficial deposits of late Quaternary age were identified within the western Hawke's Bay landscape. The established practice of dating surficial deposits within the lower North Island has been to record the lithostratigraphy and correlate it with the loessial sequences of the Rangitikei River Valley, Wanganui Basin (see Table 3.1). To elucidate the sequence of landscape-forming events within the western Hawke's Bay landscape (see section 10.5), greater resolution was needed to date geomorphic events than that obtained in Chapter Five.

In Chapter Five both macroscopic and microscopic Taupo Volcanic Zone (TVZ)-sourced andesitic and rhyolitic tephra-bearing layers were identified within the western Hawke's Bay soilscape. Tephrochronology is one tool which has been widely used to date geomorphic events within the lower North Island. The <64 000 year B.P. tephra successions around the TVZ volcanic centres (i.e. down to the Rotoehu Ash) are well known and dated (e.g. Froggatt and Lowe, 1990; Wilson, 1993). Older tephra successions (>64 000 years B.P.) however, are more poorly dated because of:

1. the lack of a reliable dating technique to use beyond the maximum age limit imposed by the radiocarbon method, and
2. many of the older tephra successions in their source areas are either deeply buried or have been destroyed by subsequent volcanic and/or Quaternary climatic events.

This study aims to establish a chronological framework for dating late Quaternary coverbed sequences in western Hawke's Bay utilising the much quoted Rangitikei River Valley alluvial and loessial stratigraphies (see Table 3.1), the Wanganui chronology (Pillans, 1991; 1994a;b; Palmer and Pillans, 1996), and the TVZ rhyolitic tephra chronologies (see Table 3.3). The tephra record in such distal, downwind settings is

often fragmentary and incomplete, making it difficult to trace an unknown tephra layer to source and to correlate it with a dated eruptive event. A number of tephra "fingerprinting" techniques (chemical and mineralogical) have been developed to help resolve the identity and hence age of individual tephra layers in distal depositional environments. The data obtained is then used to complement the field chronologies. The following sections detail:

1. the analytical procedures used to identify tephra time-lines within surficial deposits, and
2. the mineralogical and chemical "fingerprinting" methods used to match a tephra to its proximal correlative.

Once this is achieved geomorphic events within western Hawke's Bay can be dated and then correlated to the lower North Island late Quaternary climate model, described earlier (see section 3.2.1).

6.2 ANALYTICAL PROCEDURES USED IN TEPHRA IDENTIFICATION AND FINGERPRINTING

6.2.1 Approach

To elucidate which tephras have been emplaced within the western Hawke's Bay soilscape, a sequential approach was required. The first phase was to identify the presence of tephra/s by mineralogical analyses (volcanic glass counts and quantitative quartz analysis). Once this was achieved the next phase was to establish its approximate stratigraphic position and age. Tephra fingerprinting techniques (ferromagnesian mineral assemblages and electron microprobe analysis of volcanic glass shards) were then conducted to identify the unknown tephra. Sources of relevant information include:

1. tephra isopach maps (e.g. Pullar and Birrell, 1973a;b)
2. theses (Roxburgh, 1974; Robertson, 1978; Hull, 1985; Raub, 1985), and
3. published papers (Healy, *et al.*, 1964; Pullar, 1970; Howorth, *et al.*, 1980; Stewart and Neall, 1984; Froggatt and Rogers, 1990; Eden *et al.*, 1993; Carter *et al.*, 1995;

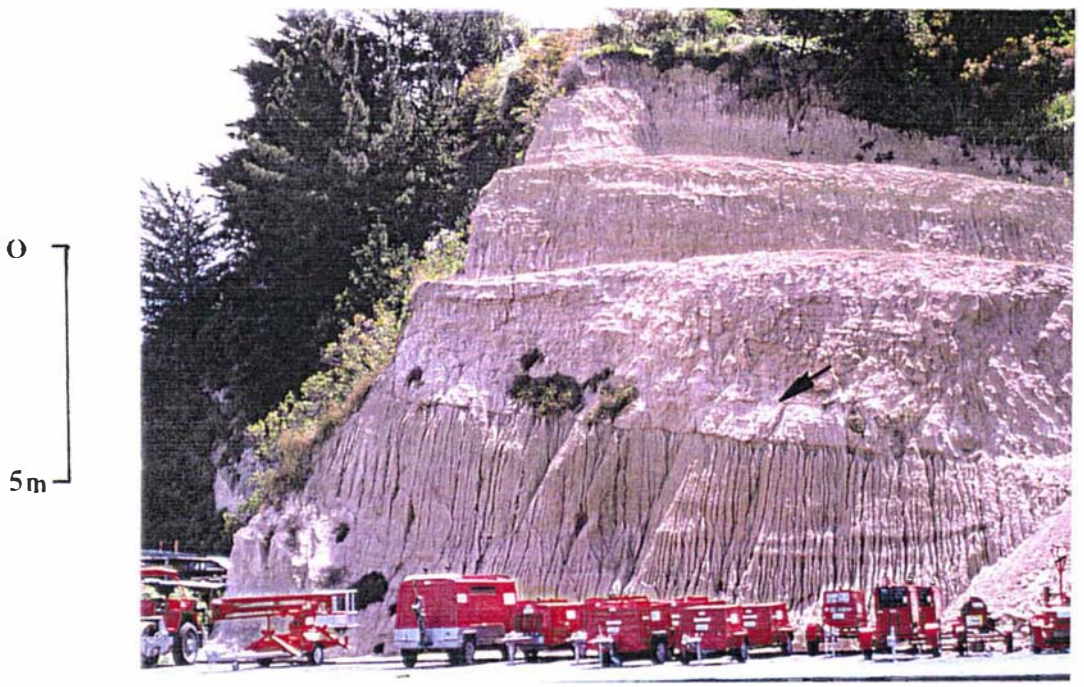

Plate 6.1: The *c.*350 ka Rangitawa Pumice (arrowed) rests within a thick loess-paleosol succession at the City Hire section (V21/451 826), Scinde Island. Estuarine mud and paleosols are present at the base of the section.

Eden and Froggatt, 1996; Shane, 1994; Shane *et al*., 1996a;b) undertaken within Hawke's Bay and its environs.

6.2.2 Sampling, sample pretreatment and preparation

Samples for tephra fingerprinting were taken from:

- reference sections (see section 5.4.3)
- a proximally reworked ignimbrite within an alluvial fan sequence bordering the Mohaka River (see section 5.5.3)
- an ignimbrite on the true right bank of Mangaonuku Stream near the Mangaonuku #1 Bridge (see section 5.5.4), and
- from a tephra near the base of a layered loess sequence blanketing Scinde Island (Plate 6.1; V21 451 826). This section is referred to as the City Hire section.

The reference sections were studied in most detail as they comprise what is thought to be the full suite of tephras seen in western Hawke's Bay.

Details of the sampling strategy and the methods of preparing loess and tephra samples for laboratory analysis are described in section 5.4.3.2. Ignimbrite and coarse-grained lapilli samples were crushed using a porcelain mortar and pestle. Samples were then chemically pretreated (cleaned) to remove coatings prior to mineralogical and chemical analyses. Allophanic Soils (allophane and ferrihydrite dominated samples) required 0.2M ammonium oxalate pretreatment (Schwertmann, 1959; 1964) for the dissolution of short-range-order clays and organic complexes (Alloway *et al.*, 1992b) whereas Pallic Soils were subjected to a cold citrate-bicarbonate-dithionite (CBD) pretreatment (Blakemore *et al.*, 1987) to remove crystalline coatings.

Following chemical pretreatment, samples were placed in an ultrasonic water bath for 10 minutes to help remove any additional adhering material. After ultrasonication, samples were washed through a 63μm diameter nylon sieve. The >63μm fractions were placed in petri-dishes and then dried in a fan oven at *c.*30°C. Once dry the >63μm fraction was dry sieved into a 63-125μm fraction and a >125μm fraction. Both

fractions were stored in plastic vials for mineralogical and chemical analysis. Fractions <63μm are commonly not retained for mineralogical and chemical analyses because they are difficult to separate using the Frantz electromagnetic separator (Froggatt and Gosson, 1982).

Froggatt and Gosson (1982) recommend the 63-250μm fraction as being the most useful for tephra fingerprinting. In this study only the 63-125μm fraction was studied because few grains were larger than 125μm. Each sample was split into a "heavy" (ferromagnesian mineral assemblage) and a "light" mineral fraction (quartz, feldspars and volcanic glass shards) using a Frantz isodynamic electromagnetic separator. Operating conditions and settings are detailed in Froggatt and Gosson (1982). Strongly magnetic grains of titanomagnetite were removed with a hand magnet prior to separation. The "light" fraction was further separated into:

1. a volcanic glass fraction, and
2. a quartz and feldspar fraction

using the Frantz isodynamic electromagnetic separator. Operating conditions and settings for these separates are also detailed in Froggatt and Gosson (1982). The purity of these splits were checked with a binocular microscope.

A bulk sample charcoal sample was obtained from the Ratan paleosol (sampled at 410-412cm depth) at the Pakaututu Road reference section (for site details refer to section 5.4.3.3), and submitted for radiocarbon assay. The purpose of the radiocarbon date was to:

- date the top of the Ratan paleosol
- date a rhyolitic tephra (Mangaone subgroup tephra) within this paleosol, and
- provide a maximum date for the last stadial (Ohakean).

This paleosol is found in many locales within the lower North Island but has not previously been dated by the radiocarbon method.

6.2.3 Mineralogical procedures

6.2.3.1 *Volcanic glass counts*

Field studies (section 5.4.2.3) indicate the presence of microscopic tephra layers within the dominantly loessial coverbed sequences at Pakaututu Road, Manaroa, Apley Road and Poraiti. Grain counts were undertaken on the chemically cleaned 63-125μm fraction at each of the reference sections to search for volcanic glass concentrations at each selected stratigraphic level.

Samples for grain counting were taken every 10cm (±1.5cm) from the current soil surface and within layers of interest. Four hundred mineral grains were counted using Galehouse's (1969) "ribbon method." The advantage of the ribbon method over point counting is that it reduces the bias towards counting larger grain sizes (Eden and Milne, 1987).

6.2.3.2 *Quantitative quartz analysis of coverbed sequences*

A rapid, quantitative x-ray diffraction (XRD) method (Alloway, 1989; Alloway *et al.*, 1992a) was utilised to assess the total quartz content present at the Pakaututu Road and Manaroa reference sections. Both sites have experienced varying inputs of tephra (andesitic and rhyolitic) and quartzo-feldspathic loess. Site details are recorded in Chapter Five. Samples for XRD analyses were taken every 10cm (±1.5cm) and within layers of interest.

X-ray diffraction (XRD) settings, procedures for the preparation of standards to draw a standard quartz regression line and the preparation of samples prior to XRD determination are detailed elsewhere (Alloway, 1989; Alloway *et al.*, 1992a; Hodgson, 1993; Palmer and Pillans, 1996). Modifications were made to the method, principally:

- the use of the chemically untreated whole (<2mm) fraction to reduce sample preparation time, and

Table 6.1: Characteristic ferromagnesian mineral assemblages for silicic Taupo Volcanic Zone eruptives since *c.*64 000 years B.P.

ASSEMBLAGE 1 **Hyp ± aug ± hbl**	ASSEMBLAGE 2 **Hyp + hbl ± aug**	ASSEMBLAGE 3 **Hyp + hbl + bio**	ASSEMBLAGE 4 **Hyp + cgt ± hbl**	ASSEMBLAGE 5 **Hyp + aug ± hbl**	ASSEMBLAGE 6 **Aegirine**
Taupo VC	**Okataina VC**	**Okataina VC**	**Okataina VC**	**Okataina VC**	**Tuhua VC**
Taupo (all members)	Mamaku	Kaharoa	Whakatane	Hauparu	Tahua
Mapara	Waiohau	Rotorua (top part)	Rotoma	Te Mahoe	
Whakaipo	Rotorua (lower part)	Rerewhakaaitu	Rotoiti (all members except Matahi)	Maketu	
Wamihia (both members)	Te Rere	Okareka			
Hinemaiaia	Ornataroa	Earthquake Flat			
Motutere	Awakeri	Rotoiti (top part)			
Opepe	Mangaone				
Poronui	Tahuna				
Karapiti	Ngamotu				
	Taupo VC	**Maroa VC**			
	Kawakawa (both members)	Puketerata			
	Poihipi				
	Okaia				
	Tihoi				
	Waihora				
	Otake				

hyp=hypersthene (orthopyroxene)

aug=augite (clinopyroxene)

hbl=hornblende

bio=biotite

Reproduced from Froggatt and Lowe (1990).

- the use of Linde-A, an aluminium oxide (α Al_2O_3 product), as an internal standard rather than sodium fluoride (NaF). The advantage of Linde-A is its purity, chemical stability and its freedom from orientation, due to its shape, in sample preparation. Linde-A is also non-toxic.

The utility of this XRD method is that it enables:

- the measurement in a sample of quartzo-feldspathic loess inputs relative to volcanic ash (rhyolitic and andesitic), and
- it helps identify microscopic tephra accessions which may not have been detected during field studies.

Previous studies (e.g. Alloway, 1989; Alloway *et al.* 1992a; Hodgson, 1993; Palmer and Pillans, 1996) have used quartz contents within stratigraphic layers as a proxy for interpreting Quaternary climatic changes. These studies have shown higher quartz contents (maxima) denote periods of maximum loess deposition (i.e. landscape instability during glacials and stadials) and lower quartz contents (minima) represent tephra (andesitic and/or rhyolitic) additions (dilution of quartz contents) and/or the presence of paleosols (i.e. landscape stability during interglacials and interstadials). Quartz contents within paleosols may be diluted by the preservation and concentration of fine andesitic ash accessions during periods of landscape stability.

6.2.3.3 *Ferromagnesian mineral assemblages*

Ferromagnesian mineral counts have routinely been used to assist the identification of an unknown tephra to its source caldera in New Zealand. Six ferromagnesian mineral assemblages are recognised (Froggatt and Lowe, 1990). These are listed in Table 6.1 by their characteristic mineral assemblages and volcanic centres. Mineral assemblages are listed in order of their abundance, followed by those minerals that may or may not be present.

Certain marker minerals such as cummingtonite are generally considered diagnostic of having been derived from the Haroharo complex within the Okataina Volcanic Centre. Cummingtonite occurs as a dominant ferromagnesian mineral in the Whakatane, Rotorua and Rotoehu Tephras. Minor amounts (<5%), however, occur in non-Haraharo tephras e.g. the Kaharoa, Waiohau, Rerewhakaaitu, Te Rere and Mangaone Tephras (Kohn, 1973).

The Pakaututu Road section was chosen as the most likely site to identify TVZ tephras because it is the most proximal to the TVZ volcanic centres. Individual tephra layers are thicker at this site and give a better tephra record. Grain counts were undertaken at selected depths on the chemically cleaned 63-125μm ferromagnesian fraction which was then identified using standard optical petrological procedures. Tephra layers recorded at other sections were then correlated with those at Pakaututu Road.

6.2.4 Chemical procedures

6.2.4.1 *Electron microprobe analysis of volcanic glass*

After volcanic glass counts had been conducted, samples were selected for electron microprobe (EMP) analyses and subsequent tephra fingerprinting. Preparation of polished volcanic glass thin sections for EMP analyses followed established procedures (Froggatt and Gosson 1982; Wallace *et al.*, 1985; Donoghue, 1991). Electron microprobe analyses were undertaken at the Analytical Facility, Victoria University of Wellington, on a fully automated JEOL JXA733 Superprobe using the settings and guidelines recommended for fingerprinting volcanic glass in New Zealand (Froggatt and Gosson, 1982; Froggatt, 1992). Microprobe operating conditions were:

- a beam current of 8nA
- an accelerating voltage of 15kV, and
- a defocussed beam diameter of 20μm to minimise volatilisation of Na, K and H_2O.

Volcanic glass analyses were calibrated against the following standards: KN-18, comenditic obsidian; VG-99, basaltic glass; and VG-568, Yellowstone rhyolitic glass.

Glass standards were frequently analysed under the same instrument settings as the unknown volcanic glass samples to check probe performance and stability.

In this study at least 10 shards were analysed per sample to check sample homogeneity (shard-to-shard variability) and whether samples were of a single or mixed population. This number of EMP analyses should reveal whether a sample from a particular depth increment is a single or mixed population (Froggatt and Gosson, 1982; Froggatt, 1983; 1992). Wherever the possibility of a mixed population existed, more than 10 analyses were undertaken.

Great care was taken to avoid including: bubbles, microlites, inclusions, vesicles, cracks, fractures and weathering products under the EMP beam. Major elements measured were SiO_2, TiO_2, Al_2O_3, FeO, MgO, CaO, Na_2O, K_2O and Cl.

6.2.4.2 *Statistical interpretation of EMP analysis*

The identification of which rhyolitic tephra/s are present within a sample was elucidated using:

- bivariate (% CaO-% FeO) plots
- ternary (% FeO-% $1/3K_2O$-% CaO) plots
- similarity coefficients (SC), and
- coefficients of variation (CV) (Borchardt *et al.*, 1971; 1972).

These methods have routinely been used in New Zealand to identify unknown tephras. The glass shard chemistry of an unknown tephra is matched with the glass chemistries of tephras at the well dated and stratigraphically constrained TVZ reference sections. Elements used to match unknown tephra samples with those at the reference sections were SiO_2, TiO_2, Al_2O_3, FeO, MgO, CaO, Na_2O, and K_2O. Chlorine was excluded as it has very low and almost invariant values.

Similarity coefficients of ≥ 0.92 and coefficients of variation of ≤ 12 for volcanic glass are defined by Froggatt (1983; 1992) as being chemically indistinguishable from that of

the reference volcanic glass datasets. In this study interpretations were made using these values, provided they complemented the field stratigraphic data. All results were interpreted only after comparison with:

- published data from the North Island reference sites
- isopach maps of tephra distributions, and
- the stratigraphic units recognised in Chapter Five.

6.3 RESULTS OF DETAILED STRATIGRAPHY AT REFERENCE AND OTHER SECTIONS

6.3.1 Volcanic glass counts and quartz determinations

Two types of volcanic glass shards were identified during the volcanic glass counts, clear glass and brown glass. Rhyolitic and dacitic glass is usually clear or light-coloured whilst andesitic glass is usually darker in colour, very often poorly preserved and only found within the upper coverbeds (i.e. within the younger Holocene ashes). In this study it was not always possible to separate rhyolitic and dacitic glass as they were often intermixed. A further problem in separating the different types of glass was that neither the 0.2M ammonium oxalate nor the CBD reagents completely cleaned the glass of adhering material. This was despite repeated chemical pretreatments being undertaken.

Rhyolitic glass shards exhibit a wide range in their degree of alteration, ranging from shards with sharply defined conchoidal fractures to shards with ill defined fractures and slight to moderate birefringence. Glass shards obtained from within former landsurfaces (paleosols) commonly show the greatest degree of alteration. This is attributed to these horizons having experienced more intense pedogenic alteration, resulting in the hydration and conversion of volcanic glass to allophane.

Volcanic glass maxima were labelled (◀) for microprobe analyses and subsequent tephra fingerprinting (Figures 6.1-6.7). A summary of the observed trends at each of the reference sections is as follows:

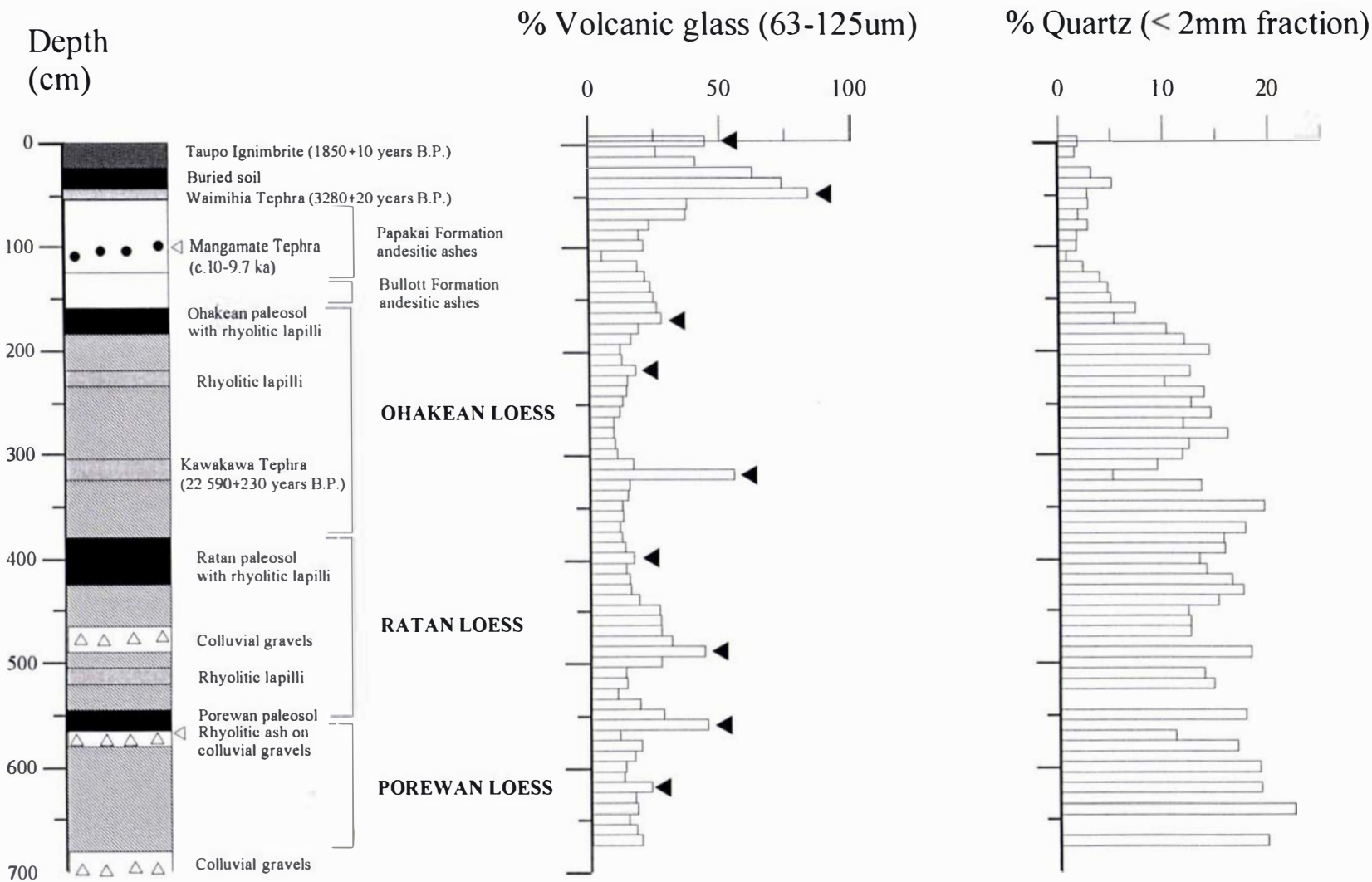

Figure 6.1: Volcanic glass and quartz contents at the Pakaututu Road reference section

Stratigraphic sequence at Pakaututu Road reference section (V20/117 125)

% Volcanic glass trends

- Volcanic glass maxima (Fig. 6.1) coincide with Taupo Ignimbrite and the macroscopic Waimihia and Kawakawa Tephras identified in Chapter Five.
- Volcanic glass maxima are also encountered within the:
  1. andesitic Papakai and Bullott Formations
  2. Ohakean paleosol
  3. Ratan paleosol, and
  4. rhyolitic ash on colluvial gravels within the Porewan paleosol.
- Andesitic glass is poorly preserved and becomes less common with depth.

% Quartz trends

- Quartz values (Fig. 6.1) are at their highest (maxima) within the Ohakean, Ratan and Porewan loess units and at those depth increments within the quartzo-feldspathic loess which are relatively undiluted by tephric (rhyolitic and andesitic) accessions
- Lower quartz levels (minima) are present within:

1. Taupo Ignimbrite
2. macroscopic rhyolitic tephra layers (e.g. Waimihia and Kawakawa Tephras and rhyolite ash (Rotoehu Ash?) on colluvial gravels within the Porewan paleosol)
3. the andesitic Papakai and Bullott Formations
4. the grey andesitic ash balls at 110cm depth (Mangamate Tephra?)
5. paleosols developed on Ohakean, Ratan and Porewan loess units, and
6. wherever a microscopic tephra layer (rhyolitic or andesitic), denoted by a volcanic glass peak (Fig. 6.1), is present.

Stratigraphic sequence at Manaroa reference section (V20/186 036)

% Volcanic glass trends

- Volcanic glass maxima (Fig. 6.2) are encountered within Taupo Ignimbrite, and the macroscopic andesitic (Papakai and Bullott Formations) and rhyolitic (Wamihia and Kawakawa Tephras) tephra layers.

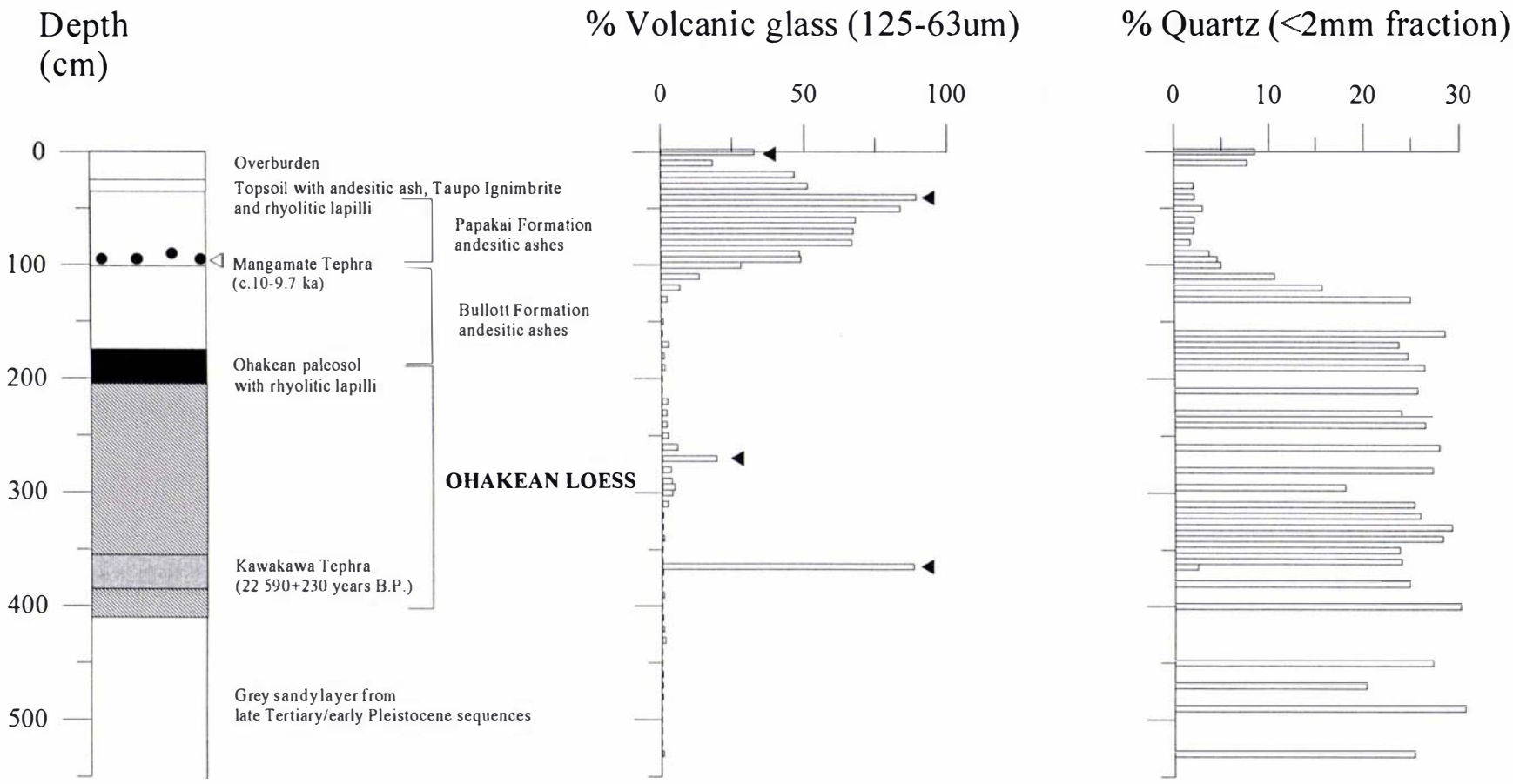

Figure 6.2: Volcanic glass and quartz contents at the Manaroa reference section

- Low levels of volcanic glass (< 5%) are present within both the Ohakean paleosol and loess, except at those depths which correspond to zones of rhyolitic lapilli (e.g. 270cm and 365cm) identified within the field (see Chapter Five, section 5.4.3.3).

% Quartz determinations

- Quartz values (Fig. 6.2) are at a minima within Taupo Ignimbrite, the macroscopic rhyolitic (e.g. Waimihia and Kawakawa Tephras) and the andesitic (e.g. Papakai Formation and Mangamate Tephra) tephra layers
- Quartz values are generally lower (<25%) within the Papakai Formation than those within the andesitic Bullott Formation and the quartzo-feldspathic Ohakean loess.
- Quartz minima coincide with volcanic glass maxima.

Stratigraphic sequence at Apley Road reference sections (V21/316 877)

% Volcanic glass trends

- At the Apley Road #1 section volcanic glass maxima (Fig. 6.3) were identified within the topsoil (Taupo and Waimihia lapilli), and Kawakawa Tephra layers. Volcanic glass values are generally low (<5%) within the Ohakean loess.
- At the Apley Road #2 section volcanic glass maxima (Fig. 6.4) were identified:
  1. at the base (0cm) of the Kawakawa Tephra
  2. near the base (110cm) of the Ohakean loess
  3. within the Ratan paleosol (160cm), and
  4. within the Porewan paleosol (320cm).
- At the Apley Road #3 section volcanic glass maxima (Fig. 6.5) were recognised within the Porewan loess (10cm) and within the highly weathered upper coversand unit (230cm).
- No discernible volcanic glass peaks (all were less than 1%) were obtained from the Apley Road No 4 section.

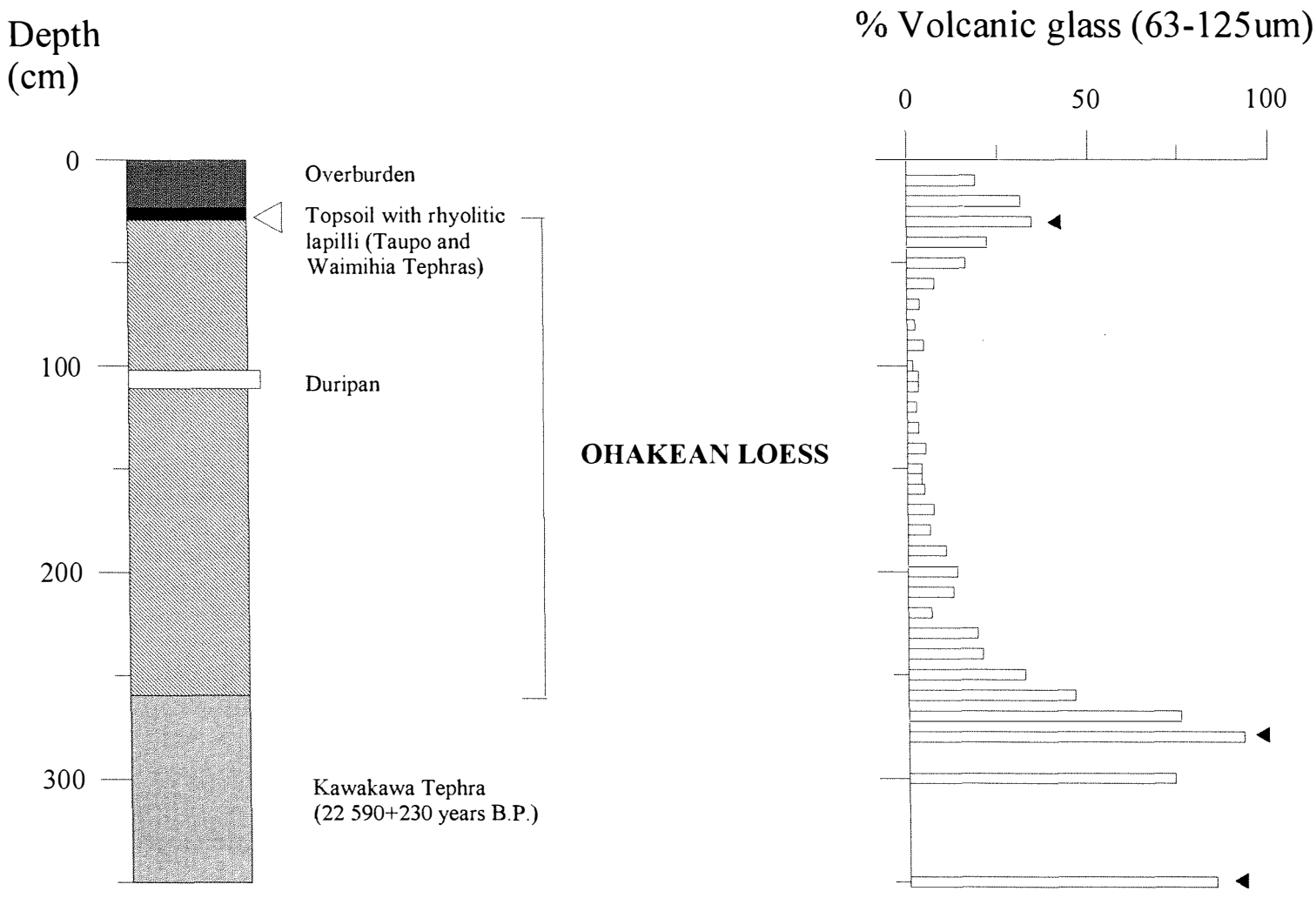

Figure 6.3: Volcanic glass concentrations within the Apley Road #1 section

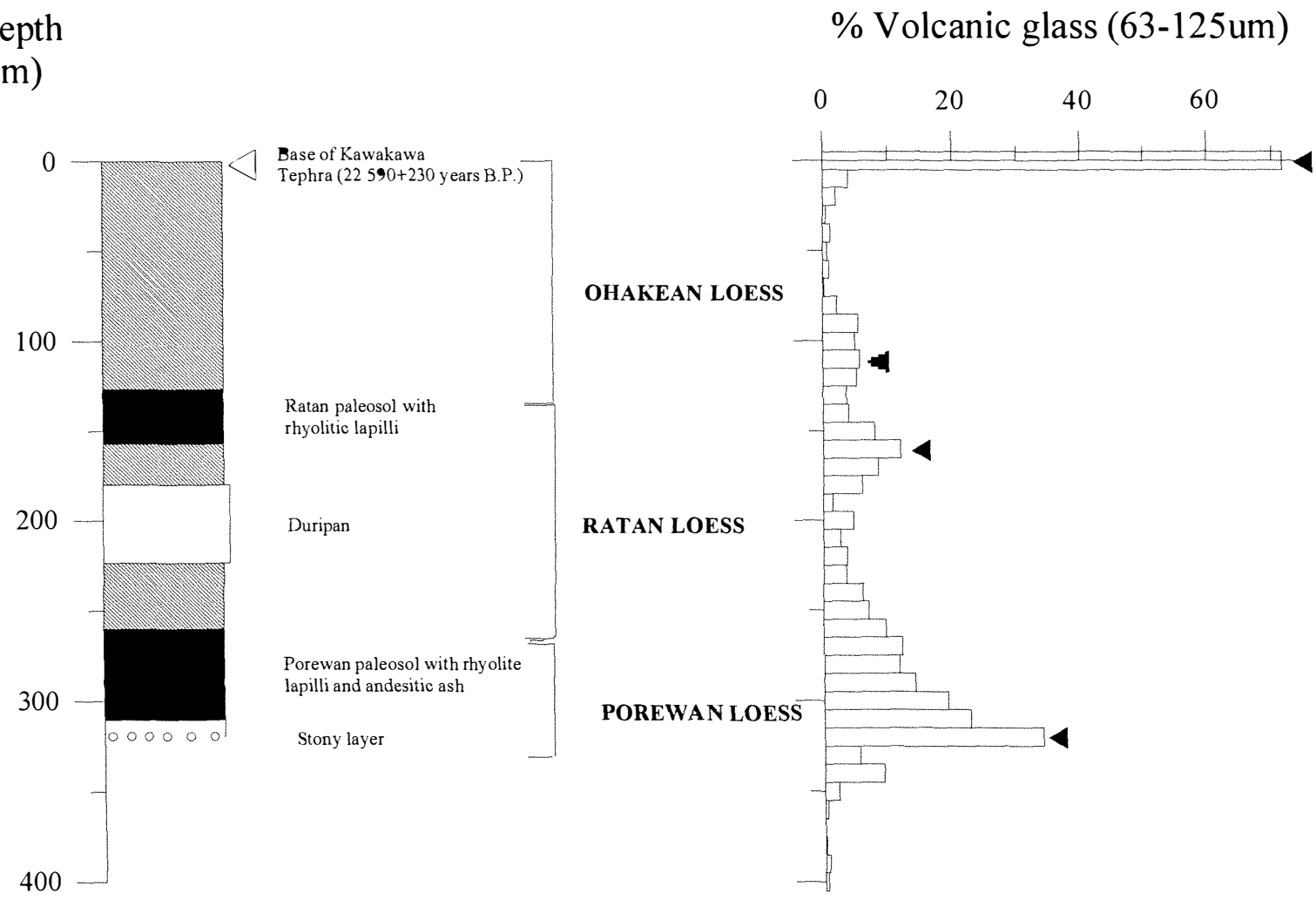

Figure 6.4: Volcanic glass concentrations within the Apley Road # 2 section

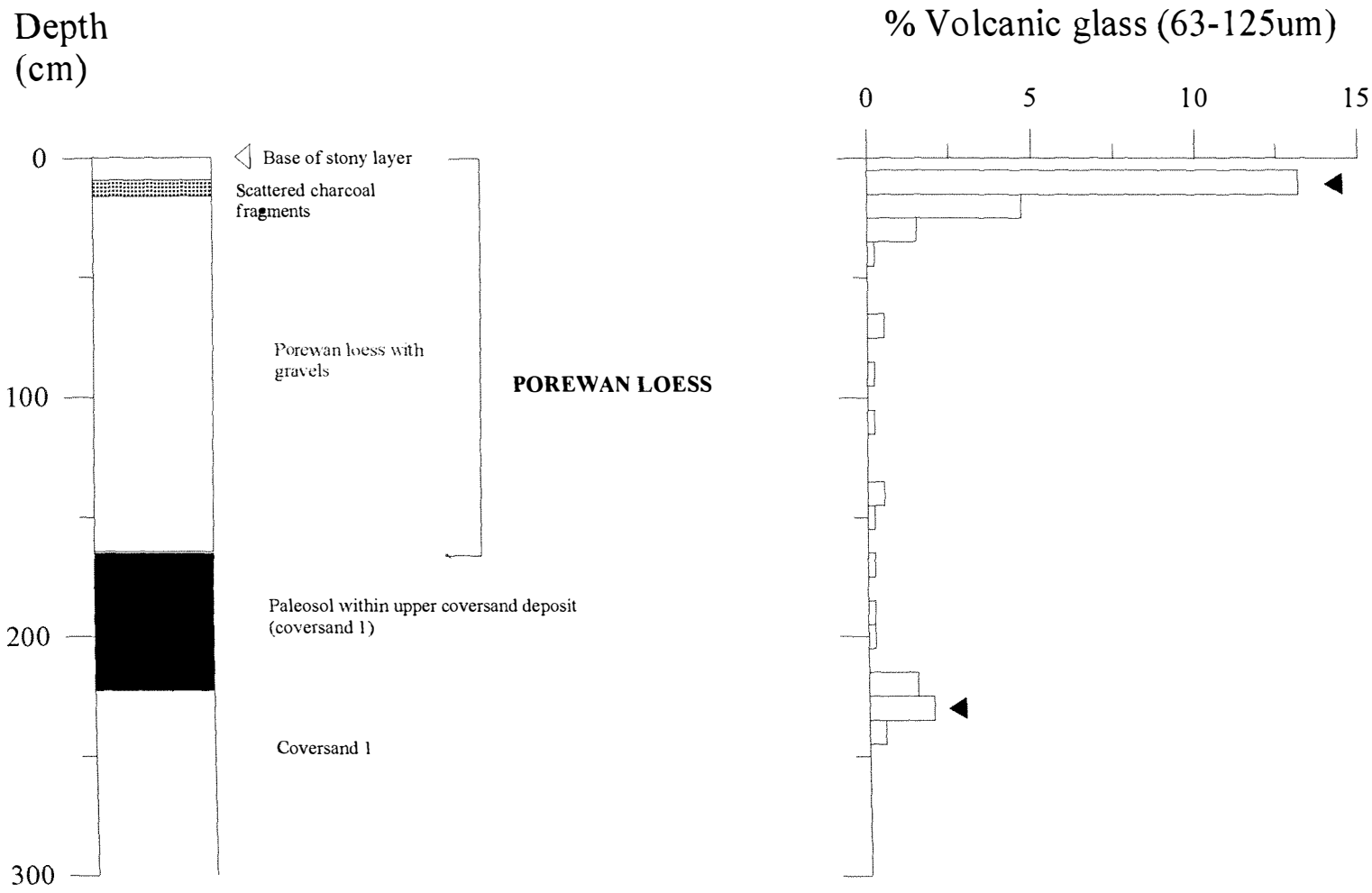

Figure 6.5: Volcanic glass concentrations within the Apley Road #3 section

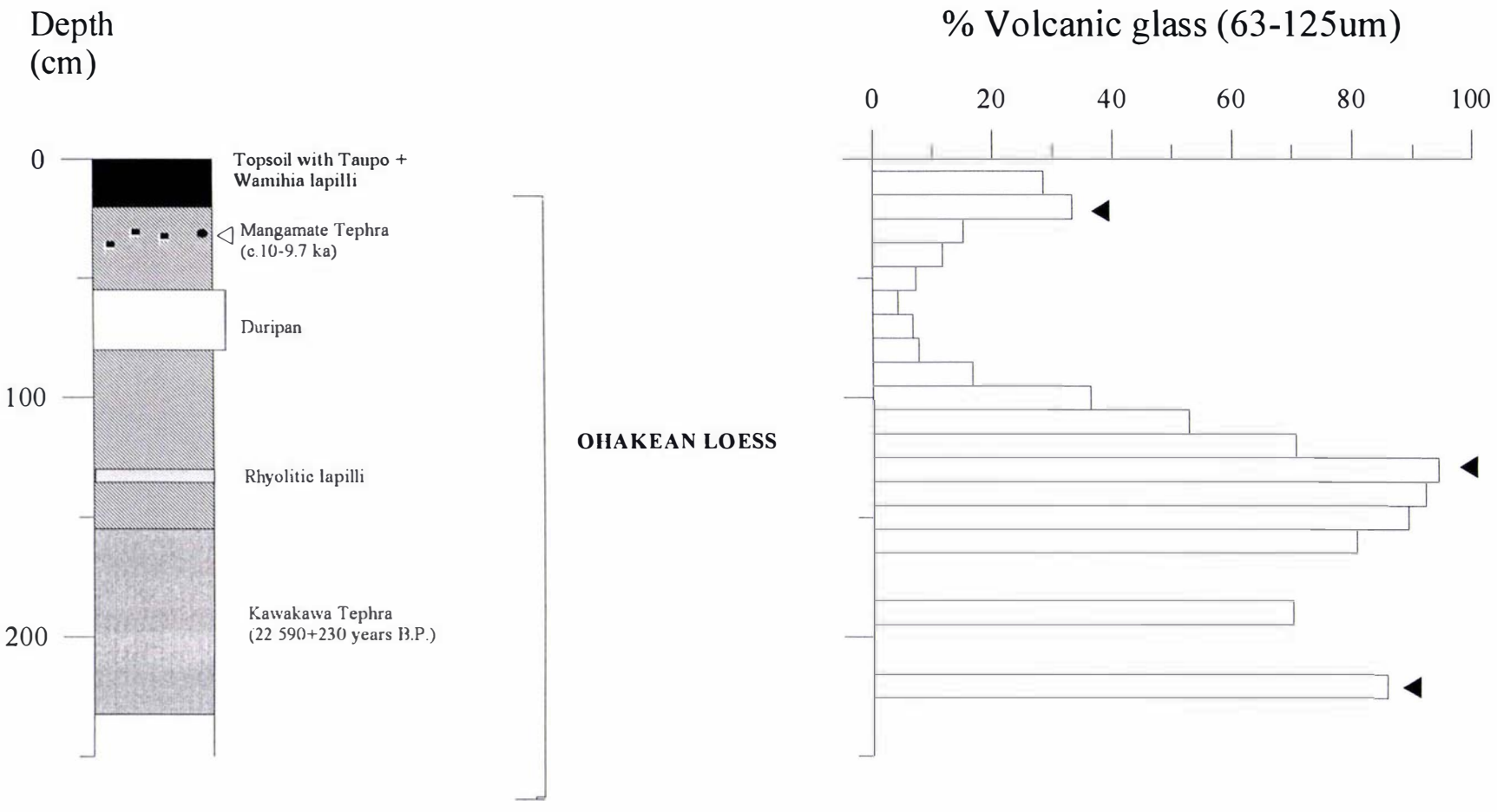

Figure 6.6: Volcanic glass concentrations within the Poraiti #1 section

Stratigraphic sequence at Poraiti reference sections (V21/398 837)

% Volcanic glass trends

- Volcanic glass maxima for the Poraiti #1 section (Fig. 6.6) are encountered within:
  1. the topsoil (Taupo and Waimihia lapilli)
  2. Ohakean loess (130cm), and
  3. within Kawakawa Tephra.
- Volcanic glass maxima within the Poraiti #2 section (Fig. 6.7) are present:
  1. at the base of the Kawakawa Tephra (0cm)
  2. near the base of the Ohakean loess (100cm)
  3 within the Ratan loess (130cm)
  4. within the Porewan loess (220cm)
  5. within Loess 4 (280cm, 330cm, 370cm), and
  6. within Loess 5 (420cm, 450cm)

6.3.2 Ferromagnesian mineral assemblages

Table 6.2 summarises the ferromagnesian minerals identified at selected depth increments within the Pakaututu Road reference section. All samples are dominated by orthopyroxene with varying quantities of clinopyroxene, hornblende, biotite, olivine and cummingtonite. Samples from within the andesitic Papakai and Bullott Formations have slightly higher clinopyroxene values than those within andesite-poor samples, reflecting their derivation from andesitic ash.

At 110cm, grains of olivine were identified within the grey balls of andesitic tephra observed in the field. The significance of this will be discussed in section 6.4.

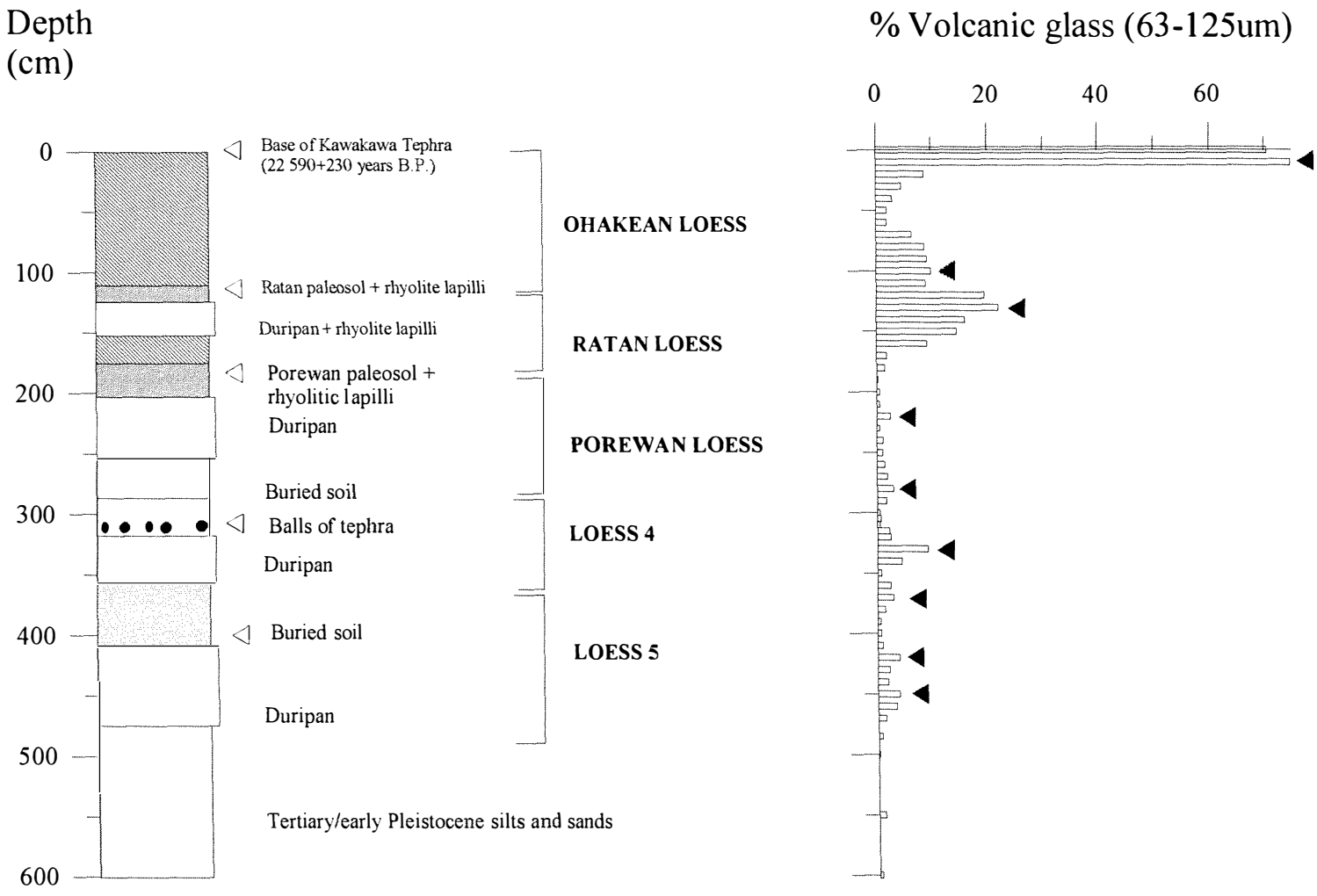

Figure 6.7: Volcanic glass concentrations within the Poraiti #2 section

Table 6.2: Ferromagnesian minerals identified at the Pakaututu Road section

Depth (cm)	% Orthopyroxene	% Clinopyroxene	% Hornblende	% Biotite	% Olivine	% Cummingtonite	Grains counted	Field studies[1]
0	76.2	10.2	6.5	0.2		6.7	400	Taupo Ignimbrite, Tufa Trig and Ngauruhoe Formations
10	72.2	19.0	8.0			0.7	400	Taupo Ignimbrite
30	55.2	29.7	15.0				400	Paleosol on Waimihia lapilli
40	53.5	26.2	19.7				400	Waimihia Tephra
60	49.7	27.0	15.7	0.7		6.2	400	Papakai Formation
70	53.0	29.7	11.7			5.5	400	Papakai Formation
110	43.0	35.4	12.2		8.2	1.3	400	Mangamate Tephra
170	58.2	18.5	20.3	4.0			400	Ohakean paleosol
290	56.2	18.5	25.2				400	Ohakean tephric loess
320	56.2	21.8	22.0				400	Kawakawa Tephra
390	62.4	9.2	28.2	0.3			400	Ratan paleosol
570	60.0	18.4	13.2	0.2		8.2	400	Rotoehu Ash

[1] stratigraphic units identified in the field (see Chapter Five)

6.3.3 Electron microprobe analysis of volcanic glass at reference sections

Electron microprobe analysis totals ranged from *c.*98% to below 90%. Low totals are common in volcanic glass and result from post-depositional hydration (Smith and Westgate, 1969; Sarna-Wojcicki *et al.*, 1987; Froggatt, 1992). In this study totals of down to 89% were accepted for grains in some weathered horizons if their normalised values were similar to those with totals of >92%, the commonly accepted threshold or rejection point.

Original and normalised EMP analysis are given in Appendix III. Mean analyses were not calculated for each sample as many of them showed mixed populations (see section 6.4). Each EMP analysis was normalised to 100% (weight-percentages of elemental oxides) on a fluid-free basis for comparison with published tephra data. FeO is total iron (i.e. FeO + Fe_2O_3 calculated as FeO, usually denoted as FeO^*).

Tables with fewer than 10 EMP analyses (see Appendix III) indicate where there was considerable difficulty in obtaining 10 reasonable quality grains in the sample and consequently contain less reliable data. Those tables with more than 10 EMP analyses are suggestive of a mixed population because more analyses were needed.

Glass chemistry results were compared to data from the tephra reference sections close to source to find a match or match/es using bivariate (%CaO-%FeO) plots, ternary (%FeO-%1/3K_2O-%CaO) plots, similarity coefficients and coefficients of variation. Tables 6.3-6.6 summarise these results. The age range of tephras identified is given using their currently accepted radiocarbon dates (refer to Table 3.3). Finally, an interpretation is made as to the estimated age of a sample at a particular depth.

Depth (cm)	Tephras identified by their glass chemistries	Age Range (in ^{14}C years B.P.) indicated by glass chemistry	Estimated Age (in ^{14}C years B.P.)
160	**Okataina Volcanic Centre is dominant** Okataina eruptives Rotorua and Rerewhakaaitu	13 080±50 to 14 700±110	*c.* 14 000
170	**Okataina Volcanic Centre is dominant** Okataina eruptives: Rerewhakaaitu	14 700±110	*c.* 14 500-15 000
190	Taupo eruptives: Kawakawa (reworked) Okataina eruptives: Rerewhakaaitu, Okareka	14 700±110 to 22 590±230	*c.* 16 000
230	Taupo eruptives: Kawakawa (reworked) Okataina eruptives: Okareka (?)	*c.* 18 000 to 22 590±230	*c.* 18 000
250	Taupo eruptives: Kawakawa (reworked)	22 590±230	*c.* 19 000
270	Taupo eruptives: Kawakawa (reworked)	22 590±230	*c.*20 000
280	Taupo eruptives: Kawakawa (reworked)	22 590±230	*c.*20 500
290	Taupo eruptives: Kawakawa (reworked)	22 590±230	*c.*21 000
320	Kawakawa	22 590±230	22 590±230
390	Omataroa and Mangaone (?)	28 220±630 to 35 300±2200	*c.*28 000-35 000
410	Omataroa and Mangaone(?)	28 220±630 to 35 300±2200	*c.*35 000
450	Reworked Tahuna	*c.*43 000	*c.*40 000
470	Undifferentiated Tahuna and/or Tihoi and/or Ngamotu	43 000 to 46 000	*c.*43 000-45 000
520	Undifferentiated Rotoehu and/or Tihoi	46 000 to 55 000	*c.*45 000-50 000
550	Undifferentiated Rotoehu and/or Otake and/or Tihoi	46 000 to 55 000	*c.*45 000-50 000
570	Rotoehu	*c.* 55 000	*c.*55 000

[1]Refer to Donoghue (1991) and Donoghue *et al.* (1995)

[2] It is likely that this glass is derived from the erosion of gullies upslope.

[3] From Donoghue *et al.* (1991).

Table 6.3: Identification of glass populations at Pakaututu Road reference section. Identification is based on glass chemistry (electron microprobe) and ferromagnesian mineral identification.

Depth (cm)	Tephras identified by their glass chemistries	Age Range (in ^{14}C years B.P.) indicated by glass chemistry	Estimated Age (in ^{14}C years B.P.)
0	**Taupo Volcanic Centre is dominant** Taupo airfall/ignimbrite, Hatepe, andesitic glass (Tufa Trig Formation[1]) and volcanic glass of unknown[2] Okataina Volcanic Centre origin.	Present day to 1850±10	Present day to 1850±10
10	**Taupo Volcanic Centre is dominant** Taupo Ignimbrite and Hatepe Ash	1850±10	1850±10
30	**Taupo Volcanic Centre is dominant** Mixture of Mapara and Waimihia Tephras with (?) Whakaipo and dacitic glass	1850±10 to 3280±20	*c.*2000-2500
40	**Taupo Volcanic Centre is dominant** Waimihia, (?) Whakaipo, Mapara and 1 dacitic glass shard	2160±25 to 3280±20	2600-3300
50	**Taupo Volcanic Centre is dominant** Waimihia, undifferentiated Hinemaiais and 2 grains of Whakatane glass.	3280±20 to 4830±20	*c.*4000
60	**Okataina Volcanic Centre is dominant** Taupo eruptives: undifferentiated Hinemaiaias. Okataina eruptives: Whakatane	4000 to 4830±20	*c.*4500-5000
70	**Okataina Volcanic Centre is dominant** Taupo eruptives: Hinemaiaias and Motutere Okataina eruptives: Whakatane	4830±20 to 5430±60	*c.*5000-5500
80	**Okataina Volcanic Centre is dominant** Taupo eruptives: Motutere Okataina eruptives: Mamaku	5430±60 to 7250±20	*c.*6000-7000
90	**Okataina Volcanic Centre is dominant** Taupo eruptives: Motutere Okataina eruptives: Mamaku	5430±60 to 7250±20	*c.*7500
100	**Okataina Volcanic Centre only** Okataina eruptive: Rotoma	8530±10	*c.*8500
110	**Tongariro Volcanic Centre** Mangamate Tephra (andesitic)	*c.*10 000[3]	*c.*10 000
120	Taupo eruptives: (?) Poronui and Karapiti Okataina eruptives: Waiohau	9810±50 to 11 850±60	*c.*10 000-11 000
130	Taupo eruptives: (?) Poronui and Karapiti Okataina eruptives: Waiohau	9810±50 to 11 850±60	*c.*11 500-12 000
140	**Okataina Volcanic Centre is dominant** Taupo eruptives: Karapiti Okataina eruptives: Waiohau and Rotorua Three dacitic grains	9810±50 to 13 080±50	*c.*12 000-13 000
150	**Okataina Volcanic Centre is dominant** Maroa eruptive: Puketerata Okataina eruptives: Waiohau and Rotorua	*c.*9810±50 to *c.*14 000	*c.*13 000

Depth (cm)	Tephras identified by their glass chemistries	Age Range (in ^{14}C years B.P.) indicated by glass chemistry	Estimated Age (in ^{14}C years B.P.)
170	**Okataina Volcanic Centre is dominant** Okataina eruptives: Predominantly Rotorua with a few shards of Rerewhakaaitu	13 080±50 to 14 700±110	*c.* 13 000-14 000
190	Taupo eruptives: reworked Kawakawa Okataina eruptives: reworked Te Rere	14 700±110 to 22 590±230	*c.* 15 000
240	Undifferentiated Te Rere and/or Kawakawa	21 100±320 to 22 590±230	*c.* 17 000-18 000
270	Undifferentiated Te Rere and/or Kawakawa	21 100±320 to 22 590±230	*c.* 19 000-20 000
295	Predominantly Te Rere with a few shards of Kawakawa (reworked ?)	21 100±320 to 22 590±230	*c.* 21 100
320	Okataina eruptive: Te Rere (2 analyses only)	21 100±320	*c.* 21 500
330	Taupo eruptive: Kawakawa	22 590±230	22 590±230
365	Taupo eruptive: Kawakawa	22 590±230	22 590±230

[1]It is likely that this glass is derived from the erosion of gullies upslope.

[2]Refer to Donoghue (1991) and Donoghue *et al.* (1995)

Table 6.4: Identification of glass populations at Manaroa reference section. Identification is based on glass chemistry (electron microprobe) and ferromagnesian mineral identification

Depth (cm)	Tephras identified by their glass chemistries	Age Range (in ^{14}C years B.P.) indicated by glass chemistry	Estimated Age (in ^{14}C years B.P.)
0	Mixed assemblage of glass which does not fit the stratigraphy	Overburden or erosion products from elsewhere (Recent)	<100
10	Taupo eruptives: Taupo Ignimbrite, Hatepe, Mapara, Whakaipo and Waimihia Okataina eruptives: volcanic glass of unknown[1] origin.	≤ 3280±20	≤ 3280±20
30	Taupo eruptives: Hatepe, Mapara, Whakaipo and Waimihia. Okataina eruptives:Whakatane reworked (?).	2160±25 to 4830±20	2160±25-3280±20
40	**Okataina Volcanic Centre is dominant** Taupo eruptives: undifferentiated Hinemaiaias Okataina eruptives: Whakatane Andesitic glass (Bullott Formation[2])	*c.*4000 to 4830±20	*c.*3500-5000
50	Taupo eruptives: undifferentiated Hinemaiaias Okataina eruptives: Whakatane	*c.*4000 to 4830±20	*c.*4000-5000
60	Taupo eruptives: Motutere Okataina eruptives: undifferentiated Whakatane, Mamaku and/or Rotoma	5430±60 to 8530±10	*c.*5500-7000
70	Taupo eruptives: Opepe and/or Poronui (reworked ?) Okataina eruptives: Mamaku and Rotoma	7250±20 to 9810±50	*c.*7000-8000
80	Taupo eruptives: Opepe, Poronui Okataina eruptives: Mamaku and Rotoma	7250±20 to 9810±50	*c.*8500-9500
90	Taupo eruptives: undifferentiated Opepe, Poronui and/or Karapiti Okataina eruptives: Waiohau (reworked)	9050±40 to 11 850±60	*c.*9000-10 000
100	**Okataina Volcanic Centre is dominant** Taupo eruptives: Karapiti (1 shard) Okataina eruptives: Waiohau 2 dacitic glass shards of Egmont Volcano chemistry	9820±80 to 11 850±60	*c.* 10 000-11 000
110	**Okataina Volcanic Centre is dominant** Taupo eruptives: Karapiti (1 shard) Okataina eruptives: Waiohau	9820±80 to 11 850±60	*c.* 11 000-12 000
120	**Okataina Volcanic Centre is dominant** Okataina eruptives: Waiohau and few reworked Rotorua (?) shards 2 dacitic glass shards of Egmont Volcano chemistry	11 850±60 to 13 080±50	*c.* 12 000

Table 6.5: Identification of glass populations at Apley Road reference sections. Identification is based on glass populations (electron microprobe).

Depth (cm)	Tephras identified by their glass chemistries	Age Range (in ^{14}C years B.P.) indicated by glass chemistry	Estimated Age (in ^{14}C years B.P.)
1AR10	Unknown tephras[1]	?	?
1AR20	Taupo, Mapara, Whakaipo and Waimihia. Tephra of unknown origin was also present. This too may be derived from older tephras upslope.	1850±10 ≤ 3280±20	1850±10 ≤ 3280±20
1AR40	Whakaipo, Mapara, Waimihia and Hinemaiaias (Stent, Unknown Taupo)	2685±20 to 4510±20	*c.*3000-4500
1AR50	Mapara, Waimihia and Hinemaiaias (Stent, Unknown Taupo	2160±25 to 4510±20	*c.*3500-4500
1AR60	Hinemaiaias (Stent, Unknown Taupo), Motutere, Whakatane, and (?)Rotoma and (?)Mamaku	4510±20 to 7250±20	*c.*4500-6000
1AR130	Waiohau, Rotorua and (?) Rerewhakaaitu	11 850±60 to 14 700±110	*c.*12 000-13 000
1A 155	Rotorua and minor Rerewhakaaitu	13 080±50 to 14 700±110	*c.* 13 000-14 000
1AR170	Rotorua and minor Rerewhakaaitu	13 080±50 to 14 700±110	*c.*13 000-14 000
1AR180	Rotorua and Rerewhakaaitu	13 080±50 to 14 700±110	*c.*13 500-14 500
1AR190	Rotorua and Rerewhakaaitu with possible reworked Te Rere and Kawakawa	13 080±50 to 22 590±230	*c.*15 000
1AR200	Rotorua and Rerewhakaaitu with possible reworked Te Rere and Kawakawa	13 080±50 to 22 590±230	*c.*15 000-16 000
1AR240	Te Rere and reworked Kawakawa	21 100±320 to 22 590±230	*c.*21 000
1AR260	Kawakawa	22 590±230	22 590±230
1AR280	Kawakawa	22 590±230	22 590±230
1AR350	Kawakawa	22 590±230	22 590±230
2AR90	Okaia with reworked Omataroa	*c.*23 000 to 28 220±630	*c.*23 000-25 000
2AR110	Okaia with reworked Omataroa	28 220±630	*c.*25 000
2AR130	Reworked Omataroa	28 220±630	*c.*25 000-27 000
2AR160	Omataroa	28 220±630	28 220±630
2AR170	Omataroa and Mangaone	28 220±630 to 35 3500±1270	*c.*30 000
2AR200	Undifferentiated Tahuna and/or Ngamotu and/or Tihoi	*c.*43 000 to 46 000	*c.*43 000
2AR240	Tihoi and reworked Rotoehu	*c.*46 000 to 60 000	*c.*46 000
2AR260	Reworked Rotoehu	*c.*60 000	*c.*50 000
2AR280	Rotoehu	*c.*60 000	*c.*60 000
2AR300	Rotoehu	*c.*60 000	*c.*60 000
2AR320	Reworked Tephra A[2]	*c.*100 000	*c.*80 000 to 100 000
2AR340	Tephra A[2]	*c.*100 000	*c.*100 000
3AR20	Tephra A[2]	*c.*100 000	*c.*100 000

Unknown tephras[1]. These were later shown to be derived from upslope and from road-making activities

Tephra A[2]may relate to the Copenhagen Tephra of Manning (1996)

Table 6.6: Identification of glass populations at Poraiti reference sections. Identification is based on glass populations (electron microprobe).

Depth (cm)	Tephras identified by their glass chemistries	Age Range (in ^{14}C years B.P.) indicated by glass chemistry	Estimated Age (in ^{14}C years B.P.)
1Por10	Taupo eruptives: Whakaipo (?), Waimihia 2 dacitic glass shards (Egmont Volcano source?) Glass from unknown[1] source/s	2685±20 to 3280±20	*c.*3000
1Por 30	1 dacitic glass shard Undifferentiated glass shards from Waimihia to Poronui	3280±20 to 9810±50	*c.*5000-7000
1Por 40	Taupo eruptives: Poronui (?) Okataina eruptives: Rotoma(?), Mamaku (?)	7250± 20 to 9810±50 to	*c.*9000
1Por 70	Okataina eruptives: Waiohau (?), Rotorua(?) and Puketerata	11 850±60 to *c.* 14 000	*c.*12 000
1Por 100	Okataina eruptives: Rotorua, Rerewhakaaitu(?), Te Rere(?) Taupo eruptive: reworked Kawakawa	13 080±50 to 22 590±230	*c.*14 000
1Por 110	Okataina eruptives: Rotorua, Rerewhakaaitu(?), Te Rere (?) Taupo eruptive: reworked Kawakawa	13 080±50 to 22 590±230	*c.*14 000-16 000
120	Okataina eruptives: Rotorua, Rerewhakaaitu (?), Te Rere (?) Taupo eruptive: reworked Kawakawa	13 080±50 to 22 590±230	*c.*15 000-17 000
1Por 221	Kawakawa	22 590±230	22 590±230
2Por0	Kawakawa	22 590±230	22 590±230
2Por 40	Okaia, Poihipi, and Omataroa (reworked)	*c.*23 000 to 28 220±630	*c.*24 000
2Por 80	Okaia and reworked Omataroa	*c.*23 500 to 28 220±630	*c.*26 000
2Por 100	Omataroa	28 220±630	*c.*27 000-28 000
2Por 120	Omataroa 1 shard of dacitic glass	28 220±630	*c.*28 000-28 500
2Por 130	Reworked Tahuna, Ngamotu and Tihoi (undifferentiated)	*c.*43 000 to 46 000	*c.*35 000-40 000
2Por 150	Tahuna, Ngamotu and Tihoi (undifferentiated)	*c.*43 000 to 46 000	*c.* 40 000-45 000
2Por 160	Rotoehu 1 shard of dacitic glass	*c.*50 000-60 000	*c.*50 000-60 000
2Por 220	Mixture of Tephra A[1] and Tephra B[2]	*c.*105 000 to 115 000*	*c.*100 000
2Por 280	Tephra B[2]	*c.* 115 000	*c.* 110 000
2Por 320	Tephra C[3] and Tephra D[4] (reworked)		*c.*115 000
2Por 340	Tephra C[3] and Tephra D[4] (reworked)		*c.*115 000
2Por 370	Tephra C[3] and Tephra D[4] (reworked)		*c.*130 000
2Por 420	Tephra C[3] and Tephra D[4] (reworked)		*c.*140 000
2Por 450	Tephra D[4]	*c.*160 000	*c.*160 000

Tephra A[1] may relate to Torere Tephra of Manning (1996)

Tephra B[2] may relate to Copenhagen Tephra of Manning (1996)

Tephra C[3] unknown rhyolitic tephra

Tephra D[4] may relate to Reid's Reserve Tephra of Manning (1996)

*From Manning (1996a)

Table 6.7: Variation Matrix for Mohaka River (Tarawera Farm) ignimbrite (refer to section 5.5.3 for site details)

Numbers above unit diagonal are SIMILARITY COEFFICIENTS, below are COEFFICIENTS OF VARIATION.

	Taupo	Hatepe	Kawakawa	Matahiwi	Pipiriki	MOr1	MOr2	MOr3	MOr4	MOr5	MOr6	MOr7	MOr8	MOr9	MOr10
Taupo[1]	--	0.94	0.77	0.76	0.76	0.85	0.84	0.76	0.74	0.75	0.75	0.81	0.79	0.82	0.77
Hatepe[1]	5.87	--	0.76	0.77	0.75	0.85	0.86	0.77	0.76	0.76	0.78	0.81	0.81	0.85	0.78
Kawakawa[2]	18.49	15.39	--	0.98	0.97	0.86	0.88	0.94	0.90	0.92	0.94	0.88	0.90	0.89	0.91
Matahiwi[3]	17.10	15.13	2.89	--	0.97	0.86	0.89	0.94	0.92	0.92	0.94	0.90	0.90	0.89	0.93
Pipiriki[3]	18.85	16.33	2.58	3.09	--	0.86	0.87	0.93	0.91	0.93	0.93	0.90	0.89	0.87	0.93
MOr1	9.94	8.12	14.42	13.74	16.14	--	0.90	0.87	0.84	0.83	0.85	0.89	0.90	0.89	0.89
MOr2	12.45	11.13	14.74	13.68	15.42	11.93	--	0.91	0.86	0.86	0.88	0.93	0.89	0.93	0.91
MOr3	16.65	16.02	4.47	5.63	6.01	13.80	16.70	--	0.89	0.92	0.97	0.89	0.94	0.90	0.93
MOr4	20.86	20.46	12.89	13.22	11.19	20.33	18.97	14.60	--	0.90	0.89	0.87	0.86	0.87	0.90
MOr5	21.14	19.60	7.49	9.51	8.00	17.89	18.92	7.26	13.75	--	0.91	0.87	0.90	0.86	0.91
MOr6	17.48	17.56	5.12	5.47	4.57	14.19	15.95	2.81	12.92	6.38	--	0.89	0.92	0.90	0.93
MOr7	15.92	14.76	12.95	12.56	13.73	16.43	9.26	14.95	12.74	16.98	13.69	--	0.86	0.90	0.93
MOr8	16.15	15.63	11.73	12.64	13.74	12.45	19.06	10.32	19.89	13.08	11.47	19.91	--	0.88	0.88
MOr9	13.73	12.98	9.72	7.71	9.92	10.51	6.97	11.50	16.23	14.69	12.11	7.85	14.19	--	0.90
MOr10	15.67	14.92	5.99	5.10	7.46	14.58	11.89	9.14	11.35	13.33	8.48	7.48	15.50	7.03	--

Taupo[1]=Taupo Ignimbrite+lapilli (Stokes *et al.*, 1992)

Hatepe[1]=ash+lapilli (Stokes *et al.*, 1992)

Kawakawa[2] (Pillans and Wright, 1992)

Matahiwi[3]=Pumiceous alluvium from Oruanui Ignimbrite (Pillans *et al.*, 1993)

Pipiriki[3]=Pumiceous alluvium from Oruanui Ignimbrite (Pillans *et al.*, 1993)

MOr=Mohaka River (?) Oruanui Ignimbrite

6.3.4 Electron microprobe analysis of volcanic glass at other sections

In Chapter Five, two ignimbrites, and a tephra of unknown age at the base of Napier Hill were sampled. Glass samples were electron microprobed to elucidate their identities and hence age. The results are presented in Appendix III. The chemistry of individual glass shards was compared to those of likely correlatives at the reference sections using the statistical and plotting techniques described in section 6.2.4.2.

The proximally reworked ignimbrite sample taken from within an alluvial fan sequence bordering the Mohaka River (Tarawera Farm, refer to section 5.5.4 for site details) showed a good correlation ($SC \geq 0.92$ and $CV \leq 12$) with Oruanui Ignimbrite and Kawakawa Tephra samples (see Table 6.7).

The ignimbrite sample taken from the Mangaonuku Stream section (refer to section 5.5.4 for details) showed good correlations ($SC \geq 0.92$ and $CV \leq 12$) with the Rabbit Gully and Potaka Ignimbrites (see Table 6.8).

A tephra sample obtained from near the base of a layered loess sequence at the City Hire section showed good correlations ($SC \geq 0.92$ and $CV \leq 12$) with a number of tephras and ignimbrites (see Table 6.9).

6.4 DISCUSSION

6.4.1 Volcanic glass variations

In Chapter Five a low resolution time-stratigraphic framework was outlined for correlating surficial deposits within western Hawke's Bay. A major limitation was the sole use of easily identified macroscopic tephra layers (e.g. Taupo Ignimbrite, Taupo Tephra, Hatepe Tephra, Waimihia Tephra, Papakai Formation, Bullott Formation and Kawakawa Tephra) as chronohorizons. These macroscopic tephras are often either widely spaced in time or not present within critical time periods (i.e. within paleosols).

Table 6.8: Variation Matrix for ignimbrite at Mangaonuku Stream section (refer to section 5.5.4 for site details)

Numbers above unit diagonal are SIMILARITY COEFFICIENTS, below are COEFFICIENTS OF VARIATION.

	Rabbit	Potaka	Rewa	Pot1	Pot2	Pot3	Pot4	Pot5	Pot6	Pot7	Pot8	Pot9	Pot10	Pot11
Rabbit[1]	--	0.91	0.93	0.88	0.86	0.88	0.94	0.88	0.93	0.93	0.94	0.94	0.90	0.72
Potaka[1]	8.46	--	0.92	0.93	0.92	0.89	0.91	0.87	0.95	0.86	0.88	0.92	0.94	0.75
Rewa[1]	8.82	5.57	--	0.92	0.88	0.87	0.89	0.90	0.89	0.91	0.92	0.93	0.93	0.74
Pot1	8.23	4.14	7.35	--	0.89	0.86	0.89	0.89	0.91	0.85	0.86	0.91	0.94	0.73
Pot2	16.85	12.24	10.83	9.93	--	0.84	0.86	0.88	0.90	0.82	0.84	0.86	0.92	0.79
Pot3	11.81	15.50	11.84	15.17	18.91	--	0.87	0.86	0.86	0.87	0.84	0.87	0.87	0.69
Pot4	5.41	10.32	10.76	10.36	18.98	11.92	--	0.90	0.94	0.90	0.92	0.90	0.92	0.74
Pot5	12.63	10.12	9.01	9.98	12.49	11.76	14.58	--	0.86	0.89	0.87	0.90	0.93	0.79
Pot6	6.21	8.69	9.33	10.05	17.52	16.50	8.70	15.54	--	0.88	0.91	0.91	0.91	0.73
Pot7	6.12	10.05	8.14	10.93	16.58	9.29	8.96	14.11	10.73	--	0.93	0.94	0.86	0.72
Pot8	5.60	10.44	12.05	12.69	18.19	12.48	8.00	15.99	7.50	6.80	--	0.93	0.87	0.73
Pot9	4.66	6.30	5.56	8.46	14.06	12.78	6.78	10.86	7.91	8.79	7.66	--	0.92	0.74
Pot10	10.66	6.65	6.44	4.21	10.66	12.83	13.03	6.31	13.18	11.40	13.81	9.11	--	0.77
Pot11	24.97	23.85	23.36	22.92	21.11	23.61	27.05	24.38	25.47	26.34	26.81	24.66	24.24	--

Rabbit[1] (Shane *et al.*, 1996a;b)

Potaka[1] (Shane et al., 1996a;b)

Rewa[1] (Shane et al., 1996a;b)

Pot =Potaka Ignimbrite sample

	Rangitawa	Mt. Curl	Kid.A	Kid.B	Kid.C	Kid.D	Kid.E	Kid.F	Rabbit	Potaka	Rewa	CH9	CH10	CH11	CH12
Rangitawa[1]	--	0.97	0.94	0.83	0.95	0.93	0.87	0.87	0.92	0.95	0.91	0.94	0.93	0.87	0.89
Mt. Curl[1]	2.71	--	0.92	0.82	0.95	0.92	0.85	0.86	0.91	0.94	0.90	0.92	0.92	0.86	0.89
Kid.A[2]	5.21	4.87	--	0.83	0.94	0.93	0.88	0.91	0.92	0.98	0.94	0.93	0.91	0.86	0.89
Kid.B[2]	9.17	9.87	10.02	--	0.80	0.89	0.93	0.88	0.90	0.82	0.86	0.86	0.83	0.82	0.81
Kid.C[2]	4.88	3.92	6.17	11.30	--	0.90	0.84	0.88	0.89	0.95	0.90	0.92	0.91	0.85	0.88
Kid.D[2]	6.95	6.55	8.35	10.01	7.37	--	0.92	0.88	0.96	0.92	0.93	0.91	0.89	0.88	0.87
Kid.E[2]	9.74	9.40	13.24	4.58	12.42	9.94	--	0.89	0.93	0.86	0.89	0.91	0.86	0.88	0.85
Kid.F[2]	8.56	9.23	7.22	11.84	11.05	11.84	14.17	--	0.88	0.90	0.93	0.87	0.87	0.80	0.84
Rabbit[3]	7.25	6.22	8.63	8.72	8.37	4.68	8.75	10.24	--	0.91	0.93	0.91	0.89	0.88	0.88
Potaka[3]	4.80	4.37	2.57	10.04	5.21	8.77	12.67	7.09	8.46	--	0.92	0.93	0.92	0.86	0.90
Rewa[3]	7.61	7.51	4.49	9.35	7.78	9.32	11.47	4.12	8.82	5.57	--	0.91	0.90	0.83	0.86
CH9	8.46	7.85	12.13	8.63	10.92	8.14	8.06	9.40	9.82	11.84	8.09	--	0.95	0.90	0.86
CH10	6.45	5.85	9.24	11.17	7.86	9.21	9.22	8.95	10.39	9.64	7.96	3.53	--	0.87	0.85
CH11	16.99	16.31	20.02	9.90	18.60	13.97	10.24	18.45	14.21	20.04	17.42	15.44	17.09	--	0.87
CH12	11.09	11.94	10.56	11.85	13.25	9.77	14.24	13.51	10.11	11.23	12.96	16.13	15.69	18.56	--

	Rangitawa	Mt. Curl	Kid.A	Kid.B	Kid.C	Kid.D	Kid.E	Kid.F	Rabbit	Potaka	Rewa	CH13	CH14	CH15
Rangitawa[1]	--	0.97	0.94	0.83	0.95	0.93	0.87	0.87	0.92	0.95	0.91	0.90	0.88	0.88
Mt. Curl[1]	2.71	--	0.92	0.82	0.95	0.92	0.85	0.86	0.91	0.94	0.90	0.89	0.86	0.87
Kid.A[2]	5.21	4.87	--	0.83	0.94	0.93	0.88	0.91	0.92	0.98	0.94	0.87	0.88	0.87
Kid.B[2]	9.17	9.87	10.02	--	0.80	0.89	0.93	0.88	0.90	0.82	0.86	0.83	0.85	0.78
Kid.C[2]	4.88	3.92	6.17	11.30	--	0.90	0.84	0.88	0.89	0.95	0.90	0.87	0.85	0.86
Kid.D[2]	6.95	6.55	8.35	10.01	7.37	--	0.92	0.88	0.96	0.92	0.93	0.90	0.90	0.85
Kid.E[2]	9.74	9.40	13.24	4.58	12.42	9.94	--	0.89	0.93	0.86	0.89	0.87	0.90	0.83
Kid.F[2]	8.56	9.23	7.22	11.84	11.05	11.84	14.17	--	0.88	0.90	0.93	0.83	0.83	0.80
Rabbit[3]	7.25	6.22	8.63	8.72	8.37	4.68	8.75	10.24	--	0.91	0.93	0.90	0.89	0.85
Potaka[3]	4.80	4.37	2.57	10.04	5.21	8.77	12.67	7.09	8.46	--	0.92	0.88	0.86	0.88
Rewa[3]	7.61	7.51	4.49	9.35	7.78	9.32	11.47	4.12	8.82	5.57	--	0.87	0.85	0.83
CH13	14.23	14.18	15.94	10.39	16.41	11.68	10.73	16.68	11.79	16.27	16.88	--	0.91	0.83
CH14	14.20	13.73	18.06	8.66	16.02	11.28	7.76	17.58	11.93	17.33	15.75	10.41	--	0.86
CH15	25.00	24.53	25.41	19.40	24.69	23.24	19.78	22.60	23.19	25.91	22.84	25.34	21.02	--

Rangitawa[1] (Alloway *et al.*, 1993)

Mt. Curl[1](Alloway et al., 1993)

Kid.A[2] (Black, 1992)

Kid.B[2](Black, 1992)

Kid.C[2](Black, 1992)

Kid.D[2] (Black, 1992)

Kid.E[2] (Black, 1992)

Kid.F[2](Black, 1992)

Rabbit[3](Shane *et al.*, 1996a;b)

Potaka[3](Shane et al., 1996a;b)

Rewa[3](Shane et al., 1996a;b)

CH=City Hire section

Table 6.9: Variation Matrix for tephra within City Hire section (refer to Plate 6.1).

Numbers above unit diagonal are SIMILARITY COEFFICIENTS, below are COEFFICIENTS OF VARIATION.

	Rangitawa	Mt. Curl	Kid.A	Kid.B	Kid.C	Kid.D	Kid.E	Kid.F	Rabbit	Potaka	Rewa	CH1	CH2	CH3	CH4
Rangitawa[1]	--	0.97	0.94	0.83	0.95	0.93	0.87	0.87	0.92	0.95	0.91	0.88	0.92	0.93	0.93
Mt. Curl[1]	2.71	--	0.92	0.82	0.95	0.92	0.85	0.86	0.91	0.94	0.90	0.86	0.91	0.91	0.93
Kid.A[2]	5.21	4.87	--	0.83	0.94	0.93	0.88	0.91	0.92	0.98	0.94	0.86	0.89	0.89	0.90
Kid.B[2]	9.17	9.87	10.02	--	0.80	0.89	0.93	0.88	0.90	0.82	0.86	0.87	0.82	0.86	0.88
Kid.C[2]	4.88	3.92	6.17	11.30	--	0.90	0.84	0.88	0.89	0.95	0.90	0.85	0.90	0.89	0.90
Kid.D[2]	6.95	6.55	8.35	10.01	7.37	--	0.92	0.88	0.96	0.92	0.93	0.88	0.92	0.91	0.90
Kid.E[2]	9.74	9.40	13.24	4.58	12.42	9.94	--	0.89	0.93	0.86	0.89	0.92	0.85	0.90	0.91
Kid.F[2]	8.56	9.23	7.22	11.84	11.05	11.84	14.17	--	0.88	0.90	0.93	0.85	0.85	0.84	0.88
Rabbit[3]	7.25	6.22	8.63	8.72	8.37	4.68	8.75	10.24	--	0.91	0.93	0.89	0.90	0.92	0.91
Potaka[3]	4.80	4.37	2.57	10.04	5.21	8.77	12.67	7.09	8.46	--	0.92	0.87	0.88	0.89	0.91
Rewa[3]	7.61	7.51	4.49	9.35	7.78	9.32	11.47	4.12	8.82	5.57	--	0.85	0.88	0.88	0.90
CH1	12.61	12.31	14.90	8.44	15.62	9.01	8.19	16.40	8.59	15.66	14.43	--	0.89	0.93	0.92
CH2	12.20	12.01	12.80	10.97	13.02	8.04	11.67	16.83	9.24	12.37	14.90	9.71	--	0.92	0.86
CH3	9.21	8.37	11.57	8.26	12.00	5.72	5.80	12.33	7.07	11.82	11.56	5.33	7.86	--	0.94
CH4	6.42	7.76	8.91	8.30	9.87	7.04	6.14	8.81	6.03	8.86	7.69	11.64	11.65	7.87	--

	Rangitawa	Mt. Curl	Kid.A	Kid.B	Kid.C	Kid.D	Kid.E	Kid.F	Rabbit	Potaka	Rewa	CH5	CH6	CH7	CH8
Rangitawa[1]	--	0.97	0.94	0.83	0.95	0.93	0.87	0.87	0.92	0.95	0.91	0.95	0.90	0.88	0.87
Mt. Curl[1]	2.71	--	0.92	0.82	0.95	0.92	0.85	0.86	0.91	0.94	0.90	0.94	0.89	0.87	0.87
Kid.A[2]	5.21	4.87	--	0.83	0.94	0.93	0.88	0.91	0.92	0.98	0.94	0.96	0.87	0.85	0.90
Kid.B[2]	9.17	9.87	10.02	--	0.80	0.89	0.93	0.88	0.90	0.82	0.86	0.85	0.87	0.87	0.83
Kid.C[2]	4.88	3.92	6.17	11.30	--	0.90	0.84	0.88	0.89	0.95	0.90	0.94	0.87	0.86	0.87
Kid.D[2]	6.95	6.55	8.35	10.01	7.37	--	0.92	0.88	0.96	0.92	0.93	0.94	0.89	0.88	0.85
Kid.E[2]	9.74	9.40	13.24	4.58	12.42	9.94	--	0.89	0.93	0.86	0.89	0.87	0.93	0.91	0.83
Kid.F[2]	8.56	9.23	7.22	11.84	11.05	11.84	14.17	--	0.88	0.90	0.93	0.91	0.83	0.84	0.91
Rabbit[3]	7.25	6.22	8.63	8.72	8.37	4.68	8.75	10.24	--	0.91	0.93	0.92	0.90	0.88	0.87
Potaka[3]	4.80	4.37	2.57	10.04	5.21	8.77	12.67	7.09	8.46	--	0.92	0.96	0.87	0.86	0.90
Rewa[3]	7.61	7.51	4.49	9.35	7.78	9.32	11.47	4.12	8.82	5.57	--	0.95	0.86	0.85	0.89
CH5	5.45	5.79	4.49	9.40	6.40	6.47	9.89	8.09	6.62	5.59	4.03	--	0.87	0.87	0.87
CH6	11.50	11.69	13.73	9.38	13.60	11.00	6.18	13.44	11.01	13.95	12.82	11.44	--	0.92	0.84
CH7	13.15	12.78	15.08	8.84	16.10	9.33	7.47	16.32	8.62	15.59	14.12	14.21	8.21	--	0.81
CH8	10.47	11.16	6.84	16.17	8.76	12.50	16.10	8.70	13.53	6.42	9.15	9.23	17.85	18.36	--

To refine the time resolution fine microscopic tephra accessions within paleosols and between the macroscopic tephra layers were identified.

Volcanic glass variations present within the andesitic Papakai and Bullott Formations and within the Ohakean, Ratan, Porewan, Loess 4 and Loess 5 loess layers are assumed to mark the sequential accessions of tephra to each site.

The highest volcanic glass concentrations coincide with the presence of macroscopic rhyolitic tephras at sites more proximal to source (e.g. Taupo Ignimbrite, Waimihia Tephra and Kawakawa Tephras at the Pakaututu Road and Manaroa reference sites) and the Kawakawa Tephra which is visible at all the reference sections.

Volcanic glass counts and quartz determinations undertaken at the Pakaututu Road and Manaroa reference sections show an expected inverse relationship, volcanic glass maxima corresponding to quartz minima. A good example of this may be seen at 320cm, where a sample was taken from the white base of the Kawakawa Tephra (Fig. 6.1). Quartz maxima thus correspond to relatively undiluted quartzo-feldspathic loess. Conversely, quartz minima correspond to macroscopic and microscopic tephra layers and paleosols.

6.4.2 Quartz variations

In New Zealand, variations in the accumulation rates of aerosolic quartz grains have been used to construct a record of Quaternary climatic change which extends as far back as *c.*500 ka (Stewart and Neall, 1984; Nelson *et al.*, 1985; Alloway *et al.*, 1992a; Hodgson, 1993; Palmer and Pillans, 1996). Periods of increased quartz accumulation are interpreted as stadials or glacial climatic conditions and have been correlated to the marine oxygen isotope stratigraphy (Palmer and Pillans, 1996).

In this study quartz values were generally higher when the Ohakean, Ratan and Porewan loess sheets were emplaced (>10% quartz for the Pakaututu Road and Manaroa

reference sections) relative to the post-glacial period (<10% quartz at the Pakaututu Road and Manaroa reference sections). High quartz values are attributed to considerable landscape instability when loess originated from aggrading alluvial fans and terraces was blown onto the downlands, and also direct erosion from quartzo-feldspathic country rock. Quartz peaks are thus correlated with the cold periods (Ohakean, Ratan and Porewan stadials) during the last glacial.

Quartz values obtained from the paleosols developed on or within the Ohakean, Ratan and Porewan loesses are marginally lower than their surrounding loess sheets (see Figs. 6.1-6.2). One interpretation, supported by palynological studies (Heusser and van de Geer, 1994), is that climatic amelioration resulted in landscape stabilisation during interstadials and the present post-glacial. Consequently, the rate of quartzo-feldspathic loess production slowed and tephras (andesitic and rhyolitic) became more significant components of the air-fall accession.

To summarise, the quartz content measured in this and other studies (Stewart and Neall, 1984; Nelson *et al.*, 1985; Alloway *et al.*, 1992a; Palmer and Pillans, 1996) reflects the degree to which quartzo-feldspathic sediments were exposed to erosion and records landscape destabilisation during glacial and stadial times.

6.4.3 Ferromagnesian mineral assemblages

Samples obtained from macroscopic tephra layers show ferromagnesian mineral assemblages (Table 6.2) which concur with the field identifications. For example:

- an assemblage 1 mineralogy (Froggatt and Lowe, 1990) for Taupo Ignimbrite (10cm)
- an assemblage 1 mineralogy (Froggatt and Lowe, 1990) for Waimihia Tephra (40cm)
- an assemblage 2 mineralogy (Froggatt and Lowe, 1990) for Kawakawa Tephra (320cm), and
- an assemblage 4 (Froggatt and Lowe, 1990) mineralogy for the rhyolite ash resting on colluvial gravels within the Porewan paleosol. The presence of cummingtonite within this layer indicated it to be Rotoehu Ash (570cm). Electron microprobe

analysis of glass shards taken from this layer (see Table 6.3) concur with this identification.

It was not, however, always possible to use the characteristic ferromagnesian mineral assemblages in Table 6.1 to identify individual microscopic tephra layers because they are likely to have been subjected to:

- contamination with continued accessions of andesitic ash
- the effects of sedimentary fractionation and winnowing during transport (hydraulic sorting)
- weathering, and
- post-depositional reworking with older tephras eroded from gullies upslope.

A good example may be seen within the 0cm sample from the Pakaututu Road section (see Table 6.2). The presence of biotite and cummingtonite is at odds with the stratigraphic units identified at this depth (Taupo Ignimbrite, Tufa Trig and Ngauruhoe Formations) and raises the possibility of older tephras having been eroded from gullies upslope and redeposited. Electron microprobe analyses of volcanic glass obtained at this level show glass shards with an Okataina Volcanic Centre origin (Table 6.3). The only volcanic glass of this origin, younger than the Taupo Ignimbrite, is Kaharoa Tephra. Statistical analysis of the glass chemistry shows it not to be Kaharoa Tephra (see Appendix III). It is therefore likely that this glass is derived from either an older reworked tephra or part of a more widely sourced aeolian assemblage.

Grey balls of andesitic ash, present at the base of the Papakai Formation (110cm) at the Pakaututu Road section (refer to section 5.4.2.3 for site details), are easily recognised and may be found as far east as the Poraiti reference section. Ferromagnesian mineral counts on samples from this lithology show the significant presence of olivine (8.2%). Olivine is a distinctive mineral within the Mangamate Formation tephras which erupted from Mount Tongariro *c.*10 000-9700 years B.P. The olivine grains seen in these samples are quite weathered hence it was not possible to equate their shapes to any of the olivine quench shapes described in Donoghue *et al.* (1991).

A sample taken for EMP analysis directly under (120cm) the grey ash balls shows a mixed glass assemblage of (?) Poronui (9810±50 years B.P.), Karapiti (9820±80 years B.P.) and Waiohau (11 850±60 years B.P.) Tephras (see Table 6.3). From this evidence it is interpreted that the grey balls belong to the Mangamate Tephra of Donoghue *et al.* (1991).

6.4.4 Volcanic glass sources

In this discussion it is unnecessary to describe each tephric sample fingerprinted. Rather the approach has been to choose a few tephric samples from selected depth increments which both relate to and help date the major depositional and erosional geomorphic surfaces (refer to section 4.3.5 for this concept) observed within the district's surficial deposits. Geomorphic surfaces recognised in western Hawke's Bay are:

- Taupo Ignimbrite (1850±10 years B.P.)
- Waimihia paleosol (3280±20 to 1850±10 years B.P)
- Waimihia Tephra (3280±20 years B.P.)
- Mangamate Tephra (*c.* 10 000-9700 years B.P.)
- Rerewhakaaitu Tephra (14 700±110 years B.P.) within the Ohakean paleosol (*c.*15 000-14 000 years B.P.)
- Kawakawa Tephra (22 590±230 years B.P.)
- Omataroa Tephra (28 220±630 years B.P.) within the Ratan paleosol (*c.*30 000-26 000 years B.P.)
- Rotoehu Ash (64 ka) in the Porewan paleosol (60 000-70 000 years B.P.)

An age range of *c.*26ka to 30ka was estimated for the Ratan paleosol. This is based on two lines of evidence:

- a radiocarbon date of 26 380±370 years B.P. (NZA 5042) obtained on charcoal from within the Pakaututu Road Ratan paleosol, and

- the identification of Omataroa Tephra, dated at 28 220±630 years B.P. (see Table 3.3), also within this paleosol. Ages for the Ratan paleosol have only been estimates to date.

Within the Poraiti section a number of previously undescribed rhyolitic tephras were identified (numbered A, B, C, D) in Loess 4 (accumulated during marine oxygen isotope stages 5d and 5b) and Loess 5 (accumulated during marine oxygen isotope stage 6) and within a paleosol developed on the upper coversand at the Apley Road number 3 section.

There is no published information on these tephras for comparison purposes. Some tentative correlations with the tephras identified by Manning (1996a) within the Bay of Plenty, based on glass shard similarities, were made. These are:

- Tephra A may relate to the Torere Tephra (*c.*105 ka)
- Tephra B may relate to the Copenhagen Tephra (*c.*110 ka)
- Tephra C, is probably an uncorrelated tephra (*c.*115 ka) , and
- Tephra D may relate to the Reid's Reserve Tephra, emplaced near the end of the penultimate glacial (Dr David Manning, pers. comm. 1994).

The sample taken from the proximally reworked ignimbrite within the alluvial fan sequence bordering the Mohaka River (refer to section 5.5.4 for site details) is correlated with the 22 590±230 years B.P. Oruanui Ignimbrite because its glass chemistry (SC≥0.92, CV≤12) is indistinguishable from that of pumiceous Oruanui alluvium (Matahiwi and Pipiriki samples of Pillans *et al.*, 1993), and Kawakawa Tephra (Pillans and Wright, 1992). This is one of the most easterly occurrences of Oruanui Ignimbrite and the first report of it having reached Hawke's Bay via the Mohaka River.

The ignimbrite sample taken from near the Mangaonuku #1 Bridge is correlated with the *c.*1Ma year B.P. Potaka Ignimbrite (=Kidnappers A Ignimbrite), a widespread ignimbrite deposit in both the Wanganui and East Coast Basins (Shane, 1994). The Rabbit Gully Ignimbrite (=Kidnappers D tephra) (Black, 1992) is excluded, even though it's chemistry is indistinguishable (SC≥0.92, CV≤12) from that of Potaka Ignimbrite

(see Appendix III), because it is not found within the Salisbury gravel lithofacies. The ignimbrite found within the Salisbury gravels has been identified elsewhere in the district as being Potaka Ignimbrite and dated at 1Ma (Erdman and Kelsey, 1992; Shane, 1994; Shane *et al.*, 1996a;b).

The tephra identified near the base of the City Hire loess sequence is correlated to the *c.*350 ka Rangitawa Tephra (=Mount Curl Tephra) on two grounds. Firstly, it is found within Loess 10 which is consistent with other studies (Kohn *et al.*, 1992; 1996; Pillans *et al.*, 1996), and it has SC and CV's of $\geq$0.92 and $\leq$12, respectively. Other tephras (see Table 6.9) compared with that found at the City Hire section were excluded, despite their good glass chemistry matches (SC$\geq$0.92, CV$\leq$12) because as they are now known to be too old (Shane *et al.*, 1996a;b).

6.5: CONCLUSIONS

The quantitative analysis of quartz undertaken at the Pakaututu Road and Manaroa reference sections reflects the degree to which quartzo-feldspathic sediments were exposed to erosion. Quartz values of >10% indicate landscape destabilisation at these sites during the cold periods of the last glacial (i.e. during the Ohakean, Ratan and Porewan stadials). Upon climatic amelioration during the interstadials or post-glacial the landscape was stabilised by vegetation. Loess deposition ceased about 14 ka, as evidenced by the presence of Rerewhakaaitu Tephra within Ohakean paleosols, and a gentle accession of andesitic tephras became dominant (i.e. Papakai and Bullott Formations).

The overall geographic extent of many known tephra layers (see Tables 6.3-6.7) has been significantly expanded into a district, previously not studied in detail, during the course of this study. Furthermore, this is one of the few studies where microscopic tephra time-lines have been used in an aeolian depositional environment.

Volcanic glass counts undertaken during this study proved a powerful tool in the identification of microscopic tephras within:

- the Papakai and Bullott Formations at the Pakaututu Road and Manaroa reference sections, and
- within the Ohakean, Ratan, Porewan, Loess 4 and Loess 5 paleosols at all four reference sites.

The macroscopic grey balls of andesitic tephra identified within the Bullott Formation tephras in the western parts of the district were shown to be olivine bearing. These are here correlated to the Mangamate Tephra, a *c.*10 000-9700 years B.P. eruptive from Tongariro Volcano (Donoghue, 1991; Donoghue *et al.*, 1991; 1995).

The identification and dating of two new occurrences of ignimbrite were made possible by chemically fingerprinting (by EMP) their glass shards. The younger is recognised as proximally reworked Oruanui Ignimbrite which erupted from the Taupo Volcanic Centre 22 590±230 years B.P. This is the most easterly occurrence of Oruanui Ignimbrite and the first record of it entering Hawke's Bay. The older ignimbrite is identified as Potaka Ignimbrite which was erupted from a Mangakino source *c.*1Ma years B.P. and flowed as far east as Cape Kidnappers (Black, 1992; Shane *et al.*, 1996a;b).

At the City Hire section (refer to section 6.4) Rangitawa Tephra (0.35±0.04 Ma, Kohn *et al.*, 1992) was identified within Loess 10. This is the first positive identification of Rangitawa Tephra in Hawke's Bay and one of the few sites where the full succession of 10 loess layers may be seen.

Four new tephra layers are identified within Loess 4 and Loess 5 at the Poraiti reference sections. Some tentative correlations have been made with the pre-Rotoiti tephras identified by Manning (1996a) within the Bay of Plenty.

CHAPTER SEVEN:
CHEMICAL AND ELEMENTAL CHARACTERISTICS OF COVERBEDS AT TYPE SECTIONS

7.1 INTRODUCTION

In Chapters Five and Six the loessial coverbeds at the four reference sites were shown to be a product of Quaternary climatic events. Glacial and stadial periods were times of environmental destabilisation, loess accumulation and reduced chemical weathering whilst warm periods (interglacials and interstadials) were marked by much reduced rates of climatically induced erosion and deposition resulting in a stabilisation of landsurfaces. Soil forming processes were thereby able to proceed at an intensified rate. From this strong interrelationship between climate, weathering and subsequent soil formation, it should be possible to characterise the western Hawke's Bay coverbeds using major oxides, trace elements and selected elemental and chemical dissolution parameters to augment the pedologic, stratigraphic and mineralogical interpretations already made, so refining our understanding of the magnitude and duration of paleoclimatic events in western Hawke's Bay.

Studies, both in New Zealand (Runge *et al.*, 1974; Childs, 1975; Childs and Searle, 1975; Palmer, 1982a; Vucetich and Stevens, 1985a; Qizhong *et al.*, 1992; Palmer and Pillans, 1996) and overseas (Busacca and Singer, 1989; Eden *et al.*, 1994), have used major and trace element distributions to:

- identify the presence of loess/buried soil discontinuities
- measure losses and gains of elements resulting from soil development
- evaluate parent material uniformity within layered soils
- identify soil parent material provenance, and
- act as a proxy to interpret late Quaternary climatic fluctuations.

A study of major oxides and trace elements was undertaken to refine the pedological and stratigraphic interpretations made in earlier chapters that the western Hawke's Bay

coverbeds comprise of multiple loess layers, each terminating in a buried soil (paleosol). A buried soil represents a former groundsurface during a period of relatively low loess accumulation where chemical weathering processes exceeded those of physical weathering. Former groundsurfaces within a loess column can be identified by their characteristic major oxide and trace element distribution patterns with depth. Chemical and physical weathering processes result in the translocation, dissolution, leaching and hydrolysis of more mobile oxides and trace elements and the preferential increase in less mobile oxides and trace elements within the solum of each loess layer. Implicit to this is the assumption that each loess layer originally had a uniform composition hence differences in elemental content between horizons can be ascribed to pedogenesis. The addition of extraneous material such as tephra to the loess makes any interpretations based solely on pedogenic processes problematic.

Studies of major oxides and trace elements were conducted at the Pakaututu Road and Poraiti sections (refer to Chapter Five for reference section details). Both sites have multiple layers of quartzofeldspathic loess, derived from Mesozoic greywacke sandstone/argillite and Neogene marine sequences, as their dominant soil parent material. Intercalated within the loess are andesitic and rhyolitic tephra layers of varying thickness. These are described in Chapters Five and Six. The Pakaututu Road section is more proximal to the Taupo Volcanic Zone (TVZ) than the Poraiti sections hence it has experienced more frequent and often appreciable inputs of andesitic and rhyolitic tephra. Major oxide and trace element distribution patterns are interpreted in view of these volcanic inputs to the loess columns at these sections. The Pakaututu Road section receives a higher mean annual rainfall (*c.*1400mm/annum) than the Poraiti sections (*c.*800mm/annum) hence the leaching regime at the former section has been higher.

A number of attempts have been made to relate stratigraphic variations in dissolution chemistry to the influence of past environments, especially climate change within the late Quaternary (see review in Lowe, 1986). Allophane-rich (Al/Si ratio $\geq$2.0) beds are considered to have weathered under warm, moderate to high rainfall conditions during interglacials and interstadials (hence promoting strong Si leaching) whereas halloysite-

rich (Al/Si ratios=1.0) beds weathered under cold, low rainfall conditions (hence promoting weak Si leaching) during glacials and stadials (Stevens and Vucetich, 1985b).

In Chapter Five allophane was detected within tephra-rich layers at the Pakaututu Road and Manaroa reference sections (see Chapter Five and Appendix I) using the NaF test of Fieldes and Perrott (1966). Allophane is a short-range-order weathering product of tephric material and, under favourable circumstances, of quartzofeldspathic parent material (see reviews in Lowe, 1986; Parfitt, 1990). The NaF test is not specific for allophane. Fluoride also reacts with Al in Al-humus complexes (Parfitt and Saigusa, 1985), hence verification as to its presence along with that of associated ferrihydrite (for reviews of ferrihydrite formation see Childs, 1985; 1992a) was required. Differential x-ray diffraction (DXRD) has shown acid-oxalate to be the most effective reagent for dissolving allophane and ferrihydrite-like constituents in soils (Campbell and Schwertmann, 1985).

Chemical dissolution analyses were undertaken on the tephra and loess layers at the Pakaututu Road and Manaroa reference sections (see Chapter Five and Appendix I for site details and soil profile descriptions) to:

- characterise and quantify the soil minerals within the clay-size fraction (allophane and ferrihydrite), and
- to determine whether there has been any chemical weathering and/or downward movement of material from surface horizons.

These procedures are routinely undertaken in soil studies.

An estimate of the amount of allophane (short-range-order aluminosilicates and imogolites) present within the samples was calculated by the method of Parfitt and Henmi (1982) and Parfitt and Wilson (1985) using acid-oxalate and sodium pyrophosphate reagents. Acid-oxalate extracts poorly crystalline (short-range-order) organic and inorganic Fe, Al and Si (abbreviated as Fe_o, Al_o and Si_o) whilst pyrophosphate extracts organically complexed forms of Fe and Al (abbreviated as Fe_p and Al_p) (Schwertmann, 1959; 1964; McKeague and Day, 1966; McKeague, 1967;

McKeague *et al.*, 1971; Parfitt and Childs, 1988). The established methodology (i.e. Parfitt and Henmi, 1982; Parfitt and Wilson, 1985) is to assess the Al/Si ratio for allophane from $(Al_o\text{-}Al_p)/Si_o$ multiplied by 28/27 to give the atomic ratio. The allophane content of a sample is then calculated by multiplying the Si_o content by a factor corresponding to the atomic ratio. Good agreement has been found between this method and that obtained by infra-red spectroscopy (Parfitt and Henmi, 1982). Ferrihydrite concentrations were estimated by multiplying acid-oxalate extractable Fe (Fe_o) values by 1.7% (Childs, 1985; Parfitt and Childs, 1988).

7.2 ANALYTICAL PROCEDURES

7.2.1 Sampling, sample pretreatment and preparation

Details of the sampling strategy and the methods of preparing loess and tephra samples for laboratory analysis are described in section 5.4.2.2.

7.2.2 Analytical techniques

(a) *Major oxides and trace element analysis*

Financial constraints meant that only a limited number of samples could be analysed by the x-ray fluorescence (XRF) technique. Consequently, samples were selected from as many different horizons as possible. More rigorous procedures such as replicate analyses and the analyses of various particle size fractions could not be undertaken.

Six grams of each sample (<2mm diameter) were ground in a tungsten carbide ring mill for 2 minutes. Samples were then split into two subsamples. Loss on ignition (LOI) determinations were determined on one subsample by weight loss on heating to 1000°C. On the other subsample major oxide determinations (SiO_2, TiO_2, Al_2O_3, Fe_2O_3, MnO_2, MgO, CaO, Na_2O, K_2O, P_2O_5) were conducted using a fused glass disc and trace element determinations (As, Ba, Ce, Cr, Cu, Ga, La, Nb, Ni, Pb, Rb, Sc, Sr, Th, U, V, Y, Zn, Zr) on a lithium tetraborate backed pressed pellet (Roser, 1983). Analyses were undertaken on a Philips PW 1404 automatic sequential x-ray spectrometer at the

Analytical Facility, Victoria University of Wellington. Standard soil and rock samples were analysed and used for calibration. The detection limit for most oxides and trace elements is on the order of 2ppm, while precision errors are about $\pm$3ppm (Palmer, 1990).

(b) *Dissolution chemistry*

The chemical dissolution methods used are described in Blakemore *et al.* (1987), unless otherwise stated. All chemical analyses were duplicated and the average value presented.

(i) Oxalate-extractable Fe (Fe_o), Al (Al_o) and Si (Si_o)

1g of soil (<2mm, air-dried) and 100ml of 0.2M acidified ammonium oxalate were shaken in the dark for two hours on a reciprocating shaker (Schwertmann, 1959; 1964; Schwertmann *et al.*, 1982). After adding "Superfloc" to prevent clay dispersion, then centrifuging, aliquots were determined for Fe and Al by atomic absorption spectroscopy (AAS). Oxalate-extractable Si values were determined colorimetrically (Weaver *et al.*, 1968).

(ii) Pyrophosphate extractable-Fe and -Al (Fe_p, Al_p)

1g of soil (<2mm, air-dried) and 100ml of 0.1M sodium pyrophosphate were shaken overnight (16h) on an end-over-end shaker. After addition of "Superfloc," centrifuging and suitable dilution, Fe and Al aliquots were measured by atomic absorption spectroscopy.

7.3 RESULTS

7.3.1 Presentation of results

X-ray fluorescene and chemical dissolution data are presented in Appendix IV. For ease of comparison and interpretation, data are presented as either major oxide, trace element or soil chemical property versus soil-depth plots. Depth measurements were taken from the current soil surface at the Pakaututu Road and Poraiti #1 sections and

Table 7.1: Ratings for chemical properties

Rating	**Fe_o (%)**	**Al_o (%)**	**Si_o (%)**	**Fe_p (%)**	**Al_p (%)**
Very high	>2.0	>3.0		>1.2	>2.0
High	1.0-2.0	1.0-3.0	>0.5	0.6-1.2	0.8-2.0
Medium	0.5-1.0	0.5-1.0	0.15-0.5	0.3-0.6	0.4-0.8
Low	0.2-0.5	0.2-0.5	0.05-0.15	0.1-0.3	0.1-0.4
Very low	<0.2	<0.2	<0.05	<0.1	<0.1

Reproduced from Blakemore *et al.* (1987)

from the base of the *c.*22 600 year B.P. rhyolitic Kawakawa Tephra at the Poraiti #2 section. Interpretations were made with respect to the horizons described in Chapter Five.

The major oxide analyses include loss on ignition (LOI) values. As LOI results incorporate later additions of carbon and water to the primary parent material, data had to be recalculated on a LOI free basis and then normalised to 100%. Normalisation of data does not account for water bound in micas, amphiboles and volcanic glasses (Wallace, 1987). This, however, represents only a relatively minor component of the whole soil. Normalisation calculations were not undertaken on the trace element data.

Chemical values are reported and rated (see Table 7.1) according to the guidelines set out for New Zealand soils by Blakemore *et al.* (1987).

7.3.2 Major oxides and trace element distributions

7.3.2.1 *Major oxides*

Pakaututu Road section

Macroscopic andesitic tephra-rich horizons comprising the Papakai (80cm depth), Mangamate (110cm depth) and Bullott (120, 170cm depths) Formations at Pakaututu Road are readily identified by their lower SiO_2 and K_2O values and higher TiO_2, Al_2O_3, Fe_2O_3, MnO_2, MgO, CaO, P_2O_5 and LOI values than that of quartzofeldspathic loess and rhyolitic tephra-rich horizons (Fig. 7.1).

Macroscopic rhyolitic tephras such as the Waimihia (40cm depth), Kawakawa (315cm depth) and Rotoehu (570cm depth) Tephras are identified by their lower TiO_2, Al_2O_3 (higher for Rotoehu Tephra) and Fe_2O_3 and higher CaO and Na_2O values, relative to that of the enclosing quartzofeldspathic loess and andesitic tephras (Fig. 7.1). SiO_2, MnO_2, MgO, K_2O and P_2O_5 values within rhyolitic tephra layers do not show any significant differences to those within quartzofeldspathic loess or andesitic tephras.

Table 7.2: Major oxide trends within the current soil and paleosols at the Pakaututu Road section

Major oxide	Current soil	Soil buried by Taupo Ignimbrite	Ohakean paleosol	Ratan paleosol	Porewan paleosol
SiO_2	lower	lower	lower	higher	higher
TiO_2	higher	higher	higher	higher	higher
Al_2O_3	lower	higher	higher	n.d.	lower
Fe_2O_3	higher	higher	higher	lower	higher
MnO_2	n.d.	higher	higher	higher	higher
MgO	higher	higher	higher	n.d.	higher
CaO	higher	higher	higher	lower	lower
Na_2O	lower	lower	lower	lower	lower
K_2O	lower	lower	lower	higher	higher
P_2O5	higher	higher	higher	lower	higher
LOI	higher	higher	higher	lower	lower

n.d. = no difference

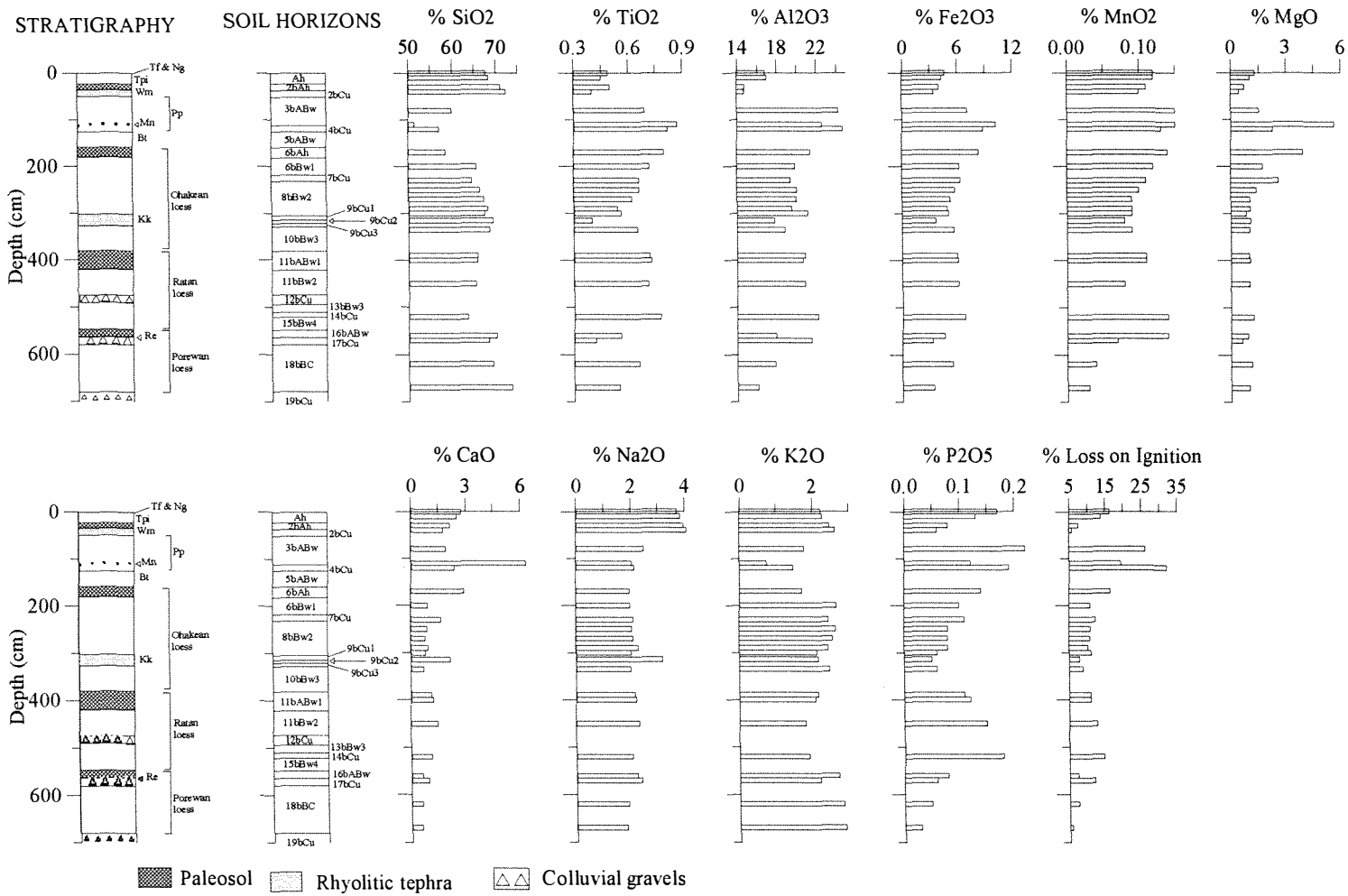

Figure 7.1: Major oxide distributions at the Pakaututu Road section.
(Tf=Tufa Trig Formation, Ng=Ngauruhoe Formation, Tpi=Taupo Ignimbrite, Wm=Waimihia Tephra, Pp=Papakai Formation, Mn=Mangamate Formation, Bt=Bullot Formation, Kk=Kawakawa Tephra, Re=Rotoehu Tephra. Refer to Chapters Five and Six for details.)

Table 7.3: Major oxide trends within the current soil/Ohakean paleosol and paleosols at the Poraiti sections

Major oxides	Ohakean paleosol	Ratan paleosol	Porewan paleosol	Loess 4 paleosol	Loess 5 paleosol
SiO_2	higher	higher	lower	lower	higher
TiO_2	lower	n.d.	lower	higher	n.d.
Al_2O_3	lower	lower	higher	higher	higher
Fe_2O_3	lower	lower	higher	higher	higher
MnO_2	higher	lower	lower	lower	n.d.
MgO	lower	lower	lower	lower	lower
CaO	higher	higher	lower	lower	lower
Na_2O	higher	higher	lower	lower	higher
K_2O	higher	lower	lower	lower	lower
P_2O5	higher	lower	n.d.	lower	lower
LOI	higher	lower	higher	higher	lower

n.d. = no difference

Microscopic tephra layers (andesitic and rhyolite) are intermixed with quartzofeldspathic loess (e.g 230cm depth) hence their rhyolite or andesite-like trends are not always apparent.

Table 7.2 summarises the major oxide trends within the: current soil developed on Taupo Ignimbrite (0cm depth); soil buried by Taupo Ignimbrite (30cm depth), Ohakean paleosol (170cm depth), Ratan paleosol (390, 400cm depths) and the Porewan paleosol (560cm depth) (refer to Fig. 7.1 and Appendix 4.1). All values are termed "higher" or "lower," depending upon whether they are higher or lower than their respective parent materials (lower B and C horizons).

Poraiti # 1 and #2 sections

The only macroscopic rhyolitic tephra layer present at the Poraiti sections (see Fig. 7.2) is that of the *c.*22 600 year B.P. Kawakawa Tephra (190, 221cm depths). There are significant variations in major oxide values even within Kawakawa Tephra samples (e.g. SiO_2, Al_2O_3, MgO, CaO, and K_2O). Kawakawa Tephra displays slightly higher SiO_2 (221cm depth), CaO (190cm depth), Na_2O and K_2O (221cm depth) values and lower TiO_2 and Fe_2O_3 values than the enclosing quartzofeldspathic-rich Ohakean loess (Fig. 7.2). The remaining major oxide values are similar to those within the Ohakean loess.

Macroscopic andesitic tephra-rich horizons at the Poraiti #2 section (e.g. 300, 310cm depths) have lower SiO_2, MnO_2, MgO, CaO, Na_2O, K_2O and higher TiO_2, Al_2O_3, Fe_2O_3 and LOI values than those of the enclosing quartzofeldspathic-rich loess (Fig. 7.3).

Table 7.3 summarises the major oxide trends within the current soil/Ohakean paleosol (10cm depth) at the Poraiti #1 section and the Ratan (120cm depth), Porewan (180cm depth), Loess 4 (300, 310cm depths) and Loess 5 (360cm depth) paleosols at the Poraiti #2 section (refer to Figs. 7.2-7.3 and Appendices 4.3 and 4.4). Major oxide values are termed "higher" or "lower," depending upon whether they are higher or lower than their respective subsoils (B and C horizons).

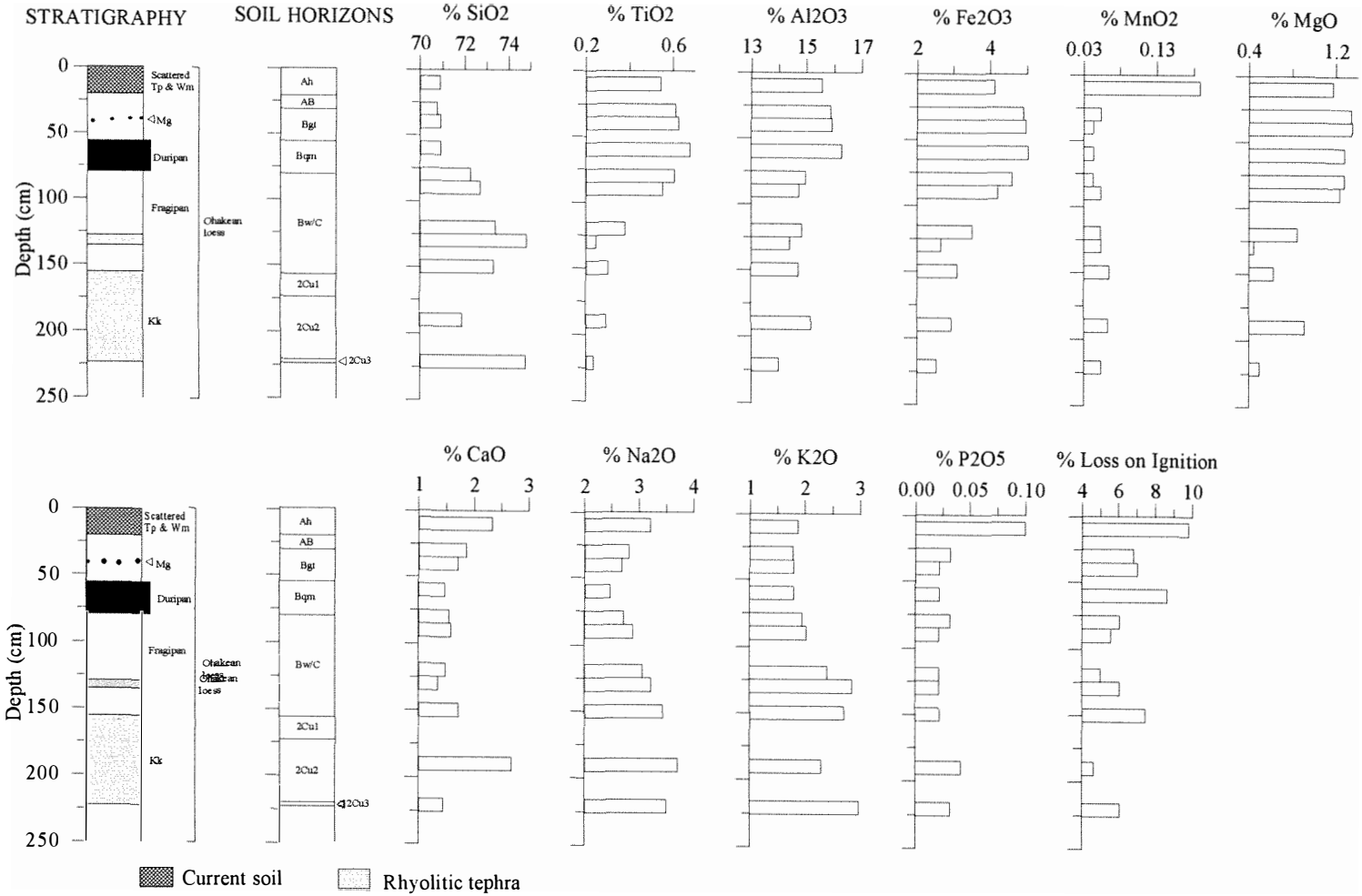

Figure 7.2: Major oxide distributions at the Poraiti #1 section.
(Tp=Taupo Tephra, Wm=Waimihia Tephra, Kk=Kawakawa Tephra. Refer to Chapters Five and Six for details.)

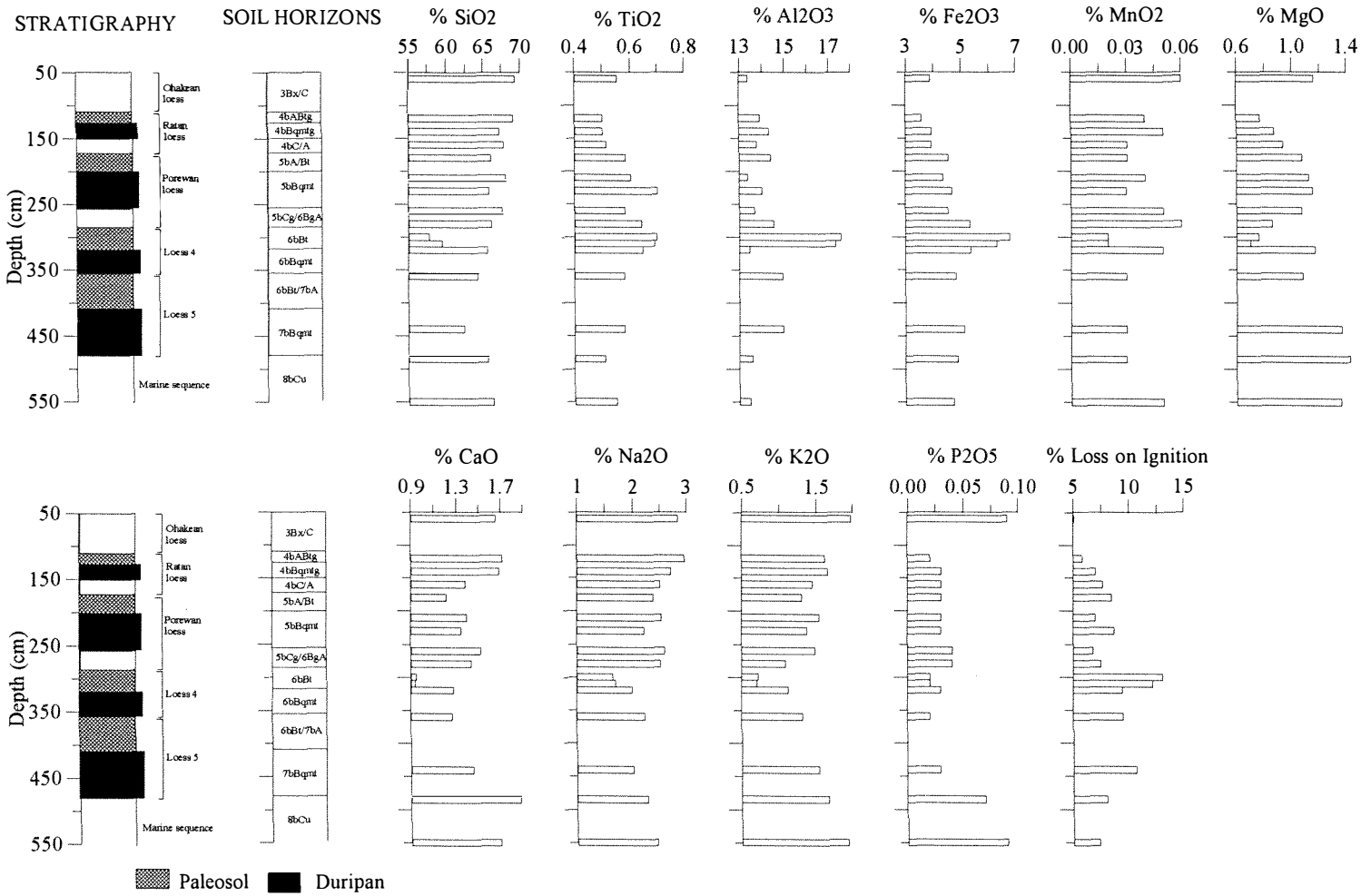

Figure 7.3: Major oxide distributions at the Poraiti #2 section.
(Refer to Chapters Five and Six for details.)

The marine sequence underlying the loess column at the Poraiti #2 section (485, 550cm depths) has SiO_2, TiO_2, Al_2O_3, Fe_2O_3, MnO_2, MgO, Na_2O and LOI values which are similar to those of the overlying quartzofeldspathic-rich loess sheets whereas its CaO, K_2O and P_2O_5 values are slightly higher than those of the overlying loess and tephra units (Fig. 7.3).

SiO_2, TiO_2, Fe_2O_3, MgO, CaO, and Na_2O values at the Pakaututu Road section are similar to those at the Poraiti sections whereas Al_2O_3, MnO_2, K_2O, P_2O_5 and LOI values at the Pakaututu Road section are generally higher than those at the Poraiti sections (see Appendices 4.1, 4.3 and 4.4).

7.3.2.2 *Trace elements*

Pakaututu Road section

Taupo Ignimbrite (10cm depth) and macroscopic rhyolitic tephras such as the Waimihia (40cm depth), Kawakawa (315cm depth) and Rotoehu (570cm depth) tephras have lower Pb, Rb, As, Sc, V, Cr, La, Ce, Ni, Cu, Zn and Zr values than those of quartzofeldspathic loess (Figs 7.4a,b). The other trace elements measured exhibit similar values to those of loess.

The macroscopic andesitic tephra-rich layers of the Papakai (80cm depth), Mangamate (110cm depth) and Bullott (120, 170cm depths) Formations show considerable variations in their trace elements. Hence, consistent differences with those of the overlying rhyolite tephras and underlying quartzofeldspathic loess are not always possible (see Appendix 4.2). Andesitic tephras do, however, exhibit higher Sc, V, Cr, La (80, 120cm depths only), Ce (80cm depth only), Ni, Cu, Zn (110, 170cm depths only) and lower Rb, Ba and Zr values than those of the overlying Taupo Ignimbrite and Waimihia Tephra. The andesitic tephra-rich layers have higher V (except 80cm depth), Cr (110cm depth only), La (80, 120cm depths only), and lower Pb, Rb, Sr, Th, As, Ba, Ni (80, 120cm depths only), Zr and Nb than the underlying quartzofeldspathic-rich Ohakean loess.

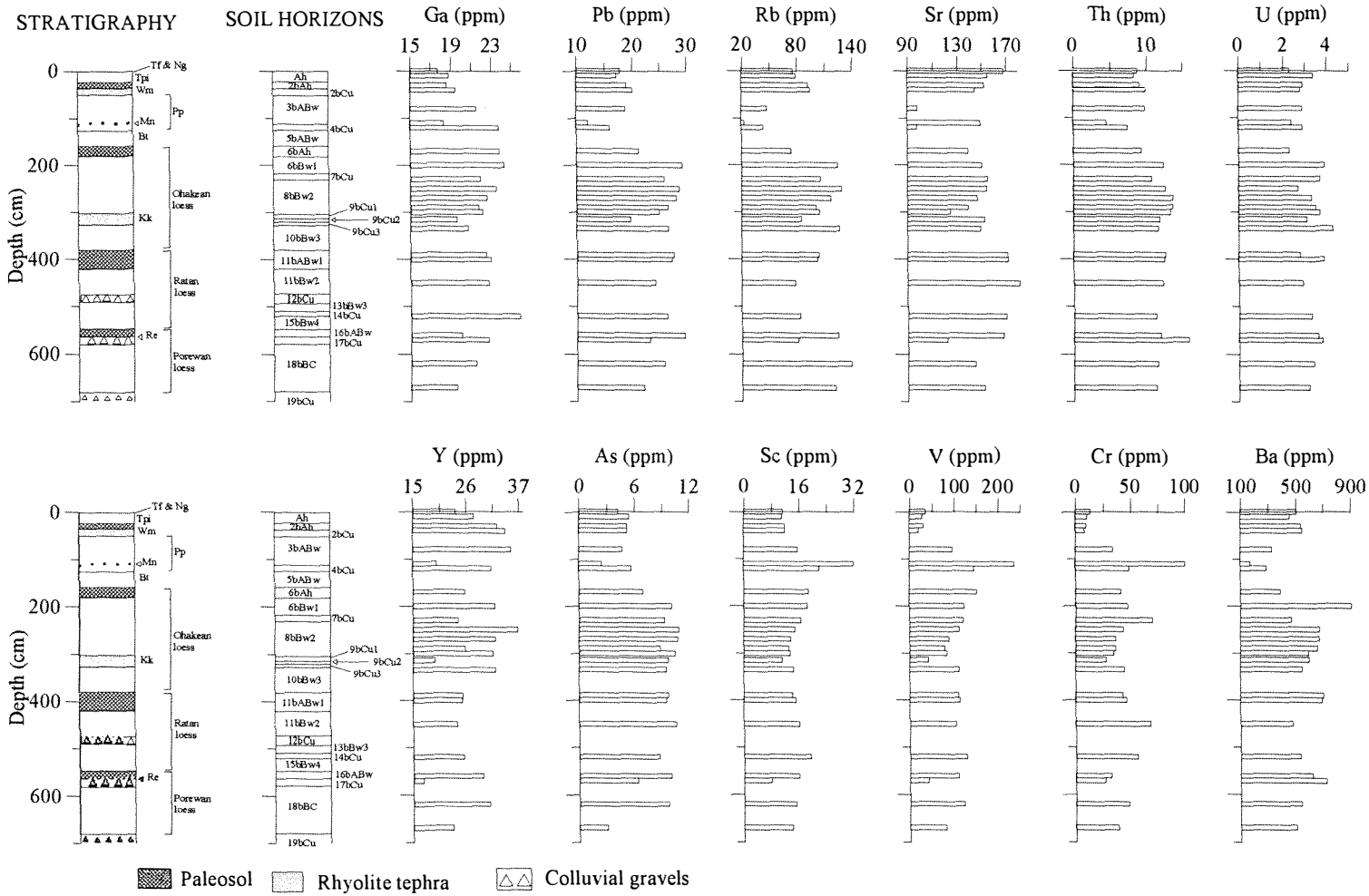

Figure 7.4a: Trace element distributions at the Pakaututu Road section.
(Tf=Tufa Trig Formation, Ng=Ngauruhoe Formation, Tpi=Taupo Ignimbrite, Wm=Waimihia Tephra, Pp=Papakai Formation, Mn=Mangamate Formation, Bt=Bullot Formation, Kk=Kawakawa Tephra, Re=Rotoehu Tephra. Refer to Chapters Five and Six for details.)

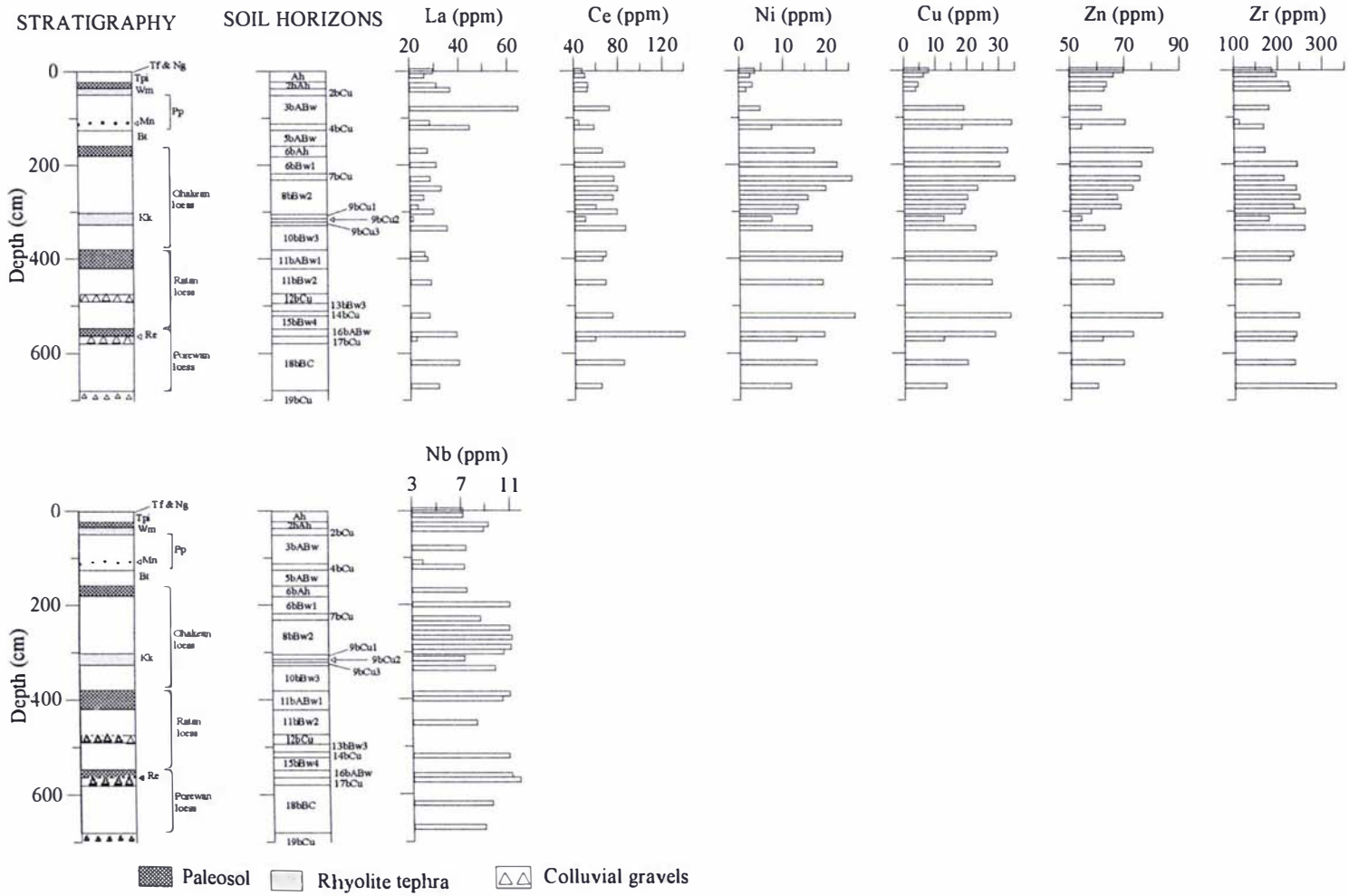

Figure 7.4b: Trace element distributions at the Pakaututu Road section.
(Tf=Tufa Trig Formation, Ng=Ngauruhoe Formation, Tpi=Taupo Ignimbrite, Wm=Waimihia Tephra, Pp=Papakai Formation, Mn=Mangamate Formation, Bt=Bullot Formation, Kk=Kawakawa Tephra, Re=Rotoehu Tephra. Refer to Chapters Five and Six for details.)

Table 7.4: Trace element trends within the current soil and paleosols at the Pakaututu Road section

Trace element	Current soil	Soil buried by Taupo Ignimbrite	Ohakean paleosol	Ratan paleosol	Porewan paleosol
Ga	lower	lower	lower	n.d.	lower
Pb	higher	lower	lower	higher	higher
Rb	lower	lower	lower	higher	higher
Sr	higher	higher	lower	lower	higher
Th	higher	lower	lower	higher	lower
U	lower	higher	lower	higher	lower
Y	lower	lower	lower	higher	higher
As	lower	n.d.	lower	lower	higher
Sc	higher	n.d.	higher	lower	higher
V	higher	higher	higher	higher	higher
Cr	higher	higher	lower	lower	higher
Ba	higher	lower	lower	higher	lower
La	higher	lower	lower	lower	higher
Ce	lower	higher	lower	higher	higher
Ni	higher	higher	lower	higher	higher
Cu	higher	higher	higher	higher	higher
Zn	higher	higher	higher	higher	higher
Zr	lower	lower	lower	higher	higher
Nb	n.d.	higher	lower	higher	lower

n.d. = no difference

Table 7.4 summarises the trace element trends within the: current soil developed on Taupo Ignimbrite (0cm depth); soil buried by Taupo Ignimbrite (30cm depth); Ohakean paleosol (170cm depth); Ratan paleosol (390, 400cm depth) and the Porewan paleosol (560cm depth) (refer to Figs. 7.4a,b and Appendix 4.2). All values are termed "higher" or "lower," depending upon whether they are higher or lower than their respective subsoils (B and C horizons).

Poraiti #1 and #2 sections

There is considerable variation in trace element values within the Kawakawa Tephra (compare trace element values taken at 190 and 221cm depths) at the Poraiti #1 section (see Appendix 4.5). The fine white basal ash of the Kawakawa Tephra (221cm depth) has higher Rb (221cm depth), U (221cm depth) and lower V (221cm depth) and Cr (221cm depth) values than that of Ohakean loess (Figs. 7.5a,b). These trends are not apparent within the Kawakawa Tephra sample taken at 190cm depth. Other trace elements measured (see Appendix 4.5) do not show any marked differences in their contents relative to that of Ohakean loess.

The macroscopic andesitic layer (300, 310cm depth) within Loess 4 at the Poraiti #2 section has higher Ga, Sc, V, Cr, Ni, Cu and lower Rb, Sr, Y, Ba, La, Ce, Zn and Zr values than that of quartzofeldspathic loess (Figs. 7.6a,b).

Table 7.5 summarises the trace element trends within the current soil/Ohakean paleosol (10cm depth) at the Poraiti #1 section and the Ratan (120cm depth), Porewan (180cm depth), Loess 4 (300, 310cm depths) and Loess 5 (360cm depth) paleosols at the Poraiti #2 section (refer to Figs. 7.5a,b and Figs. 7.6a,b). All values are termed "higher" or "lower," depending upon whether they are higher or lower than their respective subsoils (B and C Horizons).

The marine sequence at the Poraiti #2 section has slightly lower Ga and higher Y, As, Ba, La, Ce, Ni (550cm depth) and Zn (550cm depth) values than that of the overlying coverbeds (Fig. 7.6a,b). No major differences are evident within the other trace elements measured.

Table 7.5: Trace element trends within the current soil/Ohakean paleosol and paleosols at the Poraiti sections

Trace element	Ohakean paleosol	Ratan paleosol	Porewan paleosol	Loess 4 paleosol	Loess 5 paleosol
Ga	lower	lower	higher	higher	higher
Pb	higher	lower	higher	lower	lower
Rb	higher	lower	lower	lower	lower
Sr	lower	higher	lower	lower	higher
Th	higher	lower	lower	higher	lower
U	lower	lower	lower	higher	higher
Y	higher	lower	lower	lower	lower
As	lower	lower	lower	lower	lower
Sc	lower	lower	higher	higher	lower
V	lower	lower	higher	higher	higher
Cr	lower	higher	lower	higher	lower
Ba	higher	lower	lower	lower	lower
La	higher	lower	lower	lower	lower
Ce	higher	lower	lower	lower	lower
Ni	lower	higher	lower	lower	lower
Cu	lower	lower	higher	higher	higher
Zn	higher	lower	lower	lower	lower
Zr	lower	higher	lower	lower	higher
Nb	lower	higher	lower	higher	higher

n.d. = no difference

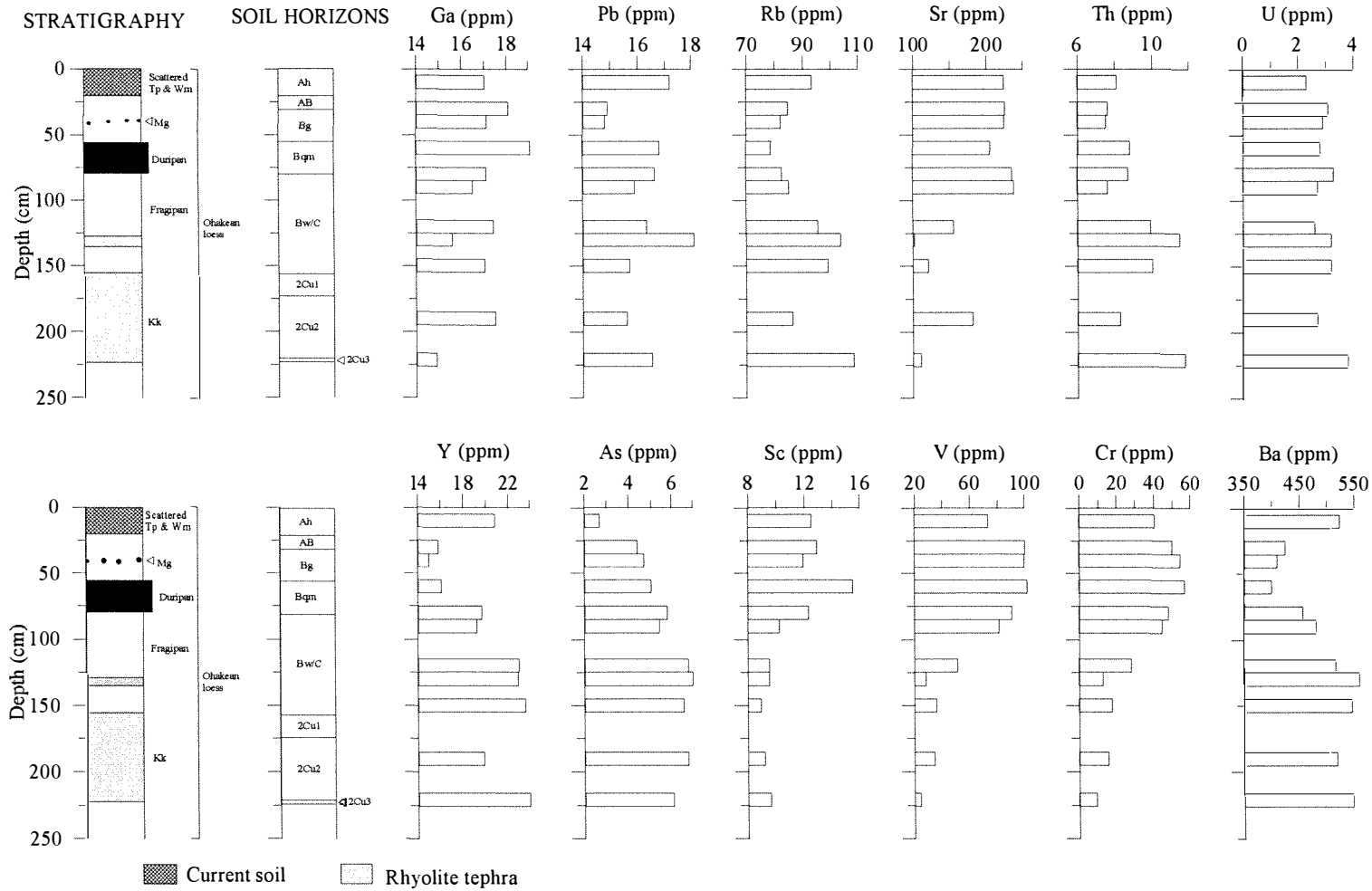

Figure 7.5a: Trace element distributions at the Poraiti #1 section.
(Tp=Taupo Tephra, Wm=Waimihia Tephra, Kk=Kawakawa Tephra. Refer to Chapters Five and Six for details.)

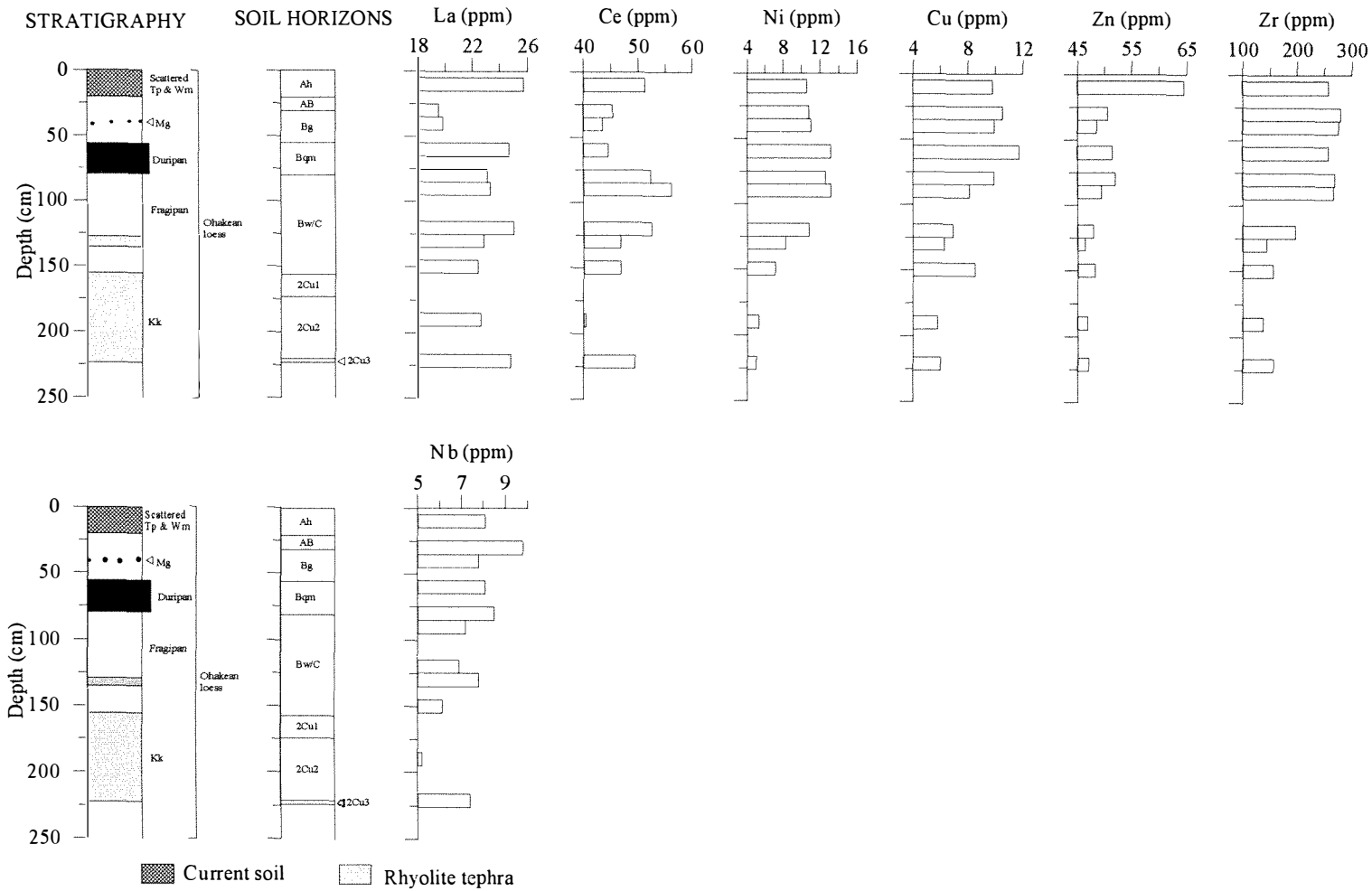

Figure 7.5b: Trace element distributions at the Poraiti #1 section.
(Tp=Taupo Tephra, Wm=Waimihia Tephra, Kk=Kawakawa Tephra. Refer to Chapters Five and Six for details.)

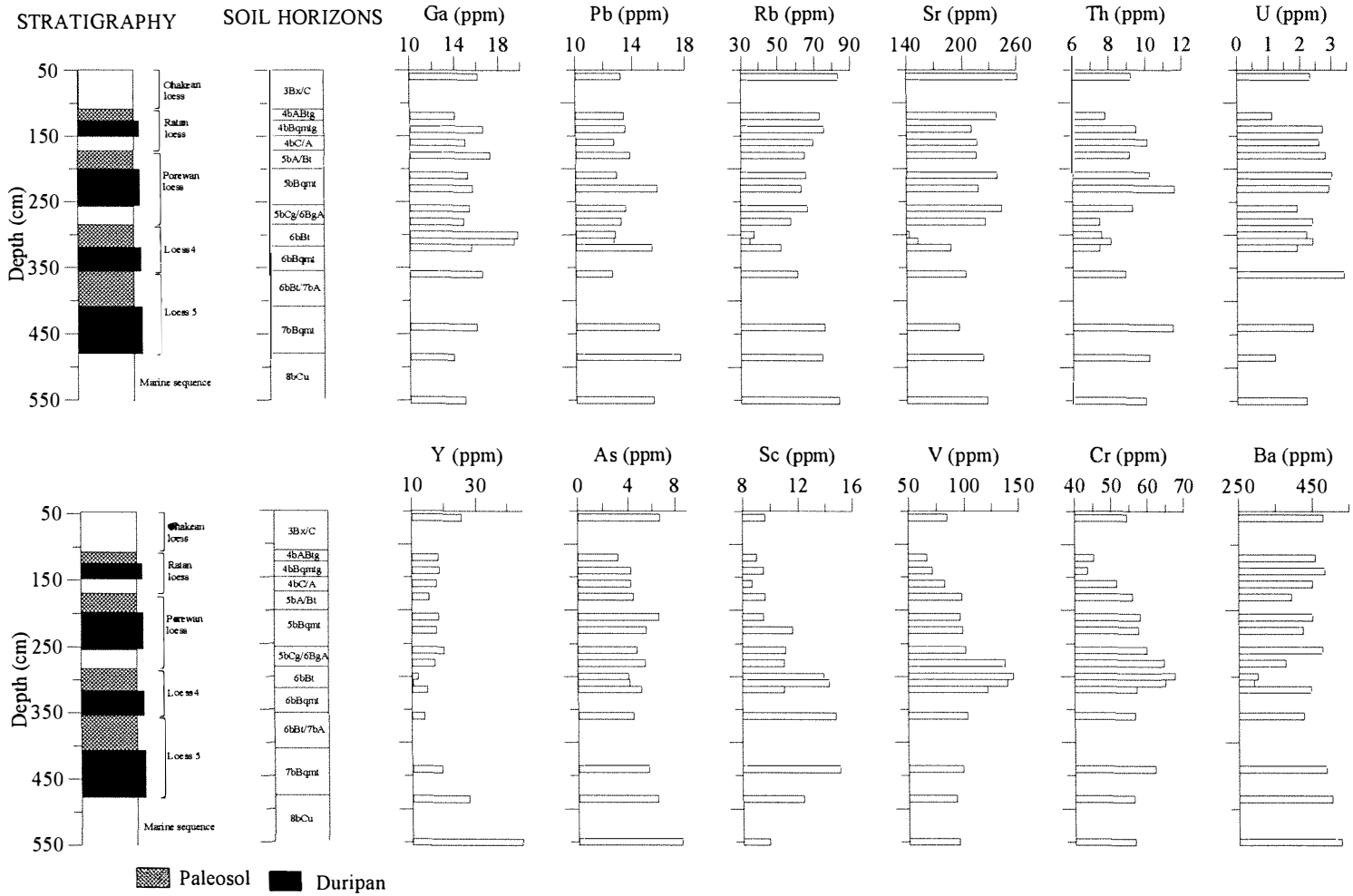

Figure 7.6a: Trace element distributions at the Poraiti #2 section.
(Refer to Chapters Five and Six for details.)

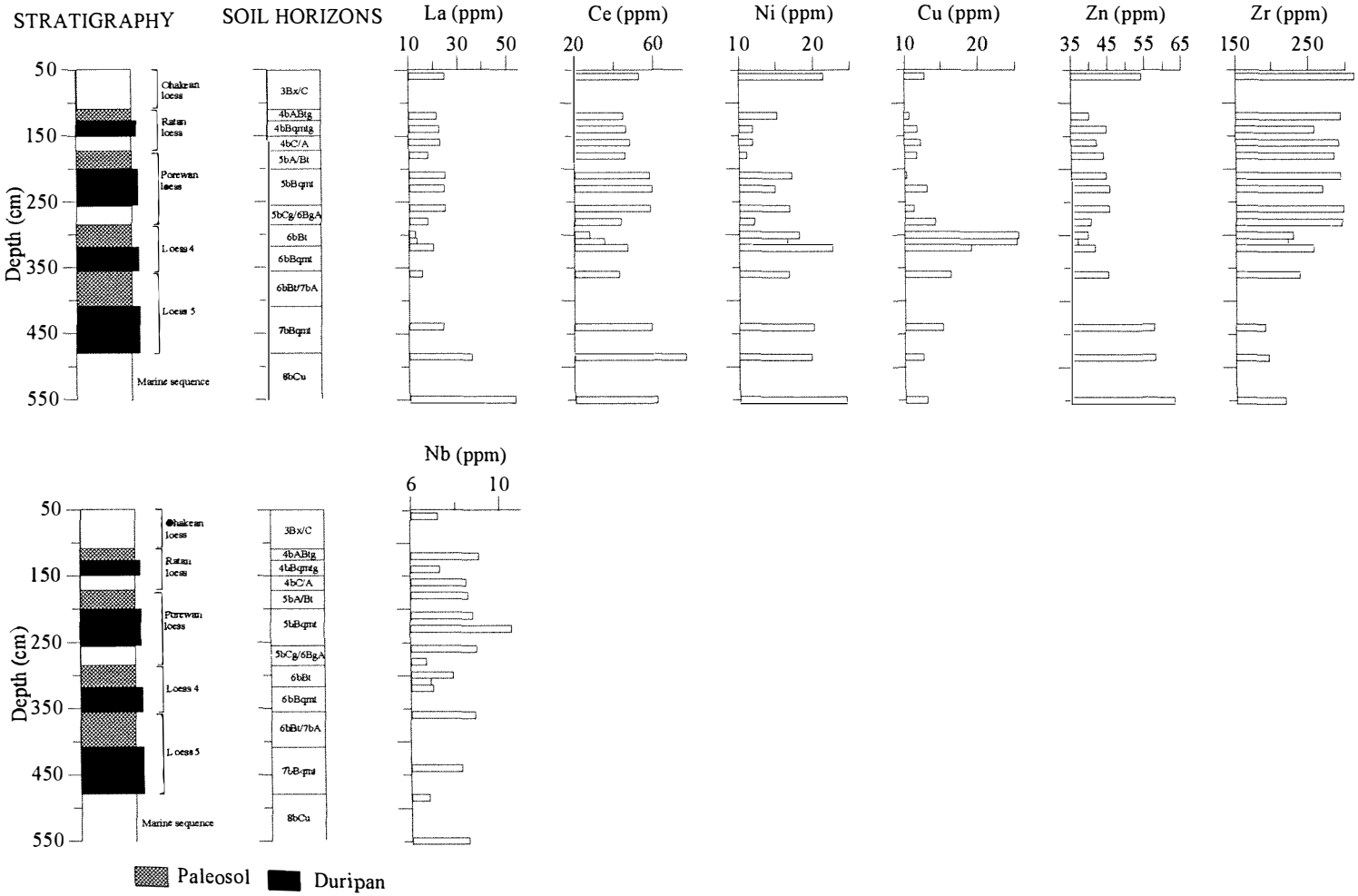

Figure 7.6b: Trace element distributions at the Poraiti #2 section.
(Refer to Chapters Five and Six for details.)

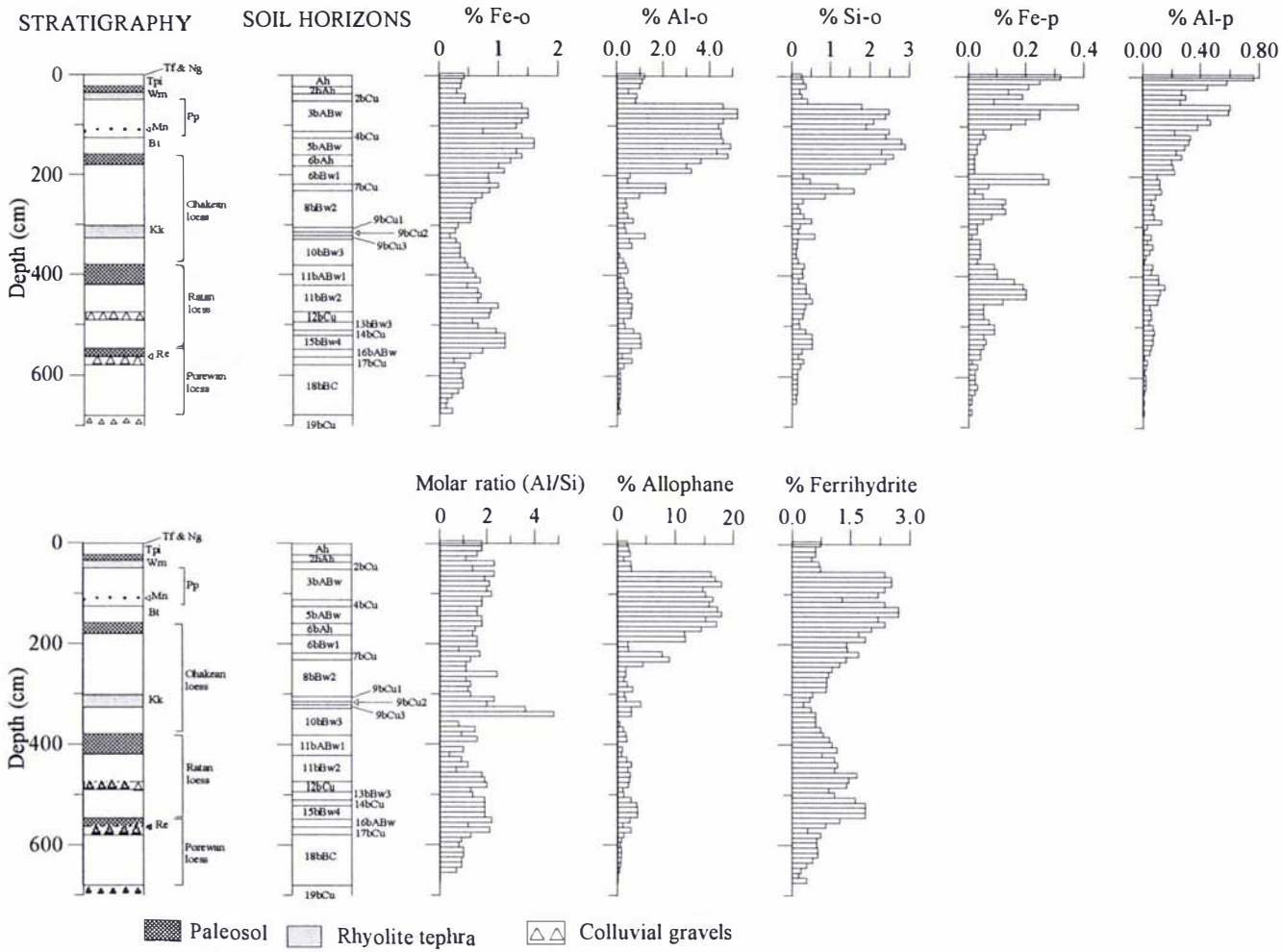

Figure 7.7: Dissolution chemistry at the Pakaututu Road section.
(Tf=Tufa Trig Formation, Ng=Ngauruhoe Formation, Tpi=Taupo Ignimbrite, Wm=Waimihia Tephra, Pp=Papakai Formation, Mn=Mangamate Formation, Bt=Bullot Formation, Kk=Kawakawa Tephra, Re=Rotoehu Tephra. Refer to Chapters Five and Six for details.)

The quartzofeldspathic loess at the Pakaututu Road section generally has higher Ga, Pb, Rb, Th, Y, As, Sc, Ba, La, Ce, Cu, Zn and Nb and lower Sr, Cr and Zr values than those within their corresponding loess units at the Poraiti sections (see Appendices 4.2, 4.5 and 4.6). Ni, U and V loess values at these sections are similar.

7.3.3 Dissolution chemistry

7.3.3.1 *Pakaututu Road section*

In Chapter Five the Pakaututu section was subdivided into 3 zones:

- an upper zone (0-50cm depth) comprising: a thin veneer of andesitic tephras (Tufa Trig and Ngauruhoe Formations) overlying Taupo Ignimbrite (0-22cm depth), and two macroscopic rhyolite tephras (Taupo and Waimihia Tephras);
- a predominantly andesitic zone (50-158cm depth) comprising accessions of the Papakai, Mangamate and Bullot Formations with very fine dustings of rhyolitic tephra; and
- a predominantly loessial zone (158-680cm depth) comprising three loess units termed Ohakean loess, Ratan loess and Porewan loess. Each loess unit is separated by a paleosol. The loess units and paleosols are intercalated by both macroscopic and microscopic rhyolitic and andesitic tephra layers. These have been used as time planes (see Chapter Six).

Oxalate-extractable Fe (Fe_o), Al (Al_o) and Si (Si_o)

Oxalate-extractable Fe (Fe_0) values are: low within the Taupo Ignimbrite and the macroscopic rhyolitic (Waimihia, Kawakawa and Rotoehu) tephra layers; medium to high within the andesitic tephra layers (Papakai, Mangamate and Bullot Formations); and very low to medium within the quartzofeldspathic loess (see Fig. 7.7 and Appendix 4.7). High Fe_o values are, however, encountered towards the base of the Ratan loess (520-540cm depth).

Oxalate-extractable Al (Al_0) values are: high within the Taupo Ignimbrite; low to high within the macroscopic rhyolitic tephra layers (Waimihia, Kawakawa and Rotoehu);

very high within andesitic tephra layers (Papakai, Mangamate and Bullot Formations); and very low to medium within quartzofeldspathic loessial units (see Fig. 7.7).

Oxalate-extractable Si (Si_0) values are: medium within the Taupo Ignimbrite; medium to high within macroscopic rhyolite tephra layers (Waimihia, Kawakawa and Rotoehu Tephras); high within macroscopic andesitic tephra layers (Papakai, Mangamate and Bullott Formations); and very low to medium within the quartzofeldspathic loessial units (Fig. 7.7). Si_0 values are generally greater (>2%) within the andesitic layers than in the rhyolitic or loessial parts of the section. Si_o peaks seen within the loess coincide with tephra inputs, both macroscopic (e.g. Kawakawa Tephra) and microscopic (e.g. 450cm depth).

Al_o, Si_o and Al_p values are generally much lower below 2-3m depth than above (Fig. 7.7).

Pyrophosphate-extractable Fe (Fe_p) and Al (Al_p)

Pyrophosphate-extractable Fe (Fe_p) values are: low to medium within the topsoil containing Taupo Ignimbrite; very low to low within macroscopic rhyolitic tephras (Waimihia. Kawakawa and Rotoehu Tephras); very low to medium within macroscopic andesitic tephra layers; and very low to low within quartzofeldspathic loess (see Fig. 7.7, Appendix 4.7).

Pyrophosphate-extractable Al (Al_p) values are: medium within Taupo Ignimbrite; very low to low within macroscopic rhyolitic tephras (Waimihia, Kawakawa and Rotoehu Tephras); low to medium within andesitic tephra-rich zones; and very low to low within quartzofeldspathic loess (Fig. 7.7, Appendix 4.7). Al_p values are generally higher than Fe_p values within andesitic tephra layers. Both Fe_p and Al_p values decrease with depth, especially within the loess. The Ratan and Porewan paleosols show slight increases in their Fe_p and Al_p values. No marked trend is evident in the Ohakean paleosol.

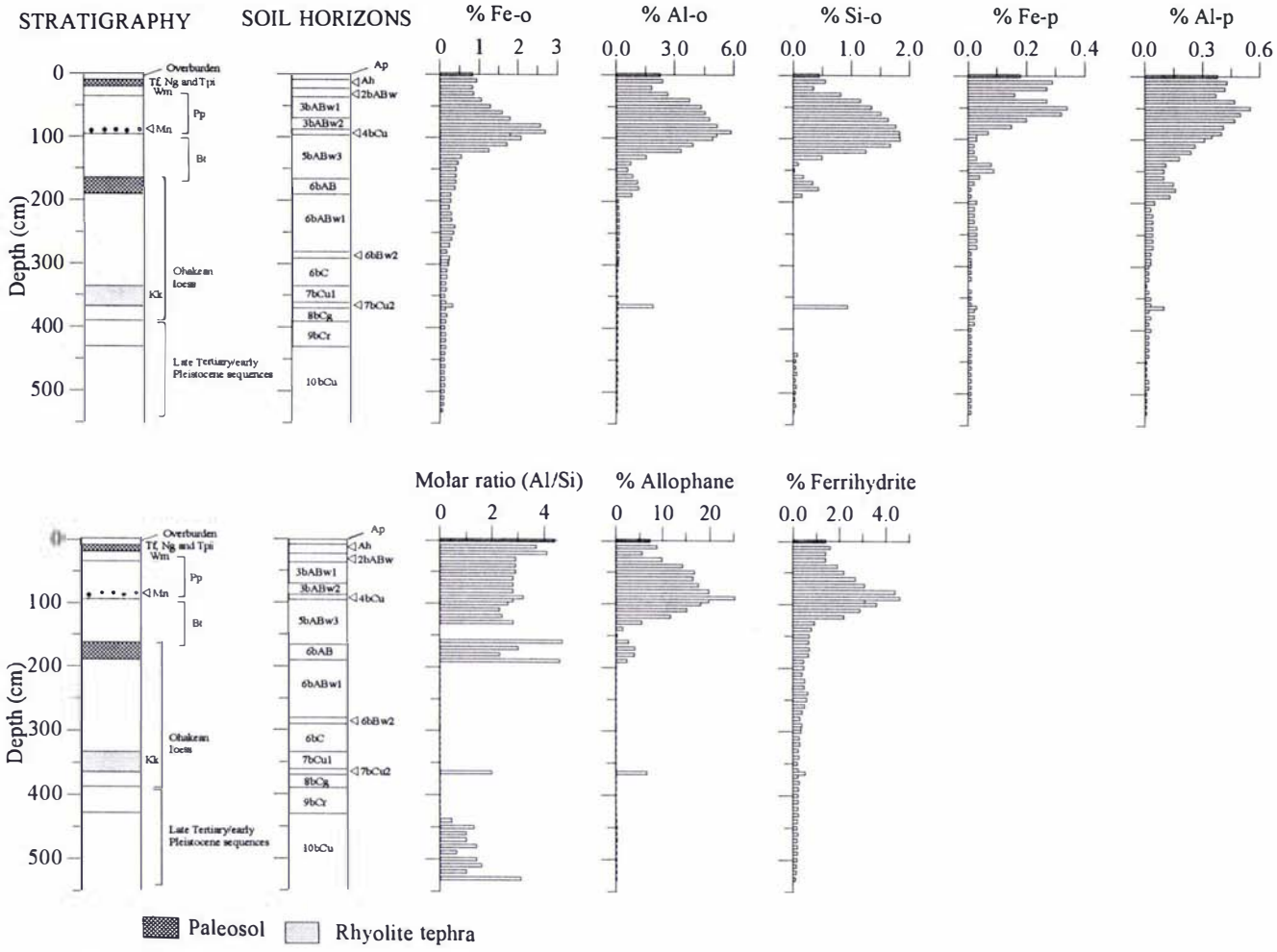

Figure 7.8: Dissolution chemistry at the Manaroa section.
(Tf=Tufa Trig Formation, Ng=Ngauruhoe Formation, Tpi=Taupo Ignimbrite, Wm=Waimihia Tephra, Pp=Papakai Formation, Mn=Mangamate Formation, Bt=Bullot Formation, Kk=Kawakawa Tephra. Refer to Chapters Five and Six for details.)

Molar ratios (Al/Si), % allophane and % ferrihydrite

Molar ratios within Taupo Ignimbrite and the rhyolitic and andesitic tephra layers are usually >1.5 whereas ratios for quartzofeldspathic loess average 1.0 but may increase to >2.0 if diluted by tephra (Fig. 7.7). The allophane content within Taupo Ignimbrite and Waimihia Tephra ranges from 1.0-2.4%. A marked increase in allophane content (14.7-18.0%) is seen within the andesitic Papakai, Mangamate and Bullott Formations relative to the overlying rhyolitic units. The allophane content within quartzofeldspathic loess is highly variable but less than that of Taupo Ignimbrite, rhyolitic and andesitic tephra layers (i.e. <1%). Wherever a tephric layer is encountered within loess the allophane content increases substantially (e.g. 4.7% for the Kawakawa Tephra at 320cm). Ferrihydrite values are typically <1% within Taupo Ignimbrite, Waimihia, Kawakawa and Rotoehu Tephras. Values within the andesitic Papakai, Mangamate and Bullott Formations are substantially higher (>2%) than those within rhyolitic tephras and quartzofeldspathic loess layers.

7.3.3.2 Manaroa section

The Manaroa section was subdivided into 3 zones:

- an upper predominantly andesitic zone (0-165cm depth) comprising the Tufa Trig, Ngauruhoe, Papakai, Mangamate and Bullot Formations with minor admixtures of Taupo and Waimihia Tephras within the upper part (0-26cm depth) of the section;
- a layer of quartzofeldspathic Ohakean loess (165-390cm depth); and
- possible (?) marine sands (390cm+) which underlie the loess.

The loess is intercalated with both macroscopic and microscopic rhyolitic and andesitic tephra layers (e.g. Kawakawa Tephra at 335-368cm depth). Chemical values within the uppermost 10cm of the Manaroa section were not interpreted as this layer was later found to have been disturbed by road-making activities.

Oxalate-extractable Fe (Fe_o), Al (Al_o) and Si (Si_o)

Oxalate-extractable Fe (Fe_0) values are medium within the upper part (0-30cm) of the section where there is mixing of andesitic and rhyolitic tephras (Fig. 7.8, Appendix 4.8).

Values are high to very high within the andesitic rich Papakai, Mangamate and Bullott Formations. Fe_0 values within the Ohakean loess decrease progressively with depth from very low to low values, except for a slight increase (0.31%) associated with the fine white base of the Kawakawa Tephra at 365cm depth.

Oxalate-extractable Al (Al_0) values are high within the mixed rhyolitic and andesitic zone (0-36cm depth), becoming very high (>3%) within the andesitic-rich (36-120cm depth) part of the section (see Fig.7.8). From 130cm depth Al_0 decreases to medium values. Values within the quartzofeldspathic loess are very low (<0.2%) and show a progressive decrease with depth except at 365cm depth (Kawakawa Tephra) where they are high (1.9%).

Si_0 values are medium to high within the upper part of the profile (0-36cm depth), increasing to >1% in the andesitic-rich Papakai, Mangamate and Bullot Formations (Fig. 7.8). Values then drop steadily with depth from medium to very low within the quartzofeldspathic loess. The only deviation from this general trend is when a tephra layer is encountered (e.g. Kawakawa Tephra at 365cm depth) and high Si_0 values are subsequently recorded.

Pyrophosphate-extractable Fe (Fe_p) and Al (Al_p)

Pyrophosphate-extractable Fe (Fe_p) values are low within the upper part of the profile (0-80cm) and become very low (<0.1%) within the lower part (Fig. 7.8) of the section (>80cm depth).

Pyrophosphate-extractable Al (Al_p) values are low to medium within the upper part of the section (0-190cm) and very low within the underlying loess (Fig. 7.8). A slight increase in Al_p content within the Ohakean loess is associated with the Kawakawa Tephra (0.10%).

Molar ratios (Al/Si), % allophane and % ferrihydrite

Molar ratios (Fig. 7.8) are >2.0 within the tephric-rich upper part of the section (0-190cm depth). Within the quartzofeldspathic Ohakean loess molar ratios are <1.0

except within the Kawakawa Tephra (365cm) and in the underlying marine sequence (440-530cm depth).

Considerable quantities of allophane (>10% allophane) are present within the more andesitic-rich tephra layers (40-120cm depth). Values are low to insignificant within the quartzofeldspathic loess. A substantial increase in allophane content is, however, seen within the Kawakawa Tephra layer (365cm depth).

Ferrihydrite values are >1.0% within the andesitic part of the section but fall quite dramatically (<1.0%) at 130cm depth (Fig. 7.8). Below 130cm depth ferrihydrite values decrease steadily to 0.1%, except for a slight increase (0.5%) associated with the Kawakawa Tephra (365cm depth).

7.4 DISCUSSION

7.4.1 Major oxides and trace element distributions

SiO_2, Al_2O_3, TiO_2, Y and Zr are considered to be relatively immobile in most weathering environments (e.g. Gerrard, 1992). Within the Pakaututu Road and Poraiti loess columns these oxides and trace elements show considerable variations with depth. Differences in oxide values coincide with changes in parent material, such as the presence of macroscopic andesitic and rhyolitic tephra layers within the loess columns. These trends become more difficult to discern in the eastern parts of the district where tephra layers thin and become intermixed with quartzofeldspathic material (e.g. at the Poraiti sections).

The marine sequence which underlies the Poraiti #2 loess column has stable oxide and trace element values (TiO_2, Al_2O_3, SiO_2 and Zr) which are similar to those of loess, implying that the marine and loessial sediments may originally have been derived from similar source rocks. The marine sequence does, however, have lower Ga values and higher CaO, K_2O, P_2O_5, LOI, Y, As, Ba, La, Ce and Zn values relative to that of the

overlying loess. These rises are consistent with this sediment having been in contact with sea-water and having additional CaO and P_2O_5 from the shells of marine organisms.

The more basic (andesitic tephra-rich) layers at Pakaututu Road and Poraiti show anticipated rises in their transition metal concentrations (TiO_2, Fe_2O_3, MnO_2, Sc, V, Cr and Cu) relative to that of quartzofeldspathic loess, rhyolitic tephra and ignimbrite. Similar trends were reported for andesitic ash layers within the Wairarapa (Palmer, 1982a), Table Flat (Childs and Searle, 1975) and Kimbolton (Qizhong *et al.*, 1992) loess columns within the North Island of New Zealand.

As the Poraiti sections are more distal to the TVZ, macroscopic andesitic tephra layers seen at Pakaututu Road (Tufa Trig, 0cm; Ngauruhoe, 0cm; Papakai, 80cm; Mangamate, 110cm; and Bullott, 120, 170cm; Formations) are thinner or absent. Transition metal values should thus either be masked by or are only marginally higher than those of loess. A further complication is that the loess may contain dustings of andesitic tephra redeposited by wind erosion from older andesitic material.

Slight increases in Fe_2O_3, MnO_2, Sc, V and Cr are seen within the upper part (0-60cm depth) of the Ohakean loess at the Poraiti #1 section and within the Porewan (230cm depth) and Loess 4 (300, 310cm depths) loess units at the Poraiti #2 section. These rises are likely to be derived from fine dustings of andesitic material corresponding to the Tufa Trig, Ngauruhoe, Papakai, Mangamate and Bullott Formations (0-60cm depth). The andesitic layers identified within the Porewan and Loess 4 units are likely to correlate with stratigraphically-equivalent layers around the Tongariro Volcanic Zone (Hodgson, 1993; Cronin *et al.*, 1996a; 1997; Hobden *et al.*, 1996).

When the major oxide values at the Pakaututu Road and Poraiti sections are compared (see Appendix IV) some striking differences within their concentrations became apparent. The Pakaututu Road loess has higher Al_2O_3, MnO_2, K_2O, P_2O_5, LOI, Ga, Pb, Th, Y, As, Sc, Ba, La, Ce, Cu, Zn, and Nb values than loess present at the Poraiti sections. Conversely, the Poraiti loess has higher CaO, Sr, Cr and Zr concentrations

than that at Pakaututu Road. It has already been shown that the coverbeds at all the sections have received varying inputs of andesitic and rhyolitic tephra. Consequently, those sites closer to the TVZ (e.g Pakaututu Road) have been enriched in those oxides and trace elements associated with tephra, namely the transition elements for andesitic tephras and Na_2O for the rhyolitic tephras. It is proposed that the Pakaututu Road loess may have a greater greywacke sandstone/argillite component than that at the Poraiti sections. The Pakaututu Road section is located east of the greywacke sandstone/argillite axial ranges (see Chapter Five for site location), in close proximity to these loess source areas. Loess at the Poraiti sections, in addition to a greywacke sandstone/argillite component, may also have received inputs derived from the erosion of Neogene marine sequences within the hill country to the west.

The distribution patterns of the more readily mobilised major oxides (K_2O, P_2O_5, MgO, Na_2O) have been shown in the literature (e.g. Runge *et al.*, 1974; Childs and Searle, 1975; Palmer, 1982a; Palmer and Pillans, 1996) to respond sensitively to chemical weathering and are thus useful in reflecting soil development within individual loess layers. These oxides have been used in these studies to provide quantitative evidence for identifying or confirming the presence of a paleosol. Two considerations need to be taken into account when interpreting major oxide trends at the Pakaututu Road and Poraiti sections. The first is that paleosols are generally tephric-rich whereas their subsoils are usually tephra poor. This non-uniformity in parent material makes it difficult to relate major oxide levels within a paleosol to that of its subsoil solely in terms of mobilisation and translocation. The second consideration is that the Poraiti site presently receives, and presumably did during the cold periods of the Quaternary, a lower mean annual rainfall than that at the Pakaututu Road site (see section 7.1 for mean annual rainfalls at these sections). Consequently, paleosol development and hence element mobilisation within the solum of each loess layer at Poraiti is not as pronounced as that at Pakaututu Road. Furthermore, interpretations would have been easier had finances allowed more samples to be analysed. Samples were sometimes taken from widely spaced increments within a loess layer. Interpretations based on pedogenic processes are thus problematic and need to be considered in view of these limitations.

The depth distribution patterns of alkali metals (e.g. K_2O) within the Pakaututu and Poraiti loess columns show similar trends to the Rangitatau East loess column (Palmer and Pillans, 1996), namely lower concentrations in paleosols and relatively higher concentrations within the C horizons of loess. This trend is attributed to weathering during paleosol formation whereby elements such as K are either released by K-bearing minerals (e.g. mica and K-feldspars) into the soil solution or are incorporated into secondary clay minerals. Deviations from this trend (e.g. Ratan and Porewan paleosols at Pakaututu Road) are attributed to the presence of rhyolitic tephra.

The alkaline earth metals (Mg, Ca, Sr and Ba) and non-metals of group 5A (e.g. P) exhibit some of their highest concentrations within the current soil and in buried soils. High Mg, Ca and P values within the topsoils may, in part, be attributed to fertiliser applications. High concentrations in paleosols may result from plant uptake whereby these elements are transported from the rooting zone (B horizon) to the former soil surface (A horizon). Deviations from this trend may be attributed to tephra inputs. For example, rhyolitic tephra layers (e.g. Kawakawa Tephra) have Ca-bearing feldspars and volcanic glass. Despite the greater number of layers and amount of tephra, and hence Ca-bearing volcanic feldspars at the Pakaututu Road site, loess at the Poraiti site has slightly higher CaO values than that at Pakaututu Road. This may relate to the lower rainfall at Poraiti (*c.*800mm/annum) where the loess is less leached and conditions conducive to the formation of pedogenic carbonates. In Chapter Nine numerous calcite rhombs of possible pedogenic origin were noted within the Poraiti loess column.

Non-metals of Groups 3A (Al_2O_3, Ga) and 4A (SiO_2, Pb) show a variety of trends, none of which relate to the presence of a paleosol. Changes in values with depth relate primarily to changes in parent material, notably the presence of tephra or organic matter.

Transition metals, as described earlier, show distinct variations in their concentrations. Maximum concentrations generally occur in the current soil and in paleosols whilst minimum concentrations appear in their loess layers (see Tables 7.1-7.4). The slightly higher transition metals concentrations within paleosols result both from the presence

of andesitic tephras and slightly higher levels of organic matter, as measured by LOI values. Andesitic tephras are rich in titanomagnetite and ferromagnesian minerals whereas organic matter fixes transition metals by adsorption or complex formation. This process tends to inhibit the translocation of these elements by soil processes.

Elements of the lanthanide or rare earth (Ce, Nd) and actinide (Th, U) series do not appear to show any obvious trends associated with the presence of paleosols.

7.4.2 Dissolution chemistry

Many of the chemical trends seen at the Pakaututu Road and Manaroa sections can be interpreted if the coverbeds at these sites are recognised as being accretionary soils. During stadials (i.e. Ohakean, Ratan and Porewan) there was rapid accretion of quartzofeldspathic loess at these sites. Tephric material derived from the TVZ during stadials was mixed or diluted by the loess. Voluminous rhyolitic eruptions such as the *c.*22 600 year B.P. Kawakawa Tephra, however, left a distinctive layer within the Ohakean loess as its accretion rate was greater than that of loess. During warmer climates (interglacials and interstadials) rates of loess accretion slowed, the landsurface was stabilised by vegetation and recognisable soils (now paleosols) developed on the loess. Tephric material settling on the landscape during this time was less prone to erosion, resulting in an accretionary volcanic succession (e.g. volcanic ashes of the Papakai, Mangamate and Bullott Formations). The high and low rates of loess accretion are considered to represent cold-warm climates respectively and are identified by loess-paleosol sequences.

At both the Pakaututu Road and Manaroa sections minima in Al_o, Si_o, Fe_p, and Al_p values correspond to tephra-poor quartzofeldspathic loess deposited during the Ohakean, Ratan and Porewan stadials. Loess accretion rates were high during these times whereas chemical weathering (i.e. soil formation) and organic matter levels were low.

Increases (maxima) in Al_o, Si_o, Fe_p, and Al_p values correspond to the Ohakean, Ratan and Porewan paleosols identified in the field (see Chapter Five) and the presence of macro- and microscopically visible andesitic and rhyolitic tephra layers (see Chapter Six). During interstadials the rate of loess accretion slowed hence vegetation became established on landsurfaces resulting in an increase in tephra accumulation rates (e.g. andesitic ashes) and in organic matter levels, as indicated by slightly raised Fe_p and Al_p levels within these horizons.

Both Fe_p and Al_p values decrease with depth, especially within the loessial units, reflecting a decrease in organic matter with depth. This indicates that pyrophosphate-extractable Fe and Al species associated with organic matter are not present in large amounts within the loess. The low to very low Fe_p and Al_p values within the loess supports the contention of its glacial or cold climate origin and the interpretation of an unstable landsurface lacking a stabilising vegetative cover.

Rhyolite tephras, unlike andesitic tephras have low ferromagnesian:felsic mineral ratios hence the low Fe_o accumulations, except for a Kawakawa Tephra sample (365cm depth) taken at the Manaroa section. Slight increases within Fe_o values, associated with andesitic tephra accessions, are evident within the Ohakean paleosol at Manaroa and the Ohakean and Porewan paleosols at Pakaututu Road but not evident within the Ratan paleosol at this section. The presence of rhyolitic tephra within the Ratan paleosol at Pakaututu Road (see section 5.4.3.3) has resulted in low Fe_o values being recorded. A further complication to weathering trends within the Ratan loess is the presence (detected only after major oxide, trace element and dissolution chemistries had been conducted) of a major andesitic eruptive period which correspond to the Middle Tongariro Ashes (Milne and Smalley, 1979; Cronin *et al.*, 1995). These ashes have raised the levels of transition elements, Fe_o, Al_o and Si_o within the Ratan loess.

The amount and composition of the dominant primary minerals within a sample, notably plagioclase, volcanic glass and ferromagnesian minerals determines the initial Al/Si ratios. Which of these variables has the predominant effect varies from site to site, especially as the relative abundances of rhyolitic and andesitic ashes in sections

change geographically. Molar ratios within the rhyolitic and andesitic tephra layers indicate the presence of Al-rich allophanes (referred to as imogolite-like allophanes, Parfitt, 1990) whereas ratios within quartzofeldspathic-rich loess ($\leq$1.0) indicate the presence of Si-rich allophanes (referred to as halloysite-like allophanes, Parfitt, 1990). Allophane and ferrihydrite contents within the Pakaututu Road and Manaroa sections are highly variable. The highest allophane and ferrihydrite contents are within the uppermost part of the Pakaututu Road and Manaroa sections which are consistent with their appreciable andesitic character. High values also correspond to paleosols, especially if weatherable andesitic ash layers are present.

The rapid weathering rates of andesitic glass (half-life of less than 300 years, Kirkman, 1975; 1980) and mafic minerals has resulted in the release of large amounts of iron into soil solution. This, in turn, has led to the over-saturation of the soil solution to the point that metastable phases like ferrihydrite are formed. Levels of ferrihydrite within the quartzofeldspathic loess are low implying that the rates of chemical weathering during stadials (e.g. Ohakean, Ratan and Porewan) were either low or not conducive to soil formation. A slight increase (0.5%) in ferrihydrite is, however, associated with the presence of Kawakawa Tephra. Ferrihydrite formation in this instance is related to the release of iron oxides produced by the weathering of rhyolitic glass.

The molar ratios determined in this study are consistent with existing models of allophane formation whereby low Al/Si ratios ($\leq$1.0) indicate the formation of halloysite within quartzofeldspathic loess and high Al/Si ratios ($\geq$2.0) the formation of allophane from andesitic tephras. This model does not, however, require allophane to be formed as an intermediary which later transforms to halloysite, as in the model of Kirkman (1975). In this study Al-rich allophanes are found to coexist with Si-rich allophanes within the Ohakean loess (compare Ohakean loess molar ratios with those of Kawakawa Tephra). The presence of allophane ranges in age from present day to 64 000 years B.P. (age of Rotoehu Tephra at Pakaututu Road section) and hereby shows the stability of allophane over this time period.

Table 7.6: Table of major oxides and trace element trends within the Pakaututu Road loess column

Trend	Oxides and trace elements
High in paleosols	TiO_2, V, Cu, Zn
Low in paleosols	Na_2O
High in andesitic tephras	TiO_2, Al_2O_3, Fe_2O_3, MnO_2, MgO, CaO, P_2O_5, LOI>loess, rhyolite tephras Sc, V, Cr, Ni, Cu>rhyolite tephras
Low in andesitic tephras	SiO_2, K_2O<loess, rhyolite tephras Rb, Ba, Zr<rhyolite tephras Pb, Rb, Sr, Th, As, Ba, Zr, Nb<loess
High in rhyolitic tephras	CaO, Na_2O>loess, andesitic tephras
Low in rhyolitic tephras	TiO_2, Fe_2O_3<loess, andesitic tephras Pb, Rb, As, Sc, V, Cr, La, Ce, Ni, Cu, Zn, Zr<loess
Variations inconclusive in: rhyolitic tephras andesitic tephras	 Al_2O_3, SiO_2, MnO_2, MgO, K_2O, P_2O_5 La, Ce, Zn, V, Cr, La, Ni

Table 7.7: Table of major oxides and trace element trends within the the Poraiti sections

Trends	Oxides and trace elements
High in paleosols	Variations inconclusive
Low in paleosols	MgO, As
High in andesitic tephras	TiO_2, Al_2O_3, Fe_2O_3, LOI, Ga, Sc, V, Cr, Ni, Cu>loess
Low in andesitic tephras	SiO_2, MnO_2, MgO, CaO, Na_2O, K_2O, Rb, Sr, Y, Ba, La, Ce, Zn, Zr<loess
High in rhyolitic tephras	Na_2O>loess
Low in rhyolitic tephras	TiO_2, Fe_2O_3<loess
High in marine sequence	CaO, K_2O, P_2O_5, Y, As, Ba, La, Ce, Zn>loess, tephra
Low in marine sequence	Ga<loess, tephra
Variations inconclusive in: rhyolite tephras marine sequence	 SiO_2, Al_2O_3, MgO, CaO, K_2O, Rb, U, V, Cr SiO_2, TiO_2, Al_2O_3, Fe_2O_3, MnO_2, MgO, Na_2O, LOI, SiO_2, TiO_2, Al_2O_3, Ni, U, V, Zn

7.5 CONCLUSIONS AND AVENUES FOR FUTURE RESEARCH

Major oxides, trace element and dissolution results have shown there is a considerable tephric component, both rhyolitic and andesitic, within the loessial soils of western Hawke's Bay. This is more pronounced within the more western parts of the district which are more proximal to the TVZ.

Major oxide and trace element studies confirm the pedological and stratigraphic subdivisions made at the reference sections in Chapter Five. Trends are, however, complicated by the addition of varying quantities of tephra (both andesitic and rhyolitic).

Major oxide and trace element analyses confirm the presence of macro- and microscopically visible tephra layers seen in the field. Trace elements, major oxides and dissolution analyses identifed an andesitic layer/s at the base of the Ratan loess at Pakaututu Road. The position of this andesitic layer corresponds to the Middle Tongariro Ashes identified within Ratan loess deposits elsewhere within the lower North Island (Milne and Smalley, 1979; Cronin *et al.*, 1995).

Tables 7.6 and 7.7 summarise the major oxides and trace element trends seen within Pakaututu Road and Poraiti sections.

Both major oxides and trace element analyses indicate compositional differences between the loess sheets at Pakaututu Road and those at the Poraiti sections. These differences relate to the amount and type of tephric inputs to the loess columns and may also reflect differences in loess source rocks. It is proposed that the loess from the Pakaututu Road section has a greater greywacke sandstone/argillite component whereas the loess at the Poraiti sections, besides a greywacke sandstone/argillite component, comprises a component from Neogene marine sequences. A further avenue of research, still to be pursued, is to obtain compositional XRF data on the major source rocks within the district. This data can then be computed by statistical techniques, such as

discriminant function analyses, to give an indication of the provenance of the different loess units at each of these sections.

Dissolution analyses indicate that the main short-range-order materials present in western Hawke's Bay soils are allophane, ferrihydrite and Al-humus complexes. These are associated with tephras, particularly the andesitic tephras (i.e. Papakai, Mangamate and Bullott Formations).

Maxima in Al_o, Si_o, Fe_p and Al_p are associated with tephra, both andesitic and rhyolitic, within the loess columns. Increases and decreases within these values cannot be attributed solely to the presence of a paleosol as tephra layers frequently coincide with paleosols which tend to overprint the pedogenic signature within the loess.

Increases in pyrophosphate-extractable Fe and Al values may be used to infer a period of stability within a landscape whereby vegetation was able to establish itself and soil organic matter able to accumulate (i.e. paleosols).

CHAPTER EIGHT:
DATING OF OHAKEAN TERRACES:
MOHAKA RIVER, WESTERN HAWKE'S BAY

8.1 INTRODUCTION

Extensive alluvial surfaces of last stadial (Ohakean) age are present adjacent to a number of rivers within the lower North Island (Te Punga, 1952; Rhea, 1968; Cowie and Milne, 1973; Milne, 1973a;b; Milne and Smalley, 1979; Kaewyana, 1980; Palmer, 1982a; Marden, 1984; Raub, 1985; Vella *et al.*, 1988; Palmer *et al.*, 1989; Warnes, 1992). Two to three alluvial surfaces are often identified within the last stadial. These are termed Ohakean 1 (Oh_1), Ohakean 2 (Oh_2) and Ohakean 3 (Oh_3) terraces, in order of decreasing height and by inference age, after Milne's (1973a;b) work on the Rangitikei River terraces in the Wanganui Basin. The dating of Ohakean terrace treads is important as it represents the time of crossing the critical power threshold as a river's operation changes from aggradation to degradation.

Milne (1973a) estimated the ages of Oh_1, Oh_2 and Oh_3 terrace treads to be 15 000 years B.P., 15 000-13 000 years B.P. and 13 000-12 000 years B.P., respectively from the thickness of the coeval Ohakean loess. These ages are based on two lines of evidence. Firstly, in the Rangitikei River Valley the base of the Ohakea loess is radiocarbon dated at 25 500$\pm$800 years B.P. (NZ3188A) and the top (NZ3165A) at 9 480$\pm$100 years B.P. (Milne and Smalley, 1979). Secondly, the Kawakawa Tephra (22 590$\pm$230 years B.P., Wilson *et al.*, 1988) is absent within Oh_1, Oh_2 and Oh_3 terrace coverbeds. The best estimates of Oh_1, Oh_2 and Oh_3 terrace tread ages were obtained by Marden and Neall (1990). They obtained radiocarbon dates of 10 350$\pm$100 years B.P. (NZ5320A) and 12 650$\pm$150 years B.P. (NZ5591A) from wood within Oh_3 and Oh_2 terrace gravels at Ballantrae, near the township of Woodville in southern Hawke's Bay. From these dates they estimated an age of *c.*18 000 years B.P. for the Oh_1 terrace tread.

Until now tephra layers within coverbeds blanketing Oh_1, Oh_2 and Oh_3 terraces have not been utilised to obtain minimum dates for their respective terrace treads. In this study an attempt was made to identify the oldest tephra chronohorizon within Ohakean terrace coverbeds by applying the various tephra "fingerprinting" techniques used in Chapter Six. Field and laboratory methods used to characterise coverbeds on Oh_1, Oh_2 and Oh_3 terrace treads are outlined and dating is discussed. Postulated differences in terrace tread ages and their consistency with the dates and chronologies obtained in other studies are also examined.

8.2 MATERIALS AND METHODS

8.2.1 Field studies

Studies were focussed on a set of Ohakean aged fluvial surfaces adjacent to the Mohaka River in western Hawke's Bay (see Fig. 1.1 for location). The identification of Ohakean-aged fluvial surfaces were based on four criteria:

1. they were the broadest, most extensive alluvial fan surfaces in the district
2. they are often paired, aggradational surfaces (using the terminology of Bull, 1991)
3. they lack Kawakawa Tephra (22 590±230 years B.P.) within their coverbeds, and
4. they have a very thin (<0.5m) alluvial silt or tephric loess (post-glacial) cover.

Sites were selected on Oh_1, Oh_2 and Oh_3 terraces along the true left bank of the Mohaka River near the Mohaka Bridge (see Fig. 1.1 for location). Grid references for the three sections chosen for further study were taken from a 1:50 000 topographic map (NZMS 260 V20 Esk). These are:

- 235 192 for the Oh_1 terrace
- 238 189 for the Oh_2 terrace, and
- 237 184 for the Oh_3 terrace.

Sections were selected at sites which had readily identifiable macroscopic tephras present. This facilitates the dating of the underlying fluvial surface. Ohakean aged fluvial surfaces observed elsewhere in the district (see section 5.3.2.3) had thinner coverbeds and lacked readily identifiable macroscopic tephra marker beds.

The subdivision of Ohakean aged surfaces into Oh_1, Oh_2 and Oh_3 terraces were based purely on their close vertical (riser) separation from one other, usually less than 2-3m. These surfaces are the last set of paired aggradational terraces, separated by marked downcutting ($\geq$30m) into the Nukumaruan country rock, until the present day river channel is reached. Numerous flights of low-lying Holocene terraces are present, commonly on meander bends close to the current flood-plain. These Holocene terraces are discontinuous and often unpaired. Aerial photographs (1:25 000 scale) were used as an aid to help delineate Ohakean surfaces in the field.

8.2.2 Laboratory studies

8.2.2.1 *Sampling and sample preparation*

Samples for laboratory analysis were bulk sampled either over a 5 or 10cm depth range. To cut down on the number of analyses samples were taken from the base of the Waimihia Tephra at the Oh_1 section and from beneath the Mangamate Tephra (grey balls of olivine-bearing andesitic tephra, refer to Chapter Six and later this chapter) within the Oh_2 and Oh_3 sections, to the alluvial silts, sands and gravels on the underlying terrace treads.

Samples for analyses were air-dried, gently crushed and then sieved to separate the coarse (>2mm diameter) fraction from the fine earth (<2mm diameter) fraction. Fine earth fractions were retained for mineralogical (volcanic glass and ferromagnesian mineral counts) and chemical (electron microprobe) analyses. To aid mineral identification all samples were chemically pretreated with 0.2M ammonium oxalate solution (Schwertmann, 1959; 1964) to remove amorphous oxide and oxyhydroxide coatings (Alloway *et al.*, 1992b). Samples for ferromagnesian mineral identification and electron microprobe analysis were concentrated by Frantz electromagnetic separation. Details of the 0.2M ammonium oxalate procedure and subsequent electromagnetic separation of samples are similar to those used in section 6.2.2.

8.2.2.2 *Mineralogical and chemical procedures*

Volcanic glass counts were conducted on 0.2M ammonium oxalate cleaned 63-125μm fractions using similar criteria to that discussed in section 6.2.3.1. This was undertaken on all samples.

Tephra fingerprinting techniques were conducted on samples from the lowermost depth increment at which a volcanic glass concentration was present. The objective was to identify the oldest tephra/s overlying each of the Oh_1, Oh_2 and Oh_3 terrace treads so minimum tread ages could be obtained.

Techniques applied on these basal samples included:

1. the identification of the ferromagnesian mineral assemblage present, and
2. the electron microprobe (EMP) analysis of volcanic glass shards.

Details about these techniques, the procedures followed along with the electron microprobe operating conditions, are similar to those used in section 6.2. The objective was to use a number of techniques to assist in resolving the identities of these unknown tephras.

Results from EMP analysis were plotted as bivariate (%CaO-%FeO) graphs, ternary (%FeO-%1/3K_2O-%CaO) diagrams, and subjected to statistical treatment (similarity coefficients and coefficients of variation; Borchardt and Harward, 1971; Borchardt *et al.*, 1971; 1972). Similarity coefficients (SC) of $\geq$0.92 and coefficients of variation (CV) of $\leq$12 for volcanic glass are defined by Froggatt (1992) as being chemically indistinguishable from that of the reference volcanic glass data-sets. Interpretations were made after comparison with:

- isopach maps and published data from the established North Island reference sites (Pullar and Birrell, 1973a;b; Froggatt and Lowe, 1990; Donoghue, 1991; Donoghue *et al.*, 1991; 1995), and
- the alluvial, loess and tephra stratigraphy of the district obtained in Chapters Five and Six.

8.3 RESULTS

8.3.1 Stratigraphy and volcanic glass counts

Of the three Ohakean terraces, the Oh_3 terraces are the least extensive and usually only seen on meander bends. The Oh_1 and Oh_2 terraces are more extensive, often paired, and seen along most reaches of the Mohaka River and other rivers within the district.

The stratigraphic units recognised overlying Oh_1, Oh_2 and Oh_3 terrace treads, along with graphs of their volcanic glass content, are depicted in Figures 8.1-8.3. Coverbeds on all three Ohakean terraces comprise:

- a dark black topsoil developed in 1850±10 years B.P. year B.P. Taupo Ignimbrite (Froggatt and Lowe, 1990) and its associated plinian eruptives. The topsoil also comprises fine andesitic ash accessions (<1mm) from the Tufa Trig and Ngauruhoe Formations (Donoghue, 1991; Donoghue *et al.*, 1995)
- a buried soil (paleosol) between the Taupo Ignimbrite and the underlying 3280±20 years B.P. Waimihia Tephra (Froggatt and Lowe, 1990)
- a buried soil (paleosol) developed on andic Papakai Formation ashes (Donoghue, 1991; Donoghue *et al.*, 1995)
- grey balls (≤10mm diameter) of andesitic ash at the base of the Papakai Formation ashes. This ash is olivine-bearing and has been correlated with the *c.*10 000-9700 year B.P. Mangamate Tephras derived from the Tongariro Volcanic Centre (see Chapters Five and Six). The Mangamate Tephra is a widespread tephra layer within western Hawke's Bay and provides a distinctive chronohorizon for inter-site correlations.
- beneath the Mangamate Tephra a further andesitic ash unit is encountered. This is correlated to the *c.*22 600-10 000 years B.P. Bullott Formation (Donoghue, 1991; Donoghue *et al.*, 1995), and
- beneath the coverbeds an alluvial fill of dominantly greywacke sandstone gravels immediately overlies mudstone and siltstone strath-cut surfaces of Nukumaruan age.

At the Oh_1 section distinctive sand and silt layers overlie the greywacke sandstone alluvial gravels. At the Oh_2 and Oh_3 sections, however, sand and silt are intermixed

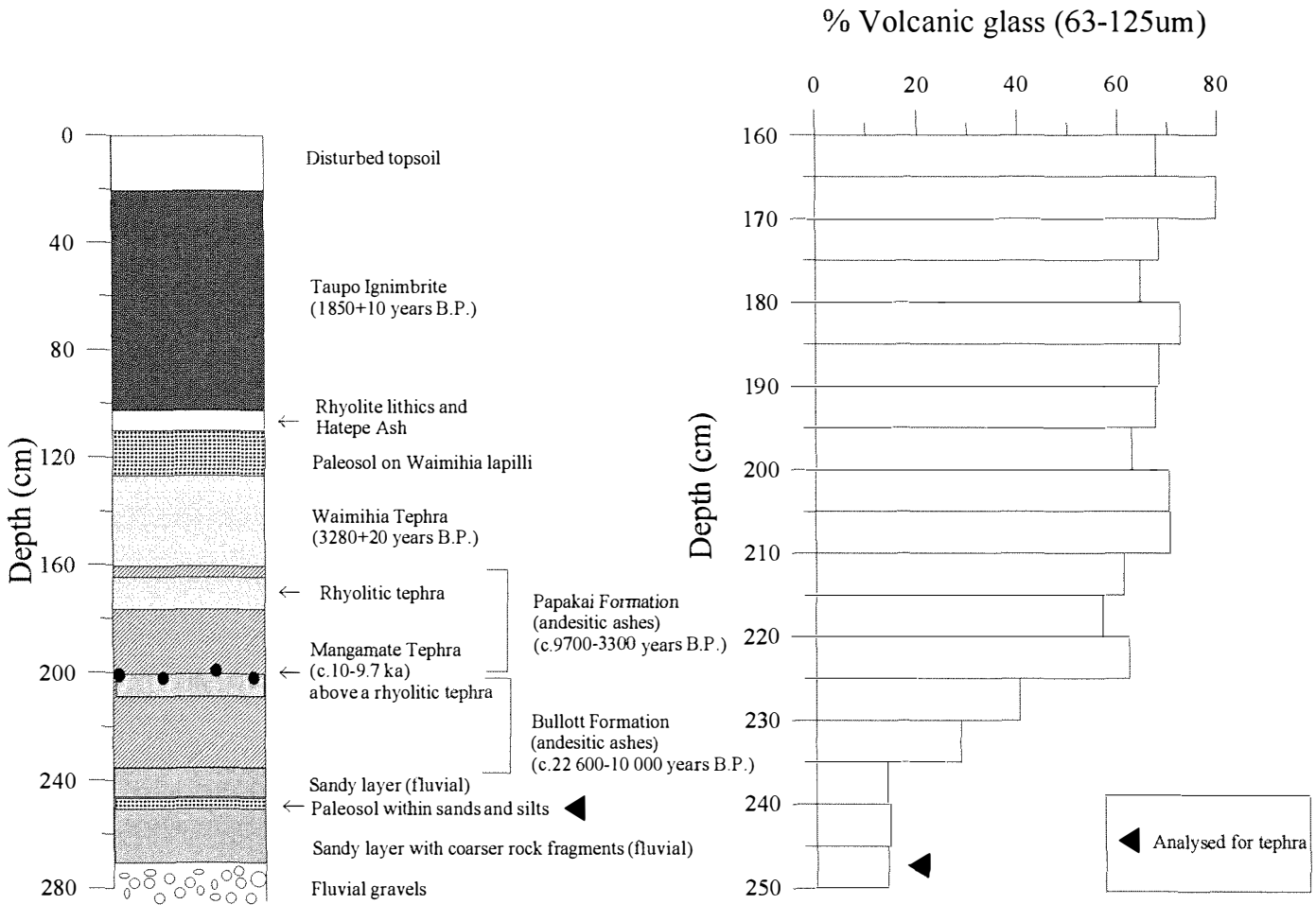

Figure 8.1: Stratigraphy and volcanic glass concentrations for the Ohakean 1 terrace (GRID REFERENCE: V20/235 192)

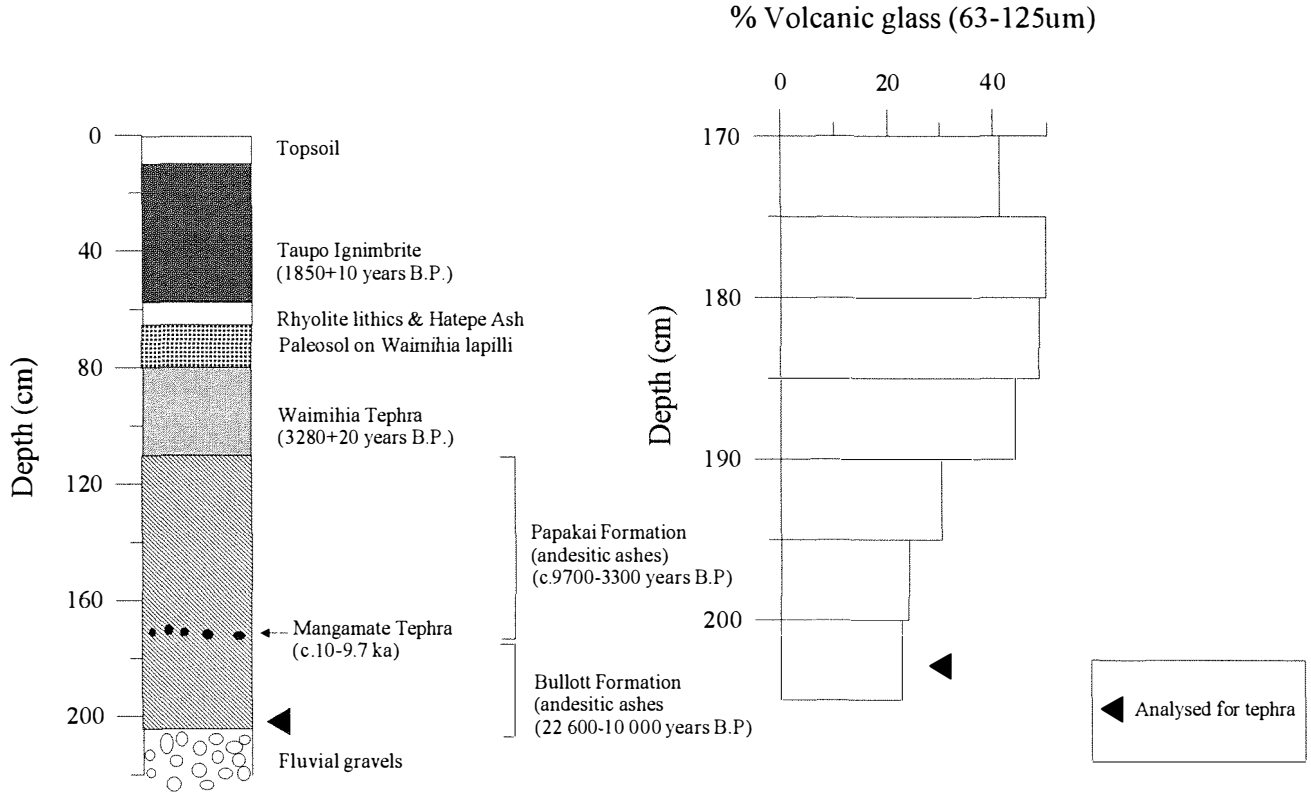

Figure 8.2: Stratigraphy and volcanic glass counts for the Ohakean 2 terrace (GRID REFERENCE: V20/238 189)

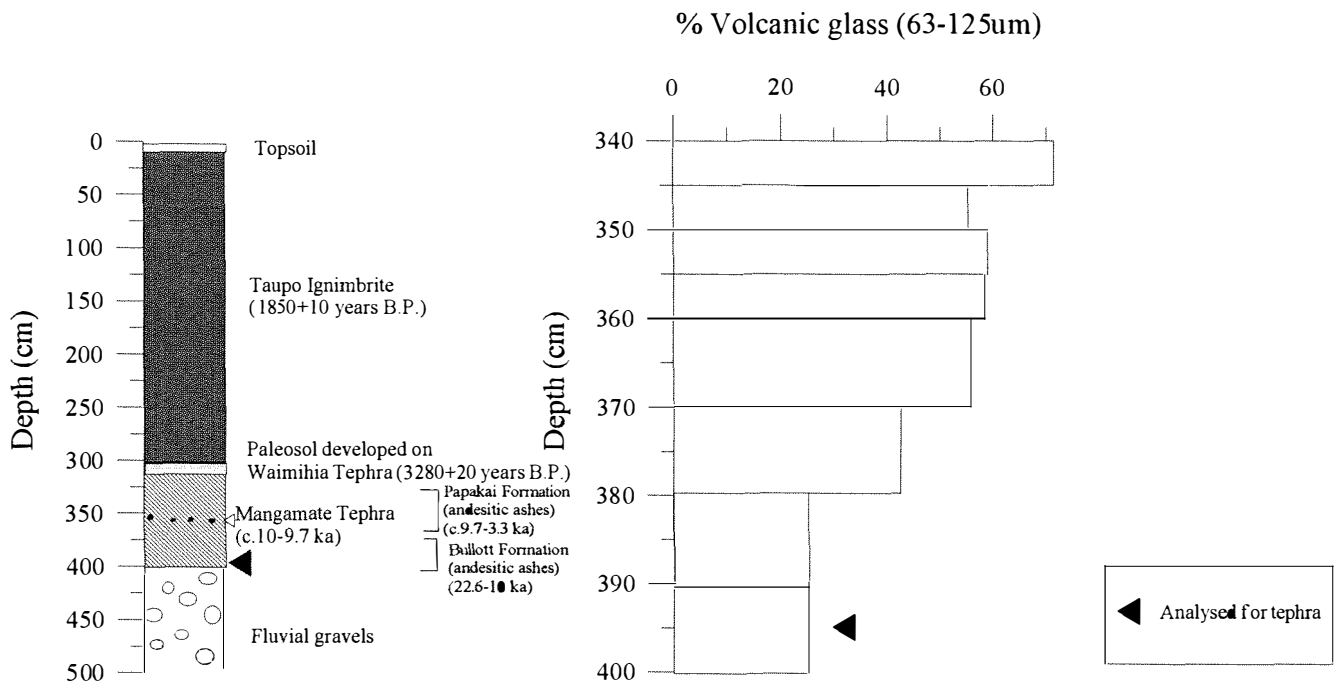

Figure 8.3: Stratigraphy and volcanic glass counts for the Ohakean 3 terrace (GRID REFERENCE: V20/237 184)

within the andic ash, as evidenced by an increasing grittiness towards the base of the Bullott Formation. These gritty andic sediments presumably are overbank sediments but some loessial or cover-sand inputs cannot be discounted. As reported in Chapter Five, silt and sand can be observed being winnowed around the Ngaruroro River floodplain on a windy day. Root channels, some minor bioturbation, and other pedogenic features associated with soil development are present in a paleosol lying on the supposed overbank and aeolian sediments. The time interval between the top of this buried soil (paleosol) and the base of the andic Bullott Formation is unknown.

The percentage of rhyolitic volcanic glass (63-125μm fraction) within the andesitic Papakai and Bullot Formations at all three sections was high (see Figs. 8.1-8.3). Volcanic glass peaks obtained at 165-175cm and 200-210cm depths in Oh_1 coverbeds correspond to two macroscopic rhyolitic tephras seen within the andic Papakai and Bullott Formation ashes, respectively (see Fig. 8.1). The most likely candidate for the rhyolite tephra in the Papakai Formation is the Whakatane Tephra (4830±20 years B.P.) and that in the Bullott Formation is either the Karapiti Tephra (9820±80 years B.P.) or the Waiohau Tephra (11 850±60 years B.P.) (see Table 3.3). These interpretations are based on the known distributions and volumes of these rhyolitic tephras and the known stratigraphic positions they occupy within the Papakai and Bullott Formations elsewhere (see Pullar and Birrell, 1973a;b; Donoghue, 1991; Donoghue *et al.*, 1995). Tephra fingerprinting was not undertaken on these tephras to verify their identities.

Good volcanic glass concentrations for electron microprobe analyses and subsequent tephra fingerprinting were obtained from the basal paleosol within the Oh_1 (14.0%) coverbeds and at the base of the Oh_2 (22.7%) and Oh_3 (22.7%) coverbeds (see Figs 8.1-8.3).

8.3.2 Ferromagnesian mineral assemblages

Ferromagnesian mineral counts conducted on samples from the base of the Oh_1, Oh_2 and Oh_3 coverbeds show a significant amount of clinopyroxene present with lesser

Table 8.1: Ferromagnesian minerals identified within samples taken from the base of the coverbeds overlying Ohakean terraces

Ohakean Terrace	Depth (cm)	% Orthopyroxene	% Clinopyroxene	% Hornblende	% Biotite	% Cummingtonite	Grains counted
Oh_1	245	12.8	76.5	7.5	3.3	-	400
Oh_2	200	4.8	86.5	5.2	3.0	0.5	400
Oh_3	390	3.5	94.5	2.0	-	-	400

Table 8.2: Sourcing of volcanic glass within coverbeds overlying Ohakean terraces

Ohakean terrace	Source of volcanic glass
Oh_1	OkVC>TpVC>MI
Oh_2	OkVC>TpVC
Oh_3	OkVC>TpVC

TpVC=Taupo Volcanic Centre

OkVC=Okataina Volcanic Centre

MI=Mayor Island

Table 8.3: Tephras within the 22 600-10 000 year B.P. age range

Tephra	Symbol	Source	Volume	Age (ka)
Karapiti Tephra	Kp	Taupo	2	9820±80
Waiohau Tephra	Wh	Okataina	18	11 850±60
Rotorua Tephra	Rr	Okataina	7	13 080±50
Rerewhakaaitu Tephra	Rk	Okataina	7	14 700±110
Okareka Tephra	Ok	Okataina	8	*c.*18 000
Te Rere Tephra	Te	Okataina	6	21 100±320
Kawakawa Tephra	Kk	Taupo	[220]	22 590±230
Oruanui Ignimbrite	Ou		150	
Aokautere Ash	Ao		70	

Reproduced from Manning (1996a).

quantities of orthopyroxene, hornblende, biotite and cummingtonite, respectively (Table 8.1). Correlation of these mineral assemblages with those from the central North Island master chronologies (Table 3.3) was attempted and are discussed in section 8.4.

8.3.3 Electron microprobe analysis of volcanic glass shards

Results from electron microprobe analysis of individual volcanic glass shards obtained from the base of the Oh_1, Oh_2 and Oh_3 coverbeds are presented in Appendices 3.12-3.14. No attempt was made to prune the data, a common feature in these studies, as there was no justification to do so.

Similarity coefficients (SC), coefficients of variation (CV), ternary diagrams (%FeO-%1/3K_2O-%CaO), and bivariate plots (%CaO-%FeO) indicate that at each of the sections the chemistry of the volcanic glass indicates derivation from more than one volcanic centre (Table 8.2).

8.4 DISCUSSION

The presence of olivine-bearing Mangamate Tephra (*c.*10 000-9700 years B.P.) and absence of a macroscopic Kawakawa Tephra (22 590±230 years B.P.) layer within any of the coverbeds indicates that the basal tephra/s on each terrace tread are between *c.*22 600 and 10 000 years B.P. Published data from all large volume tephra units which are likely to be encountered within the district and lie within this time frame-work were considered (see Table 8.3).

The elucidation as to which microscopic tephra/s are present at the base of the coverbeds is difficult as:

- both statistical treatment (CV, SC) and graphical representation (ternary diagrams and bivariate plots) of the glass shard chemistry indicates derivation from more than

Table 8.4: Variation matrix for tephras in the 22 600-10 000 years B.P. age range
Numbers above unit diagonal are SIMILARITY COEFFICIENTS, below are COEFFICIENTS OF VARIATION.

	Kp	Wh	Rr	Rk	Ok	Te	Kk
Kp*	-	0.81	0.89	0.76	0.75	0.91	0.83
Wh*	13.76	-	0.86	0.92	0.89	0.89	0.89
Rr*	9.20	11.73	-	0.80	0.78	0.93	0.88
Rk*	16.09	10.39	17.22	-	0.97	0.84	0.89
Ok*	17.48	9.23	16.49	4.12	-	0.81	0.87
Te*	12.06	7.52	6.34	14.13	13.43	-	0.89
Kk#	12.00	7.23	16.45	7.74	9.89	11.07	-

*Stokes *et al.* (1992)

#Pillans and Wright (1992)

Table 8.5: Summary of data obtained by the various tephra fingerprinting techniques

Terrace	Ca-Fe plot	Ternary plot	Ferromagnesian minerals	SC (≥0.92)	CV (<12)	Estimated age (years B.P.)
Oh_1	Kp-Wh	Kp-Kk	Ok±Rk±Rr	Rr-Ok Average: Rk	Rr-Kk Average: Rk or Rr	16 000-14 000
Oh_2	Kp-Kk	Kp-Kk	Wh-Te	Kp-Kk Average: Rr	Kp-Kk Average: Rr	14 000-11 000
Oh_3	Wh-Kk	Kp-Kk	Wh-Rr	Wh-Kk Average: Rr	Kp-Kk Average: Rr	11 000-10 000

one eruptive event and more than one volcanic centre (see Appendices 3.12-3.14 and Table 8.2)

- tephras emplaced within the 22 600-10 000 years B.P. time range have overlapping glass chemistries providing two or more possible correlatives (Table 8.4).
- the expectation that Kawakawa Tephra has been redeposited and comprises a significant component of any aeolian or water-laid post 22 600 years B.P. deposit, and
- ferromagnesian mineral counts conducted on Oh_1, Oh_2 and Oh_3 samples exhibit very high clinopyroxene numbers (Table 8.1). Samples were enriched in clinopyroxene from the Bullot Formation ashes.

Despite these difficulties the list of possible candidates can be narrowed down. Table 8.5 summarises the tephras identified by the various tephra fingerprinting techniques used in this study. Bivariate (Figs. 8.4a-c) and ternary plots (Figs. 8.5a-c) were generally of little use as they do not allow sufficient discrimination of the data.

Age estimates obtained in this study are:

- 16 000-14 000 years B.P. for the Oh_1 terrace tread
- 14 000-11 000 years B.P. for the Oh_2 terrace tread, and
- 11 000-10 000 years B.P. for the Oh_3 terrace tread.

These ages are not unequivocal but are based on the best evidence available. The evidence for a 16 000-14 000 year B.P. age estimate for the Oh_1 terrace tread is:

- the presence of volcanic glass ranging in age from the Kawakawa Tephra (22 590$\pm$230 years B.P.) to the Rerewhakaaitu Tephra (14 700$\pm$110 years B.P.). Kawakawa Tephra is known to have blanketed the district in a *c.* 1m thick mantle 22 590$\pm$230 years B.P. (Pullar and Birrell, 1973a;b). As Kawakawa Tephra is not present as a primary deposit within these coverbeds, it is likely that Kawakawa Tephra glass shards were derived from elsewhere during the last stadial.
- the predominance of Rerewhakaaitu Tephra (14 700$\pm$110 years B.P.) grains as demonstrated by a high number of SC (>0.92) and CV ($\leq$12) values.
- the presence of a paleosol on the Oh_1 terrace tread. The occurrence of a paleosol on Ohakean terrace treads (e.g. Ngaruroro River Ohakean terraces) and on last stadial

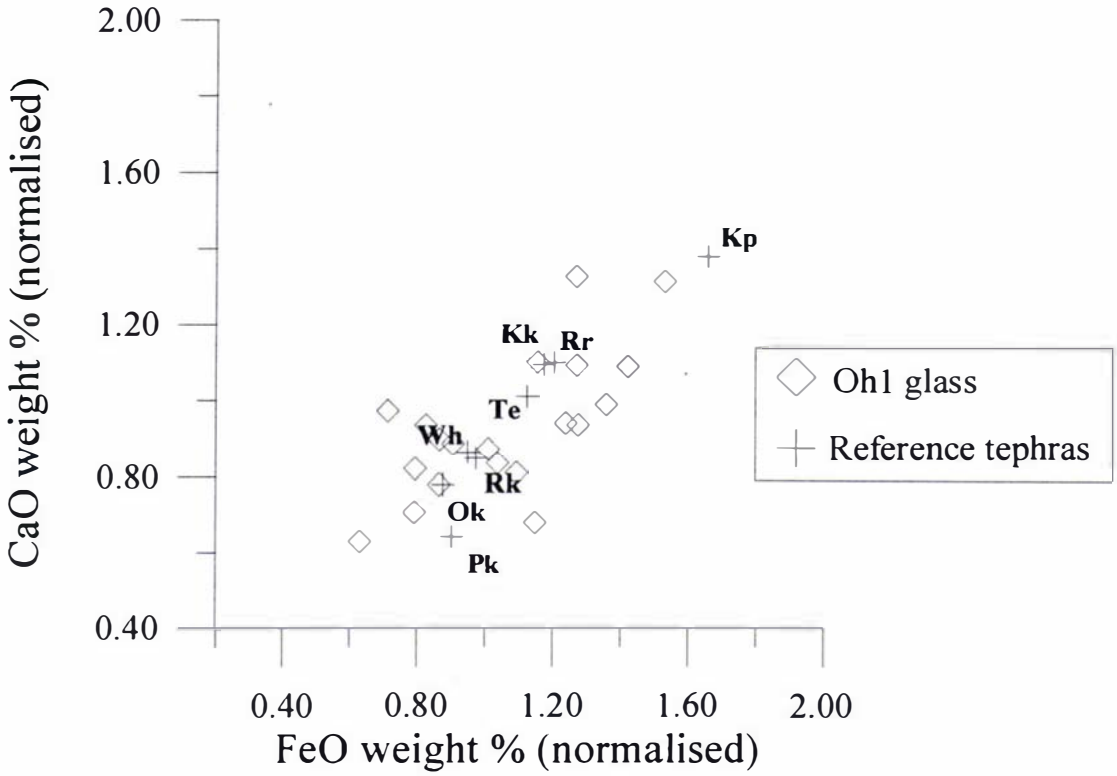
2.00
1.60
1.20
0.80
0.40
CaO weight % (normalised)
0.40
0.80
1.20
1.60
2.00
FeO weight % (normalised)
Kp
Kk
Rr
Te
Wh
Rk
Ok
Pk
Oh1 glass
Reference tephras

(a)

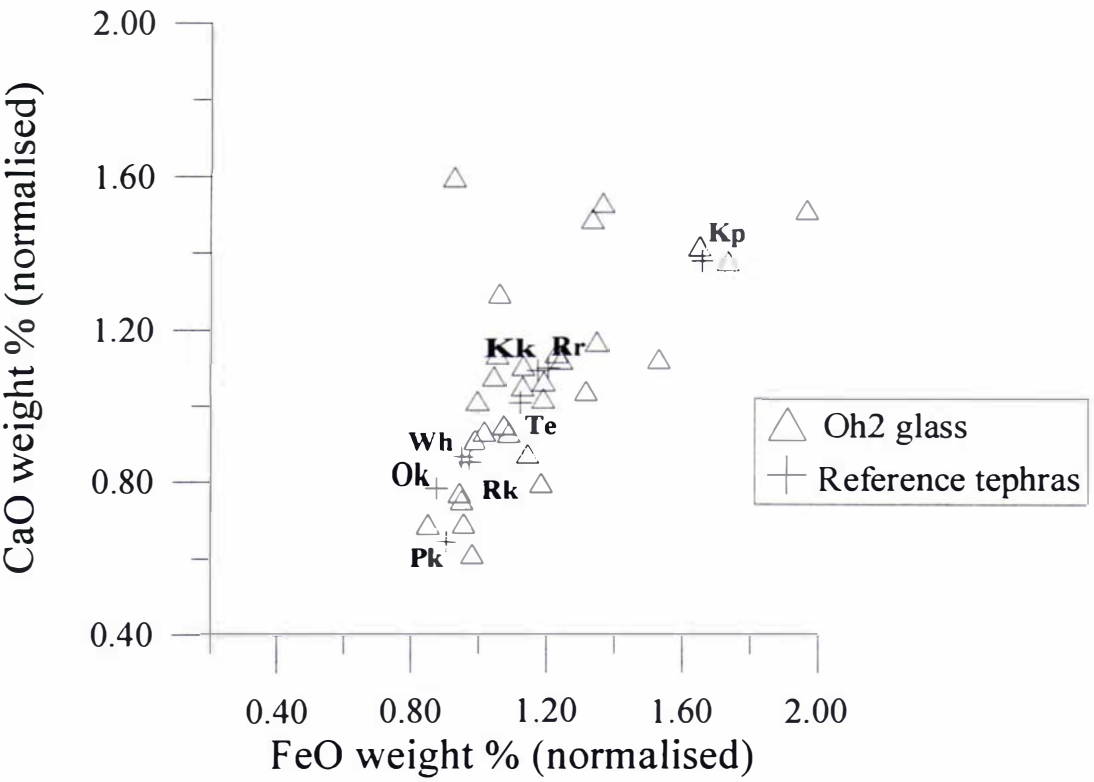
2.00
1.60
1.20
0.80
0.40
CaO weight % (normalised)
0.40
0.80
1.20
1.60
2.00
FeO weight % (normalised)
Kp
Kk
Rr
Te
Wh
Ok
Rk
Pk
Oh2 glass
Reference tephras

(b)

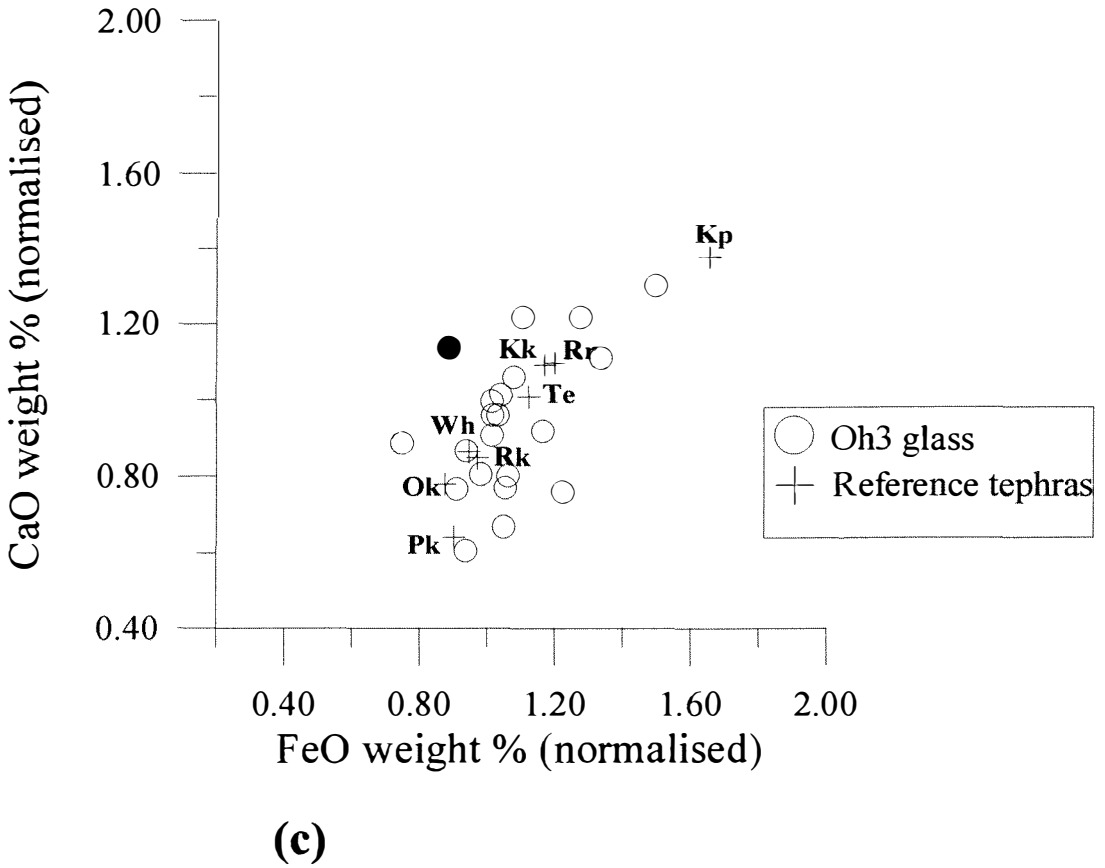

Figures 8.4a-c: Bivariate plots for silicic tephras in the 10 000 to 22 600 years B.P. age range against Oh1, Oh2 and Oh3 glass chemistries

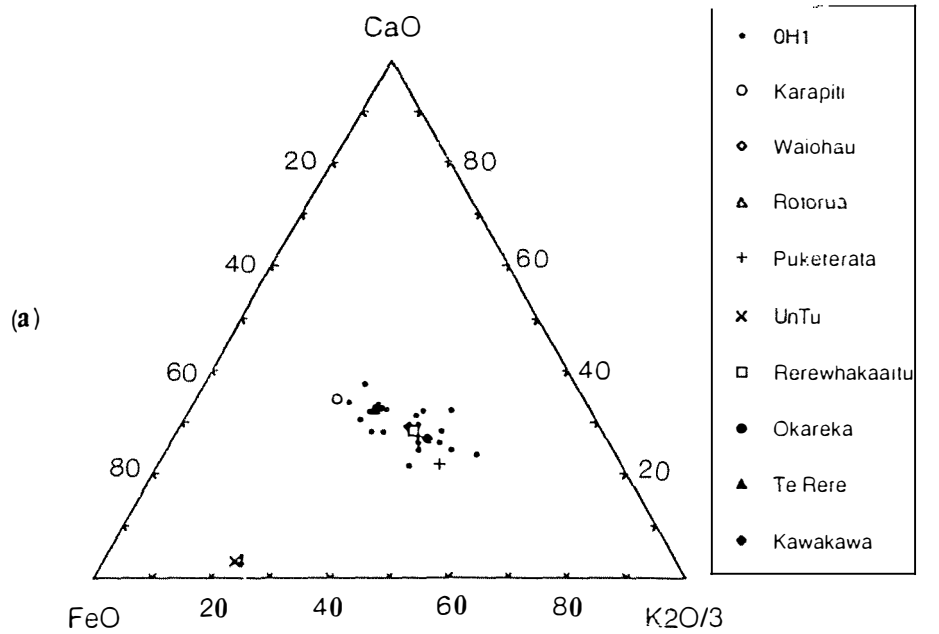

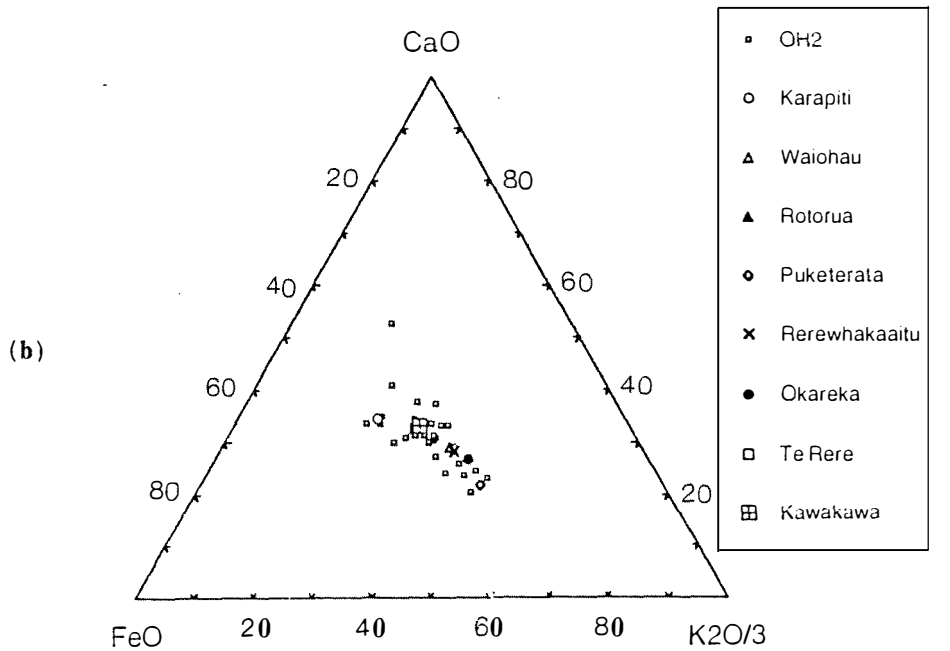

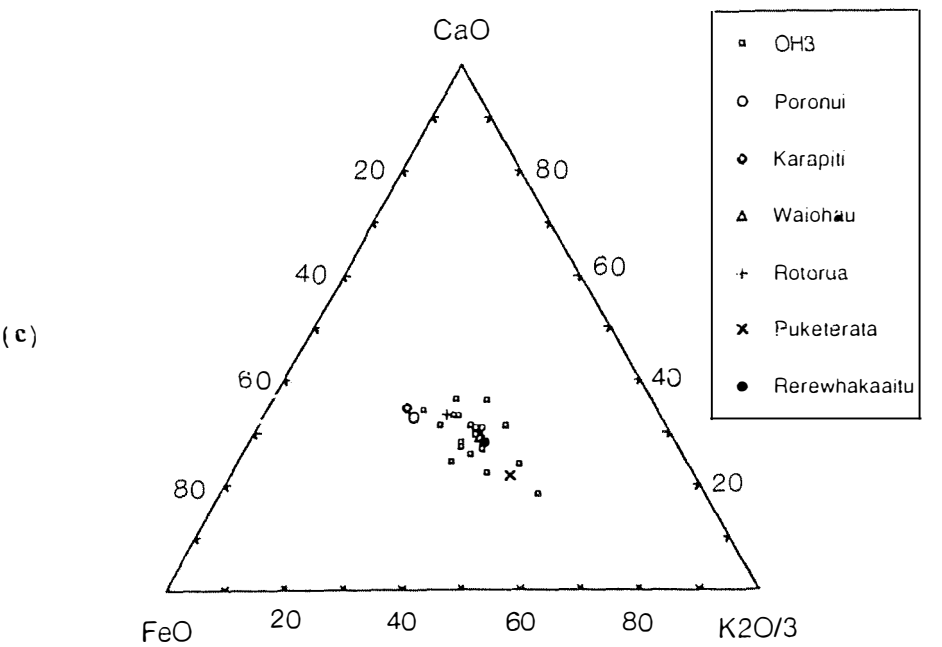

Figures 8.5a-c: Ternary diagrams of Oh_1, Oh_2 and Oh_3 volcanic glass chemistries matched against possible correlatives from Taupo Volcanic Zone reference sections.

loess is widespread in western Hawke's Bay. It denotes a hiatus, between the landscape instability associated with the last stadial and the stability of the present stadial/interglacial. This resulted in the intensification of pedogenesis and the subsequent expression of soil features. Similar findings have been reported in the Rotorua district (Kennedy, 1988; 1994). Aggradation of the Oh_1 surface ceased during this time. This was followed by incision or degradation to form the Oh_2 surface.

- the presence of two dacitic glass shards (grains 12 and 21 in Appendix 3.12). Both glass shards were matched with an unnamed tephra (untu) from Mayor Island (see Fig. 8.5). Similarity coefficient and coefficient of variation values for these two grains, however, are less than optimum (see Appendix 3.12). One possible explanation is that these grains may have shown signs of hydration which was not detected during the microprobe work.
- if the high clinopyroxene contents are ignored (contamination by andesitic ash) the Oh_1 sample indicates an assemblage 3 mineral content of: **hypersthene+hornblende+biotite** (see Table 6.1). One or more of the following tephras: Rotorua (13 080±50 years B.P.), Rerewhakaaitu (14 700±100 years B.P.) and/or Okareka (*c.*18 000 years B.P.) are thus likely to be present. As the Rotorua Tephra does not have a significant biotite load, the presence of biotite in a distal setting such as this should be significant (Dr. Bob Stewart, pers. comm. 1997). Consequently, the biotite grains seen within the ferromagnesian mineral assemblage are most likely to have been derived from the major biotite-bearing tephras within this time range, namely the Rerewhakaaitu and Okareka Tephras.

Tread ages in this study were compared with those obtained by Milne (1973a) and Pillans (1994a) for the Ohakea terrace treads adjacent to the Rangitikei River (see Table 3.1) and those along the Manawatu River by Marden and Neall (1990). Estimates of tread ages made in this study are similar to those estimated by Milne (1973a) but are at variance with those estimated by Pillans (1994a) and Marden and Neall (1990). It is argued that the ages obtained for the Oh_1 terrace tread in this study, 16 000-14 000 years B.P., are more reasonable as they correlate well with the climatic evidence (warming) at the end of the last stadial.

Stewart and Neall (1984) demonstrated that after the last glacial maxima (*c.*18 000 years B.P.) a global climatic amelioration began *c.*16 200 years B.P. Consequently, the rate of glacial erosion within the mountains decreased and river regimes changed from aggradational to degradational. The Oh_1 terrace tread should therefore mark the cross-over from a dominantly aggradational regime to a degradational one *c.*16 200 years B.P. Tephra cover beds on Oh_1 treads concur with this date. Stewart and Neall (1984) state that a poleward contraction of the prevailing westerly wind system occurred towards the end of the last stadial *c.*14 700 years B.P. This too is consistent with the field observations which show loess sheets to be either thin (<0.25m) or absent on Ohakean terraces.

The presence of Rerewhakaaitu Tephra (14 700±110 years B.P.) within the paleosol on the Oh_1 terrace tread is consistent with its occurrence elsewhere in the district and within the central North Island (Vucetich, 1968; Kennedy, 1988; 1994). This tephra commonly overlies a widespread erosion break in central North Island tephra sequences and occurs within paleosols on last stadial (Ohakean) loess. The Rerewhakaaitu Tephra is thus an important chronohorizon which marks the onset of landscape stability at the termination of the last stadial. Further support for this contention can be found in palynological studies which show forest expansion to have started in the lower North Island about this time (McGlone and Topping, 1973; 1977).

The Oh_2 and Oh_3 treads could not be easily separated in age from one another based on their glass chemistries. Similarity coefficient and coefficient of variation values (see Appendices 3.13-3.14) indicated Waiohau Tephra and Rotorua Tephra as being the youngest and most common tephras present. Older tephras present are presumed to have been reworked from older tephra sequences. The low number of Karapiti Tephra grains found in each of the Oh_2 and Oh_3 samples (1 grain each) is consistent with this being a smaller volume eruption (see Table 8.3) with samples being taken from a distal setting. It is also likely that this Karapiti Tephra glass may have been reworked from above by any one of a number of processes, for example the inversion of the bolus around a tree/shrub after it had toppled over.

The trace amount of cummingtonite present in the Oh_2 (0.5%) sample is most likely to have been derived from the Rotorua Tephra. It is considered that other cummingtonite suppliers, for example the Waiohau Tephra, Rerewhakaaitu Tephra or the Te Rere Tephra would have supplied a negligible amount, especially in a distal environment such as this (Donoghue, 1991; Dr. Bob Stewart, pers. comm. 1997). The absence of cummingtonite in the Oh_3 sample indicates that this tread post-dates the Rotorua Tephra in age. Further refinement/resolution as to which tephra/s overlies each terrace tread was not possible as the samples analysed are from sampling intervals in which mixed glass populations occur and from a distal source area which has been subjected to the effects of sedimentary fractionation and winnowing during transport. Furthermore, these microscopic tephra layers are also likely to be composite and subjected to post depositional fluvial and aeolian reworking and contamination with older tephras.

It is postulated that Oh_2 and Oh_3 terraces resulted from the removal during the post glacial (<14 000 years B.P.) of last stadial derived fluvial gravels out of the mountains and along the various reaches of the fluvial system. The movement and temporary storage of these gravels through the fluvial system would have been controlled by the migration of knick-points as the river tried to achieve a steady state. It is further postulated that the Oh_2 and Oh_3 terraces were formed by internal feedback mechanisms within the catchments rather than by external environmental changes. Once this had been achieved the river valley was subject to a period of deep incision, with minor perturbations (Holocene terraces) associated with storm events (Grant, 1985; 1996), until the river had achieved its present day river course and channel.

Dates obtained for the Oh_2 tread coincide with those dates for the Younger Dryas climatic oscillation (11.2-12Ka). Palynological and pedological studies, however, do not support the contention of a late glacial (Younger Dryas) climatic oscillation within the lower North Island (McGlone, 1995). In this study no convincing or well-dated evidence could be found for an erosion break/s denoting cold-climate erosion within western Hawke's Bay coverbeds of this age range.

8.5 CONCLUSIONS AND FUTURE AVENUES OF RESEARCH

The presence of Mangamate Tephra (*c.*10 000-9700 years B.P.) and absence of Kawakawa Tephra (22 590±230 years B.P.) helped constrain the age estimates of Ohakean terrace treads. Basal tephra/s identified at each section are greater than 10 000 years B.P. and less than 22 600 years B.P.

Ohakean terraces along a reach of the Mohaka River adjacent to the Mohaka Bridge have the following tread ages:

- Oh_1: *c.*16 000-14 000 years B.P.
- Oh_2: *c.*14 000-11 000 years B.P., and
- Oh_3: *c.*11 000-10 000 years B.P.

An age of 16 000-14 000 years B.P. for the Oh_1 terrace tread is in agreement with:

- the timing of the amelioration in global climate after the last stadial (Stewart and Neall, 1994)
- palynological evidence (McGlone and Topping, 1973; 1977; Heusser and van de Geer, 1994), and
- the presence of Rerewhakaaitu Tephra overlying a widespread erosion break in central North Island tephra and last stadial sequences (Vucetich, 1968; Kennedy, 1988; 1994).

The Oh_2 and Oh_3 terraces result from a time-lag in which last stadial erosion products were still being moved through the fluvial system *c.*14 000-10 000 years B.P. before more widespread stability could be achieved.

Oh_1, Oh_2 and Oh_3 terrace treads were dated using stratigraphy and mineralogy rather than glass chemistry. Glass chemistry was insufficient to add to the conclusions gained from stratigraphy and mineralogy.

Further research is being undertaken to use more sophisticated statistical techniques (e.g. discriminant function analysis, Stokes *et al.*, 1992; Shane and Froggatt, 1994; Cronin *et al.*, 1997) to help better resolve the identities and hence ages of the volcanic

glass at the Oh_1, Oh_2 and Oh_3 sections with those from the North Island reference sections.

CHAPTER NINE:
DURIPAN STUDY

9.1 INTRODUCTION

Indurated, massive to coarse platy pans (hard pans) immediately overlie prismatic structured fragipans within the loessial soils of Hawke's Bay. The pans impede water movement, act as an impediment to root penetration, restrict digging and tillage and are resistant to erosion. The distribution of these pans within the eastern parts of the region coincide with the loessial soils experiencing: a rainfall of 600-1000mm/annum; a seasonal water deficit and a decreasing input of volcanic ash accessions.

The hard-pans were first recognised during early soil surveys made in the district (Pohlen *et al.*, 1947) but were interpreted as being part of the fragipan which had been case-hardened and did not soften, even under prolonged wetting (Taylor and Pohlen, 1979). During the late 1970's and early 1980's the concepts and criteria of the American soil classification "Soil Taxonomy" (Soil Survey Staff, 1975; 1994) were applied to a range of New Zealand soils. Blakemore (1982) demonstrated that hard-pans, within the Pallic Soils (formerly classified as central yellow-grey earths) of Hawke's Bay, are cemented. Unlike fragipan horizons they do not slake or fracture when placed in water. In Blakemore's study the cemented horizons were shown to have properties similar to those of duripan horizons described within Soil Taxonomy. Until now, no further work was undertaken to elucidate the composition of the material making up the cement nor the mechanism/s for its emplacement.

The current New Zealand Soil Classification (Hewitt, 1992) recognises a duripan as a diagnostic horizon within the Pallic Soils of New Zealand. It defines a duripan as a: *subsurface horizon that is cemented by silica or other opaque or uncoloured material and has all of the following requirements, but does not meet the requirements of a*

calcareous horizon:

1. *dry fragments do not slake in water, even during prolonged wetting, and*
2. *it does not react visibly with 10% HCl, and*
3. *the average lateral distance between any fractures is 100mm or more.*

Furthermore, it states that duripans are: *recognised where the cementing materials are apparently related to the presence of siliceous tephra in the parent material or high exchangeable sodium in the soil.*

No thorough New Zealand study of the distribution and properties of indurated horizons has been reported beyond the field definitions and criteria used to identify duripan horizons in the current New Zealand soil classification system. The focus of this study is to: characterise some of the morphological, physical, chemical and mineralogical properties of a typical Hawke's Bay duripan; to deduce the nature of the cementing agent/s involved; and to determine whether the mechanism/s for duripan formation, alluded to in the current New Zealand soil classification (Hewitt, 1992), are valid.

9.2 MATERIALS AND METHODS

9.2.1 Site selection and field studies

The impetus to undertake a study of duripans within the soils of Hawke's Bay arose during the course of field work to elucidate the late Quaternary coverbed stratigraphy of the region. Numerous road-cuts were investigated and described in order to ascertain the areal distribution and range of properties within duripan horizons. Road-cuts were the best sites for description and sampling as digging with hand-tools into the cemented subsoils was difficult.

The Poraiti reference site (Poraiti #1 and #2 sections, see Chapter Five) was selected to conduct detailed field and laboratory analyses because not only does it have a number of well developed duripans within its various loess layers but also because extensive field, chemical and mineralogical data have already been obtained from this site which may aid interpretations. Details are available in Chapters Five to Seven and in the

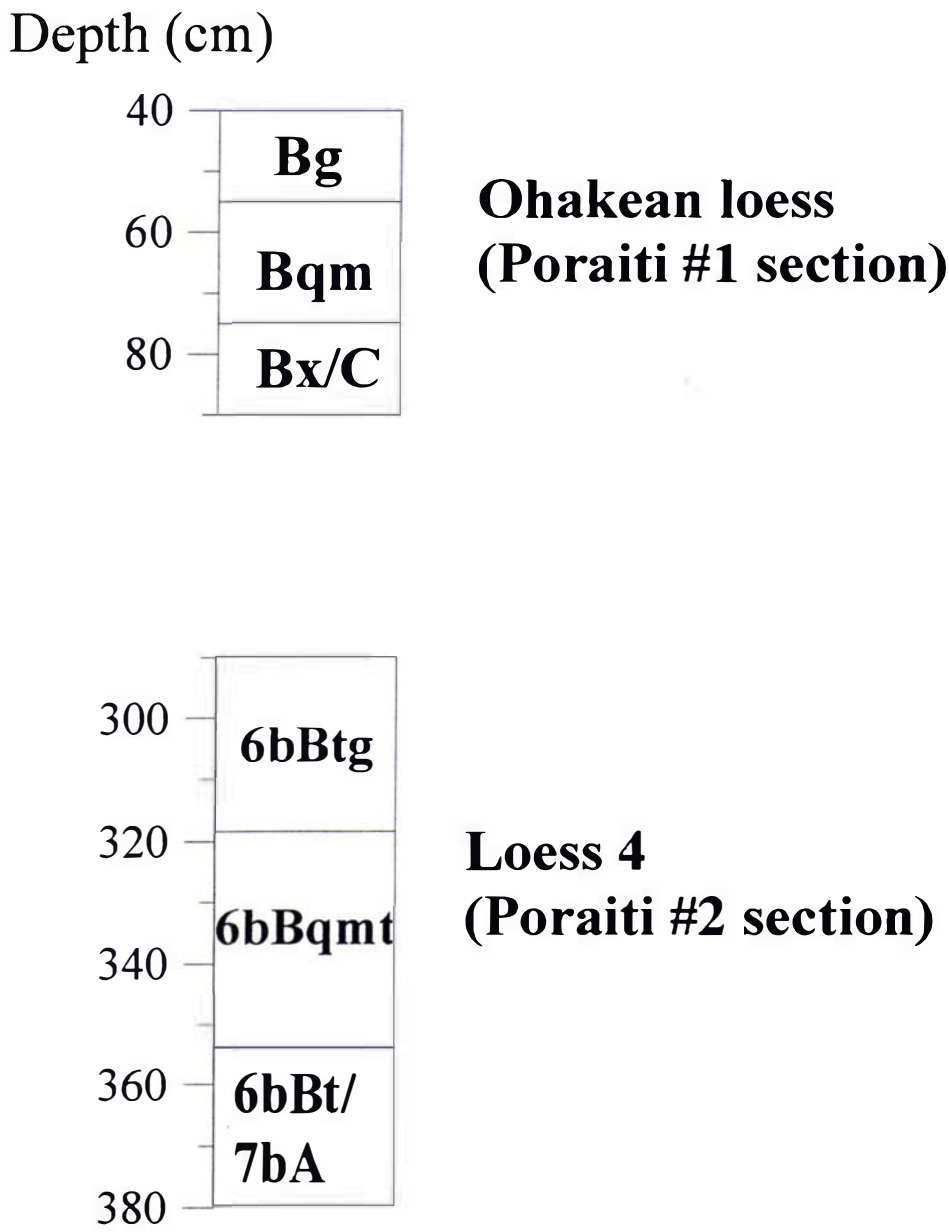

Figure 9.1: Horizonation of Ohakean (upper) and Loess 4 (lower) duripans and their enclosing horizons. Note the depths for the soil horizons within Loess 4 are taken from the base of the Kawakawa Tephra (=0cm)

Appendices. A detailed morphological description of the soil properties at this site is available in Appendix 1.

Samples for laboratory analyses were taken from horizons immediately above, within and below the duripan (Bqm horizon) in the Ohakean (Loess 1) and Loess 4 loess sheets (Fig. 9.1). These horizons are also referred to as the "upper" or "lower" duripans, respectively. Comparisons were then made between the two duripan horizons and the non-cemented horizons enclosing them and also between the two duripans, so as to ascertain a possible mechanism for their genesis. Methods of field sampling and sample preparation, prior to laboratory analyses, are similar to those outlined in Chapter Five.

9.2.2 Laboratory studies

9.2.2.1 *Methodology*

The choice as to which analytical techniques to use to characterise quantitatively the duripans of Hawke's Bay and hence offer a possible explanation to their formation, were made taking into account Blakemore's (1982) recommendations for further study, as well as studies conducted on similar soil horizons overseas (Flach *et al.*, 1969; 1974; McKeague and Sprout, 1975; McKeague and Protz, 1980; Chadwick *et al.*, 1987a;b; 1989; Blank and Fosberg, 1991). These studies have utilised a range of analytical techniques to characterise the cement, a presumed amorphous aluminosilicate binding agent, and have emphasised the distinctness of duripan horizons from those of their overlying and underlying horizons.

In this study analyses were undertaken to:

1. verify that these horizons are cemented and hence meet the requirements of a duripan horizon within the current New Zealand Soil Classification (Hewitt, 1992)
2. evaluate the role of amorphous components, principally forms of Fe, Al and Si in effecting bonding between soil particles within duripan horizons. Standard chemical dissolution techniques were undertaken to extract the amorphous compounds

because coatings are too thin to be analysed morphometrically. Values were then contrasted with those obtained from overlying and underlying horizons

3. describe the physical and mineralogical arrangement of the various components within the duripan. Mineralogical descriptions involving conventional petrographic observations were coupled with scanning electron microscopy (SEM), energy dispersive x-ray analysis (EDXRA) and electron microprobe (EMP) analysis to study the nature and composition of the cement within the duripans.

9.2.2.2 *Chemical and physical procedures*

Slaking and soil pH

Air-dry clods were immersed in water. Their degree of slaking/non-slaking was recorded over a 24 hour period. Samples were then taken from the Ohakean (60cm depth) and Loess 4 (330cm depth) duripans and immersed in: 10% HCl; hot, concentrated KOH; and a mixture of HCl and KOH. The purpose of this was to see whether the samples conformed to the diagnostic horizon criteria listed for duripan horizons within the New Zealand (Hewitt, 1992) and American soil classifications (Soil Survey Staff, 1975; 1994; Thomas *et al.* 1979). Slaking is considered one of the key criteria for differentiating between non-cemented (i.e. fragipans) and cemented (duripans) horizons.

Soil pH measurements were made above, within and below the duripans on a 1:2.5 (soil:water) suspension (Blakemore *et al.*, 1987).

Soil physical procedures

Bulk densities of the duripans and their enclosing horizons were determined by the clod method on air-dry samples and reported on an oven dry basis (Blake and Hartge, 1986; Houghton *et al.*, 1988), after corrections for gravimetric water content. The clods were coated in a water repellent (silicone-based) aerosol and weighed first in air and then whilst immersed in water. The spray is assumed to contribute negligible mass and volume to a clod.

Other soil physical parameters measured were: particle density; gravimetric water content; and pore space ratios (PSR) using laboratory methods provided by Dr D.R. Scotter, Soil Science Department, Massey University.

Dissolution chemistry

Extracts from various alkali and acid solutions may be used to characterise amorphous mineral colloids within soils. Three procedures in common practice are:

1. the acid ammonium oxalate procedure of Schwertmann (1964) to extract poorly ordered (short-range-order) oxides and hydroxides;
2. the sodium citrate-bicarbonate and sodium dithionite (CBD) procedure of Mehra and Jackson (1960), as modified by Whitton and Churchman (1987), to extract both crystalline oxides and x-ray amorphous (poorly crystallised) silicates;
3. the hot 0.5M NaOH procedure of Hashimoto and Jackson (1960), after CBD extraction above, to extract poorly crystalline, opaline silica (SiO_2) and aluminium hydroxy compounds.

All extracts were analysed for Fe, Al and Si. Extractable-Si was determined colorimetrically by the molybdate method of Weaver *et al.* (1968) and extractable-iron and aluminium contents by atomic absorption spectrophotometry (AAS). Standard curves were based on standards with similar matrices.

X-ray fluorescence (XRF) analyses

Major element distributions across the duripan horizons were performed by XRF. Details of the procedures used are presented in Chapter Seven.

9.2.2.3 *Mineralogical procedures*

Petrography

Microscope studies have been undertaken on the fine sand fraction (63-125μm) to elucidate the mineralogical composition of the loess and tephra layers within the Poraiti reference sections and are reported in Chapter Six. The identification and

quantification of the amount of volcanic glass and type of ferromagnesian minerals present within the Ohakean and Loess 4 duripans and their enclosing horizons were made on grain mounts by the point count method using a petrographic microscope. Details of the procedures followed and results obtained are reported in Chapter Six.

Scanning electron microscopy (SEM) and energy dispersive x-ray analysis (EDXRA)

Scanning electron microscopy was undertaken on clod samples. This provides greater detail of specific features and a three-dimensional view of natural aggregates. Clod samples from above the Ohakean duripan (50cm depth), within the Ohakean duripan (60cm depth) and from within the Loess 4 duripan (330cm depth) were coated with a layer, a few Angstroms thick, of gold for SEM studies and carbon for EDXRA.

Photomicrographs were taken of the cementing material that formed bridges between mineral grains, around pores and voids and at grain-to-grain contacts at a series of magnifications, from 150 to 4000x. Features were identified by making use of an SEM soil interpretation atlas (Smart and Tovey, 1981). Semi-quantitative characterisation of the cementing material was undertaken by EDXRA.

Electron microprobe (EMP) analysis

Undisturbed ped and clod samples from the duripans were impregnated with epoxy resin for thin section preparation. Quantitative chemical analyses of the cement were then undertaken by EMP. Operating conditions for the EMP are outlined in Chapter Six, except that the electron beam was narrowed to 2-3μm.

X-ray diffraction (XRD) and differential thermal analyses (DTA)

Prior to XRD and DTA analyses, samples were subject to CBD pretreatment to remove iron oxide coatings and then to ultrasonic dispersion to maximise clay removal from the coarser particles (Whitton and Churchman, 1987). X-ray diffraction traces were obtained using the methods and machine operating conditions outlined in Whitton and Churchman (1987) to determine the presence and quantity of mica, vermiculite, chlorite, smectite and other interstratified minerals.

Plate 9.1: A typical Pallic Soil within Hawke's Bay. Note the coarse platy duripan (Bqm horizon) overlying a prismatic-structured fragipan (Bx horizon). (U21/080 738).

9.3 RESULTS AND DISCUSSION

9.3.1 Field characteristics

9.3.1.1 *General field occurrences and observations*

As one progresses eastwards, across Hawke's Bay, towards the lower rainfall areas (<1000mm/annum) of the Heretaunga and Takapau-Ruataniwha Plains, a hard, apparently cemented horizon (duripan or Bqm horizon), emerges within the Pallic Soils at the same time as did the fragipan horizon (Bx). The hard, apparently cemented horizons, common within the Poporangi and Matapiro soil sets, are conspicuous by their protruding, massive or coarse platy structures which in turn overlie columnar or prismatically structured fragipans (Plate 9.1). The appearance of a duripan in the eastern parts of the study area also coincides with a seasonal moisture deficit and a thinning of rhyolitic and andesitic tephra accessions. Holocene andesitic tephra beds form a distinctive layer overlying the upper (Ohakean) loess unit in the western parts of the district but merge with the upper horizons of the Ohakean loess in the east (see Chapter Five).

A typical profile consists of a Bg or Btg horizon overlying a duripan (Bqm) which in turn overlies a fragipan (Bx). This sequence may repeat itself a number of times within a section, depending on the number and thickness of loess layers present. Duripans usually have an abrupt upper boundary to the overlying Bg or Btg horizon and a diffuse boundary with the underlying fragipan. Prominent coatings cap or cement the upper boundary of the duripan. Cementation is usually strongest at a duripan's upper boundary or a few centimetres below it and decreases gradually with depth within any one loess sheet or layer. Duripan colour/s usually differ little from that of their enclosing horizons (see Appendix 1).

Duripans appear not to be penetrated by roots. Root mats are frequently seen growing on top of the pan or down the cracks separating overlapping cemented pans and into the polygonal cracks within the underlying fragipan. Root pseudomorphs are common within many of the duripans and possibly relate to a period when the soil was less indurated and hence conducive to root extension. Duripans are impermeable to water

as seen by it seeping out laterally along road-cuts or along prism faces after rainfall. The size, contrast and abundance of mottling increases towards the lower part of the Bg or Btg horizon. This denotes a seasonal perching of the water table. No evidence of reduction is, however, present at the interface of the duripan and the overlying B horizon. This is probably because once downward moving water encounters a duripan, it is deflected laterally outwards and downslope in response to the hydraulic gradient. Some of the water is also subject to evapotranspiration and upward capillary movement.

Morphologically there appears to be a continuum of properties between a duripan and a fragipan. Morphological differences between duripan and fragipan horizons are limited primarily to structure, consistence and brittleness characteristics. Duripans differ principally from fragipans in that they have: a platy structure; a very firm or extremely firm moist consistence; and are always brittle, even after a prolonged period of saturation by rain in winter.

A number of degrees of cementation occur in subsoils, making it difficult to decide whether a subsoil horizon is sufficiently hard to be designated as a duripan i.e. different degrees of cementation in soils of different texture. An example of this may be seen in the so-called "incipient pans" within massive, shower-bedded Kawakawa Tephra. These pans are readily broken by hand, more easily than pans from within the finer textured loess and tephra.

Immediately above each duripan there is an increase in clay content. This increase may result from decreased permeability after the duripan has formed, or it may be an essential requirement for the formation of more strongly developed fragipans and duripans. Argillic horizons are common immediately above the duripan, especially within the pre-Ohakean loess layers. Such horizons exhibit subangular blocky structures, have clay coatings and a clay-loam texture. They are generally more intensely mottled than the underlying duripan and fragipan thus indicating a perched water table. Clay coatings may continue into duripan and fragipan horizons. The lower zones of fragipans commonly have silt loam textures.

Table 9.1: Soil classification and site factors at the Poraiti reference site (V21/398 837)

Soil and classification	Annual rainfall Climatic class	Parent material	Topography (Altitude, slope and aspect)	Past vegetation	Present vegetation
Matapiro silt loam. A moderately leached Pallic Soil (central yellow-grey earth)	840mm Subhumid mesothermal 1	Moderately weathered Pleistocene loess and tephra over fossiliferous Neogene marine silts and muds	150m *c.*10° southeast	Broadleaved forest or fernland	Grasses and pasture

Particle size analyses were not conducted on the duripans because harsh chemical pretreatments would be needed to remove the cement and the resultant particles might not reflect the original particle size distribution, instead being an artefact of the pretreatment procedures.

The upper boundary of the Ohakean duripan is commonly 50-80cm from the surface. The rooting depth of trees growing on these surfaces is shallow, so such trees are liable to windthrow. Duripans do restrict the erosion or dissection of geomorphic surfaces by forming a base level to which ephemeral streams can incise to, hence they have strongly influenced landscape evolution within the Pallic Soils of Hawke's Bay.

9.3.1.2 *Field characteristics and observations made at the Poraiti reference section*

The Poraiti reference site comprises five loess layers or sheets, each of which is intercalated by varying thicknesses of andesitic and rhyolitic tephra originating from the Taupo Volcanic Zone (TVZ) and Egmont Volcano. Each loess layer is separated by a paleosol which denotes a still-stand in loess deposition and a period of marked pedogenic horizon differentiation. A detailed stratigraphy of the various coverbeds, the timing of their deposition, and a description of the soil horizons and soil morphological properties are discussed in Chapters Five and Six. Table 9.1 summarises the main soil and site factors at the Poraiti reference site.

The Loess 4 loess sheet is different in that it does not have a fragipan underlying the duripan. The duripan, however, is very well cemented. One possible interpretation is that the fragipan has become so cemented over time (it has undergone weathering during and since the Last Interglacial) that it has acquired the morphology and properties of a duripan.

Besides a massive to coarse platy soil structure, duripans are characterised by their consistence properties. These are: a very strong to rigid soil strength, a brittle characteristic failure, and strong cementation. Stickiness and plasticity ratings could

Table 9.2: Slaking characteristics of air-dry clods over time, after immersion in water. Duripan samples are in bold type

Depth (cm)	5 minutes	2 hours	24 hours
40	0	1	2
50	0	0	1
60	**0**	**0**	**0**
70	**0**	**0**	**0**
80	0	0	0
90	0	0	1
290	1	3	4
300	4	4	4
305	1	2	3
310	4	4	4
320	**0**	**0**	**0**
330	**0**	**0**	**0**
340	**0**	**0**	**0**
350	**0**	**1**	**1**
360	1	2	2
370	2	3	4

0=no slaking

1=minor fissuring

2=marked fissuring and minor disintegration of clod

3=marked fissuring and major disintegration of clod

4=total disintegration of clod

not be estimated due to the very strong cementation of the duripans. The degree of cementation increases within the older duripans which have experienced greater periods of weathering.

9.3.2 Laboratory characterisation

9.3.2.1 *Presentation of data*

The Poraiti reference site comprises two overlapping sections, Poraiti #1 and Poraiti #2 (see section 5.4.3.3). The reporting and rating of results follow the recommendations of Blakemore *et al.* (1987). However, no ratings are available in Blakemore *et al.* (1987) for CBD extractable-Si and NaOH extractable-Fe, -Al and -Si, so terms like "higher" and "lower" are used for comparative purposes. Dissolution chemistry results are prefixed by the extractant used. For example: Fe_o is acid ammonium oxalate extractable-iron; Fe_d is CBD extractable-iron; and Fe_{NaOH} is sodium hydroxide extractable-iron.

All slaking, pH, chemical dissolution and physical analyses were performed in duplicate and the mean value presented.

9.3.2.2 *Chemical and physical characterisation*

Slaking experiments

Results from the immersion of air-dry clods in water are presented in Table 9.2. These indicate that duripan horizons (Bqm and 6bBqmt) recognised in the field are indeed cemented as they do not slake in water, even after prolonged saturation (24 hours).

Clods from the overlying B horizons (Bg and 6bBtg horizons in the Ohakean and Loess 4 loess sheets, respectively) and underlying horizons (Bx/C and 6bBt/7bA horizons) do, however, slake when immersed in water. Slaking characteristics are more pronounced between duripans and their overlying horizons than between them and their underlying

Table 9.3: Soil chemical attributes of the Ohakean and Loess 4 duripans at the Poraiti reference site. Duripan samples are in bold type.

Depth (cm)	% Glass	pH (H_2O) (1:2.5)	% Fe_o	% Al_o	% Si_o	% Fe_d	% Al_d	% Si_d	% Fe_{NaOH}	% Al_{NaOH}	% Si_{NaOH}
40	11.7	6.1	0.14	0.11	0.00	0.21	0.07	0.62	0.15	2.3	4.6
50	7.2	5.5	0.08	0.11	0.00	0.21	0.06	0.63	0.10	1.4	2.6
60	**4.2**	**4.8**	**0.09**	**0.14**	**0.00**	**0.22**	**0.07**	**0.66**	**0.09**	**1.1**	**2.2**
70	**6.7**	**4.9**	**0.11**	**0.15**	**0.00**	**0.29**	**0.07**	**0.63**	**0.19**	**1.4**	**7.0**
80	7.7	5.2	0.12	0.11	0.00	0.41	0.06	0.59	0.14	0.99	3.7
90	36.2	4.7	0.12	0.09	0.00	0.41	0.04	0.55	0.10	0.95	2.0
290	1.7	6.6	0.05	0.03	0.09	0.42	0.04	0.29	0.15	1.6	4.2
300	0.5	6.4	0.06	0.06	0.12	0.12	0.05	0.33	0.14	2.1	6.3
305	0.7	6.6	0.10	0.05	0.03	0.67	0.03	0.35	0.17	1.5	8.3
310	0.5	6.5	0.06	0.05	0.10	0.24	0.04	0.16	0.21	1.9	10.9
315	2.2	6.6	0.06	0.04	0.00	0.37	0.02	0.38	0.16	1.1	7.3
320	**2.5**	**6.5**	**0.05**	**0.05**	**0.12**	**0.40**	**0.02**	**0.43**	**0.15**	**0.89**	**6.8**
330	**9.2**	**6.4**	**0.04**	**0.06**	**0.13**	**0.28**	**0.03**	**0.40**	**0.21**	**1.8**	**13.7**
340	**4.5**	**6.6**	**0.03**	**0.05**	**0.12**	**0.36**	**0.02**	**0.39**	**0.18**	**1.2**	**7.8**
350	**0.7**	**6.8**	**0.03**	**0.03**	**0.03**	**0.26**	**0.02**	**0.40**	**0.17**	**1.2**	**6.5**
360	2.5	6.9	0.03	0.05	0.07	0.18	0.01	0.36	0.14	1.3	5.9
370	3.0	6.7	0.03	0.05	0.09	0.22	0.02	0.43	0.18	1.5	5.5

Table 9.4: Soil physical properties of the Ohakean and Loess 4 duripans at the Poraiti reference section. Duripan samples are in bold type.

Depth (cm)	Particle density gcm^{-3}	Grav. water	Bulk density gcm^{-3}	PSR
40	2.68	0.029	1.68	0.37
50	2.67	0.030	1.74	0.35
60	**2.69**	**0.035**	**1.71**	**0.36**
70	**2.65**	**0.034**	**1.70**	**0.36**
80	2.64	0.028	1.69	0.36
90	2.70	0.024	1.60	0.41
290	2.68	0.032	1.89	0.29
300	2.80	0.057	1.77	0.37
305	2.71	0.047	1.65	0.39
310	2.70	0.056	1.75	0.35
315	2.33	0.047	n.d.	n.d.
320	**2.57**	**0.046**	**1.74**	**0.32**
330	**2.60**	**0.043**	**n.d.**	**n.d.**
340	**2.63**	**0.036**	**1.85**	**0.30**
350	**2.64**	**0.039**	**1.86**	**0.30**
360	2.65	0.055	1.80	0.32
370	2.70	0.059	1.79	0.34

n.d.= not determined. This was due to insufficient sample left for analyses.

horizons. Fragipan horizons, unlike duripans, are not cemented because they do slake after prolonged soaking.

Duripan horizons do not slake when immersed in 10% HCl, even after prolonged soaking (24 hours) but do exhibit minor slaking when immersed in hot, concentrated KOH or in alternating acid and alkali (10% HCl and KOH). This is consistent with the key criteria for duripan identification described in Soil Taxonomy (Soil Survey Staff, 1975; 1994; Thomas *et al.*, 1979). Overseas studies (e.g. Flach *et al.*, 1974) have shown the cementing material in duripans to be amorphous Fe, Al and Si oxides and hydroxides.

Further quantification of slaking may be helpful in differentiating between fragipan and duripan horizons as there appears to be an overlap in properties between the two horizons, especially where loess sheets are thin.

Soil pH

All of the horizons measured were acidic (Table 9.3). The duripan horizon within the Ohakean loess is strongly acidic whereas that within Loess 4 is only slightly acidic to near neutral, a natural consequence of establishment of equilibrium at depth. Within the Ohakean loess (40-90cm) pH decreased with depth, rising only slightly at the duripan/fragipan boundary (70-80 cm) and then falling again within the underlying fragipan. Soil pH values within Loess 4 do not vary appreciably with depth (pH values 6.4-6.6) but increase slightly at the boundary between the duripan and the underlying horizon. Overall, pH values for duripans are not markedly different from those of non-duripan horizons. In summary, the pH has equilibrated in Loess 4 whereas in the Ohakean loess soil formation is ongoing.

Physical analysis

The physical properties of the Poraiti section are shown in Table 9.4. Bulk density values for all samples were high (1.60-1.89gcm^{-3}), confirming the close-packing observed within the soil horizons. The highest bulk density values within the Ohakean loess are from immediately above the duripan (50cm). Values are slightly lower within

the Bqm and Bx horizons. Bulk density values for Loess 4 are also high, yet no major contrast occurs between non-cemented and cemented horizons. The values obtained, however, are complicated by both the addition of andesitic tephra, which tend to lower bulk density values, and the loading of 5-6 metres of loess above.

Gravimetric water contents are slightly higher within the better structured, clay-rich B horizons than within duripans. This relates partially to water adsorption by the clays and the low porosities of duripans.

The bulk densities of the pans did not relate to their resistance to slaking; some horizons were dense but slaked easily. Nettleton and Peterson (1983) state that silica cementation does not necessarily result in higher bulk densities unless also accompanied by carbonate accumulation. No macroscopic accumulations of carbonate are present at the Poraiti reference section. Microscope studies, however, showed calcite rhombs present within the 63-125μm fraction. The significance of these in duripan formation is assumed to be negligible because this fraction is small.

Particle densities are fairly consistent with depth, despite the presence of minor inputs of volcanic ash. Overall, the values obtained are similar to those obtained by other workers for soils of predominantly quartzo-feldspathic mineralogy (Scotter *et al.*, 1979). Where the volcanic inputs become more appreciable (e.g. 315cm) values fall.

Particle and bulk densities were used to calculate pore space ratios (PSR). The very low porosities obtained (Table 9.4) explain the poor internal drainage in the subsoil and the subsequent perching of water above the duripan. Bulk density and pore space ratios also confirm the qualitative morphological descriptions and observations made in these layered soils, particularly the dense, closely packed nature of the duripans.

Dissolution chemistry

The amounts of Fe, Al and Si extracted are shown in Table 9.3. The following trends in amounts were noted: $Fe_o < Fe_{NaOH} < Fe_d$; $Al_d < Al_o < Al_{NaOH}$; and $Si_o < Si_d < Si_{NaOH}$.

Oxalate-extractable iron (Fe_o) and aluminium (Al_o) values are very low within the duripans and their enclosing horizons. Fe_o values show a slight decrease at the Bg/Bqm horizon boundary (50-60cm) within the Ohakean loess but there are no marked differences in values between the lower part of the Ohakean duripan and those within its underlying fragipan.

Slightly higher Fe_o values within the Bg horizon of the Ohakean loess may be attributed to the weathering of fine laminations of Holocene andesitic ash, as evidenced by their remnant ferromagnesian and magnetic mineral assemblages seen under the microscope. Likewise, a slight increase in Fe_o at 305cm depth also corresponds to the presence of a macroscopic andesitic tephra layer. Fe_o values within the Loess 4 duripan and its enclosing horizons are markedly lower (half) than those within the Ohakean duripan and its surrounding horizons.

Al_o values are slightly higher within the upper part of the Ohakean duripan (60-70cm), corresponding to the most indurated or intensely coated part of the pan. Values within the Loess 4 duripan do not appear to change appreciably with depth. They are, however, markedly lower (half to a third) than those within the Ohakean duripan.

Oxalate-extractable Si values within the Ohakean loess show no release of Si into the extractant, indicating negligible cementation by short-range-order (poorly crystalline) siliceous minerals. Values within Loess 4 are generally low (0.03-0.13%) but do, however, rise very slightly within the upper part of the duripan (320-340cm).

This preliminary evaluation of acid ammonium oxalate extractable-Fe, -Al and -Si in duripan and non duripan horizons therefore provides little evidence for poorly-ordered aluminosilicates as a major binding agent.

Values for Fe_d are ranked as very low (0.18-0.67%) yet they are markedly higher than those extracted by acid oxalate. Fe_d values within the Ohakean loess rise markedly within the underlying Bx horizon (0.41%). The Loess 4 duripan has slightly higher Fe_d values (0.18-0.40%) than those in the Ohakean duripan (0.22-0.29%). The highest Fe_d

value is from 305cm depth and may relate to the presence of a ferromagnesian-rich andesitic tephra. No marked Fe_d trends with depth are obvious.

CBD aluminium values are very low and do not vary appreciably with depth in either loess sheet but are lower in the Loess 4 duripan. The highest Al_d values within Loess 4 are within the overlying 6bBtg horizon (280-318cm). It was noted during the application of extractants to the soils that air-dry clods placed in a CBD solution showed marked slaking, more so than the oxalate, although oxalate extracted more Al.

CBD-extractable Si values are markedly higher than those extracted by oxalate. Si_d values show an overall decrease in values with depth within the Ohakean loess sheet. A slight increase in Si_d is, however, noted at the top of the duripan (60cm) which corresponds with the field evidence of more intense cementation there. Likewise, a slight increase in Si_d content may be seen within the Loess 4 duripan (6bBqmt horizon) relative to its 6bBtg horizon. Values within the 6bBt/7bA horizon, however, are not appreciably different to those of the 6bBqmt horizon. Si_d values within the Loess 4 duripan and its enclosing horizons are about half those of corresponding horizons within the Ohakean loess sheet.

Fe_{NaOH} values range from 0.09-0.21% and show no depth trends. Values between the two duripans are similar. Al_{NaOH} values range from 0.89-2.3%. The highest Al_{NaOH} value for the Ohakean duripan was obtained from the Bg horizon. Al_{NaOH} values then steadily decrease with depth. Likewise, the 6bBtg horizon overlying the Loess 4 duripan has the highest (2.1%) value within this loess sheet, but does not show any appreciable depth trend. Overall, Al_{NaOH} values in the Ohakean and Loess 4 duripans are quite similar.

The sodium hydroxide extracted the greatest quantity of Si from the soil. Values obtained from the lower Bg and upper Bqm horizons within the Ohakean loess were slightly lower than those from surrounding depths. Si_{NaOH} values within the Loess 4 duripan are slightly higher (4.2-13.7%) than those in the Ohakean duripan (2.2-7.0%), which is consistent with the Loess 4 duripan having experienced a longer period of

Table 9.5: Fusion analyses of soil horizons within a Matapiro soil

Depth	0-6in. (A1)	12-15in. (A2)	Hard Pan	Cemented layer at top of pan
SiO_2	70.14	72.15	68.99	69.93
Al_2O_3	16.22	15.24	15.90	14.97
Fe_2O_3	4.71	4.47	5.51	6.49
Other constituents	8.90	8.14	9.60	8.61

Reproduced from Table IX (page 38) in Pohlen *et al.* (1947).

Table 9.6: Selected XRF elemental data for the Ohakean and Loess 4 loess sheets
Duripan layers are in bold type

Depth (cm)	% SiO_2	% TiO_2	% Al_2O_3	% Fe_2O_3	% MnO_2	% MgO	% CaO	% Na_2O	% K_2O	% P_2O_5	TOTAL (%)
40	70.92	0.62	15.93	4.95	0.04	1.35	1.70	2.68	1.79	0.02	100.00
60	**70.93**	**0.68**	**16.28**	**5.03**	**0.04**	**1.28**	**1.47**	**2.47**	**1.80**	**0.02**	**100.00**
80	72.27	0.61	14.96	4.60	0.04	1.28	1.54	2.72	1.95	0.03	100.00
90	72.71	0.55	14.72	4.22	0.05	1.23	1.57	2.88	2.03	0.02	100.00
300	57.77	0.70	17.55	6.77	0.02	0.76	0.95	1.65	0.72	0.02	100.00
310	59.48	0.69	17.31	6.29	0.02	0.70	0.94	1.70	0.70	0.02	100.00
320	**65.57**	**0.65**	**13.45**	**5.34**	**0.05**	**1.17**	**1.28**	**2.00**	**1.13**	**0.03**	**100.00**
360	64.22	0.58	14.93	4.81	0.03	1.08	1.27	2.23	1.32	0.02	100.00

weathering and hence cementation. Extractable-silica falls to its lowest levels within the Ohakean fragipan despite it having the highest volcanic glass content. A slight increase in $Si_{Na\bullet H}$ content at 310cm depth, however, corresponds to the presence of a highly weathered rhyolitic tephra (see Table 9.3).

Hot 0.5M NaOH extracted much more Al and especially Si than either the oxalate or CBD extractants. Extraction with NaOH removed about 10-40 times more Si than CBD.

XRF

For XRF comparative purposes the fusion analyses reported by Pohlen *et al.* (1947) are presented in Table 9.5. In Pohlen *et al.*'s study the cemented top of the pan yielded a slightly higher iron oxide content than the overlying A horizons or the underlying hard pan (fragipan) despite the lack of any appreciable iron oxide staining within the pan. No comment was made about the mechanism for cementation or its origin.

Table 9.6 details the XRF major element contents within the Ohakean and Loess 4 duripans and their enclosing horizons. The contribution of each of these elements, along with their depth trends has been discussed in Chapter Seven. The Ohakean duripan, like the cemented layer in Table 9.5, also shows a slight increase in Fe_2O_3 content relative to that of its enclosing horizons. This trend is not evident within the Loess 4 duripan. Some caution is needed, however, when interpreting these results because variations in elemental content with depth may not relate solely to eluvial/illuvial trends. It may also relate to the presence of varying quantities of rhyolitic and/or andesitic tephra present within the quartzofeldspathic loess.

9.3.2.3 *Mineralogical characterisation*

Petrography

Loessial soils of Hawke's Bay have been shown in Chapters Five to Seven to have a significant tephric component. Weathered volcanic glass shards showed similar

(a)

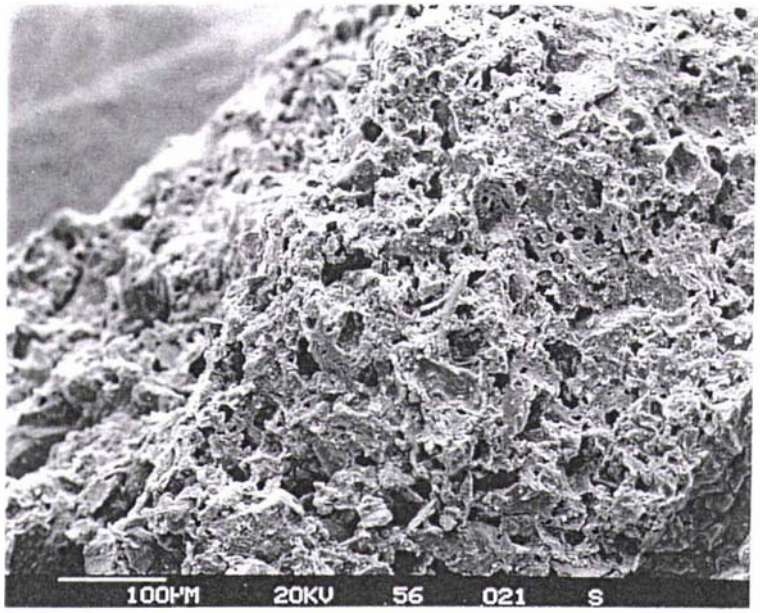

(b)

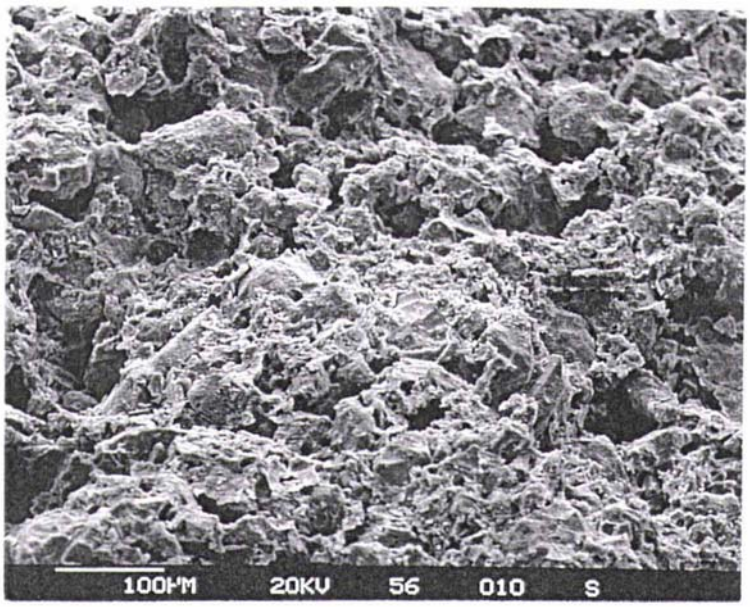

(c)

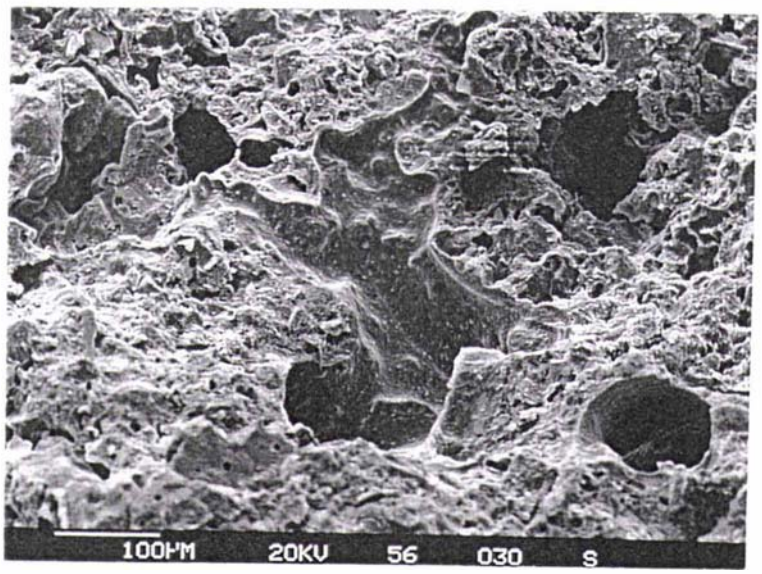

Plates 9.2a-c: SEM images of the soil fabric within samples **(a)** immediately above the Ohakean duripan **(b)** within the Ohakean duripan and **(c)** within the Loess 4 duripan. Duripan horizons have a less porous structure. Grains within duripans are cemented or bridged by silica-rich cements.

properties to those reported in Chadwick *et al.* (1989), namely: rounded or invaginated edges which indicate solution and reprecipitation; obscured plane-light transmission because of partial alteration to supposed aluminosilicate clays, sesquioxides and/or opaline silica; and birefringence in cross-polarised light caused by neoformed clays.

The cement in duripan thin sections appears as extremely thin (micron thicknesses), weakly birefringent "stringers or flocs" throughout the matrix. Under plane-polarised light this cement has a pale-brown colour, probably due to occluded clay and/or Fe oxides.

SEM and EDXRA

Mineral grains within the duripans were easily recognised with the SEM at magnifications >150x. The soil fabric within the Bg horizon (50cm depth) of the Ohakean loess is less cemented and hence more porous than that within the Ohakean and Loess 4 duripan horizons (Plates 9.2a-c). SEM examination of the pores and grains at magnifications of 400 to 4000x showed them to be infilled or bridged by an amorphous clay-sized material. This amorphous material is presumed to have been derived from weathering and illuviation products.

Energy dispersive spectra of these infillings or intergrain bridges were always dominated by Si peaks with lesser peaks for Al, K, Ca, Ti and Fe. The Al content was somewhat variable which may be due to different amounts of Al contained in the bridge or to differing amounts of associated silicate clay minerals. Similar EDXRA traces were reported by Norton *et al.* (1984) for fragipans within the loessial soils of Ohio and by Chartres *et al.* (1990) for case-hardened soils in Australia.

EMP characterisation

Results of electron microprobe analysis of the cement in the Ohakean and Loess 4 duripans are presented in (Table 9.7). These results corroborate the EDXRA results, showing the cement within the duripan to be primarily a siliceous cement.

Table 9.7: Electon microprobe analysis of Ohakean and Loess 4 duripan cements

Ohakean loess: Duripan cement													
	1	2	3	4	5	6	7	8	9	10	11	12	13
SiO_2	79.813	80.718	80.308	80.933	79.917	74.881	79.473	79.685	80.077	79.379	77.222	75.988	78.606
TiO_2	0.134	0.054*	0.047*	0.040*	0.064	0.081	0.087	0.056	0.082	0.100	0.090	0.064	0.096
Al_2O_3	1.424	1.309	1.252	1.232	1.271	1.222	1.263	1.265	1.242	1.223	1.208	1.219	1.378
FeO	0.003*	0.003*	0.042*	0.201	0.086*	0.013*	0.012*	0.025*	0.094	0.048*	0.142	0.114	0.082*
MnO	0.046*	0.095	0.116	0.000*	0.100	0.138	0.044*	0.000	0.118	0.079*	0.032*	0.000*	0.003*
MgO	4.512	4.326	4.606	4.745	4.749	4.787	4.492	4.561	4.705	4.586	4.805	4.450	4.280
CaO	7.526	6.640	6.311	7.081	6.506	7.571	6.433	6.945	6.866	6.904	6.886	6.906	7.536
Na_2O	4.745	5.918	6.473	5.694	6.210	11.263	6.056	4.757	6.243	7.093	5.652	2.606	9.471
K_2O	1.014	0.694	0.898	1.019	1.044	0.992	0.933	0.880	1.139	1.100	1.326	1.379	1.087
P_2O_5		0.206	0.059*	0.459	0.072*	0.225	0.101	0.073*	0.348	0.125	0.160	0.162	0.166
SrO			0.000*	0.000*	0.000*	0.000*	0.000*	0.000*	0.000*	0.000*	0.000*	0.082*	0.000*
BaO			0.348	0.217*	0.331	0.007*	0.396	0.269*	0.244*	0.203*	0.000*	0.003*	0.048*
Total	99.216	99.962	100.460	101.620	100.351	101.178	99.290	98.516	101.157	100.841	97.522	92.974	102.753

Loess 4: Duripan cement										
	1	2	3	4	5	6	7	8	9	10
SiO_2	79.219	79.420	80.788	80.199	81.269	80.652	81.632	80.659	81.275	80.972
TiO_2	0.098	0.050*	0.061	0.097	0.025*	0.140	0.051*	0.077	0.091	0.037*
Al_2O_3	1.206	1.323	1.294	1.244	1.267	1.415	1.254	1.270	1.234	1.305
FeO	0.056*	0.114	0.085*	0.043*	0.100	0.036*	0.103	0.050*	0.010*	0.081*
MnO	0.000*	0.008*	0.045*	0.098	0.052*	0.075*	0.119	0.024*	0.106	0.089
MgO	4.627	4.480	4.560	4.611	4.608	4.451	4.503	4.587	4.459	4.502
CaO	6.410	5.983	5.977	6.089	6.025	6.470	5.937	6.194	6.132	6.219
Na_2O	5.193	4.113	4.890	4.148	5.536	4.373	5.119	5.896	5.394	4.955
K_2O	0.597	0.570	0.744	0.595	0.616	0.573	0.531	0.702	0.694	0.638
P_2O_5	0.226	0.266	0.116	0.189	0.273	0.038*	0.211	0.243	0.298	0.154
SrO	0.178*	0.000*	0.009*	0.000*	0.017*	0.000*	0.004*	0.000*	0.000*	0.000*
BaO	0.179*	0.310	0.220*	0.098*	0.265	0.095*	0.156*	0.123*	0.141*	0.121*
Total	97.988	96.637	98.791	97.411	100.054	98.317	99.620	99.825	99.833	99.073

Electron microprobe operating conditions are detailed in section 6.2.4.1
* denotes at detection limit

Table 9.8: Silt mineralogy of the Ohakean and Loess 4 duripans and their enclosing horizons. Duripan horizons are in bold type.

Depth (cm)	% Quartz	% Feldspar	% Kandite	% Mica	% Smectite	% Mica-Smectite	% Vermiculite	% Mica-Vermiculite	Total
40	54	34	0	5	0	7	0	0	100
50	50	35	0	4	0	5	0	6	100
60	**51**	**34**	**0**	**4**	**0**	**6**	**0**	**5**	**100**
70	**50**	**35**	**0**	**5**	**0**	**5**	**0**	**5**	**100**
80	47	38	0	3	0	9	0	3	100
90	48	35	0	8	0	9	0	0	100
290	58	30	2	2	5	3	0	0	100
300	45	32	8	3	12	0	0	0	100
305	50	30	4	2	10	4	0	0	100
310	50	30	7	0	10	3	0	0	100
315	45	32	5	0	15	3	0	0	100
320	**46**	**37**	**2**	**0**	**10**	**5**	**0**	**0**	**100**
330	**50**	**35**	**2**	**4**	**4**	**5**	**0**	**0**	**100**
340	**46**	**42**	**2**	**3**	**3**	**4**	**0**	**0**	**100**
350	**50**	**38**	**0**	**2**	**5**	**5**	**0**	**0**	**100**
360	48	36	0	2	8	4	0	2	100
370	48	32	0	0	4	0	8	8	100

Table 9.9: Clay mineralogy of the Ohakean and Loess 4 duripans and their enclosing horizons. Duripan horizons are in bold type.

Depth (cm)	% Quartz	% Feldspar	% Kandite	% Mica	% Smectite	% Mica-Smectite	% Vermiculite	% Mica-Vermiculite	Total
40	4.7	5.8	20	18	4	48	0	0	100.5
50	4.7	5.1	20	15	5	50	0	0	99.8
60	**4.4**	**3.0**	**22**	**11**	**8**	**52**	**0**	**0**	**100.4**
70	**4.0**	**2.8**	**15**	**20**	**0**	**58**	**0**	**0**	**99.8**
80	5.5	4.4	10	18	8	54	0	0	99.9
90	7.1	5.5	12	16	10	50	0	0	100.6
290	9.7	7.2	43	0	34	6	0	0	99.9
300	5.0	5.4	43	0	47	0	0	0	100.4
305	5.5	5.4	41	0	48	0	0	0	99.9
310	4.6	3.9	45	0	47	0	0	0	100.5
315	2.3	2.4	38	0	50	8	0	0	100.7
320	**3.8**	**3.3**	**23**	**5**	**35**	**30**	**0**	**0**	**100.1**
330	**5.3**	**3.7**	**24**	**7**	**30**	**30**	**0**	**0**	**100**
340	**3.7**	**5.6**	**20**	**10**	**28**	**32**	**0**	**0**	**99.3**
350	**5.5**	**4.8**	**22**	**4**	**34**	**30**	**0**	**0**	**100.3**
360	6.6	5.0	16	5	55	12	0	0	99.6
370	6.2	5.1	17	0	24	0	27	21	100.3

XRD and DTA characterisation

The relative proportions of minerals in the silt and clay fractions of the CBD-treated samples, as estimated by XRD and DTA, are indicated in Tables 9.8 and 9.9.

X-ray diffraction analyses of the silt fractions indicate that quartz (diagnostic peaks at 0.334 and 0.426nm) and feldspars (several unresolved peaks near 0.320nm) are the dominant minerals present. Mineralogical distributions in the <2μm clay fractions are dominated by kandite, mica, mica-smectite and smectite. There is a tendency for increased mica-smectite in duripan horizons. The formation of smectites in the presence of excess silica is expected from thermodynamic stability considerations (Kittrick, 1969). The high smectite content of the duripans contrasts with its rheological properties, low permeability and lack of slaking in water and lower gravimetric water contents. The silica does not prevent expansion of the clays upon Mg^{2+} saturation and glycerol solvation.

Mica-smectite is a common interstratified mineral in Pallic Soils and is accounted for by the weathering of mica and loss of interlayer potassium (Fieldes, 1968; Churchman, 1978). A low degree of weathering is indicated by the presence of feldspars in all of the samples analysed.

9.3.3 Proposed genesis and mechanism of duripan formation

9.3.3.1 *Source and composition of the cement*

Slaking experiments confirmed that the horizons identified in the field as being cemented did qualify as duripans using the horizon criteria of the New Zealand (Hewitt, 1992) and American (Soil Survey Staff, 1975; 1992; Thomas *et al.*, 1979) soil classifications.

Scanning electron microscopy and energy dispersive x-ray analysis revealed Si-rich bridges between the silt and sand grains within these duripans. These horizons are also frequently associated with CBD and NaOH extractable-Si maxima. Overseas studies,

conducted on similar cemented (duripan) horizons, favour silica as playing a crucial role in the binding of soil particles together (Flach *et al.*, 1969; 1974; Harlan *et al.*, 1977; Norton and Franzmeier, 1978; Steinhardt and Franzmeier, 1979; McKeague and Protz, 1980; Steinhardt *et al.*, 1982; Norton *et al.*, 1984; Chadwick *et al.*, 1987a;b, 1989; Karathanasis, 1987a;b). In order to elucidate the mechanism/s involved in duripan formation the origin of the cement needs to be considered and then evaluated with that proposed in the New Zealand Soil Classification (Hewitt, 1992).

In Hawke's Bay the silica cemented soil horizons (duripans) have developed in soils of loessial and tephric origin (see Chapters Five and Six). The absence of duripans in other regions experiencing similar climatic conditions and with loess of similar quartzofeldspathic composition has led some researchers (Hewitt, 1992) to conclude that the tephric additions to the soils may be a primary cause. Further evidence to support the proposition that the weathering or hydrolysis of volcanic glass is a major source of silica for soil cementation and duripan formation are:

1. volcanic glass is thermodynamically less stable than most alumino-silicate minerals of similar composition (Lindsay, 1979)
2. the weathering activation energies of volcanic glasses are about half those of feldspars with similar chemical composition (White, 1983)
3. laboratory studies show volcanic glass rapidly releases silica to solutions at near neutral pH (White and Claassen, 1980) and at a much higher rate than do feldspars and ferromagnesian minerals (Keller and Reeseman, 1963), and
4. tephra is present in all of the soils in which silica cementation occurs.

Other possible sources of silica for the cementation of soil horizons include:

1. dissolution of soil clays and plant silica
2. the hydrolysis of primary minerals, and
3. post-depositional weathering of aeolian dust (Blank and Fosberg, 1991).

It is here considered unlikely that these sources of silica contribute as much rapidly available silica to the soil solution as volcanic glass because duripan horizons have not been described in other regions of New Zealand with similar climate and soils of loessial origin.

The New Zealand Soil Classification (Hewitt, 1992) states that the cement in duripans is derived from either siliceous tephra or sodium. Sodium, presumably, is derived from the weathering of volcanic feldspars and albite in the greywacke loess. No mention is made in the New Zealand Soil Classification of the contribution of andesitic tephra to the genesis of the cement. Andesitic glass has been shown in a number of studies (e.g. Kirkman, 1980; Kirkman and McHardy, 1980) to devitrify more readily than rhyolitic glass under a moderate intensity of weathering. Rhyolitic glass may persist in soils for thousands of years whereas the half-life of andesitic glass in Taranaki is less than 300 years (Kirkman, 1975; 1980). Andesitic glass is rare or absent at the Poraiti reference site. Ferromagnesian minerals associated with andesitic ash have, however, been detected above, within and below the duripans and correlated with eruptives from the Tongariro Volcanic Centre (see Chapters Five and Six). The absence of andesitic glass signifies that it has been destroyed by weathering.

It is here proposed that most of the silica within the cement is derived from the weathering of andesitic glass and to a lesser degree rhyolitic glass, volcanic feldspars and ferromagnesian minerals.

9.3.4 *Proposed mechanism/s for duripan formation*

In this study field observations coupled with laboratory data have led to the following hypothesis being proposed for the formation of Si-rich duripans in the Pallic Soils of Hawke's Bay. The conditions needed to do this, along with the mechanism/s for Si emplacement within the upper part of the fragipan, form the major basis for this discussion.

From the evidence presented EDXRA, EMP and dissolution chemistry have shown duripans to be Si-rich. It is here interpreted that duripans form within the upper part of a fragipan due to cementation with Si-rich material. Preconditions for duripan formation, appear to be:

1. a low precipitation (<1000mm/annum)

2. a seasonal moisture deficit
3. a fragipan which impedes the free drainage of weathering products, and
4. a source of weatherable tephra within the loess column.

In this mechanism tephra (glass, feldspars and ferromagnesian minerals) is weathered under acid conditions and Fe, Al and Si move into solution. It is proposed that the solutes move as an iron oxide sol, a hypothesis of long standing in pedology. The oxidic surfaces of Fe are much more reactive than the silicate surfaces of clay minerals in adsorbing silica from the solution phase. Hence, they act as loci for Si bridging by providing a surface for initial $Si(OH)_4$ adsorption. $Si(OH)_4$ is adsorbed on exposed hydroxyl groups on the surfaces of clays, sesquioxides and weathered surfaces of primary silicate and aluminosilicate minerals and then, in turn, acts as a template for further adsorption.

The iron oxide sol moves downwards and probably laterally before the wetting front is impeded by the slow draining, low porosity, high bulk density fragipan. This results in a solute laden saturated zone perched above the fragipan, a condition known as episaturation (McDaniel and Falen, 1994). When the soil dries out in late spring and in summer, some of the water is slowly drained away (low PSR and high bulk densities) but most is utilised by the vegetative cover via the process of evapotranspiration. As water is removed, the adsorbed $Si(OH)_4$ molecules increase in concentration prior to precipitation to form weakly hydrous SiO_2 compounds generally known as opaline silica (Chadwick *et al.*, 1987a;b). Likely points of precipitation for the SiO_2 supersaturated solution are in the meso and micropores of the soil where bridges (menisci) form between adjacent grains. During particularly dry conditions overgrowths of these SiO_2 coatings bind particles together by plugging up small pores, resulting in progressively larger soil masses acquiring some rigidity, cementation and brittleness and eventually leading to the development of a duripan.

Amorphous SiO_2 shields adsorption surfaces from rewetting and effectively inhibits desorption. To break the Si-O bonds and rehydrate these polymers during the next soil wetting, relatively high activation energies ($c.61 kJmol^{-1}$) are needed (Rimstidt and

Barnes, 1980). Consequently, the rewetting of these soils during the following autumn and winter is often insufficient to dissolve the precipitated SiO_2 and thus weaken the soil. Thus, the eventual loci of silica deposition is determined by both the depth to which water can readily infiltrate and the amount of adsorption surface area. Slightly higher Si contents in argillic horizons (Bt), as evidenced by their slightly higher CBD and NaOH extractable Si contents, provide many adsorbing surfaces to "catch" downward moving solutes.

Alternatively, the cement may have resulted from the weathering *in situ* of the subsoil materials. The presence of weatherable volcanic material (glass, feldspars and ferromagnesian minerals) and the acid pH values within the duripans are consistent with the postulate of *in situ* weathering. Furthermore, the clay mineralogy of the subsoils also indicates weak weathering. The mechanism/s for cementation are not obvious but the best assumption is that it was derived from the short-distance translocation/illuviation of weathering products from the overlying horizons and from some *in situ* weathering. The close packing of the fragipans (high bulk densities, low PSR) indicates that very little cement would be required to bring about void closure and eventual cementation.

In terms of the influence of Na^+ on duripan formation, Karathanasis (1987a) showed that excess soluble Na^+ and Mg^{2+}, released from the dissolution of Na-feldspars and micas, and not released from the soil due to restricted drainage conditions (i.e. presence of a duripan), may have induced amorphous SiO_2 precipitation and cementation by increasing particle dispersivity and plugging of the pores.

9.5 CONCLUSIONS AND RECOMMENDATIONS

Field and laboratory studies show that the cemented horizons seen within the Pallic Soils qualify as duripans, a diagnostic horizon within New Zealand.

Laboratory studies of these duripans showed that they are cemented by an amorphous to poorly crystalline Si-rich solute which is derived from the weathering and dissolution of tephra (glass, feldspars and ferromagnesian minerals) which is leached as $Si(OH)_4$ molecules.

This leached material becomes perched above the fragipan where it is subject to evapotranspiration and desiccation during late spring and summer. Consequently, this supersaturated $Si(OH)_4$ solution precipitates as fine coatings on very thin bridges (menisci) between adjacent grains. Subsequent rewetting is often not sufficient to rehydrate the strong Si-O bonds. Over a number of wetting and drying cycles these horizons acquire unique properties which include: brittleness; coarse platy structures above fragipans; and Si cementation.

Further laboratory studies are needed to:

1. characterise the surface chemistry of these thin coatings and menisci between grains
2. to study the role of $CaCO_3$ and silica within the drier end members of these soils. Overseas studies suggest a continuum exists (Soil Survey Staff, 1975).
3. and to quantify the role of fragipans in landscape hydrology, especially during periods of low potential evapotranspiration.

CHAPTER TEN:
LATE QUATERNARY LANDSCAPE EVOLUTION OF WESTERN HAWKE'S BAY

10.1 INTRODUCTION

A number of late Quaternary aged geomorphic surfaces are recognised within the western Hawke's Bay soilscape. These are characterised and dated in Chapters Five to Nine. Few New Zealand studies have described the soil-landscape models used to unravel the late Quaternary landscape evolution of a region or district. Most studies have been preoccupied with the general distribution and stratigraphy of Quaternary deposits, the relationships between landform elements (e.g. slopes and regolith types) or land-use aspects of earth science. The models used in these studies have usually been conceptual models in the mind of the investigator/s and are rarely expressed, besides sketchy outlines in the physiographic legend or brief discussions of soil-landscape relationships buried in the text of a report.

In this study the much quoted lower North Island loess deposition model (Te Punga, 1952; Vella, 1963b; Milne, 1973a;b), along with selected soil-geomorphic models from the literature (see Chapter Four), are incorporated into an integrated soil-landscape model which can be used to elucidate the late Quaternary history of western Hawke's Bay. The objective is to present a conceptual framework within which geomorphic processes and soil-regolith patterns in the western Hawke's Bay landscape can be viewed.

This chapter is subdivided into two parts. Part A outlines the integrated soil-landscape model and describes the geomorphological processes and soilscape patterns seen in a transect across the Hawke's Bay landscape. Part B outlines the chronological sequence of landscape-forming events within the district. The timing of events were facilitated by the use of loess stratigraphy and tephra chronohorizons identified within coverbed

sequences in Chapters Five and Six. Future avenues of research, which arose during the course of and as a consequence of this study, are suggested in the conclusions.

PART A: AN INTEGRATED SOIL-LANDSCAPE MODEL

10.2 CONCEPTUAL FRAMEWORK FOR MODEL DEVELOPMENT

10.2.1 Approach

The concepts and principles described in the formulation of this integrated soil-landscape model for western Hawke's Bay are not new. Most are derived from soil geomorphology and soil stratigraphy (see Chapter Four). Authors of individual concepts will be referred to where applicable. Further details may be derived from the review in Chapter Four. Data for measuring and developing the integrated model are detailed in Chapters Five to Nine.

10.2.2 Land systems approach

Scale plays an important role in the application of soil-landscape models because what we see is totally conditioned by how close we are viewing it (Tonkin, 1994). Two scales are recognised within this study. The first is the scale of the overall soil-landscape architecture and the second is the scale of the models used.

The land system concept of Christian and Stewart (1953) is a convenient means of indicating the scale of the western Hawke's Bay soil-landscape architecture. The western Hawke's Bay landscape was subdivided into four broad zones (land systems) in a west (mountains) to east (sea) transect. Differences in physiography were the primary

criteria for delineating the land systems seen. The land systems identified in this transect are:

Ranges: comprise the Ruahine Ranges to the south and the Kaweka and Black Birch Ranges to the north. Most mountain slopes below the present tree-line (*c.*1000m a.s.l.) are vegetated with either indigenous (e.g. Kaweka Forest) or exotic forests (e.g. Gwavas State Forest) rooted in tephra. Above the tree-line mass movement is common. The eastern boundary of this land system is marked by the trace of the Ruahine Fault, a range-bounding strike-slip fault. The lithology of the ranges land system consists almost entirely of indurated sandstones (greywacke) and argillites with localised limestone and volcanics. Podzols, Pumice, Allophanic and Brown Soils are common.

Inland basins: a series of tectonically warped and faulted eastward tilting depressions extend from the range-front to the Mohaka Fault trace. From north to south these are the Puketitiri, Kohurau and Ohara depressions (Kingma, 1957a;b). These depressions are discontinuous and not connected. Landsurfaces are blanketed by Holocene tephras (andesitic and rhyolitic) which are underlain by Pleistocene loess-paleosol and tephra sequences. In toe-slope positions coverbeds can exceed 3m in depth (e.g. Pakaututu Road reference section). Parts of the Kohurau and Puketitiri depressions are veneered in Taupo Ignimbrite. Up to 7m of Taupo Ignimbrite (primary and reworked) may be seen overlying terraces near the confluence of the Mohaka and Ripia rivers (see section 5.5.2). Pumice and Allophanic Soils are the most prevalent soils in this land system.

Hill-country: comprises the uplifted eastern flank of the Mohaka Fault and a series of NNE-SSW trending late Pliocene limestone-capped ridges or cuestas with steep north-west facing scarp slopes and long gentle south-west facing dipslopes (e.g. Maniaroa, Te Waka and Maungaharuru Ranges) on the eastward dipping limb of the Hawke's Bay Syncline. Within the hill-country land system Neogene beds have an overall NNE-SSW strike, dipping 5-20°SE towards Hawke Bay.

The strike becomes increasingly easterly to the north resulting in a drainage pattern that converges in a radial fashion on Hawke Bay. Partially blanketing this land system are Taupo Ignimbrite, andesitic and rhyolitic ashes and loess-paleosol sequences of varying thicknesses. Taupo Ignimbrite, andesitic (e.g. Tufa Trig, Ngauruhoe, Papakai, Mangamate and Bullott Formations) and rhyolitic (e.g. Taupo and Waimihia Tephras) tephras thin towards the east. Parallelling this eastward thinning of Holocene tephras, is the emergence at the current land surface of the underlying Ohakean loess layer. Landslide erosion (see section 5.6.2 for main types) is common within the hill-country. There are more than 16 large (>100ha) deep-seated landslides recognised within the district (e.g. Maungaharuru landslide, see Plate 5.18), most of which are found down dip. Pumice, Allophanic, Brown and Recent Soils predominate in the more western parts of this land system whereas Pallic and Recent Soils are seen to the east. The hill-country land system merges with the plains land system in the east.

Plains: comprises the Heretaunga Plains around Napier and Hastings cities, and the Takapau-Ruataniwha Plains south of the Ngaruroro River. These plains are formed by a series of coalescing alluvial fans built by the aggrading Tutaekuri, Ngaruroro and Waipawa-Tukituki rivers exiting the ranges and hill-country land systems. The Heretaunga Plains are composed of: Mesozoic greywacke sandstone/argillite (predominantly); Neogene sandstone, siltstone, mudstone, conglomerate and limestone; and reworked Taupo Ignimbrite aggradation gravels. The Takapau-Ruataniwha Plains are composed of: Mesozoic greywacke sandstone/argillite (predominantly); Potaka Ignimbrite (both primary and reworked); and Neogene sandstone, siltstone, mudstone, conglomerate and limestone aggradation gravels. Both plains are progradational, owing their formation to the infilling of the Petane Trough (see section 2.2.3) with aggradation gravels derived from the ranges and hill-country land systems and ignimbrite

from the Taupo Volcanic Zone. Swamp, estuary, lagoon and beach deposits are seen in the vicinity of the coastline bordering Napier City. These deposits interfinger with the alluvial fan deposits. Stony Brown Soils dominate on Ohakean surfaces, Pallic Soils on colluvium or loess, and Pumice and Recent Soils on the younger surfaces.

The ranges land system corresponds to the frontal ridge and the inland basins, hill-country and plains land systems correspond to the forearc basin in the plate tectonic model proposed for the district (see Chapter Two). Further details pertaining to the tectonic and physiographic settings within this west to east transect are available in sections 2.2.1 and 2.2.2, respectively.

Field work was centred mainly within the inland basins, principally within the Puketitiri depression, and within the hill-country land system (see Chapter Five). Consequently, these land systems became the main focus for the formulation of the integrated soil-landscape model and landscape evolution interpretations. A further objective was to determine the factors influencing the soil-regolith distributions within each land system. These are discussed in the following sections.

10.3 REGIMES OPERATIVE IN HAWKE'S BAY

10.3.1 Introduction

The architecture and physiography of many of the landforms observed within the four land systems owe their origins to the tectonic regime (see Chapter Two). Landforms have subsequently been sculptured by the climatic regime. It is often difficult to separate the climatic imprint from that of the tectonic regime, frequently they operate in tandem or one overprints the other. A volcanic input is associated with the tectonic regime and fluvial and aeolian inputs with the climatic regime.

Erosion products from the ranges and hill-country land systems have been transported eastwards via the alluvial fans of five large rivers. From north to south these are the

Mohaka, Esk, Tutaekuri, Ngaruroro and the Waipawa-Tukituki rivers. Loess, blown up from point-bars on the alluvial fan floodplains of these rivers during glacial periods, and also probably directly from the hill-country, has blanketed the landscape, especially the hill-country land system and its associated terrace-lands. Interbedded within the loess layers are intermittent accessions of volcanic tephra (andesitic and rhyolitic) from the volcanic centres of the Taupo Volcanic Zone (see Chapters Five and Six). Taupo and Mangakino sourced ignimbrites (e.g. Taupo, Oruanui, Rabbit Gully and Potaka Ignimbrites) have also contributed to the formation of past and present landscapes within the inland basins, hill-country and plains land systems. Chapters Five and Six detail the distributions and ages of these deposits.

The supply of sediment to the forearc basin (inland basins, plains and Hawke Bay) is largely controlled by the tectonic regime and Quaternary climatic cycles. Water has been, and still is, the primary means of transporting material from the tectonically elevated ranges and hill-country land systems, sculpturing the landscape during its eastward progress.

10.3.2 Tectonic regime

In section 2.2.1 the plate tectonic setting of Hawke's Bay was reviewed. The focus of this section is to describe how the tectonic regime dictates the physiography which, in turn, influences soil and regolith distributions within each land system.

Oblique subduction and subsequent underplating of the Pacific Plate beneath the Australian Plate began in the late Miocene and continues to the present day (see section 2.2). This resulted in the regional uplift of the frontal ridge (ranges land system) and the forearc basin (inland basins, hill-country and plains land systems), creating a basin-and-range topography. Folding and tilting dominates the structure of the Neogene rocks exposed in coastal Hawke's Bay. The intensity of folding decreases westward. The eastern boundary of the frontal ridge is bounded by two transcurrent fault traces, the Ruahine and Mohaka Faults. Both are steep, reverse oblique slip faults which exhibit

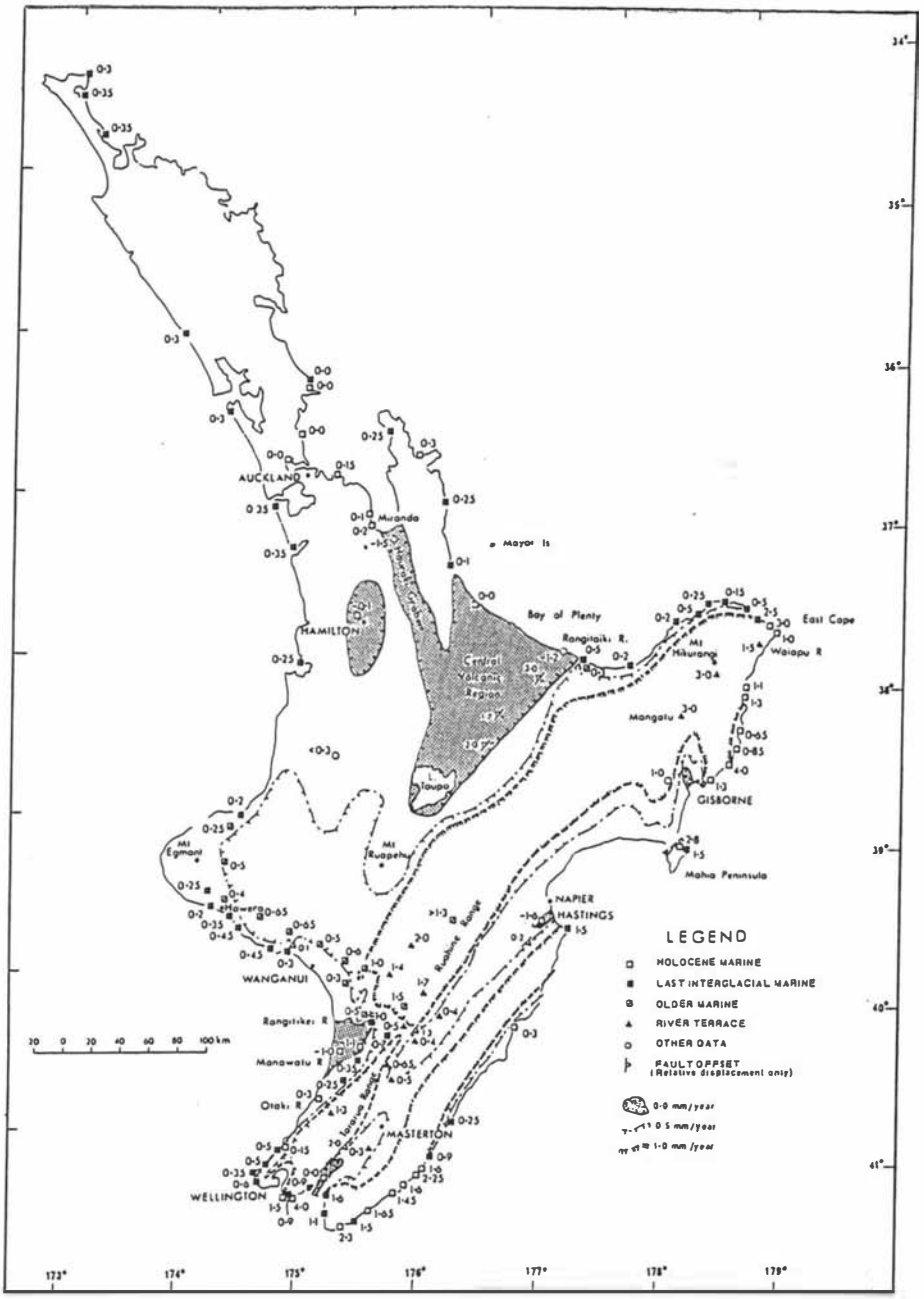

Figure 10.1: A late Quaternary uplift map for the North Island of New Zealand. All uplift values are in mm/year. Reproduced from Pillans (1986).

uplift to the southeast during the Holocene. The structural and geomorphic effects of these faults merging, side-stepping and scissoring are presented elsewhere (e.g. Raub, 1985; Raub *et al.*, 1987; Erdman and Kelsey, 1992; Hanson, 1994; thesis in preparation; Neall *et al.*, 1994).

In Figure 10.1. Pillans (1986) present a late Quaternary uplift map for the North Island of New Zealand. The highest uplift rates (*c.*2mm/yr) are within the ranges land system whereas the forearc basin has an overall uplift rate of *c.*1mm/yr. Uplift resulted in the elevation of river and stream base levels, followed by the progressive erosion of soil and regolith from upper slope positions and its deposition downslope and downstream. Earthflows are common on both scarp- and dip-slopes of the hill-country land system (e.g. Maniaroa, Te Waka and Maungaharuru Ranges) whereas block slides are more common on the SE dipping dip-slopes (e.g. Maungaharuru Range). Thin soils (<0.5m) are found on scarp slopes. These have developed in volcanic ash and skeletal colluvium. In contrast, dip slopes are generally mantled with thicker (>1.0m) volcanic ash and loess deposits. Fluvial dissection, driven by Holocene downcutting, has frequently removed support from down-dip sites along potential failure surfaces. This has resulted in at least 16 Holocene landslides >100ha and landslide dammed lakes, for example Lake Pohue near the Te Pohue settlement (see Fig. 1.1).

The Hawke's Bay Syncline (=Matapiro Syncline) is a major structural feature within western Hawke's Bay (Lillie, 1953; Grindley, 1960; Kingma, 1971). Neogene strata, cyclothemic sequences of sandstone, siltstone, mudstone, conglomerate and limestone dip towards the synclinal axis. These sediments become older and dip more steeply (up to 20° SE) nearer to the ranges. The axis of the Hawke's Bay Syncline curves northeastwards from the Ngaruroro River, through the junction of Matapiro Road with the Napier-Taihape Road, out into Hawke Bay through the cliffs bordering the former Ahuriri lagoon (Grindley, 1960; Kingma, 1971). This results in a drainage pattern that converges in a radial fashion on Hawke Bay. Nearer to the Ruahine Ranges the western limb of this syncline stops abruptly at the Mohaka fault scarp. To the north there is no structural boundary. The syncline passes gradually northwards into the deep-water Nukumaruan mudstones of the Wairoa district. To the south the syncline terminates

abruptly at the Ngaruroro River where it lies opposite the axis of the Mason Ridge Anticline. The greatest amount of uplift (3-4mm/year) is along the Mohaka Fault, currently being studied by Hanson (1994; thesis in preparation), resulting in the steepening of the adjacent western limb of the Hawke's Bay Syncline. Consequently, the major rivers of the district have incised deeply into Ohakean-aged alluvial fan aggradational gravels and into the underlying Neogene strata. Most of this incision has occurred since the Ohakean gravels (i.e. Oh_3 terrace) were emplaced (see Chapter Eight). The net result is the isolation of Ohakean (Oh_1 Oh_2 and Oh_3) and pre-Ohakean aggradation gravels from present-day floodplain processes (see section 5.3.2.3).

The eastward drainage of the major Hawke's Bay rivers is controlled by the NNE/SSW structural trend of the Neogene hill-country sequences. For example, the Mohaka River meanders eastwards but is deflected north by the NNE/SSW trending Maungaharuru Range before resuming its eastward course near its confluence with the Te Hoe River, to the north of the field area.

The Ohara, Kohurau and Puketitiri depressions lie to the east of the ranges land system, between the Ruahine and Mohaka fault traces. These depressions are interpreted as being pull-apart basins or half-grabens (Raub, 1985; Ballance, 1993) which owe their formation to transpression and strike-slip fault movement along the Ruahine and Mohaka faults. The basins or depressions have acted as depositories for material eroding from the slopes of the ranges and hill-country land systems and for airfall (volcanic and loessial) accessions. The maximum thickness of late Quaternary material in these depressions was not determined as observations were limited to road and stream cuttings. Coverbed sequences within toeslope positions, seen in road cuttings (e.g. Pakaututu Road reference section), commonly exceed 3m in thickness.

Water plays a key role in the dissection of the uplifted landscape, evacuating soils and regolith from colluvium-filled hollows and undercutting hill-slopes and stream-banks in toe-slope positions. The inland basins and plains land systems serve as "temporary" storage facilities or depositories for this material. Eroded material (soils, regolith and bedrock) is transported eastwards via the fluvial network (see section 10.4).

10.3.3 Climatic regime

The climatic regime has had a major influence on geomorphic processes within the ranges and hill-country land systems and on the waterways draining these landscapes. Changes in the amount and type of precipitation alter the magnitudes and rates of weathering, erosion, transportation and deposition, thereby changing the morphologies of the hill-slopes and streams within these land systems.

Throughout the Quaternary there have been episodes or mega-cycles of erosion and deposition seen within the soil and regolith record of drainage basins within the ranges and hill-country land systems. These cycles correspond to cold stages within the Quaternary (glacials, stadials). Material is ultimately eroded from the ranges and hill-country land systems and subsequently deposited as aggradational sediments onto the lowlands to form valley fills, fans and piedmont plains. Valley fills have subsequently been tectonically elevated and then fluvially dissected to form valley terraces. Smaller climatic cycles, which relate to climatic perturbations of a smaller scale, are recognised within the megacycles, especially within the more recent record which is better preserved. Grant's cycles of erosion and alluvial sedimentation, reviewed in section 3.2.1, are an example of this.

The general model of alluvial aggradation and loess deposition in the lower North Island states that during cold climates (glacials, stadials) erosion is at a maximum within drainage basins, rivers aggrade and dust is blown up from point-bars and directly from the eroding hill-country and deposited as loess sheets on higher surfaces (Te Punga, 1952; Vella, 1963b; Milne, 1973a;b). During warmer climates (interglacials, interstadials) landsurfaces were stabilised by vegetation reestablishing itself. Consequently, loess accretion slowed or ceased. Soils subsequently developed on the loess whilst rivers and streams, no longer actively aggrading, began to incise into the loess mantled aggradational surfaces. Loess-paleosol and aggradational-degradational sequences recognised are considered to represent cold-warm climates, respectively. The recognition and dating of tephra chronohorizons within Chapters Five and Six

confirms the general tenets of this climatic model for loess production and paleosol formation.

Erosion rates of those portions of hill-slopes immediately adjacent to streams increase during periods of stream entrenchment (warm climates-interstadials, interglacials), removing soil and regolith from swale sites (foot- and toe-slopes), and decrease during periods of aggradation (cold climates-stadials, glacials). However, erosion on areas of hill-slopes more distant from stream channels may be unrelated to, and even out of phase with, changes within the stream channel and may be more closely related to vegetational changes (DeRose *et al.*, 1991).

During the coldest phase of the Last Glacial period (25 000-15 000 years B.P.) a grassland-shrubland vegetation is likely to have dominated the landscape in western Hawke's Bay with only pockets of beech forest surviving on sheltered north-facing hill-slopes. This would have left the deforested hill-slopes more prone to erosion than those under a forest canopy.

During glacial and stadial episodes sea-levels around New Zealand dropped as much as 150m, initiating major cycles of river and stream incision with accompanying drainage basin rejuvenation and the reactivation or initiation of landslides. Interglacial and interstadial episodes were marked by a rise in river base-levels within lower reaches to maintain grade. The history of sea-level changes has affected the drainage development in Hawke's Bay in the following way: the major rivers of Hawke's Bay have downcut in their lower reaches when sea-level fell (stadials, glacial), and have aggraded when sea-level rose (interstadials, interglacials).

Water is a major agent of the climatic regime. It controls the movement of material from production sites to sites of eventual deposition, dissecting the loess and tephra mantled landscape on its eastward (coastward) journey.

10.4 FLUVIAL SYSTEM MODEL

10.4.1 Introduction

Many of the landforms seen in western Hawke's Bay are fluvially derived or modified, for example the alluvial fans and terraces along the Mohaka, Tutaekuri, Ngaruroro and Waipawa-Tukituki rivers. The fluvial system model of Schumm (1977) is a hierarchical model. It forms a convenient means of describing the geomorphic processes operative in western Hawke's Bay and viewing the interrelationships of soil-regolith patterns to the landforms recognised within each land system. The utility of applying this model to the western Hawke's Bay situation lies in the fact that it:

- describes the movement or transfer of material through the various reaches of the fluvial system and relates these to the landforms seen (i.e. drainage basins, valley floors, terraces and alluvial fans)
- recognises a number of spatially linked, cascading subsystems, each of which may impact on the evolution of another linked subsytem (i.e. feedback mechanisms), and
- it recognises landforms as providing the foundation from which the regolith, soils and soil patterns evolve.

Schumm (1977) subdivided the fluvial system into three zones, each dominated by different geomorphic and dynamic processes (see Fig. 4.5). Zone 1 is the drainage basin from which sediment and water are derived; Zone 2, the major river channel, is the transfer zone; and Zone 3 is the area of deposition or sediment sink. The transfer of sediment down-stream or river through these three zones proceeds in a discontinuous manner, transportation events being separated by periods of inactivity, during which sediment accumulates awaiting further remobilisation.

The drainage basin subsystem (Schumm, 1977) is a convenient means of viewing the zone of sediment production (zone 1). Landforms within this subsytem comprise hill- and mountain-slopes and the stream network draining the slopes. Two drainage basin subsystems are recognised in western Hawke's Bay, one in the ranges land system and the other in the hill-country land system. Both subsystems are major sources of sediment to the plains land system.

Tonkin (1994) subdivided the evolution of a typical drainage basin subsystem into three time periods. These are:

1. a period of sediment accumulation (Recovery Time)
2. a period of soil development and soil catenary differentiation (Residence Time), and
3. a period/s of erosion (Evacuation Time).

The K-cycle model of Butler (1959) provides a means of viewing the spatial and temporal organisation of erosion-depositional cycles within a drainage basin subsystem (see section 4.3.3). Slopes within a first order drainage basin subsytem can be stratified using Ruhe's hill-slope components (see section 4.3.6). Periods of instability (Evacuation Time) may result in the evacuation of material (in storage) from colluvial-filled bedrock depressions on slopes, creating a complex array of erosional and depositional geomorphic surfaces on slopes (see section 4.3.5 for geomorphic surface concept). It should also be noted, that periods of gravel fill evacuation (e.g. in terraces) occur during downcutting when all else seems stable (e.g. interglacials, interstadials) and there is a reduction in the supply of eroded material and the vegetation cover is at a maximum. Evacuation times are followed by period/s of metastability during which a soil mantle evolves (Recovery and Residence Times). An unstable (Evacuation Time) and metastable (Recovery and Residence Times) couplet constitutes one K-cycle.

During sediment accumulation exposed bedrock is weathered and colluvium from sideslopes infills bedrock hollows. Airfall accessions (loess and tephra) and Taupo Ignimbrite interstratify and overlie the colluvium-filled bedrock hollows and the colluvium on the sideslopes. Aggrading and composite soils are seen on side-slopes and in colluvium-filled bedrock hollows. Soil horizon differentiation and catenary gradients develop during sediment storage when there is relative stability within the subsystem. Prolonged weathering (Residence Time) however, results in a decrease in macroporosity and soil strength making the soil and regolith more vulnerable to disturbance events (e.g. cyclonic storms, seismic shaking and tectonic uplift). An example of this is the weathering of loess to form Pallic Soils in low rainfall areas.

Tonkin (1994) subdivided disturbance events into:

1. microscale erosion and deposition events (e.g. smaller cyclones that regularly impact upon the East Coast of the North Island)
2. mesoscale erosion and deposition events (larger cyclones e.g. Cyclone Bola of 1988), and
3. megascale erosion and deposition events. These encompass major changes in landform evolution, reflecting significant tectonic (e.g. uplift of ranges) and climatic changes (e.g. glacial-interglacial and stadial-interstadial cycles) occurring over tens of thousands of years.

Disturbance events result in the partial or complete evacuation of soil and regolith from colluvium-filled bedrock depressions (Evacuation Time) by recurrent landsliding into higher order streams. Having removed material from the hollow, slope failure progressively works its way up the sideslopes, refilling the bedrock hollows. During the unstable phase new erosional and depositional geomorphic surfaces are created. These surfaces are often of a transitory nature until a new stability is established. A complex array of simple, compound and composite soil profiles (Morrison, 1978) may be seen. When the supply of erodible soil and regolith are exhausted, bedrock surfaces are exposed and a period of recovery starts. Field studies show the nose and interfluve slope elements may retain part of their original soil and regolith cover.

The general model of progressive backfilling of hollows from sideslopes is complicated by airfall (loess and tephra) accessions. In this situation aggrading and composite soils are seen over the whole slope, depending on the rates and frequency of airfall additions. Variations in the rates of airfall deposition may be related to slope angle and slope orientation which, in turn, affects the resultant soil-regolith pattern. Studies conducted in the Taranaki-country (DeRose *et al.*, 1991) have shown landslide frequency increases on deforested hill-slopes above 28°.

Detailed studies on "representative" drainage basin subsystems within each of the ranges and hill-country land systems were beyond the scope of this study. The purpose of this study was twofold, firstly to record the main landscape-forming processes

operative in Hawke's Bay and secondly to act as a fore-runner to more detailed soil-regolith studies in representative drainage basin subsytems in the future.

10.4.2 The ranges drainage basin subsystem

Within the ranges land system mountain slopes are typically steep and ridges narrow and sharp-crested, bedrock outcrops and scree slopes are common. The main source of aggradational gravels which infill the forearc basin are from the substantial quantities of highly shattered, coarse greywacke sandstone/argillite colluvium held in temporary storage on steep scree slopes awaiting evacuation. The highly shattered nature of this rock is the result of it being uplifted, intensely folded and faulted during two major orogenies, and then subjected to physical weathering during the fluctuating climates of the Quaternary. Sediment yields of more than 4500 cubic metres per square kilometre per year have been recorded within the forested northern Ruahine Range (McKelvey, 1995).

A variety of mass movement types occur within the ranges land system. Rockfalls and debris avalanches are the dominant mass movement processes operative in the erosion of material from slopes, particularly above the tree-line. In forest and scrub-covered areas soil and regolith failures are mainly episodic debris avalanches, slides and flows and are associated with high intensity rainfalls, earthquake shaking and a variety of other active processes. Long linear debris avalanche scars are common on mountain-slopes (e.g. in the Upper Waipawa River Basin). These slopes have a wide variety of ages, as seen by the mosaic of vegetation and soils on them. Uplift and continual fluvial downcutting maintains the steep slopes. Slow, continuous mass movements are also common. Deep-seated movement on steeply dipping joints causes mass creep of greywacke sandstone and argillite sequences on the eastern side of the Ruahine and Kaweka Ranges. Tension cracks seen across steep slopes indicate creep. Windthrow occurs throughout the ranges land system, affecting individual and small groups of trees.

The transfer and distribution of erosion products along the various reaches of the fluvial system are controlled by the incising river. Rivers flowing through the ranges land system have high gradients and occupy steep gravel-filled ravines (e.g. the Waipawa River), often they have braided channels when supply of eroded material is high. Once a river exits the range front its behaviour changes. It is no longer confined by its bedrock channel or the steep valley sides within a gorge (e.g. Ngaruroro River) and spreads out laterally, producing an alluvial fan apex.

Four broad zones corresponding to the four zones recognised within Butler's soil periodicity (erosional-depositional) model (see Fig. 4.2) are recognised from ridge crest or interfluve divide (e.g. Makahu Saddle in the Kaweka Range) to the low order drainage channel exiting at the base of a scree slope (e.g. headwaters of the Waipawa River in the Ruahine Range and the Ripia River in the Ahimanawa Range). A persistent zone is seen along ridge tops and interfluves. It typically consists of a tephric mantle which is underlain by a highly fractured or shattered bedrock surface (collectively termed the debris mantle regolith). Tephra sequences recognised, from current soil surface, are: Tufa Trig and Ngauruhoe Formation andesitic tephras; Taupo Ignimbrite and/or Taupo airfall tephra; a buried soil developed on Waimihia lapilli; Waimihia Tephra; and andesitic tephras of the Papakai, Mangamate and Bullott Formations. Loess sequences are generally absent. This implies that stabilisation of these surfaces occurred after the climate ameliorated *c.*16-14 ka. The main soil groups recognised within the persistent zone are Podzols, Pumice, Allophanic and Brown Soils.

The steepest part, typically higher up on the slopes of a mountain, corresponds to the sloughing or erosion zone. This zone typically has little to no soil present (e.g. R or A/R profiles). Tephra sequences recognised are Tufa Trig and Ngauruhoe Formation andesitic tephras, Taupo Tephra and Waimihia Tephra. Soil groups present are Raw (e.g. Rocky Raw Soils) and Recent Soils.

The alternating zone is subject to both erosion and deposition (the inputs of mass wasting products derived from upslope). Where erosion and deposition are continuous or residence times are less than decades, K-cycles may be unrecognisable. This results

in aggrading or composite soils in depositional zones and ephemeral A/C or A/R soil profiles in erosional zones. In contrast, where erosion-deposition cycles are episodic residence times may be hundreds to thousands of years long. K-cycles may be recognised by arrays of geomorphic and buried surfaces. Composite and compound soil profiles are present in the alternating and depositional zones. Soil groups recognised are Raw, Recent, Pumice and Allophanic Soils.

The depositional zone, at the base of a scree slope (foot or toe-slope positions), serves as a temporary storage facility for erosion products derived from upslope. Often this zone lies below the tree-line on less steep, vegetated sites. Colluvial deposits within this zone are either blanketed or interstratified with tephra. Soil groups encountered are Podzols, Pumice, Allophanic and Recent Soils. Frequently, the depositional zone corresponds to a stream or river terrace which is being undercut and partly removed by streambank erosion. Soil patterns within the alternating and depositional zones are often complex. Grant (1985; 1990; 1994; 1996) believes that these depositional zones are often cyclic in age.

10.4.3 The hill-country drainage basin subsystem

Oblique subduction and compression has resulted in strike-slip fault movement along the Ruahine and Mohaka Faults within the forearc basin. The compression vector is manifest in the physiography of the hill-country land system as a series of NNE-SSW trending hills on the western limb of the Hawke's Bay Syncline. Strike-slip movement, combined with uplift along the Ruahine and Mohaka Faults, has resulted in the western limb of the Hawke's Bay Syncline becoming steepened. Blanketing this landscape is loess derived from the floodplains of alluvial fans during cold climates (glacials, stadials) and tephra accessions from the volcanic centres of the Taupo Volcanic Zone.

Hill-tops and ridges are commonly narrow, occupying only a small percentage of the total area. Many of these have a Pliocene limestone cap which is permeable but relatively resistant to erosion. Underlying the limestones are softer, impermeable

Neogene rocks of sandstone, siltstone, mudstone and conglomerate (Haywick, 1990; Carter *et al.*, 1991; Haywick *et al.*, 1991; 1992; Beu, 1995) which are highly susceptible to erosion. Valley bottoms are narrow and show entrenchment of first order stream channels. These often broaden along higher order stream channels grading into narrow terraces along major streams and rivers. The main cause of erosion within hill-country drainage basins is from water (i.e. from streams, rivers and high intensity, low-frequency cyclonic storms). Seismic shaking resulting from earthquakes is another means of slope erosion. Dislodged erosion debris builds up (aggrades) in the beds of low-order streams. This "stored" material is moved through various reaches of the drainage basin subsystem into higher-order tributaries by low-intensity, high frequency events. The rate of movement of material into higher order streams depends on the storage capacity in the low-order catchments and the frequency of triggering events.

Tectonic uplift has resulted in many of the steeper hill-slopes within the hill-country land system being prone to mass wasting and earth flow processes. Many of the steeper hill-slopes are veneered in colluvial deposits. Colluvial deposits comprise reworked loess and tephra (slope-wash) interstratified with limestone and mudstone blocks from the Neogene strata which outcrop upslope. Erosion processes and landforms often differ on scarp- and dip-slopes. Rockfall is common on the steeper scarp slopes whilst debris avalanching are common features on dip-slopes. At the Pakaututu Road and Apley Road reference sites (see section 5.4.3.3) the accessions of loess/tephra are greater than those of slope debris. Consequently, these slopes were used to maximise tephra and dating control (see Chapters Five and Six). Those slopes where colluvial debris are greater than loess/tephra accessions (e.g. colluvial fans and footslopes) contain an as yet unexplored record of climatic and tectonic events, but will be more difficult to date.

Loess and tephra cover on the hilly topography of western Hawke's Bay is often thin and highly variable in thickness. Thickness gradients are difficult to establish because the loess often fell on steep and undulating surfaces. Much of the loess and tephra has subsequently been redistributed by erosion processes from upper slopes into bedrock hollows and downslope. On lower slopes airfall accessions are augmented by

solifluction, soil-creep and wash from upslope. Consequently, the thickness of a mantle at a particular site can be highly variable. A few broad trends in thickness were observed, however. Soil depths to the top of duripan and fragipan horizons within Pallic Soils are thinnest on ridges, spurs and shoulder slopes and thickest on swales, foot and toeslopes (sites of net sediment accumulation). This relates to the erosion of material from shoulder slopes and its subsequent deposition (temporary storage) into hollows, footslopes or further downslope into ephemeral waterways. Loess deposits thicken markedly near the present rivers, the floodplains of which acted as loess sources, and towards the coast. Since loess and tephra were deposited as accessionary drapes on a hilly landsurface old drainage patterns and relief features have been inherited from the underlying landsurface (i.e. antecedent).

The hill-country drainage basin subsystem is a major source of sediment, especially suspended sediment loads, to the depositional zones (plains land system) in the east. Fluvial dissection, along with complementary slope development under mass failure, are the dominant processes in this land system. The downslope transport of material from side-slopes and evacuation of colluvium-filled bedrock hollows within low order drainage basins requires a trigger. Triggers are provided by the tectonic (e.g. seismic shaking and uplift) and climatic regimes (e.g. Quaternary climatic changes and cyclonic storms). The overall rate of sediment removal is controlled by the weathering process. During an unstable phase new erosional and depositional geomorphic surfaces are created. A complex array of simple, compound and composite soil-profile forms may be seen.

Hill-slopes within a typical hill-country drainage basin subsystem can be stratified using Ruhe's hill-slope components (see section 4.3.6). The temporal and spatial patten of erosion-deposition on hill-slopes can be elucidated using Butler's K-cycle concept (see section 4.3.3), in much the same way as used in the ranges drainage basin subsystem.

The persistent zone comprises Melanic, Allophanic, Pumice and Pallic Soils. Melanic Soils are associated with Pliocene limestone bedrock along the summits of many of the hills. Allophanic Soils are found in the more western parts of the district where the

tephra deposits are thicker. Pallic Soils predominate in the eastern parts of the district where the tephra deposits thin and the Ohakean loess is exposed at the current soil surface.

The sloughing or erosion zone has little to no soil present (i.e. A/R or R profiles). Recent Soils are the predominant soil group seen. These are commonly found on the steeper fault-bounded scarp slopes which are more prone to erosion.

The alternating zone shows similar soil patterns to that seen in the ranges land system (see section 10.4.2) although the textures are generally much finer grained (from Neogene sequences). Soil groups recognised are Pumice, Allophanic and Pallic Soils.

The depositional zone (foot and toe-slopes) comprises thicker, multiple loess-paleosol layers e.g. Pakaututu Road and Apley Road, the focus of study as they offer maximum stratigraphy and chronology. These are interstratified and blanketed with tephras (andesitic and rhyolitic) and colluvium. Soil groups encountered are Pumice and Allophanic Soils in the western parts of the district and Pallic Soils farther to the east.

Tephra coverbeds within the drainage basin subsystem are restricted to stable sites such as hill-crests, colluvium-filled hollows and toe-slopes and are rare on the steeper slopes. On steeper parts of the hill-slope (i.e. erosional or sloughing zones) landslide erosion is common. Regolith and soil derived from the steeper parts of the slope enters streams at the base of the hill-slope, accumulates on colluvial footslopes or in interspur hollows. Channel erosion is common within the hill-country land system. This is marked by the headward extension of stream channels and the downcutting of the stream bed through the coverbeds into the underlying Neogene strata. Material eroded is eventually deposited on the valley floor.

10.4.4 Valley floor subsystem: alluvial fans and terraces

A series of large, coalescing and inset alluvial fans may be seen debouching eastwards away from the range front (ranges land system). These alluvial fans correspond to both former and present courses of the eastward-flowing Mohaka, Esk, Tutaekuri, Ngaruroro and Waipawa-Tukituki Rivers. Terracing is common within the mid- to upper reaches of these fans. The eastward progress of these alluvial fans has been constrained by the Neogene topography of the forearc basin, active tectonics (uplift, range-bounding faults and growing folds) and the supply of material from the ranges (greywacke sandstone and argillite) and hill-country (limestone, sandstone, siltstone, conglomerate and mudstone) land systems and from the Taupo Volcanic Zone (ignimbrites). The morphologies of the alluvial fans are similar to those described in the standard literature (e.g. Bull, 1977; Schumm, 1977) with proximal areas dissected by a fan-head trench, convergence of fan surface and channel to an intersection point in mid-fan, and aggradation in distal areas (e.g. the Ngaruroro River fan).

Between the alluvial fans, minor rivers and streams drain the loess and tephra-mantled hill-country and high terrace edges. These converge on the major eastward flowing rivers. In the fluvial system model alluvial fans act as transfer zones whereby material is being conveyed from the ranges and hill-country land systems to the sites of eventual deposition (i.e. the plains land system and the Pacific Ocean) via the fan-head trench. The transfer zone also acts as a temporary storage zone where considerable material is held in temporary storage (i.e. in valley fills) before being mobilised and carried eastwards.

Sites of temporary sediment deposition (i.e river terraces) are seen adjacent to many of these water-courses. Gravels within the alluvial fans have infilled the Hawke's Bay Synclinal basin. Oceanographic studies have shown some of these alluvial fans to extend up to 20km beyond the present coastline into Hawke Bay (Lewis, 1971; Lewis, 1980; Lewis and Pettinga, 1993).

The best preserved sequence of alluvial fan deposits seen in the study area is along the mid-upper reaches of the Ngaruroro River (see section 5.3.2), where there are at least four alluvial fan aggradation surfaces. At the point where the Ngaruroro River emerges from the ranges (near Big Hill Station), the present floodplain is entrenched more than 50m below an Ohakean (Oh_3) terrace surface. This river entrenchment decreases eastwards. The eastward progress of these fans is controlled by the supply of aggradational gravels from the ranges land system and the steepening of the western limb of the Hawke's Bay Syncline associated with uplift along the Mohaka Fault. Ohakean-aged aggradation surfaces dip eastwards, beneath Holocene-aged deposits (i.e. reworked Taupo Ignimbrite alluvium) within the Heretaunga Plains in the vicinity of the settlement of Maraekakaho. The pronounced eastward dip of aggradation surfaces is accentuated by them overlying eastward dipping Neogene strata on the western limb of the Hawke's Bay Syncline. Likewise, a number of pre-Ohakean aged alluvial fans are seen to dip beneath the present surface of the Takapau-Ruataniwha Plains. State Highway 50 cuts across the toes of many of these fans e.g. mid-Pleistocene Salisbury fan.

The available evidence (see Chapter Five) shows major periods of fan aggradation to have coincided with Quaternary cold phases, and fan dissection with periods of lower sediment supply during warmer phases. The most important climatic parameter is the effectiveness of storm rainfall, in that it influences the generation of sediment and runoff in the mountain catchment, and the stream power through the fan environment. This is a parameter about which little is known in relation to previous climatic conditions, and one that is often beyond the scope of climate change models.

Instability within the valley fill is seen by gullying and slumping, the excavation of coverbeds and valley fill and headward erosion into tributaries. The resulting debris formed new, lower level fans at the outer, eastern edge of the prograding Ohakean and pre-Ohakean alluvial fans. The extent of terrace dissection by fluvial processes increases up the terrace flight until terrace surfaces are completely dissected. Drainage development proceeds through headward sapping of first order streams. The sapping process is controlled by ground water outflow from beneath permeable terrace deposits

overlying impermeable Neogene strata. Material slumping from valley sides is largely responsible for infilling the valley floor. This has increased with the clearing of the natural forest cover and replacing it with pasture species (see DeRose *et al.*, 1993; Page *et al.*, 1994a;b).

10.4.5 Piedmont subsystem: plains land system

The Heretaunga and Takapau-Ruataniwha Plains comprise a series of coalescing aggradation fans (alluvial fan-delta) which infill the Hawke's Bay Syncline. Rivers issuing from the ranges land system built these alluvial fans during stadial periods, and when mass wasting processes decreased during interglacials and interstadials the fans were dissected. The Heretaunga Plains are built up principally from the products of the Tutaekuri and Ngaruroro Rivers, whereas the Takapau-Ruataniwha Plains from the Waipawa and Tukituki Rivers. Pumice, Recent and Raw Soils are the main soil groups recognised within this land system.

The Heretaunga and Takapau-Ruataniwha Plains are interpreted as being composed of a composite "stack" of numerous, possibly cross-cutting, cut-and-fill deposits. The architecture of the cut-and-fill is controlled by the varying rates of climatic, tectonic, and sedimentary processes operating on the system.

PART B: TIMING OF LANDSCAPE EVOLUTION

10.5 LANDSCAPE FORMING EVENTS

10.5.1 Miocene-early Pleistocene

By the late Miocene Hawke's Bay had been structurally differentiated into a western basement high (present-day axial ranges), a central depression (Petane Trough) and an eastern high (present-day coastal ranges). Further details are available in the review, section 2.2.3.

The regional trend through the Pliocene and early Pleistocene is one of gradual uplift of the present-day axial and coastal ranges above sea-level, decelerated subsidence in the inland depressions and progressive withdrawal of the sea (i.e. a marine regression) from the Petane Trough (see section 2.2.3). A possible mechanism for regional uplift is the overthickening of the Australian Plate crust by incorporation of material from the downward moving Pacific Plate (Walcott, 1987). This "underplating" process would have the effect of buoying up the forearc region (Berryman, 1988).

10.5.2 Middle Pleistocene (1.0-0.17Ma)

A marine environment persisted in the Petane Trough until the middle Pleistocene when the trend of basin subsidence reversed. The adjacent, more rapidly rising Wakarara and Ruahine Ranges (frontal ridge) shed orogenic gravels (e.g. Salisbury gravel lithofacies of Erdman and Kelsey, 1992) as prograding alluvial fans (Salisbury and Wahora Terraces of Kingma, 1971) into the Petane Trough. The lack of significant greywacke gravels within the underlying Nukumaruan sequences (*c.*2.4-1.2Ma) indicates that uplift of the ranges occurred after the early Pleistocene.

It is difficult to pin-point accurately the commencement and duration of the present phase of tectonic uplift within the ranges land system. Potaka Ignimbrite, dated at *c.*1.0

Ma, has been reported within alluvial fan gravels at a number of East Coast localities (see Chapter Five; Raub, 1985; Erdman and Kelsey, 1992; Shane, 1994). In this study Potaka Ignimbrite was found within the hill-country land-system around Gwavas State Forest and beneath the Takapau-Ruataniwha Plains (see section 5.5.4). The thick gravel sequences overlying Potaka Ignimbrite indicate the ranges were rapidly rising and shedding gravels eastwards onto the forearc basin, about the time Potaka Ignimbrite was emplaced. Applying models outlined in section 10.3.3. the erosion of material from the ranges was probably enhanced by climatic changes. Further paleoenvironmental interpretation of the mid-Pleistocene strata is needed to resolve this. At Cape Kidnappers Potaka Ignimbrite overlies a dunal sequence (Maraetotora Sands). This is the most easterly exposure of Potaka Ignimbrite and was close to paleocoastline at that time. The presence of logs within the ignimbrite suggests that the district was forested at the time of the eruption.

Since Potaka Ignimbrite was emplaced the forearc region has undergone folding, faulting and uplift in response to accelerated transpression across the inner arc. The forearc basin is transected by a zone of major strike-slip faulting (North Island Shear Belt). This belt is regarded as the western limit of movement induced by subduction of the Pacific Plate beneath the Australian Plate.

The Petane Trough became fully terrestrial about 0.5 Ma (Krieger, 1992; Ballance, 1993). Krieger (1992) demonstrated that the marine regression was punctuated by at least 10 fifth- and six-order glacio-eustatic cycles representing oxygen isotope stages 21 to 39 (1.2-0.7 Ma).

The Rabbit Gully Ignimbrite, identified at Cape Kidnappers (see section 5.5.4), was not identified within the western hill-country. Future studies within the hill-country land system will be directed towards locating it and other tephras.

The Whakamaru group of ignimbrites (*c.*1000km^3 volume), which erupted *c.*0.35Ma (Houghton *et al.*, 1995), were unable to reach the forearc region. This is presumably because the axial ranges were sufficiently high so as to be a major influence on the

redirection of volcaniclastic transport routes but it did flow well into the Kaimanawa mountains and got close to Te Haroto on the Napier-Taupo road (State Highway 5). The Rangitawa Ash (*c.*0.35Ma), an airfall equivalent of one of the Whakamaru Ignimbrites, is located within loessial coverbeds at the City Hire Section, Napier City (refer to Chapter Six for details). The absence of Whakamaru Ignimbrite within Hawke's Bay sequences gives a minimum estimate for the duration of major uplift within the frontal ridge.

No loess-paleosol sequences of 0.35-0.17 Ma were found within the western Hawke's Bay hill-country. The absence of deposits of this age range may relate to the fact that the hill-country, previously beneath the sea in the Petane Trough, is relatively youthful (i.e. it was being uplifted during this time period). Hence, a coverbed record of this age range is likely to have been eroded during ensuing uplift and climatic events.

A thick (>20m) loess-paleosol section was found at the City Hire section, Napier (see Chapter Six and Plate 6.1 for details). In this section at least 10 loess-paleosol layers, intercalated by tephras were identified. As this section was located only towards the final stages of this thesis detailed studies of the loess-paleosol layering were not attempted. This will form a future research project.

10.5.3 Late Pleistocene and Holocene (170 ka-present)

The evidence for late Pleistocene stadial-interstadial climatic cycles within the western Hawke's Bay soilscape is less fragmentary and better preserved than for earlier climatic cycles. Consequently, a more detailed record of landscape-forming events may be unravelled. The subsections which follow outline the sequence of events.

Stadials were marked by widespread erosion in drainage basins and the deposition of material from these subsystems onto the forearc basin as large, aggradational alluvial fans. Aggradational alluvial fans are seen along the Mohaka, Esk, Tutaekuri, Ngaruroro and Waipawa-Tukituki Rivers. Loess, blown up from point-bars within rivers and

streams and directly from the eroding hill-country (e.g. the Manaroa site), blanketed terrace surfaces and hill-slopes. Interstadials were marked by warmer climates which led to the revegetation and eventual stabilisation of sediment production zones. Consequently, rivers had increased competency, incising into the aggradational fan gravels. This, combined with tectonic uplift, produced the flights of terraces seen today (refer to the Ngaruroro River study in Chapter Five). Loess production during interstadial periods slowed or ceased. The combination of warmer climate and general landscape stability led to an intensification of pedogenic processes and the development of a soil on individual loess sheets.

One of the main difficulties in dating Hawke's Bay colluvial fan sequences is the absence of Kawakawa Tephra and multiple loess-paleosol sequences on what are clearly pre-Ohakean aggradational surfaces (see Chapter Five). Consequently, reliable correlations could not be made with the Rangitikei River Valley sequences. Loess-paleosol sequences in foot- and toe-slope positions within the hill-country land-system, however, provided a more extensive coverbed record (see Chapter Five). The most complete stratigraphic records are from sequences found on footslopes with aspects towards the east and southeast. Coverbeds within the hill-country land system have successfully been correlated to the Rangitikei River Valley loess sequences using tephra layers as chronohorizons (see Chapters Five and Six). Five loess layers are recognised within the west to east transect. A brief account of each follows.

170 000-140 000 years B.P.

Loess 5, accumulated during marine oxygen isotope stage 6 and has an estimated age range of 170 000-140 000 years B.P. It is correlated to the Marton Loess within the Rangitikei River Valley. A rhyolitic tephra found within this loess layer at the Poraiti #2 reference section has been identifed as being chemically similar to Manning's (1996a;b) Reid's Reserve Tephra in the Bay of Plenty. Manning (pers. comm. 1994; 1996a;b) reports this tephra to have erupted near the end of the penultimate glacial (*c.*140Ka), marine oxygen isotope stage 6 or in the marine oxygen isotope stage 5e soil. Tephras described in this time range are in distal sites and are correlated with those close to source for the first time.

120 000-90 000 years B.P.

An age of 120 000-100 000 years B.P. is estimated for the accumulation of Loess 4, during marine oxygen isotope stage 5d and 5b. Three rhyolitic tephra layers, termed Unknown tephras A, B, C are found within Loess 4 (see Chapter Six). An attempt was made to correlate the glass chemistries of these tephras with the pre-Rotoehu sequences of Manning (1996a;b) in the Bay of Plenty district. Manning (written communication, 1994) analysed the glass chemistries of Tephras A and B and gave a provisional correlation to his Torere and Copenhagen Tephras respectively (dated between *c.*105 000-115 000 years B.P.). Again, these tephras are described in distal sites and correlated to source for the first time.

80 000-70 000 years B.P.

The Porewan loess accumulated during marine oxygen isotope stage 4, 70 000-80 000 years B.P. Rotoehu Tephra, dated *c.*64 ka by Wilson *et al.* (1992), is found within the paleosol developed on Porewan loess and within the base of the overlying Ratan loess. The position of the Rotoehu Tephra is consistent with its position in the Rangitikei River Valley and Wanganui Basin sequences.

50 000-30 000 years B.P.

This interval is marked by the Ratan stadial, marine oxygen stage 3. The soil on the Ratan loess is weak suggesting that the soil forming period (interstadial) between the Ratan and Ohakean stadials was either of short duration or of lower intensity than the preceding Porewan stadial. A comparison of loess stratigraphy, the eustatic sea-level and oxygen isotope curves indicates that the paleoclimate during the Ratan stadial was not as severe as either the preceding Porewan stadial or the Ohakean stadial that followed.

Two dates were obtained for the Ratan paleosol. The first was a radiocarbon date of 26 380±370 years B.P. (NZA5042) obtained on charcoal fragments collected from within the paleosol. Charcoal, however, is known to readily absorb younger organic contaminants, mainly in the form of humic and fulvic acids. It is therefore likely that the radiocarbon date obtained from the charcoal may be younger than the true age. A

second date (see Chapter Six) was obtained after glass shards from within the paleosol were identified as being from the Omataroa Tephra, dated elsewhere at 28 220±630 years B.P. (Froggatt and Lowe, 1990). An age range of 30 000-26 000 years B.P is proposed for the Ratan paleosol. This age is consistent with that proposed by Milne (1973a) for the Ratan paleosol within the Rangitikei River Valley sequence.

26 000-15 000 years B.P. (Ohakean loess)

The last stadial in New Zealand was a time of low mean annual temperatures, estimated from snowlines to be 4-5°C cooler than present (Soons, 1979). Scrub and grassland were the typical vegetation at the time. These indicate a cooler, drier climate than present (McGlone, 1988).

In the Wellington district to the south, solifluction was widespread during glacial periods (Cotton and Te Punga, 1955). Similar periglacial conditions are likely to have existed in the Hawke's Bay ranges land system. Milne (1973a) calculated that the lower North Island mountains during this time to have been largely devegetated above the 900m contour.

Climatic conditions during the last stadial resulted in widespread erosion within drainage basins. Extensive alluvial fan deposits of Ohakean age (see Chapter Five) debouched eastwards from the range-front onto the forearc basin. These Ohakean-aged alluvial fans are the most extensive surfaces seen within the district.

Loess deposits, derived from actively aggrading alluvial fan flood plains, blanketed the landscape. Ohakean loess, deposited between *c.*26 000-15 000 years B.P., is readily identified. It is the uppermost loess layer and commonly has Kawakawa Tephra, dated *c.*22 600 years B.P., located at two thirds depth within it. Kawakawa Tephra is a widespread, easily identified macroscopic tephra found throughout the Hawke's Bay district. This eruptive was so voluminous (220km^3) that it overwhelmed much of the last stadial landscape, blanketing surfaces with up to 1m of tephra. As this tephra fell immediately prior to the Last Glacial maximum it was subsequently subject to intense erosion. Those sites located at higher elevations, closer to the ranges (e.g. Pakaututu

Road reference site), were subject to the most instability. Hence, a much thinner Kawakawa Tephra layer is seen at these sites than those in more coastal environs (e.g. the Poraiti sections) where there is likely to have been a more widespread vegetative cover.

Erosion of the upper part of the Kawakawa Tephra is borne out by the highly tephric nature of the overlying Ohakean loess. Glass counts and chemical analysis of individual glass shards, extracted from Ohakean loess samples immediately above the macroscopically visible Kawakawa Tephra, showed a glass chemistry indistinguishable from Kawakawa Tephra (see Chapter Six).

The best preserved Ohakean loess exposures are found on colluvial footslopes within the hill-country land system. Ohakean loess found on Ratan and older aggradation surfaces (see Ngaruroro River study in Chapter Five) postdate Kawakawa Tephra deposition. The absence of Kawakawa Tephra within Ohakean and pre-Ohakean loessial coverbeds on terrace treads indicates that these surfaces have had their loess removed, probably during the onset of the Ohakean stadial and remained as non accumulating sites (see Chapter Five).

Many of the colluvial foot- and toe-slopes, seen along road-cuttings which traverse the hill-country land system, are blanketed by Ohakean loess. Kawakawa Tephra is commonly seen overlying Neogene sequences. This is indicative of a period of sediment evacuation immediately prior to Kawakawa Tephra deposition. It is postulated that a change in vegetation (from forest to shrubland and grasses), brought about by the onset of the Ohakean stadial, destabilised the Ratan paleosol resulting in the removal of it and all underlying loess. Foot and toe-slopes within the hill-country around Napier and Taradale, however, have multiple loess-paleosol layers. These sites presumably were stabilised by a better vegetative cover than those further inland.

15 000-14 000 years B.P.

The period 15 000-14 000 years B.P. was marked by widespread landscape stability in western Hawke's Bay. Many loess sections, especially those buried by andesitic tephras in the more western parts of the district, show a paleosol developed on Ohakean loess. Electron microprobe analyses indicate the presence of Rerewhakaaitu Tephra (14 700±110 years B.P.) in this paleosol (see Chapters Six and Eight). Many of the Ohakean 1 (Oh_1) terraces have a soil developed on their treads (see Chapter Nine). Microprobe analysis of glass shards within this terrace tread soil indicate the presence of Rerewhakaaitu Tephra.

Studies by Stewart and Neall (1984) on offshore core P69 have shown an ameliorating climate at the end of the last stadial (16 200-14 700 years B.P.) led to increased channel flow out of the ranges land system, the decline of polar westerlies and the reestablishment of a forest cover at higher elevations. These factors led to a reduction in sediment discharge in source areas. Consequently, rivers had increased competency and incised into Ohakean deposits and the underlying Neogene deposits in their upper reaches (e.g. the Ngaruroro River) and deposited this material as aggradation gravels on the plains land system.

14 000-3300 years B.P.

Vegetation re-establishment and hence landscape stabilisation occurred later within the ranges land system than within the inland basins and hill-country land systems. Palynological studies (Lees, 1986; Rogers and McGlone, 1989) have shown forest vegetation returned to high mountain slopes *c.*13 000 years B.P. Froggatt and Rogers (1990) showed Karapiti Tephra, dated at 9820±80 years B.P., to be the oldest tephra preserved in peat bogs near the summits of the ranges. There appears to be a time-lag in terms of forest vegetation reestablishing itself on the higher slopes within the ranges land system than within the inland basins, hill-country and on the terrace lands. These dates concur with the view of Milne (1973a) who inferred a time-lag of 2000-3000 years between the onset of major retreat of South Island valley glaciers and the onset of revegetation of the higher parts of North Island mountains.

Above the tephric-rich Ohakean paleosol (16-14 ka) a seemingly continuous layer of andesitic ash accessions are seen within the more western parts of the district. Three andesitic tephra formations are recognised. From the Ohakean paleosol upwards they are the Bullott (15 000-10 000 years B.P.), Mangamate (10 000-9500) and Papakai (9500-3300 years B.P.) Formations (see Chapter Five). Fine dustings of rhyolitic tephra are present within the andesitic ashes (see Chapter Six). Andesitic ash accessions thin rapidly towards the east and are not detectable as discrete layers within sections near the coast (e.g. Poraiti sections).

Charcoal is commonly found within the Papakai Formation ashes (refer to the Pakaututu Road, Manaroa and Apley Road sections in Chapter Six). It is likely that vegetation growing on Papakai Formation ashes were set alight by fires induced by lightening strikes associated with the active volcanism at the time (see section 5.4.3.3).

The post Ohakean period (10 000 years B.P -present) is marked by considerable stream and river channel entrenchment into Ohakean gravels and the underlying Neogene strata. Along the upper reaches of the major Hawke's Bay rivers flights of localised, discontinuous and often unmatched terrace surfaces, incised below the level of the youngest Ohakean (Oh_3) surface, may be seen. Most of these terraces present brief still-stands during a general phase of river downcutting. It is likely that many of the Holocene terraces were formed by self-arresting internal feedback mechanisms within drainage basin subsystems rather than having to invoke purely external changes (e.g. tectonics and climate). Post-Ohakean terraces are stony and often devoid of a loess cover. The lack of a loess cover on these surfaces is consistent with the glacial theory that loess production during the Holocene was considerably less than during stadials.

3300-1800 years B.P.

The eruption of the rhyolitic Waimihia Tephra *c.*3300 years B.P punctuated the steady andesitic tephra accessions of the Papakai Formation. Waimihia Tephra is a distinctive often laterally extensive layer in the ranges, inland basins and hill-country land systems of western Hawke's Bay. Farther to the east it thins becoming a composite with that of Taupo Tephra and the Ohakean paleosol layer (e.g. at the Apley and Poraiti sections).

The period 3300-1800 years B.P. is marked by a soil developed on Waimihia lapilli. This soil is found over a variety of slopes and elevations. It is an easily recognisable geomorphic surface in the ranges, inland basins and the western parts of the hill-country land systems, denoting a period of relative slope stability. Glass counts and electron microprobe analyses of glass shards within this layer indicate the presence of fine rhyolitic (e.g. Whakaipo and Mapara Tephras) and andesitic tephra dustings.

1800 years B.P.

The eruption of Taupo Ignimbrite from Lake Taupo 1800 years B.P. had a marked impact upon the western Hawke's Bay landscape. Ignimbrite flowed eastwards overtopping low points in the ranges land system (up to 1500m a.s.l., see Chapter Five) more than 45km from its vent. Flows also extended down the Mohaka and Ngaruroro Rivers, both these rivers have their headwaters in close proximity to Lake Taupo (see Chapter Five).

Taupo Ignimbrite is absent within the higher parts of the ranges land system signifying that these were a significant barrier to their eastward progress. East of the ranges land system is the Mohaka fault scarp on the eastern flank of the Maniaroa, Te Waka and Maungaharuru Ranges (see Chapter Five). These ranges (part of the hill-country land system) were a further barrier to those flows which managed to overtop the low points in the ranges land system (e.g. Gentle Annie Saddle) and those that flowed eastwards via the Mohaka and Ngaruroro River valleys (see Chapter Five).

The presence of Taupo Ignimbrite had a major impact on the western Hawke's Bay landscape. It inundated western mountain slopes, river valleys and the Puketitiri depression, smothering pre-existing landforms and incinerating vegetation rooted within the groundsurface developed on Waimihia lapilli. Charred logs and charcoal fragments are seen within the Taupo Ignimbrite flow.

1800 years B.P.-present

Following deposition of Taupo Ignimbrite rapid fluvial incision into these easily erodible products took place. Cut-and-fill terraces may be seen along the Mohaka and

Ngaruroro Rivers. Once Taupo Ignimbrite had been incised into the rate of stream incision probably slowed down to about its pre-Taupo rate. Gullying and stream bank collapse are the main mechanisms whereby Taupo Ignimbrite is presently being eroded by the fluvial system and moved eastwards. Low-level Taupo Pumice alluvial aggradational terraces can be seen along the Mohaka and Ngaruroro Rivers. Up to 15m of Taupo Pumice alluvium (Griffiths, 1982) has infilled the Hawke's Bay synclinal basin. Pumice soils are seen on the Heretaunga Plains (e.g. the Pakipaki series). Sites that were completely devastated by the Taupo Ignimbrite were revegetated, returning to compositions typical of pre-eruption forests within 120 to 225 (radiocarbon) years (Wilmshurst and McGlone, 1996).

Overlying Taupo Ignimbrite are thin <1mm layers of andesitic tephra, correlated to the Tufa Trig and Ngauruhoe Formations (1800 years B.P to present)(Donoghue, 1991; Donoghue *et al.*, 1995). These andesitic tephras form a minor contribution to the overall evolution of the western Hawke's Bay landscape. Their presence is noted by a slightly deeper, dark topsoil on Taupo Ignimbrite which may serve to protect Taupo Ignimbrite from erosion.

Cyclonic storms, for example Esk (1938) and Bola (1988), have had a marked impact upon the western Hawke's Bay landscape. These have acted as triggers evacuating the material held in storage in colluvium-filled hollows and have helped initiate the expansion of gullies (see Page *et al.*, 1994a;b).

The 1931 M_s 7.8 Napier Earthquake resulted in the uplift of a north-east trending dome *c.*90km in length and 17km wide (Hull, 1990). Approximately 1300ha of the bed of the old Ahuriri Lagoon was uplifted and drained during the 1931 earthquake. The mouths of the Tutaekuri and Esk Rivers were diverted southward (Hull, 1986; 1990). Ground breakage associated with this event is poorly preserved today. Hull (1990) showed that although 15km of surface faulting occurred during this earthquake, only 3km of fault trace could be confidently recognised 53 years later. This means that the evidence for past earthquake events may be underestimated if surface rupture is the only key to their presence.

Charcoal fragments are common within topsoils. Their presence is related to man-induced firing, both Maori and European. Deforestation, combined with changing landuses (i.e conversion of forest to pasture-land) of the hill-country land system and some of the mountain slopes within the ranges land system has resulted in a lowering of the threshold slope angle. Consequently, many slopes are now more prone to erosion (i.e. shortening of soil-regolith residence times and the evacuation of bedrock hollows). Measurements of residence and evacuation times were beyond the scope of this study. These type of studies have been conducted in the Taranaki district (DeRose *et al.*, 1991) and the Tutira catchment in northern Hawke's Bay (Page *et al.* 1994a;b). Measurements of this type would form the next stage of research in the landscapes of western Hawke's Bay.

Agricultural activities late last century and early this century have resulted in some quite severe erosion of Pumice and Allophanic Soils. In many places frost, rain and wind, in concert, have stripped off the more friable volcanic layers, exposing highly fractured, erodible greywacke sandstone and argillite on the slopes of the ranges land system. In the more eastern parts of the hill-country land system the upper soil horizons within Pallic soils have been removed exposing silica-cemented duripan horizons (see Chapter Nine).

Pedestals and local "blowouts," features of wind erosion may be seen within the Kuripapango and Puketitiri areas. These relate to deforestation (burning), the subsequent overstocking by early pastoralists and finally the depletive impact of rabbits, goats, deer and opossums.

10.6 CONCLUSIONS AND FUTURE AVENUES OF RESEARCH

The variation in the character of the landscape across western Hawke's Bay is a result of the interaction of tectonics, mountain-building produced by plate convergence at an active plate boundary, and global atmospheric circulations. Soils and landforms seen reflect tectonics, stadial-interstadial history, the presence of man and introduced species and underlying lithologic and structural controls.

Table 10.1: Summary of the major stability and instability events instrumental in the evolution of the western Hawke's Bay landscape.

PERIOD (ka)	MAJOR ALLUVIAL TERRACES*	LOESS LAYER	BURIED SOIL+	TEPHRA MARKER LAYERS
0-10	Waipawa (1950 A.D.- present)• Tamaki (1870-1900 A.D.)• Wakarara (180-150yrs B.P)• Matawhero (450-330 yrs B.P.)• Waihirere (680-600 yrs B.P.)• Pre Kaharoa II (1000-950 yrs B.P.)• Pre Kaharoa I (1250-1200 yrs B.P.)• Post Taupo (1600-1500 yrs B.P.)• Taupo (1764 yrs B.P.)•		Top soil Pre Taupo/Post Waimihia	Tufa Trig Formation Ngauruhoe Formation Taupo Ignimbrite & Tephra (1.9ka) Waimihia Tephra (3.3ka) Papakai Formation (3.3-9.5ka) Mangamate Tephra (9.5-10ka) Bullott Formation (10-15ka)
10-30	Obakea III terrace Ohakea II terrace Ohakea I terrace	Ohakean	Ohakean soil	Waiohau Tephra (11.9ka) Rerewhakaaitu Tephra (14.7ka) Kawakawa Tephra & Ignimbrite (22.6ka) Mangaone Tephras (28-32ka)
30-50	Ratan terrace	Ratan	Ratan soil	Mangaone Tephras (32-45ka)
70-80	Porewan terrace	Porewan	Porewan soil	Rotoehu Tephra (64ka)
90-120	Terrace 4	Loess 4	Loess 4 soil	Unknown Tephras A & B (*c.*100ka)
140-170		Loess 5	Loess 5 soil	Unknown Tephra C (*c.*120ka) Unknown Tephra D (=Reid's Reserve Tephra#) (*c.*140ka)
170-340		Loess 6, 7, 8, and 9	Loess 6, 7, 8 and 9 soils	A number of uncorrelated tephra layers within the City Hire section, Napier. Future research will be conducted to resolve their identities
340-350		Loess 10	Loess 10 soil	Rangitawa Tephra (*c.*350ka)
c.1 Ma				Potaka Ignimbrite (*c.*1Ma)

* These names are interim for western Hawke's Bay. They are used primarily for the lower North Island.

• Late Holocene alluvial terraces of Grant (1996).

+ In areas of thin tephra cover the Ohakean soil extends to ground surface.

Correlated to the Bay of Plenty sequences of Manning (1996a;b)

Future research needs to be directed towards locating "representative" drainage basin subsystems within both the ranges and hill-country land systems. Detailed soil and geomorphic mapping, along with digital elevation models (DEMs), need to be undertaken within selected drainage basin subsytems. More detailed information may then be gleaned as to the residence and excavation times of coverbeds infilling colluvial hollows on different slope components, as undertaken in studies elsewhere (e.g Dietrich and Dorn, 1984; Reneau *et al.*, 1986; Trustrum and DeRose, 1988; Trustrum *et al.*, 1989; 1990; DeRose *et al.*, 1991; 1993; McLeod *et al.*, 1995; DeRose, 1996). Research efforts also need to be directed towards seeing whether a relationship exists between periods of erosion in the ranges land system versus that in the hill-country land system.

At present very little structural and stratigraphic work has been undertaken on the Neogene strata within the forearc basin besides the work of Haywick to the north within the Tangaio Block (Haywick, 1990; Haywick and Henderson, 1991; Haywick *et al.*, 1991; 1992;), Kelsey and co-workers on the coastal accretionary ridge (Cashman and Kelsey, 1990; Cashman *et al.*, 1992; Kelsey *et al.*, 1993; 1995; Beu, 1995) and the area to the south of the Ngaruroro River (Erdman and Kelsey, 1992; Beu, 1995). This information then needs to be related to current concepts on sequence stratigraphy and plate tectonics. From this more accurate analysis on the tectonic controls on soil-regolith distributions in the forearc basin can be gleaned.

A further avenue of research would be to compile an atlas of the major soil-landscapes seen in western Hawke's Bay. From these the residence, recovery and evacuation times for various drainage basins within the district could be calculated.

The following table (Table 10.1) summarises the major stability and instability events instrumental in the evolution of the western Hawke's Bay landscape.

CHAPTER ELEVEN:
CONCLUSIONS

11.1 SUMMARY OF CONCLUSIONS

The main conclusions borne out of this study are:

- The architecture and subsequent sculpturing of land systems within Hawke's Bay are controlled by a complex interplay of five regimes: tectonics, climate, fluvial, aeolian and volcanic with the recent imprint of humans and their introduced species.
- The Hawke's Bay landscape can be subdivided into four zones, the ranges, inland basins, hill-country and plains, using the land systems concept. This enabled the geomorphological processes and soil patterns within each of these land systems to be described. The ranges and hill-country land systems are the major suppliers of aggradational gravels and sediment to the Heretaunga and Takapau-Ruataniwha Plains.
- The fluvial system model of Schumm (1977) is a convenient means of describing the geomorphic processes operative in western Hawke's Bay and viewing the interrelationships of soil-regolith patterns to the landforms recognised within each land system.
- This is one of the few soilscape characterisation studies undertaken on the East Coast hill-country where the soil-landscape models used are presented
- Loess-paleosol layers recognised within Hawke's Bay (Ohakean, Ratan, Porewan, Loess 4 and Loess 5) correlate well with Milne's (1973a;b) loess model for the Rangitikei River Valley in the Wanganui Basin. Multiple loess-paleosol layers, unlike those in the Rangitikei River Valley, are not found on terrace sequences but on colluvial toe-slopes within the hill-country land system.
- The overall geographic extent of many known tephra layers (see Tables 6.3-6.7) has been significantly expanded into a district, previously not studied in detail, during the course of this study. Furthermore, this is one of the few studies where microscopic tephra time-lines have been used to decipher the timing of landscape history in an aeolian erosional-depositional environment.

- A set of three terraces associated with the last stadial (Ohakean), are commonly seen along the reaches of many Hawke's Bay rivers. A study undertaken to date Ohakean terraces along the Mohaka River near the Mohaka Bridge yielded the following tread ages:

  Oh_1: *c.*16 000-14 000 years B.P.

  Oh_2: *c.*14 000-11 000 years B.P., and

  Oh_3: *c.*11 000-10 000 years B.P.

  The Oh_1, Oh_2 and Oh_3 tread ages are within the age ranges estimated by Milne (1973a) for Ohakean terraces along the Rangitikei River. The Oh_1 tread age is younger than the 18 ka age obtained by Marden and Neall (1990) near Woodville.
- Rerewhakaaitu Tephra (14 700±110 years B.P.) is present in Hawke's Bay. It is present within the Ohakean paleosol and on the treads of Oh_1 terraces along the Mohaka River. This tephra helps date an amelioration in Hawke's Bay climate towards the end of the last stadial *c.*15 000 years B.P. Higher slopes within the ranges land system were revegetated after this date
- An age range of *c.*26-30 ka were estimated for the Ratan paleosol. This was based on two lines of evidence, a radiocarbon date of 26 380±370 years B.P. (NZA 5042) obtained on charcoal from within the Ratan paleosol, and the identification of Omataroa Tephra, dated at 28 220±630 years B.P. (Froggatt and Lowe, 1990), also within this paleosol. Previous ages for the Ratan paleosol have been estimates.
- One of the most easterly occurrences of Oruanui Ignimbrite (22 590±230 years B.P.) is recorded within a fan sequence along the Mohaka River. This is the first record of Oruanui Ignimbrite having reached Hawke's Bay.
- Four previously unrecognised tephra layers are identified. They are from within Loess 4 and Loess 5 at the Apley Road and Poraiti reference sections. These are:

  Tephra A of *c.*100 000 years B.P.

  Tephra B of *c.*100 000 years B.P.

  Tephra C of *c.*120 000 years B.P., and

  Tephra D of *c.*140 000 years B.P.

  Tephras, A, B and D are correlated through glass chemistry and stratigraphic position to Manning's (1996a;b) Torere, Copenhagen and Reid's Reserve Tephras, respectively in the Bay of Plenty district. Tephra C has no known correlatives.

- Rangitawa (=Mount Curl) Tephra was identified within loess layer 10 (Loess 10) within Hawke's Bay. This is the first recorded occurrence of this tephra within the district.
- Potaka Ignimbrite (*c.*1 Ma years B.P.) is a widespread flow deposit within Hawke's Bay, reaching as far east as Cape Kidnappers. This deposit underlies much of the hill-country and plains (Takapau-Ruataniwha Plains) land systems within western and southern Hawke's Bay. It is a major constructional landform.
- Dissolution chemistry and XRF results confirm the stratigraphic and pedological subdivisions made at the reference sections. These show the loessial coverbeds within Hawke's Bay to have considerable tephric (andesitic and rhyolitic) inputs. This is more pronounced within the more western parts of the district which are more proximal to the volcanic centres of the Taupo Volcanic Zone. Dissolution analyses indicate the main short-range-order materials present in western Hawke's Bay soils are allophane, ferrihydrite and Al-humus complexes. These are associated with tephras, particularly the andesitic Papakai, Mangamate and Bullott Formations. Dissolution chemistry and XRF proved to be of limited use in delimiting paleosols within loess. Weathering trends within the loessial coverbeds are complicated by the addition of varying quantities of andesitic and rhyolitic tephra.
- This was the first study undertaken within New Zealand which both characterises and offers a possible mechanism for the formation of duripans within the loessial soils of Hawke's Bay. It is proposed that the siliceous cement present within these horizons is derived from the weathering of tephra. This is borne out by the absence of duripans in other regions which experience similar climatic conditions, have loess of similar quartzofeldspathic composition but little to no input of tephra.

REFERENCES

Adams, R. D., and Ware, D. E. (1977). Subcrustal earthquakes beneath New Zealand: locations determined with a laterally inhomogenous velocity model. *New Zealand Journal of Geology and Geophysics* **20,** 59-83.

Alloway, B. V. (1989). "Late-Quaternary cover-bed stratigraphy and tephrochronology of north-eatern and central Taranaki." Unpublished Ph.D. thesis, Massey University, New Zealand.

Alloway, B. V., Lowe, D. J., Chan, R. P. K., Eden, D. N., and Froggatt, P. C. (1994). Stratigraphy and chronology of the Stent Tephra, a *c.*4000 year distal silicic tephra from Taupo Volcanic Centre, New Zealand. *New Zealand Journal of Geology and Geophysics* **37,** 37-47.

Alloway, B. V., Neall, V. E., and Vucetich, C. G. (1992b). Particle size analyses of late Quaternary allophane-dominated andesitic deposits from New Zealand. *Quaternary International* **13/14,** 167-174.

Alloway, B. V., Neall, V. E., and Vucetich, C. G. (1995). Late Quaternary (post 28,000 year B.P.) tephrostratigraphy of northeast and central Taranaki, New Zealand. *Journal of the Royal Society of New Zealand* **25,** 385-458.

Alloway, B. V., Pillans, B. J., Sandhu, A., and Westgate, J. A. (1993). Revision of the marine chronology in the Wanganui Basin, New Zealand, based on the isothermal plateau fission-track dating of tephra horizons. *Sedimentary Geology* **82,** 299-310.

Alloway, B. V., Stewart, R. B., Neall, V. E., and Vucetich, C. G. (1992a). Climate of the Last Glaciation in New Zealand, based on aerosolic quartz influx in an andesitic terrain. *Quaternary Research* **38,** 170-179.

Alloway, B. V., Westgate, J. A., and Sandhu, A. S. (1992a). Isothermal plateau fission-track age and revised distribution of the widespread mid-Pleistocene Rockland Tephra in west-central United States. *Geophysical Research Letters* **19,** 569-572.

Alloway, B. V., Neall, V. E., and Vucetich, C. G. (1992b). Particle size analyses of late Quaternary allophane-dominated andesitic deposits from New Zealand. *Quaternary International* **13/14,** 167-174.

American Commission on Stratigraphic Nomenclature (1961). Code of stratigraphic nomenclature. *American Association of Petroleum Geologists Bulletin* **45,** 645-665.

Bakker, L., Lowe, D. J., and Jongmans, A. G. (1996). A micromorphological study of pedogenic processes in an evolutionary soil sequence formed on late Quaternary rhyolitic tephra deposits, North Island, New Zealand. *Quaternary International* **34-36,** 249-261.

Ballance, P. F. (1993). The New Zealand Neogene Forearc Basins. *In* "South Pacific Sedimentary Basins of the World." (P. F. Ballance, Ed.), pp. 177-193. Elsevier Science Publishers B.V., Amsterdam.

Bannister, S. C. (1988). Microseismicity and velocity structure in the Hawke's Bay region, New Zealand: fine structure of the subducting Pacific Plate. *Geophysical Journal* **95,** 45-62.

Basher, L. R., and Tonkin, P. J. (1985). Soil formation, soil erosion and revegetation in the central South Island hill and mountain lands. *In* "Proceedings of the soil dynamics and land use seminar, Blenheim, May 1985. New Zealand Society of Soil Science and New Zealand Soil Conservators Association." (I. B. Campbell, Ed.), pp. 154-169. Blenheim Printing Company Limited, Blenheim, New Zealand.

Beanland, S., and Berryman, K. R. (1987). Ruahine Fault Reconnaissance. *Geological Survey Report* **EDS 109**.

Beckmann, G. G. (1984). Paleosols, pedoderms, and problems in presenting pedological data. *Australian Geographer* **16,** 15-21.

Berger, G. W., Pillans, B.J. and Palmer, A.S. (1992). Dating loess up to 800 ka by thermoluminescence. *Geology* **20,** 403-406.

Berger, G. W., Pillans, B.J. and Palmer, A.S. (1994). Test of thermoluminescence dating of loess from New Zealand and Alaska. *Quaternary Science Reviews* **13,** 309-333.

Berry, J. A. (1928). The volcanic deposits of Scinde Island. With special reference to the pumice bodies called chalazoidites. *Transactions of the New Zealand Institute* **59,** 571-608.

Berryman, K. R. (1988). Tectonic geomorphology at a plate boundary: a transect across Hawke Bay, New Zealand. *Zeitschrift fur Geomorphologie Supplementband* **69,** 69-86.

Berryman, K. R. (1992). A stratigraphic age of Rotoehu Ash and late Pleistocene climate interpretation based on marine terrace chronology, Mahia Peninsula, North Island, New Zealand. *New Zealand Journal of Geology and Geophysics* **35,** 1-7.

Berryman, K. R., Ota, Y., and Hull, A. G. (1989). Holocene paleoseismicity in the fold and thrust belt of the Hikurangi subduction zone, eastern North Island, New Zealand. *Tectonophysics* **163,** 185-195.

Beu, A. G. (1995). Pliocene limestones and their scallops. Lithostratigraphy, pectinid biostratigraphy and paleogeography of eastern North Island late Neogene limestone. *Institute of Geological and Nuclear Sciences Monograph* **10**.

Beu, A. G., Browne, G. H., and Grant-Taylor, T. L. (1981). New Chlamys delicatula localities in the central North Island and uplift of the Ruahine Range. *New Zealand Journal of Geology and Geophysics* **24,** 127-132.

Beu, A. G., and Edwards, A. G. (1984). New Zealand Pleistocene and late Pliocene glacio-eustatic cycles. *Palaeogeography, Palaeoclimatology, Palaeoecology* **46,** 119-142.

Beu, A. G., Grant-Taylor, T. L., and Hornibrook, N. d. B. (1980). The Te Aute Limestone Facies (Poverty Bay to Northern Wairarapa). *New Zealand Geological Survey Miscellaneous Serial, Map 13*.

Birkeland, P. W. (1984). "Soils and geomorphology." Oxford University Press, New York.

Birkeland, P. W. (1990). Soil-geomorphic research-a selective overview. *Geomorphology* **3,** 207-224.

Birrell, K. S., and Packard, R. Q. (1953). Some physical properties of New Zealand "loess". *New Zealand Journal of Science and Technology* **B35,** 30-35.

Birrell, K. S., and Pullar, W. A. (1973). Weathering of paleosols in Holocene and late Pleistocene tephras in central North Island, New Zealand. *New Zealand Journal of Geology and Geophysics* **16,** 687-702.

Black, R. (1991). Esk River catchment- the influence of lithology and land use on water yield. *In* "Proceedings of the international conference on sustainable land management, November 17-23, 1991." (P. Henriques, Ed.), pp. 259-267, Napier.

Black, T. M. (1992). Chronology of the Middle Pleistocene Kidnappers Group, New Zealand and correlation to global oxygen isotope stratigraphy. *Earth and Planetary Science Letters* **109,** 573-584.

Blake, G. R., and Hartge, K. H. (1986). Bulk density. *In* "Methods of soil analysis. Part 1." (A. Klute, Ed.), pp. 363-375. ASA and SSSA, Madison, Wisconsin.

Blakemore, L. C. (1982). Some analytical data on fragipans and duripans. *In* "New Zealand Soil Science Society 1982 Annual Conference." (E. Griffiths, Ed.), pp. 76-80. New Zealand Society of Soil Science, Hastings, Hawke's Bay.

Blakemore, L. C., Searle, P. L., and Daly, B. K. (1987). Methods for chemical analysis of soils. *New Zealand Soil Bureau Scientific Report* **80**.

Blank, R. R., and Fosberg, M. A. (1991). Duripans of Idaho, U.S.A.: in situ alteration of eolian dust (loess) to an opal-A/X-ray amorphous phase. *Geoderma* **48,** 131-149.

Bockheim, J. G. (1980). Solution and use of chronofunctions in studying soil development. *Geoderma* **24,** 71-85.

Boellstorff, J. D., and Te Punga, M. T. (1977). Fission-track ages and correlation of middle and lower Pleistocene sequences from Nebraska and New Zealand. *New Zealand Journal of Geology and Geophysics* **20,** 47-58.

Borchardt, G. A., Aruscavage, P. J., and Millard, J., H.T. (1972). Correlation of the Bishop Ash, a Pleistocene marker bed, using instrumental neutron activation analysis. *Journal of Sedimentary Petrology* **42,** 301-306.

Borchardt, G. A., and Harward, M. E. (1971). Trace element correlation of volcanic ash soils. *Soil Science Society of America Proceedings* **35,** 626-631.

Borchardt, G. A., Harward, M. E., and Schmitt, R. A. (1971). Correlation of volcanic ash deposits by activation analysis of glass separates. *Quaternary Research* **1,** 247-260.

Bos, R. H. G., and Sevink, J. (1975). Introduction of gradational and pedogeomorphic features in description of soils. A discussion of the soil horizon concept with special reference to paleosols. *Journal of Soil Science* **26,** 223-233.

Brewer, R. (1972). Use of macro- and micromorphological data in soil stratigraphy to elucidate surficial geology and soil genesis. *Journal of the Geological Society of Australia* **19,** 331-344.

Brewer, R., Crook, K. A. W., and Speight, J. G. (1970). Proposal for soil-stratigraphic units in the Australian stratigraphic code. *Journal of the Geological Society of Australia* **17,** 103-109.

Bryan, W. H., and Teakle, L. J. H. (1946). Pedogenic inertia-a concept in soil science. *Nature* **164,** 969.

Buhay, W. M., Clifford, P.M. and Schwarcz, H.P. (1992). ESR dating of the Rotoiti Breccia in the Taupo Volcanic Zone, New Zealand. *Quaternary Science Reviews* **11,** 267-271.

Bull, W. B. (1977). The alluvial-fan environment. *Progress in physical geography* **1,** 222-270.

Bull, W. B. (1990). Stream-terrace genesis: implications for soil development. *Geomorphology* **3,** 351-367.

Bull, W. B. (1991). "Geomorphic responses to climatic change." Oxford University Press, New York.

Bull, W. L., and Knuepfer, P. L. K. (1987). Adjustments by the Charwell River, New Zealand, to uplift and climatic changes. *Geomorphology* **1,** 15-32.

Burns, S. F., and Tonkin, P. J. (1982). Soil geomorphic models and the spatial distribution and development of alpine soils. *In* "Space and time in geomorphology. The Binghampton Symposium in geomorphology: International Series No. 12." (C. E. Thorn, Ed.), pp. 25-43. George Allen and Unwin, London.

Busacca, A. J. (1989). Long Quaternary record in eastern Washington, U.S.A., interpreted from multiple buried paleosols in loess. *Geoderma* **45,** 105-122.

Busacca, A. J., and Singer, M. J. (1989). Pedogenesis of a chronosequence in the Sacramento Valley, California, U.S.A., II. Elemental chemistry of silt fractions. *Geoderma* **44,** 43-75.

Bussell, M. R. (1988). "Quaternary vegetational and climatic changes recorded in cover beds of the South Wanganui Basin marine terraces, New Zealand." Unpublished Ph.D. thesis, Australian National University, Australia.

Butler, B. E. (1959). Periodic phenomena in landscapes as a basis for soil studies. *C.S.I.R.O Soil Publication* **14**.

Butler, B. E. (1982). A new system for soil systems. *Journal of soil science* **33,** 581-595.

Cameron, R. J. (1964). Destruction of the indigenous forest for Maori agriculture during the Nineteenth Century. *New Zealand Journal of Forestry* **9,** 98-109.

Campbell, A. S., and Schwertmann, U. (1985). Evaluation of selective dissolution extractants in soil chemistry and mineralogy by differential x-ray diffraction. *Clay Mineralogy* **20,** 515-519.

Campbell, I. B. (1973). Pattern of variation in steepland soils: variation on a single slope. *New Zealand Journal of Science* **16,** 413-434.

Campbell, I. B. (1975). Pattern of variation in steepland soils: soil differences in complex topography. *New Zealand Journal of Science* **18,** 53-66.

Carter, R. M., Abbott, S. T., Fulthorpe, C. S., Haywick, D. W., and Henderson, R. A. (1991). Application of global sea-level and sequence-stratigraphic models in southern hemisphere Neogene strata from New Zealand. *Special Publication International Association of Sedimentologists* **12,** 41-65.

Carter, L., Nelson, C. S., Neil, H. L., and Froggatt, P. C. (1995). Correlation, dispersal, and preservation of the Kawakawa Tephra and other late Quaternary tephra layers in the southwest Pacific Ocean. *New Zealand Journal of Geology and Geophysics* **38,** 29-46.

Cashman, S. M., and Kelsey, H. M. (1990). Forearc uplift and extension, southern Hawke's Bay, New Zealand: Mid-Pleistocene to present. *Tectonics* **9,** 23-44.

Cashman, S. M., Kelsey, H. M., Erdman, C. F., Cutten, H. N. C., and Berryman, K. R. (1992). Strain partitioning between structural domains in the forearc of the Hikurangi subduction zone, New Zealand. *Tectonics* **11,** 242-257.

Catt, J. A. (1979). Soils and Quaternary geology in Britain. *Journal of Soil Science* **30,** 607-642.

Catt, J. A. (1986). "Soils and Quaternary geology: a handbook for field scientists." Clarendon Press, Oxford.

Chadwick, O. A., Hendricks, D. M., and Nettleton, W. D. (1987a). Silica in Duric soils: I. A depositional model. *Soil Science Society of America Journal* **51,** 975-982.

Chadwick, O. A., Hendricks, D. M., and Nettleton, W. D. (1987b). Silica in Duric soils: II. Mineralogy. *Soil Science Society of America Journal* **51,** 982-985.

Chadwick, O. A., Hendricks, D. M., and Nettleton, W. D. (1989). Silicification of Holocene soils in northern Monitor Valley, Nevada. *Soil Society of America Journal* **53,** 158-164.

Chartres, C. J., Kirby, J. M., and Raupach, M. (1990). Poorly ordered silica and aluminosilicates as temporary cementing agents in hard- setting soils. *Soil Science Society of America Journal* **54,** 1060-1067.

Childs, C. W. (1973). Patterns of total element concentrations in Quaternary loess columns. *Proceedings IX INQUA Congress, Abstracts,* 61-62.

Childs, C. W. (1975). Distribution of elements in two New Zealand Quaternary loess columns. *In* "Quaternary Studies: a selection of papers presented at IX INQUA Congress, New Zealand 1973." (R. P. Suggate, and M. M. Cresswell, Eds.), pp. 95-99. Royal Society of New Zealand, Wellington.

Childs, C. W. (1985). Towards understanding soil mineralogy. II Notes on ferrihydrite. *New Zealand Soil Bureau Laboratory Report* **CM7**.

Childs, C. W. (1992a). Ferrihydrite: a review of structure, properties and occurrence in relation to soils. *Z. Pflanzenernahr. Bodenk* **155,** 441-448.

Childs, C. W. (1992b). Soil- and geo-chemistry: rattling nodules to heat engines. *New Zealand Soil News* **40,** 5-16.

Childs, C. W., and Searle, P. L. (1975). Element distributions in loess columns at Claremont, Table Flat, and Stewart's Claim, New Zealand. *New Zealand Soil Bureau Scientific Report* **20**.

Christian, C. S., and Stewart, G. A. (1953). General report on survey of Katherine-Darwin region, 1946. *Australian Land Resources Survery* **1**.

Christiansen, R. L. (1980). Eruption of Mount St. Helens. Volcanology. *Nature* **285,** 531-533.

Churchman, G. J. (1978). Studies on a climosequence of soils in tussock grasslands. 21. Mineralogy. *New Zealand Journal of Science* **21,** 467-480.

Churchward, H. M. (1961). Soil studies at Swan Hill, Victoria, Australia. I. Soil Layering. *Journal of Soil Science* **12,** 73-86.

Cole, J. W., Darby, D.J. and Stern, T.A. (1995). Taupo Volcanic Zone and central volcanic region backarc structures of North Island, New Zealand. *In* "Backarc Basins: Tectonics and Magmatism." (B. Taylor, Ed.), pp. 1-28. Plenum Press, New York.

Cole, J. W., and Lewis, K. B. (1981). Evolution of the Taupo-Hikurangi subduction system. *Tectonophysics* **72,** 1-21.

Colman, S. M., Pierce, K. L., and Birkeland, P. W. (1987). Suggested terminology for Quaternary dating methods. *Quaternary Research* **28,** 314-319.

Costa, J. E., and Baker, V. R. (1981). "Surficial geology, building with the earth." John Wiley and Sons, New York.

Cotton, C. A. (1942). "Geomorphology." Whitcombe and Toombs, Christchurch.

Cotton, C. A., and Te Punga, M. T. (1955). Solifluxion and periglacially modified landforms at Wellington, New Zealand. *Transactions of the Royal Society of New Zealand* **82,** 1001-1031.

Coulter, J. D. (1962). Easterly and westerly rainfalls in Hawke's Bay. *New Zealand Meteorological Service Technical Note* **146**.

Cowie, J. D. (1962). Age of Ohakea Terrace, Rangitikei River. *New Zealand Journal of Geology and Geophysics* **5,** 617-619.

Cowie, J. D. (1964a). Aokautere Ash in the Manawatu district, New Zealand. *New Zealand Journal of Geology and Geophysics* **7,** 67-77.

Cowie, J. D. (1964b). Loess in the Manawatu district, New Zealand. *New Zealand Journal of Geology and Geophysics* **7,** 389-396.

Cowie, J. D. (1978). Soils and agriculture of Kairanga County, North Island, New Zealand. *New Zealand Soil Bureau Bulletin* **33**.

Cowie, J. D., and Milne, J. D. G. (1973). Maps and sections showing the stratigraphy of North Island loess and associated deposits. *New Zealand Soil Survey Report* **6**.

Cronin, S. J., Hedley, M. J., and Neall, V. E. (1996d). Impact of October 1995 Ruapehu Ash fall on soil fertility. Part 1: preliminary estimates of elemental deposition rates. Massey University, Palmerston North, New Zealand.

Cronin, S. J., Neall, V. E., and Palmer, A. S. (1995). Investigation of an aggrading paleosol developed into andesitic ring-plain deposits, Ruapehu volcano, New Zealand. *Geoderma* **69,** 119-135.

Cronin, S. J., Neall, V. E., and Palmer, A. S. (1996a). Geological history of the north-eastern ring plain of Ruapehu Volcano, New Zealand. *Quaternary International* **34-36,** 21-28.

Cronin, S. J., Neall, V. E., Palmer, A. S., and Stewart, R. B. (1997). Methods of identifying late Quaternary rhyolitic tephras on the ring plains of Ruapehu and Tongariro volcanoes, New Zealand. *New Zealand Journal of Geology and Geophysics* **40,** 175-184.

Cronin, S. J., Neall, V. E., Stewart, R. B., and Palmer, A. S. (1996b). A multiple-parameter approach to andesitic tephra correlation, Ruapehu volcano, New Zealand. *Journal of Volcanology and Geothermal Research* **72,** 199-215.

Cronin, S. J., Wallace, R. C., and Neall, V. E. (1996c). Sourcing and identifying andesitic tephras using major oxide titanomagnetite and hornblende chemistry, Egmont volcano and Tongariro Volcanic Centre, New Zealand. *Bulletin of Volcanology* **58,** 33-40.

Crook, K. A. W., and Coventry, R. J. (1967). Climatically controlled Quaternary sedimentation and soils in Ryan Creek Valley, N.S.W. *Australian New Zealand Association Advancement of Science Section C. Abstracts* **T,** 9-11.

Crozier, M. J., Eyles, R. J., Marx, S. L., McConchie, J. A., and Owen, R. C. (1980). Distribution of landslips in the Wairarapa hill country. *New Zealand Journal of Geology and Geophysics* **23,** 575-586.

Dan, J., and Yaalon, D. H. (1968). Pedomorphic forms and pedomorphic surfaces. *Transactions 9th International Congress of Soil Science* **4,** 577-584.

Daniels, R. B., Gamble, E. E., and Cady, J. G. (1971). The relation between geomorphology and soil morphology and genesis. *Advances in Agronomy* **23,** 51-88.

Daniels, R. B., and Hammer, R. D. (1992). "Soil Geomorphology." John Wiley and Sons, New York.

de Lisle, J. F., and Patterson, D. I. (1971). The climate and weather of the Hawke's Bay region, New Zealand. *New Zealand Meteorological Service Miscellaneous Publication* **115**.

De Mets, C., Gordon, R. G., Argus, D. F., and Stein, S. (1990). Current plate motions. *Geophysical Journal International* **101,** 425-478.

DeRose, R. C., Trustrum, N.A. and Blaschke, P.M. (1991). Geomorphic change implied by regolith-slope relationships on steepland hillslopes, Taranaki, New Zealand. *Catena* **18,** 489-514.

DeRose, R. C. (1996). Relationships between slope morphology, regolith depth, and the incidence of shallow landslides in eastern Taranaki hill country. *Zeitschrift fur Geomorphologie Supplementband* **105,** 49-60.

DeRose, R. C., Trustrum, N. A., and Blaschke, P. M. (1993). Post-deforestation soil loss from steepland hillslopes in Taranaki, New Zealand. *Earth Surface Processes and Landforms* **18,** 131-144.

Dietrich, W. E., and Dorn, R. (1984). Significance of thick deposits of colluvium on hillslopes: a case study involving the use of pollen analysis in the coastal mountains of Northern California. *Journal of Geology* **92,** 147-158.

Dijkerman, J. C. (1974). Pedology as a science: the role of data, models and theories in the study of natural soil systems. *Geoderma* **11,** 73-93.

Ding, Z., Yu, Z., Rutter, N. W., and Liu, T. (1994). Towards an orbital time scale for Chinese loess deposits. *Quaternary Science Reviews* **13,** 39-70.

Donoghue, S. L. (1991). "Late Quaternary volcanic stratigraphy of the southeastern sector of the Mount Ruapehu ring plain, New Zealand." Unpublished Ph.D. thesis, Massey University, New Zealand.

Donoghue, S. L., and Neall, V. E. (1996). Tephrostratigraphic studies at Tongariro Volcanic Centre, New Zealand: an overview. *Quaternary International* **34-36,** 13-20.

Donoghue, S. L., Neall, V. E., and Palmer, A. S. (1995). Stratigraphy and chronology of late Quaternary andesitic tephra deposits, Tongariro Volcanic Centre, New Zealand. *Journal of the Royal Society of New Zealand* **25,** 115-206.

Donoghue, S. L., Stewart, R. B., and Palmer, A. S. (1991). Morphology and chemistry of olivine phenocrysts of Mangamate Tephra, Tongariro Volcanic Centre, New Zealand. *Journal of the Royal Society of New Zealand* **21,** 225-236.

Duchaufour, P. (1982). "Pedology pedogenesis and classification." George Allen and Unwin, London.

Eden, D. N. (1987). Stratigraphy and chronology of Seaview Formation, Awatere Valley, South Island, New Zealand. *In* "Aspects of loess research." (L. Tungsheng, Ed.), pp. 216-230. China Ocean Press, Beijing.

Eden, D. N. (1989). River terraces and their loessial cover beds, Awatere River Valley, South Island, New Zealand. *New Zealand Journal of Geology and Geophysics* **32,** 487-497.

Eden, D. N., and Froggatt, P. C. (1996). A 6500-year history of tephra deposition recorded in the sediments of Lake Tutira, eastern North Island, New Zealand. *Quaternary International* **34-36,** 55-64.

Eden, D. N., Froggatt, P. C., and McIntosh, P. D. (1992). The distribution and composition of volcanic glass in late Quaternary loess deposits of southern South Island, New Zealand, and some possible correlations. *New Zealand Journal of Geology and Geophysics* **35,** 69-79.

Eden, D. N., Froggatt, P. C., Trustrum, N. A., and Page, M. J. (1993). A multiple-source Holocene tephra sequence from Lake Tutira, Hawke's Bay, New Zealand. *New Zealand Journal of Geology and Geophysics* **36,** 233-242.

Eden, D. N., and Milne, J. D. G. (1987). Rationale and methods for the determination of volcanic glass content. *New Zealand Soil Bureau Laboratory Report CM16.*

Eden, D. N., Qizhong, W., Hunt, J. L., and Whitton, J. S. (1994). Mineralogical and geochemical trends across the Loess Plateau, North China. *Catena* **21,** 73-90.

Eggleston, G. W. (1989). "Models of soil development and distribution on alluvial, composite and debris-flow fans. Case studies: central Canterbury intermontane region." Unpublished M.Appl.Sc. thesis, University of Canterbury, New Zealand.

Eiby, G. A. (1971). Seismic regions of New Zealand. *Royal Society of New Zealand* **9,** 155-160.

Erdman, C. F., and Kelsey, H. M. (1992). Pliocene and Pleistocene stratigraphy and tectonics, Ohara Depression and Wakarara Range, North Island, New Zealand. *New Zealand Journal of Geology and Geophysics* **35,** 177-192.

Ewart, A. (1963). Petrology and petrogenesis of the Quaternary pumice ash in the Taupo area, New Zealand. *Journal of Petrology* **4,** 392-431.

Eyles, R. J. (1971). Mass movement in Tangoio conservation reserve northern Hawke's Bay. *Earth Science Journal* **5,** 79-91.

Fenner, J., Carter, L. and Stewart, R.B. (1992). Late Quaternary paleoclimatic and paleoceanographic change over northern Chatham Rise, New Zealand. *Marine Geology* **108,** 383-404.

Fenwick, I. M. (1981). Paleosols. *In* "Geomorphological Techniques." (A. Goudie, Ed.), pp. 342-345. George Allen Unwin, Hemel Hampsted.

Fenwick, I. M. (1985). Paleosols: problems of recognition and interpretation and interpretation. *In* "Soils and Quaternary landscape evolution." (J. Boardman, Ed.), pp. 3-21. John Wiley and Sons, Chichester.

Fieldes, M. (1968). Clay mineralogy. *New Zealand Soil Bureau Bulletin* **26,** 22-39.

Fieldes, M., and Perrott, K. W. (1966). The nature of allophane in soils. Part 3. Rapid field and laboratory test for allophane. *New Zealand Journal of Science* **9,** 623-629.

Finkl, C. W. J. (1980). Stratigraphic principles and practices as related to soil mantles. *Catena* **7,** 169-194.

Finkl, C. W. J. (1984). Chronology of weathered materials and soil age determination in pedostratigraphic sequences. *Chemical Geology* **44,** 311-335.

Flach, K. W., Nettleton, W. D., Gile, L. H., and Cady, J. G. (1969). Pedocementation: induration by silica, carbonates, and sesquioxides in the Quaternary. *Soil Science* **107,** 442-453.

Flach, K. W., Nettleton, W. D., and Nelson, R. E. (1974). The micromorphology of silica-cemented soil horizons in western North America. *In* "Soil Microscopy. Proceedings of the Fourth International Working-Meeting on Soil Micromorphology." (G. K. Rutherford, Ed.), pp. 714-729. Limestone Press, Ontario, Canada.

Fleming, C. A. (1953). "The geology of the Wanganui Subdivision." Government Printer, Wellington.

Follmer, L. R. (1978). The Sangamon soil in its type area- a review. *In* "Quaternary Soils." (W. C. Mahaney, Ed.), pp. 125-165. Geo Abstracts, Norwich.

Follmer, L. R. (1982). The geomorphology of the Sangamon surface: its spatial and temporal attributes. *In* "Space and time in geomorphology." (C. E. Thorn, Ed.), pp. 117-146. The Binghampton symposia in geomorphology, International Series No 12. George Allen and Unwin, London.

Follmer, L. R. (1983). Sangamon and Wisconsinan pedogenesis in midwestern United States. *In* "Late Quaternary environments of the United States. Volume 1: The late Pleistocene." (H. E. J. Wright, Ed.), pp. 138-144. University of Minnesota Press, Minneapolis.

Froggatt, P. C. (1979). Lake Taupo-probable source of Taupo Pumice Formation (Note). *New Zealand Journal of Geology and Geophysics* **22,** 763-764.

Froggatt, P. C. (1983). Toward a comprehensive upper Quaternary tephra and ignimbrite stratigraphy in New Zealand using electron microprobe analysis of glass shards. *Quaternary Research* **19,** 188-200.

Froggatt, P. C. (1992). Standardization of the chemical analysis of tephra deposits. Report of the ICCT Working Group. *Quaternary International* **13/14,** 93-96.

Froggatt, P. C., and Gosson, G. J. (1982). Techniques for the preparation of tephra samples for mineral and chemical analysis and radiometric dating. *Victoria University of Wellington Department of Geology Publication* **23**.

Froggatt, P. C., Nelson, C.S., Carter, L., Greggs, G. and Black, K.P. (1986). An exceptionally large late Quaternary eruption from New Zealand. *Nature* **319,** 578-582.

Froggatt, P. C., and Lowe, D. J. (1990). A review of late Quaternary silicic and some other tephra formations from New Zealand: their stratigraphy, nomenclature, distribution, volume and age. *New Zealand Journal of Geology and Geophysics* **33,** 89-109.

Froggatt, P. C., and Rogers, G. M. (1990). Tephrostratigraphy of high-altitude peat bogs along the axial ranges, North Island, New Zealand. *New Zealand Journal of Geology and Geophysics* **33,** 111-124.

Frye, J. C. (1959). Climate and Lester King's "Uniformitarian nature of hillslopes". *Journal of Geology* **67,** 111-113.

Galehouse, J. S. (1969). Counting grain mounts: number percentage vs. number frequency. *Journal of Sedimentary Petrology* **39,** 812-815.

Gerrard, A. J. (1992). "Soil geomorphology: an integration of pedology and geomorphology." Chapman and Hall, London.

Ghani, M. A. (1974). "Late Cenozoic vertical crustal movement in the central part of New Zealand." Unpublished Ph.D. thesis, Victoria University of Wellington.

Ghani, M. A. (1978). Late Cenozoic vertical crustal movements in the southern North Island, New Zealand. *New Zealand Journal of Geology and Geophysics* **21,** 117-125.

Gibbs, H. S. (1971). Nature of paleosols in New Zealand and their classification. *In* "Paleopedology." (D. H. Yaalon, Ed.), pp. 229-244. Israel University Press, Jerusalem.

Gibbs, H. S. (1980). "New Zealand Soils-An Introduction." Oxford University Press, Wellington.

Goh, K. M. (1972). Amino acid levels as indicators of paleosols in New Zealand soil profiles. *Geoderma* **7,** 33-47.

Grant, P. J. (1963). Forests and recent climatic history of the Huiarau Range, Urewera region, North Island. *Transactions of the Royal Society of New Zealand (Botany)* **2,** 143-172.

Grant, P. J. (1965). Major regime changes of the Tukituki River, Hawke's Bay, since about 1650 A.D. *Journal of Hydrology (N.Z.)* **4,** 17-30.

Grant, P. J. (1966). Variations of rainfall frequency in relation to erosion in eastern Hawke's Bay. *Journal of Hydrology (N.Z.)* **5,** 73-86.

Grant, P. J. (1985). Major periods of erosion and alluvial sedimentation in New Zealand during the Late Holocene. *Journal of the Royal Society of New Zealand* **15,** 67-121.

Grant, P. J. (1990). Major periods of erosion and alluvial sedimentation in New Zealand during the late Holocene. *Geological Society of New Zealand Miscellaneous Publication* **50A,** 57.

Grant, P. J. (1991). Disturbance in the forests of the Ruahine Range since 1770. *Journal of the Royal Society of New Zealand* **21,** 385-404.

Grant, P. J. (1994). Late Holocene histories of climate, geomorphology and vegetation, and their effects on the first New Zealanders. *In* "The origins of the first New Zealanders." (D. G. Sutton, Ed.), pp. 164-194. Auckland University Press, Auckland.

Grant, P. J. (1996). "Hawke's Bay forests of yesterday: a description and interpretation." P.J. Grant, Havelock North.

Grant-Taylor, T. L., and Rafter, T. A. (1971). New Zealand radiocarbon measurements-6. *New Zealand Journal of Geology and Geophysics* **14,** 364-402.

Griffiths, E. (1982). Soil pattern and environment in Hawke's Bay. *In* "New Zealand Soil Science Society 1982 annual conference Hastings, Hawke's Bay 22-26 November 1982:." (E. Griffiths, Ed.). New Zealand Society of Soil Science, Hastings.

Griffiths, E. (1984). The influence of climate on the distribution of yellow-grey earths and other soil groups in Hawke's Bay. *In* "Soil Groups of New Zealand Part 7." (J. G. Bruce, Ed.), pp. 20-24. New Zealand Society of Soil Science, Wellington.

Grindley, G. W. (1960). Sheet 8 Taupo (1st edition) Geological Map of New Zealand 1:250 000. DSIR, Wellington.

Hall, G. F. (1983). Pedology and geomorphology. *In* "Pedogenesis and Soil Taxonomy. 1. Concepts and interactions." (L. P. Wilding, N. E. Smeck, and G. F. Hall, Eds.), pp. 117-140. Elsevier Science Publishers B.V., Amsterdam.

Hall, G. F., and Olson, C. G. (1991). Predicting variability of soils from landscape models. *In* "Spatial variabilities of soils and landforms." (S. S. S. o. America, Ed.), pp. 9-24. Soil Science Society of America. Soil Science Society of America Special Publication No., Madison.

Hancox, G. T., and Berryman, K. R. (1986). Interim assessment of seismotectonic hazards at possible hydro-electric power development sites on the Mohaka River, Hawke's Bay. *EG Immediate Report* **86/036**.

Hanson, J. (1994). Paleoseismicity on the Wellington Fault in western Hawke's Bay. *Geological Society of New Zealand Miscellaneous Publication* **80,** 79.

Hardcastle, J. (1889). Origin of the loess deposits of the Timaru Plateau. *Transactions and Proceedings of the New Zealand Institute* **22,** 406-414.

Hardcastle, J. (1890). On the Timaru loess as a climatic indicator. *Transactions and Proceedings of the New Zealand Institute* **23,** 324-332.

Harden, J. W. (1982). A quantitative index of soil development from field descriptions: examples from a chronosequence in central California. *Geoderma* **28,** 1-28.

Harden, J. W., and Taylor, E. M. (1983). A quantitative comparison of soil development in four climatic regimes. *Quaternary Research* **20,** 342-359.

Harlan, P. W., Franzmeier, D. P., and Roth, C. B. (1977). Soil formation on loess in southwestern Indiana: II. Distribution of clay and free oxides and fragipan formation. *Soil Science Society of America Journal* **41,** 99-103.

Hashimoto, I., and Jackson, M. L. (1960). Rapid dissolution of allophane and kaolinite-halloysite after dehydration. *Clays Clay Minerals* **7,** 102-113.

Haywick, D. W. (1990). "Stratigraphy, sedimentology, palaeoecology and diagenesis of the Petane Group (Plio-Pleistocene) in the Tangoio Block, central Hawke's Bay, New Zealand." Unpublished Ph.D. thesis, James Cook University, Australia.

Haywick, D. W., Carter, R. M., and Henderson, R. A. (1992). Sedimentology of 40 000 year Milankovitch-controlled cyclothems from central Hawke's Bay, New Zealand. *Sedimentology* **39,** 675-696.

Haywick, D. W., and Henderson, R. A. (1991). Foraminiferal paleobathymetry of Plio-Pleistocene cyclothemic sequences, Petane Group, New Zealand. *Palaios* **6,** 586-599.

Haywick, D. W., Lowe, D. A., Beu, A. G., Henderson, R. A., and Carter, R. M. (1991). Plio-Pleistocene (Nukumaruan) lithostratigraphy of the Tangoio block, and origin of sedimentary cyclicity, central Hawke's Bay, New Zealand. *New Zealand Journal of Geology and Geophysics* **34,** 213-225.

Head, P. S., and Nelson, C. S. (1994). A high resolution oxygen isotope record for the past 6.4 million years B.P. at DSDP Site 593, Challenger Plateau, southern Tasman Sea. *In* "Evolution of the Tasman Sea Basin." (G. J. Van der Lingen, K. M. Swanson, and R. J. Muir, Eds.), pp. 159-179. A. A. Balkema, Rotterdam.

Healy, J., Vucetich, C. G., and Pullar, W. A. (1964). Stratigraphy and chronology of late Quaternary volcanic ash in Taupo, Rotorua, and Gisborne districts. *New Zealand Geological Survey Bulletin* **73**.

Henderson, J. (1933). Geological aspects of the Hawke's Bay earthquakes. *New Zealand Journal of Science and Technology* **15,** 38-75.

Heusser, L. E., and van de Geer, G. (1994). Direct correlation of terrestrial and marine paleoclimatic records from four glacial-interglacial cycles-DSDP Site 594 southwest Pacific. *Quaternary Science Reviews* **13,** 273-282.

Hewitt, A. E. (1992). New Zealand soil classification (Version 3.0). *DSIR Land Resources Scientific Report* **19**.

Hobden, B. J., Houghton, B. F., Lanphere, M. A., and Nairn, I. A. (1996). Growth of the Tongariro volcanic complex: new evidence from K-Ar age determinations. *New Zealand Journal of Geology and Geophysics* **39,** 151-154.

Hodgson, J. M. (1976). Soil survey field handbook. *Soil Survey Technical Monograph* **No 5**.

Hodgson, K. A. (1993). "Later Quaternary lahars from Mount Ruapehu in the Whangaehu River Valley, North Island, New Zealand." Unpublished Ph.D. thesis, Massey University, New Zealand.

Hogg, A. G., and McCraw, J. D. (1983). Late Quaternary tephras of Coromandel Peninsula, North Island, New Zealand: a mixed peralkaline and calcalkaline tephra sequence. *New Zealand Journal of Geology and Geophysics* **26,** 163-187.

Houghton, B. F., Wilson, C. J. N., and Hassan, M. (1988). Density measurements for pyroclasts and pyroclastic rocks. *New Zealand Geological Survey Record* **35,** 73-76.

Houghton, B. F., Wilson, C. J. N., Williams, M. O., Lanphere, M. A., Weaver, S. D., Briggs, R. M., and Pringle, M. S. (1995). Chronology and dynamics of a large silicic magmatic system: central Taupo Volcanic Zone, New Zealand. *Geology* **23,** 13-16.

Hovan, S. A., Rea, D. K., Pisias, N. G., and Shackleton, N. J. (1989). A direct link between the China loess and marine d18O records: aeolian flux to the north Pacific. *Nature* **340,** 296-298.

Howorth, R., Froggatt, P. C., and Robertson, S. M. (1980). Late Quaternary volcanic ash stratigraphy of the Poukawa area, central Hawke's Bay, New Zealand. *New Zealand Journal of Geology and Geophysics* **23,** 487-491.

Hubbard, C. B., Marden, M., Neall, V. E., and Pollok, J. A. (1979). The relationship of geology and soils to erosion in the south-eastern Ruahine range. *New Zealand Journal of Ecology* **2,** 88-89.

Hubbard, C. B., and Neall, V. E. (1980). A reconstruction of late Quaternary erosional events in the West Tamaki River catchment, southern Ruahine Range, North Island, New Zealand. *New Zealand Journal of Geology and Geophysics* **23,** 587-593.

Huggett, R. J. (1975). Soil landscape systems: a model of soil genesis. *Geoderma* **13,** 1-22.

Hughes, H. A., Hodgson, L., and Harris, A. C. (1939). Soil survey of the Heretaunga Plains. *In* "Land Utilisation report of the Heretaunga Plains." (N. Z. D. o. S. a. I. R. Bulletin, Ed.), pp. 18-43. Government Printer, Wellington.

Hull, A. G. (1985). "Late Quaternary geology of the Cape Kidnapper's area, Hawke's Bay, New Zealand." Unpublished M.Sc. thesis, Victoria University of Wellington, New Zealand.

Hull, A. G. (1987). A late Holocene uplifted shore platform on the Kidnapper's coast, North Island, New Zealand: some implications for shore platform development processes and uplift mechanism. *Quaternary Research* **28,** 183-195.

Hull, A. G. (1986). Pre-A.D. 1931 tectonic subsidence of Ahuriri Lagoon, Napier, Hawke's Bay, New Zealand. *New Zealand Journal of Geology and Geophysics* **29,** 75-82.

Hull, A. G. (1990). Tectonics of the 1931 Hawke's Bay earthquake. *New Zealand Journal of Geology and Geophysics* **33,** 309-320.

Jenny, H. (1941). "Factors of soil formation-a system of quantitative pedology." McGraw-Hill, New York.

Jenny, H. (1980). "The soil resource, origin and behaviour." Springer-Verlag, New York.

Johnson, D. L., and Watson-Stegner, D. (1987). Evolution model of pedogenesis. *Soil Science* **143,** 349-366.

Kaewyana, W. (1980). "Late Quaternary alluvial terraces and their coverbed stratigraphy, Eketahuna and Pahiatua districts, New Zealand." Unpublished M.Sc. thesis, Victoria University of Wellington, New Zealand.

Kamp, P. J. J. (1978). "Stratigraphy and sedimentology of conglomerates in the Pleistocene Kidnappers Group, Hawke's Bay." Unpublished M.Sc. thesis, University of Waikato, New Zealand.

Kamp, P. J. J. (1984). Neogene and Quaternary extent and geometry of the subducted Pacific Plate beneath North Island, New Zealand: Implications for Kaikoura tectonics. *Tectonophysics* **108,** 241-266.

Kamp, P. J. J. (1988). Tectonic geomorphology of the Hikurangi Margin: surface manifestations of different modes of subduction. *Zeitschrift fur Geomorphologie Supplementband* **69,** 55-67.

Kamp, P. J. J. (1990). Kidnappers Group (middle Pleistocene), Hawke's Bay. *Geological Society of New Zealand Miscellaneous Publication* **50B,** 105-118.

Kamp, P. J. J. (1992a). Landforms of Hawke's Bay and their origin: a plate tectonic interpretation. *In* "Landforms of New Zealand." (J. M. Soons, and M. J. Selby, Eds.), pp. 343-366. Longman Paul Limited, Auckland.

Kamp, P. J. J. (1992b). Landforms of Wairarapa: a geological perspective. *In* "Landforms of New Zealand." (J. M. Soons, and M. J. Selby, Eds.), pp. 367-381. Longman Paul Limited, Auckland.

Kamp, P. J. J., Harmsen, F. J., Nelson, C. S., and Boyle, S. F. (1988). Barnacle-dominated limestone with giant cross-beds in a non-tropical, tide-swept, Pliocene forearc seaway, Hawke's Bay, New Zealand. *Sedimentary Geology* **60,** 173-195.

Kamp, P. J. J., and Nelson, C. S. (1987). Tectonic and sea-level controls on non-tropical Neogene limestones in New Zealand. *Geology* **15,** 610-613.

Kamp, P. J. J., and Nelson, C. S. (1988). Nature and occurrence of modern and Neogene active margin limestones in New Zealand. *New Zealand Journal of Geology and Geophysics* **31,** 1-20.

Karathanasis, A. D. (1987a). Mineral solubility relationships in Fragiudalfs of western Kentucky. *Soil Science Society of America Journal* **51,** 474-481.

Karathanasis, A. D. (1987b). Thermodynamic evaluation of amorphous aluminosilicate binding agents in fragipans of western Kentucky. *Soil Science Society of America Journal* **51,** 819-824.

Keller, W. D., and Reesman, A. L. (1963). Dissolved products of artificially pulverised silicate minerals and rocks: Part II. *Journal of Sedimentary Petrology* **33,** 426-437.

Kelsey, H. M., Cashman, S. M., Beanland, S., and Berryman, K. R. (1995). Structural evolution along the inner forearc of the obliquely convergent Hikurangi margin, New Zealand. *Tectonics* **14,** 1-18.

Kelsey, H. M., Erdman, C. F., and Cashman, S. M. (1993). Geology of southern Hawke's Bay from the Maraetotara Plateau and Waipawa westward to the Wakarara Range and the Ohara Depression. *Institute of Geological and Nuclear Sciences Science Report* **93/2**.

Kemp, R. A. (1984). "Quaternary soils in southern East Anglia and Lower Thames Basin." Unpublished Ph.D. thesis, University of London, England.

Kemp, R. A. (1985). A consideration of the terms "paleosol" and "rubification". *Quaternary Newsletter* **45,** 6-11.

Kennedy, N. M. (1988). Late Quaternary loess associated with the Mamaku Plateau, North Island, New Zealand. *In* "Loess: its distribution, geology and soils." (D. N. Eden, and R. J. Furkert, Eds.), pp. 71-80. A.A. Balkema, Rotterdam.

Kennedy, N. M. (1994). New Zealand tephro-chronology as a tool in geomorphic history of the c.140ka Mamaku Ignimbrite Plateau and in relating oxygen isotope stages. *Geomorphology* **9,** 97-115.

King, L. C. (1953). Canons of landscape evolution. *Bulletin of the Geological Society of America* **64,** 721-751.

Kingma, J. T. (1957a). The North Island Geanticline in the Hawke's Bay sector. *New Zealand Journal of Science and Technology* **B38,** 496-499.

Kingma, J. T. (1957b). The tectonic setting of the Ruahine-Rimutaka Range. *New Zealand Journal of Science and Technology* **B38,** 858-861.

Kingma, J. T. (1959). The tectonic history of New Zealand. *New Zealand Journal of Geology and Geophysics* **2,** 1-55.

Kingma, J. T. (1960). Outline of the Cretaceo-Tertiary sedimentation in the eastern basin of New Zealand. *New Zealand Journal of Geology and Geophysics* **3,** 222-234.

Kingma, J. T. (1971). Geology of Te Aute subdivision. *New Zealand Geological Survey Bulletin* **70**.

Kirkman, J. H. (1975). Clay mineralogy of some tephra beds of Rotorua area, North Island, New Zealand. *Clay Minerals* **10,** 437-449.

Kirkman, J. H. (1980). Clay mineralogy of a sequence of andesitic tephra beds of western Taranaki, New Zealand. *Clay Minerals* **15,** 157-163.

Kirkman, J. H., and McHardy, W. J. (1980). A comparative study of the morphology, chemical composition and weathering of rhyolitic and andesitic glass. *Clay Minerals* **15,** 165-173.

Kittrick, J. A. (1969). Soil minerals in the Al2O3-SiO2-H2O system and a theory of their formation. *Clays Clay Minerals* **17,** 157-167.

Kohn, B. P. (1970). Identification of New Zealand tephra layers by emission spectrographic analysis of their titanomagnetites. *Lithos* **3,** 361-368.

Kohn, B. P. (1973). "Studies of New Zealand Quaternary pyroclastic rocks." Unpublished Ph.D. thesis, Victoria University of Wellington, New Zealand.

Kohn, B. P., Pillans, B.J. and McGlone, M.S. (1992). Zircon fission track age for middle Pleistocene Rangitawa Tephra, New Zealand: stratigraphic and paleoclimatic significance. *Palaeogeography, Palaeoclimatology, Palaeoecology* **95,** 73-94.

Kohn, B. P., and Glasby, G. P. (1978). Tephra distribution and sedimentation rates in the Bay of Plenty, New Zealand. *New Zealand Journal of Geology and Geophysics* **21,** 49-70.

Kohn, B. P., and Neall, V. E. (1973). Identification of late Quaternary tephras for dating Taranaki lahar deposits. *New Zealand Journal of Geology and Geophysics* **16,** 781-792.

Kohn, B. P., Pillans, B. J., and Alloway, B. V. (1996). Letter to the Editor. Fission track age estimates for Mount Curl Tephra. Reply. *New Zealand Journal of Geology and Geophysics* **39,** 333-335.

Kottlowski, F. E., Cooley, M.E. and Ruhe, R.V. (1965). Quaternary geology of the Southwest. *In* "Quaternary of the United States." (H. E. J. Wright, and R. B. Morrison, Eds.), pp. 287-298. Princeton University Press, Princeton.

Krieger, F. W. (1992). "Sedimentology and paleoenvironmental analysis of Castlecliffian strata in the Dannevirke Basin." Unpublished M.Sc. thesis, Massey University, New Zealand.

Kukla, G., and Cilek, V. (1996). Plio-Pleistocene megacycles: record of climate and tectonics. *Palaeogeography, Palaeoclimatology, Palaeoecology* **120,** 171-194.

Kukla, G. J. (1975). Loess stratigraphy of central Europe. *In* "After the Australopithecines." (K. W. Butzer, and G. L. Isaac, Eds.), pp. 99-188. Mouton, The Hague.

Kukla, G. J. (1977). Pleistocene land-sea correlations. I. Europe. *Earth Science Reviews* **13,** 307-374.

Kukla, G. J. (1987). Loess stratigraphy in central China. *Quaternary Science Reviews* **6,** 191-219.

Laffan, M. D., and Cutler, E. J. B. (1977a). Landscapes, soils, and erosion of a small catchment in the Wither Hills, Marlborough. 1. landscape periodicity, slope deposits, and soil pattern. *New Zealand Journal of Science* **20,** 37-48.

Lamarche, G., and Froggatt, P. C. (1993). New eruptive vents for the Whakamaru Ignimbrite (Taupo Volcanic Zone) identified from magnetic fabric study. *New Zealand Journal of Geology and Geophysics* **36,** 213-222.

Lambert, M. G., Trustrum, N.A. and Costall, D.A. (1984). Effect of soil slip erosion on seasonally dry Wairarapa hill pastures. *New Zealand Journal of Agricultural Research* **27,** 57-64.

Leamy, M. L. (1975). Paleosol identification and soil stratigraphy in South Island, New Zealand. *Geoderma* **13,** 53-60.

Leamy, M. L., and Burke, A. S. (1973). Identification and significance of paleosols in cover deposits in central Otago. *New Zealand Journal of Geology and Geophysics* **16,** 623-635.

Leamy, M. L., Milne, J. D. G., Pullar, W. A., and Bruce, J. G. (1973). Paleopedology and soil stratigraphy in the New Zealand Quaternary succession. *New Zealand Journal of Geology and Geophysics* **16,** 723-744.

Lees, C. M. (1986). Late Quaternary palynology of the southern Ruahine Range, North Island, New Zealand. *New Zealand Journal of Botany* **24,** 315-329.

Lewis, K. B. (1971). Sediments on the continental shelf and slope between Napier and Castlepoint, New Zealand. *New Zealand Journal of Marine and Freshwater Research* **7,** 183-208.

Lewis, K. B. (1980). Quaternary sedimentation on the Hikurangi oblique-subduction and transform margin, New Zealand. *Special Publication of the International Association of Sedimentologists* **4,** 171-189.

Lewis, K. B., and Pettinga, J. R. (1993). The emerging, imbricate frontal wedge of the Hikurangi margin. *In* "Sedimentary Basins of the World." (P. F. Ballance, Ed.), pp. 225-250. Elsevier, Amsterdam.

Lillie, A. R. (1953). The geology of the Dannevirke Subdivision. *New Zealand Geological Survey Bulletin* **n.s. 46**.

Limmer, A. W., and Wilson, A. T. (1980). Amino acids in buried paleosols. *Journal of Soil Science* **31,** 147-153.

Lindsay, W. L. (1979). "Chemical equilibria in soils." John Wiley and Sons, New York.

Lowe, D. J. (1986). Controls on the rates of weathering and clay mineral genesis in airfall tephras: a review and New Zealand case study. *In* "Rates of chemical weathering of rocks and minerals." (S. M. Colman, and D. P. Dethier, Eds.), pp. 265-330. Academic Press, Orlando.

Lowe, D. J. (1990). Tephra studies in New Zealand: a historical review. *Journal of the Royal Society of New Zealand* **20,** 119-150.

Lowe, D. J. (1994). Conference Tour Guides. *In* "International Inter-INQUA Field Conference and Workshop on Tephrochronology, Loess, and Paleopedology." (D. J. Lowe, Ed.), pp. 186, University of Waikato, Hamilton, New Zealand.

Lowe, D. J., and Hogg, A. G. (1992). Application of new technology liquid scintillation spectrometry to radiocarbon dating of tephra deposits, New Zealand. *Quaternary International* **13/14,** 135-142.

Manning, D. A. (1996a). "Middle-late Pleistocene tephrostratigraphy of the eastern Bay of Plenty region, New Zealand." Unpublished Ph.D. thesis, Victoria University of Wellington, New Zealand.

Manning, D. A. (1996b). Middle-late Pleistocene tephrostratigraphy of the eastern Bay of Plenty, New Zealand. *Quaternary International* **34-36,** 3-12.

Marden, M. (1984). "Geology and its relationship to erosion in the southern Ruahine Range, North Island, New Zealand." Unpublished Ph.D. thesis, Massey University, New Zealand.

Marden, M., and Neall, V. E. (1990). Dated Ohakean terraces offset by the Wellington Fault, near Woodville, New Zealand. *New Zealand Journal of Geology and Geophysics* **33,** 449-453.

Marden, M., Paintin, I. K., Lees, C. M., and Neall, V. E. (1986). Woodville neotectonics and Quaternary stratigraphy field trip. *Geological Society of New Zealand Miscellaneous Publication* **No.35B,** B3/1-20.

Marden, M., Phillips, C., and Rowan, D. (1991). Declining soil loss with increasing age of plantation forests in the Uawa catchment, east coast region, North Island, New Zealand. *In* "Proceedings of the international conference on sustainable land management, November 17-23, 1991." (P. Henriques, Ed.), pp. 358-361, Napier.

Marden, M., and Rowan, D. (1993). Protective value of vegetation on Tertiary terrain before and during Cyclone Bola, East Coast, North Island, New Zealand. *New Zealand Journal of Forestry Science* **23,** 255-263.

Marshall, P. (1933). Effects of earthquake on coastline near Napier. *New Zealand Journal of Science and Technology* **15,** 79-92.

McArthur, J. L., and Shepherd, M. J. (1990). Late Quaternary glaciation of Mt Ruapehu, North Island, New Zealand. *Journal of the Royal Society of New Zealand* **20,** 287-296.

McDaniel, P. A., and Falen, A. L. (1994). Temporal and spatial patterns of episaturation in a fragixeralf landscape. *Soil Science Society of America Journal* **58,** 1451-1457.

McDonald, E. V., and Busacca, A. J. (1992). Late Quaternary stratigraphy of loess in the channelled Scabland and Palouse regions of Washington State. *Quaternary*
McGlone, M. S. (1978). Forest destruction by early Polynesians, Lake Poukawa, Hawkes Bay, New Zealand. *Journal of the Royal Society of New Zealand* **8,** 275-281.

McGlone, M. S. (1978). Forest destruction by early Polynesians, Lake Poukawa, Hawkes Bay, New Zealand. *Journal of the Royal Society of New Zealand* **8,** 275-281.

McGlone, M. S. (1983). Polynesian deforestation of New Zealand: A preliminary synthesis. *Archaeology in Oceania* **18,** 11-25.

McGlone, M. S. (1988). New Zealand. *In* "Vegetation History." (B. a. W. I. Huntley, T., Ed.), pp. 557-599. Kluwer Academic Publishers, The Hague.

McGlone, M. S. (1989). The Polynesian settlement of New Zealand in relation to environmental and biotic changes. *New Zealand Journal of Ecology* **12 (Supplement),** 115-129.

McGlone, M. S. (1995). LateGlacial landscape and vegetation change and the Younger Dryas climatic oscillation in New Zealand. *Quaternary Science Reviews* **14,** 867-881.

McGlone, M. S., Howorth, R., and Pullar, W. A. (1984b). Late Pleistocene stratigraphy, vegetation and climate of the Bay of Plenty and Gisborne regions, New Zealand. *New Zealand Journal of Geology and Geophysics* **27,** 327-350.

McGlone, M. S., Neall, V. E., and, and Pillans, B. J. (1984a). Inaha Terrace deposits: a late Quaternary terrestrial record in South Taranaki, New Zealand. *New Zealand Journal of Geology and Geophysics* **27,** 35-49.

McGlone, M. S., and Topping, W. W. (1973). Late Otiran/early Aranuian vegetation in the Tongariro area, central North Island, New Zealand. *New Zealand Journal of Botany* **11,** 283-290.

McGlone, M. S., and Topping, W. W. (1977). Aranuian (post-glacial) pollen diagrams from the Tongariro region, North Island, New Zealand. *New Zealand Journal of Botany* **15,** 749-760.

McIntosh, P. D., Eden, D. N., Burgham, S. J., and Froggatt, P. C. (1988). Volcanic glass and terrace chronology in the Gore region, Southland. *Geological Society of New Zealand Newsletter* **80,** 54-56.

McIntyre, B. M. (1975). "Upper Quaternary loess stratigraphy at two exposures in the southern Manawatu." Unpublished B.Sc. (Hons) thesis, Massey University, New Zealand.

McKeague, J. A. (1967). An evaluation of 0.1M pyrophosphate and pyrophosphate-dithionite in comparison with oxalate as extractants of the accumulation products in podzols and some other soils. *Canadian Journal of Soil Science* **47,** 95-99.

McKeague, J. A., Brydon, J. E., and Miles, N. M. (1971). Differentiation of forms of extractable iron and aluminium in soils. *Soil Science Society of America Proceedings* **35,** 33-38.

McKeague, J. A., and Day, J. H. (1966). Dithionite- and oxalate-extractable Fe and Al as aids in differentiating various classes of soils. *Canadian Journal of Soil Science* **46,** 13-22.

McKeague, J. A., and Protz, R. (1980). Cement of duric horizons, micromorphology and energy dispersive analysis. *Canadian Journal of Soil Science* **60,** 45-52.

McKeague, J. A., and Sprout, P. N. (1975). Cemented subsoils (duric horizons) in some soils of British Columbia. *Canadian Journal of Soil Science* **55,** 189-203.

McKelvey, P. (1995). "Steepland forests: a historical perspective of protection forestry in New Zealand." Canterbury University Press, Christchurch.

McLeod, M., Rijkse, W.C. and Dymond, J.R. (1995). A soil-landscape model for close-jointed mudstone, Gisborne-East Cape, North Island, New Zealand. *Australian journal of soil research* **33,** 381-396.

Mehra, O. P., and Jackson, M. L. (1960). Iron oxide removal from soils and clays by a dithionite-citrate system buffered with sodium bicarbonate. *Clays and Clay Minerals* **7,** 317-327.

Milne, G. (1935a). Some suggested units of classification and mapping particularly for East African soils. *Soils Research* **4,** 183-198.

Milne, G. (1935b). Composite units for the mapping of complex soil association. *Transactions of the 3rd International Congress of Soil Science* **1,** 345-357.

Milne, G. (1936). Normal erosion as a factor in soil profile development. *Nature* **138,** 548-549.

Milne, J. D. G. (1973a). "Upper Quaternary geology of the Rangitikei drainage basin, North Island, New Zealand." Unpublished Ph.D. thesis, Victoria University of Wellington, New Zealand.

Milne, J. D. G. (1973b). Maps and sections of river terraces in Rangitikei Basin, North Island, New Zealand. *New Zealand Soil Survey Report* **4**.

Milne, J. D. G. (1973c). Mount Curl Tephra, a 230 000-year-old marker bed in New Zealand, and its implications for Quaternary chronology. *New Zealand Journal of Geology and Geophysics* **16,** 519-532.

Milne, J. D. G., and Smalley, I. J. (1979). Loess deposits in the southern part of the North Island of New Zealand: an outline stratigraphy. *Acta Geologica Academiae Scientiarum Hungaricae, Tomus* **22,** 197-204.

Ministry of Works (1971). "National Resources Survey. Part VI, Hawke's Bay Region." Government Printer, Wellington, New Zealand

Molloy, L. (1988). "Soils in the New Zealand landscape-the living mantle." Mallinson Rendel Ltd., Wellington.

Morrison, R. B. (1967). Principles of Quaternary soil stratigraphy. *In* "Quaternary Soils, International Association for Quaternary Research (INQUA), VII Congress, 1965." (R. B. Morrison, and H. E. J. Wright, Eds.), pp. 1-69. Centre for Water Resources Research, Desert Research Institute, University of Nevada, Reno, Nevada.

Morrison, R. B. (1978). Quaternary soil stratigraphy-concepts, methods, and problems. *In* "Quaternary Soils." (W. C. Mahaney, Ed.), pp. 77-108. Geo Abstracts, Norwich.

Neall, V. E., Hanson, J., and Palmer, A. S. (1994). Paleoseismicity on the Ruahine Fault in western Hawke's Bay. *Geological Society of New Zealand Miscellaneous Publication* **80,** 143.

Nelson, C. S., Hendy, C. H., Jarrett, G. R., and Cuthbertson, A. M. (1985). Near-synchroneity of New Zealand alpine glaciations and Northern Hemisphere continental glaciations during the past 750kyr. *Nature* **318,** 361-363.

Nettleton, W. D., and Peterson, F. F. (1983). Aridisols. *In* "Pedogenesis and soil taxonomy: II. The soil orders." (L. P. Wilding, N. E. Smeck, and G. F. Hall, Bureau, N. Z. S. (1954). General survey of the soils of the North Island. *New Zealand Soil Bureau Bulletin* **5,** 1-286.

New Zealand Soil Bureau (1954). General survey of the soils of the North Island. *New Zealand Soil Bureau Bulletin* **5,** 1-286.

New Zealand Soil Bureau (1968). Soils of New Zealand. Part 1. *New Zealand Soil Bureau Bulletin* **26,** 47-88.

Nikiforoff, C. C. (1942). Fundamental formula of soil formation. *American Journal of Science* **240,** 847-866.

Noble, K. E. (1985). Land Use Classification of the southern Hawke's Bay-Wairarapa Region: a bulletin to accompany New Zealand Land Resource Inventory Worksheets. *Water and Soil Miscellaneous Publication No.* **74**.

Nomenclature, A. C. o. S. (1961). Code of stratigraphic nomenclature. *American Association of Petroleum Geologists Bulletin* **45,** 645-665.

Norton, L. D., and Franzmeier, D. P. (1978). Toposequences of loess-derived soils in southwestern Indiana. *Soil Science Society of America Journal* **42,** 622-627.

Norton, L. D., Hall, G. F., Smeck, N. E., and Bigham, J. M. (1984). Fragipan bonding in a late-Wisconsinan loess-derived soil in east- central Ohio. *Soil Science Society of America Journal* **48,** 1360-1366.

O'Loughlin, C. L., and Ziemer, R. R. (1982). The importance of root strength and deterioration rates upon edaphic stability in steepland forests. *In* "Carbon uptake and allocation in subalpine ecosystems as a key to management. Proceedings of International Union of Forest Research Organisations August 1982.", pp. 70-78. Oregon State University, Corvalis, Oregon.

Ota, Y., Omura, A., and Iwata, H. (1989). 230Th-238U age of Rotoehu Ash and its implications for marine terrace chronology of eastern bay of Plenty, New Zealand. *New Zealand Journal of Geology and Geophysics* **32,** 327-331.

Oyama, M., and Takehara, H. (1967). "Revised standard soil charts." Frank McCarthy Colour Ltd., Melbourne.

Page, M. J. (1988). Land Use Classification of the northern Hawke's Bay Region: a bulletin to accompany the New Zealand Land Resource Inventory Worksheets. *Water and Soil Miscellaneous Publication No.* **109**.

Page, M. J., Trustrum, N. A., and Dymond, J. R. (1994a). Sediment budget to assess the geomorphic effect of a cyclonic storm, New Zealand. *Geomorphology* **9,** 169-188.

Page, N. J., Trustrum, N. A., and DeRose, R. C. (1994b). A high resolution record of storm-induced erosion from lake sediments, New Zealand. *Journal of Paleoliminology* **11,** 333-348.

Palmer, A. S. (1982a). "The stratigraphy and selected properties of loess in Wairarapa, New Zealand." Unpublished Ph.D. thesis, Victoria University of Wellington, New Zealand.

Palmer, A. S. (1982b). Kawakawa Tephra in Wairarapa, New Zealand, and its use for correlating Ohakea loess. *New Zealand Journal of Geology and Geophysics* **25,** 305-315.

Palmer, A. S., and Barker, P. R. (1984). Dry bulk density, natural water content and tip penetration resistance data for four Wairarapa loess cores. *New Zealand Soil Bureau Scientific Report* **68**.

Palmer, A. S., Barnett, R., Pillans, B. J., and Wilde, R. H. (1988). Loess, river aggradation terraces and marine benches at Otaki, southern North Island, New Zealand. *In* "Loess, its distribution, geology and soils." (D. N. Eden, and R. J. Furkert, Eds.), pp. 163-174. A.A. Balkema, Rotterdam.

Palmer, A. S., and Pillans, B. J. (1996). Record of climatic fluctuations from ca. 500ka loess deposits and paleosols near Wanganui, New Zealand. *Quaternary International* **34-36,** 155-162.

Palmer, A. S., Vucetich, C. G., McGlone, M., and Harper, M. A. (1989). Last Glacial loess and early Last Glacial vegetation history of Wairarapa Valley, New Zealand. *New Zealand Journal of Geology and Geophysics* **32,** 499-513.

Palmer, K. (1990). XRF analysis of granatoids and associated rocks St Johns Range, South Victoria Land, Antarctica. *Wellington: Victoria University of Wellington, Research School of Earth Science, Geology Board of Studies Publication* **5,** 1-23.

Parfitt, R. L. (1990). Allophane in New Zealand-a review. *Australian Journal of Soil Research* **28,** 343-360.

Parfitt, R. L., and Childs, C. W. (1988). Estimation of forms of Fe and Al: a review, and analysis of contrasting soils by dissolution and Moessbauer methods. *Australian Journal of Soil Research* **26,** 121-144.

Parfitt, R. L., and Henmi, T. (1982). Comparison of an oxalate-extraction method and an infrared spectroscopic method for determining allophane in soil clays. *Soil Science and Plant Nutrition* **28,** 183-190.

Parfitt, R. L., and Saigusa, M. (1985). Allophane and humus-aluminium in Spodosols and Andepts formed from the same volcanic ash beds in New Zealand. *Soil Science* **139,** 149-155.

Parfitt, R. L., and Wilson, A. D. (1985). Estimation of allophane and halloysite in three sequences of volcanic soils, New Zealand. *Catena Supplement* **7,** 1-8.

Pettinga, J. R. (1982). Upper Cenozoic structural history, coastal southern Hawke's Bay, New Zealand. *New Zealand Journal of Geology and Geophysics* **25,** 149-191.

Pettinga, J. R. (1987a). Waipoapoa Landslide: a deep-seated complex block slide in Tertiary weak-rock flysch, southern Hawke's Bay, New Zealand. *New Zealand Journal of Geology and Geophysics* **30,** 401-414.

Pettinga, J. R. (1987b). Poniu Landslide: a deep-seated wedge failure in Tertiary weak-rock flysch, southern Hawke's Bay, New Zealand. *New Zealand Journal of Geology and Geophysics* **30,** 415-430.

Pettinga, J. R., and Bell, D. H. (1991). Engineering geological assessment of slope instability for rural land-use, Hawke's Bay, New Zealand. *In* "Landslides." (D. H. Bell, Ed.), pp. 1467-1480. A.A. Balkema, Rotterdam.

Pillans, B., and Kohn, B. (1981). Rangitawa Pumice: a widespread (?) Quaternary marker bed in Taranaki-Wanganui. *Victoria University of Wellington Geology Department Publication* **20,** 94-104.

Pillans, B. J. (1983). Upper Quaternary marine terrace chronology and deformation, South Taranaki, New Zealand. *Geology* **11,** 292-297.

Pillans, B. J. (1986). A late Quaternary uplift map for North Island, New Zealand. *Royal Society of New Zealand Bulletin* **24,** 409-417.

Pillans, B. J. (1988a). Loess chronology in Wanganui Basin, New Zealand. *In* "Loess: its distribution, geology and soils." (D. N. Eden, and R. J. Furkert, Eds.), pp. 175-191. A.A. Balkema, Rotterdam.

Pillans, B. J. (1991). New Zealand Quaternary stratigraphy: an overview. *Quaternary Science Reviews* **10,** 405-418.

Pillans, B. J. (1994a). Direct marine-terrestrial correlations, Wanganui Basin, New Zealand: the last 1 million years. *Quaternary Science Reviews* **13,** 189-200.

Pillans, B. J. (1994b). New Zealand Quaternary stratigraphy: integrating marine and terrestrial records of environmental changes. *Japanese Journal of Geography* **103,** 760-769.

Pillans, B. J., Kohn, B. P., Berger, G., Froggatt, P. C., Duller, G., Alloway, B. V., and Hesse, P. (1996). Multi-method comparison for mid-Pleistocene Rangitawa Tephra, New Zealand. *Quaternary Science Reviews (Quaternary Geochronology)* **15,** 641-653.

Pillans, B. J., McGlone, M., Palmer, A. S., Mildenhall, D., Alloway, B. V., and Berger, G. (1993). The Last Glacial Maximum in central and southern North Island, New Zealand: a palaeoenvironmental reconstruction using the Kawakawa Tephra Formation as a chronostratigraphic marker. *Palaeogeography, Palaeoclimatology, Palaeoecology* **101,** 283-304.

Pillans, B. J., Pullar, W. A., Selby, M. J., and Soons, J. M. (1992). The age and development of the New Zealand landscape. *In* "Landforms of New Zealand." (J. M. Soons, and M. J. Selby, Eds.), pp. 31-62. Longman Paul, Auckland.

Pillans, B. J., and Wright, I. C. (1990). 500 000 year paleomagnetic record from New Zealand loess. *Quaternary Research* **33,** 178-187.

Pillans, B. J., and Wright, I. C. (1992). Late Quaternary tephrostratigraphy from the southern Havre Trough-Bay of Plenty, northeast New Zealand. *New Zealand Journal of Geology and Geophysics* **35,** 129-143.

Pohlen, I. J., Harris, C. S., Gibbs, H. S., and Raeside, J. D. (1947). Soils and some related agricultural aspects of mid-Hawke's Bay. *New Zealand Department of Industrial Research Bulletin* **94**.

Pringle, M. S., McWilliams, M., Houghton, B.F., Lanphere, M.A. and Wilson, C.J.N. (1992). 40Ar/39Ar dating of Quaternary feldspar: examples from the Taupo Volcanic Zone, New Zealand. *Geology* **20,** 531-534.

Pullar, W. A. (1970). Pumice ash beds and peaty deposits of archaeological significance near Lake Poukawa, Hawke's Bay. *New Zealand Journal of Science* **13,** 687-705.

Pullar, W. A., and Birrell, K. S. (1973a). Age and distribution of late Quaternary pyroclastic and associated cover deposits of the Rotorua and Taupo area, North Island, New Zealand. *New Zealand Soil Survey Report* **1**.

Pullar, W. A., and Birrell, K. S. (1973b). Age and distribution of late Quaternary pyroclastic and associated cover deposits of central North Island, New Zealand. *New Zealand Soil Survey Report* **2**.

Pullar, W. A., Birrell, K. S., and Heine, J. C. (1973). Named tephras and tephra formations occurring in the central North Island, with notes on derived soils and buried paleosols. *New Zealand Journal of Geology and Geophysics* **16,** 497-518.

Pullar, W. A., and Heine, J. C. (1971). Ages, inferred from 14C dates, of some tephra and other deposits from Rotorua, Bay of Plenty, Gisborne, and Hawke's Bay districts. *In* "Proceedings of radiocarbon user's conference." (R. S. o. N. Zealand, Ed.), pp. 119-138. Royal Society of New Zealand, Lower Hutt.

Pye, K., and Krinsley, D. (1984). Petrographic examination of sedimentary rocks in the SEM using backscattered detectors. *Journal of Sedimentary Petrology* **54,** 877-888.

Qizhong, W., Eden, D. N., and Hunt, J. L. (1992). A comparison of the geochemical features of some loess sections in New Zealand and China. *Chinese Journal of Geochemistry* **11,** 201-213.

Raeside, J. D. (1964). Loess deposits of the South Island, New Zealand, and soils formed on them. *New Zealand Journal of Geology and Geophysics* **7,** 811-838.

Rait, G., Chanier, F., and Waters, D. W. (1991). Landward- and seaward-directed thrusting accompanying the onset of subduction beneath New Zealand. *Geology* **19,** 230-233.

Raub, M. L. (1985). "The neotectonic evolution of the Wakarara area, southern Hawke's Bay, New Zealand." Unpublished M.Phil. thesis, University of Auckland, New Zealand.

Raub, M. L., Cutten, H. C. N., and Hull, A. G. (1987). Seismotectonic hazard analysis of the Mohaka Fault, North Island, New Zealand. *In* "Proceedings of the Pacific Conference on earthquake engineering.", pp. 219-230, Wairaki, New Zealand, 5-8 August 1987.

Reid, R. (1983). Origin of the rhyolitic rocks of the Taupo Volcanic Zone, New Zealand. *Journal of Volcanology and Geothermal Research* **15,** 315-338.

Reneau, S. L., Dietrich, W. E., Dorn, R. I., Berger, C. R., and Rubin, M. (1986). Geomorphic and paleoclimatic implications of latest Pleistocene radiocarbon dates from colluvium-mantled hollows, California. *Geology* **14,** 655-658.

Revell, C. G. (1981). Tropical cyclones in the south-west Pacific November 1969-April 1979. *New Zealand Meteorological Service Miscellaneous Publication* **170**.

Reyners, M. A. (1980). A microearthquake study of the plate boundary, North Island, New Zealand. *Geophysical Journal of the Royal Astronomical Society* **63,** 1-22.

Reyners, M. A. (1983). Lateral segmentation of the subducted plate at the Hikurangi Margin, New Zealand: seismological evidence. *Tectonophysics* **96,** 203-223.

Rhea, K. P. (1968). Aokautere Ash, loess, and river terraces in the Dannevirke district, New Zealand. *New Zealand Journal of Geology and Geophysics* **11,** 685-692.

Richmond, G. M., and Frye, J. C. (1957). Stratigraphic Commission. Note 19-Status of soils in stratigraphic nomenclature. *Bulletin of the American Association of Petroleum Geologists* **41,** 758-763.

Riecken, F. F., and Poetsch, E. (1960). Genesis and classification considerations of some prairie formed soil profiles from local alluvium in Adair County, Iowa. *Proceedings of the Iowa Academy of Sciences* **67,** 268-276.

Rijkse, W. C. (1972). Soils of Takapau Agricultural Research Farm, Hawke's Bay, New Zealand. *New Zealand Journal of Agricultural Research* **15,** 329-340.

Rijkse, W. C. (1980). Soils of part Mohaka-Aropaoanui area, North Island, New Zealand. *New Zealand Soil Survey Report 55.*

Rimstidt, J. D., and Barnes, H. L. (1980). The kinetics of silica-water reactions. *Geochimica et Cosmochimica Acta* **44,** 1683-1699.

Robertson, S. M. (1978). "A study of late Quaternary history of Poukawa basin." Unpublished M.Sc. thesis, Victoria University of Wellington, New Zealand.

Rogers, G. M., and McGlone, M. S. (1989). A postglacial vegetation history of the southern-central uplands of North Island, New Zealand. *Journal of the Royal Society of New Zealand* **19,** 229-248.

Roser, B. P. (1983). "Comparative studies of copper and manganese mineralisation in Torlesse, Waipapa and Haast Schist terrains, New Zealand." Unpublished Ph.D. thesis, Victoria University of Wellington, New Zealand.

Roxburgh, H. J. (1974). "Characterisation of late Pleistocene tephra at Te Mata Peak, Havelock North." Unpublished B.Sc. (Hons) thesis, Victoria University of Wellington, New Zealand.

Ruellan, A. (1971). The history of soils: some problems of definition and interpretation. *In* "Paleopedology: origin, nature and dating of paleosols." (D. H. Yaalon, Ed.), pp. 3-13. International Society of Soil Science and Israel Universities Press, Jerusalem.

Ruhe, R. V. (1956). Geomorphic surfaces and the nature of soils. *Soil Science* **82,** 441-455.

Ruhe, R. V. (1959). Stone lines in soils. *Soil Science* **87,** 223-231.

Ruhe, R. V. (1960). Elements of the soil landscape. *Transactions 7th International Congress of Soil Science* **4,** 165-170.

Ruhe, R. V. (1969a). "Quaternary landscapes in Iowa." Iowa State University Press, Ames, Iowa.

Ruhe, R. V. (1969b). Principles for dating pedogenic events in the Quaternary. *Soil Science* **107,** 398-402.

Ruhe, R. V. (1975). "Geomorphology." Houghton Mifflin, Boston.

Ruhe, R. V., and Olson, C. G. (1980). Soil welding. *Soil Science* **130,** 132-139.

Ruhe, R. V., and Walker, P. H. (1968). Hillslope models and soil formation: I. Open systems. *Transactions 9th International Congress of Soil Science* **4,** 551-560.

Runge, E. C. A., Walker, T. W., and Howarth, D. T. (1974). A study of late Pleistocene loess deposits, south Canterbury, New Zealand. Part 1. Forms and amounts of phosphorous compared with other techniques for identifying paleosols. *Quaternary Research* **4,** 76-84.

Sarna-Wojcicki, A. M., Morrison, S. D., Meyer, C. E., and Hillhouse, J. W. (1987). Correlation of upper Cenozoic tephra layers between sediments of the western United States and eastern Pacific Ocean and comparison with biostratigraphic and magnetostratigraphic age data. *Geological Society of America Bulletin* **98,** 207-223.

Schumm, S. A. (1977). "The fluvial system." John Wiley and Sons, New York.

Schwertmann, U. (1959). Die fractionierte extraktion der freien eisenoxyde in boden ihre mineralogischen formen und ihre entstehungsweisen. *Zeitschrift fur Pflanzenernahrung, Dungung und Bodenkunde* **84,** 194-204.

Schwertmann, U. (1964). Differenzierung der eisenoxide des bodens durch photochemische extraktion mit saurer ammoniumoxalat-losung. *Zeitschrift fur Pflanzenernahrung, Dungung und Bodenkunde,* **105,** 194-202.

Schwertmann, U., Schulze, D. G., and Murad, E. (1982). Identification of ferrihydrite in soils by dissolution kinetics, differential x-ray diffraction, and Mossbauer spectroscopy. *Soil Science Society of America Journal* **46,** 869-875.

Scotter, D. R., Clothier, B. E., and Corker, R. B. (1979). Soil water in a Fragiaqualf. *Australian Journal of Soil Research* **17,** 443-453.

Seward, D. (1974). Age of New Zealand Pleistocene substages by fission-track dating of glass shards from tephra horizons. *Earth and Planetary Science Letters* **24,** 242-248.

Seward, D. (1975). Fission-track ages of some tephras from Cape Kidnappers, Hawke's Bay, New Zealand (Note). *New Zealand Journal of Geology and Geophysics* **18,** 507-510.

Seward, D. (1976). Tephrostratigraphy of the marine sediments in the Wanganui Basin, New Zealand. *New Zealand Journal of Geology and Geophysics* **7,** 479-482.

Seward, D. (1979). Comparison of zircon and glass fission-track ages from tephra horizons. *Geology* **7,** 470-482.

Seward, D., Christoffel, D. A., and Lienert, B. (1986). Magnetic polarity stratigraphy of a Plio-Pleistocene sequence of North Island, New Zealand. *Earth and Planetary Science Letters* **80,** 353-360.

Shane, P. A. R. (1991). Remobilised silicic tuffs in middle Pleistocene fluvial sediments, southern North Island, New Zealand. *New Zealand Journal of Geology and Geophysics* **34,** 489-499.

Shane, P. A. R. (1993). "Tephrostratigraphy, magnetostratigraphy and geochronology of some early and middle Pleistocene deposits in New Zealand." Unpublished Ph.D. thesis, Victoria University of Wellington, New Zealand.

Shane, P. A. R. (1994). A widespread, early Pleistocene tephra (Potaka tephra, 1 Ma) in New Zealand: character, distribution, and implications. *New Zealand Journal of Geology and Geophysics* **37,** 25-35.

Shane, P. A. R., Alloway, B. V., Black, T. M., and Westgate, J. A. (1996b). Isothermal plateau fission-track ages of tephra beds in an early-middle Pleistocene marine and terrestrial sequence, Cape Kidnappers, New Zealand. *Quaternary International* **34-36,** 49-53.

Shane, P. A. R., Black, T. M., B.V, A., and Westgate, J. A. (1996a). Early to middle Pleistocene tephrochronology of North Island, New Zealand: Implications for volcanism, tectonism and paleoenvironments. *Geological Society of America Bulletin* **108,** 915-925.

Shane, P. A. R., Black, T. M., and Westgate, J. A. (1994). Isothermal plateau fission-track age for a paleomagnetic excursions in the Mamaku Ignimbrite, New Zealand, and implications for late Quaternary stratigraphy. *Geophysical Research Letters* **21,** 1695-1698.

Shane, P. A. R., and Froggatt, P. C. (1991). Glass chemistry, paleomagnetism and correlation of middle Pleistocene tuffs in southern North Island, New Zealand, and western Pacific. *New Zealand Journal of Geology and Geophysics* **34,** 203-211.

Shane, P. A. R., and Froggatt, P. C. (1994). Discriminant function analysis of glass chemistry of New Zealand and North American tephra deposits. *Quaternary Research* **41,** 70-81.

Shane, P. A. R., Froggatt, P. C., Black, T. M., and Westgate, J. A. (1995). Chronology of Pliocene and Quaternary bioevents and climatic events from fission track ages on tephra beds, Wairarapa, New Zealand. *Earth and Planetary Science Letters* **130,** 141-154.

Shawcross, K. (1967). Fern root and the total scheme of 18th century Maori food production in agricultural areas. *Journal of the Polynesian Society* **76,** 330-352.

Shell raod maps of New Zealand.Simarco Maps Limited, Timaru.

Shepherd, M. J. (1987). Glaciation of the Tararuas-fact or fiction? *In* "Proceedings of the 14th New Zealand Geography Conference.", pp. 114-115, Palmerston North.

Smart, P., and Tovey, N. K. (1981). "Electron microscopy of soils and sediments: examples." Clarendon Press, Oxford.

Smeck, N. E., Runge, E. C. A., and MacKintosh, E. E. (1983). Dynamics and genetic modelling of soil systems. *In* "Pedogenesis and Soil Taxonomy. 1. Concepts and Interactions." (L. P. Wilding, N. E. Smeck, and G. F. Hall, Eds.), pp. 51-81. Developments in Soil Science 11a. Elsevier, Amsterdam.

Smith, D. G. W., and Westgate, J. A. (1969). Electron probe technique for characterising pyroclastic deposits. *Earth and Planetary Science Letters* **5,** 313-319.

Soengkono, S., Hochstein, M. P., Smith, I. E. M., and Itaya, T. (1992). Geophysical evidence for widespread reversely magnetised pyroclastics in the western Taupo Volcanic Zone (New Zealand). *New Zealand Journal of Geology and Geophysics* **35,** 47-55.

Soil Survey Staff (1975). "Soil Taxonomy: A basic system of soil classification for making and interpreting soil surveys. USDA-SCS Agriculture Handbook No. 436." U.S. Government Printing Office, Washington D.C.

Soil Survey Staff (1992). "Keys to Soil Taxonomy. Soil Management Support Service Technical Monograph 19." Pocahontas Press, Blacksburg, Virginia.

Soil Survey Staff (1994). "Keys to Soil Taxonomy. Soil Management Support Services Technical Monograph 19." USDA-SCS, Washington D.C.

Soons, J. M. (1979). Late Quaternary environments in the central South Island of New Zealand. *New Zealand Geographer* **35,** 16-23.

Speden, I. (1978). Geology and erosion in the Ruahine Range. *New Zealand Geological Survey Report* **G20**.

Spörli, K. B., and Ballance, P. F. (1989). Mesozoic-Cenozoic ocean floor/continent interaction and terrane configuration, southwest Pacific area around New Zealand. *Oxford Monographs on Geology and Geophysics* **8,** 176-190.

Steinhardt, G. C., and Franzmeier, D. P. (1979). Chemical and mineralogical properties of the fragipans of the Cincinnati catena. *Soil Science Society of America Journal* **43,** 1008-1013.

Steinhardt, G. C., Franzmeier, D. P., and Norton, L. D. (1982). Silica associated with fragipan and non-fragipan horizons. *Soil Science Society of America Journal* **46,** 656-657.

Stevens, K. (1989). "Chemical, physical and mineralogical properties of the cover bed sequence on the Pahiatua Terrace north-western Wairarapa." Unpublished M.Sc. thesis, Victoria University of Wellington, New Zealand.

Stevens, K. F., and Vucetich, C. G. (1985b). Weathering of upper Quaternary tephras in New Zealand. 2. Clay minerals and their climatic interpretation. *Chemical Geology* **53,** 237-247.

Stevens, K. F., and Vucetich, G. C. (1985a). Pedogenic weathering of upper Quaternary tephras in New Zealand. I. Isovolumetric geochemical evidence of cation movement. *Chemical Geology* **47,** 285-302.

Stevens, P. R., and Walker, T. W. (1970). The chronosequence concept and soil formation. *Quarterly Review of Biology* **45,** 333-350.

Stewart, R. B., and Neall, V. E. (1984). Chronology of palaeoclimatic change at the end of the Last Glaciation. *Nature* **311,** 47-48.

Stokes, S., and Lowe, D. J. (1988). Discriminant function analysis of late Quaternary tephras from five volcanoes in New Zealand using glass shard major element chemistry. *Quaternary Research* **30,** 270-283.

Stokes, S., Lowe, D. J., and Froggatt, P. C. (1992). Discriminant function analyses and correlation of late Quaternary rhyolitic tephras from Taupo and Okataina volcanoes, New Zealand, using glass shard major element composition. *Quaternary International* **13/14,** 103-117.

Suggate, R. P. (1965). "Late Pleistocene geology of the northern part of the South Island, New Zealand." Government Printer, Wellington.

Taylor, N. H., and Pohlen, I. J. (1979). Soil survey method: a New Zealand handbook for the field study of soils. *New Zealand Soil Bureau Bulletin* **25**.

Te Punga, M. T. (1952). The geology of the Rangitikei Valley. *New Zealand Geological Survey Memoir* **8**.

Te Punga, M. T. (1984). Seven climatic cycles in New Zealand during the last half-million years. *New Zealand Geological Survey Report* **G79**.

Thomas, R. F., Blakemore, L. C., and Kinloch, D. I. (1979). Flow-diagram keys for "Soil Taxonomy." A. Diagnostic horizons and properties: mineral soils. *New Zealand Soil Bureau Scientific Report* **39A**.

Thompson, C. S. (1987a). The climate and weather of Hawke's Bay. *New Zealand Meteorological Service Miscellaneous Publication* **115**.

Thompson, C. S. (1987b). Extreme rainfall frequencies in New Zealand. *New Zealand Meteorological Service Miscellaneous Publication* **191**.

Tonkin, P. J. (1984). "Studies of soil development and distribution in the eastern hill country, central South Island, New Zealand." Unpublished Ph.D. thesis, University of Canterbury, New Zealand.

Tonkin, P. J. (1985). Studies of soil development with respect to aspect, and rainfall, eastern hill country, South Island, New Zealand. *In* "Proceedings of the soil dynamics and land use seminar, Blenheim, May 1985. New Zealand Society of Soil Science and New Zealand Soil Conservators Association." (I. B. Campbell, Ed.), pp. 1-18. Blenheim Printing Company Limited, Blenheim, New Zealand.

Tonkin, P. J. (1994). Principles of soil-landscape modelling and their applications in the study of soil-landform relationships within drainage basins. *In* "Soil-landscape modelling in New Zealand." (T. H. Webb, Ed.), pp. 20-37. Landcare Research Science Series No. 5. Manaaki Whenua Press, Lincoln.

Tonkin, P. J., and Basher, L. R. (1990). Soil-stratigraphic techniques in the study of soil and landform evolution across the Southern Alps, New Zealand. *Geomorphology* **3,** 547-575.

Tonkin, P. J., Harrison, J. B. J., Whitehouse, I. E., and Campbell, A. S. (1981). Methods for assessing late Pleistocene and Holocene erosion history in glaciated mountain drainage basins. *In* "Erosion and sediment transport in Pacific rim steeplands." (T. R. H. Davies, and A. J. Pearce, Eds.), pp. 527-543. International Association of Scientific Hydrology.

Tonkin, P. J., Young, A. W., McKie, D. A., and Campbell, A. S. (1977). Conceptual models of soil development and soil distribution in hill country, central South Island, New Zealand. Part 1. Analysis of the changes in soil pattern. *New Zealand Soil News* **25,** 170-172.

Topping, W. W., and Kohn, B. P. (1973). Rhyolite tephra marker beds in the Tongariro area, North Island, New Zealand. *New Zealand Journal of Geology and Geophysics* **16,** 375-395.

Trustrum, N. A., Blaschke, P. M., DeRose, R. C., and West, A. (1990). Regolith changes and pastoral productivity declines following deforestation in steeplands of North Island, New Zealand. *Transactions 14th International Congress of Soil Science, Kyoto, Japan* **1,** 125-130.

Trustrum, N. A., and DeRose, R. C. (1988). Soil depth-age relationship of landslides on deforested hillslopes, Taranaki, New Zealand. *Geomorphology* **1,** 143-160.

Trustrum, N. A., and Page, M. J. (1991). The long-term erosion history of Lake Tutira watershed: implications for sustainable land use management. *In* "Proceedings of the international conference on sustainable land management, November 17-23, 1991." (P. Henriques, Ed.), pp. 212-215, Napier.

Trustrum, N. A., Wallace, R. C., and DeRose, R. C. (1989). Tephrochronological dating of regolith in landslide prone steeplands, New Zealand. *In* "Proceedings of international symposium on erosion and volcanic debris flow technology.", Yogyakarta, Indonesia.

Valentine, K. W. G., and Dalrymple, J. B. (1975). The identification, lateral variation, and chronology of two buried paleocatenas at Woodhall Spa and West Runton, England. *Quaternary Research* **5,** 551-590.

Valentine, K. W. G., and Dalrymple, J. B. (1976). Quaternary buried paleosols: a critical review. *Quaternary Research* **6,** 209-222.

van der Lingen, G. J., and Pettinga, J. R. (1980). The Makara Basin: a Miocene slope-basin along the New Zealand sector of the Australian-Pacific obliquely convergent plate boundary. *Special Publication of the International Association of Sedimentologists* **4,** 191-215.

Van Dijk, D. C., Riddler, A. M. H., and Rowe, R., K,. (1968). Criteria and problems of ground surface correlations with reference to a regional correlation in south-eastern Australia. *Transactions 9th International Congress of Soil Science* **4,** 131-138.

Vella, P. (1963a). Plio-Pleistocene cyclothems, Wairarapa, New Zealand. *Transactions Royal Society New Zealand, Geology* **2,** 15-50.

Vella, P. (1963b). Upper Pleistocene succession in the inland part of Wairarapa Valley, New Zealand. *Transactions of the Royal Society of New Zealand, Geology* **2,** 63-78.

Vella, P., Kaewyana, W., and Vucetich, C. G. (1988). Late Quaternary terraces and their cover beds, north-western Wairarapa, New Zealand, and provisional correlations with oxygen isotope stages. *Journal of the Royal Society of New Zealand* **18,** 309-324.

Vreeken, W. J. (1973). Soil variability in small loess watersheds: clay and organic carbon content. *Catena* **1,** 181-196.

Vreeken, W. J. (1975a). Principal kinds of chronosequences and their significance in soil history. *Journal of Soil Science* **26,** 378-394.

Vreeken, W. J. (1975b). Quaternary evolution in Tama County, Iowa. *Annals of the Association of American Geographers* **65,** 283-296.

Vreeken, W. J. (1984). Relative dating of soils and paleosols. *In* "Quaternary dating methods." (W. C. Mahaney, Ed.), pp. 269-281. Elsevier, Amsterdam.

Vucetich, C. G. (1968). Soil-age relationships for New Zealand based on tephrochronology. *Transactions 9th International Congress of Soil Science Society* **IV,** 121-130.

Vucetich, C. G., and Howarth, R. (1976b). Proposed definition of Kawakawa Tephra, the c. 20 000 years B.P. marker horizon in the New Zealand region. *New Zealand Journal of Geology and Geophysics* **19,** 43-50.

Vucetich, C. G., and Howorth, R. (1976a). Late Pleistocene tephrostratigraphy in the Taupo district, New Zealand. *New Zealand Journal of Geology and Geophysics* **19,** 51-69.

Vucetich, C. G., and Pullar, W. A. (1969). Stratigraphy and chronology of late Pleistocene volcanic ash beds in central North Island, New Zealand. *New Zealand Journal of Geology and Geophysics* **12,** 784-837.

Vucetich, C. G., and Pullar, W. A. (1973). Holocene tephra formations erupted in the Taupo area, and interbedded tephras from other volcanic sources. *New Zealand Journal of Geology and Geophysics* **16,** 745-780.

Vucetich, C. G., Vella, P., and Warnes, P. N. (1996). Antepenultimate glacial to last glacial deposits in southern Wairarapa, New Zealand. *Journal of the Royal Society of New Zealand* **26,** 469-482.

Walcott, R. I. (1987). Geodetic strain and the deformation history of the North Island of New Zealand during the late Cenozoic. *Philosophical Transactions of the Royal Society London, Serial A* **321,** 459-471.

Walker, G. P. L., Heming, R. F., and Wilson, C. J. N. (1980a). Low-aspect ratio ignimbrites. *Nature* **283,** 286-287.

Walker, P. H., Beckmann, G. G., and Brewer, R. (1984). Definition and use of the term "pedoderm". *Journal of Soil Science* **35,** 505-510.

Walker, P. H., and Ruhe, R. V. (1968). Hillslope models and soil formation. II. Closed systems. *Transactions 9th International Conference on Soil Science* **4,** 561-568.

Wallace, R. C. (1987). "The mineralogy of the Tokomaru silt loam and the occurrence of cristobalite and tridymite in selected North Island soils." Unpublished Ph.D. thesis, Massey University, New Zealand.

Wallace, R. C., Stewart, R. B., and Neall, V. E. (1985). Volcanic glass field laboratory test and procedure to prepare thin section of the sand fraction of soils. *Massey University Department of Soil Science Occasional Report Number 7.*

Warnes, P. N. (1992). Last interglacial and last glacial stage terraces on the eastern side of Wairarapa Valley between Waiohine and Waingawa Rivers. *Journal of the Royal Society of New Zealand* **22,** 217-228.

Weaver, R. M., Syers, J. K., and Jackson, M. L. (1968). Determination of silica in citrate-bicarbonate-dithionite extracts of soils. *Soil Science Society of America Proceedings* **32,** 497-501.

Webb, T. H. (1994). Review of studies of soil-landscape relationships in New Zealand. *In* "Soil-landscape modelling in New Zealand." (T. H. Webb, Ed.), pp. 12-19. Landcare Research Science Series No. 5. Manaaki Whenua Press, Lincoln.

Webb, T. H., Campbell, A. S., and Fox, F. B. (1986). Effect of rainfall on pedogenesis in a climosequence of soils near Pukaki, New Zealand. *New Zealand Journal of Geology and Geophysics* **29,** 323-334.

White, A. F. (1983). Surface chemistry and dissolution kinetics of glassy rocks at 25o. *Geochimica et Cosmochimica Acta* **47,** 805-815.

White, A. F., and Claassen, H. C. (1980). Kinetic model for the short-term dissolution of a rhyolitic glass. *Chemical Geology* **28,** 91-109.

Whitehead, N. E., and Ditchburn, R. G. (1994). Note. Revision of some ages for the Rotoehu Ash. *New Zealand Journal of Geology and Geophysics* **37,** 381-383.

Whitton, J. S., and Churchman, G. J. (1987). Standard methods for mineral analysis of soil survey samples for characterisation and classification in New Zealand Soil Bureau. *New Zealand Soil Bureau Scientific Report* **79**.

Wilde, R. H., and Vucetich, C. G. (1988). Aeolian cover beds of marine terraces in the western Wanganui district, North Island, New Zealand. *In* "Loess: its distribution, geology and soils." (D. N. Eden, and R. J. Furkert, Eds.), pp. 215-232. A.A. Balkema, Rotterdam.

Wilmshurst, J. M., and McGlone, M. S. (1996). Forest disturbance in the central North Island, New Zealand, following the 1850 BP Taupo eruption. *The Holocene* **6,** 399-411.

Wilson, C. J. N. (1985). The Taupo eruption, New Zealand II. The Taupo Ignimbrite. *Philosophical Transactions of the Royal Society of London* **A314,** 229-310.

Wilson, C. J. N. (1986). Reconnaissance stratigraphy and volcanology of ignimbrites from Mangakino Volcano. *Royal Society of New Zealand Bulletin* **23,** 179-193.

Wilson, C. J. N. (1993). Stratigraphy, chronology, styles and dynamics of late Quaternary eruptions from Taupo volcano, New Zealand. *Philosophical Transactions of the Royal Society of London* **A343,** 205-306.

Wilson, C. J. N., Houghton, B. F., Lanphere, M. A., and Weaver, S. D. (1992). A new radiometric age estimate for the Rotoehu Ash from Mayor Island volcano, New Zealand. *New Zealand Journal of Geology and Geophysics* **35,** 371-374.

Wilson, C. J. N., Rogan, A. M., Smith, I. E. M., Northey, D. J., Nairn, I. A., and Houghton, B. F. (1984). Caldera volcanoes of the Taupo Volcanic Zone, New Zealand. *Journal of Geophysical Research* **89,** 8463-8484.

Wilson, C. J. N., Switsur, V. R., and Ward, A. P. (1988). A new 14C age for the Oruanui (Wairakei) eruption, New Zealand. *Geological Magazine* **125,** 297-300.

Wilson, C. J. N., and Walker, G. P. L. (1985). The Taupo eruption, New Zealand I. General Aspects. *Philosophical Transactions of the Royal Society of London* **A314,** 199-228.

Wood, A. (1942). The development of hillside slopes. *Geological Association Proceedings* **53,** 128-138.

Working Group on the Occurrence and Nature of Paleosols (1971). Criteria for the recognition and classification of paleosols. *In* "Paleopedology: origin, nature and dating of paleosols." (D. H. Yaalon, Ed.), pp. 153-158. International Society of Soil Science and Israel Universities Press, Jerusalem.

Young, A. W., Tonkin, P. J., McKie, D. A., and Campbell, A. S. (1977). Conceptual models of soil development and soil distribution in hill country, central South Island, New Zealand. Part 2: Chemical and mineralogical properties. *New Zealand Soil News* **25,** 173-175.

Young, D. J. (1967). Loess deposits of the West Coast of the South Island, New Zealand. *New Zealand Journal of Geology and Geophysics* **10,** 647-658.

APPENDIX I:
SOIL PROFILE DESCRIPTIONS

TERMS USED FOR SOIL PROFILE DESCRIPTIONS

Soil horizon symbols (indicates a common subordinate horizon)	O, L, F, H (surface organic horizons) A (b, h, p) (surface mineral horizons) E B (b, c, g, f, h, k, m, n, p, q, r, s, t, u, w, x, y, z) C R					
Depth or Thickness (measured in cm)						
Boundary	Distinctness (mm)	sharp (<5)	abrupt (5-20)	clear (20-50)	gradual (50-120)	diffuse (>120)
	Shape	smooth	wavy	irregular	broken	
Soil Colour	From soil colour charts					
Mottling	Abundance (%)	few (<2)	common (2-20)	many (20-40)	very many (>40)	
	Size (mm)	fine (<5)	medium (5-15)	coarse (>15)		
	Contrast	faint	distinct	prominent		
Texture	Organic modifier (%)	peat (>50)	peaty (35-50)	humic (15-35)	not applicable (<15)	
	Skeletal material (mm)	lapilli (2-64)*	pumice clasts (>64)*	gravels (2-20)	stones (20-200)	boulders (>200)
	Estimated volume (%)	slightly (2-15)	moderately (15-50)	very (50-90)	gravel (>90)	
	Shape	angular	subangular	subrounded	round	
	Weathering	fresh	slightly	moderately	highly	
	Fine earth	sand (s)	loamy sand (ls)	sandy loam (sl)	loam (l)	silt loam (zl)
		clay loam (cl)	clay (c)			
Consistence	Soil strength	loose	weak	firm	strong	
	Characteristics of failure	brittle	semi-deformable	deformable	slightly fluid	moderately fluid
		fluid				
	Cementation	non	very weak	weakly	strong	very strongly
	Maximum stickiness	non	slightly	moderately	very	
	Maximum plasticity	non	slightly	moderately	very	
Structure	Grade	(non pedal)	single grained	massive		
		(pedal)	weakly developed	moderately developed	strongly developed	
	Size class (mm)		prism-like	block-like	spheroidal	
		very fine	<10	<5	<1	
		fine	10-20	5-10	1-2	
		medium	20-50	10-20	2-5	
		coarse	50-100	20-50	5-10	
		very coarse	>100	>50	>10	
	Type		prismatic	blocky	granular	
			columnar	nut	crumb	
Cutans	Kind of coat	clay	sand or silt	oxidic	organic	carbonate
		stress orientated				
	Abundance (% of surface)	none	few (<10)	common (10-50)	many (>50)	
	Continuity	patchy	discontinuous	continuous	entire	
	Distinctness	faint	distinct	prominent		
Roots	Abundance	few	common	many	abundant	
	Size	very fine-fine (1-2mm)	medium-coarse (>2mm)			

Soil profile notation and terms are adapted from Hodgson (1976)

* Dictionary of Geological Terms (1976)

SOIL PROFILE DESCRIPTION: PAKAUTUTU ROAD SECTION

SOIL HORIZON Symbols	Ah	2bAh	2bCu	3bABw	4bCu	5bABw		6bAh	6bBw1	7bCu	8bBw2	9bCu1	9bCu2
DEPTH or THICKNESS VARIATION (cm)	0-22	22-36	36-48/50	48/50-110	110-125	125-158		158-182	182-218	218-231	231-305	305-313	313-322
BOUNDARY Distinctness Shape	sharp wavy	sharp wavy	clear wavy	gradual wavy	discontinuous wavy	gradual wavy		gradual wavy	gradual wavy	gradual wavy	clear wavy	clear wavy	clear wavy
COLOUR(S) Field	7.5YR3/2	7.5YR-10YR3/4	7.5YR5/8 to 10YR5/8 (pumice) 7.5YR3/4 (matrix)	7.5YR4/6	2.5Y4/1-4/2	10YR5/8		10YR5/6-4/6	10YR5/6	10YR5/8	10YR5/8	10YR5/6	10YR6/3
MOTTLING Abundance Size Contrast													
TEXTURE Organic modifier Skeletal material Est. volume Shape Weathering Fine earth	pumice clasts moderately sub angular slightly sandy loam	lapilli & pumice slightly angular slight-moderately loamy sand	lapilli very angular slightly fine lapilli	sandy loam	andesitic ash balls (1-3cm) sandy loam	sandy loam		sandy loam	sandy silt loam	silty clay loam	silty clay loam	lapilli few sandy loam (ash)	lapilli common slight loamy sand (ash)
CONSISTENCE Soil strength Char. failure Cementation Stickiness Plasticity	weak non non non	weak non non non	loose non non non	weak brittle non non non	strong brittle non non non	firm brittle non non non		firm brittle non non non	firm brittle non slightly plastic	firm brittle non slightly plastic	firm brittle non slightly plastic	weak brittle non non non	weak brittle non non non
STRUCTURE Grade Size Type	weak mod-coarse granular + nut	moderate med-coarse granular	non pedal	moderate coarse-med. blocky	non pedal	weak coarse blocky		weak coarse blocky	weak coarse blocky	weak coarse blocky	weak coarse blocky	massive	massive
CUTANS Colour Kind Abundance Continuity Distinctness Thickness (mm)				reddish organic/Fe few patchy distinct <2mm		reddish organic/Fe few patchy distinct <2mm	pale brown Si few patchy distinct <2mm	orange Si few patchy distinct <2mm	orange Si/Allophane? few patchy distinct <2mm				
ROOTS/CHANNELS Abundance Size	abundant very fine	many very fine	common very fine	few very fine				common very fine	few very fine	few very fine			

SOIL PROFILE DESCRIPTION: PAKAUTUTU ROAD SECTION

SOIL HORIZON Symbols	9bCu3	10bBw3	11bABw1	11bBw2	12bCu	13bBw3	14bCu	15bBw4	16bABw	17bCu	18bBC	19bCu
DEPTH or THICKNESS VARIATIONS (cm)	322-326	326-380/385	380/385-423	423-474	474-496	496-508	508-521	521-547	547-563	563-578/580	578/580-680	680+
BOUNDARY Distinctness Shape	clear wavy	gradual wavy	gradual wavy	abrupt smooth-wavy	clear smooth-wavy	clear wavy	clear wavy	sharp wavy	clear irregular		sharp wavy	
COLOUR(S) Field	10YR7/2	10YR5/8	10YR5/8	10YR5/8	10YR4/6	10YR5/6	10YR5/6	10YR5/6	10YR5/6		10YR5/5	
MOTTLING Abundance Size Contrast												
TEXTURE Organic modifier Skeletal material Est. volume Shape Weathering Fine earth	loamy sand (ash)	silty clay loam	not applicable lapilli silty clay loam	fine sand sandy loam	gravels, stones very angular moderate	silt loam	lapilli silty clay loam	silt loam	humic gravels very subangular slight-moderately sandy loam	gravels very subangular slight-moderately	not applicable silt loam	not applicable gravels/stones very subangular slight-moderately
CONSISTENCE Soil strength Char. failure Cementation Stickiness Plasticity	weak brittle non non non	firm brittle non slightly plastic	firm brittle non slight-moderately very	firm brittle non slight- moderately moderately	loose non slightly very slightly	weak brittle non slightly moderately	firm brittle non slight-moderately very	weak brittle non slightly moderately				
STRUCTURE Grade Size Type	massive	weak med-coarse blocky	moderate med-coarse blocky	weak-moderate medium blocky		weak coarse blocky	weak coarse blocky	weak coarse blocky				
CUTANS Colour Kind Abundance Continuity Distinctness Thickness (mm)		organic	organic, humic, clay, Si, allophane	organic,humic,S i, allophane	Si, clay, humic,organic, allophane	Humic, Si, allophane	Humic, Si, allophane	Humic, Si, allophane	Mn			
ROOTS/CHANNELS Abundance Size			common very fine-coarse (charcoal present	few very fine-fine					few very fine			

SOIL PROFILE DESCRIPTION: MANAROA SECTION

SOIL HORIZON Symbols	Ap	Ah	2bABw	3bABw1	3bABw2	4bCu	5bABw	6bAB	6bBw1	6bBw2	6bC
DEPTH or THICKNESS VARIATION (cm)	0-10	10-21	21-36	36-70	70-95	90-95	95-165	165-190	190-280	280-292	292-335
BOUNDARY Distinctness Shape		abrupt wavy	abrupt wavy	gradual wavy	gradual wavy	discontinuous wavy	gradual wavy	clear wavy	gradual wavy	abrupt wavy	abrupt wavy
COLOUR(S) Field		7.5YR2/2	7.5YR3/4	10YR3/4	10YR4/6	10YR4/2-3	10YR5/6- 2.5Y5/6	2.5Y4/6	10YR5/4	10YR5/6	10YR5/5
MOTTLING Abundance Size Contrast		orange common fine distinct		orange/black few fine black-sharp orange-faint							
TEXTURE Organic modifier Skeletal material Est. volume Shape Weathering Fine earth		humic lapilli sandy loam	lapilli 10% loamy sand	lapilli 15% sandy silt loam	lapilli, ferromags sandy loam	balls of andesitic ash sandy loam	 silty clay loam	 sandy loam	 sandy loam	 sandy loam	 loamy sand
CONSISTENCE Soil strength Char. failure Cementation Stickiness Plasticity		weak brittle non non non	weak brittle non non non	weak brittle non very slightly slightly	firm brittle non slightly slightly	firm brittle non non non	firm brittle non slightly plastic	firm brittle non non slightly	firm brittle non non non	weak brittle non non non	weak brittle non non non
STRUCTURE Grade Size Type		moderate fine nutty-crumb	weak fine nutty-crumb	moderate medium blocky	weak-moderate medium blocky	massive	weak coarse blocky	moderate coarse blocky	weak coarse blocky	weak coarse blocky	massive
CUTANS Colour Kind Abundance Continuity Distinctness Thickness (mm)			brown humic	brown humic, organic, sesquioxides, allophane	brown humic, allophane, sesquioxides		orange few in root channels	yellow common in root channels	reddish/brown few in root channels		
ROOTS/CHANNELS Abundance Size		many fine	common very fine	common very fine			few very fine-fine	common fine	few fine		

SOIL PROFILE DESCRIPTIONS: MANAROA SECTION

SOIL HORIZON Symbols	7bCu1	7bCu2	8bCg	9bCr	10bCu
DEPTH OR THICKNESS VARIATION (cm)	335-362	362-368	368-390	390-430	430+
BOUNDARY Distinctness Shape	broken wavy	broken wavy	diffuse		
COLOUR(S) Field	10YR5/4	7.5YR6/8-10YR7/3	7.5YR6/8 (50%) 2.5Y6/2 (50%)	10YR5/1	
MOTTLING Abundance Size Contrast		Black Mn streaks along peds	common medium prominent	few (2.5Y6/2) fine-coarse distinct	
TEXTURE Organic modifier Skeletal material Est. volume Shape Size Weathering Fine earth	lapilli few loamy sand	 fine sandy loam (ash)	 fine sandy loam	 sandy loam	 sand
CONSISTENCE Soil strength Char. failure Cementation Stickiness Plasticity	weak brittle non non non	weak brittle non non non	weak brittle non non slightly	weak brittle non non non	weak brittle non non non
STRUCTURE Grade Size Type	massive	massive	massive	massive	massive
CUTANS Colour Kind Abundance Continuity Distinctness Thickness (mm)					
ROOTS/CHANNELS Abundance Size					

SOIL PROFILE DESCRIPTION: APLEY ROAD #1 SECTION

SOIL HORIZON Symbols	Ap	Ah	AB	Bg1	Bg2	Bf	Bqm	Bx/C
DEPTH or THICKNESS VARIATION (cm)	0-22	22-31	31-42	42-71 (71-77)	71-101 (101-106)	101-101.3	101.3-112	112-260
BOUNDARY Distinctness Shape	sharp	sharp wavy	abrupt wavy	sharp wavy	sharp wavy	sharp wavy	gradual wavy	gradual wavy-irregular
COLOUR(S) Field		10YR2/3	10YR4/4	2.5Y6/4	2.5Y6/4 &10YR4/6	7.5YR5/8	10YR5/6	10YR5/4
MOTTLING Abundance Size Contrast		few (<2) medium (5-15) distinct	common fine-medium distinct-prominent	common medium faint-distinct	many-very many coarse prominent-distinct			
TEXTURE Organic modifier Skeletal material Est. volume Shape Size Weathering Fine earth		humic sandy loam	 sandy loam	 silt loam	non gravel <2% subangular fresh silty clay loam		 silt loam	 silt loam
CONSISTENCE Soil strength Char. failure Cementation Stickiness Plasticity		weak-loose semideformable non non slightly	weak semideformable non non moderately	firm semideformable non slightly mod.-very	moderate-strong brittle weak slight-moderate very		moderately firm brittle weak-strong non very	moderately firm brittle non non moderately
STRUCTURE Grade Size Type		mod-strongly fine nut-crumb	weak-moderately fine blocky,nut,crumb	strong medium-coarse blocky	strong coarse blocky		massive tabular	massive
CUTANS Colour Kind Abundance Continuity Distinctness Thickness (mm)				 organic few patchy distinct <1mm	 oxidic few patchy distinct <1mm		 clay, humic few continuous distinct <1mm	
ROOTS Abundance Size		abundant very fine	common very fine-coarse	common very fine-coarse	few medium-coarse		few very fine and fine	

SOIL PROFILE DESCRIPTIONS: APLEY ROAD #1 SECTION

SOIL HORIZON Symbols	2bCu1	2bCu2	2bCu3	2bCu4	2Cu5	2Cu6	2Cu7	2Cu8	2Cu9
DEPTH OR THICKNESS VARIATION (cm)	260-292	292-313	313-315	315-321	321-325	325-334	334-345	345-347	347-352
BOUNDARY Distinctness Shape	sharp gradual	sharp smooth	sharp wavy	sharp wavy	sharp wavy	abrupt wavy	sharp-abrupt wavy	sharp wavy	sharp wavy
COLOUR(S) Field	7.5YR6/4	7.5YR6/3	7.5YR6/8	7.5YR7/2	7.5 YR6/3	red band (7.5YR7/8) base (7.5YR7/3)	7.5YR6/3	7.5YR7/2	7.5YR8/2
MOTTLING Abundance Size Contrast	7.5YR5/6 common fine faint-distinct								
TEXTURE Organic modifier Skeletal material Est. volume Shape Size Weathering Fine earth	none lapilli rounded 2-3mm fresh-slightly sandy	none lapilli rounded 2-5mm slightly sandy	none lapilli rounded 5-12mm slightly sandy	none lapilli rounded <1mm slightly sandy	none lapilli rounded 2-5mm slightly sandy	none lapilli rounded <1mm slightly sandy	none lapilli rounded 2-5mm slightly sandy	none lapilli	none lapilli
CONSISTENCE Soil strength Char. failure Cementation Stickiness Plasticity	very weak brittle non non non	very weak brittle non non non	very weak brittle non non non	very weak brittle non non non	very weak brittle non non non	very weak brittle non non non	very weak brittle non non non	very weak brittle non non non	very weak brittle none nonnon
STRUCTURE Grade Size Type	massive	massive	massive	massive	massive	massive	massive	massive	massive
CUTANS Colour Kind Abundance Continuity Distinctness Thickness (mm)	oxidic few patchy- discontinuous faint-distinct <1mm								
ROOTS Abundance Size									

SOIL PROFILE DESCRIPTION: APLEY ROAD #2 SECTION

SOIL HORIZON Symbols	3bCx	3bC/4bA	4bBt	4bBqm		4bBx/C		5bAB	5bABw1		6bCu
DEPTH or THICKNESS VARIATION (cm)	0-125	125-155	155-178	178-222		222-260		260-308	308-318		318-320
BOUNDARY Distinctness Shape	abrupt wavy	clear wavy-irregular	abrupt wavy	clear wavy		gradual irregular		clear-gradual wavy	sharp wavy+broken		sharp wavy+broken
COLOUR(S) Field	10YR6/4	10YR6/4	10YR4/4	10YR4/6		10YR5/6		10YR4/4	10YR6/4		
MOTTLING Abundance Size Contrast			5YR3/6 common medium faint-distinct			common Fine-medium faint-distinct					
TEXTURE Organic modifier Skeletal material Est. volume Shape Size (mm) Weathering Fine earth	silt loam	silty clay loam	clay loam	too hard		stones slightly subrounded 2-20 slightly sandy loam		gravels rare angular fresh silt loam	lapilli+gravels slightly rounded fresh silt loam		stony moderately rounded fresh
CONSISTENCE Soil strength Char. failure Cementation Stickiness Plasticity	moderately firm brittle non slightly moderately	very firm brittle non moderately very	moderately weak brittle non moderately very	very strong brittle strong too hard too hard		moderately firm brittle non non very		moderately firm brittle non slightly very	moderately -very firm brittle non non very		
STRUCTURE Grade Size Type	massive	massive	moderately medium blocky	tabular		massive		massive	massive		
CUTANS Colour Kind Abundance Continuity Distinctness Thickness (mm)	organic few-common patchy distinct <1mm	Mn, organic few-common patchy prominent <1mm	clay many entire prominent <1mm	clay many continuous-entire prominent 1mm	Si many continuous-entire prominent 1mm	Mn rare patchy-discontinuous distinct <1mm	clay common-many continuous-entire distinct- prominent <1mm	organic many ~~continuous-entire~~ distinct-prominent <1mm	organic common continuous distinct <1mm	Mn few discontinuous distinct <1mm	
ROOTS Abundance Size	few very fine and fine	common very fine and fine	few very fine and fine					common very fine and fine	common very fine and fine		

SOIL PROFILE DESCRIPTION: APLEY ROAD #3 SECTION

SOIL HORIZON Symbols	7bBw2	8bBw	9bAB	
DEPTH OR THICKNESS VARIATION (cm)	0-70	70-165	165-223	
BOUNDARY Distinctness Shape	 gradual wavy	 gradual wavy	 gradual wavy	
COLOUR(S) Field	10YR6/6	10YR5/6	10YR4/4	
MOTTLING Abundance Size Contrast				
TEXTURE Organic modifier Skeletal material Est. volume Shape Size Weathering Fine earth	 lapilli subrounded 1-2mm slightly silty clay loam	 stones slightly subrounded fresh silty clay loam	 stones rare subrounded-rounded fresh sandy clay loam	
CONSISTENCE Soil strength Char. failure Cementation Stickiness Plasticity	 very firm brittle non slightly very	 moderately weak brittle non slightly very	 moderately weak brittle non slightly very	
STRUCTURE Grade Size Type	 massive	 weakly medium-coarse blocky	 moderately medium-coarse blocky	
CUTANS Colour Kind Abundance Continuity Distinctness Thickness (mm)	 Mn, clay, organic common discontinuous distinct-prominent >1mm	 organic common discontinuous faint-distinct >1mm	 Mn few discontinuous distinct >1mm	 organic, clay common continuous prominent >1mm
ROOTS/CHANNELS Abundance Size	 few very fine and fine	 few very fine and fine	 common very fine and fine	

SOIL PROFILE DESCRIPTION: APLEY ROAD #4 SECTION

SOIL HORIZON Symbols	9bBt			10bABt	10bBt
DEPTH or THICKNESS VARIATION (cm)	0-150			150-178	178-338
BOUNDARY Distinctness Shape	 gradual wavy			 gradual wavy	 gradual wavy
COLOUR(S) Field	2.5Y5/4			2.5Y5/4	2.5Y5/4
MOTTLING Abundance Size Contrast					
TEXTURE Organic modifier Skeletal material Est. volume Shape Size Weathering Fine earth	 gravels, stones rare subrounded fresh sandy clay loam			 gravels, stones rare subrounded fresh sandy clay loam	 gravels, stones rare subrounded fresh sandy clay loam
CONSISTENCE Soil strength Char. failure Cementation Stickiness Plasticity	 moderately weak semideformable non moderate very			 moderately weak semideformable non moderate very	 moderately weak semideformable non moderate very
STRUCTURE Grade Size Type	 moderately medium-coarse blocky			 strongly developed medium blocky	 moderately medium-coarse blocky
CUTANS Colour Kind Abundance Continuity Distinctness Thickness (mm)	 Mn common discontinuous prominent <1mm	 clay many entire prominent <1mm	 organic common continuo us distinct <1mm	Same as 9bBt	Same as 9bBt
ROOTS/CHANNELS Abundance Size	 few very fine and fine			 common fine and medium	 few very fine and fine

SOIL PROFILE DESCRIPTIONS: PORAITI #1 SECTION

SOIL HORIZON Symbols	Ah	ABg	Bg	Bqm	Bx/C	2bCu1	2bCu2	2bCu3
DEPTH OR THICKNESS VARIATION (cm)	0-20	20-32	32-55	55-75(80)	75-155	155-173	173-219	219-223
BOUNDARY Distinctness Shape	 abrupt wavy	 clear wavy	 sharp wavy	 gradual wavy	 sharp-abrupt wavy	 sharp-abrupt wavy	 sharp smooth-wavy	 sharp wavy
COLOUR(S) Field	7.5Y3/1	10YR5/4	10YR7/3	2.5Y7/4	2.5Y6/4	5Y7/3 and 5YR5/8	5Y8/1	2.5Y8/2
MOTTLING Colour Abundance Size Contrast		7.5YR5/8, 7.5YR4/6 common medium prominent	 10YR5/8 very many medium-coarse distinct-prominent					
TEXTURE Organic modifier Skeletal material Est. volume Shape Size Weathering Fine earth	 humic silt loam	 silt loam	 silty clay loam	 silt loam	 lapilli (129-135cm) rounded moderately silt loam	 lapilli rounded very slightly sandy loam	 lapilli sub-rounded slight/moderate <5mm sandy loam	 fine ash 100% sandy loam
CONSISTENCE Soil strength Char. failure Cementation Stickiness Plasticity	 very weak semideformable non non very	 moderately weak brittle non very slightly very	 moderately strong brittle non slightly very	 very strong brittle very strongly too hard too hard	 moderately weak brittle non slightly moderately	 moderately firm brittle non very slightly slightly	 very firm brittle non non non	 very firm brittle non moderately moderately
STRUCTURE Grade Size Type	 moderately fine-coarse granular / moderately fine-very fine crumb	 moderately medium-very coarse blocky	 weak-moderately medium-coarse blocky	 tabular	 moderately very coarse columnar	 massive	 massive	 massive
CUTANS Colour Kind Abundance Continuity Distinctness Thickness (mm)		 organic common discontinuous distinct <1mm	 organic common patchy faint-distinct <1mm	 organics in cracks few patchy faint-distinct <1mm	 organic few patchy faint <1mm			
ROOTS/CHANNELS Abundance Size	 many very fine and fine	 many very fine and fine	 common very fine and fine	 few very fine and fine	 very few very fine and fine			

SOIL PROFILE DESCRIPTIONS: PORAITI #2 SECTION

SOIL HORIZON Symbols	3bBx/C	4bABtg		4bBqmg	4bC/5bA			5bA/Bt	5bBqmt	5bCg/6bBg		6bBtg	
DEPTH OR THICKNESS VARIATION (cm)	1-110	110-125		125-150	150-173			173-200	200-255	255-285		285-318	
BOUNDARY Distinctness Shape	clear wavy	sharp wavy		clear wavy	clear-gradual wavy			sharp wavy	clear wavy	clear wavy		abrupt wavy	
COLOUR(S) Field	2.5Y7/4	10YR5/6		10YR8/2	10YR5/6			2.5YR5/4	10YR4/4	10YR5/8		10YR5/4	
MOTTLING Colour Abundance Size Contrast		2.5Y8/2 common fine-medium faint		10YR6/8 common medium-coarse faint-distinct						7.5YR5/8 few medium very faint		balls of ash 7.5YR4/6 up to 2cm diameter	
TEXTURE Organic modifier Skeletal material Est. volume Shape Size Weathering Fine earth	silt loam	lapilli silty clay loam		lapilli silt loam	lapilli silt loam			 clay loam	lapilli silt loam	lapilli silt loam		lapilli rounded slight clay loam	
CONSISTENCE Soil strength Char. failure Cementation Stickiness Plasticity	strong brittle non slightly very	moderately weak brittle-semideformable non slightly very		very strong brittle strongly too hard too hard	moderately strong brittle non slightly very			moderately weak brittle non moderately very	strong-rigid brittle strongly too hard too hard	firm brittle non slightly very		moderately firm semideformable non slightly-moderately very	
STRUCTURE Grade Size Type	massive very coarse columnar	moderately medium-coarse blocky		 tabular	massive			moderately-weak medium-coarse blocky	tabular	weakly very coarse blocky		moderately very coarse blocky	
CUTANS Colour Kind Abundance Continuity Distinctness Thickness (mm)	 organic few patchy faint-distinct <1mm	 organic common patchy- discontinuous distinct <1mm	 clay few patchy faint- distinct <1mm	 organic+clay common discontinuous distinct <1mm	 clay few patchy faint <1mm	 organic common discontinuous distinct <1mm	 Fe oxides few patchy faint- distinct <1mm	 clay common continuous distinct- prominent <1mm	along ped faces clay+organic common continuous distinct <1mm	 organic common discontinuou s faint-distinct <1mm	(along ped faces) clay many continuous prominent <1mm	 organic common continuous prominent <2mm	 clay many continuous prominent <1mm
ROOTS/CHANNELS Abundance Size	few-common very fine and fine	common very fine-medium		rare very fine and fine	few very fine and fine			common very fine and fine	few very fine and fine	common very fine and fine		few-common very fine and fine	

SOIL PROFILE DESCRIPTIONS: PORAITI #2 SECTION

SOIL HORIZON Symbols	6bBqmt	6bBt/7bA		7bBqmt		8bCu
DEPTH or THICKNESS Variation (cm)	318-355	355-408		408-478		478-base
BOUNDARY Distinctness Shape	 abrupt wavy	 abrupt wavy		 gradual wavy		
COLOUR(S) Field	10YR4/4	10YR5/8		2.5Y8/4		10YR6/8
MOTTLING Abundance Size Contrast						Mn mottles common fine-medium distinct-prominent
TEXTURE Organic modifier Skeletal material Est. volume Shape Weathering Fine earth	 lapilli rounded slight too hard	 silty clay loam		 too hard		 sandy loam
CONSISTENCE Soil strength Char. failure Cementation Stickiness Plasticity	 rigid brittle strongly too hard too hard	 moderately weak semideformable non slightly very		 very strong brittle strongly too hard too hard		 moderately weak-moderately firm brittle non non very
STRUCTURE Grade Size Type	 tabular	 weak-moderate medium-very coarse blocky		 tabular		 massive
CUTANS Colour Kind Abundance Continuity Distinctness Thickness (mm)	 clay+organic few patchy-discontinuous faint-distinct <1mm	 organic common continuou s prominent <1mm	 clay many entire prominent <1mm	 clay many entire prominent <1mm	 organic common discontinuous distinct <1mm	
ROOTS/CHANNELS Abundance Size	 very few very fine and fine	 common very fine and fine		 very few very fine and fine		

APPENDIX II:

VOLCANIC GLASS AND QUARTZ DETERMINATIONS

2.1	Pakaututu Road reference section	p. A
2.2	Manaroa reference section	p. A
2.3	Apley Road reference section	p. A
2.4	Poraiti reference section	p. A

Pakaututu Road reference section

Depth (cm)	% Glass	% Quartz	% >125um	% 125-63um	% <63um
0	96.2	1.9	44.6	21.8	33.7
10	94.5	1.5	25.8	13.3	60.9
20	90.0		41.0	17.5	41.4
30	80.7	3.1	62.5	8.1	29.4
40	71.0	5.1	73.8	4.5	21.7
50	81.0	2.8	83.9	1.3	14.8
60	86.7	2.8	37.7	10.4	51.8
70	91.0	1.9	37.1	15.0	47.9
80	84.2	2.8	23.1	15.4	61.6
90	83.7	1.7	19.0	13.7	67.3
100	82.5	1.7	20.8	14.6	64.5
110	1.5	0.7	4.7	17.1	78.3
120	68.0	2.3	18.3	9.9	71.9
130	62.2	3.9	21.1	9.8	69.1
140	57.0	4.7	23.2	9.7	67.0
150	23.7	5.0	24.4	10.3	65.3
160	44.5	7.3	25.7	11.9	62.4
170	31.0	5.3	27.4	15.9	56.7
180	21.2	10.3	18.6	19.2	62.2
190	39.0	11.9	15.6	19.1	65.4
200	10.7	14.3	11.3	19.1	69.6
210	6.2		12.0	18.0	70.1
220	20.2	12.5	17.5	24.0	58.5
230	37.0	10.1	14.2	18.9	66.9
240	25.7	13.8	13.8	21.3	64.9
250	27.0	12.5	12.2	18.7	69.1
260	25.5	14.5	11.1	18.7	70.2
270	32.2	11.8	8.7	19.4	71.9
280	56.7	16.0	8.7	20.4	70.9
290	41.0	12.4	9.1	23.1	67.8
300	39.2	11.7	10.1	19.6	70.3
310	62.0	9.3	16.5	19.8	63.8
320	66.2	5.0	54.9	12.5	32.6
330	4.5	13.5	14.9	22.4	62.7
340	4.5		14.2	24.6	61.2
350	2.2	19.5	11.9	26.0	62.1
360	3.5		12.4	24.1	64.0
370	4.7	17.6	11.0	11.4	77.6
380	6.0	15.6	11.9	19.5	68.7
390	18.7	15.7	12.9	14.9	72.2
400	10.7	13.3	16.4	14.3	69.3
410	16.7	13.9	13.4	15.7	71.0
420	11.2	16.4	14.7	16.7	68.7
430	8.0	17.4	15.2	15.3	69.6
440	25.2	15.1	18.5	11.9	69.7
450	24.5	12.2	26.3	13.3	60.4
460	31.2	12.4	26.8	12.4	60.9
470	40.5	12.4	27.0	11.5	61.5
480	12.5		31.1	10.1	58.8
490	3.0	18.2	43.4	9.4	47.2
500	3.5		27.0	12.3	60.6
510	9.0	13.8	13.3	11.0	75.8
520	10.7	14.7	13.7	10.5	75.9
530	14.5		10.0	10.3	79.7
540	11.7		18.8	11.3	69.8
550	15.7	17.7	28.1	12.1	59.9
560	6.5		44.6	11.5	43.9
570	73.2	11.0	10.8	14.7	74.6
580	23.5	16.9	19.3	17.0	63.7
590	5.0		16.5	16.9	66.7
600	2.0	19.0	13.0	16.4	70.6
610	2.7		12.2	15.0	72.7
620	0.7	19.2	23.0	14.3	62.7
630	1.7		16.8	20.1	63.2
640	1.0	22.3	17.5	27.4	55.1
650	0.0		14.2	24.6	61.2
660	0.0		17.3	28.1	54.6
670	0.2	19.8	19.4	25.5	55.1

Manaroa reference section

Depth (cm)	% Glass	% Quartz	% >125um	% 125-63um	% <63um
0	32.7	8.5	40.7	17.8	41.5
10	18.5	7.7	39.7	14.9	45.4
20	46.5		43.8	14.6	41.6
30	51.2	2.1	49.3	7.1	43.6
40	89.2	2.2	42.1	7.3	50.6
50	83.7	3.0	36.9	7.7	55.4
60	68.0	2.2	32.6	7.5	59.9
70	67.2	2.1	31.1	8.1	60.8
80	66.7	1.7	28.0	7.7	64.3
90	48.2	3.7	22.2	10.4	67.4
95	48.7	4.5	25.0	11.3	63.7
100	28.0	4.9	23.9	13.0	63.1
110	13.5	10.6	14.8	20.5	64.7
120	6.7	15.7	11.8	25.9	62.3
130	2.0	24.9	8.5	33.0	58.5
140	0.0		6.9	36.7	56.3
150	0.7		6.6	38.3	55.1
160	0.5	28.5	5.1	39.0	55.9
170	2.5	23.7	6.1	38.6	55.3
180	1.0	24.6	6.4	40.8	52.8
190	1.2	26.3	5.4	46.0	48.7
200	0.2		3.3	48.3	48.4
210	0.0	25.6	3.8	48.4	47.8
220	2.0		5.3	45.8	48.9
230	1.7	23.9	3.6	49.0	47.4
240	1.7	26.4	8.6	42.7	48.8
250	2.2		9.3	41.5	49.3
260	5.5	27.9	13.2	38.4	48.4
270	19.2		24.6	37.6	37.8
280	3.2	27.2	30.9	37.1	32.0
290	3.5		28.7	38.7	32.5
295	4.5	18.0	29.4	41.9	28.7
300	3.7		24.4	44.9	30.7
310	2.0	25.3	20.0	51.5	28.6
320	0.5	25.9	15.3	54.5	30.3
330	0.5	29.1	17.1	55.7	27.2
340	0.7	28.2	22.6	55.8	21.7
350	0.2	23.7	25.5	53.6	20.9
360	0.2	23.9	25.8	46.6	27.7
365	88.0	2.4	22.1	14.6	63.3
370	0.5		30.8	35.6	33.7
380	0.2	24.7	19.7	38.3	42.0
390	0.7		12.9	43.8	43.3
400	0.0	30.1	7.6	55.5	36.9
410	0.5		7.1	53.4	39.4
420	0.7		7.0	50.9	42.2
430	1.2		8.5	50.6	41.0
440	0.0		11.2	55.3	33.5
450	0.0	27.2	15.3	56.5	28.2
460	0.5		20.8	54.0	25.2
470	0.5	20.3	17.5	53.5	29.0
480	0.5		21.0	50.1	29.0
490	0.0	30.6	24.4	42.8	32.8
500	0.0		39.4	36.9	23.8
510	0.0		62.2	19.5	18.3
520	0.0		68.7	17.3	13.9
530	0.7	25.3	74.8	15.9	9.3

Apley Road #1 reference section

Depth (cm)	% Glass	% >250um	% 250-125um	% 125-63um	% <63um
10	19.0	13.37	15.38	26.24	45.02
20	31.5	16.94	16.12	25.74	41.20
30	34.5	10.74	15.54	24.41	49.32
40	22.0	7.14	15.09	23.98	53.80
50	16.0	5.86	12.79	23.33	58.03
60	7.5	2.06	9.56	22.52	65.86
70	3.5	0.80	9.08	27.04	63.08
80	2.2	0.38	7.92	34.74	56.96
90	4.5	0.50	7.03	33.47	59.00
100	1.5	0.46	8.20	26.99	64.36
105	3.0	0.82	7.42	34.14	57.63
110	3.0	0.85	7.99	29.62	61.53
120	2.5	0.34	7.09	40.30	52.28
130	3.0	0.40	6.93	33.05	59.62
140	5.0	0.22	7.16	35.43	57.20
150	4.0	0.32	8.27	36.17	55.24
155	4.0	0.28	7.15	39.21	53.36
160	4.7	0.34	6.94	36.32	56.40
170	7.2	0.38	9.51	35.89	54.23
180	6.0	0.38	7.58	37.76	54.27
190	10.5	0.30	6.06	38.24	55.40
200	13.5	0.27	5.45	34.71	59.57
210	12.5	0.20	6.00	35.28	58.52
220	6.5	0.30	6.61	38.78	54.31
230	19.2	0.34	7.40	33.70	58.57
240	20.5	0.52	7.89	34.49	57.10
250	32.2	0.42	6.96	35.86	56.76
260	46.2	3.94	7.93	32.72	55.41
270	75.5	17.33	17.43	17.29	47.96
280	93.0	14.84	9.32	12.99	62.85
300	74.0	55.29	20.78	5.97	17.96
350	85.2	47.78	18.60	6.55	27.07

Depth (cm)	% Glass	% >250um	% 250-125um	% 125-63um	% <63um
0	71.7	42.50	21.28	11.22	25.01
10	4.0	1.05	7.71	33.60	57.65
20	2.0	0.20	5.73	38.01	56.06
30	0.5	0.10	4.76	37.00	58.14
40	1.2	0.12	5.33	36.73	57.83
50	0.7	0.08	4.54	37.00	58.38
60	1.0	0.04	5.84	37.50	56.61
70	0.2	0.08	5.06	36.17	58.70
80	2.2	0.14	6.64	36.74	56.48
90	5.5	0.22	7.15	31.95	60.68
100	5.0	0.34	6.69	26.95	66.03
110	5.7	0.33	8.53	29.41	61.73
120	5.2	0.40	7.34	31.84	60.42
130	3.7	0.52	7.81	26.30	65.37
140	4.0	1.20	7.26	18.90	72.64
150	8.0	1.16	10.14	20.08	68.62
160	12.0	1.54	9.07	19.78	69.60
170	8.5	2.20	12.10	42.92	42.78
180	6.0	1.85	12.07	31.83	54.25
190	1.5	0.91	9.84	31.74	57.51
200	4.7	0.30	10.94	26.82	61.94
210	2.7	0.44	6.81	28.96	63.79
220	3.7	0.69	7.12	32.04	60.14
230	3.5	1.05	9.38	28.99	60.58
240	6.2	1.06	8.07	30.96	59.90
250	7.0	1.27	12.81	28.65	57.27
260	9.7	1.43	9.42	32.58	56.57
270	12.2	2.56	14.27	27.91	55.26
280	11.7	2.24	10.16	31.00	56.60
290	14.2	1.54	9.74	26.64	62.08
300	19.2	0.93	12.49	32.08	54.51
310	22.7	0.84	11.61	27.09	60.46
320	34.0	1.14	8.42	21.78	68.66
330	5.5	0.91	16.91	28.36	53.83
340	9.2	2.30	10.67	24.43	62.60
350	2.2	0.50	11.21	36.73	51.57
360	0.5	0.96	11.64	28.60	58.80
370	0.0	0.30	11.94	31.44	56.33
380	0.2	0.16	8.26	37.94	53.63
390	0.7	0.28	9.14	32.50	58.08
400	0.5	0.30	9.74	35.27	54.69

Apley Road #3 reference section

Depth (cm)	% Glass	% >250um	% 250-125um	% 125-63un	% <63um
0					
10	13.2	0.78	8.68	24.97	65.57
20	4.7	0.95	10.57	32.82	55.66
30	1.5	0.98	13.00	37.06	48.96
40	0.2	1.14	9.72	28.84	60.29
50	0.0	0.70	25.01	30.78	43.52
60	0.0	1.03	12.62	27.20	59.15
70	0.5	0.59	17.09	36.56	45.76
80	0.00	0.57	18.63	29.91	50.89
90	0.2	0.66	9.47	40.31	49.55
100	0.00	1.67	14.03	35.32	48.99
110	0.2	0.72	10.07	34.53	54.68
120	0.0	0.37	8.66	38.94	52.02
130	0.0	0.49	13.48	30.47	55.55
140	0.5	0.58	9.92	36.25	53.25
150	0.2	0.63	19.73	34.00	45.65
160	0.00	0.65	19.20	36.74	43.41
170	0.2	0.36	14.09	36.42	49.13
180	0.00	0.65	11.96	37.68	49.70
190	0.2	0.71	19.59	32.23	47.47
200	0.2	0.55	22.38	34.21	42.87
210	0.0	0.51	24.03	27.74	47.72
220	1.5	0.98	24.14	25.95	48.93
230	2.0	0.58	26.41	26.78	46.23
240	0.5	0.51	18.59	25.95	54.95
250	0.0	1.48	18.73	26.13	53.66

Depth (cm)	% Glass	% >250um	% 250-125um	% 125-63um	% <63um
0	0.2	1.07	13.64	31.23	54.06
20	0	0.42	12.23	26.53	60.82
40	0.2	0.27	19.03	31.09	49.61
60	0	0.33	25.76	22.99	50.92
80	0	0.45	24.84	34.44	40.27
100	0.5	0.37	13.33	24.95	61.34
120	0.2	0.35	23.46	21.44	54.74
140	0.2	0.35	10.82	24.74	64.10
160	0	0.36	13.00	25.68	60.96
180	0.2	0.46	13.24	22.96	63.34
200	0	0.50	15.03	17.82	66.65
220	0	0.29	15.00	29.10	55.61
240	0	0.34	23.85	22.69	53.12
260	0.2	0.21	22.43	21.83	55.53
280	0.2	0.43	27.24	25.12	47.22
300	0	0.33	15.82	18.37	65.49
320	0	0.22	17.47	32.98	49.33
340	0	0.45	23.41	33.17	42.97
360	0	0.51	16.90	31.68	50.92
380	0	0.36	19.41	34.27	45.96

Poraiti #1 reference section

Depth (cm)	% Glass	% >250um	% 250-125um	% 125-63um	% <63um
10	28.5	7.55	12.72	33.93	45.79
20	33.2	6.67	11.11	24.54	57.68
30	15.2	3.87	14.15	30.36	51.63
40	11.7	1.50	9.03	36.62	52.85
50	7.2	0.42	6.65	39.04	53.89
60	4.2	0.53	5.66	42.52	51.29
70	6.7	2.10	12.15	38.18	47.57
80	7.7	0.44	5.04	39.14	55.38
90	36.2	0.33	4.84	38.23	56.60
100	16.7	0.96	5.89	37.16	55.99
110	52.7	0.37	6.73	33.88	59.02
120	70.5	0.95	7.52	37.59	53.94
130	94.2	0.44	7.01	29.37	63.18
140	92	2.14	19.16	30.23	48.48
150	89	16.00	27.41	23.14	33.45
160	80.5	19.14	14.77	16.82	49.27
190	70	52.06	21.19	8.38	18.37
221	85.5	4.65	12.13	20.61	62.61

Poraiti #2 reference section

Depth (cm)	% Glass	% >250um	% 250-125um	% 125-63um	% <63um
0	70.5	50.49	16.84	8.10	24.57
10	74.7	16.51	13.00	15.65	54.84
20	8.7	0.06	2.48	40.67	56.79
30	4.7	0.00	4.00	43.77	52.24
40	3.0	0.06	3.42	52.51	44.01
50	2.0	0.08	6.08	46.11	47.73
60	2.0	0.08	2.58	43.87	53.48
70	6.5	0.06	2.11	42.25	55.59
80	8.7	0.33	5.07	40.89	53.71
90	9.2	0.78	4.84	40.13	54.25
100	10.0	1.08	4.36	38.51	56.05
110	9.0	1.13	5.05	36.89	56.94
120	19.5	1.93	8.46	34.16	55.45
130	22.0	1.07	5.49	25.88	67.56
140	16.0	3.10	3.10	32.16	61.63
150	14.5	1.75	1.75	32.41	64.09
160	9.2	0.62	8.38	38.96	52.05
170	2.0	0.10	2.05	36.91	60.94
180	1.5	0.17	8.41	42.33	49.08
190	0.2	0.04	11.86	44.79	43.30
200	0.5	0.42	6.36	51.35	41.87
210	0.5	0.13	3.41	41.45	55.00
220	2.5	0.21	9.04	44.06	46.69
230	0.5	0.14	6.77	41.03	52.07
240	1.2	0.18	8.56	44.63	46.63
250	1.0	0.12	7.66	40.77	51.45
260	1.5	0.17	3.36	39.38	57.09
270	2.0	0.44	2.72	43.81	53.02
280	3.0	0.43	4.03	46.59	48.94
290	1.7	0.51	4.62	48.57	46.31
300	0.5	1.03	14.84	48.70	35.43
305	0.7	0.41	6.77	44.21	48.61
310	0.5	0.42	14.54	35.80	49.24
315	2.2	4.82	13.90	44.40	36.89
320	2.5	8.69	15.06	31.58	44.67
330	9.2	17.61	14.66	26.45	41.28
340	4.5	4.98	13.59	34.18	47.24
350	0.7	0.78	8.22	43.24	47.76
360	2.5	0.89	6.75	43.95	48.41
370	3.0	6.90	3.91	55.38	33.81
380	1.5	0.32	14.85	46.80	38.03
390	0.5	0.58	3.00	56.90	39.52
400	0.7	1.21	23.31	41.91	33.57
410	1.0	0.36	14.20	34.23	51.21
420	4.0	0.88	8.91	40.20	50.01
430	2.2	0.36	3.81	45.26	50.56
440	2.0	0.71	4.46	39.54	55.29
450	4.0	1.20	3.84	50.64	44.32
460	3.5	1.03	3.63	48.49	46.85
470	1.5	0.66	8.12	43.55	47.68
485	0.7	1.06	19.11	44.76	35.06
500	0.2	1.02	17.14	45.56	36.27
550	1.2	0.37	19.67	42.88	37.08
600	0.5	0.32	9.73	49.39	40.56

APPENDIX III:

ELECTRON MICROPROBE ANALYSES OF VOLCANIC GLASS SHARDS

Pakaututu Road:0cm

	1	2	3	4	5	6	7	8	9	10	11	12	13	14	15	16	17
SiO_2	71.46	68.42	74.75	73.19	75.55	75.63	73.17	73.35	74.13	72.96	75.18	73.00	71.77	73.27	72.79	69.39	73.64
TiO_2	0.18	0.15	0.29	0.29	0.07	0.18	0.31	0.23	0.13	0.27	0.18	0.14	0.26	0.16	0.13	0.26	0.26
Al_2O_3	13.48	17.62	13.32	13.02	12.22	11.99	12.89	13.14	11.96	13.05	12.10	11.54	12.82	12.99	12.36	16.39	13.17
FeO	1.52	1.32	1.92	1.89	1.10	1.10	1.98	1.81	1.26	1.87	0.90	1.07	1.91	1.81	1.62	1.40	1.73
MgO	0.20	0.22	0.27	0.21	0.14	0.11	0.24	0.29	0.11	0.32	0.15	0.20	0.25	0.20	0.05	0.20	0.25
CaO	1.58	3.70	1.51	1.49	1.00	1.03	1.31	1.55	1.01	1.49	0.88	0.94	1.47	1.54	1.13	2.90	1.27
Na_2O	4.48	5.48	4.38	4.58	4.13	4.16	4.46	4.62	4.08	4.27	3.87	3.66	4.36	4.70	3.52	5.08	4.39
K_2O	2.54	1.94	2.82	2.74	3.01	3.19	2.63	2.77	3.11	3.07	3.81	3.08	2.46	2.82	3.70	2.00	2.67
Cl	0.09	0.14	0.12	0.15	0.14	0.20	0.16	0.15	0.16	0.13	0.20	0.16	0.22	0.14	0.13	0.15	0.19
Totals	95.53	98.99	99.37	97.56	97.37	97.58	97.13	97.90	95.94	97.42	97.25	93.78	95.51	97.63	95.43	97.78	97.56
Analyses normalised to 100% loss free																	
SiO_2	74.80	69.11	75.23	75.02	77.59	77.50	75.33	74.92	77.26	74.89	77.30	77.84	75.15	75.05	76.28	70.97	75.48
TiO_2	0.18	0.15	0.29	0.30	0.07	0.19	0.31	0.23	0.13	0.28	0.19	0.15	0.27	0.17	0.14	0.27	0.26
Al_2O_3	14.11	17.80	13.41	13.35	12.55	12.29	13.27	13.42	12.47	13.40	12.44	12.31	13.42	13.31	12.95	16.77	13.50
FeO	1.59	1.34	1.93	1.94	1.13	1.12	2.04	1.85	1.31	1.92	0.92	1.14	2.00	1.85	1.69	1.43	1.77
MgO	0.21	0.23	0.27	0.21	0.14	0.11	0.25	0.30	0.11	0.32	0.15	0.21	0.26	0.20	0.05	0.21	0.25
CaO	1.66	3.74	1.52	1.53	1.02	1.05	1.35	1.58	1.05	1.53	0.90	1.00	1.54	1.57	1.19	2.96	1.30
Na_2O	4.69	5.53	4.40	4.69	4.25	4.27	4.59	4.72	4.25	4.38	3.98	3.91	4.57	4.81	3.69	5.20	4.50
K_2O	2.66	1.95	2.83	2.81	3.09	3.27	2.71	2.83	3.24	3.15	3.92	3.28	2.57	2.89	3.87	2.04	2.74
Cl	0.10	0.14	0.12	0.15	0.15	0.21	0.16	0.15	0.17	0.14	0.20	0.17	0.23	0.15	0.14	0.16	0.19
Totals	100.00	100.00	100.00	100.00	100.00	100.00	100.00	100.00	100.00	100.00	100.00	100.00	100.00	100.00	100.00	100.00	100.00

Pakaututu Road:10cm

	1	2	3	4	5	6	7	8	9	10	11	12	13	14
SiO_2	73.05	75.48	73.20	72.33	72.07	73.04	73.00	73.21	72.80	73.12	72.77	71.09	72.69	73.10
TiO_2	0.11	0.15	0.19	0.36	0.32	0.31	0.19	0.27	0.34	0.28	0.26	0.20	0.34	0.29
Al_2O_3	12.00	12.04	13.04	12.79	12.73	13.11	12.32	12.49	12.99	13.17	13.01	11.48	12.88	13.31
FeO	1.25	1.19	1.74	1.83	1.69	1.90	1.40	1.56	1.84	1.90	1.90	1.22	1.97	1.96
MgO	0.15	0.11	0.31	0.30	0.26	0.24	0.16	0.18	0.27	0.29	0.29	0.14	0.23	0.32
CaO	1.03	0.98	1.51	1.44	1.42	1.42	1.40	1.27	1.46	1.40	1.58	1.07	1.41	1.59
Na_2O	4.02	4.24	4.66	4.69	4.37	4.56	3.93	3.97	4.46	4.49	3.26	3.74	4.39	4.83
K_2O	2.81	3.25	2.75	2.68	2.43	2.93	2.91	3.25	2.67	2.79	2.54	2.98	2.59	2.95
Cl	0.19	0.22	0.16	0.17	0.17	0.17	0.24	0.15	0.17	0.19	0.12	0.21	0.20	0.18
Totals	94.61	97.67	97.56	96.58	95.45	97.67	95.54	96.33	97.00	97.64	95.74	92.14	96.70	98.52
Analyses normalised to 100% loss free														
SiO_2	77.21	77.28	75.04	74.88	75.50	74.78	76.41	76.00	75.05	74.89	76.01	77.15	75.17	74.19
TiO_2	0.12	0.15	0.19	0.37	0.33	0.32	0.19	0.28	0.35	0.29	0.27	0.21	0.35	0.30
Al_2O_3	12.68	12.33	13.37	13.24	13.34	13.42	12.89	12.97	13.39	13.49	13.59	12.46	13.32	13.51
FeO	1.32	1.22	1.78	1.89	1.77	1.95	1.46	1.62	1.90	1.95	1.99	1.33	2.03	1.99
MgO	0.16	0.11	0.32	0.31	0.28	0.24	0.17	0.18	0.28	0.30	0.31	0.15	0.24	0.32
CaO	1.08	1.01	1.55	1.49	1.48	1.45	1.46	1.32	1.50	1.44	1.65	1.17	1.46	1.61
Na_2O	4.25	4.35	4.77	4.86	4.58	4.67	4.11	4.12	4.59	4.60	3.40	4.05	4.54	4.90
K_2O	2.96	3.33	2.82	2.78	2.55	3.00	3.04	3.37	2.76	2.85	2.66	3.24	2.68	2.99
Cl	0.20	0.23	0.16	0.18	0.17	0.17	0.25	0.15	0.17	0.19	0.13	0.23	0.21	0.18
Totals	100.00	100.00	100.00	100.00	100.00	100.00	100.00	100.00	100.00	100.00	100.00	100.00	100.00	100.00

Pakututu Road:30cm

	1	2	3	4	5	6	7	8	9	10	11	12	13	14	15
SiO_2	74.21	73.26	72.78	71.33	62.94	73.97	74.30	75.42	73.51	73.87	72.52	73.16	73.29	72.53	74.40
TiO_2	0.15	0.29	0.31	0.16	0.10	0.18	0.17	0.17	0.29	0.20	0.21	0.25	0.33	0.24	0.31
Al_2O_3	13.42	13.05	13.31	12.09	20.03	13.33	11.35	13.25	12.61	12.04	11.69	13.12	12.76	12.82	13.24
FeO	1.91	1.72	1.84	1.60	1.01	2.02	1.73	1.60	2.02	1.63	2.11	1.84	1.72	1.73	1.76
MgO	0.17	0.14	0.26	0.21	0.15	0.18	0.17	0.18	0.30	0.17	0.25	0.40	0.31	0.31	0.25
CaO	1.25	1.23	1.60	1.21	4.79	1.38	0.73	1.25	1.53	1.03	1.18	1.61	1.36	1.53	1.32
Na_2O	4.31	4.28	4.66	4.63	5.90	4.55	4.47	4.42	4.65	4.36	4.53	4.95	4.22	4.67	4.62
K_2O	2.89	2.68	2.94	3.05	1.52	2.77	2.90	2.98	2.80	2.99	2.94	2.78	3.02	2.84	2.41
Cl	0.15	0.28	0.27	0.28	0.20	0.14	0.22	0.17	0.16	0.18	0.19	0.25	0.09	0.19	0.23
Totals	98.47	96.92	97.97	94.55	96.63	98.50	96.04	99.44	97.88	96.47	95.61	98.34	97.09	96.86	98.54
Analyses normalised to 100% loss free															
SiO_2	75.36	75.59	74.29	75.45	65.14	75.10	77.37	75.85	75.11	76.57	75.85	74.39	75.48	74.88	75.51
TiO_2	0.16	0.30	0.31	0.17	0.11	0.18	0.18	0.17	0.30	0.21	0.22	0.25	0.33	0.25	0.31
Al_2O_3	13.63	13.46	13.59	12.79	20.73	13.53	11.82	13.32	12.88	12.48	12.23	13.34	13.14	13.23	13.44
FeO	1.94	1.77	1.88	1.69	1.04	2.05	1.80	1.61	2.07	1.69	2.21	1.87	1.77	1.79	1.79
MgO	0.18	0.14	0.26	0.22	0.15	0.18	0.18	0.18	0.30	0.18	0.26	0.41	0.32	0.31	0.25
CaO	1.27	1.27	1.64	1.27	4.95	1.40	0.76	1.26	1.56	1.07	1.23	1.63	1.40	1.58	1.34
Na_2O	4.37	4.41	4.76	4.90	6.10	4.61	4.66	4.44	4.75	4.52	4.73	5.03	4.34	4.82	4.69
K_2O	2.94	2.77	3.00	3.22	1.58	2.81	3.02	3.00	2.86	3.10	3.07	2.82	3.11	2.93	2.44
Cl	0.15	0.29	0.27	0.29	0.20	0.14	0.23	0.17	0.16	0.19	0.20	0.25	0.09	0.20	0.24
Totals	100.00	100.00	100.00	100.00	100.00	100.00	100.00	100.00	100.00	100.00	100.00	100.00	100.00	100.00	100.00

	16	17	18	19	20	21	22	23	24	25	26	27	28	29
SiO_2	74.13	73.61	73.49	74.07	70.59	74.85	72.43	72.26	74.16	72.51	72.94	73.16	74.61	74.21
TiO_2	3.22	0.21	0.30	0.49	0.18	0.33	0.33	0.27	0.41	0.31	0.19	0.24	0.09	0.15
Al_2O_3	11.33	11.95	12.50	13.02	11.88	11.92	13.01	12.51	14.35	13.57	13.13	12.76	12.11	13.42
FeO	1.26	1.25	1.98	1.79	1.56	1.82	1.76	1.68	2.14	2.17	1.91	1.93	0.90	1.91
MgO	0.16	0.16	0.11	0.27	0.16	0.14	0.27	0.31	0.31	0.19	0.09	0.21	0.14	0.15
CaO	0.96	1.02	1.29	1.33	0.95	1.09	1.47	1.44	1.25	1.26	1.28	1.31	1.05	1.19
Na_2O	3.90	3.89	4.40	4.48	4.15	3.82	4.76	4.52	4.35	4.59	4.63	3.93	4.22	4.52
K_2O	2.98	2.82	2.96	3.17	2.84	3.05	2.61	2.58	2.79	2.69	2.60	3.63	2.92	2.95
Cl	0.26	0.31	0.14	0.22	0.27	0.12	0.17	0.24	0.16	0.18	0.20	0.17	0.24	0.21
Totals	98.19	95.21	97.15	98.82	92.57	97.15	96.81	95.80	99.93	97.46	96.97	97.32	96.27	98.73
Analyses normalised to 100% loss free														
SiO_2	75.50	77.31	75.64	74.95	76.25	77.05	74.81	75.42	74.22	74.40	75.22	75.17	77.49	75.17
TiO_2	3.28	0.22	0.31	0.49	0.19	0.34	0.34	0.28	0.41	0.31	0.19	0.25	0.09	0.16
Al_2O_3	11.54	12.55	12.87	13.17	12.83	12.27	13.44	13.06	14.36	13.92	13.54	13.11	12.58	13.60
FeO	1.29	1.31	2.04	1.81	1.68	1.88	1.81	1.76	2.14	2.22	1.97	1.98	0.93	1.93
MgO	0.16	0.17	0.11	0.27	0.17	0.15	0.28	0.32	0.31	0.20	0.10	0.21	0.14	0.15
CaO	0.97	1.07	1.33	1.34	1.03	1.13	1.52	1.51	1.25	1.29	1.32	1.35	1.09	1.21
Na_2O	3.97	4.09	4.52	4.54	4.48	3.93	4.91	4.72	4.36	4.71	4.77	4.03	4.39	4.58
K_2O	3.03	2.96	3.05	3.20	3.07	3.14	2.69	2.70	2.80	2.76	2.68	3.73	3.04	2.99
Cl	0.26	0.32	0.14	0.22	0.29	0.12	0.18	0.25	0.16	0.18	0.21	0.17	0.25	0.22
Totals	100.00	100.00	100.00	100.00	100.00	100.00	100.00	100.00	100.00	100.00	100.00	100.00	100.00	100.00

Pakaututu Road:40cm (10um)

	1	2	3	4	5	6	7	8	9	10	11
SiO_2	77.00	75.88	75.11	75.20	73.43	73.81	76.38	76.37	74.20	74.07	75.47
TiO_2	0.13	0.18	0.17	0.16	0.09	0.04	0.08	0.19	0.15	0.20	0.14
Al_2O_3	12.34	12.53	11.54	12.26	12.28	12.44	12.34	12.49	12.12	12.53	12.37
FeO	1.54	1.55	1.58	1.63	1.88	1.70	1.65	1.76	1.73	2.05	1.92
MgO	0.11	0.17	0.18	0.14	0.23	0.11	0.14	0.20	0.19	0.17	0.15
CaO	1.02	1.31	1.08	1.35	1.26	1.41	1.06	1.51	1.26	1.28	1.29
Na_2O	4.10	4.15	3.64	4.18	4.31	4.16	4.12	4.20	4.07	4.39	4.15
K_2O	3.12	2.73	2.90	2.55	2.52	2.88	3.16	2.89	2.75	2.85	2.96
Cl	0.20	0.12	0.15	0.16	0.12	0.13	0.08	0.16	0.15	0.11	0.14
Totals	99.57	98.61	96.34	97.62	96.12	96.68	99.01	99.77	96.60	97.64	98.60
Analyses normalised to 100% loss free											
SiO_2	77.34	76.95	77.96	77.03	76.40	76.34	77.15	76.54	76.81	75.85	76.55
TiO_2	0.13	0.18	0.17	0.16	0.09	0.04	0.08	0.19	0.16	0.20	0.14
Al_2O_3	12.39	12.70	11.98	12.56	12.77	12.87	12.46	12.52	12.54	12.83	12.54
FeO	1.55	1.58	1.64	1.67	1.96	1.76	1.67	1.77	1.79	2.10	1.95
MgO	0.11	0.17	0.19	0.14	0.24	0.12	0.14	0.20	0.19	0.17	0.16
CaO	1.03	1.32	1.12	1.38	1.31	1.46	1.07	1.51	1.31	1.31	1.31
Na_2O	4.12	4.21	3.78	4.28	4.48	4.31	4.16	4.21	4.22	4.50	4.21
K_2O	3.14	2.77	3.01	2.61	2.63	2.98	3.19	2.90	2.84	2.92	3.00
Cl	0.20	0.12	0.15	0.16	0.13	0.14	0.08	0.16	0.15	0.11	0.14
Totals	100.00	100.00	100.00	100.00	100.00	100.00	100.00	100.00	100.00	100.00	100.00

Pakaututu Road:40cm (20um)

	1	2	3	4	5	6	7	8	9	10	11	12	13	14	15	16	17	18	19	20
SiO_2	75.12	74.06	73.38	73.28	73.82	73.83	74.31	74.17	74.97	73.94	71.63	72.77	73.29	74.50	72.19	69.06	71.58	70.73	73.90	64.34
TiO_2	0.27	0.28	0.27	0.16	0.27	0.28	0.29	0.31	0.27	0.20	0.27	0.27	0.15	0.20	0.25	0.20	0.19	0.25	0.37	0.27
Al_2O_3	13.27	11.64	12.40	12.67	12.62	12.37	12.81	12.94	12.75	12.62	12.36	12.57	12.88	12.05	12.54	11.84	12.16	11.85	13.03	16.30
FeO	1.97	1.45	1.85	1.81	1.74	1.63	1.87	1.86	1.59	1.67	1.62	1.91	1.79	1.46	1.35	1.25	1.44	0.91	1.72	0.77
MgO	0.25	0.05	0.41	0.27	0.30	0.19	0.30	0.25	0.30	0.20	0.20	0.22	0.19	0.22	0.15	0.28	0.23	0.10	0.25	0.37
CaO	1.33	0.67	1.29	1.40	1.19	1.17	1.19	1.31	0.98	1.06	1.32	1.26	1.32	1.08	1.10	1.20	1.12	1.15	1.37	2.34
Na_2O	4.10	3.19	3.70	3.95	3.92	3.77	3.79	3.77	3.68	4.21	3.82	3.86	3.99	3.73	4.00	3.62	3.99	4.42	3.51	4.67
K_2O	2.57	4.25	3.10	2.52	2.83	3.05	2.78	2.67	2.99	2.99	3.14	2.71	2.96	3.01	2.65	2.32	2.67	2.08	2.98	3.83
Cl	0.27	0.21	0.26	0.13	0.23	0.16	0.19	0.11	0.16	0.15	0.09	0.13	0.21	0.19	0.12	0.10	0.19	0.16	0.13	0.18
Totals	99.16	95.80	96.66	96.19	96.92	96.45	97.54	97.37	97.68	97.03	94.46	95.69	96.78	96.43	94.36	89.86	93.56	91.64	97.26	93.07
Analyses normalised to 100% loss free																				
SiO_2	75.76	77.31	75.92	76.19	76.17	76.54	76.19	76.17	76.75	76.20	75.83	76.05	75.73	77.25	76.50	76.86	76.51	77.17	75.98	69.13
TiO_2	0.27	0.29	0.28	0.17	0.28	0.29	0.30	0.32	0.28	0.20	0.28	0.29	0.15	0.20	0.26	0.22	0.20	0.27	0.38	0.29
Al_2O_3	13.38	12.16	12.83	13.17	13.02	12.82	13.14	13.29	13.05	13.01	13.09	13.13	13.31	12.50	13.29	13.17	13.00	12.93	13.39	17.51
FeO	1.98	1.52	1.92	1.88	1.80	1.69	1.92	1.91	1.63	1.73	1.72	2.00	1.85	1.52	1.43	1.39	1.54	0.99	1.77	0.83
MgO	0.25	0.05	0.43	0.28	0.31	0.20	0.31	0.25	0.31	0.20	0.22	0.23	0.20	0.22	0.16	0.31	0.24	0.11	0.26	0.40
CaO	1.35	0.70	1.33	1.45	1.22	1.21	1.22	1.34	1.00	1.09	1.39	1.31	1.36	1.12	1.17	1.34	1.20	1.26	1.41	2.51
Na_2O	4.14	3.33	3.82	4.10	4.04	3.91	3.88	3.87	3.77	4.34	4.05	4.03	4.13	3.87	4.24	4.03	4.26	4.82	3.61	5.02
K_2O	2.60	4.43	3.21	2.62	2.92	3.16	2.85	2.74	3.06	3.08	3.32	2.83	3.06	3.12	2.81	2.58	2.85	2.27	3.06	4.12
Cl	0.27	0.22	0.27	0.14	0.23	0.16	0.19	0.11	0.16	0.16	0.10	0.13	0.22	0.20	0.13	0.11	0.21	0.18	0.14	0.19
Totals	100.00	100.00	100.00	100.00	100.00	100.00	100.00	100.00	100.00	100.00	100.00	100.00	100.00	100.00	100.00	100.00	100.00	100.00	100.00	100.00

Pakaututu Road: 50cm

	1	2	3	4	5	6	7	8	9	10	11	12	13	14	15	16	17
SiO_2	75.92	75.05	70.32	67.06	72.94	72.77	71.19	72.41	72.89	69.19	70.04	69.75	70.01	66.78	70.90	73.04	72.76
TiO_2	0.20	0.32	1.32	0.24	0.19	0.20	0.28	0.23	0.33	0.14	0.21	0.12	0.26	0.23	0.24	0.30	0.31
Al_2O_3	13.25	12.57	11.85	11.34	12.15	12.05	11.88	11.09	12.21	11.17	11.66	10.47	11.58	11.41	11.98	12.19	12.31
FeO	1.89	1.94	1.69	1.60	1.99	1.57	1.81	0.88	1.69	1.66	1.82	0.80	1.69	1.43	1.92	1.65	1.91
MgO	0.24	0.21	0.20	0.18	0.20	0.25	0.27	0.19	0.23	0.12	0.22	0.12	0.15	0.02	0.20	0.25	0.27
CaO	1.66	1.29	1.33	1.05	1.21	1.31	1.32	0.71	1.20	1.13	1.28	0.91	1.38	1.141	1.24	1.26	1.22
Na_2O	3.53	4.12	3.77	3.81	4.08	4.15	3.68	3.60	4.06	3.69	3.56	3.46	3.77	3.54	3.87	4.24	4.15
K_2O	2.48	2.75	2.71	2.65	3.41	2.97	2.81	3.28	3.09	2.77	2.68	3.42	3.08	3.08	2.78	2.88	3.09
Cl	0.13	0.16	n.d.	n.d.	n.d.	n.d.	n.d.	n.d.	n.d.	n.d.	n.d.	n.d.	n.d.	n.d.	n.d.	n.d.	n.d.
Totals	99.28	98.40	93.20	87.93	96.17	95.26	93.26	92.38	95.71	89.87	91.47	89.05	91.92	87.63	93.12	95.82	96.01
Analyses normalised to 100% loss free																	
SiO_2	76.47	76.27	75.46	76.27	75.84	76.39	76.34	78.38	76.16	76.99	76.57	78.33	76.17	76.21	76.14	76.22	75.79
TiO_2	0.20	0.32	1.41	0.27	0.20	0.20	0.30	0.24	0.35	0.16	0.22	0.14	0.28	0.26	0.26	0.31	0.32
Al_2O_3	13.34	12.78	12.72	12.90	12.63	12.65	12.74	12.01	12.76	12.42	12.75	11.76	12.59	13.02	12.87	12.73	12.82
FeO	1.90	1.97	1.82	1.82	2.07	1.64	1.95	0.95	1.76	1.85	1.99	0.90	1.83	1.63	2.06	1.72	1.98
MgO	0.24	0.21	0.22	0.20	0.21	0.27	0.29	0.20	0.24	0.13	0.24	0.14	0.17	0.02*	0.21	0.26	0.28
CaO	1.67	1.31	1.43	1.19	1.26	1.38	1.42	0.76	1.25	1.26	1.40	1.02	1.50	1.30	1.33	1.32	1.27
Na_2O	3.55	4.19	4.04	4.33	4.24	4.35	3.95	3.89	4.25	4.10	3.89	3.88	4.10	4.04	4.15	4.43	4.32
K_2O	2.49	2.79	2.91	3.01	3.55	3.12	3.02	3.55	3.23	3.08	2.93	3.84	3.36	3.52	2.98	3.01	3.22
Cl	0.13	0.16	n.d.	n.d.	n.d.	n.d.	n.d.	n.d.	n.d.	n.d.	n.d.	n.d.	n.d.	n.d.	n.d.	n.d.	n.d.
Totals	100.00	100.00	100.00	100.00	100.00	100.00	100.00	100.00	100.00	100.00	100.00	100.00	100.00	100.00	100.00	100.00	100.00

Pakaututu Road:60cm

	1	2	3	4	5	6	7	8	9	10
SiO_2	73.54	73.83	73.07	71.14	73.83	74.66	71.29	74.36	72.81	76.61
TiO_2	0.09	0.29	0.09	0.20	0.06	0.21	0.13	0.32	0.22	0.11
Al_2O_3	11.65	11.60	11.85	12.80	11.70	11.96	11.81	12.50	12.06	12.09
FeO	0.82	0.79	0.73	1.76	0.76	0.91	1.03	1.26	1.13	0.76
MgO	0.04	0.17	0.11	0.21	0.21	0.25	0.32	0.19	0.15	0.13
CaO	0.66	0.90	0.66	1.36	0.93	0.90	0.92	1.25	1.02	0.71
Na_2O	3.93	4.20	4.28	4.48	3.35	2.97	4.13	4.05	2.99	4.39
K_2O	3.73	2.90	2.87	2.64	2.99	2.87	2.43	2.77	2.58	3.05
Cl	0.14	0.14	0.14	0.12	0.10	0.12	0.12	0.13	0.22	0.18
Totals	94.59	94.82	93.80	94.72	93.92	94.82	92.17	96.81	93.18	98.03
Analyses normalised to 100% loss free										
SiO_2	77.74	77.86	77.90	75.06	78.61	78.73	77.34	76.81	78.15	78.15
TiO_2	0.10	0.30	0.10	0.21	0.06	0.22	0.14	0.33	0.24	0.11
Al_2O_3	12.31	12.24	12.64	13.51	12.46	12.61	12.81	12.91	12.95	12.33
FeO	0.87	0.83	0.78	1.85	0.80	0.96	1.12	1.30	1.21	0.78
MgO	0.05	0.18	0.11	0.22	0.22	0.26	0.34	0.20	0.16	0.14
CaO	0.69	0.95	0.70	1.44	0.99	0.95	1.00	1.29	1.09	0.72
Na_2O	4.15	4.43	4.57	4.73	3.57	3.13	4.48	4.18	3.21	4.48
K_2O	3.94	3.06	3.05	2.79	3.18	3.02	2.64	2.86	2.77	3.11
Cl	0.15	0.14	0.15	0.20	0.10	0.12	0.13	0.13	0.23	0.18
Totals	100.00	100.00	100.00	100.00	100.00	100.00	100.00	100.00	100.00	100.00

Pakaututu Road:70cm

	1	2	3	4	5	6	7	8	9	10	11	12	13	14	15	16	17	18
SiO_2	76.14	75.14	75.35	74.22	75.76	72.98	70.19	75.39	74.50	73.63	74.52	76.86	76.65	75.48	76.90	74.96	73.05	76.35
TiO_2	0.14	0.26	0.15	0.24	0.15	0.26	0.19	0.22	0.17	0.26	0.25	0.14	0.17	0.12	0.10	0.10	0.18	0.14
Al_2O_3	12.25	12.49	12.52	12.78	11.71	11.31	12.11	13.89	12.60	11.55	12.85	12.51	12.30	11.99	11.93	13.20	11.88	12.24
FeO	0.92	1.22	1.05	1.45	0.86	0.93	1.60	1.53	1.02	1.04	1.95	0.92	1.04	0.87	0.84	1.46	0.63	0.83
MgO	0.10	0.28	0.10	0.14	0.21	0.17	0.19	0.14	0.14	0.14	0.22	0.13	0.15	0.16	0.16	0.17	0.11	0.14
CaO	0.81	1.49	0.73	1.19	0.73	0.74	1.45	1.26	0.81	0.76	1.49	0.80	0.75	0.81	0.84	1.22	0.71	0.76
Na_2O	4.11	4.35	4.45	4.08	4.30	4.28	4.36	4.34	3.97	4.10	4.57	4.44	4.46	4.19	4.30	4.22	4.27	4.47
K_2O	3.20	2.96	3.39	3.15	3.37	3.18	2.89	2.92	3.55	3.13	2.77	3.30	3.08	3.40	3.63	2.94	3.35	3.16
Cl	0.30	0.16	0.20	0.20	0.20	0.23	0.32	0.14	0.19	0.23	0.13	0.15	0.18	0.21	0.24	0.18	0.20	0.23
Totals	97.97	98.36	97.95	97.44	97.28	94.07	93.30	99.82	96.95	94.85	98.73	99.23	98.78	97.22	98.95	98.45	94.36	98.32
Analyses normalised to 100% loss free																		
SiO_2	77.72	76.39	76.93	76.17	77.88	77.58	75.23	75.52	76.84	77.63	75.47	77.45	77.60	77.64	77.72	76.14	77.41	77.65
TiO_2	0.14	0.27	0.16	0.24	0.15	0.28	0.20	0.22	0.18	0.28	0.26	0.14	0.17	0.12	0.11	0.10	0.20	0.14
Al_2O_3	12.51	12.70	12.79	13.12	12.04	12.02	12.98	13.91	13.00	12.18	13.01	12.61	12.46	12.34	12.06	13.41	12.59	12.45
FeO	0.94	1.24	1.07	1.49	0.89	0.99	1.72	1.53	1.06	1.10	1.97	0.92	1.06	0.89	0.84	1.49	0.67	0.85
MgO	0.10	0.28	0.11	0.14	0.21	0.18	0.21	0.14	0.14	0.15	0.22	0.13	0.15	0.16	0.16	0.17	0.11	0.14
CaO	0.83	1.52	0.74	1.22	0.75	0.79	1.56	1.26	0.83	0.80	1.51	0.81	0.76	0.83	0.85	1.24	0.75	0.78
Na_2O	4.20	4.42	4.54	4.19	4.42	4.55	4.67	4.34	4.09	4.32	4.62	4.47	4.51	4.30	4.35	4.29	4.52	4.54
K_2O	3.27	3.01	3.47	3.23	3.46	3.38	3.10	2.92	3.66	3.30	2.80	3.33	3.12	3.50	3.67	2.99	3.55	3.21
Cl	0.31	0.17	0.20	0.20	0.21	0.25	0.34	0.14	0.20	0.24	0.13	0.15	0.18	0.21	0.24	0.18	0.21	0.23
Totals	100.00	100.00	100.00	100.00	100.00	100.00	100.00	100.00	100.00	100.00	100.00	100.00	100.00	100.00	100.00	100.00	100.00	100.00

Pakaututu Road:80cm

	1	2	3	4	5	6	7	8	9	10	11	12	13	14	15
SiO_2	76.91	75.90	72.60	75.88	75.48	75.26	75.69	75.57	77.30	74.90	75.72	72.30	76.59	75.73	73.17
TiO_2	0.14	0.17	0.14	0.24	0.16	0.15	0.11	0.07	0.14	0.05	0.11	0.22	0.18	0.12	0.16
Al_2O_3	12.30	11.99	11.69	12.05	12.72	12.90	12.04	12.16	12.41	12.00	11.99	12.25	12.35	12.14	11.85
FeO	0.91	0.95	1.10	0.97	1.50	1.59	1.06	0.89	0.95	0.91	0.91	1.56	0.89	0.92	0.86
MgO	0.15	0.12	0.12	0.18	0.24	0.15	0.13	0.12	0.08	0.12	0.15	0.22	0.14	0.17	0.12
CaO	0.67	0.77	1.01	0.65	1.33	1.43	0.92	0.77	0.81	0.70	0.73	1.23	0.80	0.84	0.82
Na_2O	4.20	4.01	4.00	4.22	4.27	4.19	4.24	4.17	4.20	3.96	4.35	4.02	4.32	3.80	4.14
K_2O	3.07	3.04	2.87	3.12	2.82	3.11	3.17	3.28	3.39	3.20	3.14	3.11	3.13	3.29	3.18
Cl	0.13	0.10	0.20	0.12	0.12	0.17	0.11	0.16	0.13	0.11	0.21	0.10	0.20	0.19	0.16
Totals	98.49	97.07	93.73	97.44	98.64	98.95	97.46	97.19	99.41	95.94	97.30	95.00	98.59	97.19	94.45
Analyses normalised to 100% loss free															
SiO_2	78.09	78.20	77.45	77.88	76.52	76.05	77.67	77.75	77.76	78.07	77.82	76.10	77.69	77.92	77.47
TiO_2	0.15	0.17	0.15	0.25	0.17	0.15	0.11	0.07	0.14	0.05	0.11	0.23	0.18	0.13	0.17
Al_2O_3	12.49	12.35	12.48	12.37	12.90	13.04	12.35	12.51	12.49	12.50	12.33	12.89	12.53	12.49	12.54
FeO	0.92	0.98	1.17	1.00	1.52	1.61	1.09	0.92	0.95	0.95	0.93	1.64	0.90	0.95	0.91
MgO	0.16	0.12	0.13	0.18	0.24	0.16	0.13	0.13	0.08	0.13	0.15	0.23	0.14	0.17	0.13
CaO	0.68	0.80	1.08	0.67	1.35	1.45	0.94	0.79	0.82	0.73	0.75	1.29	0.81	0.86	0.86
Na_2O	4.26	4.13	4.26	4.33	4.32	4.24	4.35	4.29	4.22	4.13	4.47	4.23	4.38	3.91	4.38
K_2O	3.11	3.13	3.07	3.21	2.86	3.14	3.25	3.38	3.41	3.33	3.23	3.27	3.18	3.38	3.36
Cl	0.14	0.11	0.21	0.12	0.12	0.17	0.11	0.16	0.13	0.11	0.21	0.11	0.20	0.19	0.17
Totals	100.00	100.00	100.00	100.00	100.00	100.00	100.00	100.00	100.00	100.00	100.00	100.00	100.00	100.00	100.00

Pakaututu Road:90cm

	1	2	3	4	5	6	7	8	9	10
SiO_2	74.52	77.68	78.17	76.01	76.01	76.19	77.04	77.11	77.57	77.42
TiO_2	0.18	0.13	0.08	0.08	0.21	0.13	0.10	0.23	0.19	0.22
Al_2O_3	12.47	12.17	12.11	12.00	12.68	12.12	11.74	12.39	12.28	12.42
FeO	1.61	0.94	0.94	0.86	1.78	1.21	0.85	1.67	0.72	0.88
MgO	0.19	0.15	0.15	0.13	0.29	0.15	0.13	0.19	0.11	0.17
CaO	1.22	0.85	0.71	0.72	1.32	0.77	0.84	1.15	0.84	0.76
Na_2O	4.31	4.21	4.24	4.20	4.50	4.38	4.40	4.12	4.41	4.49
K_2O	2.92	3.39	3.32	3.18	2.91	3.03	3.09	3.05	3.18	2.94
Cl	0.09	0.10	0.26	0.19	0.25	0.16	0.14	0.09	0.14	0.18
Totals	97.52	99.63	99.97	97.36	99.94	98.15	98.33	100.00	99.44	99.47
Analyses normalised to 100% loss free										
SiO_2	76.42	77.97	78.20	78.08	76.05	77.63	78.35	77.11	78.01	77.83
TiO_2	0.18	0.13	0.08	0.08	0.21	0.14	0.10	0.23	0.19	0.22
Al_2O_3	12.79	12.22	12.11	12.33	12.68	12.34	11.94	12.39	12.35	12.49
FeO	1.65	0.94	0.94	0.88	1.78	1.24	0.86	1.67	0.72	0.88
MgO	0.20	0.15	0.15	0.13	0.29	0.16	0.13	0.19	0.11	0.17
CaO	1.25	0.85	0.71	0.73	1.32	0.79	0.85	1.15	0.84	0.76
Na_2O	4.42	4.23	4.25	4.32	4.50	4.47	4.48	4.12	4.43	4.51
K_2O	2.99	3.40	3.32	3.27	2.91	3.09	3.14	3.05	3.19	2.96
Cl	0.09	0.10	0.26	0.19	0.25	0.16	0.14	0.09	0.14	0.18
Totals	100.00	100.00	100.00	100.00	100.00	100.00	100.00	100.00	100.00	100.00

Pakaututu Road;100cm

	1	2	3	4	5	6	7	8	9	10	11	12	13	14	15
SiO_2	74.48	75.70	75.26	75.93	74.90	75.26	75.65	73.76	71.79	72.11	74.06	76.13	72.90	76.84	75.95
TiO_2	0.19	0.19	0.21	0.07	0.11	0.07	0.11	0.16	0.15	0.12	0.18	0.09	0.13	0.15	0.08
Al_2O_3	12.05	12.19	12.02	12.45	12.07	12.03	11.71	11.69	11.40	11.57	11.86	12.25	12.13	12.05	12.08
FeO	0.83	1.00	0.90	0.92	0.89	0.82	0.80	0.80	0.82	0.81	0.87	0.75	0.74	1.01	0.89
MgO	0.11	0.17	0.10	0.14	0.16	0.18	0.11	0.17	0.11	0.15	0.10	0.09	0.15	0.14	0.09
CaO	0.70	0.77	0.79	0.86	0.79	0.72	0.80	0.74	0.66	0.70	0.87	0.77	0.84	0.83	0.71
Na_2O	4.21	4.17	4.35	4.08	3.98	4.08	4.04	3.95	3.48	3.92	4.23	4.17	4.21	4.03	4.02
K_2O	3.47	3.29	3.24	3.20	3.14	3.22	3.17	3.18	3.87	3.33	3.20	3.46	3.23	3.14	3.25
Cl	0.12	0.14	0.14	0.14	0.14	0.10	0.13	0.18	0.13	0.20	0.19	0.19	0.12	0.15	0.19
Totals	96.16	97.61	96.99	97.80	96.17	96.47	96.51	94.61	92.42	92.91	95.54	97.89	94.44	98.33	97.26
Analyses normalised to 100% loss free															
SiO_2	77.46	77.55	77.59	77.65	77.88	78.02	78.38	77.96	77.67	77.60	77.52	77.77	77.20	78.14	78.09
TiO_2	0.20	0.19	0.22	0.08	0.11	0.07	0.12	0.17	0.17	0.13	0.19	0.09	0.14	0.15	0.09
Al_2O_3	12.53	12.48	12.40	12.73	12.55	12.47	12.13	12.36	12.33	12.45	12.41	12.51	12.84	12.25	12.42
FeO	0.86	1.02	0.92	0.94	0.92	0.85	0.82	0.84	0.89	0.87	0.91	0.77	0.79	1.03	0.91
MgO	0.11	0.18	0.10	0.15	0.16	0.19	0.12	0.18	0.12	0.16	0.10	0.09	0.16	0.15	0.10
CaO	0.73	0.79	0.81	0.88	0.82	0.75	0.83	0.78	0.72	0.76	0.91	0.79	0.89	0.85	0.73
Na_2O	4.38	4.27	4.48	4.18	4.14	4.22	4.19	4.17	3.77	4.22	4.42	4.26	4.45	4.09	4.14
K_2O	3.60	3.37	3.34	3.27	3.27	3.34	3.28	3.36	4.19	3.58	3.35	3.53	3.41	3.19	3.34
Cl	0.12	0.14	0.14	0.14	0.14	0.10	0.14	0.18	0.14	0.22	0.19	0.20	0.12	0.15	0.20
Totals	100.00	100.00	100.00	100.00	100.00	100.00	100.00	100.00	100.00	100.00	100.00	100.00	100.00	100.00	100.00

Pakaututu Road:110cm

	1
SiO_2	75.01
TiO_2	0.39
Al_2O_3	11.70
FeO	1.45
MgO	0.09
CaO	0.75
Na_2O	3.28
K_2O	5.23
Cl	0.12
Totals	98.00
Analyses normalised to 100% loss free	
SiO_2	76.54
TiO_2	0.40
Al_2O_3	11.93
FeO	1.48
MgO	0.09
CaO	0.76
Na_2O	3.35
K_2O	5.34
Cl	0.12
Totals	100.00

Pakaututu Road:120cm

	1	2	3	4	5	6	7	8	9	10	11	12
SiO_2	75.67	76.19	72.99	73.43	77.63	77.00	76.63	74.38	77.78	78.13	77.75	76.42
TiO_2	0.11	0.20	0.15	0.00	0.20	0.17	0.16	0.17	0.12	0.17	0.22	0.19
Al_2O_3	12.07	12.59	12.06	12.66	11.99	12.20	12.68	11.91	12.16	12.09	12.07	12.69
FeO	0.88	1.81	1.64	1.62	0.89	0.81	1.46	1.50	1.07	0.95	0.91	1.63
MgO	0.15	0.17	0.22	0.25	0.06	0.14	0.18	0.12	0.13	0.19	0.11	0.12
CaO	0.75	1.30	1.32	1.30	0.82	0.80	1.35	1.15	0.82	0.75	0.71	1.45
Na_2O	4.24	4.30	4.21	3.53	4.02	4.06	4.31	4.24	4.46	4.05	4.32	4.25
K_2O	3.13	2.85	2.80	4.25	3.30	3.33	2.95	2.98	3.31	3.30	3.24	3.00
Cl	0.18	0.16	0.14	0.11	0.03	0.17	0.14	0.16	0.12	0.18	0.14	0.19
Totals	97.17	99.57	95.52	97.14	98.93	98.66	99.86	96.61	99.97	99.80	99.47	99.94
Analyses normalised to 100% loss free												
SiO_2	77.87	76.52	76.41	75.59	78.48	78.04	76.74	76.99	77.80	78.28	78.17	76.47
TiO_2	0.12	0.20	0.16	0.00	0.20	0.17	0.16	0.18	0.12	0.17	0.23	0.19
Al_2O_3	12.42	12.65	12.63	13.03	12.12	12.36	12.70	12.33	12.17	12.11	12.13	12.70
FeO	0.91	1.82	1.72	1.66	0.90	0.82	1.46	1.55	1.07	0.96	0.91	1.63
MgO	0.16	0.17	0.23	0.25	0.06	0.14	0.18	0.12	0.13	0.19	0.11	0.12
CaO	0.77	1.30	1.38	1.34	0.83	0.81	1.35	1.19	0.82	0.75	0.71	1.45
Na_2O	4.36	4.32	4.40	3.63	4.07	4.12	4.31	4.39	4.46	4.06	4.34	4.25
K_2O	3.22	2.86	2.93	4.37	3.33	3.37	2.95	3.09	3.31	3.30	3.26	3.00
Cl	0.19	0.16	0.14	0.12	0.03	0.17	0.14	0.17	0.12	0.18	0.14	0.19
Totals	100.00	100.00	100.00	100.00	100.00	100.00	100.00	100.00	100.00	100.00	100.00	100.00

Pakaututu Road:130cm

	1	2	3	4	5	6	7	8	9	10	11	12	13	14	15	16
SiO_2	74.00	74.24	73.66	76.78	74.04	74.08	73.72	71.90	76.26	72.96	77.18	74.21	76.16	74.24	75.31	74.76
TiO_2	0.00	0.16	0.15	0.13	0.21	0.24	0.23	0.14	0.28	0.16	0.08	0.12	0.18	0.26	0.13	0.24
Al_2O_3	12.45	12.44	12.59	12.20	12.72	12.79	12.64	12.06	12.46	11.58	12.50	11.83	12.13	12.80	12.97	12.78
FeO	1.56	1.60	1.77	0.82	1.43	1.60	1.40	1.70	0.98	0.98	0.91	0.77	0.73	1.93	1.82	1.65
MgO	0.15	0.33	0.10	0.18	0.20	0.18	0.23	0.15	0.16	0.16	0.16	0.18	0.15	0.14	0.16	0.21
CaO	1.27	1.45	1.39	0.75	1.47	1.28	1.42	1.28	0.79	0.75	0.83	0.70	0.72	1.32	1.45	1.39
Na_2O	4.24	4.07	4.12	4.17	3.83	4.07	4.07	3.76	4.17	4.21	4.39	4.27	4.24	4.17	4.24	3.94
K_2O	3.20	3.33	3.03	3.48	2.98	3.09	3.12	2.83	3.44	2.97	3.36	3.28	3.29	3.13	3.36	3.25
Cl	0.10	0.15	0.19	0.14	0.14	0.14	0.14	0.15	0.15	0.23	0.16	0.20	0.13	0.18	0.16	0.19
Totals	96.98	97.77	97.01	98.64	97.02	97.47	96.96	93.96	98.68	93.99	99.57	95.57	97.72	98.17	99.60	98.41
Analyses normalised to 100% loss free																
SiO_2	76.31	75.94	75.93	77.84	76.32	76.00	76.04	76.53	77.28	77.62	77.52	77.65	77.94	75.62	75.62	75.97
TiO_2	0.00	0.16	0.16	0.13	0.21	0.25	0.23	0.14	0.28	0.17	0.08	0.13	0.18	0.27	0.13	0.24
Al_2O_3	12.84	12.72	12.98	12.37	13.11	13.12	13.03	12.83	12.62	12.32	12.56	12.38	12.41	13.04	13.02	12.98
FeO	1.61	1.63	1.83	0.83	1.48	1.64	1.44	1.81	1.00	1.04	0.92	0.80	0.75	1.96	1.82	1.68
MgO	0.16	0.34	0.10	0.18	0.20	0.19	0.23	0.16	0.16	0.17	0.16	0.19	0.15	0.14	0.16	0.21
CaO	1.31	1.48	1.44	0.76	1.51	1.31	1.46	1.36	0.80	0.80	0.83	0.74	0.74	1.35	1.46	1.42
Na_2O	4.38	4.17	4.25	4.23	3.95	4.17	4.20	4.00	4.22	4.48	4.41	4.47	4.33	4.25	4.25	4.01
K_2O	3.30	3.40	3.13	3.53	3.07	3.17	3.21	3.01	3.49	3.16	3.37	3.44	3.36	3.19	3.37	3.30
Cl	0.11	0.16	0.19	0.14	0.15	0.14	0.14	0.15	0.15	0.24	0.16	0.21	0.13	0.18	0.16	0.19
Totals	100.00	100.00	100.00	100.00	100.00	100.00	100.00	100.00	100.00	100.00	100.00	100.00	100.00	100.00	100.00	100.00

Pakaututu Road:140cm

	1	2	3	4	5	6	7	8	9	10	11	12	13	14	15
SiO_2	72.13	73.84	73.97	71.11	76.30	74.77	77.33	75.37	75.79	76.31	74.39	77.13	72.61	77.35	73.55
TiO_2	0.24	0.23	0.26	0.42	0.10	0.22	0.16	0.24	0.22	0.11	0.07	0.10	0.12	0.18	0.17
Al_2O_3	12.10	13.41	12.07	12.76	12.49	11.92	11.85	11.26	11.69	12.05	11.87	11.96	11.42	12.30	12.42
FeO	3.40	2.03	1.61	2.55	0.72	1.14	0.92	1.05	1.26	1.07	0.83	0.98	0.85	1.05	1.55
MgO	0.23	0.37	0.24	0.39	0.18	0.18	0.20	0.12	0.12	0.13	0.07	0.18	0.18	0.15	0.15
CaO	1.60	1.83	1.43	1.82	0.68	1.02	1.01	1.20	1.17	1.06	0.73	0.87	0.87	0.89	1.34
Na_2O	4.20	4.23	4.15	4.70	3.68	4.27	4.01	3.61	4.02	4.30	3.98	4.25	4.08	4.35	4.20
K_2O	2.84	2.83	3.06	3.13	3.91	3.15	3.20	3.29	3.19	3.20	4.08	3.09	2.92	3.22	2.79
Cl	0.17	0.16	0.13	0.18	0.17	0.12	0.17	0.19	0.22	0.21	0.21	0.20	0.20	0.14	0.14
Totals	96.92	98.93	96.91	97.05	98.22	96.78	98.85	96.33	97.67	98.43	96.23	98.75	93.24	99.64	96.30
Analyses normalised to 100% loss free															
SiO_2	74.42	74.64	76.33	73.28	77.68	77.26	78.23	78.24	77.60	77.52	77.31	78.10	77.87	77.64	76.38
TiO_2	0.25	0.23	0.26	0.43	0.10	0.23	0.16	0.25	0.22	0.11	0.07	0.10	0.13	0.18	0.18
Al_2O_3	12.49	13.55	12.45	13.14	12.71	12.32	11.99	11.68	11.96	12.24	12.33	12.11	12.24	12.35	12.89
FeO	3.51	2.05	1.66	2.63	0.74	1.17	0.93	1.09	1.29	1.08	0.86	0.99	0.91	1.05	1.60
MgO	0.24	0.38	0.24	0.40	0.18	0.18	0.21	0.12	0.12	0.13	0.07	0.18	0.19	0.15	0.15
CaO	1.65	1.85	1.48	1.87	0.69	1.06	1.02	1.25	1.20	1.08	0.76	0.88	0.93	0.89	1.39
Na_2O	4.33	4.27	4.28	4.84	3.75	4.41	4.05	3.75	4.12	4.37	4.14	4.30	4.38	4.36	4.37
K_2O	2.93	2.86	3.15	3.22	3.98	3.25	3.24	3.41	3.26	3.25	4.24	3.12	3.13	3.24	2.89
Cl	0.18	0.16	0.14	0.18	0.17	0.13	0.18	0.20	0.23	0.21	0.22	0.21	0.21	0.14	0.15
Totals	100.00	100.00	100.00	100.00	100.00	100.00	100.00	100.00	100.00	100.00	100.00	100.00	100.00	100.00	100.00

Pakaututu Road;150cm

	1	2	3	4	5	6	7	8	9	10	11	12	13	14
SiO_2	76.63	76.93	76.93	75.02	76.03	75.45	76.38	76.50	76.30	74.37	72.57	75.30	75.67	74.55
TiO_2	0.13	0.16	0.10	0.18	0.13	0.14	0.14	0.28	0.16	0.13	0.23	0.13	0.31	0.00
Al_2O_3	12.12	11.99	12.19	11.75	11.86	11.92	11.84	12.65	11.98	11.47	11.51	11.85	12.39	11.58
FeO	1.31	1.06	0.78	1.19	1.04	1.25	1.28	1.57	0.84	1.06	1.11	1.36	1.50	1.25
MgO	0.12	0.15	0.09	0.12	0.16	0.10	0.16	0.16	0.22	0.09	0.15	0.13	0.15	0.16
CaO	1.11	0.99	0.68	1.11	1.05	1.14	0.86	1.26	0.87	0.81	1.03	1.15	1.34	1.16
Na_2O	4.22	4.30	3.61	4.03	3.61	3.80	4.08	4.29	4.69	3.99	3.86	3.85	4.11	3.96
K_2O	3.12	3.17	4.17	2.84	3.01	3.28	3.11	3.10	4.35	2.87	2.62	3.03	3.03	2.98
Cl	0.27	0.16	0.11	0.19	0.25	0.19	0.18	0.17	0.23	0.14	0.24	0.12	0.17	0.20
Totals	99.00	98.91	98.65	96.43	97.15	97.26	98.02	99.99	99.63	94.92	93.30	96.92	98.67	95.83
Analyses normalised to 100% loss free														
SiO_2	77.40	77.78	77.98	77.80	78.26	77.57	77.92	76.51	76.58	78.35	77.78	77.70	76.68	77.80
TiO_2	0.13	0.16	0.10	0.18	0.13	0.14	0.14	0.28	0.16	0.13	0.24	0.14	0.31	0.00
Al_2O_3	12.24	12.13	12.35	12.18	12.21	12.26	12.07	12.65	12.03	12.08	12.34	12.22	12.56	12.08
FeO	1.32	1.07	0.79	1.23	1.07	1.29	1.30	1.57	0.84	1.11	1.18	1.40	1.52	1.30
MgO	0.12	0.15	0.09	0.12	0.16	0.10	0.17	0.16	0.22	0.09	0.16	0.13	0.15	0.16
CaO	1.12	1.00	0.69	1.15	1.08	1.17	0.87	1.26	0.87	0.86	1.11	1.18	1.36	1.21
Na_2O	4.26	4.35	3.66	4.18	3.72	3.91	4.17	4.29	4.70	4.20	4.13	3.97	4.17	4.13
K_2O	3.15	3.21	4.23	2.94	3.10	3.37	3.17	3.10	4.37	3.02	2.80	3.13	3.07	3.11
Cl	0.27	0.16	0.11	0.20	0.26	0.20	0.19	0.17	0.23	0.15	0.26	0.12	0.17	0.21
Totals	100.00	100.00	100.00	100.00	100.00	100.00	100.00	100.00	100.00	100.00	100.00	100.00	100.00	100.00

Pakaututu Road:160cm

	1	2	3	4	5	6	7	8	9	10	11	12	13
SiO_2	73.21	75.85	75.91	76.72	74.57	74.99	71.34	73.04	70.27	70.99	75.27	74.26	73.90
TiO_2	0.09	0.20	0.19	0.27	0.22	0.29	0.13	0.18	0.21	0.16	0.24	0.16	0.17
Al_2O_3	11.68	12.42	11.87	12.10	11.91	12.05	11.48	11.68	11.31	12.27	12.37	12.60	11.90
FeO	0.94	0.77	0.87	1.14	0.90	0.98	1.18	0.97	1.08	1.93	1.00	1.27	1.04
MgO	0.05	0.11	0.11	0.16	0.12	0.17	0.11	0.18	0.08	0.16	0.13	0.14	0.13
CaO	0.68	0.93	0.86	0.89	0.82	0.78	0.96	0.92	0.97	1.47	0.89	1.39	0.88
Na_2O	3.46	3.85	3.91	3.92	3.90	3.90	3.67	3.64	3.62	4.05	3.95	4.07	3.87
K_2O	4.10	3.28	3.15	3.24	3.06	3.24	3.02	3.11	3.09	3.06	3.16	3.14	3.21
Cl	0.18	0.13	0.09	0.14	0.14	0.08	0.17	0.13	0.23	0.17	0.15	0.17	0.16
Totals	94.39	97.53	96.96	98.57	95.63	96.49	92.05	93.85	90.87	94.24	97.14	97.20	95.24
Analyses normalised to 100% loss free													
SiO_2	77.56	77.77	78.30	77.83	77.98	77.72	77.50	77.83	77.33	75.32	77.49	76.40	77.59
TiO_2	0.10	0.20	0.19	0.27	0.23	0.30	0.14	0.19	0.23	0.17	0.24	0.16	0.17
Al_2O_3	12.38	12.73	12.24	12.27	12.45	12.49	12.47	12.44	12.45	13.02	12.73	12.96	12.49
FeO	1.00	0.79	0.90	1.16	0.95	1.02	1.28	1.04	1.19	2.05	1.03	1.31	1.09
MgO	0.05	0.11	0.12	0.16	0.12	0.18	0.12	0.19	0.09	0.17	0.13	0.14	0.14
CaO	0.72	0.95	0.89	0.90	0.85	0.81	1.04	0.98	1.06	1.55	0.91	1.43	0.92
Na_2O	3.66	3.94	4.03	3.98	4.08	4.04	3.99	3.88	3.98	4.29	4.06	4.19	4.06
K_2O	4.34	3.37	3.24	3.28	3.19	3.35	3.28	3.32	3.40	3.25	3.25	3.23	3.37
Cl	0.19	0.14	0.09	0.14	0.15	0.09	0.18	0.14	0.25	0.18	0.15	0.17	0.16
Totals	100.00	100.00	100.00	100.00	100.00	100.00	100.00	100.00	100.00	100.00	100.00	100.00	100.00

Pakaututu Road:170cm

	1	2	3	4	5	6	7	8	9	10	11	12
SiO_2	76.45	78.06	77.06	76.34	74.43	74.15	76.55	75.55	76.61	75.86	73.94	75.05
TiO_2	0.31	0.10	0.26	0.15	0.13	0.14	0.16	0.12	0.13	0.13	0.14	0.09
Al_2O_3	11.82	12.12	12.01	11.70	12.05	12.14	12.06	12.08	11.74	11.76	11.70	11.63
FeO	1.17	1.04	0.93	1.15	0.91	1.08	0.81	0.81	1.19	1.16	1.27	1.01
MgO	0.16	0.14	0.13	0.08	0.09	0.05	0.13	0.06	0.16	0.10	0.16	0.18
CaO	1.13	0.87	0.84	0.86	0.72	0.68	0.87	0.57	1.15	0.85	0.99	1.02
Na_2O	3.96	3.91	4.18	3.85	3.75	3.97	4.18	3.93	3.78	3.95	4.06	4.08
K_2O	3.67	3.42	3.14	3.40	3.96	3.83	3.06	4.19	3.01	2.88	2.63	3.29
Cl	0.17	0.13	0.22	0.21	0.12	0.22	0.11	0.13	0.28	0.19	0.18	0.25
Totals	98.85	99.80	98.78	97.73	96.15	96.27	97.93	97.45	98.04	96.88	95.09	96.61
Analyses normalised to 100% loss free												
SiO_2	77.34	78.22	78.01	78.11	77.41	77.03	78.17	77.53	78.14	78.31	77.76	77.68
TiO_2	0.32	0.10	0.27	0.15	0.13	0.15	0.16	0.13	0.13	0.14	0.15	0.10
Al_2O_3	11.96	12.15	12.16	11.97	12.53	12.61	12.32	12.40	11.97	12.14	12.31	12.04
FeO	1.19	1.05	0.94	1.18	0.95	1.12	0.82	0.83	1.22	1.20	1.34	1.05
MgO	0.16	0.14	0.13	0.08	0.10	0.05	0.13	0.06	0.16	0.10	0.17	0.18
CaO	1.14	0.87	0.85	0.88	0.75	0.70	0.89	0.58	1.17	0.88	1.04	1.06
Na_2O	4.01	3.92	4.24	3.94	3.90	4.13	4.27	4.03	3.85	4.08	4.27	4.23
K_2O	3.71	3.42	3.18	3.47	4.11	3.98	3.12	4.30	3.07	2.97	2.77	3.41
Cl	0.17	0.13	0.22	0.22	0.12	0.23	0.11	0.14	0.29	0.20	0.19	0.26
Totals	100.00	100.00	100.00	100.00	100.00	100.00	100.00	100.00	100.00	100.00	100.00	100.00

Pakaututu Road:190cm

	1	2	3	4	5	6	7	8	9	10	11	12	13
SiO_2	73.06	72.01	72.68	73.56	72.11	77.00	73.77	75.89	69.74	71.99	74.11	72.59	69.22
TiO_2	0.17	0.15	0.12	0.11	0.11	0.23	0.12	0.23	0.27	0.18	0.12	0.19	0.08
Al_2O_3	12.11	11.50	11.69	11.65	11.49	12.24	12.38	12.98	11.20	11.12	11.37	11.15	11.54
FeO	0.95	1.20	1.13	0.98	1.06	0.97	1.02	1.30	0.76	1.12	1.53	0.86	0.68
MgO	0.10	0.11	0.17	0.05	0.16	0.16	0.10	0.23	0.20	0.12	0.16	0.11	0.09
CaO	1.22	0.95	0.98	0.83	1.14	0.96	1.02	1.18	0.83	0.83	0.92	0.65	0.78
Na_2O	3.92	3.86	3.99	3.91	4.13	4.22	4.24	4.26	3.95	3.91	3.88	3.42	3.45
K_2O	3.18	2.89	3.13	3.74	3.02	3.07	3.28	2.93	2.94	3.22	3.19	4.27	3.71
Cl	0.17	0.25	0.21	0.21	0.13	0.17	0.28	0.11	0.16	0.13	0.17	0.24	0.33
Totals	94.88	92.90	94.09	95.05	93.33	99.01	96.21	99.11	90.06	92.61	95.46	93.48	89.87
Analyses normalised to 100% loss free													
SiO_2	77.00	77.51	77.25	77.39	77.26	77.77	76.68	76.57	77.44	77.74	77.64	77.65	77.02
TiO_2	0.17	0.16	0.13	0.12	0.11	0.23	0.12	0.24	0.30	0.19	0.13	0.20	0.09
Al_2O_3	12.77	12.38	12.42	12.26	12.31	12.36	12.87	13.09	12.44	12.00	11.91	11.93	12.84
FeO	1.00	1.29	1.20	1.03	1.13	0.97	1.06	1.31	0.85	1.21	1.60	0.92	0.76
MgO	0.10	0.12	0.18	0.06	0.17	0.16	0.10	0.24	0.23	0.13	0.17	0.12	0.09
CaO	1.29	1.02	1.04	0.87	1.22	0.97	1.06	1.19	0.92	0.90	0.97	0.70	0.87
Na_2O	4.13	4.15	4.24	4.12	4.43	4.27	4.41	4.30	4.39	4.22	4.06	3.66	3.84
K_2O	3.35	3.11	3.33	3.93	3.23	3.10	3.41	2.96	3.26	3.47	3.34	4.57	4.13
Cl	0.18	0.26	0.22	0.23	0.14	0.18	0.29	0.11	0.18	0.14	0.18	0.26	0.37
Totals	100.00	100.00	100.00	100.00	100.00	100.00	100.00	100.00	100.00	100.00	100.00	100.00	100.00

Pakaututu Road:230cm

	1	2	3	4	5	6	7	8	9	10	11	12
SiO_2	71.90	70.83	73.64	72.44	73.55	72.97	72.98	73.55	73.18	72.56	72.05	72.58
TiO_2	0.13	0.10	0.30	0.13	0.23	0.09	0.11	0.18	0.16	0.13	0.10	0.20
Al_2O_3	11.57	11.59	11.80	11.65	11.74	11.93	11.75	11.76	11.88	11.61	11.63	12.03
FeO	1.30	1.24	0.98	1.00	0.95	1.31	1.04	1.14	1.12	1.22	1.00	1.19
MgO	0.17	0.19	0.12	0.11	0.18	0.17	0.16	0.12	0.13	0.16	0.18	0.16
CaO	1.08	1.03	0.99	0.91	0.97	1.14	0.94	1.10	0.97	1.04	0.91	0.84
Na_2O	3.71	3.68	3.72	3.62	3.80	3.93	3.64	3.81	3.67	3.63	3.76	3.53
K_2O	2.68	3.13	3.04	3.12	3.22	3.00	3.28	3.20	3.21	3.17	3.20	3.79
Cl	0.13	0.20	0.18	0.15	0.18	0.19	0.23	0.18	0.21	0.21	0.19	0.10
Totals	92.67	91.98	94.77	93.10	94.81	94.72	94.13	95.05	94.52	93.73	93.02	94.43
Analyses normalised to 100% loss free												
SiO_2	77.59	77.01	77.71	77.80	77.57	77.04	77.53	77.38	77.43	77.42	77.46	76.86
TiO_2	0.14	0.10	0.31	0.14	0.24	0.10	0.12	0.19	0.17	0.14	0.11	0.21
Al_2O_3	12.48	12.60	12.46	12.51	12.38	12.59	12.49	12.37	12.56	12.39	12.50	12.74
FeO	1.40	1.34	1.03	1.07	1.00	1.38	1.11	1.20	1.18	1.30	1.07	1.26
MgO	0.18	0.20	0.13	0.11	0.19	0.18	0.17	0.13	0.14	0.17	0.19	0.17
CaO	1.16	1.12	1.04	0.97	1.02	1.20	1.00	1.16	1.03	1.11	0.98	0.89
Na_2O	4.01	4.00	3.93	3.88	4.01	4.14	3.87	4.00	3.88	3.87	4.04	3.74
K_2O	2.89	3.41	3.21	3.35	3.40	3.17	3.49	3.37	3.40	3.38	3.44	4.01
Cl	0.14	0.21	0.19	0.16	0.19	0.20	0.24	0.19	0.22	0.22	0.21	0.10
Totals	100.00	100.00	100.00	100.00	100.00	100.00	100.00	100.00	100.00	100.00	100.00	100.00

Pakaututu Road: 250cm

	1	2	3	4	5	6	7	8	9	10	11	12	13	14
SiO_2	72.88	74.74	72.62	74.27	72.32	74.01	72.95	71.83	71.01	72.18	73.28	74.07	73.31	68.43
TiO_2	0.12	0.24	0.15	0.20	0.21	0.12	0.16	0.16	0.18	0.21	0.11	0.18	0.19	0.22
Al_2O_3	11.55	12.41	11.93	12.30	12.01	11.71	11.67	11.56	11.63	12.17	11.97	11.67	11.69	11.14
FeO	1.24	1.13	1.18	1.19	1.18	1.16	1.01	1.07	1.15	1.55	1.02	1.10	1.33	0.86
MgO	0.13	0.14	0.19	0.14	0.13	0.21	0.09	0.15	0.15	0.12	0.09	0.16	0.11	0.11
CaO	1.15	0.94	1.10	1.06	1.04	1.02	1.12	1.01	1.00	0.79	1.11	1.01	1.10	0.93
Na_2O	3.79	4.09	3.93	3.38	3.77	3.87	3.83	4.01	3.38	3.67	3.62	3.91	3.69	3.65
K_2O	3.22	3.12	2.84	4.05	3.15	3.33	3.13	3.12	3.64	3.62	3.22	3.27	3.21	3.10
Cl	0.19	0.18	0.25	0.14	0.24	0.21	0.14	0.19	0.20	0.23	0.17	0.18	0.19	0.29
Totals	94.27	96.98	94.19	96.74	94.06	95.66	94.09	93.09	92.32	94.54	94.59	95.55	94.81	88.73
Analyses normalised to 100% loss free														
SiO_2	77.31	77.07	77.10	76.77	76.89	77.37	77.53	77.16	76.91	76.35	77.47	77.52	77.32	77.12
TiO_2	0.12	0.25	0.16	0.21	0.22	0.12	0.17	0.17	0.19	0.22	0.12	0.19	0.20	0.24
Al_2O_3	12.25	12.79	12.67	12.71	12.77	12.24	12.40	12.41	12.59	12.87	12.65	12.21	12.33	12.55
FeO	1.32	1.16	1.25	1.23	1.26	1.22	1.07	1.15	1.25	1.64	1.08	1.16	1.40	0.97
MgO	0.14	0.14	0.20	0.15	0.14	0.22	0.09	0.16	0.16	0.13	0.09	0.16	0.12	0.13
CaO	1.22	0.97	1.17	1.10	1.11	1.07	1.19	1.08	1.08	0.84	1.17	1.06	1.16	1.05
Na_2O	4.02	4.22	4.18	3.49	4.01	4.05	4.07	4.30	3.66	3.88	3.83	4.09	3.89	4.11
K_2O	3.41	3.21	3.02	4.19	3.35	3.48	3.32	3.35	3.94	3.83	3.40	3.43	3.38	3.49
Cl	0.20	0.18	0.26	0.15	0.26	0.22	0.15	0.21	0.22	0.24	0.18	0.19	0.20	0.33
Totals	100	100	100	100	100	100	100	100	100.00	100.00	100.00	100	100	100.00

Pakaututu Road: 270cm

	1	2	3	4	5	6	7	8	9	10	11	12
SiO_2	77.256	71.825	76.711	73.713	73.836	73.077	73.600	75.968	73.286	72.658	73.391	74.842
TiO_2	0.127	0.132	0.124	0.068	0.098	0.138	0.093	0.268	0.174	0.242	0.193	0.161
Al_2O_3	11.599	11.686	11.697	11.753	11.542	11.723	11.945	11.828	11.576	12.078	11.483	11.757
FeO	1.115	1.188	1.115	1.191	1.126	1.220	1.160	1.315	0.967	1.013	1.092	1.154
MgO	0.167	0.130	0.139	0.144	0.125	0.163	0.088	0.163	0.140	0.134	0.156	0.096
CaO	1.117	1.039	0.904	1.015	1.136	0.925	0.856	1.002	0.957	0.938	1.026	0.886
Na_2O	3.813	3.886	3.813	3.842	4.155	3.881	4.114	4.230	3.794	3.707	4.061	3.834
K_2O	2.955	3.072	3.183	3.381	3.213	3.031	3.324	3.534	3.333	2.935	3.137	3.193
Cl	0.123	0.251	0.183	0.225	0.127	0.179	0.199	0.178	0.262	0.220	0.152	0.154
Totals	98.272	93.209	97.869	95.332	95.358	94.337	95.379	98.486	94.489	93.925	94.691	96.077
Analyses normalised to 100% loss free												
SiO_2	78.61	77.06	78.38	77.32	77.43	77.46	77.17	77.14	77.56	77.36	77.51	77.90
TiO_2	0.13	0.14	0.13	0.07	0.10	0.15	0.10	0.27	0.18	0.26	0.20	0.17
Al_2O_3	11.80	12.54	11.95	12.33	12.10	12.43	12.52	12.01	12.25	12.86	12.13	12.24
FeO	1.13	1.27	1.14	1.25	1.18	1.29	1.22	1.34	1.02	1.08	1.15	1.20
MgO	0.17	0.14	0.14	0.15	0.13	0.17	0.09	0.17	0.15	0.14	0.16	0.10
CaO	1.14	1.11	0.92	1.06	1.19	0.98	0.90	1.02	1.01	1.00	1.08	0.92
Na_2O	3.88	4.17	3.90	4.03	4.36	4.11	4.31	4.30	4.02	3.95	4.29	3.99
K_2O	3.01	3.30	3.25	3.55	3.37	3.21	3.49	3.59	3.53	3.12	3.31	3.32
Cl	0.13	0.27	0.19	0.24	0.13	0.19	0.21	0.18	0.28	0.23	0.16	0.16
Totals	100	100	100	100	100	100	100	100	100	100	100	100

Pakaututu Road: 280cm

	1	2	3	4	5	6	7	8	9	10	11	12	13	14	15
SiO_2	72.06	71.76	72.84	71.75	73.16	73.11	73.56	74.21	72.96	71.88	70.89	73.12	71.53	72.38	72.87
TiO_2	0.11	0.11	0.20	0.11	0.15	0.23	0.08	0.18	0.18	0.16	0.33	0.21	0.21	0.12	0.17
Al_2O_3	11.42	11.90	11.77	11.66	11.95	11.97	11.97	11.78	11.61	11.84	11.69	11.84	11.51	11.80	11.94
FeO	0.96	0.97	1.11	1.49	3.34	1.10	1.67	1.12	1.14	0.96	0.81	1.09	1.02	1.13	1.18
MgO	0.11	0.13	0.16	0.13	0.11	0.15	0.14	0.18	0.17	0.16	0.19	0.09	0.14	0.17	0.17
CaO	0.97	1.05	0.91	0.99	0.92	0.89	0.95	0.94	0.89	0.90	0.93	1.03	1.14	0.93	1.13
Na_2O	3.66	3.88	3.69	2.84	4.68	2.73	2.50	3.81	3.69	3.69	3.94	3.68	3.92	3.69	3.90
K_2O	3.45	3.03	3.07	3.29	4.04	2.98	3.14	3.14	3.41	3.17	2.74	3.18	3.18	3.31	3.18
Cl	0.16	0.17	0.24	0.22	0.12	0.22	0.14	0.22	0.23	0.29	0.20	0.20	0.26	0.29	0.18
Totals	92.89	92.98	93.98	92.49	98.46	93.38	94.16	95.58	94.28	93.05	91.72	94.44	92.90	93.82	94.72
Analyses normalised to 100% loss free															
SiO_2	77.58	77.17	77.50	77.58	74.30	78.29	78.13	77.64	77.39	77.25	77.29	77.42	77.00	77.15	76.93
TiO_2	0.12	0.11	0.21	0.12	0.15	0.25	0.09	0.19	0.20	0.17	0.36	0.22	0.22	0.13	0.18
Al_2O_3	12.30	12.80	12.52	12.61	12.14	12.82	12.71	12.32	12.31	12.73	12.75	12.54	12.39	12.57	12.61
FeO	1.03	1.04	1.18	1.62	3.40	1.18	1.77	1.17	1.21	1.03	0.89	1.16	1.10	1.21	1.24
MgO	0.12	0.14	0.17	0.14	0.12	0.16	0.15	0.18	0.18	0.18	0.20	0.09	0.15	0.19	0.18
CaO	1.04	1.13	0.97	1.07	0.94	0.96	1.01	0.99	0.95	0.97	1.01	1.09	1.22	0.99	1.19
Na_2O	3.93	4.17	3.92	3.07	4.75	2.92	2.66	3.99	3.92	3.96	4.29	3.89	4.22	3.93	4.11
K_2O	3.71	3.26	3.27	3.56	4.10	3.19	3.33	3.29	3.61	3.41	2.99	3.37	3.42	3.52	3.36
Cl	0.17	0.18	0.26	0.23	0.12	0.23	0.15	0.23	0.24	0.31	0.22	0.22	0.28	0.31	0.19
Totals	100.00	100.00	100.00	100.00	100.00	100.00	100.00	100.00	100.00	100.00	100.00	100.00	100.00	100.00	100.00

Pakaututu Road: 290cm

	1	2	3	4	5	6	7	8	9	10	11	12	13	14	15	16	17
SiO_2	74.20	74.29	76.29	75.50	72.13	74.91	76.18	74.44	75.71	75.66	73.71	73.19	73.82	73.42	74.97	71.93	75.43
TiO_2	0.12	0.14	0.17	0.18	0.17	0.11	0.11	0.16	0.15	0.10	0.21	0.16	0.09	0.18	0.14	0.10	0.17
Al_2O_3	11.86	11.95	12.24	12.03	11.64	12.25	12.26	12.01	12.02	12.23	12.11	11.94	12.06	12.37	12.41	11.64	12.42
FeO	1.10	1.17	1.03	1.11	1.00	1.34	1.24	1.08	1.10	1.29	1.33	1.08	1.03	1.23	1.04	1.06	1.35
MgO	0.17	0.18	0.13	0.24	0.16	0.42	0.09	0.12	0.20	0.20	0.16	0.15	0.10	0.14	0.17	0.19	0.17
CaO	1.06	1.02	1.06	1.02	0.90	1.06	1.07	1.10	0.97	0.95	1.18	0.94	1.03	1.00	1.06	1.01	1.04
Na_2O	3.88	3.98	4.12	3.73	3.96	3.86	3.92	3.96	3.88	4.19	3.86	4.12	3.97	3.88	4.01	3.91	4.10
K_2O	3.17	3.19	3.10	3.60	3.12	3.40	3.28	3.18	3.31	3.24	3.08	3.24	3.29	3.21	3.03	3.12	3.05
Cl	0.24	0.17	0.23	0.21	0.29	0.17	0.18	0.19	0.19	0.21	0.22	0.18	0.19	0.24	0.20	0.28	0.19
Totals	95.80	96.09	98.37	97.62	93.36	97.49	98.32	96.25	97.53	98.06	95.85	94.98	95.59	95.67	97.04	93.24	97.92
Analyses normalised to 100% loss free																	
SiO_2	77.45	77.30	77.56	77.35	77.26	76.83	77.48	77.34	77.63	77.15	76.90	77.06	77.23	76.74	77.26	77.14	77.03
TiO_2	0.13	0.15	0.17	0.18	0.18	0.11	0.11	0.17	0.16	0.10	0.22	0.17	0.10	0.19	0.14	0.11	0.17
Al_2O_3	12.38	12.44	12.44	12.33	12.47	12.56	12.46	12.47	12.33	12.47	12.63	12.57	12.62	12.93	12.79	12.49	12.69
FeO	1.15	1.21	1.05	1.13	1.07	1.37	1.26	1.12	1.13	1.31	1.38	1.13	1.08	1.28	1.07	1.13	1.38
MgO	0.17	0.19	0.13	0.24	0.17	0.43	0.09	0.13	0.20	0.20	0.17	0.16	0.10	0.15	0.18	0.20	0.17
CaO	1.11	1.07	1.07	1.05	0.96	1.08	1.09	1.14	1.00	0.97	1.24	0.99	1.08	1.05	1.09	1.09	1.06
Na_2O	4.05	4.14	4.19	3.82	4.24	3.96	3.99	4.12	3.98	4.27	4.02	4.33	4.15	4.06	4.13	4.19	4.19
K_2O	3.31	3.32	3.15	3.69	3.34	3.49	3.34	3.31	3.39	3.31	3.21	3.41	3.45	3.36	3.12	3.35	3.12
Cl	0.25	0.18	0.24	0.21	0.31	0.17	0.18	0.20	0.19	0.21	0.23	0.19	0.20	0.25	0.21	0.30	0.19
Totals	100.00	100.00	100.00	100.00	100.00	100.00	100.00	100.00	100.00	100.00	100.00	100.00	100.00	100.00	100.00	100.00	100.00

Pakaututu Road: 320cm (10um)

	1	2	3	4	5	6	7	8	9	10	11	12	13	14
SiO_2	74.46	76.07	74.72	75.80	74.08	74.21	73.37	73.56	73.15	72.00	77.66	74.03	75.99	74.80
TiO_2	0.11	0.08	0.11	0.15	0.10	0.13	0.17	0.10	0.13	0.12	0.07	0.16	0.04	0.10
Al_2O_3	11.55	11.87	11.60	11.76	11.59	11.58	12.09	11.82	11.45	11.36	12.09	11.86	11.65	11.52
FeO	0.99	1.03	1.27	1.23	1.24	1.17	1.02	0.92	1.22	0.77	1.12	0.96	1.11	1.35
MgO	0.07	0.10	0.15	0.06	0.12	0.19	0.18	0.18	0.13	0.08	0.06	0.13	0.13	0.09
CaO	1.03	1.25	1.19	0.99	1.01	1.11	1.11	1.12	1.10	0.60	0.93	1.00	1.20	1.10
Na_2O	3.77	4.16	4.11	4.18	3.74	3.83	4.35	4.18	3.90	3.55	4.25	3.83	3.93	3.94
K_2O	2.93	2.78	2.61	2.84	2.90	2.97	3.16	2.73	2.77	3.92	3.09	2.74	2.78	3.00
Cl	0.13	0.19	0.13	0.12	0.11	0.21	0.21	0.18	0.19	0.17	0.15	0.15	0.13	0.18
Totals	95.04	97.51	95.89	97.12	94.89	95.40	95.65	94.80	94.03	92.57	99.41	94.85	96.95	96.09
Analyses normalised to 100% loss free														
SiO_2	78.34	78.01	77.93	78.04	78.08	77.79	76.70	77.60	77.80	77.78	78.12	78.05	78.38	77.84
TiO_2	0.12	0.08	0.11	0.15	0.10	0.14	0.17	0.11	0.14	0.13	0.07	0.17	0.05	0.11
Al_2O_3	12.15	12.17	12.09	12.11	12.21	12.14	12.64	12.47	12.18	12.27	12.16	12.50	12.01	11.99
FeO	1.04	1.05	1.32	1.27	1.30	1.22	1.06	0.97	1.29	0.83	1.13	1.01	1.14	1.41
MgO	0.07	0.10	0.16	0.06	0.12	0.20	0.19	0.19	0.13	0.08	0.06	0.13	0.13	0.09
CaO	1.09	1.28	1.25	1.01	1.07	1.17	1.16	1.18	1.17	0.65	0.94	1.05	1.23	1.15
Na_2O	3.97	4.26	4.28	4.30	3.94	4.02	4.55	4.41	4.15	3.84	4.27	4.04	4.05	4.10
K_2O	3.09	2.85	2.72	2.93	3.06	3.11	3.31	2.88	2.95	4.23	3.10	2.89	2.87	3.13
Cl	0.13	0.19	0.13	0.12	0.12	0.21	0.22	0.19	0.20	0.18	0.15	0.16	0.14	0.18
Totals	100.00	100.00	100.00	100.00	100.00	100.00	100.00	100.00	100.00	100.00	100.00	100.00	100.00	100.00

	15	16	17	18	18	20	21	22	23	24	25	26	27
SiO_2	74.60	75.15	76.89	74.02	74.81	76.89	75.92	75.33	75.07	76.60	75.83	75.44	73.72
TiO_2	0.05	0.14	0.05	0.13	0.09	0.04	0.11	0.03	0.14	0.16	0.08	0.07	0.15
Al_2O_3	11.41	11.42	11.65	11.73	11.65	11.92	11.38	11.49	11.41	11.38	11.65	11.50	11.39
FeO	0.94	1.06	1.03	1.18	1.11	1.21	0.98	0.98	0.99	1.11	1.09	1.15	1.83
MgO	0.08	0.19	0.10	0.10	0.16	0.11	0.09	0.09	0.01	0.09	0.12	0.10	0.24
CaO	1.19	0.99	0.96	1.17	0.93	1.03	1.10	1.02	1.13	0.96	1.04	1.00	1.19
Na_2O	4.04	3.94	4.13	4.01	3.66	3.67	3.91	3.74	3.43	3.73	4.03	3.82	3.32
K_2O	2.71	3.01	3.26	2.59	3.10	3.40	3.17	3.01	2.87	3.13	2.98	3.05	3.18
Cl	0.17	0.23	0.19	0.21	0.13	0.17	0.17	0.15	0.08	0.19	0.18	0.13	0.10
Totals	95.18	96.12	98.26	95.12	95.63	98.44	96.85	95.86	95.13	97.35	97.01	96.26	95.12
Analyses normalised to 100% loss free													
SiO_2	78.38	78.19	78.26	77.81	78.23	78.11	78.40	78.59	78.91	78.69	78.17	78.37	77.50
TiO_2	0.05	0.15	0.05	0.13	0.10	0.04	0.11	0.03	0.15	0.17	0.08	0.07	0.15
Al_2O_3	11.99	11.88	11.85	12.33	12.18	12.11	11.75	11.99	12.00	11.69	12.01	11.95	11.98
FeO	0.99	1.10	1.05	1.24	1.16	1.23	1.01	1.03	1.04	1.14	1.12	1.19	1.93
MgO	0.08	0.19	0.10	0.10	0.17	0.11	0.09	0.09	0.01	0.09	0.13	0.10	0.25
CaO	1.25	1.03	0.98	1.23	0.97	1.05	1.13	1.07	1.18	0.98	1.08	1.04	1.25
Na_2O	4.24	4.10	4.21	4.21	3.82	3.73	4.04	3.90	3.61	3.83	4.15	3.96	3.49
K_2O	2.85	3.13	3.32	2.72	3.24	3.45	3.28	3.14	3.01	3.21	3.08	3.17	3.34
Cl	0.18	0.24	0.19	0.22	0.14	0.17	0.18	0.16	0.09	0.19	0.19	0.14	0.11
Totals	100.00	100.00	100.00	100.00	100.00	100.00	100.00	100.00	100.00	100.00	100.00	100.00	100.00

Pakaututu Road: 320cm(20um)

	1	2	3	4	5	6	7	8	9	10	11	12
SiO_2	71.13	73.67	71.62	71.88	70.20	70.57	72.90	71.79	71.85	71.68	74.53	71.54
TiO_2	0.28	0.23	0.18	0.20	0.14	0.22	0.23	0.16	0.12	0.13	0.11	0.18
Al_2O_3	11.65	11.57	11.67	11.38	11.54	11.36	11.90	11.75	11.54	11.53	11.75	11.43
FeO	1.05	1.14	1.21	1.03	1.18	1.23	1.24	1.15	1.03	1.02	1.16	1.00
MgO	0.14	0.14	0.12	0.11	0.11	0.14	0.14	0.14	0.14	0.08	0.15	0.07
CaO	1.06	1.01	1.02	0.95	0.98	1.15	0.96	1.13	1.07	0.85	1.12	0.94
Na_2O	3.64	3.62	3.93	3.64	3.47	3.67	4.01	3.81	3.72	3.74	4.15	3.79
K_2O	2.69	3.41	2.76	2.81	2.89	2.63	3.11	2.91	2.86	2.82	2.72	2.83
Cl	0.19	0.18	0.20	0.19	0.17	0.23	0.15	0.18	0.16	0.16	0.15	0.98
Totals	91.82	94.98	92.71	92.18	90.68	91.19	94.63	93.02	92.49	92.00	95.84	92.76
Analyses normalised to 100% loss free												
SiO_2	77.46	77.57	77.25	77.97	77.41	77.39	77.04	77.18	77.69	77.91	77.76	77.13
TiO_2	0.30	0.25	0.20	0.22	0.16	0.24	0.24	0.17	0.13	0.14	0.11	0.20
Al_2O_3	12.69	12.18	12.59	12.35	12.72	12.45	12.58	12.64	12.48	12.53	12.26	12.32
FeO	1.14	1.20	1.31	1.12	1.31	1.35	1.31	1.24	1.11	1.11	1.21	1.08
MgO	0.16	0.15	0.13	0.12	0.12	0.15	0.15	0.15	0.15	0.08	0.16	0.08
CaO	1.16	1.06	1.10	1.03	1.08	1.26	1.02	1.22	1.16	0.92	1.17	1.01
Na_2O	3.97	3.81	4.24	3.94	3.82	4.03	4.24	4.09	4.02	4.06	4.33	4.09
K_2O	2.93	3.59	2.98	3.05	3.19	2.88	3.28	3.13	3.09	3.06	2.84	3.05
Cl	0.20	0.19	0.21	0.20	0.19	0.25	0.15	0.19	0.17	0.18	0.16	1.06
Totals	100.00	100.00	100.00	100.00	100.00	100.00	100.00	100.00	100.00	100.00	100.00	100.00

Pakaututu Road: 390cm

	1	2	3	4	5	6	7	8	9	10	11	12	13	14	15	16
SiO_2	71.45	72.28	69.45	72.64	72.52	72.03	72.46	72.40	69.68	72.13	72.52	75.08	71.29	70.22	73.11	66.37
TiO_2	0.20	0.11	0.21	0.11	0.06	0.19	0.06	0.22	0.40	0.15	0.11	0.14	0.09	0.18	0.12	0.23
Al_2O_3	12.19	11.54	11.74	11.62	11.79	11.38	11.56	11.82	11.56	11.80	11.74	11.96	11.59	12.54	11.94	11.67
FeO	1.09	0.99	1.27	1.15	0.85	1.23	0.99	1.72	1.11	1.17	1.07	0.99	0.87	1.42	1.09	2.12
MgO	0.21	0.15	0.16	0.21	0.05	0.13	0.07	0.18	0.18	0.24	0.07	0.19	0.15	0.23	0.13	0.11
CaO	0.81	1.26	1.08	1.09	0.62	0.90	0.74	0.71	1.05	1.04	0.71	1.06	0.94	1.62	0.79	1.40
Na_2O	3.50	3.50	3.15	3.67	3.58	3.67	3.33	3.04	3.34	3.37	3.55	3.51	3.47	3.77	3.75	3.31
K_2O	3.58	3.27	3.45	2.72	3.87	3.18	4.04	4.55	3.51	3.73	3.94	3.80	3.67	3.35	3.22	3.36
Cl	0.20	0.17	0.22	0.18	0.12	0.25	0.21	0.19	0.20	0.20	0.18	0.13	0.21	0.17	0.19	0.27
Totals	93.22	93.27	90.72	93.39	93.46	92.94	93.46	94.85	91.03	93.83	93.88	96.86	92.28	93.51	94.35	88.85
Analyses normalised to 100% loss free																
SiO_2	76.65	77.49	76.55	77.79	77.60	77.50	77.53	76.34	76.54	76.87	77.25	77.51	77.25	75.10	77.49	74.70
TiO_2	0.21	0.12	0.23	0.11	0.07	0.20	0.07	0.23	0.44	0.16	0.11	0.14	0.10	0.19	0.13	0.26
Al_2O_3	13.08	12.37	12.94	12.44	12.62	12.25	12.37	12.47	12.70	12.58	12.51	12.35	12.56	13.42	12.65	13.14
FeO	1.16	1.07	1.40	1.23	0.91	1.32	1.06	1.82	1.21	1.25	1.14	1.02	0.94	1.52	1.16	2.39
MgO	0.22	0.16	0.17	0.23	0.05	0.14	0.07	0.19	0.20	0.25	0.07	0.20	0.16	0.24	0.14	0.12
CaO	0.86	1.35	1.19	1.17	0.66	0.97	0.79	0.75	1.16	1.10	0.76	1.09	1.02	1.73	0.84	1.58
Na_2O	3.75	3.75	3.48	3.93	3.83	3.95	3.56	3.21	3.66	3.59	3.78	3.63	3.76	4.03	3.97	3.72
K_2O	3.84	3.50	3.80	2.91	4.14	3.42	4.32	4.80	3.86	3.98	4.19	3.92	3.98	3.59	3.42	3.79
Cl	0.21	0.18	0.24	0.19	0.13	0.26	0.23	0.20	0.22	0.22	0.19	0.14	0.22	0.18	0.21	0.30
Totals	100.00	100.00	100.00	100.00	100.00	100.00	100.00	100.00	100.00	100.00	100.00	100.00	100.00	100.00	100.00	100.00

Pakututu Road: 410cm

	1	2	3	4	5	6	7	8	9	10	11	12	13
SiO_2	70.76	68.46	69.44	72.77	74.00	71.43	72.55	70.15	72.77	73.08	70.88	72.99	72.95
TiO_2	0.10	0.16	0.76	0.09	0.20	0.06	0.16	0.13	0.17	0.12	0.07	0.11	0.16
Al_2O_3	11.69	12.00	12.69	11.59	11.62	11.62	11.87	11.53	11.94	12.00	13.51	11.54	11.84
FeO	0.94	1.54	3.27	0.97	0.93	0.92	1.09	3.66	0.99	1.21	0.36	0.89	0.92
MgO	0.19	0.20	0.56	0.15	0.12	0.14	0.12	0.17	0.17	0.15	0.05	0.14	0.12
CaO	0.95	1.18	2.03	1.02	0.77	1.05	1.01	0.89	0.95	1.10	0.52	0.93	0.72
Na_2O	3.30	3.74	3.14	3.52	3.99	3.45	3.36	3.99	3.56	4.11	4.41	3.35	3.24
K_2O	3.73	3.12	4.41	3.74	3.19	4.15	3.96	3.33	3.80	2.92	5.08	3.77	3.81
Cl	0.13	0.26	0.21	0.14	0.18	0.15	0.16	0.19	0.19	0.24	0.06	0.17	0.17
Totals	91.79	90.66	96.50	93.98	95.00	92.96	94.28	94.02	94.53	94.94	94.93	93.90	93.93
Analyses normalised to 100% loss free													
SiO_2	77.10	75.51	71.96	77.43	77.90	76.84	76.96	74.61	76.98	76.98	74.66	77.73	77.66
TiO_2	0.11	0.18	0.79	0.10	0.21	0.06	0.17	0.14	0.18	0.13	0.07	0.12	0.17
Al_2O_3	12.74	13.23	13.15	12.33	12.23	12.50	12.59	12.26	12.63	12.64	14.23	12.29	12.60
FeO	1.02	1.70	3.38	1.03	0.98	0.99	1.16	3.90	1.04	1.28	0.37	0.95	0.98
MgO	0.21	0.22	0.58	0.16	0.13	0.15	0.12	0.18	0.18	0.15	0.05	0.15	0.13
CaO	1.04	1.30	2.11	1.09	0.81	1.13	1.07	0.94	1.00	1.16	0.55	0.99	0.76
Na_2O	3.60	4.12	3.26	3.75	4.20	3.71	3.56	4.24	3.76	4.33	4.64	3.57	3.45
K_2O	4.06	3.44	4.57	3.98	3.36	4.46	4.20	3.54	4.02	3.08	5.35	4.01	4.06
Cl	0.14	0.29	0.22	0.14	0.19	0.17	0.17	0.20	0.20	0.25	0.06	0.18	0.18
Totals	100.00	100.00	100.00	100.00	100.00	100.00	100.00	100.00	100.00	100.00	100.00	100.00	100.00

	14	15	16	17	18	19	20	21	22
SiO_2	71.60	70.72	73.67	73.49	69.51	72.62	71.18	71.90	67.95
TiO_2	0.17	0.19	0.14	0.23	0.72	0.48	0.13	0.20	0.11
Al_2O_3	11.65	11.60	11.92	12.51	12.46	11.89	11.45	11.56	11.24
FeO	0.64	1.02	1.07	1.00	2.90	1.09	1.16	1.10	1.00
MgO	0.22	0.15	0.12	0.16	0.45	0.17	0.06	0.16	0.14
CaO	0.83	1.01	0.99	1.08	1.72	0.88	0.77	1.05	0.91
Na_2O	3.19	3.33	3.47	2.97	3.37	3.62	3.47	3.44	3.14
K_2O	4.01	3.69	3.86	2.71	4.70	4.06	4.09	3.90	3.51
Cl	0.14	0.16	0.13	0.25	0.18	0.19	0.19	0.23	0.38
Totals	92.46	91.86	95.37	94.39	96.00	94.99	92.49	93.53	88.38
Analyses normalised to 100% loss free									
SiO_2	77.44	76.99	77.25	77.85	72.41	76.45	76.96	76.87	76.89
TiO_2	0.18	0.21	0.14	0.25	0.75	0.51	0.14	0.21	0.13
Al_2O_3	12.60	12.63	12.50	13.25	12.98	12.52	12.38	12.36	12.71
FeO	0.69	1.11	1.12	1.06	3.02	1.15	1.25	1.18	1.14
MgO	0.24	0.16	0.13	0.17	0.47	0.17	0.06	0.17	0.16
CaO	0.90	1.10	1.04	1.15	1.79	0.93	0.83	1.12	1.03
Na_2O	3.45	3.62	3.64	3.14	3.51	3.82	3.75	3.68	3.56
K_2O	4.34	4.01	4.05	2.87	4.89	4.27	4.42	4.17	3.97
Cl	0.15	0.17	0.14	0.27	0.18	0.20	0.21	0.25	0.42
Totals	100.00	100.00	100.00	100.00	100.00	100.00	100.00	100.00	100.00

Pakaututu Road: 450cm

	1	2	3	4	5	6	7	8	9	10	11	12
SiO_2	74.69	74.49	74.69	73.22	73.70	73.90	73.35	74.51	75.69	75.11	75.13	73.34
TiO_2	0.15	0.16	0.12	0.16	0.12	0.17	0.22	0.16	0.14	0.20	0.19	0.16
Al_2O_3	11.90	12.09	12.13	12.11	11.98	11.94	11.71	12.11	12.20	12.08	12.16	11.85
FeO	1.05	1.21	1.13	0.98	1.08	1.07	1.08	1.04	1.21	1.22	0.87	1.01
MgO	0.10	0.16	0.14	0.18	0.16	0.10	0.16	0.16	0.11	0.18	0.16	0.11
CaO	0.90	0.91	0.93	1.01	0.94	0.98	0.88	0.97	1.10	0.93	1.12	0.91
Na_2O	3.68	3.53	3.39	3.72	3.69	3.44	3.31	3.63	3.65	3.76	3.57	3.85
K_2O	3.93	3.95	3.78	3.79	3.80	3.76	3.92	3.93	4.00	4.04	4.28	3.65
Cl	0.12	0.10	0.12	0.16	0.13	0.16	0.21	0.10	0.20	0.18	0.12	0.15
Totals	96.51	96.60	96.42	95.31	95.59	95.51	94.83	96.61	98.31	97.70	97.60	95.03
Analyses normalised to 100% loss free												
SiO_2	77.39	77.11	77.46	76.82	77.10	77.38	77.35	77.13	76.99	76.88	76.98	77.18
TiO_2	0.15	0.17	0.13	0.17	0.13	0.17	0.23	0.16	0.15	0.21	0.19	0.17
Al_2O_3	12.33	12.51	12.58	12.71	12.53	12.50	12.35	12.54	12.41	12.37	12.46	12.47
FeO	1.09	1.25	1.17	1.03	1.13	1.12	1.14	1.07	1.23	1.25	0.90	1.06
MgO	0.10	0.16	0.15	0.18	0.16	0.10	0.17	0.16	0.11	0.18	0.16	0.12
CaO	0.93	0.95	0.96	1.06	0.98	1.03	0.92	1.00	1.12	0.95	1.15	0.95
Na_2O	3.81	3.66	3.52	3.90	3.86	3.60	3.49	3.76	3.72	3.85	3.66	4.05
K_2O	4.08	4.09	3.92	3.97	3.97	3.93	4.13	4.07	4.07	4.14	4.39	3.84
Cl	0.12	0.10	0.12	0.16	0.14	0.17	0.22	0.11	0.21	0.18	0.12	0.16
Totals	100.00	100.00	100.00	100.00	100.00	100.00	100.00	100.00	100.00	100.00	100.00	100.00

Pakaututu Road: 470cm

	1	2	3	4	5	6	7	8	9	10	11	12	13	14
SiO_2	72.15	73.85	70.72	73.93	71.33	72.19	72.18	71.45	72.89	72.95	73.87	72.45	72.73	72.72
TiO_2	0.17	0.20	0.08	0.17	0.19	0.16	0.20	0.19	0.21	0.16	0.13	0.12	0.14	0.15
Al_2O_3	11.53	11.48	11.56	12.02	11.77	11.90	11.74	11.88	11.95	11.76	12.02	11.95	11.94	12.17
FeO	1.20	0.87	1.13	1.12	0.95	1.02	0.76	1.11	1.11	1.26	1.11	1.14	1.02	1.02
MgO	0.20	0.14	0.11	0.12	0.23	0.14	0.10	0.17	0.16	0.14	0.17	0.17	0.17	0.16
CaO	1.00	0.75	0.83	0.94	0.98	1.09	1.06	1.04	0.86	1.01	0.96	0.96	1.01	0.92
Na_2O	3.25	3.44	3.52	3.47	3.32	3.42	3.46	3.36	3.66	3.58	3.25	3.18	3.52	3.46
K_2O	3.74	3.79	3.35	3.81	3.88	3.62	3.84	3.61	3.85	3.47	3.98	3.96	3.87	3.82
Cl	0.18	0.20	0.20	0.19	0.36	0.13	0.22	0.17	0.18	0.15	0.15	0.21	0.08	0.19
Totals	93.42	94.72	91.49	95.76	93.00	93.66	93.57	92.97	94.87	94.48	95.63	94.13	94.48	94.61
Analyses normalised to 100% loss free														
SiO_2	77.24	77.97	77.30	77.20	76.69	77.08	77.15	76.85	76.83	77.22	77.25	76.97	76.99	76.86
TiO_2	0.18	0.21	0.09	0.18	0.20	0.17	0.21	0.20	0.22	0.17	0.13	0.13	0.15	0.16
Al_2O_3	12.35	12.12	12.63	12.55	12.65	12.70	12.55	12.77	12.60	12.45	12.56	12.69	12.63	12.86
FeO	1.29	0.92	1.24	1.17	1.02	1.08	0.82	1.20	1.17	1.33	1.16	1.21	1.08	1.08
MgO	0.21	0.14	0.12	0.13	0.25	0.15	0.11	0.18	0.17	0.15	0.18	0.18	0.18	0.17
CaO	1.07	0.79	0.90	0.98	1.05	1.16	1.14	1.12	0.90	1.07	1.00	1.01	1.07	0.98
Na_2O	3.47	3.63	3.85	3.62	3.57	3.65	3.70	3.62	3.85	3.79	3.40	3.37	3.72	3.65
K_2O	4.00	4.00	3.66	3.98	4.18	3.87	4.10	3.88	4.06	3.67	4.16	4.21	4.09	4.03
Cl	0.19	0.21	0.22	0.20	0.39	0.14	0.23	0.18	0.19	0.16	0.15	0.22	0.08	0.21
Totals	100.00	100.00	100.00	100.00	100.00	100.00	100.00	100.00	100.00	100.00	100.00	100.00	100.00	100.00

Pakaututu Road: 520cm

	1	2	3	4	5	6	7	8	9	10	11	12
SiO_2	71.61	72.54	70.89	69.75	71.72	73.79	72.62	71.23	71.94	72.91	71.82	70.17
TiO_2	0.09	0.08	0.13	0.22	0.13	0.16	0.10	0.10	0.09	0.27	0.12	0.11
Al_2O_3	10.94	10.86	11.16	10.62	11.04	11.13	10.85	10.78	11.20	11.11	11.09	10.77
FeO	0.78	1.17	0.64	0.98	1.04	0.89	0.80	0.85	0.83	0.70	1.03	0.89
MgO	0.09	0.11	0.10	0.15	0.05	0.10	0.08	0.14	0.10	0.11	0.04	0.08
CaO	0.76	0.77	0.71	0.67	0.80	0.74	0.72	0.81	0.78	0.69	0.70	0.65
Na_2O	3.54	3.35	3.78	2.94	3.25	3.68	3.40	3.64	3.74	3.82	3.56	3.56
K_2O	2.84	3.11	2.46	3.54	3.09	2.75	2.77	3.03	3.03	2.62	3.21	3.05
Cl	0.25	0.18	0.20	0.31	0.22	0.21	0.21	0.31	0.21	0.20	0.26	0.28
Totals	90.88	92.18	90.05	89.16	91.34	93.45	91.54	90.88	91.91	92.44	91.82	89.55
Analyses normalised to 100% loss free												
SiO_2	78.79	78.70	78.72	78.22	78.52	78.96	79.33	78.37	78.27	78.88	78.22	78.35
TiO_2	0.10	0.09	0.14	0.24	0.14	0.17	0.11	0.11	0.10	0.29	0.13	0.12
Al_2O_3	12.03	11.78	12.39	11.91	12.08	11.91	11.85	11.86	12.18	12.02	12.07	12.03
FeO	0.86	1.27	0.71	1.10	1.14	0.95	0.88	0.93	0.91	0.76	1.12	1.00
MgO	0.10	0.12	0.11	0.17	0.06	0.10	0.09	0.15	0.11	0.12	0.05	0.09
CaO	0.83	0.84	0.79	0.75	0.88	0.79	0.78	0.89	0.85	0.74	0.76	0.72
Na_2O	3.90	3.63	4.19	3.30	3.56	3.93	3.72	4.01	4.07	4.14	3.88	3.97
K_2O	3.12	3.37	2.73	3.97	3.38	2.94	3.02	3.33	3.29	2.83	3.50	3.40
Cl	0.27	0.20	0.22	0.35	0.24	0.23	0.23	0.34	0.23	0.22	0.28	0.31
Totals	100.00	100.00	100.00	100.00	100.00	100.00	100.00	100.00	100.00	100.00	100.00	100.00

Pakaututu Road:550cm

	1	2	3	4	5
SiO_2	70.28	72.77	72.61	71.59	69.94
TiO_2	0.16	0.13	0.14	0.09	0.16
Al_2O_3	11.28	11.71	11.65	11.61	11.23
FeO	0.78	0.80	1.16	1.11	1.05
MgO	0.14	0.15	0.09	0.08	0.13
CaO	0.75	0.91	0.81	0.78	0.82
Na_2O	3.87	4.00	3.60	3.37	3.73
K_2O	2.86	3.00	3.97	3.90	2.74
Cl	0.20	0.22	0.20	0.14	0.27
Totals	90.30	93.67	94.22	92.67	90.06
Analyses normalised to 100% loss free					
SiO_2	77.82	77.69	77.06	77.25	77.66
TiO_2	0.17	0.14	0.15	0.10	0.18
Al_2O_3	12.49	12.50	12.36	12.53	12.47
FeO	0.86	0.85	1.23	1.19	1.16
MgO	0.15	0.16	0.09	0.09	0.14
CaO	0.83	0.97	0.86	0.84	0.90
Na_2O	4.28	4.26	3.82	3.64	4.14
K_2O	3.17	3.20	4.21	4.21	3.04
Cl	0.22	0.23	0.22	0.15	0.30
Totals	100.00	100.00	100.00	100.00	100.00

Pakututu Road: 570cm (10um)

	1	2	3	4	5	6	7	8	9	10	11	12	13	14
SiO_2	75.34	74.77	74.59	74.87	71.65	76.91	76.58	76.17	74.47	74.60	75.03	74.78	75.74	75.63
TiO_2	0.18	0.13	0.14	0.12	0.11	0.12	0.15	0.11	0.14	0.08	0.11	0.14	0.14	0.17
Al_2O_3	11.81	11.87	11.66	12.04	11.81	11.70	11.99	11.75	12.28	11.74	12.25	11.72	11.45	11.85
FeO	0.79	0.92	0.66	0.82	0.73	0.77	0.89	0.77	1.03	0.85	1.21	0.95	0.85	0.76
MgO	0.29	0.19	0.15	0.07	0.15	0.11	0.13	0.09	0.12	0.07	0.13	0.14	0.15	0.06
CaO	0.92	0.78	0.83	0.69	0.74	0.78	0.75	0.92	0.84	0.87	1.05	0.84	0.67	0.72
Na_2O	3.72	3.80	3.74	3.91	3.84	4.09	3.94	4.13	3.98	4.03	3.51	3.83	4.26	3.79
K_2O	3.40	3.19	3.05	3.78	2.92	2.85	3.10	2.73	3.13	2.68	3.84	2.81	2.68	2.99
Cl	0.21	0.15	0.23	0.15	0.19	0.21	0.20	0.21	0.15	0.19	0.15	0.20	0.26	0.13
Totals	96.66	95.80	95.05	96.45	92.13	97.53	97.72	96.86	96.14	95.10	97.27	95.40	96.19	96.10
Analyses normalised to 100% loss free														
SiO_2	77.95	78.05	78.48	77.63	77.77	78.86	78.36	78.63	77.45	78.45	77.13	78.38	78.74	78.70
TiO_2	0.19	0.13	0.15	0.12	0.12	0.12	0.15	0.11	0.14	0.08	0.11	0.14	0.15	0.18
Al_2O_3	12.22	12.39	12.27	12.48	12.81	11.99	12.27	12.13	12.77	12.35	12.59	12.28	11.90	12.33
FeO	0.82	0.96	0.69	0.85	0.79	0.79	0.91	0.80	1.07	0.89	1.25	1.00	0.89	0.79
MgO	0.30	0.20	0.16	0.07	0.16	0.11	0.13	0.09	0.13	0.07	0.13	0.15	0.15	0.06
CaO	0.95	0.82	0.88	0.72	0.80	0.80	0.77	0.95	0.88	0.91	1.08	0.88	0.69	0.75
Na_2O	3.85	3.97	3.94	4.06	4.17	4.20	4.04	4.26	4.14	4.24	3.61	4.01	4.42	3.95
K_2O	3.51	3.33	3.21	3.92	3.17	2.92	3.17	2.82	3.26	2.82	3.95	2.95	2.78	3.11
Cl	0.22	0.16	0.24	0.15	0.20	0.21	0.20	0.21	0.16	0.19	0.15	0.21	0.27	0.14
Totals	100.00	100.00	100.00	100.00	100.00	100.00	100.00	100.00	100.00	100.00	100.00	100.00	100.00	100.00

	15	16	17	18	19	20	21	22	23	24
SiO_2	76.25	76.24	72.94	74.88	74.28	76.40	72.54	69.17	73.60	74.26
TiO_2	0.16	0.12	0.09	0.11	0.12	0.00	0.04	0.09	0.10	0.18
Al_2O_3	11.43	11.14	12.06	11.64	11.66	11.83	11.69	11.78	11.92	11.89
FeO	0.84	0.86	0.74	0.67	0.90	0.88	0.84	0.99	1.23	0.54
MgO	0.15	0.13	0.11	0.10	0.12	0.00	0.04	0.15	0.12	0.14
CaO	0.75	0.67	0.89	0.65	0.68	0.91	0.81	0.89	0.93	0.87
Na_2O	4.23	3.98	3.82	3.82	3.90	3.99	4.01	4.17	3.82	3.90
K_2O	2.79	2.69	3.42	2.63	3.06	2.93	2.91	2.76	3.58	2.92
Cl	0.21	0.12	0.13	0.17	0.14	0.00	0.17	0.20	0.25	0.19
Totals	96.80	95.93	94.20	94.66	94.86	96.94	93.04	90.19	95.55	94.89
Analyses normalised to 100% loss free										
SiO_2	78.78	79.47	77.43	79.10	78.31	78.81	77.97	76.70	77.03	78.26
TiO_2	0.16	0.13	0.09	0.12	0.12	0.00	0.04	0.10	0.11	0.19
Al_2O_3	11.80	11.61	12.80	12.30	12.29	12.21	12.56	13.06	12.48	12.53
FeO	0.87	0.89	0.79	0.71	0.95	0.90	0.90	1.09	1.28	0.57
MgO	0.15	0.14	0.11	0.10	0.13	0.00	0.04	0.16	0.12	0.15
CaO	0.77	0.70	0.95	0.69	0.71	0.94	0.87	0.98	0.98	0.92
Na_2O	4.37	4.15	4.06	4.04	4.11	4.11	4.31	4.62	3.99	4.11
K_2O	2.88	2.80	3.63	2.78	3.23	3.02	3.13	3.06	3.74	3.07
Cl	0.22	0.12	0.14	0.18	0.15	0.00	0.18	0.22	0.26	0.20
Totals	100.00	100.00	100.00	100.00	100.00	100.00	100.00	100.00	100.00	100.00

Pakaututu Road: 570cm (20um)

	1	2	3	4	5	6	7	8	9	10
SiO_2	75.33	74.73	75.11	74.93	74.10	73.30	74.14	74.26	75.01	75.96
TiO_2	0.15	0.12	0.18	0.25	0.16	0.14	0.14	0.21	0.19	0.18
Al_2O_3	11.98	12.06	12.24	11.90	11.92	11.58	11.72	11.60	11.88	11.94
FeO	0.96	0.94	1.09	0.75	0.89	0.96	0.85	0.92	0.89	0.94
MgO	0.14	0.15	0.14	0.13	0.15	0.15	0.18	0.19	0.11	0.14
CaO	0.81	0.78	0.87	0.84	0.87	0.87	0.76	0.75	0.81	0.87
Na_2O	4.03	3.96	4.09	4.13	4.00	3.77	3.90	4.02	3.82	3.94
K_2O	3.03	3.35	3.13	3.18	2.80	2.79	2.85	3.02	3.04	3.06
Cl	0.14	0.17	0.21	0.22	0.27	0.17	0.15	0.22	0.25	0.17
Totals	96.56	96.27	97.07	96.34	95.14	93.72	94.69	95.19	96.01	97.20
Analyses normalised to 100% loss free										
SiO_2	78.01	77.63	77.38	77.77	77.89	78.21	78.30	78.01	78.13	78.15
TiO_2	0.16	0.13	0.19	0.26	0.16	0.15	0.14	0.22	0.20	0.19
Al_2O_3	12.41	12.53	12.61	12.35	12.52	12.36	12.38	12.19	12.38	12.28
FeO	0.99	0.98	1.13	0.78	0.94	1.02	0.90	0.97	0.93	0.97
MgO	0.14	0.15	0.14	0.14	0.15	0.16	0.19	0.20	0.12	0.14
CaO	0.84	0.81	0.89	0.87	0.91	0.92	0.80	0.79	0.85	0.89
Na_2O	4.17	4.12	4.22	4.29	4.20	4.02	4.12	4.22	3.98	4.06
K_2O	3.14	3.48	3.22	3.30	2.94	2.97	3.01	3.17	3.17	3.15
Cl	0.14	0.18	0.22	0.23	0.28	0.18	0.15	0.23	0.26	0.17
Totals	100.00	100.00	100.00	100.00	100.00	100.00	100.00	100.00	100.00	100.00

Manroa:0cm

	1	2	3	4	5	6	7	8	9	10	11	12	13	14	15
SiO_2	74.28	73.59	72.46	74.16	72.19	71.45	69.33	76.60	76.84	76.46	71.20	71.30	70.77	73.82	75.80
TiO_2	0.14	0.13	0.12	0.11	0.14	0.11	0.12	0.12	0.17	0.17	0.21	0.15	0.14	0.14	0.29
Al_2O_3	11.20	11.57	11.48	12.10	11.39	11.51	11.08	11.61	11.45	11.68	11.86	11.52	11.25	11.66	12.60
FeO	0.72	0.95	0.91	1.15	0.84	0.65	0.83	0.98	0.90	0.85	1.53	1.30	0.74	0.89	2.01
MgO	0.10	0.12	0.11	0.03	0.13	0.17	0.13	0.16	0.16	0.15	0.27	0.15	0.20	0.14	0.29
CaO	0.87	0.71	0.75	0.87	0.56	0.73	0.74	0.93	0.72	0.79	1.22	1.11	0.79	0.75	1.46
Na_2O	3.19	3.81	3.93	3.99	3.51	3.66	3.59	3.73	3.83	3.94	4.01	3.59	3.50	3.47	4.05
K_2O	3.15	3.12	2.88	3.54	3.48	3.27	2.93	3.33	3.04	3.06	2.86	2.93	2.94	3.74	2.91
Cl	0.44	0.25	0.24	0.25	0.25	0.25	0.29	0.18	0.24	0.29	0.50	0.22	0.51	0.36	0.24
Totals	94.08	94.25	92.87	96.19	92.48	91.81	89.03	97.65	97.33	97.39	93.63	92.27	90.83	94.96	99.63
Analyses normalised to 100% loss free															
SiO_2	78.95	78.08	78.03	77.10	78.06	77.83	77.87	78.45	78.95	78.51	76.04	77.27	77.92	77.73	76.08
TiO_2	0.15	0.14	0.13	0.12	0.15	0.12	0.14	0.13	0.17	0.17	0.22	0.16	0.15	0.15	0.29
Al_2O_3	11.90	12.28	12.36	12.58	12.31	12.54	12.44	11.89	11.76	11.99	12.66	12.48	12.39	12.27	12.65
FeO	0.77	1.01	0.98	1.19	0.91	0.71	0.93	1.00	0.92	0.87	1.63	1.41	0.82	0.94	2.01
MgO	0.10	0.12	0.11	0.03	0.14	0.18	0.14	0.16	0.16	0.16	0.28	0.17	0.21	0.15	0.29
CaO	0.92	0.75	0.80	0.90	0.60	0.80	0.83	0.95	0.74	0.81	1.30	1.20	0.87	0.79	1.46
Na_2O	3.39	4.05	4.23	4.14	3.80	3.99	4.03	3.82	3.93	4.05	4.28	3.89	3.85	3.66	4.06
K_2O	3.35	3.31	3.10	3.68	3.76	3.57	3.29	3.41	3.12	3.14	3.05	3.18	3.23	3.94	2.92
Cl	0.46	0.26	0.26	0.26	0.27	0.28	0.32	0.19	0.24	0.29	0.53	0.24	0.56	0.38	0.24
Totals	100.00	100.00	100.00	100.00	100.00	100.00	100.00	100.00	100.00	100.00	100.00	100.00	100.00	100.00	100.00

Manaroa:10cm

	1	2	3	4	5	6	7	8	9	10	11	12	13	14	15	16
SiO_2	70.40	68.96	67.40	73.97	72.13	71.82	71.19	68.02	70.89	71.75	70.54	72.28	70.73	69.82	71.90	69.59
TiO_2	0.21	0.15	0.18	0.13	0.16	0.37	0.15	0.28	0.17	0.22	0.30	0.20	0.21	0.25	0.27	0.20
Al_2O_3	11.21	10.21	10.98	11.04	11.73	11.68	10.63	11.20	10.63	11.47	10.41	10.77	11.10	11.39	10.74	11.18
FeO	1.52	0.95	1.63	0.98	1.77	1.95	0.99	1.62	0.90	1.79	0.62	0.97	1.85	1.71	0.79	1.70
MgO	0.25	0.06	0.38	0.29	0.24	0.36	0.04	0.06	0.12	0.22	0.25	0.05	0.17	0.17	0.08	0.19
CaO	1.25	0.76	1.12	0.91	1.19	1.24	0.40	1.23	0.75	1.23	0.68	0.78	1.27	1.26	0.74	1.23
Na_2O	3.41	3.57	3.71	3.65	3.50	3.82	3.01	3.34	3.73	3.72	3.27	3.51	3.70	3.75	3.61	3.97
K_2O	2.80	3.12	2.59	3.12	2.97	2.91	4.04	3.06	3.22	2.94	3.61	3.33	2.64	2.71	3.26	2.73
Cl	0.24	0.30	0.25	0.24	0.17	0.21	0.26	0.30	0.34	0.20	0.26	0.25	0.21	0.19	0.20	0.23
Totals	91.27	88.08	88.24	94.32	93.86	94.35	90.70	89.10	90.75	93.54	89.95	92.13	91.89	91.25	91.58	91.01
Analyses normalised to 100% loss free																
SiO_2	77.13	78.30	76.39	78.43	76.84	76.12	78.49	76.34	78.12	76.71	78.42	78.45	76.97	76.52	78.51	76.47
TiO_2	0.23	0.17	0.21	0.13	0.17	0.39	0.16	0.31	0.19	0.23	0.34	0.21	0.23	0.27	0.30	0.22
Al_2O_3	12.28	11.59	12.44	11.71	12.50	12.37	11.71	12.57	11.72	12.26	11.58	11.69	12.08	12.49	11.72	12.29
FeO	1.66	1.08	1.85	1.04	1.89	2.06	1.09	1.81	0.99	1.92	0.69	1.06	2.01	1.88	0.86	1.86
MgO	0.27	0.06	0.43	0.30	0.26	0.38	0.04	0.07	0.13	0.24	0.28	0.05	0.19	0.19	0.08	0.20
CaO	1.37	0.86	1.26	0.96	1.27	1.32	0.44	1.38	0.83	1.31	0.75	0.85	1.38	1.38	0.80	1.35
Na_2O	3.73	4.05	4.20	3.87	3.73	4.05	3.32	3.75	4.11	3.98	3.64	3.81	4.03	4.11	3.94	4.36
K_2O	3.06	3.54	2.94	3.30	3.17	3.08	4.45	3.43	3.55	3.14	4.01	3.61	2.87	2.96	3.56	3.00
Cl	0.26	0.34	0.28	0.25	0.18	0.22	0.29	0.34	0.37	0.21	0.29	0.27	0.23	0.20	0.22	0.25
Totals	100.00	100.00	100.00	100.00	100.00	100.00	100.00	100.00	100.00	100.00	100.00	100.00	100.00	100.00	100.00	100.00

Manaroa:30cm

	1	2	3	4	5	6	7	8	9	10	11	12	13	14	15	16	17	18	19	20
SiO_2	73.39	75.43	72.36	73.16	75.99	74.28	73.29	73.50	72.93	77.09	75.40	74.60	75.28	76.02	74.69	73.79	73.62	74.47	77.02	75.07
TiO_2	0.24	0.19	0.27	0.24	0.15	0.12	0.32	0.29	0.30	0.09	0.21	0.28	0.21	0.10	0.23	0.26	0.25	0.18	0.14	0.13
Al_2O_3	12.51	12.01	12.22	12.34	12.26	11.74	12.18	12.63	12.44	11.96	11.97	12.73	13.00	12.14	13.13	12.95	12.82	11.92	11.97	11.99
FeO	1.67	0.90	1.92	1.80	1.00	0.81	1.66	1.72	1.91	1.02	1.00	1.66	1.59	0.96	1.80	1.80	1.85	0.94	0.93	1.29
MgO	0.20	0.19	0.25	0.18	0.14	0.10	0.17	0.31	0.29	0.12	0.13	0.17	0.24	0.11	0.19	0.28	0.25	0.12	0.14	0.13
CaO	1.36	0.81	1.39	1.39	0.81	0.75	1.47	1.60	1.43	0.83	0.86	1.52	1.38	0.78	1.44	1.53	1.84	0.79	1.11	0.94
Na_2O	4.18	4.06	4.10	4.17	4.20	4.02	4.29	4.52	4.30	4.01	4.11	4.03	4.02	3.95	3.72	4.38	4.18	4.01	4.02	3.96
K_2O	2.81	3.31	2.66	2.77	3.13	3.15	2.85	2.73	2.77	3.36	3.48	2.88	2.76	3.16	2.67	2.79	2.10	3.25	3.05	3.27
Cl	0.26	0.15	0.13	0.13	0.20	0.19	0.18	0.17	0.28	0.24	0.34	0.25	0.21	0.25	0.17	0.24	0.35	0.19	0.26	0.23
Totals	96.63	97.03	95.30	96.19	97.89	95.16	96.40	97.46	96.66	98.70	97.50	98.11	98.69	97.47	98.04	98.02	97.26	95.86	98.62	97.01
Analyses normalised to 100% loss free																				
SiO_2	75.95	77.74	75.92	76.06	77.63	78.06	76.02	75.41	75.45	78.10	77.34	76.04	76.28	78.00	76.18	75.28	75.69	77.68	78.09	77.39
TiO_2	0.25	0.19	0.28	0.25	0.15	0.13	0.33	0.30	0.31	0.09	0.21	0.28	0.21	0.10	0.24	0.27	0.26	0.19	0.14	0.13
Al_2O_3	12.95	12.37	12.83	12.83	12.53	12.34	12.63	12.96	12.87	12.12	12.28	12.97	13.17	12.46	13.39	13.21	13.18	12.43	12.13	12.36
FeO	1.72	0.92	2.01	1.87	1.02	0.85	1.73	1.76	1.98	1.04	1.03	1.69	1.61	0.98	1.83	1.84	1.90	0.98	0.95	1.33
MgO	0.21	0.19	0.26	0.19	0.14	0.11	0.18	0.32	0.30	0.12	0.14	0.17	0.24	0.11	0.19	0.28	0.26	0.12	0.14	0.14
CaO	1.41	0.84	1.46	1.45	0.83	0.79	1.52	1.64	1.48	0.84	0.88	1.55	1.40	0.80	1.47	1.56	1.89	0.83	1.12	0.97
Na_2O	4.32	4.18	4.31	4.34	4.29	4.22	4.45	4.64	4.45	4.06	4.22	4.11	4.07	4.05	3.80	4.47	4.30	4.18	4.07	4.08
K_2O	2.91	3.41	2.79	2.88	3.20	3.31	2.96	2.80	2.87	3.40	3.57	2.94	2.80	3.24	2.73	2.85	2.15	3.39	3.09	3.37
Cl	0.27	0.16	0.13	0.13	0.20	0.20	0.19	0.17	0.29	0.24	0.35	0.25	0.21	0.26	0.17	0.24	0.36	0.20	0.26	0.23
Totals	100.00	100.00	100.00	100.00	100.00	100.00	100.00	100.00	100.00	100.00	100.00	100.00	100.00	100.00	100.00	100.00	100.00	100.00	100.00	100.00

Manaroa:50cm

	1	2	3	4	5	6	7	8	9	10	11	12	13	14	15	16	17	18
SiO_2	71.92	74.13	74.10	74.57	74.65	71.68	74.93	74.89	73.60	74.44	77.17	77.50	73.72	75.94	70.73	73.81	73.64	74.83
TiO_2	0.13	0.17	0.16	0.12	0.09	0.14	0.14	0.15	0.25	0.18	0.13	0.16	0.20	0.17	0.20	0.24	0.10	0.10
Al_2O_3	11.46	13.14	11.97	12.05	12.23	11.93	11.87	12.14	12.57	12.71	12.29	12.06	12.68	12.14	12.74	12.61	12.07	11.99
FeO	0.81	1.53	0.91	0.78	0.89	1.47	0.99	0.96	1.73	1.92	0.93	0.91	1.68	0.93	1.74	1.63	0.94	0.89
MgO	0.12	0.15	0.15	0.19	0.16	0.11	0.18	0.15	0.22	0.24	0.15	0.10	0.16	0.14	0.22	0.14	0.17	0.13
CaO	0.73	1.20	0.85	0.68	0.79	1.23	0.74	0.76	1.17	1.45	0.68	0.72	1.41	0.80	1.55	1.23	0.82	0.74
Na_2O	3.87	4.18	3.86	4.13	2.75	3.35	4.06	3.86	4.35	3.67	3.88	3.82	4.10	3.87	3.68	4.03	3.95	3.61
K_2O	2.98	3.00	3.08	3.46	3.35	2.94	3.22	3.30	3.01	3.42	3.45	3.10	2.99	3.18	3.01	3.04	3.17	3.81
Cl	0.32	0.22	0.25	0.21	0.29	0.25	0.16	0.20	0.22	0.12	0.24	0.20	0.10	0.16	0.14	0.16	0.33	0.22
Totals	92.35	97.72	95.34	96.18	95.19	93.10	96.29	96.41	97.12	98.15	98.92	98.56	97.00	97.32	94.01	96.89	95.19	96.32
Analyses normalised to 100% loss free																		
SiO_2	77.88	75.86	77.73	77.53	78.43	76.99	77.82	77.68	75.79	75.84	78.01	78.63	76.00	78.03	75.24	76.18	77.35	77.69
TiO_2	0.15	0.17	0.17	0.12	0.09	0.15	0.14	0.15	0.26	0.19	0.13	0.16	0.21	0.18	0.21	0.25	0.11	0.10
Al_2O_3	12.41	13.44	12.56	12.53	12.85	12.82	12.33	12.59	12.95	12.95	12.43	12.24	13.07	12.47	13.55	13.02	12.68	12.45
FeO	0.88	1.57	0.96	0.81	0.93	1.58	1.03	0.99	1.78	1.96	0.94	0.92	1.73	0.95	1.85	1.68	0.99	0.92
MgO	0.13	0.15	0.16	0.20	0.16	0.12	0.19	0.15	0.23	0.25	0.15	0.10	0.17	0.14	0.24	0.14	0.18	0.14
CaO	0.79	1.23	0.89	0.71	0.83	1.32	0.77	0.79	1.21	1.48	0.69	0.73	1.46	0.82	1.65	1.27	0.86	0.77
Na_2O	4.19	4.28	4.05	4.29	2.89	3.59	4.22	4.01	4.48	3.74	3.92	3.87	4.22	3.97	3.91	4.16	4.15	3.74
K_2O	3.23	3.07	3.23	3.60	3.52	3.16	3.34	3.43	3.10	3.49	3.49	3.14	3.08	3.27	3.20	3.14	3.33	3.96
Cl	0.35	0.23	0.26	0.21	0.31	0.27	0.17	0.21	0.22	0.12	0.24	0.20	0.10	0.17	0.15	0.17	0.34	0.23
Totals	100.00	100.00	100.00	100.00	100.00	100.00	100.00	100.00	100.00	100.00	100.00	100.00	100.00	100.00	100.00	100.00	100.00	100.00

Manaroa:60cm

	1	2	3	4	5	6	7	8	9	10	11	12	13	14	15	16
SiO_2	71.78	76.19	73.80	74.08	73.02	73.77	73.07	74.68	74.24	75.67	73.51	74.49	74.03	72.418	74.99	74.25
TiO_2	0.24	0.09	0.19	0.09	0.27	0.16	0.21	0.16	0.11	0.12	0.20	0.10	0.25	0.15	0.23	0.19
Al_2O_3	11.52	11.81	11.61	11.99	12.49	11.35	12.21	12.22	11.65	11.90	12.47	11.50	12.55	11.47	11.75	12.47
FeO	0.85	0.72	0.94	0.86	1.48	0.90	1.55	1.19	0.89	0.86	1.76	0.85	1.72	0.89	0.94	1.80
MgO	0.07	0.17	0.18	0.15	0.14	0.07	0.21	0.17	0.15	0.16	0.20	0.16	0.17	0.59	0.18	0.11
CaO	0.79	0.81	0.78	0.81	1.31	0.73	1.30	0.93	0.73	0.27	1.34	0.79	1.37	0.87	0.88	1.30
Na_2O	3.63	3.96	3.83	3.85	4.19	3.95	4.19	4.58	4.04	3.87	4.16	4.04	4.32	3.92	3.95	3.90
K_2O	3.09	3.18	3.03	3.24	2.83	3.46	2.90	2.73	3.29	3.06	2.88	3.32	2.49	3.27	3.25	3.08
Cl	0.21	0.22	0.20	0.15	0.25	0.20	0.14	0.25	0.28	0.35	0.22	0.22	0.30	2.05	0.34	0.00
Totals	92.17	97.15	94.56	95.22	95.96	94.59	95.77	96.90	95.37	96.27	96.73	95.45	97.20	95.63	96.51	97.10
Analyses normalised to 100% loss free																
SiO_2	77.88	78.42	78.05	77.80	76.09	77.99	76.29	77.07	77.84	78.60	76.00	78.04	76.16	75.73	77.70	76.47
TiO_2	0.26	0.09	0.20	0.09	0.28	0.16	0.22	0.17	0.11	0.12	0.20	0.10	0.26	0.16	0.24	0.20
Al_2O_3	12.50	12.15	12.28	12.59	13.01	12.00	12.75	12.61	12.21	12.36	12.89	12.04	12.91	11.99	12.17	12.85
FeO	0.92	0.74	0.99	0.90	1.54	0.95	1.62	1.22	0.93	0.90	1.82	0.89	1.76	0.93	0.97	1.86
MgO	0.08	0.18	0.19	0.16	0.14	0.07	0.22	0.18	0.16	0.16	0.20	0.16	0.18	0.62	0.19	0.11
CaO	0.85	0.84	0.82	0.85	1.37	0.77	1.36	0.96	0.77	0.28	1.38	0.83	1.41	0.91	0.91	1.33
Na_2O	3.93	4.08	4.05	4.04	4.36	4.18	4.38	4.73	4.23	4.02	4.30	4.23	4.44	4.10	4.09	4.01
K_2O	3.35	3.28	3.21	3.40	2.95	3.66	3.03	2.82	3.44	3.18	2.98	3.48	2.56	3.42	3.36	3.17
Cl	0.23	0.23	0.21	0.16	0.26	0.22	0.14	0.25	0.29	0.36	0.22	0.23	0.31	2.14	0.35	0.00
Totals	100.00	100.00	100.00	100.00	100.00	100.00	100.00	100.00	100.00	100.00	100.00	100.00	100.00	100.00	100.00	100.00

Manaroa:70cm

	1	2	3	4	5	6	7	8	9	10	11	12	13	14	15
SiO_2	75.74	74.47	76.62	74.86	75.65	73.60	76.72	75.19	75.54	73.23	72.81	75.27	74.07	76.00	74.07
TiO_2	0.15	0.16	0.28	0.18	0.11	0.12	0.17	0.25	0.02	0.18	0.19	0.18	0.27	0.12	0.25
Al_2O_3	12.03	11.94	11.85	12.36	11.81	11.45	12.13	12.74	11.78	12.30	12.47	11.95	12.14	11.91	12.67
FeO	0.84	0.88	0.90	1.51	0.89	0.80	0.75	1.83	0.96	1.54	1.63	0.73	1.71	0.86	1.65
MgO	0.11	0.12	0.19	0.19	0.11	0.14	0.08	0.19	0.14	0.16	0.14	0.14	0.21	0.15	0.14
CaO	0.75	0.88	0.75	1.44	0.71	0.73	0.74	1.44	0.78	1.53	1.24	0.75	1.17	0.84	1.21
Na_2O	4.20	4.04	4.18	4.10	3.79	4.07	4.07	3.87	3.98	4.02	4.22	4.06	4.38	4.02	4.04
K_2O	3.30	3.23	3.16	3.13	3.33	3.20	3.27	3.11	3.02	2.93	2.79	3.49	2.95	3.05	2.81
Cl	0.22	0.28	0.19	0.19	0.14	0.27	0.29	0.16	0.19	0.18	0.34	0.18	0.24	0.21	0.22
Totals	97.34	96.01	98.12	97.95	96.53	94.36	98.21	98.78	96.41	96.08	95.83	96.76	97.13	97.15	97.06
Analyses normalised to 100% loss free															
SiO_2	77.81	77.57	78.09	76.43	78.37	78.00	78.12	76.12	78.35	76.22	75.98	77.79	76.26	78.22	76.32
TiO_2	0.16	0.17	0.28	0.19	0.11	0.12	0.17	0.25	0.02	0.18	0.20	0.19	0.28	0.13	0.25
Al_2O_3	12.36	12.44	12.07	12.62	12.23	12.13	12.35	12.90	12.22	12.81	13.02	12.35	12.50	12.26	13.06
FeO	0.86	0.92	0.92	1.54	0.92	0.85	0.76	1.85	1.00	1.60	1.70	0.76	1.76	0.88	1.69
MgO	0.11	0.13	0.20	0.19	0.11	0.15	0.08	0.19	0.15	0.17	0.15	0.14	0.21	0.15	0.15
CaO	0.77	0.91	0.77	1.47	0.73	0.77	0.76	1.46	0.81	1.59	1.29	0.78	1.20	0.87	1.25
Na_2O	4.31	4.20	4.26	4.18	3.92	4.31	4.14	3.92	4.13	4.18	4.40	4.20	4.51	4.14	4.16
K_2O	3.39	3.37	3.22	3.20	3.45	3.39	3.33	3.15	3.14	3.05	2.91	3.60	3.03	3.14	2.89
Cl	0.23	0.30	0.19	0.19	0.14	0.29	0.29	0.16	0.19	0.19	0.35	0.19	0.24	0.22	0.23
Totals	100.00	100.00	100.00	100.00	100.00	100.00	100.00	100.00	100.00	100.00	100.00	100.00	100.00	100.00	100.00

Manaroa:80cm

	1	2	3	4	5	6	7	8	9	10	11	12	13	14
SiO_2	71.72	74.66	73.44	76.14	73.80	74.71	74.60	73.96	75.73	75.53	75.87	72.64	74.77	73.73
TiO_2	0.13	0.14	0.24	0.05	0.14	0.28	0.11	0.19	0.19	0.19	0.14	0.16	0.13	0.12
Al_2O_3	10.92	12.55	12.12	12.64	11.23	11.54	11.77	12.20	11.79	11.52	11.87	11.60	11.88	12.47
FeO	1.11	1.71	1.41	0.76	0.89	1.33	0.68	1.60	1.03	0.87	0.97	0.87	0.75	1.61
MgO	0.13	0.10	0.10	0.15	0.22	0.19	0.13	0.20	0.27	0.15	0.09	0.15	0.10	0.21
CaO	0.87	1.27	1.18	1.03	0.89	0.80	0.77	1.24	0.89	0.84	0.78	0.84	0.77	1.54
Na_2O	3.50	3.91	3.98	4.48	3.81	3.79	4.07	3.99	3.99	3.83	3.87	4.02	4.01	3.98
K_2O	2.92	2.95	2.85	2.87	3.00	3.12	3.12	3.44	3.17	3.06	3.27	2.99	3.15	3.08
Cl	0.27	0.12	0.14	0.11	0.16	0.14	0.18	0.20	0.16	0.18	0.13	0.17	0.10	0.08
Totals	91.56	97.41	95.44	98.22	94.13	95.90	95.42	97.01	97.24	96.17	96.97	93.44	95.66	96.81
Analyses normalised to 100% loss free														
SiO_2	78.34	76.64	76.95	77.52	78.40	77.90	78.18	76.24	77.88	78.54	78.24	77.74	78.16	76.16
TiO_2	0.14	0.15	0.25	0.05	0.15	0.29	0.12	0.19	0.20	0.20	0.14	0.18	0.13	0.12
Al_2O_3	11.93	12.88	12.69	12.86	11.93	12.04	12.33	12.57	12.13	11.97	12.24	12.42	12.42	12.88
FeO	1.21	1.75	1.48	0.78	0.94	1.39	0.72	1.65	1.06	0.90	1.00	0.93	0.78	1.66
MgO	0.14	0.10	0.10	0.15	0.23	0.20	0.13	0.20	0.28	0.15	0.10	0.16	0.11	0.22
CaO	0.94	1.30	1.23	1.05	0.95	0.84	0.81	1.28	0.92	0.88	0.80	0.90	0.80	1.59
Na_2O	3.82	4.02	4.17	4.57	4.05	3.95	4.26	4.11	4.11	3.98	3.99	4.30	4.19	4.11
K_2O	3.19	3.02	2.98	2.92	3.18	3.25	3.26	3.55	3.26	3.18	3.37	3.19	3.29	3.18
Cl	0.29	0.13	0.15	0.11	0.17	0.15	0.19	0.20	0.17	0.19	0.13	0.19	0.10	0.08
Totals	100.00	100.00	100.00	100.00	100.00	100.00	100.00	100.00	100.00	100.00	100.00	100.00	100.00	100.00

	15	16	17	18	19	20	21	22	23	24	25
SiO_2	75.35	76.26	72.88	75.21	74.50	74.39	73.67	75.56	75.39	73.86	74.29
TiO_2	0.17	0.17	0.22	0.16	0.10	0.13	0.11	0.11	0.23	0.13	0.16
Al_2O_3	12.68	12.16	12.22	12.11	12.92	12.56	11.78	12.01	11.95	11.49	11.56
FeO	2.08	0.99	1.52	0.95	1.79	1.53	0.79	0.94	0.77	1.08	1.01
MgO	0.28	0.13	0.14	0.13	0.17	0.22	0.13	0.17	0.14	0.11	0.20
CaO	1.42	0.79	1.47	0.69	1.36	1.47	0.73	0.78	0.76	0.81	0.96
Na_2O	4.11	4.12	4.12	3.91	4.03	3.96	3.95	4.06	3.87	3.96	3.77
K_2O	2.93	3.16	2.85	3.58	2.93	2.94	3.13	3.20	3.23	3.15	2.97
Cl	0.14	0.24	0.17	0.23	0.19	0.19	0.18	0.18	0.26	0.16	0.25
Totals	99.16	98.02	95.57	96.98	98.00	97.39	94.47	96.99	96.59	94.75	95.15
Analyses normalised to 100% loss free											
SiO_2	75.98	77.80	76.25	77.55	76.03	76.38	77.98	77.90	78.05	77.95	78.08
TiO_2	0.17	0.17	0.23	0.17	0.11	0.14	0.11	0.11	0.23	0.14	0.17
Al_2O_3	12.79	12.41	12.78	12.49	13.18	12.90	12.47	12.38	12.37	12.12	12.15
FeO	2.10	1.01	1.59	0.98	1.83	1.57	0.84	0.97	0.80	1.14	1.06
MgO	0.28	0.14	0.15	0.14	0.18	0.23	0.14	0.17	0.14	0.12	0.20
CaO	1.43	0.81	1.53	0.71	1.38	1.51	0.77	0.80	0.78	0.85	1.00
Na_2O	4.14	4.20	4.31	4.03	4.11	4.07	4.18	4.18	4.00	4.18	3.96
K_2O	2.95	3.22	2.98	3.69	2.99	3.02	3.31	3.29	3.35	3.32	3.12
Cl	0.15	0.24	0.17	0.24	0.20	0.19	0.19	0.19	0.27	0.17	0.26
Totals	100.00	100.00	100.00	100.00	100.00	100.00	100.00	100.00	100.00	100.00	100.00

Manaroa:90cm

	1	2	3	4	5	6	7	8	9	10	11	12	13	14	15
SiO_2	74.89	73.69	75.75	75.66	74.71	76.11	74.02	73.78	74.83	73.79	75.53	73.83	73.73	75.73	75.08
TiO_2	0.11	0.15	0.17	0.14	0.24	0.17	0.28	0.09	0.27	0.09	0.19	0.18	0.13	0.21	0.23
Al_2O_3	11.68	11.65	12.15	12.24	12.70	11.89	12.32	11.89	12.22	12.22	11.86	11.76	11.79	11.90	12.73
FeO	0.85	0.90	0.99	0.97	1.40	0.77	1.50	0.91	1.59	1.73	0.88	1.12	0.79	0.89	1.63
MgO	0.07	0.16	0.08	0.15	0.26	0.19	0.14	0.12	0.15	0.17	0.16	0.15	0.12	0.17	0.16
CaO	0.97	0.79	0.91	0.89	1.40	0.83	1.38	0.74	1.44	1.40	1.04	1.02	0.82	0.94	1.35
Na_2O	3.61	4.17	3.96	3.98	4.15	4.10	4.28	4.17	4.10	4.14	3.89	3.93	3.91	4.00	3.94
K_2O	3.03	3.05	3.00	3.18	3.00	3.52	2.88	3.26	2.91	2.87	3.06	3.14	3.21	3.28	3.27
Cl	0.15	0.17	0.18	0.22	0.22	0.18	0.34	0.24	0.18	0.17	0.17	0.21	0.30	0.21	0.23
Totals	95.37	94.73	97.19	97.44	98.08	97.76	97.14	95.19	97.68	96.58	96.75	95.33	94.78	97.31	98.62
Analyses normalised to 100% loss free															
SiO_2	78.53	77.80	77.94	77.65	76.17	77.86	76.20	77.51	76.61	76.41	78.06	77.45	77.79	77.82	76.13
TiO_2	0.12	0.16	0.17	0.14	0.25	0.17	0.29	0.09	0.28	0.09	0.20	0.19	0.13	0.21	0.23
Al_2O_3	12.25	12.30	12.50	12.57	12.94	12.16	12.68	12.49	12.51	12.65	12.26	12.34	12.44	12.22	12.91
FeO	0.90	0.95	1.02	1.00	1.42	0.78	1.55	0.96	1.62	1.79	0.90	1.17	0.83	0.91	1.66
MgO	0.07	0.17	0.09	0.15	0.26	0.19	0.14	0.12	0.15	0.17	0.16	0.16	0.12	0.17	0.16
CaO	1.02	0.84	0.94	0.92	1.43	0.84	1.42	0.78	1.48	1.45	1.07	1.07	0.86	0.96	1.36
Na_2O	3.78	4.40	4.08	4.08	4.23	4.20	4.41	4.38	4.19	4.28	4.02	4.12	4.12	4.11	4.00
K_2O	3.17	3.22	3.09	3.26	3.06	3.60	2.96	3.42	2.98	2.97	3.16	3.30	3.38	3.37	3.32
Cl	0.16	0.18	0.18	0.22	0.23	0.18	0.35	0.25	0.19	0.17	0.17	0.22	0.31	0.21	0.23
Totals	100.00	100.00	100.00	100.00	100.00	100.00	100.00	100.00	100.00	100.00	100.00	100.00	100.00	100.00	100.00

Manaroa:100cm

	1	2	3	4	5	6	7	8	9	10	11	12	13	14	15	16	17	18	19	20
SiO_2	72.97	73.50	74.60	74.83	76.41	76.23	75.00	67.35	76.89	75.90	76.10	70.67	75.86	71.14	76.29	77.30	73.94	75.91	74.75	72.38
TiO_2	0.23	0.20	0.16	0.17	0.11	0.20	0.20	0.60	0.20	0.17	0.14	0.66	0.16	0.17	0.12	0.23	0.11	0.20	0.18	0.19
Al_2O_3	12.58	11.56	11.64	12.31	11.83	11.99	11.61	12.54	12.07	11.80	11.81	13.54	11.98	11.17	11.94	11.93	11.34	12.08	11.31	11.05
FeO	1.67	0.81	0.73	1.46	0.80	1.14	0.95	2.55	1.03	0.75	1.16	2.81	0.90	0.99	0.95	0.79	0.99	1.08	0.82	0.96
MgO	0.20	0.14	0.11	0.13	0.12	0.22	0.16	0.47	0.16	0.15	0.12	0.68	0.19	0.12	0.22	0.16	0.13	0.10	0.11	0.15
CaO	2.80	0.92	0.84	1.45	0.80	0.97	0.86	2.03	0.82	1.02	0.81	2.39	0.77	0.89	0.87	0.91	0.82	0.83	0.88	0.95
Na_2O	4.17	3.87	3.79	3.91	3.91	3.91	3.90	3.53	3.84	3.96	3.98	3.65	3.86	3.83	3.80	3.76	3.68	4.07	4.02	3.70
K_2O	2.77	3.22	3.18	3.10	3.30	3.41	3.11	3.50	3.36	3.11	3.26	3.82	3.11	3.10	3.30	3.42	3.31	3.00	3.54	3.06
Cl	0.19	0.24	0.18	0.17	0.17	0.21	0.16	0.26	0.17	0.21	0.16	0.22	0.23	0.27	0.15	0.14	0.21	0.12	0.18	0.18
Totals	97.58	94.45	95.25	97.54	97.46	98.27	95.93	92.82	98.53	97.07	97.56	98.44	97.05	91.67	97.64	98.63	94.53	97.38	95.80	92.61
Analyses normalised to 100% loss free																				
SiO_2	74.78	77.83	78.33	76.72	78.41	77.57	78.18	72.56	78.04	78.19	78.00	71.80	78.16	77.61	78.13	78.38	78.22	77.95	78.02	78.15
TiO_2	0.24	0.21	0.17	0.17	0.11	0.20	0.21	0.64	0.20	0.18	0.15	0.67	0.17	0.18	0.13	0.23	0.12	0.21	0.19	0.20
Al_2O_3	12.89	12.23	12.23	12.62	12.14	12.20	12.10	13.51	12.25	12.15	12.11	13.76	12.35	12.19	12.23	12.10	11.99	12.41	11.81	11.94
FeO	1.71	0.86	0.77	1.50	0.82	1.16	0.99	2.74	1.04	0.77	1.19	2.86	0.93	1.08	0.98	0.80	1.05	1.10	0.86	1.04
MgO	0.21	0.14	0.11	0.13	0.12	0.22	0.16	0.50	0.16	0.16	0.13	0.69	0.19	0.13	0.23	0.16	0.14	0.10	0.12	0.16
CaO	2.87	0.98	0.88	1.49	0.82	0.98	0.89	2.19	0.84	1.05	0.83	2.43	0.79	0.97	0.89	0.92	0.87	0.85	0.92	1.02
Na_2O	4.27	4.10	3.98	4.01	4.02	3.98	4.07	3.81	3.89	4.08	4.08	3.70	3.98	4.17	3.89	3.81	3.89	4.18	4.20	4.00
K_2O	2.83	3.41	3.34	3.18	3.39	3.47	3.24	3.77	3.41	3.20	3.35	3.88	3.20	3.38	3.38	3.46	3.51	3.08	3.70	3.30
Cl	0.20	0.25	0.19	0.18	0.18	0.22	0.16	0.28	0.17	0.21	0.17	0.22	0.23	0.29	0.16	0.14	0.22	0.12	0.18	0.19
Totals	100.00	100.00	100.00	100.00	100.00	100.00	100.00	100.00	100.00	100.00	100.00	100.00	100.00	100.00	100.00	100.00	100.00	100.00	100.00	100.00

Manaroa:110cm

	1	2	3	4	5	6	7	8	9	10	11	12	13	14
SiO_2	75.78	74.18	73.62	74.91	75.96	74.80	75.79	73.99	73.73	73.50	74.13	73.70	71.43	74.13
TiO_2	0.20	0.20	0.16	0.17	0.01	0.08	0.19	0.23	0.18	0.19	0.19	0.22	0.24	0.25
Al_2O_3	11.91	11.47	12.08	12.34	11.96	11.79	11.75	12.46	11.74	12.48	11.86	12.72	11.88	11.63
FeO	0.94	0.84	1.40	1.69	0.79	1.03	1.00	1.04	1.10	1.28	0.78	1.28	0.92	0.86
MgO	0.13	0.11	0.24	0.23	0.16	0.15	0.11	0.31	0.16	0.29	0.18	0.33	0.09	0.19
CaO	0.83	0.80	1.42	1.38	1.32	0.90	0.90	1.46	0.96	1.44	1.01	1.47	0.73	1.08
Na_2O	3.94	3.78	3.87	3.95	3.80	3.84	4.14	4.19	3.65	4.10	3.73	3.75	3.42	3.84
K_2O	3.34	3.32	2.80	2.95	3.39	3.19	3.21	3.10	3.43	2.85	3.26	2.98	3.86	3.37
Cl	0.21	0.17	0.34	0.31	0.23	0.23	0.21	0.29	0.22	0.17	0.15	0.12	0.22	0.26
Totals	97.28	94.87	95.92	97.92	97.62	96.00	97.31	97.07	95.16	96.29	95.29	96.57	92.78	95.59
Analyses normalised to 100% loss free														
SiO_2	77.90	78.19	76.75	76.51	77.81	77.92	77.88	76.22	77.49	76.34	77.80	76.31	76.98	77.55
TiO_2	0.20	0.21	0.16	0.17	0.01	0.08	0.20	0.23	0.18	0.20	0.20	0.22	0.26	0.26
Al_2O_3	12.25	12.09	12.59	12.60	12.25	12.28	12.07	12.83	12.34	12.97	12.44	13.17	12.81	12.17
FeO	0.96	0.89	1.46	1.72	0.81	1.07	1.03	1.07	1.16	1.32	0.82	1.33	0.99	0.89
MgO	0.14	0.11	0.25	0.23	0.17	0.16	0.11	0.32	0.17	0.30	0.18	0.34	0.10	0.20
CaO	0.85	0.85	1.48	1.41	1.35	0.93	0.93	1.51	1.00	1.49	1.06	1.52	0.78	1.13
Na_2O	4.05	3.98	4.03	4.03	3.89	4.00	4.26	4.31	3.83	4.25	3.92	3.89	3.69	4.01
K_2O	3.43	3.50	2.92	3.01	3.47	3.32	3.30	3.19	3.60	2.96	3.43	3.09	4.16	3.52
Cl	0.21	0.18	0.35	0.31	0.24	0.24	0.22	0.30	0.23	0.18	0.15	0.13	0.24	0.27
Totals	100.00	100.00	100.00	100.00	100.00	100.00	100.00	100.00	100.00	100.00	100.00	100.00	100.00	100.00

	15	16	17	18	19	20	21	22	23	24	25
SiO_2	74.24	74.68	75.98	70.93	72.82	76.61	75.20	76.31	75.74	75.05	75.61
TiO_2	0.18	0.21	0.18	0.09	0.19	0.24	0.10	0.19	0.16	0.22	0.13
Al_2O_3	11.63	11.81	11.85	11.20	11.59	11.91	11.73	11.87	12.01	12.44	12.10
FeO	1.00	0.83	0.93	1.79	1.05	1.04	0.97	1.03	0.81	1.60	1.05
MgO	0.12	0.21	0.28	0.14	0.18	0.14	0.16	0.16	0.14	0.28	0.12
CaO	0.95	0.96	1.08	1.05	0.87	0.99	0.92	0.90	1.01	1.41	0.95
Na_2O	3.45	3.61	3.85	3.67	3.85	3.94	3.87	3.05	3.90	3.98	3.91
K_2O	3.91	3.45	3.24	2.76	3.19	3.21	3.03	3.23	3.04	3.50	3.13
Cl	0.17	0.13	0.15	0.22	0.22	0.25	0.14	0.21	0.20	0.78	0.17
Totals	95.65	95.89	97.53	91.86	93.95	98.02	96.12	96.94	97.00	99.26	97.16
Analyses normalised to 100% loss free											
SiO_2	77.61	77.88	77.91	77.22	77.51	78.15	78.24	78.72	78.08	75.61	77.82
TiO_2	0.19	0.22	0.18	0.10	0.20	0.24	0.11	0.20	0.17	0.22	0.13
Al_2O_3	12.16	12.32	12.15	12.20	12.33	12.15	12.20	12.25	12.38	12.53	12.46
FeO	1.05	0.86	0.95	1.95	1.11	1.06	1.01	1.06	0.83	1.62	1.08
MgO	0.13	0.21	0.29	0.15	0.19	0.15	0.17	0.17	0.14	0.28	0.13
CaO	1.00	1.00	1.11	1.14	0.93	1.01	0.95	0.93	1.04	1.42	0.97
Na_2O	3.61	3.76	3.95	4.00	4.10	4.02	4.03	3.14	4.02	4.01	4.02
K_2O	4.09	3.60	3.32	3.01	3.39	3.27	3.15	3.33	3.13	3.53	3.22
Cl	0.18	0.14	0.15	0.24	0.24	0.25	0.15	0.21	0.21	0.78	0.17
Totals	100.00	100.00	100.00	100.00	100.00	100.00	100.00	100.00	100.00	100.00	100.00

Manaroa:120cm

	1	2	3	4	5	6	7	8	9	10	11	12	13	14	15	16
SiO_2	76.62	76.90	75.33	73.83	73.37	77.52	74.59	74.71	74.84	70.72	70.71	76.08	75.13	73.10	74.16	72.84
TiO_2	0.23	0.26	0.24	0.14	0.17	0.20	0.16	0.24	0.16	0.65	0.55	0.13	0.13	0.20	0.17	0.20
Al_2O_3	10.35	11.92	12.47	11.84	10.66	11.58	10.68	11.64	13.29	12.49	12.09	12.18	11.20	11.27	9.34	11.56
FeO	1.09	0.88	0.85	0.86	0.83	0.97	0.88	0.94	1.01	3.04	2.25	0.92	0.98	0.88	0.89	0.89
MgO	0.43	0.08	0.34	0.47	0.27	0.11	0.16	0.33	0.13	0.66	0.37	0.24	0.15	0.22	0.22	0.22
CaO	1.11	0.88	0.89	0.90	0.78	0.92	0.91	0.87	0.97	2.33	1.33	0.83	0.96	0.85	0.77	0.87
Na_2O	4.22	3.85	3.89	4.02	3.28	3.95	3.98	3.85	3.90	3.66	4.15	4.05	4.06	3.87	3.77	3.99
K_2O	3.48	3.22	3.25	3.19	4.64	3.52	3.33	3.23	4.26	3.68	4.04	3.61	3.39	3.10	3.96	2.93
Cl	0.49	0.14	0.14	0.18	0.10	0.13	0.11	0.15	0.40	0.09	0.26	0.25	0.18	0.15	0.19	0.19
Totals	98.03	98.13	97.41	95.43	94.10	98.88	94.79	95.96	98.95	97.33	95.74	98.30	96.18	93.64	93.44	93.69
Analyses normalised to 100% loss free																
SiO_2	78.16	78.37	77.33	77.37	77.97	78.39	78.69	77.86	75.64	72.67	73.86	77.40	78.12	78.07	79.36	77.75
TiO_2	0.24	0.26	0.25	0.15	0.18	0.20	0.17	0.25	0.16	0.67	0.57	0.13	0.14	0.21	0.18	0.22
Al_2O_3	10.56	12.14	12.80	12.40	11.33	11.71	11.26	12.13	13.43	12.84	12.63	12.39	11.65	12.04	9.99	12.34
FeO	1.11	0.90	0.88	0.90	0.89	0.98	0.93	0.98	1.02	3.12	2.34	0.94	1.02	0.94	0.95	0.95
MgO	0.44	0.08	0.35	0.50	0.29	0.11	0.17	0.34	0.13	0.68	0.39	0.25	0.16	0.23	0.23	0.23
CaO	1.13	0.90	0.92	0.94	0.83	0.93	0.96	0.91	0.98	2.40	1.39	0.84	1.00	0.91	0.82	0.93
Na_2O	4.30	3.92	4.00	4.21	3.48	4.00	4.20	4.01	3.94	3.76	4.33	4.12	4.22	4.13	4.03	4.26
K_2O	3.55	3.28	3.33	3.34	4.93	3.55	3.51	3.36	4.30	3.78	4.21	3.67	3.52	3.31	4.23	3.12
Cl	0.50	0.14	0.15	0.19	0.11	0.14	0.11	0.16	0.41	0.10	0.27	0.25	0.19	0.16	0.20	0.20
Totals	100.00	100.00	100.00	100.00	100.00	100.00	100.00	100.00	100.00	100.00	100.00	100.00	100.00	100.00	100.00	100.00

Manaroa: 170cm

	1	2	3	4	5	6	7	8	9	10
SiO_2	72.26	73.27	71.94	72.84	72.86	73.54	75.11	71.93	76.65	77.69
TiO_2	0.17	0.21	0.19	0.10	0.22	0.08	0.15	0.16	0.12	0.09
Al_2O_3	12.09	11.53	11.55	11.35	11.25	11.46	11.43	11.26	11.74	11.52
FeO	0.97	1.37	1.26	1.14	1.12	1.14	1.30	1.22	1.13	0.93
MgO	0.14	0.18	0.17	0.13	0.14	0.19	0.21	0.16	0.00	0.16
CaO	0.94	0.83	1.23	0.93	0.99	1.16	0.91	1.08	1.25	1.02
Na_2O	3.43	3.43	3.23	3.68	3.54	3.63	3.82	3.43	3.74	3.76
K_2O	3.33	3.69	3.21	3.39	3.07	3.23	3.80	3.02	3.49	3.90
Totals	93.33	94.50	92.79	93.55	93.18	94.42	96.73	92.26	98.12	99.06
Analyses normalised to 100% loss free										
SiO_2	77.43	77.53	77.53	77.85	78.19	77.88	77.65	77.97	78.12	78.42
TiO_2	0.18	0.22	0.21	0.11	0.24	0.09	0.16	0.18	0.12	0.09
Al_2O_3	12.96	12.21	12.45	12.13	12.07	12.13	11.82	12.21	11.96	11.63
FeO	1.04	1.45	1.35	1.22	1.20	1.21	1.35	1.32	1.16	0.94
MgO	0.15	0.19	0.18	0.14	0.15	0.20	0.21	0.18	0.00	0.16
CaO	1.00	0.88	1.33	1.00	1.06	1.23	0.94	1.17	1.28	1.03
Na_2O	3.68	3.63	3.49	3.93	3.80	3.84	3.95	3.71	3.81	3.80
K_2O	3.57	3.90	3.46	3.62	3.29	3.42	3.93	3.27	3.55	3.93
Totals	100.00	100.00	100.00	100.00	100.00	100.00	100.00	100.00	100.00	100.00

Manaroa: 190cm

	1	2	3	4	5	6	7	8	9	10
SiO_2	76.83	78.37	77.27	75.04	77.08	74.09	73.83	74.62	74.72	75.26
TiO_2	0.11	0.23	0.16	0.09	0.20	0.14	0.17	0.26	0.20	0.18
Al_2O_3	11.41	11.92	11.54	11.89	11.56	11.16	11.51	11.69	11.64	11.53
FeO	1.01	1.15	1.06	1.12	0.98	1.08	1.34	1.38	1.08	1.22
MgO	0.15	0.17	0.01	0.29	0.11	0.08	0.17	0.11	0.13	0.15
CaO	1.09	0.97	1.22	1.14	0.96	0.89	1.06	1.00	1.09	1.12
Na_2O	3.60	3.30	3.73	3.67	3.68	3.56	3.52	3.57	3.58	3.83
K_2O	3.21	3.03	2.95	3.30	3.00	3.13	2.63	3.02	2.81	2.85
Cl	0.22	0.27	0.00	0.21	0.19	0.33	0.26	0.22	0.32	0.26
Totals	97.65	99.40	97.94	96.73	97.76	94.46	94.48	95.88	95.57	96.41
Analyses normalised to 100% loss free										
SiO_2	78.68	78.85	78.89	77.58	78.85	78.44	78.14	77.83	78.18	78.07
TiO_2	0.12	0.23	0.17	0.09	0.21	0.15	0.18	0.27	0.21	0.18
Al_2O_3	11.68	11.99	11.79	12.29	11.82	11.81	12.18	12.19	12.18	11.96
FeO	1.04	1.15	1.08	1.16	1.00	1.14	1.42	1.44	1.12	1.26
MgO	0.15	0.17	0.01	0.30	0.11	0.08	0.18	0.12	0.14	0.16
CaO	1.12	0.97	1.24	1.17	0.98	0.94	1.12	1.04	1.14	1.17
Na_2O	3.69	3.32	3.80	3.79	3.76	3.77	3.72	3.72	3.75	3.98
K_2O	3.29	3.05	3.01	3.41	3.06	3.31	2.78	3.15	2.94	2.96
Cl	0.23	0.27	0.00	0.22	0.20	0.35	0.27	0.23	0.34	0.27
Totals	100.00	100.00	100.00	100.00	100.00	100.00	100.00	100.00	100.00	100.00

Manaroa:240cm

	1	2	3	4	5	6	7	8	9	10	11	12	13
SiO_2	71.27	69.76	67.77	70.05	71.33	71.37	71.81	70.70	71.27	71.81	70.99	70.59	71.92
TiO_2	0.24	0.21	0.18	0.18	0.20	0.15	0.14	0.16	0.10	0.18	0.20	0.26	0.15
Al_2O_3	10.90	10.53	10.32	10.44	10.69	10.68	10.80	10.66	10.71	10.72	10.83	10.78	10.74
FeO	1.09	1.06	1.06	1.20	1.42	1.04	1.10	1.16	1.07	1.23	1.09	1.12	1.32
MgO	0.14	0.10	0.12	0.12	0.11	0.11	0.14	0.11	0.10	0.10	0.13	0.12	0.13
CaO	0.85	1.03	1.08	1.04	1.09	0.94	0.93	1.08	0.98	0.95	1.00	1.16	1.07
Na_2O	3.27	3.45	3.18	3.34	3.06	3.65	2.90	3.41	3.26	3.56	3.53	3.31	3.50
K_2O	3.06	3.02	2.86	2.94	3.20	3.13	3.56	3.16	2.88	3.06	3.35	2.77	3.08
Cl	0.25	0.25	0.27	0.20	0.24	0.19	0.28	0.20	0.20	0.26	0.24	0.33	0.26
Totals	91.05	89.42	86.83	89.51	91.33	91.27	91.66	90.63	90.56	91.86	91.36	90.42	92.18
Analyses normalised to 100% loss free													
SiO_2	78.27	78.01	78.06	78.26	78.10	78.20	78.35	78.01	78.70	78.18	77.70	78.06	78.02
TiO_2	0.26	0.24	0.20	0.20	0.21	0.17	0.15	0.18	0.11	0.19	0.22	0.28	0.16
Al_2O_3	11.97	11.78	11.89	11.67	11.70	11.71	11.78	11.76	11.82	11.67	11.85	11.92	11.65
FeO	1.20	1.18	1.22	1.34	1.56	1.13	1.20	1.28	1.18	1.34	1.20	1.24	1.44
MgO	0.16	0.11	0.14	0.14	0.12	0.12	0.15	0.12	0.11	0.11	0.14	0.14	0.14
CaO	0.93	1.15	1.24	1.16	1.19	1.03	1.02	1.19	1.08	1.03	1.10	1.28	1.16
Na_2O	3.59	3.86	3.66	3.73	3.35	4.00	3.17	3.76	3.60	3.88	3.86	3.66	3.79
K_2O	3.36	3.38	3.29	3.28	3.50	3.43	3.89	3.49	3.18	3.33	3.67	3.06	3.35
Cl	0.27	0.28	0.31	0.22	0.26	0.21	0.31	0.22	0.22	0.28	0.27	0.36	0.29
Totals	100.00	100.00	100.00	100.00	100.00	100.00	100.00	100.00	100.00	100.00	100.00	100.00	100.00

Manaroa:270cm

	1	2	3	4	5	6	7	8	9	10	11	12
SiO_2	73.18	72.67	70.85	73.69	75.41	72.99	71.29	73.97	76.08	75.01	75.00	73.90
TiO_2	0.17	0.18	0.10	0.13	0.17	0.22	0.00	0.15	0.19	0.21	0.19	0.18
Al_2O_3	11.79	11.65	11.26	11.66	12.03	11.38	11.35	11.75	12.01	11.78	11.73	11.66
FeO	1.08	1.29	1.15	1.13	1.00	1.15	1.04	1.02	1.29	1.17	1.11	1.18
MgO	0.19	0.21	0.13	0.08	0.11	0.12	0.12	0.16	0.15	0.13	0.16	0.12
CaO	1.13	1.19	0.95	1.00	1.33	1.01	1.19	1.08	1.15	1.08	1.03	1.15
Na_2O	3.84	3.82	3.48	3.95	3.95	3.86	4.00	3.99	3.21	3.75	3.82	3.84
K_2O	3.06	3.06	2.83	3.31	2.94	3.13	2.88	3.06	3.22	3.28	3.11	3.02
Cl	0.22	0.67	0.23	0.26	0.21	0.21	0.19	0.20	0.28	0.39	0.33	0.19
Totals	94.65	94.73	90.97	95.21	97.16	94.06	92.05	95.38	97.57	96.81	96.47	95.21
Analyses normalised to 100% loss free												
SiO2	77.32	76.72	77.88	77.40	77.62	77.60	77.44	77.55	77.98	77.49	77.75	77.61
TiO2	0.18	0.19	0.11	0.13	0.18	0.23	0.00	0.15	0.19	0.22	0.19	0.19
Al2O3	12.45	12.29	12.37	12.24	12.39	12.09	12.33	12.32	12.31	12.17	12.16	12.25
FeO	1.14	1.36	1.26	1.19	1.03	1.22	1.13	1.07	1.32	1.21	1.15	1.24
MgO	0.20	0.22	0.14	0.09	0.11	0.13	0.13	0.17	0.15	0.14	0.17	0.12
CaO	1.19	1.25	1.04	1.05	1.37	1.08	1.29	1.13	1.18	1.12	1.06	1.20
Na2O	4.05	4.03	3.83	4.15	4.07	4.10	4.35	4.19	3.29	3.87	3.96	4.03
K2O	3.23	3.23	3.11	3.47	3.02	3.32	3.12	3.21	3.30	3.38	3.22	3.17
Cl	0.23	0.70	0.25	0.28	0.22	0.22	0.21	0.21	0.29	0.41	0.34	0.19
Total	100.00	100.00	100.00	100.00	100.00	100.00	100.00	100.00	100.00	100.00	100.00	100.00

Manaroa:295cm

	1	2	3	4	5	6	7	8	9
SiO_2	74.01	69.69	71.53	72.94	69.51	71.19	71.87	74.62	73.38
TiO_2	0.14	0.21	0.19	0.17	0.12	0.22	0.17	0.16	0.16
Al_2O_3	11.59	10.35	10.67	10.69	10.62	10.96	10.55	12.25	11.95
FeO	0.80	0.85	1.01	1.02	1.14	1.46	0.99	0.96	1.15
MgO	0.13	0.03	0.21	0.13	0.19	0.13	0.22	0.21	0.21
CaO	0.94	0.92	0.94	0.82	0.90	1.12	0.98	1.03	1.16
Na_2O	4.22	3.03	3.47	3.59	3.68	3.47	3.51	3.34	3.76
K_2O	3.07	2.97	3.34	3.25	2.91	3.04	3.73	4.21	3.23
Cl	0.25	0.15	0.24	0.18	0.24	0.19	0.20	0.20	0.24
Totals	95.15	88.18	91.58	92.77	89.31	91.76	92.22	96.97	95.22
Analyses normalised to 100% loss free									
SiO_2	77.79	79.03	78.10	78.63	77.83	77.58	77.93	76.95	77.06
TiO_2	0.15	0.23	0.21	0.18	0.13	0.24	0.18	0.16	0.16
Al_2O_3	12.18	11.73	11.65	11.52	11.89	11.94	11.44	12.63	12.55
FeO	0.84	0.96	1.10	1.09	1.28	1.59	1.08	0.99	1.20
MgO	0.13	0.04	0.23	0.14	0.22	0.14	0.24	0.22	0.22
CaO	0.99	1.04	1.02	0.88	1.01	1.22	1.06	1.06	1.22
Na_2O	4.43	3.44	3.78	3.87	4.12	3.78	3.81	3.45	3.95
K_2O	3.22	3.36	3.65	3.50	3.25	3.31	4.04	4.34	3.39
Cl	0.26	0.17	0.26	0.19	0.27	0.21	0.22	0.20	0.25
Totals	100.00	100.00	100.00	100.00	100.00	100.00	100.00	100.00	100.00

Manaroa: 320cm

	1	2
SiO_2	71.49	70.88
TiO_2	0.17	0.16
Al_2O_3	11.70	11.73
FeO	1.03	1.14
MgO	0.25	0.19
CaO	0.92	1.11
Na_2O	3.15	3.62
K_2O	3.19	3.29
Cl	0.19	0.16
Totals	92.08	92.27
Analyses normalised to 100% loss free		
SiO_2	77.64	76.82
TiO_2	0.19	0.18
Al_2O_3	12.70	12.71
FeO	1.12	1.24
MgO	0.27	0.20
CaO	1.00	1.20
Na_2O	3.42	3.92
K_2O	3.47	3.57
Cl	0.21	0.17
Totals	100.00	100.00

Manaroa:330cm

	1	2	3	4	5	6
SiO_2	71.84	68.08	71.42	68.91	69.49	68.58
TiO_2	0.14	0.16	0.12	0.09	0.10	0.21
Al_2O_3	11.70	10.93	11.08	10.15	10.43	10.55
FeO	1.13	1.11	1.10	1.13	1.15	1.24
MgO	0.09	0.07	0.21	0.09	0.12	0.18
CaO	1.06	0.88	0.99	0.98	0.96	0.97
Na_2O	3.75	3.57	2.89	3.22	3.19	3.14
K_2O	3.07	2.93	3.90	2.56	2.79	3.12
Cl	0.14	0.47	0.19	0.23	0.21	0.21
Totals	92.91	88.20	91.87	87.36	88.44	88.22
Analyses normalised to 100% loss free						
SiO_2	77.32	77.20	77.74	78.88	78.58	77.74
TiO_2	0.15	0.18	0.13	0.10	0.12	0.24
Al_2O_3	12.59	12.39	12.06	11.62	11.79	11.96
FeO	1.22	1.26	1.19	1.29	1.29	1.41
MgO	0.10	0.08	0.22	0.10	0.13	0.21
CaO	1.14	1.00	1.07	1.13	1.09	1.10
Na_2O	4.04	4.05	3.14	3.69	3.60	3.56
K_2O	3.31	3.32	4.24	2.93	3.16	3.54
Cl	0.15	0.53	0.21	0.26	0.24	0.24
Totals	100.00	100.00	100.00	100.00	100.00	100.00

Manaros:365cm

	1	2	3	4	5	6	7	8	9	10	11	12	13	14	15
SiO_2	73.46	73.93	74.20	72.86	73.48	73.55	73.80	74.02	73.78	74.09	73.01	75.05	73.79	75.23	72.03
TiO_2	0.15	0.16	0.11	0.06	0.18	0.17	0.27	0.07	0.14	0.20	0.00	0.13	0.32	0.23	0.16
Al_2O_3	11.20	11.36	11.25	11.31	11.13	11.34	11.23	11.22	11.45	11.51	11.50	11.34	12.23	11.85	13.04
FeO	1.14	0.86	1.06	0.89	0.86	1.34	0.84	0.91	1.34	1.13	1.23	1.20	1.35	1.38	0.89
MgO	0.19	0.09	0.13	0.15	0.13	0.15	0.10	0.09	0.10	0.14	0.17	0.18	0.22	0.14	0.10
CaO	1.08	0.70	1.07	0.70	0.89	0.98	0.83	0.64	1.05	1.05	1.16	1.07	1.50	1.04	1.53
Na_2O	3.78	3.76	3.77	3.55	3.57	3.74	3.01	3.54	3.99	3.83	4.00	3.90	3.99	4.14	4.38
K_2O	2.71	3.88	2.86	3.81	3.78	2.89	4.01	3.78	2.75	2.88	2.59	3.26	2.86	3.13	3.01
Cl	0.25	0.20	0.15	0.20	0.14	0.21	0.18	0.43	0.11	0.26	0.21	0.22	0.19	0.16	0.23
Totals	93.97	94.92	94.60	93.53	94.15	94.38	94.26	94.69	94.71	95.08	93.85	96.35	96.44	97.30	95.37
Analyses normalised to 100% loss free															
SiO_2	78.17	77.88	78.43	77.90	78.05	77.93	78.29	78.17	77.90	77.92	77.80	77.89	76.51	77.32	75.52
TiO_2	0.16	0.16	0.11	0.06	0.19	0.18	0.28	0.08	0.15	0.21	0.00	0.13	0.33	0.24	0.17
Al_2O_3	11.92	11.96	11.89	12.09	11.82	12.02	11.91	11.84	12.09	12.10	12.25	11.77	12.68	12.18	13.67
FeO	1.22	0.91	1.12	0.95	0.91	1.42	0.90	0.96	1.41	1.19	1.31	1.25	1.40	1.42	0.93
MgO	0.20	0.09	0.14	0.16	0.13	0.16	0.11	0.09	0.11	0.15	0.18	0.19	0.23	0.15	0.11
CaO	1.15	0.73	1.13	0.75	0.95	1.04	0.88	0.68	1.11	1.10	1.23	1.11	1.55	1.06	1.60
Na_2O	4.02	3.96	3.99	3.79	3.79	3.96	3.19	3.73	4.21	4.03	4.26	4.05	4.14	4.26	4.60
K_2O	2.89	4.09	3.03	4.07	4.01	3.07	4.25	3.99	2.90	3.03	2.75	3.39	2.96	3.21	3.16
Cl	0.26	0.21	0.16	0.22	0.15	0.23	0.19	0.46	0.11	0.27	0.23	0.23	0.20	0.17	0.24
Totals	100.00	100.00	100.00	100.00	100.00	100.00	100.00	100.00	100.00	100.00	100.00	100.00	100.00	100.00	100.00

	16	17	18	19	20	21	22	23	24	25	26	27	28	29	30
SiO_2	72.95	72.19	75.01	73.16	72.87	74.30	72.11	71.64	72.69	76.39	71.65	73.43	71.01	72.07	71.30
TiO_2	0.23	0.14	0.07	0.14	0.23	0.19	0.18	0.14	0.28	0.17	0.10	0.17	0.20	0.21	0.07
Al_2O_3	11.40	11.21	11.76	11.41	11.87	11.56	11.14	11.60	11.29	12.27	11.09	11.54	11.41	11.24	10.82
FeO	1.15	1.21	0.96	1.00	1.38	0.96	1.10	1.23	1.16	0.98	0.96	0.95	0.80	1.36	1.11
MgO	0.17	0.16	0.16	0.13	0.15	0.14	0.15	0.25	0.18	0.04	0.09	0.11	0.10	0.12	0.08
CaO	1.05	0.86	0.63	0.75	1.18	1.06	1.04	1.38	1.24	0.93	0.81	0.63	0.59	0.86	0.67
Na_2O	3.59	3.18	3.84	3.54	3.59	3.97	3.45	3.67	3.41	3.92	3.55	3.60	3.45	3.60	3.20
K_2O	2.85	3.55	3.62	3.72	3.18	2.97	3.87	3.06	2.84	3.48	3.11	3.97	3.56	3.59	3.48
Cl	0.15	0.19	0.19	0.27	0.21	0.24	0.23	0.19	0.19	0.22	0.18	0.25	0.25	0.21	0.20
Totals	93.53	92.68	96.23	94.11	94.66	95.40	93.26	93.15	93.28	98.40	91.53	94.65	91.36	93.25	90.92
Analyses normalised to 100% loss free															
SiO_2	77.99	77.89	77.94	77.74	76.98	77.89	77.32	76.91	77.92	77.63	78.29	77.58	77.72	77.29	78.42
TiO_2	0.24	0.15	0.07	0.15	0.25	0.20	0.19	0.15	0.30	0.17	0.11	0.18	0.22	0.22	0.08
Al_2O_3	12.18	12.09	12.22	12.12	12.54	12.12	11.94	12.45	12.10	12.47	12.11	12.19	12.49	12.06	11.90
FeO	1.23	1.30	1.00	1.06	1.46	1.01	1.18	1.32	1.25	0.99	1.04	1.00	0.87	1.45	1.22
MgO	0.18	0.17	0.17	0.14	0.15	0.15	0.16	0.26	0.19	0.04	0.09	0.12	0.11	0.12	0.09
CaO	1.12	0.93	0.66	0.79	1.24	1.11	1.11	1.48	1.32	0.95	0.88	0.66	0.65	0.92	0.73
Na_2O	3.84	3.43	3.99	3.76	3.79	4.16	3.70	3.94	3.66	3.98	3.87	3.81	3.78	3.86	3.52
K_2O	3.05	3.83	3.76	3.96	3.36	3.11	4.15	3.28	3.05	3.54	3.40	4.19	3.89	3.85	3.83
Cl	0.16	0.21	0.20	0.28	0.22	0.25	0.25	0.20	0.21	0.22	0.20	0.26	0.28	0.22	0.22
Totals	100.00	100.00	100.00	100.00	100.00	100.00	100.00	100.00	100.00	100.00	100.00	100.00	100.00	100.00	100.00

Apley Road #1:10cm

	1	2	3	4	5	6	7	8	9	10	11
SiO_2	70.22	73.57	69.55	70.78	72.76	72.49	68.42	71.02	73.25	72.96	71.39
TiO_2	0.15	0.26	0.08	0.14	0.17	0.39	0.65	0.32	0.24	0.23	0.11
Al_2O_3	10.50	11.06	10.68	10.67	11.15	10.83	11.50	10.73	10.91	11.25	10.88
FeO	1.08	0.89	1.27	1.23	0.98	1.27	2.41	1.02	0.90	1.22	0.96
MgO	0.19	0.32	0.18	0.11	0.27	0.17	0.54	0.16	0.31	0.18	0.07
CaO	0.97	0.99	1.04	0.92	0.75	1.14	1.51	0.93	1.04	1.03	0.70
Na_2O	3.32	3.27	3.40	3.69	3.26	3.33	3.30	3.71	3.17	3.50	3.11
K_2O	3.35	3.22	2.89	2.71	3.96	3.05	4.21	3.21	3.15	3.20	3.87
Cl	0.24	0.20	0.23	0.22	0.25	0.24	0.17	0.17	0.22	0.20	0.23
Totals	90.02	93.77	89.32	90.46	93.54	92.90	92.72	91.27	93.18	93.77	91.32
Analyses normalised to 100% loss free											
SiO_2	78.01	78.45	77.87	78.24	77.79	78.03	73.80	77.81	78.62	77.81	78.18
TiO_2	0.16	0.28	0.09	0.16	0.18	0.42	0.71	0.35	0.26	0.24	0.12
Al_2O_3	11.67	11.80	11.95	11.79	11.92	11.66	12.40	11.76	11.71	11.99	11.91
FeO	1.20	0.95	1.42	1.36	1.04	1.37	2.60	1.12	0.96	1.31	1.05
MgO	0.21	0.34	0.20	0.12	0.29	0.18	0.59	0.18	0.33	0.19	0.07
CaO	1.08	1.06	1.17	1.02	0.80	1.23	1.63	1.02	1.11	1.10	0.77
Na_2O	3.69	3.48	3.81	4.08	3.48	3.58	3.55	4.06	3.40	3.73	3.40
K_2O	3.72	3.43	3.23	3.00	4.23	3.28	4.54	3.52	3.38	3.41	4.23
Cl	0.26	0.21	0.25	0.24	0.27	0.26	0.19	0.18	0.23	0.22	0.25
Totals	100.00	100.00	100.00	100.00	100.00	100.00	100.00	100.00	100.00	100.00	100.00

Apley Road #2:20cm

	1	2	3	4	5	6	7	8	9	10	11	12
SiO_2	73.12	75.50	71.15	76.21	77.59	73.52	73.92	60.47	70.54	72.89	71.20	67.88
TiO_2	0.19	0.18	0.13	0.19	0.19	0.25	0.28	0.21	0.15	0.11	0.18	0.21
Al_2O_3	12.14	11.42	12.21	12.03	12.10	12.44	12.34	11.07	10.50	10.92	10.80	10.86
FeO	1.96	0.87	1.03	0.95	1.05	1.77	1.51	1.39	0.96	0.75	0.83	2.00
MgO	0.24	0.18	0.16	0.18	0.17	0.16	0.25	0.19	0.16	0.16	0.14	0.19
CaO	1.33	0.72	0.77	0.92	0.90	1.39	1.16	1.22	1.03	0.88	0.69	1.30
Na_2O	3.87	3.81	3.15	3.71	3.41	3.90	4.05	2.90	2.94	3.62	3.36	3.55
K_2O	2.67	3.20	3.57	3.22	3.26	2.64	3.08	2.67	2.68	3.43	3.08	2.72
Cl	0.22	0.16	0.14	0.12	0.10	0.23	0.17	0.26	0.20	0.21	0.18	0.19
Totals	95.74	96.03	92.30	97.54	98.77	96.29	96.76	80.38	89.15	92.97	90.45	88.89
Analyses normalised to 100% loss free												
SiO_2	76.37	78.61	77.08	78.14	78.56	76.35	76.40	75.23	79.13	78.40	78.71	76.36
TiO_2	0.20	0.19	0.14	0.20	0.19	0.26	0.29	0.26	0.16	0.12	0.20	0.24
Al_2O_3	12.68	11.89	13.23	12.33	12.25	12.92	12.75	13.77	11.77	11.75	11.94	12.22
FeO	2.05	0.91	1.12	0.97	1.06	1.84	1.56	1.73	1.08	0.81	0.92	2.25
MgO	0.25	0.18	0.17	0.19	0.17	0.17	0.26	0.24	0.18	0.17	0.16	0.22
CaO	1.39	0.75	0.84	0.94	0.91	1.45	1.20	1.52	1.16	0.95	0.76	1.46
Na_2O	4.04	3.97	3.42	3.80	3.45	4.05	4.19	3.61	3.30	3.89	3.71	3.99
K_2O	2.79	3.34	3.86	3.31	3.30	2.74	3.18	3.32	3.00	3.69	3.40	3.05
Cl	0.23	0.17	0.15	0.12	0.10	0.24	0.18	0.33	0.23	0.23	0.19	0.21
Totals	100.00	100.00	100.00	100.00	100.00	100.00	100.00	100.00	100.00	100.00	100.00	100.00

Apley Road #1:40cm

	1	2	3	4	5	6	7	8	9	10
SiO_2	74.88	76.99	75.12	75.98	75.95	72.77	72.34	71.20	72.45	74.53
TiO_2	0.25	0.22	0.11	0.26	0.12	0.15	0.18	0.11	0.10	0.25
Al_2O_3	11.83	12.43	11.69	11.65	11.89	11.97	11.70	11.61	11.78	12.31
FeO	1.25	1.19	1.10	1.22	1.61	1.06	1.31	1.72	0.93	1.25
MgO	0.10	0.10	0.12	0.07	0.09	0.08	0.13	0.19	0.22	0.18
CaO	1.02	1.05	1.13	1.09	0.89	0.97	1.09	1.25	1.09	1.30
Na_2O	4.33	4.51	4.01	2.94	4.50	4.11	4.18	3.72	4.09	3.86
K_2O	3.65	2.91	3.09	2.96	3.56	3.26	2.94	2.97	3.16	2.80
Cl	0.27	0.23	0.26	0.27	0.32	0.24	0.34	0.25	0.28	0.31
Totals	97.56	99.62	96.63	96.44	98.93	94.61	94.22	93.01	94.08	96.78
Analyses normalised to 100% loss free										
SiO_2	76.75	77.28	77.74	78.79	76.77	76.91	76.78	76.55	77.01	77.01
TiO_2	0.25	0.22	0.11	0.27	0.12	0.16	0.19	0.11	0.10	0.25
Al_2O_3	12.12	12.48	12.10	12.08	12.02	12.65	12.41	12.48	12.52	12.72
FeO	1.28	1.20	1.14	1.27	1.63	1.12	1.39	1.85	0.99	1.29
MgO	0.10	0.10	0.12	0.07	0.10	0.09	0.14	0.20	0.23	0.18
CaO	1.04	1.06	1.17	1.13	0.90	1.03	1.16	1.34	1.16	1.35
Na_2O	4.44	4.52	4.14	3.05	4.55	4.35	4.44	4.00	4.34	3.99
K_2O	3.74	2.92	3.20	3.07	3.60	3.45	3.12	3.20	3.35	2.89
Cl	0.28	0.23	0.26	0.28	0.32	0.25	0.36	0.26	0.29	0.32
Totals	100.00	100.00	100.00	100.00	100.00	100.00	100.00	100.00	100.00	100.00

Apley Road #1:50cm

	1	2	3	4	5	6	7	8	9	10
SiO_2	76.52	69.75	72.74	75.54	75.56	70.24	75.23	69.43	76.74	76.60
TiO_2	0.33	0.31	0.48	0.63	0.21	0.55	0.93	0.59	0.53	0.36
Al_2O_3	11.67	12.18	12.39	11.92	13.18	12.96	12.39	11.81	11.93	11.87
FeO	0.96	1.73	1.76	0.91	1.85	1.60	1.05	1.50	1.08	1.11
MgO	0.17	0.21	0.23	0.13	0.25	0.25	0.19	0.07	0.21	0.17
CaO	0.93	1.12	1.55	1.23	1.44	1.73	0.86	1.56	0.66	0.86
Na_2O	4.31	4.24	4.30	3.52	2.90	3.89	4.29	4.14	4.36	4.05
K_2O	3.42	2.65	3.03	3.50	3.29	2.75	3.64	3.10	3.31	3.66
Cl	0.64	0.20	0.72	0.38	0.87	0.40	0.91	0.55	0.63	0.19
Totals	98.94	92.39	97.19	97.75	99.55	94.36	99.48	92.74	99.46	98.87
Analyses normalised to 100% loss free										
SiO_2	77.34	75.49	74.84	77.27	75.90	74.43	75.62	74.86	77.16	77.47
TiO_2	0.33	0.34	0.49	0.64	0.21	0.58	0.93	0.63	0.54	0.37
Al_2O_3	11.80	13.19	12.75	12.19	13.24	13.73	12.45	12.73	12.00	12.01
FeO	0.97	1.87	1.81	0.93	1.86	1.69	1.06	1.62	1.09	1.12
MgO	0.17	0.23	0.23	0.14	0.25	0.26	0.19	0.08	0.21	0.17
CaO	0.94	1.21	1.59	1.26	1.44	1.84	0.86	1.68	0.66	0.87
Na_2O	4.35	4.59	4.42	3.60	2.91	4.12	4.31	4.46	4.39	4.09
K_2O	3.45	2.87	3.12	3.58	3.30	2.92	3.66	3.34	3.33	3.71
Cl	0.65	0.21	0.74	0.39	0.87	0.42	0.91	0.59	0.63	0.20
Totals	100.00	100.00	100.00	100.00	100.00	100.00	100.00	100.00	100.00	100.00

ApleyRoad #1:60cm

	1	2	3	4	5	6	7	8	9	10	11	12
SiO_2	74.09	70.69	70.65	74.89	71.10	69.68	72.18	70.99	73.43	72.51	71.81	72.32
TiO_2	0.50	0.58	0.14	0.37	0.11	0.49	0.00	0.47	0.39	0.38	0.45	0.10
Al_2O_3	11.90	11.80	11.43	12.21	11.86	11.51	12.61	11.74	12.11	12.03	11.81	11.97
FeO	1.03	0.84	1.06	1.09	1.06	1.39	1.54	1.14	0.96	0.84	0.93	1.30
MgO	0.19	0.09	0.15	0.20	0.10	0.10	0.15	0.19	0.14	0.21	0.18	0.13
CaO	1.79	1.20	1.46	0.90	0.86	0.96	1.59	1.26	0.95	0.84	0.82	1.06
Na_2O	3.98	3.96	3.85	4.20	3.39	4.14	4.17	3.99	4.18	3.97	4.20	3.91
K_2O	4.34	3.99	2.93	3.92	3.98	3.51	3.17	3.17	3.42	4.21	3.44	3.12
Cl	0.69	0.79	0.42	0.38	0.24	0.29	0.40	0.84	0.13	0.66	0.40	0.58
Totals	98.50	93.94	92.08	98.15	92.69	92.08	95.81	93.78	95.72	95.66	94.03	94.48
Analyses normalised to 100% loss free												
SiO_2	75.22	75.25	76.72	76.31	76.70	75.67	75.34	75.70	76.71	75.80	76.37	76.55
TiO_2	0.51	0.62	0.16	0.38	0.12	0.53	0.00	0.50	0.41	0.40	0.47	0.10
Al_2O_3	12.09	12.56	12.41	12.44	12.80	12.50	13.16	12.51	12.65	12.58	12.56	12.66
FeO	1.05	0.90	1.15	1.11	1.14	1.51	1.61	1.21	1.01	0.88	0.99	1.37
MgO	0.19	0.09	0.16	0.20	0.11	0.11	0.15	0.20	0.15	0.22	0.20	0.14
CaO	1.81	1.28	1.59	0.92	0.92	1.05	1.66	1.34	0.99	0.88	0.87	1.12
Na_2O	4.04	4.22	4.18	4.28	3.66	4.49	4.35	4.26	4.37	4.15	4.46	4.14
K_2O	4.41	4.24	3.18	3.99	4.29	3.81	3.30	3.38	3.57	4.40	3.66	3.30
Cl	0.70	0.84	0.45	0.38	0.26	0.32	0.42	0.90	0.14	0.69	0.42	0.62
Totals	100.00	100.00	100.00	100.00	100.00	100.00	100.00	100.00	100.00	100.00	100.00	100.00

Apley Road #1:130cm

	1	2	3	4	5	6	7	8	9	10	11
SiO_2	69.12	69.48	74.07	69.37	70.00	70.80	71.75	73.56	72.80	71.83	72.48
TiO_2	0.15	0.13	0.10	0.11	0.07	0.13	0.13	0.19	0.13	0.18	0.21
Al_2O_3	11.34	11.78	11.77	11.79	11.57	11.67	11.47	11.78	12.01	11.83	11.66
FeO	1.14	1.17	1.10	0.97	1.11	1.02	1.10	1.16	1.19	1.02	0.98
MgO	0.21	0.14	0.14	0.10	0.09	0.14	0.11	0.13	0.08	0.09	0.08
CaO	1.08	1.10	1.13	0.82	0.83	1.08	1.05	1.20	1.09	1.12	0.84
Na_2O	3.78	3.76	3.87	3.42	2.82	4.07	4.05	3.97	4.00	3.92	3.53
K_2O	2.79	2.94	3.24	3.64	3.78	2.60	2.95	3.20	3.10	2.96	3.80
Cl	0.30	0.22	0.28	0.11	0.26	0.18	0.24	0.21	0.25	0.24	0.17
Totals	89.92	90.73	95.69	90.32	90.53	91.67	92.84	95.40	94.64	93.17	93.75
Analyses normalised to 100% loss free											
SiO_2	76.87	76.59	77.41	76.80	77.32	77.23	77.28	77.11	76.92	77.09	77.31
TiO_2	0.17	0.14	0.10	0.12	0.08	0.14	0.14	0.20	0.13	0.19	0.22
Al_2O_3	12.61	12.99	12.30	13.06	12.78	12.73	12.35	12.35	12.69	12.69	12.44
FeO	1.27	1.29	1.15	1.07	1.23	1.11	1.18	1.21	1.25	1.09	1.05
MgO	0.24	0.16	0.14	0.11	0.10	0.15	0.12	0.14	0.09	0.10	0.09
CaO	1.20	1.21	1.18	0.91	0.92	1.18	1.13	1.26	1.15	1.20	0.90
Na_2O	4.20	4.15	4.05	3.78	3.11	4.44	4.36	4.16	4.22	4.21	3.76
K_2O	3.10	3.24	3.39	4.03	4.17	2.84	3.18	3.36	3.27	3.17	4.06
Cl	0.34	0.24	0.29	0.12	0.29	0.19	0.26	0.22	0.26	0.26	0.18
Totals	100.00	100.00	100.00	100.00	100.00	100.00	100.00	100.00	100.00	100.00	100.00

Apley Road #1:150-160cm

	1	2	3	4	5	6	7	8	9	10	11	12
SiO_2	72.26	74.49	74.13	74.38	71.62	73.18	74.00	74.70	71.62	73.21	72.31	71.38
TiO_2	0.00	0.16	0.18	0.00	0.07	0.10	0.13	0.09	0.20	0.28	0.11	0.12
Al_2O_3	11.97	12.29	11.81	12.21	11.59	11.79	12.02	12.03	11.85	12.00	11.90	11.89
FeO	1.19	1.20	1.33	1.11	1.06	1.12	1.01	1.10	1.10	1.05	1.19	1.84
MgO	0.14	0.16	0.16	0.09	0.13	0.15	0.15	0.13	0.19	0.10	0.18	0.17
CaO	1.53	1.01	1.04	1.05	0.97	0.81	1.06	1.04	1.30	1.32	0.96	1.01
Na_2O	4.07	4.13	4.09	4.06	3.78	3.80	3.98	4.06	3.73	3.52	2.61	3.76
K_2O	2.62	3.14	3.10	3.26	3.08	3.89	3.25	3.24	2.99	3.84	3.23	3.06
Cl	0.24	0.35	0.23	0.30	0.20	0.22	0.00	0.18	0.27	0.17	0.27	0.27
Totals	94.00	96.92	96.07	96.45	92.50	95.06	95.60	96.56	93.24	95.48	92.76	93.50
Analyses normalised to 100% loss free												
SiO_2	76.87	76.85	77.16	77.11	77.43	76.99	77.41	77.36	76.81	76.67	77.96	76.34
TiO_2	0.00	0.16	0.19	0.00	0.08	0.11	0.13	0.09	0.21	0.30	0.12	0.13
Al_2O_3	12.73	12.68	12.30	12.66	12.53	12.40	12.57	12.46	12.71	12.57	12.83	12.72
FeO	1.26	1.24	1.38	1.15	1.14	1.18	1.06	1.14	1.18	1.10	1.28	1.97
MgO	0.14	0.16	0.17	0.09	0.14	0.16	0.15	0.14	0.21	0.10	0.19	0.18
CaO	1.63	1.04	1.09	1.09	1.05	0.85	1.11	1.07	1.40	1.38	1.03	1.08
Na_2O	4.33	4.26	4.26	4.21	4.08	4.00	4.16	4.20	4.00	3.69	2.82	4.02
K_2O	2.79	3.24	3.22	3.38	3.33	4.09	3.40	3.36	3.20	4.02	3.48	3.27
Cl	0.26	0.36	0.24	0.31	0.21	0.23	0.00	0.18	0.28	0.18	0.29	0.29
Totals	100.00	100.00	100.00	100.00	100.00	100.00	100.00	100.00	100.00	100.00	100.00	100.00

Apley Road #1: 170cm

	1	2	3	4	5	6	7	8	9	10	11	12	13	14	15	16	17	18
SiO_2	75.75	71.30	73.98	76.42	77.57	74.28	74.47	73.68	74.59	75.67	72.94	72.44	73.19	69.80	72.90	73.16	71.98	72.97
TiO_2	0.13	0.23	0.13	0.22	0.16	0.23	0.19	0.20	0.10	0.11	0.18	0.21	0.13	0.10	0.15	0.17	0.13	0.08
Al_2O_3	12.36	12.01	11.82	12.17	12.35	11.64	11.50	11.78	11.49	11.81	12.23	11.66	11.77	11.51	11.75	11.59	11.74	11.61
FeO	1.14	1.47	1.17	1.29	1.18	1.13	1.21	1.09	1.21	1.27	1.52	1.10	1.35	1.10	1.09	1.24	1.21	0.91
MgO	0.12	0.13	0.14	0.14	0.18	0.20	0.15	0.25	0.11	0.11	0.07	0.12	0.12	0.16	0.15	0.14	0.16	0.12
CaO	1.11	1.00	1.24	1.06	1.40	1.24	0.98	1.06	1.15	1.08	1.00	0.99	1.07	1.18	1.04	1.01	1.08	0.96
Na_2O	4.30	4.13	4.12	4.25	3.15	3.87	3.82	4.20	4.29	3.94	3.60	3.91	3.92	3.43	3.91	3.87	3.85	2.51
K_2O	3.16	3.16	2.94	3.16	3.28	3.30	3.00	2.76	2.98	3.75	4.07	3.00	2.80	3.24	3.12	2.91	2.93	2.88
Cl	0.20	0.37	0.20	0.15	0.26	0.31	0.27	0.37	0.21	0.25	0.27	0.23	0.33	0.28	0.25	0.32	0.22	0.27
Totals	98.28	93.80	95.76	98.84	99.54	96.19	95.59	95.40	96.13	97.89	95.86	93.66	94.67	90.80	94.35	94.41	93.28	92.29
Analyses normalised to 100% loss free																		
SiO_2	77.08	76.01	77.26	77.31	77.93	77.22	77.91	77.23	77.59	77.30	76.09	77.35	77.30	76.87	77.26	77.49	77.17	79.06
TiO_2	0.14	0.24	0.14	0.22	0.16	0.24	0.20	0.21	0.11	0.11	0.18	0.22	0.14	0.11	0.15	0.18	0.14	0.09
Al_2O_3	12.58	12.81	12.34	12.31	12.40	12.10	12.03	12.34	11.95	12.06	12.75	12.45	12.44	12.67	12.46	12.28	12.59	12.58
FeO	1.16	1.57	1.22	1.30	1.19	1.17	1.26	1.15	1.26	1.29	1.58	1.17	1.43	1.21	1.15	1.32	1.29	0.98
MgO	0.12	0.14	0.15	0.14	0.18	0.21	0.16	0.27	0.11	0.11	0.07	0.13	0.12	0.17	0.16	0.15	0.17	0.13
CaO	1.13	1.07	1.30	1.07	1.41	1.28	1.03	1.11	1.20	1.10	1.04	1.06	1.13	1.30	1.11	1.07	1.15	1.04
Na_2O	4.38	4.40	4.30	4.30	3.17	4.02	3.99	4.40	4.47	4.02	3.75	4.17	4.14	3.78	4.15	4.09	4.12	2.72
K_2O	3.22	3.36	3.07	3.20	3.30	3.43	3.14	2.90	3.10	3.83	4.25	3.20	2.95	3.57	3.30	3.08	3.14	3.12
Cl	0.21	0.39	0.21	0.15	0.26	0.32	0.28	0.39	0.21	0.26	0.28	0.24	0.35	0.31	0.26	0.34	0.23	0.29
Totals	100.00	100.00	100.00	100.00	100.00	100.00	100.00	100.00	100.00	100.00	100.00	100.00	100.00	100.00	100.00	100.00	100.00	100.00

Apley Road #1:180cm

	1	2	3	4	5	6	7	8	9	10
SiO_2	72.44	71.37	69.39	70.14	69.98	72.04	73.82	72.30	71.69	71.39
TiO_2	0.15	0.13	0.14	0.20	0.18	0.07	0.10	0.13	0.10	0.18
Al_2O_3	11.44	11.26	11.50	13.01	13.04	11.78	12.26	11.65	11.64	11.63
FeO	1.17	1.07	1.15	1.69	1.99	1.21	1.24	1.20	1.25	1.11
MgO	0.03	0.11	0.48	0.22	0.23	0.15	0.21	0.11	0.06	0.11
CaO	1.11	1.00	1.08	1.78	1.88	1.11	1.22	1.01	0.92	1.19
Na_2O	3.80	3.57	3.73	4.33	4.53	3.89	4.12	3.92	3.85	3.59
K_2O	3.23	3.04	3.11	2.57	2.10	3.34	3.34	3.00	2.87	2.87
Cl	0.17	0.20	0.27	0.22	0.22	0.12	0.22	0.24	0.24	0.19
Totals	93.55	91.74	90.85	94.16	94.15	93.70	96.53	93.55	92.61	92.26
Analyses normalised to 100% loss free										
SiO_2	77.44	77.80	76.37	74.50	74.33	76.88	76.47	77.28	77.41	77.38
TiO_2	0.16	0.14	0.15	0.21	0.19	0.08	0.10	0.14	0.11	0.20
Al_2O_3	12.23	12.27	12.66	13.82	13.85	12.57	12.70	12.45	12.57	12.60
FeO	1.25	1.17	1.27	1.79	2.12	1.29	1.29	1.28	1.35	1.20
MgO	0.03	0.12	0.53	0.23	0.24	0.16	0.21	0.12	0.07	0.12
CaO	1.19	1.09	1.19	1.89	1.99	1.18	1.27	1.08	0.99	1.29
Na_2O	4.07	3.89	4.11	4.60	4.82	4.15	4.26	4.19	4.15	3.89
K_2O	3.45	3.31	3.42	2.72	2.23	3.56	3.46	3.20	3.10	3.11
Cl	0.19	0.21	0.29	0.24	0.23	0.13	0.23	0.26	0.25	0.21
Totals	100.00	100.00	100.00	100.00	100.00	100.00	100.00	100.00	100.00	100.00

Apley Road #1:190cm

	1	2	3	4	5	6	7	8	9	10	11	12	13	14	15
SiO_2	73.83	72.87	71.87	71.25	69.18	72.09	72.24	71.78	68.24	73.38	70.42	71.97	69.49	71.79	71.75
TiO_2	0.21	0.12	0.12	0.12	0.27	0.21	0.13	0.12	0.16	0.17	0.15	0.20	0.12	0.15	0.20
Al_2O_3	11.92	12.17	11.69	10.85	10.28	10.70	11.07	10.89	10.97	11.30	10.58	10.84	10.52	10.65	10.82
FeO	1.08	0.96	0.96	1.03	1.13	0.80	1.18	1.15	1.08	1.34	1.00	1.04	0.84	1.12	1.25
MgO	0.12	0.13	0.14	0.16	0.14	0.16	0.13	0.07	0.25	0.13	0.10	0.16	0.09	0.14	0.12
CaO	1.08	1.07	1.00	1.06	1.05	0.88	1.12	0.95	1.08	1.07	0.90	1.07	0.92	0.96	1.01
Na_2O	3.82	3.80	3.91	3.03	3.30	3.35	3.47	3.42	3.02	3.23	3.07	3.53	2.84	3.01	3.58
K_2O	3.20	3.50	3.40	2.82	2.95	3.47	3.07	2.92	2.63	2.98	2.76	2.82	3.36	3.25	3.26
Cl	0.20	0.27	0.30	0.20	0.21	0.14	0.19	0.23	0.29	0.27	0.16	0.33	0.16	0.23	0.25
Totals	95.46	94.91	93.38	90.53	88.49	91.80	92.60	91.55	87.72	93.87	89.14	91.95	88.34	91.30	92.22
Analyses normalised to 100% loss free															
SiO_2	77.34	76.78	76.96	78.71	78.17	78.53	78.01	78.41	77.80	78.17	79.00	78.27	78.66	78.63	77.80
TiO_2	0.22	0.13	0.13	0.13	0.31	0.23	0.14	0.13	0.18	0.18	0.17	0.22	0.14	0.16	0.22
Al_2O_3	12.48	12.83	12.51	11.99	11.61	11.66	11.95	11.90	12.50	12.04	11.87	11.79	11.91	11.67	11.73
FeO	1.14	1.02	1.03	1.14	1.27	0.87	1.28	1.26	1.23	1.43	1.12	1.13	0.95	1.23	1.35
MgO	0.13	0.14	0.15	0.18	0.15	0.17	0.14	0.08	0.28	0.14	0.11	0.18	0.10	0.16	0.13
CaO	1.14	1.13	1.07	1.17	1.18	0.96	1.21	1.04	1.23	1.14	1.01	1.16	1.04	1.05	1.09
Na_2O	4.00	4.01	4.18	3.35	3.73	3.65	3.75	3.74	3.44	3.44	3.45	3.84	3.22	3.30	3.88
K_2O	3.36	3.69	3.64	3.12	3.33	3.78	3.31	3.19	2.99	3.17	3.10	3.07	3.80	3.56	3.53
Cl	0.21	0.28	0.32	0.22	0.24	0.15	0.21	0.25	0.33	0.29	0.18	0.36	0.18	0.25	0.27
Totals	100.00	100.00	100.00	100.00	100.00	100.00	100.00	100.00	100.00	100.00	100.00	100.00	100.00	100.00	100.00

Apley Road #1:200cm

	1	2	3	4	5	6	7	8	9	10	11
SiO_2	70.70	70.59	69.87	70.54	71.90	71.89	71.64	72.47	72.31	71.58	69.03
TiO_2	0.99	0.12	0.00	0.21	0.22	0.10	0.14	0.16	0.17	0.09	0.12
Al_2O_3	11.66	11.56	11.29	11.33	11.53	11.57	11.76	11.52	11.75	11.45	11.38
FeO	1.07	1.09	1.20	1.05	1.11	1.14	1.32	1.10	1.13	1.30	1.02
MgO	0.15	0.16	0.13	0.18	0.15	0.14	0.14	0.16	0.10	0.11	0.11
CaO	1.24	0.92	1.05	1.03	1.06	2.05	1.01	1.14	1.01	1.02	0.86
Na_2O	3.90	4.05	3.83	3.80	4.17	3.93	3.81	3.77	3.73	3.75	3.89
K_2O	3.22	2.97	3.02	2.97	2.98	2.96	2.90	3.05	2.99	3.36	2.88
Cl	0.35	0.29	0.25	0.27	0.22	0.27	0.26	0.25	0.22	0.25	0.22
Totals	93.27	91.74	90.62	91.38	93.32	94.05	92.97	93.62	93.41	92.90	89.51
Analyses normalised to 100% loss free											
SiO_2	75.80	76.94	77.10	77.20	77.05	76.44	77.05	77.41	77.40	77.05	77.12
TiO_2	1.06	0.13	0.00	0.23	0.23	0.11	0.15	0.18	0.19	0.10	0.14
Al_2O_3	12.50	12.60	12.45	12.40	12.35	12.30	12.65	12.31	12.58	12.33	12.71
FeO	1.15	1.18	1.32	1.15	1.19	1.21	1.42	1.17	1.21	1.40	1.13
MgO	0.16	0.18	0.14	0.20	0.16	0.14	0.15	0.17	0.10	0.12	0.12
CaO	1.33	1.00	1.16	1.12	1.13	2.18	1.09	1.22	1.09	1.10	0.97
Na_2O	4.18	4.41	4.23	4.15	4.47	4.18	4.09	4.02	3.99	4.04	4.34
K_2O	3.45	3.24	3.33	3.25	3.19	3.14	3.12	3.26	3.20	3.62	3.22
Cl	0.38	0.32	0.27	0.29	0.23	0.29	0.28	0.27	0.24	0.27	0.25
Totals	100.00	100.00	100.00	100.00	100.00	100.00	100.00	100.00	100.00	100.00	100.00

Apley Road #1:240cm

	1	2	3	4	5	6	7	8	9	10
SiO_2	72.51	71.90	71.11	71.62	71.60	71.76	70.90	72.43	73.25	70.95
TiO_2	0.14	0.11	0.18	0.10	0.18	0.13	0.22	0.17	0.12	0.18
Al_2O_3	11.66	11.57	11.50	11.69	11.77	11.79	11.49	11.71	11.62	11.41
FeO	1.08	1.19	1.43	1.16	1.14	1.02	1.02	1.08	0.99	1.18
MgO	0.22	0.15	0.13	0.14	0.12	0.12	0.16	0.10	0.07	0.09
CaO	1.00	1.16	1.01	1.08	1.07	1.05	0.90	0.98	0.98	0.96
Na_2O	3.77	3.79	3.76	3.76	3.87	3.96	3.52	3.93	3.72	3.80
K_2O	2.96	2.89	2.78	3.01	2.88	3.10	2.77	2.99	3.30	2.95
Cl	0.30	0.25	0.19	0.22	0.24	0.25	0.29	0.22	0.28	0.31
Totals	93.64	93.00	92.10	92.78	92.87	93.17	91.27	93.60	94.33	91.83
Analyses normalised to 100% loss free										
SiO_2	77.44	77.31	77.21	77.19	77.09	77.02	77.68	77.38	77.65	77.26
TiO_2	0.14	0.11	0.20	0.11	0.20	0.14	0.24	0.18	0.13	0.20
Al_2O_3	12.45	12.44	12.49	12.60	12.67	12.66	12.59	12.51	12.32	12.42
FeO	1.16	1.28	1.55	1.25	1.23	1.10	1.11	1.15	1.05	1.29
MgO	0.23	0.16	0.14	0.15	0.13	0.13	0.18	0.11	0.07	0.10
CaO	1.07	1.24	1.10	1.17	1.16	1.12	0.99	1.04	1.03	1.05
Na_2O	4.03	4.07	4.09	4.05	4.17	4.25	3.85	4.20	3.95	4.14
K_2O	3.16	3.11	3.02	3.25	3.10	3.33	3.04	3.19	3.50	3.21
Cl	0.32	0.27	0.21	0.23	0.26	0.27	0.32	0.23	0.30	0.33
Totals	100.00	100.00	100.00	100.00	100.00	100.00	100.00	100.00	100.00	100.00

Apley Road #1:260cm

	1	2	3	4	5	6	7	8	9	10
SiO_2	73.04	72.85	71.74	73.12	72.88	73.74	71.97	74.36	72.43	73.06
TiO_2	0.11	0.14	0.19	0.13	0.11	0.20	0.11	0.12	0.19	0.18
Al_2O_3	11.68	12.03	11.65	11.73	11.65	11.82	11.76	12.00	11.51	11.83
FeO	1.12	1.27	0.91	1.13	1.35	1.35	1.30	1.04	1.33	1.09
MgO	0.16	0.21	0.19	0.19	0.14	0.11	0.11	0.10	0.15	0.16
CaO	1.07	0.98	1.05	1.19	1.09	1.10	0.96	0.98	1.02	1.04
Na_2O	3.78	3.93	3.90	3.77	3.76	2.76	3.77	3.72	3.95	3.70
K_2O	2.83	2.75	3.08	2.69	2.63	3.18	2.80	3.14	2.99	2.87
Cl	0.23	0.19	0.24	0.25	0.21	0.21	0.24	0.24	0.35	0.21
Totals	94.00	94.34	92.94	94.21	93.81	94.47	93.02	95.69	93.93	94.12
Analyses normalised to 100% loss free										
SiO_2	77.70	77.21	77.19	77.62	77.69	78.05	77.38	77.71	77.11	77.62
TiO_2	0.12	0.15	0.20	0.14	0.11	0.21	0.12	0.12	0.20	0.19
Al_2O_3	12.42	12.75	12.54	12.45	12.41	12.51	12.64	12.54	12.26	12.56
FeO	1.19	1.34	0.98	1.20	1.44	1.43	1.40	1.08	1.42	1.15
MgO	0.16	0.22	0.20	0.20	0.15	0.11	0.12	0.10	0.16	0.17
CaO	1.13	1.04	1.13	1.27	1.16	1.17	1.03	1.02	1.09	1.10
Na_2O	4.02	4.17	4.20	4.00	4.00	2.92	4.05	3.88	4.20	3.93
K_2O	3.01	2.91	3.31	2.86	2.80	3.37	3.01	3.28	3.18	3.05
Cl	0.25	0.20	0.25	0.27	0.22	0.22	0.26	0.25	0.38	0.22
Totals	100.00	100.00	100.00	100.00	100.00	100.00	100.00	100.00	100.00	100.00

Apley Road #1:280cm

	1	2	3	4	5	6	7	8	9	10	11	12	13	14	15	16
SiO_2	69.97	69.44	70.95	70.29	71.46	69.07	69.66	70.91	70.99	69.95	69.27	71.23	70.86	69.21	67.97	68.47
TiO_2	0.21	0.10	0.17	0.13	0.12	0.19	0.20	0.13	0.07	0.09	0.11	0.15	0.14	0.20	0.13	0.10
Al_2O_3	11.62	11.43	11.87	11.26	11.33	11.34	11.43	11.55	11.35	11.41	11.37	11.72	11.45	11.27	11.22	11.05
FeO	1.16	0.99	1.48	1.07	1.15	1.07	1.19	1.12	1.22	1.01	1.12	1.16	1.32	0.98	0.73	0.94
MgO	0.16	0.15	0.14	0.08	0.12	0.01	0.13	0.19	0.14	0.11	0.12	0.13	0.16	0.09	0.12	0.14
CaO	1.06	1.09	0.87	1.09	1.07	1.07	1.09	1.10	1.10	0.99	1.27	1.14	1.09	0.95	1.02	1.02
Na_2O	3.71	3.90	4.12	3.83	3.88	3.82	3.73	4.05	3.89	4.06	3.96	3.71	3.85	3.52	3.16	3.87
K_2O	2.76	2.74	3.47	2.54	3.00	2.85	3.02	2.94	2.79	2.96	2.59	2.90	2.67	3.00	3.34	2.89
Cl	0.19	0.22	0.29	0.25	0.26	0.23	0.31	0.21	0.30	0.22	0.18	0.22	0.25	0.27	0.30	0.34
Totals	90.84	90.05	93.36	90.52	92.37	89.72	90.74	92.20	91.84	90.79	89.98	92.36	91.79	89.48	89.98	88.81
Analyses normalised to 100% loss free																
SiO_2	77.02	77.12	76.00	77.65	77.35	76.98	76.76	76.91	77.29	77.04	76.99	77.12	77.20	77.34	75.54	77.09
TiO_2	0.23	0.11	0.18	0.14	0.13	0.21	0.22	0.14	0.08	0.10	0.12	0.17	0.15	0.22	0.14	0.11
Al_2O_3	12.80	12.69	12.71	12.44	12.27	12.64	12.60	12.53	12.36	12.57	12.64	12.69	12.47	12.60	12.47	12.44
FeO	1.27	1.10	1.59	1.18	1.24	1.19	1.31	1.21	1.33	1.11	1.24	1.25	1.43	1.10	0.81	1.06
MgO	0.18	0.17	0.15	0.09	0.13	0.01	0.14	0.20	0.15	0.12	0.14	0.14	0.17	0.09	0.13	0.16
CaO	1.17	1.21	0.93	1.20	1.15	1.20	1.20	1.20	1.19	1.09	1.41	1.24	1.18	1.06	1.13	1.15
Na_2O	4.08	4.33	4.41	4.23	4.20	4.26	4.11	4.39	4.23	4.47	4.40	4.02	4.20	3.94	3.51	4.36
K_2O	3.04	3.05	3.72	2.80	3.25	3.17	3.32	3.19	3.03	3.26	2.88	3.14	2.91	3.35	3.71	3.26
Cl	0.21	0.24	0.31	0.27	0.28	0.26	0.34	0.22	0.32	0.25	0.19	0.23	0.27	0.30	0.33	0.38
Totals	100.00	100.00	100.00	100.00	100.00	100.00	100.00	100.00	100.00	100.00	100.00	100.00	100.00	100.00	100.00	100.00

Apley Road #1:350cm

	1	2	3	4	5	6	7	8	9	10	11	12	13	14	15	16
SiO_2	70.88	71.27	70.22	71.82	71.73	71.29	72.17	71.71	69.94	72.25	69.58	70.45	70.50	71.11	70.24	70.46
TiO_2	0.18	0.17	0.18	0.13	0.16	0.24	0.12	0.17	0.12	0.16	4.36	0.23	0.12	0.20	0.11	0.10
Al_2O_3	11.63	11.34	11.40	11.58	11.55	11.66	11.75	11.68	11.52	12.08	11.53	11.43	11.78	11.64	11.91	11.63
FeO	1.17	1.04	0.89	1.18	0.96	0.94	1.10	1.02	1.03	0.96	1.02	1.08	1.22	1.24	1.28	1.11
MgO	0.14	0.16	0.10	0.14	0.14	0.19	0.16	0.18	0.13	0.21	0.13	0.12	0.14	0.18	0.19	0.14
CaO	1.08	0.98	1.08	0.96	1.11	1.13	1.23	1.09	1.18	0.97	1.11	1.15	1.10	1.19	1.19	0.95
Na_2O	3.78	3.85	3.16	3.58	4.00	3.88	3.77	3.79	3.60	3.54	3.81	3.59	3.91	3.85	3.67	4.14
K_2O	2.48	2.94	3.33	2.84	2.87	2.84	2.98	2.66	2.84	3.83	2.63	2.85	2.49	2.75	2.71	3.01
Cl	0.19	0.24	0.25	0.23	0.21	0.20	0.21	0.20	0.22	0.32	0.27	0.28	0.27	0.13	0.28	0.26
Totals	91.53	91.99	90.59	92.46	92.74	92.36	93.48	92.50	90.57	94.32	94.43	91.18	91.51	92.28	91.57	91.80
Analyses normalised to 100% loss free																
SiO_2	77.44	77.47	77.51	77.68	77.35	77.19	77.20	77.53	77.22	76.60	73.69	77.27	77.04	77.06	76.71	76.75
TiO_2	0.20	0.19	0.20	0.14	0.17	0.26	0.13	0.19	0.13	0.17	4.62	0.25	0.13	0.21	0.11	0.11
Al_2O_3	12.70	12.32	12.58	12.52	12.46	12.63	12.57	12.63	12.72	12.81	12.21	12.54	12.87	12.62	13.00	12.67
FeO	1.28	1.13	0.98	1.27	1.04	1.02	1.17	1.10	1.14	1.02	1.08	1.18	1.33	1.34	1.39	1.21
MgO	0.15	0.18	0.11	0.16	0.16	0.20	0.17	0.19	0.14	0.22	0.13	0.14	0.15	0.19	0.20	0.16
CaO	1.18	1.06	1.19	1.04	1.19	1.22	1.32	1.18	1.31	1.02	1.17	1.26	1.20	1.28	1.30	1.03
Na_2O	4.13	4.19	3.49	3.87	4.32	4.20	4.03	4.09	3.98	3.75	4.03	3.93	4.27	4.17	4.01	4.51
K_2O	2.71	3.20	3.67	3.07	3.10	3.07	3.18	2.88	3.13	4.06	2.78	3.12	2.72	2.98	2.96	3.28
Cl	0.21	0.27	0.27	0.25	0.23	0.21	0.23	0.22	0.24	0.34	0.28	0.31	0.29	0.14	0.30	0.28
Totals	100.00	100.00	100.00	100.00	100.00	100.00	100.00	100.00	100.00	100.00	100.00	100.00	100.00	100.00	100.00	100.00

Apley Road #2: 90cm

	1	2	3	4	5
SiO_2	71.50	74.02	74.56	73.57	71.67
TiO_2	0.08	0.10	0.15	0.17	0.17
Al_2O_3	11.62	11.97	12.11	11.73	11.86
FeO	1.04	1.22	1.00	1.09	1.20
MgO	0.10	0.22	0.12	0.15	0.29
CaO	1.03	1.20	0.92	1.06	1.06
Na_2O	3.90	4.00	3.63	3.49	3.48
K_2O	3.34	3.22	3.68	3.66	2.82
Totals	92.61	95.95	96.17	94.90	92.54
Analyses normalised to 100% loss free					
SiO_2	77.21	77.15	77.53	77.52	77.45
TiO_2	0.08	0.11	0.15	0.17	0.18
Al_2O_3	12.55	12.47	12.60	12.36	12.81
FeO	1.12	1.28	1.04	1.14	1.29
MgO	0.10	0.23	0.13	0.16	0.32
CaO	1.11	1.25	0.96	1.11	1.14
Na_2O	4.21	4.17	3.77	3.67	3.76
K_2O	3.61	3.36	3.83	3.86	3.05
Totals	100.00	100.00	100.00	100.00	100.00

Apley Road #2:110cm

	1	2	3	4	5	6	7	8	9	10	11	12	13	14	15	16
SiO_2	67.28	71.55	70.23	73.30	72.26	69.79	70.75	70.85	71.03	71.80	71.82	71.91	71.55	71.16	71.84	70.56
TiO_2	0.17	0.18	0.16	0.06	0.13	0.17	0.13	0.15	0.06	0.09	0.13	0.08	0.18	0.20	0.12	0.19
Al_2O_3	10.12	11.51	10.50	11.08	11.28	11.22	10.72	10.70	10.98	11.05	11.13	10.82	11.11	11.33	11.38	11.03
FeO	1.29	1.78	0.90	1.19	0.97	1.13	1.06	1.06	0.98	0.96	0.95	1.15	1.00	1.72	1.20	0.96
MgO	0.21	0.09	0.00	0.20	0.33	0.27	0.45	0.00	0.09	0.16	0.41	0.13	0.32	0.20	0.46	0.13
CaO	0.74	1.41	0.90	1.29	0.96	1.03	1.03	0.73	0.63	0.71	0.97	1.22	0.91	1.26	0.89	1.46
Na_2O	2.50	4.04	2.84	3.50	3.24	2.70	2.85	3.55	3.63	2.77	3.37	3.43	3.61	2.56	3.45	3.55
K_2O	4.20	2.57	3.53	2.89	3.85	3.51	3.51	3.67	4.22	3.91	3.80	3.06	3.68	2.80	3.60	3.36
Cl	0.23	0.16	0.20	0.11	0.23	0.26	0.14	0.19	0.22	0.24	0.20	n.d.	n.d.	n.d.	n.d.	n.d.
Totals	86.73	93.28	89.26	93.63	93.25	90.08	90.65	90.91	91.85	91.69	92.76	91.79	92.37	91.22	92.92	91.25
Analyses normalised to 100% loss free																
SiO_2	77.57	76.70	78.68	78.29	77.49	77.48	78.05	77.93	77.34	78.31	77.42	78.34	77.47	78.01	77.31	77.33
TiO_2	0.19	0.20	0.18	0.07	0.14	0.19	0.15	0.17	0.07	0.09	0.14	0.09	0.20	0.22	0.12	0.21
Al_2O_3	11.67	12.34	11.76	11.84	12.09	12.46	11.83	11.77	11.96	12.05	12.00	11.79	12.03	12.42	12.25	12.09
FeO	1.49	1.91	1.01	1.27	1.04	1.26	1.17	1.16	1.07	1.05	1.02	1.26	1.09	1.88	1.29	1.05
MgO	0.25	0.10	0.00	0.22	0.36	0.30	0.49	0.00	0.10	0.17	0.44	0.14	0.35	0.22	0.49	0.15
CaO	0.85	1.51	1.01	1.38	1.03	1.14	1.14	0.81	0.69	0.78	1.04	1.33	0.99	1.38	0.95	1.60
Na_2O	2.88	4.33	3.18	3.74	3.47	3.00	3.15	3.91	3.96	3.02	3.63	3.73	3.90	2.80	3.71	3.89
K_2O	4.84	2.75	3.95	3.09	4.12	3.89	3.87	4.04	4.59	4.27	4.10	3.33	3.99	3.07	3.88	3.68
Cl	0.27	0.17	0.23	0.12	0.25	0.29	0.15	0.21	0.24	0.26	0.22	n.d.	n.d.	n.d.	n.d.	n.d.
Totals	100.00	100.00	100.00	100.00	100.00	100.00	100.00	100.00	100.00	100.00	100.00	100.00	100.00	100.00	100.00	100.00

Apley Road #2:130cm

	1	2	3	4	5	6	7
SiO_2	71.88	68.14	69.89	73.00	72.66	72.81	74.26
TiO_2	0.11	0.14	0.15	0.11	0.12	0.17	0.22
Al_2O_3	12.01	10.65	11.68	11.71	12.08	11.91	11.61
FeO	1.10	1.18	1.16	1.15	1.02	1.10	1.05
MgO	0.48	0.00	0.42	0.22	0.42	0.24	0.36
CaO	0.95	1.25	1.10	1.05	1.04	1.14	1.11
Na_2O	4.28	3.69	3.04	3.74	2.69	3.60	4.18
K_2O	3.44	3.37	3.29	3.34	3.10	3.60	3.16
Cl	0.22	0.15	0.53	0.17	0.19	0.19	0.13
Totals	94.47	88.58	91.26	94.48	93.31	94.74	96.07
Analyses normalised to 100% loss free							
SiO_2	76.09	76.92	76.59	77.26	77.87	76.85	77.30
TiO_2	0.12	0.16	0.17	0.11	0.12	0.17	0.23
Al_2O_3	12.71	12.02	12.80	12.39	12.94	12.58	12.08
FeO	1.17	1.33	1.27	1.22	1.09	1.16	1.09
MgO	0.51	0.00	0.46	0.24	0.44	0.25	0.38
CaO	1.01	1.42	1.20	1.11	1.12	1.20	1.16
Na_2O	4.53	4.17	3.33	3.96	2.88	3.80	4.35
K_2O	3.64	3.80	3.60	3.54	3.32	3.79	3.29
Cl	0.23	0.17	0.58	0.18	0.21	0.20	0.14
Totals	100.00	100.00	100.00	100.00	100.00	100.00	100.00

Apley Road #2:160cm

	1	2	3	4	5	6	7	8	9	10
SiO_2	73.86	74.51	73.79	73.88	75.10	73.48	75.20	75.66	73.11	74.66
TiO_2	0.20	3.16	0.13	0.23	0.12	0.13	0.14	0.18	0.15	0.07
Al_2O_3	11.10	11.50	11.15	11.06	11.74	11.47	11.87	11.68	11.50	11.17
FeO	0.86	0.93	1.15	1.06	0.98	1.25	0.97	1.00	0.96	0.91
MgO	0.16	0.13	0.14	0.13	0.16	0.18	0.16	0.16	0.12	0.14
CaO	0.98	0.90	0.90	0.91	0.97	1.08	0.95	1.00	0.96	0.89
Na_2O	3.49	3.51	3.57	3.36	3.48	3.42	3.61	3.58	2.99	3.56
K_2O	3.74	3.84	3.82	3.87	4.02	3.97	3.86	4.05	3.72	4.00
Cl	0.22	0.19	0.16	0.22	0.25	0.21	0.17	0.18	0.21	0.17
Totals	94.61	98.67	94.81	94.72	96.82	95.20	96.92	97.49	93.71	95.57
Analyses normalised to 100% loss free										
SiO_2	78.07	75.51	77.82	78.00	77.57	77.19	77.59	77.61	78.02	78.12
TiO_2	0.21	3.20	0.14	0.24	0.12	0.14	0.14	0.19	0.16	0.08
Al_2O_3	11.73	11.66	11.76	11.67	12.12	12.05	12.24	11.98	12.28	11.69
FeO	0.91	0.95	1.22	1.12	1.01	1.32	1.00	1.02	1.02	0.95
MgO	0.17	0.13	0.15	0.13	0.17	0.18	0.17	0.17	0.13	0.14
CaO	1.03	0.91	0.95	0.96	1.01	1.13	0.98	1.03	1.02	0.93
Na_2O	3.69	3.55	3.77	3.55	3.59	3.60	3.72	3.67	3.19	3.72
K_2O	3.95	3.89	4.03	4.09	4.15	4.17	3.98	4.16	3.96	4.19
Cl	0.23	0.19	0.17	0.23	0.26	0.22	0.18	0.18	0.22	0.18
Totals	100.00	100.00	100.00	100.00	100.00	100.00	100.00	100.00	100.00	100.00

Apley Road #2:170cm

	1	2	3	4	5	6	7	8	9	10	11	12
SiO_2	74.08	75.62	73.86	74.39	73.21	71.73	73.15	70.72	72.53	70.47	71.24	72.59
TiO_2	0.12	0.24	0.08	0.16	0.10	0.11	0.19	0.24	0.15	0.26	0.11	0.23
Al_2O_3	11.47	11.39	11.33	11.64	11.43	11.10	11.38	11.08	11.26	11.11	11.34	11.53
FeO	1.00	1.29	1.04	1.17	1.06	0.94	1.25	0.99	1.02	0.95	0.85	1.12
MgO	0.11	0.14	0.13	0.12	0.13	0.11	0.14	0.18	0.12	0.13	0.17	0.08
CaO	0.91	0.92	1.06	1.06	1.02	1.02	0.89	0.96	1.00	0.77	0.87	1.03
Na_2O	3.20	3.55	3.46	3.38	2.77	3.36	3.34	2.99	3.52	2.89	2.92	3.54
K_2O	3.61	4.16	3.85	3.97	3.94	3.93	3.86	3.75	4.16	4.48	3.81	3.94
Cl	0.25	0.13	0.28	0.17	0.24	0.16	0.17	0.16	0.19	0.24	0.22	0.20
Totals	94.75	97.42	95.09	96.05	93.91	92.46	94.35	91.06	93.95	91.30	91.53	94.26
Analyses normalised to 100% loss free												
SiO_2	78.18	77.61	77.68	77.45	77.96	77.58	77.53	77.66	77.19	77.18	77.84	77.01
TiO_2	0.13	0.25	0.08	0.16	0.11	0.12	0.20	0.26	0.16	0.28	0.12	0.24
Al_2O_3	12.11	11.69	11.92	12.12	12.17	12.00	12.06	12.16	11.98	12.17	12.39	12.23
FeO	1.05	1.32	1.09	1.21	1.13	1.02	1.32	1.08	1.09	1.04	0.93	1.19
MgO	0.12	0.14	0.13	0.12	0.14	0.12	0.15	0.19	0.12	0.14	0.18	0.08
CaO	0.96	0.95	1.12	1.11	1.09	1.10	0.94	1.06	1.07	0.85	0.95	1.09
Na_2O	3.38	3.65	3.64	3.52	2.95	3.63	3.53	3.29	3.75	3.17	3.19	3.76
K_2O	3.81	4.27	4.04	4.13	4.19	4.25	4.09	4.12	4.43	4.90	4.16	4.18
Cl	0.26	0.13	0.30	0.18	0.26	0.17	0.18	0.17	0.20	0.27	0.24	0.22
Totals	100.00	100.00	100.00	100.00	100.00	100.00	100.00	100.00	100.00	100.00	100.00	100.00

Apley Road #2:200cm

	1	2	3	4	5	6
SiO_2	71.68	71.62	72.70	72.41	72.41	73.15
TiO_2	0.12	0.10	0.14	0.16	0.19	0.22
Al_2O_3	11.16	10.78	10.94	11.83	11.79	11.66
FeO	0.74	0.66	0.90	1.01	1.19	0.74
MgO	0.19	0.13	0.19	0.88	0.98	0.89
CaO	0.83	0.87	0.80	0.93	0.74	0.77
Na_2O	3.67	2.90	4.08	3.79	4.14	3.97
K_2O	2.93	2.94	3.00	3.29	3.30	3.10
Cl	0.25	0.20	0.19	0.23	0.26	0.24
Totals	91.57	90.18	92.93	94.53	94.99	94.74
Analyses normalised to 100% loss free						
SiO_2	78.28	79.42	78.23	76.60	76.23	77.21
TiO_2	0.13	0.11	0.15	0.17	0.20	0.23
Al_2O_3	12.18	11.95	11.77	12.52	12.42	12.31
FeO	0.81	0.73	0.97	1.07	1.25	0.78
MgO	0.20	0.15	0.20	0.93	1.03	0.94
CaO	0.91	0.96	0.86	0.98	0.77	0.81
Na_2O	4.00	3.22	4.39	4.01	4.35	4.19
K_2O	3.20	3.26	3.23	3.48	3.47	3.27
Cl	0.28	0.22	0.20	0.25	0.28	0.26
Totals	100.00	100.00	100.00	100.00	100.00	100.00

Apley Road #2:240cm

	1	2	3	4	5	6	7	8	9	10
SiO_2	74.28	71.42	69.98	73.46	71.04	69.17	67.69	69.74	75.04	75.88
TiO_2	0.24	0.21	0.15	0.25	0.28	0.17	0.27	0.16	0.07	0.20
Al_2O_3	11.88	11.55	11.18	11.74	11.90	11.15	12.12	10.83	11.27	11.29
FeO	1.01	1.01	1.20	0.93	0.90	0.85	1.20	0.94	1.06	0.88
MgO	0.11	0.17	0.09	0.10	0.22	0.14	0.33	0.24	0.20	0.36
CaO	0.79	0.79	0.93	0.88	0.85	0.82	0.88	0.83	0.85	0.92
Na_2O	3.74	3.87	3.85	4.11	3.99	3.59	3.80	3.40	3.42	3.52
K_2O	3.13	3.00	3.40	3.16	3.25	2.97	2.95	2.80	3.60	3.22
Cl	0.29	0.22	0.36	0.18	0.29	0.39	0.24	0.44	0.24	0.27
Totals	95.47	92.24	91.13	94.82	92.71	89.24	89.48	89.38	95.74	96.53
Analyses normalised to 100% loss free										
SiO_2	77.80	77.42	76.79	77.47	76.63	77.51	75.65	78.03	78.38	78.61
TiO_2	0.25	0.23	0.17	0.26	0.30	0.19	0.30	0.17	0.07	0.21
Al_2O_3	12.45	12.53	12.26	12.39	12.84	12.49	13.54	12.12	11.77	11.69
FeO	1.06	1.10	1.32	0.98	0.97	0.96	1.35	1.05	1.10	0.91
MgO	0.12	0.19	0.10	0.10	0.24	0.16	0.37	0.27	0.21	0.37
CaO	0.83	0.85	1.02	0.93	0.92	0.91	0.98	0.93	0.89	0.95
Na_2O	3.92	4.20	4.22	4.34	4.30	4.03	4.24	3.80	3.57	3.64
K_2O	3.28	3.25	3.73	3.33	3.50	3.32	3.29	3.14	3.76	3.33
Cl	0.30	0.23	0.40	0.19	0.31	0.43	0.27	0.49	0.25	0.28
Totals	100.00	100.00	100.00	100.00	100.00	100.00	100.00	100.00	100.00	100.00

Apley Road #2:260cm

	1	2	3	4	5	6	7	8	9	10	11	12	13
SiO_2	72.02	70.22	70.90	68.95	72.12	72.14	72.42	72.13	73.32	70.70	70.11	72.85	71.47
TiO_2	0.13	0.10	0.09	0.21	0.21	0.16	0.14	0.17	0.14	0.20	0.18	0.15	0.15
Al_2O_3	11.48	10.93	11.00	11.12	11.01	10.95	10.82	11.09	11.06	10.87	10.65	10.69	10.83
FeO	1.04	1.11	1.01	1.02	0.92	0.90	0.72	0.86	0.77	1.17	0.95	0.88	1.02
MgO	0.14	0.12	0.09	0.22	0.09	0.14	0.10	0.20	0.15	0.22	0.14	0.16	0.16
CaO	0.84	0.77	0.88	0.86	0.74	0.84	0.01	0.78	0.74	0.70	0.85	0.73	0.76
Na_2O	3.58	3.70	3.55	3.34	3.38	3.73	3.53	3.71	3.85	2.92	3.13	3.53	3.38
K_2O	3.14	3.32	3.25	2.80	3.81	3.04	3.15	3.26	3.04	3.05	3.44	2.96	2.92
Cl	0.24	0.27	0.26	0.28	0.22	0.20	0.30	0.25	0.21	0.27	0.20	0.29	0.25
Totals	92.60	90.54	91.04	88.79	92.49	92.10	91.21	92.45	93.27	90.09	89.64	92.23	90.94
Analyses normalised to 100% loss free													
SiO_2	77.77	77.56	77.88	77.66	77.97	78.33	79.41	78.03	78.60	78.48	78.21	78.98	78.59
TiO_2	0.14	0.11	0.10	0.24	0.23	0.17	0.16	0.18	0.15	0.22	0.20	0.16	0.17
Al_2O_3	12.40	12.07	12.08	12.52	11.90	11.89	11.87	11.99	11.86	12.06	11.88	11.59	11.91
FeO	1.13	1.23	1.11	1.15	0.99	0.98	0.79	0.93	0.82	1.29	1.06	0.95	1.12
MgO	0.15	0.13	0.10	0.25	0.09	0.15	0.11	0.21	0.16	0.24	0.16	0.18	0.18
CaO	0.90	0.85	0.96	0.97	0.80	0.91	0.01	0.84	0.79	0.78	0.95	0.79	0.84
Na_2O	3.87	4.08	3.90	3.77	3.66	4.05	3.87	4.01	4.13	3.24	3.49	3.83	3.71
K_2O	3.39	3.67	3.57	3.15	4.12	3.30	3.46	3.53	3.26	3.38	3.83	3.20	3.21
Cl	0.26	0.30	0.29	0.31	0.24	0.22	0.33	0.27	0.22	0.30	0.22	0.32	0.28
Totals	100.00	100.00	100.00	100.00	100.00	100.00	100.00	100.00	100.00	100.00	100.00	100.00	100.00

Apley Road #2:280cm

	1	2	3	4	5	6	7	8	9	10
SiO_2	77.56	77.76	77.13	75.06	76.49	75.75	72.61	74.94	77.02	71.66
TiO_2	0.18	0.12	0.48	0.07	0.11	0.15	0.09	0.14	0.19	0.12
Al_2O_3	11.66	11.64	11.99	11.49	11.37	11.33	10.75	11.06	11.62	10.79
FeO	0.86	1.09	1.09	0.89	1.12	1.16	0.99	0.91	0.80	0.82
MgO	0.12	0.10	0.34	0.04	0.26	0.03	0.00	0.09	0.23	0.00
CaO	1.05	1.00	0.91	0.90	0.82	0.84	0.83	0.79	0.80	0.85
Na_2O	2.51	4.02	4.02	3.14	3.54	3.45	3.24	3.73	3.73	3.21
K_2O	3.52	3.33	3.22	3.95	3.40	3.40	3.16	3.15	2.83	3.12
Cl	0.27	0.25	0.33	0.28	0.25	0.22	0.26	0.25	0.23	0.21
Totals	97.72	99.29	99.51	95.82	97.36	96.33	91.92	95.03	97.44	90.78
Analyses normalised to 100% loss free										
SiO_2	79.37	78.31	77.52	78.34	78.56	78.64	78.99	78.86	79.04	78.93
TiO_2	0.18	0.12	0.48	0.08	0.11	0.15	0.09	0.15	0.19	0.14
Al_2O_3	11.94	11.73	12.05	11.99	11.67	11.76	11.69	11.64	11.92	11.89
FeO	0.88	1.09	1.09	0.92	1.15	1.21	1.07	0.96	0.83	0.90
MgO	0.12	0.10	0.34	0.04	0.26	0.03	0.00	0.09	0.24	0.00
CaO	1.07	1.00	0.92	0.94	0.85	0.87	0.91	0.83	0.82	0.93
Na_2O	2.56	4.04	4.04	3.28	3.64	3.58	3.53	3.92	3.82	3.54
K_2O	3.60	3.35	3.23	4.12	3.49	3.53	3.43	3.32	2.90	3.44
Cl	0.28	0.25	0.33	0.29	0.26	0.23	0.28	0.26	0.24	0.23
Totals	100.00	100.00	100.00	100.00	100.00	100.00	100.00	100.00	100.00	100.00

Apley Road #2:300cm

	1	2	3	4	5	6	7	8	9	10
SiO_2	71.40	70.00	71.88	71.36	71.38	72.94	71.65	72.04	70.67	70.30
TiO_2	0.20	0.15	0.12	0.15	0.19	0.15	0.19	0.20	0.15	0.13
Al_2O_3	11.47	11.20	11.41	11.11	10.96	11.08	11.54	11.18	11.39	11.06
FeO	0.90	0.83	0.79	0.83	0.77	0.75	0.99	0.81	0.75	0.87
MgO	0.18	0.16	0.12	0.17	0.19	0.11	0.18	0.14	0.12	0.13
CaO	0.92	0.83	0.76	0.81	0.77	0.87	0.73	0.77	0.77	0.84
Na_2O	4.08	3.75	2.61	3.86	3.61	3.89	3.96	4.27	3.94	3.83
K_2O	3.26	2.96	2.98	3.13	3.02	3.20	3.20	3.17	3.14	2.76
Cl	0.21	0.22	0.30	0.24	0.24	0.23	0.21	0.23	0.20	0.21
Totals	92.61	90.11	90.96	91.66	91.13	93.22	92.65	92.82	91.12	90.12
Analyses normalised to 100% loss free										
SiO_2	77.10	77.68	79.03	77.86	78.33	78.25	77.34	77.62	77.56	78.01
TiO_2	0.21	0.17	0.13	0.17	0.21	0.16	0.21	0.21	0.16	0.14
Al_2O_3	12.39	12.43	12.54	12.12	12.03	11.89	12.46	12.05	12.50	12.27
FeO	0.97	0.92	0.87	0.91	0.84	0.81	1.07	0.87	0.83	0.96
MgO	0.19	0.18	0.14	0.18	0.21	0.12	0.20	0.15	0.13	0.14
CaO	0.99	0.92	0.83	0.88	0.85	0.93	0.78	0.83	0.84	0.93
Na_2O	4.40	4.17	2.87	4.21	3.96	4.17	4.27	4.60	4.32	4.25
K_2O	3.52	3.28	3.27	3.42	3.31	3.43	3.46	3.42	3.45	3.06
Cl	0.23	0.25	0.33	0.26	0.26	0.25	0.23	0.25	0.21	0.24
Totals	100.00	100.00	100.00	100.00	100.00	100.00	100.00	100.00	100.00	100.00

Apley Road #2:320cm

	1	2	3	4	5	6	7	8	9	10
SiO_2	71.03	71.32	69.90	74.81	73.05	72.52	73.03	73.64	74.87	75.43
TiO_2	0.27	0.16	0.13	0.14	0.12	0.15	0.14	0.13	0.20	0.14
Al_2O_3	11.41	11.52	11.64	11.95	11.79	11.62	12.07	11.51	11.08	10.93
FeO	1.07	0.81	0.99	0.89	1.04	0.85	1.04	0.93	0.78	0.82
MgO	0.21	0.08	0.13	0.20	0.16	0.19	0.17	0.25	0.22	0.17
CaO	0.73	0.78	0.87	0.92	0.74	0.79	0.79	0.82	0.81	0.88
Na_2O	3.85	3.52	3.43	4.09	3.70	3.88	3.93	3.19	3.57	3.70
K_2O	2.80	3.92	3.43	3.22	2.97	2.98	3.26	3.05	3.04	2.96
Cl	0.28	0.40	0.20	0.30	0.21	0.21	0.23	0.29	0.17	0.28
Totals	91.64	92.50	90.71	96.50	93.79	93.20	94.66	93.80	94.74	95.32
Analyses normalised to 100% loss free										
SiO_2	77.51	77.10	77.05	77.52	77.89	77.81	77.15	78.51	79.02	79.13
TiO_2	0.29	0.17	0.14	0.14	0.13	0.17	0.15	0.14	0.21	0.15
Al_2O_3	12.45	12.46	12.83	12.38	12.57	12.47	12.75	12.27	11.70	11.47
FeO	1.16	0.87	1.09	0.92	1.11	0.91	1.10	0.99	0.82	0.86
MgO	0.23	0.09	0.14	0.20	0.17	0.20	0.18	0.27	0.24	0.18
CaO	0.80	0.84	0.96	0.95	0.79	0.85	0.84	0.87	0.85	0.92
Na_2O	4.20	3.80	3.79	4.24	3.95	4.17	4.15	3.40	3.77	3.88
K_2O	3.05	4.24	3.78	3.33	3.16	3.20	3.44	3.25	3.21	3.11
Cl	0.30	0.43	0.22	0.31	0.22	0.23	0.25	0.31	0.18	0.29
Totals	100.00	100.00	100.00	100.00	100.00	100.00	100.00	100.00	100.00	100.00

Apley Road #2:340cm

	1	2	3	4	5	6	7	8	9	10	11
SiO_2	73.62	72.52	73.62	72.29	72.39	75.63	71.90	72.69	70.91	71.85	72.22
TiO_2	0.27	0.09	0.13	0.10	0.17	0.17	0.15	0.14	0.09	0.16	0.15
Al_2O_3	13.96	11.67	11.88	11.73	11.89	11.34	11.92	11.88	11.72	11.51	11.63
FeO	0.86	0.84	0.87	0.89	0.80	0.79	1.12	0.85	0.71	0.69	0.94
MgO	0.16	0.09	0.18	0.12	0.07	0.54	0.13	0.11	0.09	0.17	0.11
CaO	0.57	0.87	0.86	0.77	0.73	0.80	0.81	0.89	0.86	0.74	0.80
Na_2O	4.69	3.93	4.20	4.09	1.88	2.88	3.57	4.11	4.14	4.06	3.63
K_2O	4.20	3.16	3.23	3.19	3.12	4.19	4.20	3.21	2.90	2.76	4.15
Cl	0.08	0.25	0.23	0.24	0.24	0.06	0.27	0.18	0.33	0.33	0.26
Totals	99.13	93.41	95.18	93.42	91.29	96.39	94.06	94.06	91.75	92.27	93.88
Analyses normalised to 100% loss free											
SiO_2	74.27	77.64	77.34	77.39	79.29	78.46	76.44	77.28	77.29	77.87	76.93
TiO_2	0.27	0.09	0.13	0.11	0.19	0.17	0.15	0.15	0.10	0.18	0.16
Al_2O_3	14.08	12.50	12.48	12.55	13.02	11.76	12.68	12.63	12.77	12.47	12.38
FeO	0.87	0.90	0.92	0.95	0.88	0.82	1.19	0.90	0.78	0.75	1.00
MgO	0.16	0.10	0.18	0.13	0.08	0.56	0.13	0.11	0.09	0.18	0.11
CaO	0.57	0.93	0.91	0.82	0.80	0.83	0.86	0.95	0.94	0.80	0.85
Na_2O	4.73	4.20	4.41	4.37	2.06	2.99	3.79	4.37	4.51	4.40	3.87
K_2O	4.23	3.38	3.39	3.41	3.42	4.35	4.46	3.41	3.16	2.99	4.42
Cl	0.08	0.26	0.24	0.26	0.27	0.06	0.29	0.20	0.36	0.36	0.28
Totals	100.00	100.00	100.00	100.00	100.00	100.00	100.00	100.00	100.00	100.00	100.00

Apley Road #3:20cm

	1	2	3	4	5
SiO_2	71.07	70.25	71.11	71.03	71.79
TiO_2	0.15	0.15	0.19	0.16	0.13
Al_2O_3	11.06	10.54	10.86	10.70	11.09
FeO	0.92	0.85	0.81	0.78	0.85
MgO	0.17	0.13	0.32	0.27	0.31
CaO	0.91	0.83	0.81	0.80	0.78
Na_2O	3.77	3.32	3.58	3.33	4.10
K_2O	3.39	3.18	3.32	3.18	2.99
Cl	0.16	0.27	0.29	0.26	0.24
Totals	91.59	89.51	91.29	90.51	92.28
Analyses normalised to 100% loss free					
SiO_2	77.59	78.48	77.89	78.48	77.80
TiO_2	0.16	0.16	0.21	0.18	0.14
Al_2O_3	12.07	11.78	11.90	11.83	12.01
FeO	1.00	0.95	0.89	0.86	0.92
MgO	0.18	0.15	0.35	0.29	0.34
CaO	0.99	0.93	0.88	0.89	0.85
Na_2O	4.12	3.71	3.92	3.68	4.45
K_2O	3.71	3.55	3.64	3.51	3.24
Cl	0.18	0.30	0.32	0.29	0.26
Totals	100.00	100.00	100.00	100.00	100.00

Poraiti #1: 10cm

	1	2	3	4	5
SiO_2	71.29	70.19	73.09	73.07	70.72
TiO_2	0.11	0.39	0.06	0.23	0.38
Al_2O_3	11.56	12.67	11.57	11.47	12.51
FeO	1.08	2.05	1.00	1.13	1.95
MgO	0.14	0.37	0.13	0.09	0.41
CaO	1.11	1.61	0.70	0.92	1.72
Na_2O	3.45	3.92	3.73	4.20	2.70
K_2O	2.56	2.92	4.02	3.01	2.82
Cl	0.34	0.22	0.18	0.32	0.19
Totals	91.64	94.33	94.48	94.44	93.40
Analyses normalised to 100% loss free					
SiO_2	77.79	74.41	77.36	77.37	75.72
TiO_2	0.12	0.41	0.07	0.24	0.41
Al_2O_3	12.62	13.43	12.25	12.15	13.40
FeO	1.17	2.18	1.06	1.20	2.09
MgO	0.16	0.39	0.13	0.10	0.43
CaO	1.21	1.71	0.75	0.97	1.84
Na_2O	3.77	4.15	3.94	4.45	2.89
K_2O	2.79	3.09	4.25	3.18	3.02
Cl	0.37	0.23	0.19	0.34	0.20
Totals	100.00	100.00	100.00	100.00	100.00

Poraiti #2: 30cm

	1	2	3	4	5	6	7	8	9	10	11	12
SiO_2	69.77	71.39	70.82	73.61	76.03	71.44	73.65	70.72	71.96	72.62	69.22	68.72
TiO_2	0.08	0.15	0.17	0.08	0.12	0.14	0.16	0.32	0.16	0.10	0.18	0.12
Al_2O_3	11.37	11.37	11.42	11.79	11.54	11.13	11.09	11.74	10.87	11.00	11.27	11.47
FeO	0.88	1.11	1.27	0.82	0.86	1.01	0.74	1.90	1.04	0.94	1.17	1.19
MgO	0.12	0.17	0.12	0.16	0.25	0.17	0.14	0.22	0.15	0.15	0.09	0.13
CaO	0.82	1.17	1.27	0.80	1.11	1.00	0.75	1.46	1.22	0.82	1.04	1.11
Na_2O	3.64	3.58	3.63	4.07	3.68	3.46	3.55	4.28	3.62	3.66	2.33	2.39
K_2O	3.25	3.01	2.92	3.69	3.40	2.88	3.08	2.68	3.01	3.32	2.90	2.70
Cl	0.17	0.26	0.20	0.19	0.30	0.23	0.20	0.19	0.26	0.24	0.27	0.24
Totals	90.09	92.22	91.82	95.22	97.28	91.46	93.36	93.51	92.29	92.83	88.47	88.07
Analyses normalised to 100% loss free												
SiO_2	77.44	77.42	77.13	77.31	78.16	78.12	78.89	75.63	77.98	78.23	78.24	78.03
TiO_2	0.09	0.17	0.19	0.09	0.13	0.15	0.17	0.34	0.17	0.10	0.21	0.14
Al_2O_3	12.62	12.33	12.44	12.39	11.86	12.16	11.88	12.55	11.78	11.85	12.73	13.02
FeO	0.98	1.21	1.38	0.86	0.89	1.10	0.79	2.03	1.13	1.01	1.32	1.35
MgO	0.13	0.18	0.13	0.16	0.26	0.18	0.15	0.23	0.16	0.16	0.10	0.14
CaO	0.91	1.27	1.38	0.84	1.14	1.10	0.80	1.56	1.33	0.88	1.18	1.26
Na_2O	4.04	3.89	3.95	4.28	3.78	3.79	3.80	4.58	3.93	3.94	2.64	2.72
K_2O	3.61	3.27	3.18	3.87	3.49	3.15	3.30	2.87	3.26	3.57	3.28	3.07
Cl	0.19	0.28	0.22	0.20	0.31	0.25	0.21	0.21	0.28	0.25	0.31	0.27
Totals	100.00	100.00	100.00	100.00	100.00	100.00	100.00	100.00	100.00	100.00	100.00	100.00

Poraiti #1: 40cm

	1	2	3	4	5	6	7	8	9	10	11	12	13	14	15	16	17	18	19	20
SiO_2	73.12	73.69	75.14	76.25	76.89	71.49	75.60	73.01	72.51	73.10	73.28	74.59	74.99	74.67	76.70	71.58	71.77	75.38	74.21	74.34
TiO_2	0.14	0.12	0.19	0.20	0.25	0.31	0.16	0.11	0.25	0.20	0.09	0.15	0.16	0.18	0.19	0.12	0.13	0.20	0.18	0.14
Al_2O_3	11.70	11.73	11.90	12.04	11.71	11.09	11.57	11.52	11.42	12.21	11.82	11.39	11.47	11.38	11.95	11.54	11.24	11.51	11.46	11.64
FeO	1.37	1.09	1.12	0.95	1.16	1.26	0.86	1.19	0.94	1.47	0.90	1.07	0.80	1.60	0.84	1.16	1.05	0.77	1.04	0.87
MgO	0.06	0.14	0.13	0.15	0.29	0.20	0.11	0.10	0.16	0.17	0.08	0.01	0.15	0.03	0.17	0.15	0.14	0.18	0.15	0.15
CaO	0.75	1.02	1.01	0.85	1.00	1.21	0.70	0.98	0.97	1.24	0.67	0.92	0.92	0.79	0.72	1.04	1.02	0.86	0.87	0.94
Na_2O	3.72	3.80	3.72	3.97	4.08	3.48	4.05	4.09	3.76	4.26	3.79	3.92	4.38	3.82	4.32	3.65	3.61	4.16	3.96	4.09
K_2O	3.82	3.12	3.36	3.47	3.36	3.07	3.70	2.73	2.94	2.81	4.12	3.01	3.23	3.60	3.52	2.90	2.87	3.15	3.12	3.30
Cl	0.30	0.27	0.11	0.17	0.18	0.21	0.16	0.19	0.22	0.15	0.22	0.13	0.13	0.19	0.19	0.27	0.24	0.18	0.18	0.20
Totals	94.98	94.98	96.67	98.02	98.93	92.31	96.90	93.91	93.17	95.61	94.95	95.19	96.23	96.25	98.59	92.41	92.08	96.39	95.16	95.67
Analyses normalised to 100% loss free																				
SiO_2	76.99	77.59	77.73	77.78	77.72	77.44	78.02	77.74	77.82	76.46	77.18	78.36	77.93	77.58	77.80	77.46	77.95	78.20	77.98	77.71
TiO_2	0.14	0.13	0.19	0.20	0.25	0.34	0.17	0.12	0.27	0.21	0.09	0.15	0.16	0.18	0.19	0.13	0.14	0.21	0.19	0.14
Al_2O_3	12.32	12.35	12.31	12.28	11.84	12.01	11.94	12.27	12.26	12.77	12.45	11.97	11.92	11.82	12.12	12.49	12.21	11.95	12.04	12.16
FeO	1.44	1.14	1.16	0.97	1.18	1.37	0.89	1.26	1.01	1.54	0.95	1.13	0.83	1.66	0.85	1.26	1.14	0.79	1.09	0.91
MgO	0.06	0.14	0.13	0.15	0.30	0.21	0.11	0.11	0.17	0.18	0.08	0.01	0.15	0.03	0.17	0.16	0.16	0.18	0.15	0.16
CaO	0.79	1.08	1.05	0.87	1.01	1.31	0.72	1.05	1.04	1.30	0.70	0.97	0.96	0.82	0.73	1.12	1.11	0.90	0.91	0.99
Na_2O	3.92	4.00	3.85	4.04	4.12	3.77	4.17	4.36	4.03	4.45	3.99	4.11	4.56	3.96	4.38	3.95	3.92	4.32	4.16	4.27
K_2O	4.02	3.29	3.47	3.53	3.40	3.32	3.82	2.90	3.16	2.94	4.33	3.16	3.35	3.74	3.57	3.14	3.12	3.27	3.28	3.45
Cl	0.32	0.29	0.11	0.17	0.18	0.23	0.16	0.20	0.24	0.15	0.23	0.14	0.14	0.20	0.19	0.30	0.26	0.18	0.19	0.21
Totals	100.00	100.00	100.00	100.00	100.00	100.00	100.00	100.00	100.00	100.00	100.00	100.00	100.00	100.00	100.00	100.00	100.00	100.00	100.00	100.00

Poraiti #1: 70cm

	1	2	3	4	5	6	7	8	9	10	11
SiO_2	70.55	75.21	74.68	77.30	76.61	73.00	75.22	71.53	73.96	73.07	75.73
TiO_2	0.17	0.10	0.07	0.00	0.08	0.03	0.08	0.12	0.20	0.03	0.18
Al_2O_3	11.70	11.51	10.90	12.07	11.70	11.26	11.91	11.70	11.86	11.92	12.31
FeO	1.09	1.19	1.15	1.23	1.13	1.20	1.03	1.03	1.16	0.86	0.88
MgO	0.16	0.01	0.10	0.20	0.26	0.12	0.19	0.15	0.14	0.28	0.09
CaO	0.99	1.06	0.65	1.13	1.06	0.82	0.84	0.87	0.91	0.87	1.16
Na_2O	3.91	3.79	3.34	4.31	3.83	3.75	4.02	3.68	3.59	4.02	3.89
K_2O	2.45	2.80	3.84	3.22	3.18	3.19	3.21	3.09	3.35	3.71	3.21
Totals	91.02	95.66	94.73	99.47	97.84	93.36	96.49	92.16	95.17	94.76	97.44
Analyses normalised to 100% loss free											
SiO_2	77.52	78.62	78.83	77.71	78.30	78.20	77.96	77.61	77.72	77.11	77.72
TiO_2	0.19	0.10	0.08	0.00	0.08	0.03	0.08	0.13	0.21	0.03	0.18
Al_2O_3	12.85	12.03	11.51	12.14	11.96	12.06	12.34	12.70	12.46	12.58	12.63
FeO	1.20	1.24	1.22	1.24	1.16	1.28	1.06	1.12	1.22	0.91	0.91
MgO	0.17	0.01	0.10	0.20	0.26	0.12	0.19	0.17	0.15	0.29	0.09
CaO	1.09	1.11	0.69	1.14	1.08	0.88	0.87	0.94	0.96	0.91	1.19
Na_2O	4.30	3.96	3.52	4.33	3.91	4.01	4.16	3.99	3.77	4.24	3.99
K_2O	2.69	2.93	4.05	3.24	3.25	3.42	3.32	3.35	3.52	3.92	3.29
Totals	100.00	100.00	100.00	100.00	100.00	100.00	100.00	100.00	100.00	100.00	100.00

Poraiti #1: 100cm

	1	2	3	4	5	6	7	8	9	10	11	12	13
SiO_2	77.78	72.19	72.47	74.70	73.01	72.24	75.13	74.42	73.17	74.17	77.68	73.37	73.61
TiO_2	0.09	0.18	0.15	0.24	0.21	0.12	0.11	0.18	0.11	0.07	0.18	0.16	0.15
Al_2O_3	11.92	11.65	11.49	11.59	11.41	11.04	11.86	11.74	11.76	11.58	12.60	11.49	11.93
FeO	1.05	1.01	1.18	1.11	1.16	1.31	1.02	0.94	1.29	1.07	1.15	0.98	0.98
MgO	0.11	0.12	0.20	0.17	0.18	0.13	0.15	0.10	0.17	0.12	0.22	0.13	0.14
CaO	1.03	0.97	1.07	1.04	1.06	1.12	1.10	0.93	1.09	1.09	0.90	0.91	1.06
Na_2O	4.02	3.66	3.67	3.89	3.88	3.59	4.10	3.75	3.90	3.59	3.87	2.59	4.05
K_2O	3.29	2.98	3.09	3.13	2.77	2.96	2.83	3.10	2.70	3.19	3.24	3.09	3.03
Cl	0.31	0.25	0.32	0.25	0.21	0.20	0.17	0.43	0.21	0.21	0.12	0.17	0.25
Totals	99.61	93.00	93.62	96.13	93.89	92.70	96.46	95.59	94.38	95.09	99.95	92.88	95.20
Analyses normalised to 100% loss free													
SiO_2	78.09	77.62	77.41	77.71	77.76	77.93	77.88	77.86	77.53	78.00	77.72	79.00	77.32
TiO_2	0.09	0.19	0.16	0.25	0.22	0.13	0.12	0.19	0.11	0.07	0.18	0.17	0.16
Al_2O_3	11.97	12.52	12.27	12.06	12.16	11.91	12.29	12.28	12.46	12.18	12.61	12.37	12.53
FeO	1.06	1.09	1.26	1.15	1.24	1.41	1.06	0.98	1.37	1.12	1.15	1.06	1.03
MgO	0.11	0.13	0.21	0.18	0.19	0.14	0.15	0.10	0.18	0.13	0.22	0.14	0.15
CaO	1.04	1.04	1.14	1.09	1.13	1.20	1.14	0.98	1.15	1.15	0.90	0.98	1.11
Na_2O	4.03	3.93	3.92	4.04	4.13	3.87	4.25	3.92	4.13	3.78	3.87	2.79	4.25
K_2O	3.30	3.20	3.30	3.26	2.95	3.19	2.93	3.24	2.86	3.35	3.24	3.32	3.18
Cl	0.32	0.27	0.34	0.25	0.22	0.22	0.18	0.45	0.22	0.22	0.12	0.18	0.26
Totals	100.00	100.00	100.00	100.00	100.00	100.00	100.00	100.00	100.00	100.00	100.00	100.00	100.00

Poraiti #1: 110cm

	1	2	3	4	5	6	7	8	9	10	11
SiO_2	70.42	69.11	72.59	70.45	71.26	73.33	71.73	73.84	70.97	71.85	68.03
TiO_2	0.08	0.18	0.17	0.20	0.11	0.11	0.11	0.19	0.16	0.19	0.15
Al_2O_3	11.31	11.48	11.56	10.89	11.48	11.67	11.48	12.03	11.32	11.36	11.10
FeO	1.09	1.33	0.97	1.10	1.01	1.19	1.23	0.96	1.05	1.31	1.15
MgO	0.11	0.15	0.17	0.18	0.14	0.16	0.18	0.17	0.13	0.07	0.16
CaO	1.03	1.09	0.94	1.10	1.01	0.93	1.09	0.76	1.09	0.73	0.85
Na_2O	3.91	3.69	4.52	3.72	3.93	3.91	3.77	3.83	3.82	4.16	3.62
K_2O	3.09	2.78	3.07	3.18	2.88	3.15	2.66	4.39	2.73	3.55	3.49
Cl	0.21	0.26	0.26	0.26	0.23	0.23	0.20	0.45	0.28	0.25	0.47
Totals	91.24	90.06	94.24	91.09	92.05	94.67	92.44	96.61	91.55	93.47	89.01
Analyses normalised to 100% loss free											
SiO_2	77.17	76.74	77.03	77.35	77.42	77.46	77.59	76.43	77.52	76.87	76.43
TiO_2	0.08	0.19	0.18	0.22	0.12	0.11	0.12	0.19	0.17	0.20	0.17
Al_2O_3	12.40	12.75	12.26	11.96	12.47	12.33	12.42	12.45	12.36	12.16	12.47
FeO	1.20	1.48	1.02	1.20	1.10	1.25	1.33	0.99	1.14	1.40	1.29
MgO	0.12	0.17	0.18	0.20	0.15	0.17	0.19	0.18	0.14	0.08	0.18
CaO	1.13	1.21	1.00	1.21	1.10	0.98	1.18	0.79	1.19	0.78	0.95
Na_2O	4.28	4.09	4.80	4.09	4.26	4.13	4.07	3.96	4.18	4.45	4.07
K_2O	3.39	3.09	3.25	3.49	3.13	3.33	2.88	4.54	2.99	3.80	3.92
Cl	0.23	0.28	0.27	0.28	0.25	0.24	0.22	0.47	0.30	0.26	0.53
Totals	100.00	100.00	100.00	100.00	100.00	100.00	100.00	100.00	100.00	100.00	100.00

Poraiti #1: 120cm

	1	2	3	4	5	6	7	8	9	10	11	12	13	14	15
SiO_2	72.68	74.58	75.21	75.06	75.16	73.36	72.60	73.28	72.87	73.47	72.87	75.29	75.17	72.77	72.84
TiO_2	0.18	0.23	0.26	0.11	0.14	0.18	0.16	0.08	0.14	0.12	0.06	0.33	0.09	0.24	0.22
Al_2O_3	11.59	11.81	12.64	11.89	11.74	11.98	11.89	11.89	11.54	11.64	11.71	11.48	11.57	11.79	11.85
FeO	0.91	1.10	1.03	1.36	1.38	1.21	1.22	1.18	1.17	1.07	1.07	1.23	1.00	1.23	1.17
MgO	1.45	0.17	0.62	0.17	0.14	0.17	0.13	0.16	0.11	0.13	0.15	0.18	0.12	0.12	0.14
CaO	1.74	1.03	0.82	1.20	1.02	1.08	1.04	1.05	0.94	1.03	1.01	0.99	1.05	1.08	1.13
Na_2O	4.13	3.86	3.74	4.03	3.67	3.69	3.72	3.94	3.64	3.34	3.80	3.73	3.76	3.70	4.00
K_2O	3.12	3.04	4.35	3.01	3.11	2.92	2.74	2.76	2.77	2.89	2.77	3.07	2.80	3.27	3.06
Cl	0.17	0.21	0.28	0.29	0.25	0.24	0.24	0.23	0.24	0.19	0.18	0.26	0.25	0.26	0.24
Totals	95.95	96.03	98.94	97.12	96.61	94.84	93.73	94.58	93.40	93.88	93.63	96.56	95.80	94.45	94.64
Analyses normalised to 100% loss free															
SiO_2	75.74	77.66	76.02	77.28	77.80	77.36	77.45	77.49	78.01	78.26	77.83	77.97	78.46	77.04	76.96
TiO_2	0.18	0.24	0.26	0.12	0.14	0.19	0.17	0.08	0.15	0.13	0.07	0.34	0.09	0.25	0.23
Al_2O_3	12.07	12.30	12.77	12.24	12.15	12.64	12.68	12.57	12.36	12.40	12.50	11.88	12.07	12.48	12.52
FeO	0.95	1.14	1.04	1.40	1.43	1.28	1.30	1.25	1.25	1.14	1.15	1.28	1.05	1.30	1.24
MgO	1.51	0.18	0.62	0.17	0.15	0.18	0.14	0.17	0.12	0.14	0.16	0.18	0.13	0.13	0.15
CaO	1.81	1.08	0.82	1.24	1.06	1.14	1.11	1.11	1.01	1.10	1.08	1.03	1.09	1.14	1.19
Na_2O	4.30	4.02	3.78	4.15	3.80	3.89	3.96	4.17	3.89	3.56	4.06	3.87	3.92	3.91	4.23
K_2O	3.25	3.16	4.39	3.10	3.22	3.08	2.92	2.91	2.96	3.08	2.96	3.18	2.92	3.46	3.23
Cl	0.18	0.22	0.28	0.29	0.26	0.25	0.26	0.24	0.25	0.20	0.19	0.27	0.26	0.28	0.25
Totals	100.00	100.00	100.00	100.00	100.00	100.00	100.00	100.00	100.00	100.00	100.00	100.00	100.00	100.00	100.00

Poraiti #1: 221cm

	1	2	3	4	5	6	7	8	9	10	11
SiO_2	74.35	71.11	72.02	71.09	70.85	71.80	71.18	72.57	72.53	71.17	71.16
TiO_2	0.16	0.20	0.20	0.26	0.26	0.28	0.19	0.22	0.22	0.19	0.14
Al_2O_3	11.68	10.65	10.70	10.60	10.81	11.52	10.64	11.04	10.85	10.65	10.76
FeO	1.34	1.16	1.08	0.88	1.00	1.41	1.24	1.30	1.19	0.96	1.14
MgO	0.12	0.13	0.13	0.16	0.20	0.27	0.25	0.42	0.08	0.17	0.35
CaO	0.98	1.01	0.92	0.60	0.88	1.30	0.74	0.94	1.09	0.69	1.25
Na_2O	3.93	3.64	3.63	3.42	3.14	3.48	2.86	3.18	3.76	2.82	3.48
K_2O	3.12	2.89	2.88	3.89	3.19	2.87	4.08	3.59	3.03	3.93	2.85
Cl	0.30	0.22	0.20	0.22	0.27	0.21	0.19	0.20	0.21	0.20	0.25
Totals	95.97	90.99	91.74	91.10	90.60	93.14	91.37	93.45	92.95	90.78	91.37
Analyses normalised to 100% loss free											
SiO_2	77.47	78.15	78.50	78.04	78.20	77.09	77.91	77.65	78.03	78.40	77.88
TiO_2	0.16	0.21	0.21	0.28	0.29	0.30	0.21	0.23	0.24	0.20	0.15
Al_2O_3	12.17	11.70	11.66	11.63	11.93	12.37	11.64	11.81	11.67	11.73	11.77
FeO	1.40	1.28	1.18	0.96	1.10	1.51	1.36	1.39	1.28	1.06	1.24
MgO	0.12	0.14	0.14	0.17	0.22	0.29	0.27	0.44	0.08	0.18	0.38
CaO	1.02	1.11	1.00	0.66	0.97	1.39	0.81	1.01	1.17	0.76	1.37
Na_2O	4.10	4.00	3.96	3.75	3.46	3.74	3.13	3.41	4.05	3.11	3.81
K_2O	3.25	3.17	3.14	4.27	3.53	3.08	4.47	3.84	3.26	4.33	3.12
Cl	0.31	0.24	0.22	0.24	0.30	0.22	0.21	0.22	0.22	0.22	0.28
Totals	100.00	100.00	100.00	100.00	100.00	100.00	100.00	100.00	100.00	100.00	100.00

Poraiti #2: 0cm

	1	2	3	4	5	6	7	8	9	10	11	12	13
SiO_2	72.73	73.60	73.14	73.29	75.25	76.58	76.33	76.72	77.19	74.12	71.82	73.77	74.35
TiO_2	0.17	0.21	0.12	0.17	0.11	0.25	0.20	0.10	0.20	0.25	0.20	0.14	0.16
Al_2O_3	12.35	11.76	11.92	12.06	11.45	11.57	11.41	12.31	12.51	11.72	14.14	12.41	11.68
FeO	1.20	1.17	1.16	1.12	1.05	1.14	1.05	1.21	1.15	1.12	1.08	1.21	1.38
MgO	0.11	0.21	0.28	0.14	0.13	0.15	0.10	0.15	0.06	0.15	0.10	0.15	0.12
CaO	1.03	0.91	1.07	0.93	1.04	1.13	1.08	0.91	0.98	0.99	2.11	1.10	0.98
Na_2O	4.04	4.31	4.09	4.24	4.05	4.05	4.18	3.90	4.12	3.95	4.57	3.91	3.93
K_2O	2.56	3.05	2.71	2.73	2.97	2.90	2.53	2.63	2.63	2.74	2.14	2.79	3.12
Cl	0.19	0.18	0.11	0.21	0.14	0.21	0.16	0.16	0.22	0.23	0.25	0.24	0.30
Totals	94.38	95.39	94.61	94.89	96.20	97.97	97.03	98.09	99.06	95.26	96.42	95.70	96.01
Analyses normalised to 100% loss free													
SiO_2	77.06	77.16	77.31	77.23	78.23	78.16	78.67	78.21	77.92	77.80	74.49	77.08	77.44
TiO_2	0.18	0.21	0.13	0.18	0.11	0.26	0.20	0.11	0.20	0.26	0.21	0.15	0.16
Al_2O_3	13.09	12.32	12.60	12.71	11.91	11.81	11.75	12.55	12.63	12.30	14.66	12.97	12.17
FeO	1.27	1.22	1.23	1.18	1.09	1.17	1.08	1.23	1.16	1.17	1.12	1.26	1.44
MgO	0.11	0.22	0.29	0.15	0.13	0.15	0.11	0.15	0.06	0.16	0.11	0.15	0.12
CaO	1.09	0.96	1.14	0.98	1.08	1.15	1.11	0.93	0.99	1.04	2.19	1.15	1.02
Na_2O	4.28	4.52	4.33	4.47	4.21	4.13	4.30	3.97	4.16	4.15	4.74	4.08	4.09
K_2O	2.72	3.19	2.87	2.87	3.09	2.96	2.61	2.69	2.66	2.88	2.22	2.91	3.25
Cl	0.20	0.19	0.11	0.22	0.15	0.22	0.16	0.16	0.22	0.24	0.26	0.25	0.31
Totals	100.00	100.00	100.00	100.00	100.00	100.00	100.00	100.00	100.00	100.00	100.00	100.00	100.00

Poraiti #2: 40cm

	1	2	3	4	5	6	7	8
SiO_2	75.25	70.76	68.14	69.90	69.65	67.91	70.32	70.11
TiO_2	0.16	0.16	0.14	0.27	0.11	0.18	0.15	0.17
Al_2O_3	12.07	11.44	12.03	10.79	10.70	11.26	10.58	10.51
FeO	1.37	1.18	1.29	1.20	1.19	1.92	0.83	1.12
MgO	0.07	0.16	0.06	0.26	0.20	0.24	0.46	0.29
CaO	1.01	1.11	0.87	1.08	1.12	0.96	0.77	1.09
Na_2O	3.95	3.44	4.04	3.65	3.29	3.34	3.73	3.33
K_2O	3.72	2.96	3.34	2.77	2.63	4.26	2.66	2.66
Cl	0.25	0.24	0.25	0.18	0.17	0.33	0.22	0.21
Totals	97.86	91.43	90.15	90.10	89.05	90.40	89.72	89.49
Analyses normalised to 100% loss free								
SiO_2	76.90	77.39	75.58	77.58	78.21	75.12	78.37	78.35
TiO_2	0.16	0.17	0.15	0.30	0.12	0.20	0.17	0.19
Al_2O_3	12.33	12.51	13.34	11.98	12.01	12.45	11.80	11.74
FeO	1.40	1.29	1.43	1.34	1.34	2.12	0.93	1.25
MgO	0.07	0.17	0.06	0.28	0.22	0.26	0.51	0.32
CaO	1.03	1.21	0.97	1.20	1.26	1.06	0.86	1.22
Na_2O	4.04	3.76	4.48	4.05	3.70	3.70	4.16	3.72
K_2O	3.81	3.23	3.71	3.07	2.95	4.72	2.96	2.97
Cl	0.25	0.26	0.28	0.20	0.20	0.37	0.24	0.23
Totals	100.00	100.00	100.00	100.00	100.00	100.00	100.00	100.00

Poraiti #2;80cm

	1	2	3	4	5	6	7	8	9	10	11
SiO_2	71.31	72.90	72.25	72.28	72.51	70.66	71.36	73.13	71.89	74.32	76.26
TiO_2	0.11	0.14	0.18	0.14	0.14	0.22	0.08	0.08	0.14	0.10	0.15
Al_2O_3	10.71	11.13	11.03	11.42	11.83	11.88	11.52	11.88	11.48	12.22	11.68
FeO	0.96	1.28	1.32	0.81	1.03	1.23	0.86	1.12	1.08	1.02	0.99
MgO	0.07	0.13	0.20	0.18	0.31	0.25	0.13	0.13	0.29	0.26	0.14
CaO	0.72	1.01	0.93	0.75	0.98	1.20	1.00	0.90	0.84	0.95	1.07
Na_2O	3.08	3.17	3.10	3.41	3.96	3.99	3.24	3.73	3.38	4.32	3.38
K_2O	3.87	3.89	3.69	4.53	3.85	3.06	3.57	4.03	3.38	3.27	4.20
Cl	0.26	0.14	0.18	n.d.	n.d.	n.d.	n.d.	n.d.	n.d.	n.d.	n.d.
Totals	91.10	93.78	92.87	93.50	94.61	92.48	91.75	94.98	92.48	96.45	97.85
Analyses normalised to 100% loss free											
SiO_2	78.28	77.73	77.79	77.30	76.64	76.40	77.78	76.99	77.74	77.06	77.93
TiO_2	0.12	0.14	0.20	0.15	0.15	0.24	0.08	0.08	0.15	0.10	0.15
Al_2O_3	11.76	11.87	11.88	12.21	12.51	12.84	12.56	12.50	12.42	12.66	11.93
FeO	1.06	1.36	1.42	0.86	1.08	1.33	0.93	1.17	1.16	1.05	1.01
MgO	0.08	0.14	0.21	0.19	0.33	0.27	0.14	0.13	0.31	0.27	0.14
CaO	0.79	1.08	1.00	0.80	1.04	1.30	1.09	0.95	0.91	0.98	1.09
Na_2O	3.38	3.38	3.34	3.64	4.18	4.31	3.53	3.93	3.65	4.48	3.45
K_2O	4.25	4.15	3.97	4.84	4.06	3.30	3.89	4.24	3.65	3.39	4.29
Cl	0.28	0.15	0.19	n.d.	n.d.	n.d.	n.d.	n.d.	n.d.	n.d.	n.d.
Totals	100.00	100.00	100.00	100.00	100.00	100.00	100.00	100.00	100.00	100.00	100.00

Poraitl #2: 100cm

	1	2	3	4	5	6	7	8	9	10	11	12	13	14
SiO_2	76.16	72.21	74.07	75.60	72.94	72.84	77.03	74.77	74.45	75.79	76.80	75.71	73.86	74.45
TiO_2	0.15	0.17	0.12	0.23	0.15	0.17	0.16	0.31	0.16	0.24	0.14	0.18	0.12	0.24
Al_2O_3	12.27	12.20	12.54	12.66	11.13	11.33	12.58	11.78	11.43	11.04	11.71	12.05	12.34	12.18
FeO	0.82	0.96	1.04	1.26	0.75	1.19	0.94	0.95	0.99	0.99	1.22	0.89	0.96	0.80
MgO	0.15	0.19	0.22	0.23	0.11	0.15	0.15	0.17	0.20	0.21	0.23	0.17	0.18	0.14
CaO	0.76	1.00	1.07	1.12	0.73	0.77	0.91	0.91	0.98	0.51	1.07	0.78	0.97	0.97
Na_2O	4.40	3.78	3.82	3.72	4.18	3.76	3.97	4.05	3.41	3.82	3.56	4.07	3.34	3.66
K_2O	3.21	3.57	3.78	3.92	3.16	3.54	3.35	3.13	3.75	3.29	4.23	3.39	3.60	3.88
Cl	0.16	0.20	0.19	0.17	0.22	0.31	0.18	0.26	0.08	0.11	0.23	0.13	0.19	0.12
Totals	98.08	94.25	96.84	98.91	93.36	94.06	99.26	96.33	95.43	96.00	99.18	97.36	95.57	96.44
Analyses normalised to 100% loss free														
SiO_2	77.65	76.61	76.48	76.44	78.12	77.45	77.60	77.62	78.01	78.94	77.43	77.76	77.28	77.21
TiO_2	0.15	0.18	0.12	0.24	0.16	0.18	0.16	0.32	0.17	0.25	0.14	0.18	0.13	0.25
Al_2O_3	12.51	12.94	12.95	12.79	11.92	12.05	12.67	12.23	11.98	11.50	11.80	12.38	12.91	12.62
FeO	0.84	1.02	1.07	1.27	0.80	1.27	0.95	0.99	1.03	1.03	1.23	0.91	1.00	0.83
MgO	0.15	0.20	0.23	0.23	0.12	0.16	0.15	0.18	0.21	0.21	0.23	0.18	0.19	0.15
CaO	0.78	1.06	1.11	1.13	0.78	0.82	0.92	0.94	1.02	0.53	1.08	0.80	1.02	1.01
Na_2O	4.49	4.01	3.94	3.76	4.47	3.99	4.00	4.21	3.57	3.98	3.59	4.18	3.50	3.79
K_2O	3.27	3.79	3.90	3.96	3.38	3.76	3.37	3.25	3.92	3.43	4.26	3.48	3.77	4.02
Cl	0.17	0.21	0.20	0.17	0.24	0.33	0.18	0.27	0.08	0.12	0.23	0.13	0.20	0.12
Totals	100.00	100.00	100.00	100.00	100.00	100.00	100.00	100.00	100.00	100.00	100.00	100.00	100.00	100.00

	15	16	17	18	19	20	21	22	23	24	25
SiO_2	75.78	76.06	75.83	75.85	74.32	75.82	75.46	75.47	75.50	75.19	74.82
TiO_2	0.18	0.25	0.23	0.24	0.19	0.19	0.19	0.20	0.28	0.24	0.18
Al_2O_3	12.43	11.80	12.27	12.42	12.31	12.47	10.82	12.33	13.01	11.51	11.41
FeO	0.91	0.93	0.89	1.03	1.15	1.01	0.99	0.90	0.85	0.92	1.01
MgO	0.22	0.21	0.15	0.15	0.11	0.20	0.16	0.22	0.10	0.19	0.17
CaO	0.89	1.01	0.93	1.03	0.90	0.89	0.97	0.93	1.08	1.12	0.89
Na_2O	4.31	3.62	3.60	2.90	3.68	3.88	3.54	4.13	3.75	3.72	3.46
K_2O	3.35	3.57	3.86	3.80	3.74	3.17	3.78	3.02	3.03	3.77	4.06
Cl	0.21	0.17	0.18	0.09	0.15	0.25	0.19	0.15	0.13	0.14	0.09
Totals	98.27	97.63	97.94	97.52	96.54	97.88	96.09	97.36	97.72	96.81	96.08
Analyses normalised to 100% loss free											
SiO_2	77.11	77.91	77.42	77.78	76.99	77.47	78.53	77.52	77.27	77.67	77.87
TiO_2	0.18	0.26	0.24	0.25	0.20	0.20	0.19	0.21	0.28	0.25	0.19
Al_2O_3	12.65	12.09	12.52	12.74	12.75	12.74	11.26	12.67	13.31	11.89	11.88
FeO	0.93	0.96	0.91	1.06	1.19	1.03	1.03	0.93	0.87	0.95	1.05
MgO	0.23	0.22	0.16	0.15	0.11	0.20	0.16	0.22	0.10	0.20	0.17
CaO	0.90	1.03	0.94	1.06	0.93	0.91	1.01	0.96	1.10	1.16	0.92
Na_2O	4.38	3.71	3.67	2.97	3.81	3.96	3.68	4.25	3.84	3.84	3.60
K_2O	3.40	3.66	3.94	3.90	3.87	3.24	3.93	3.10	3.10	3.90	4.23
Cl	0.22	0.18	0.19	0.09	0.15	0.26	0.20	0.15	0.13	0.14	0.09
Totals	100.00	100.00	100.00	100.00	100.00	100.00	100.00	100.00	100.00	100.00	100.00

Poraiti #2:120cm

	1	2	3	4	5	6	7	8	9	10	11	12	13	14	15	16	17	18	19
SiO_2	74.73	74.25	75.91	75.28	74.69	73.37	73.80	75.63	74.49	74.45	74.53	72.98	74.43	73.64	74.56	75.18	76.83	75.84	74.59
TiO_2	0.19	0.20	0.27	0.23	0.31	0.33	0.24	0.21	0.17	0.18	0.25	0.17	0.20	0.20	0.16	0.13	0.22	0.23	0.22
Al_2O_3	11.95	12.20	11.32	12.15	11.78	11.18	11.86	12.56	11.90	12.00	11.55	10.99	12.07	11.32	11.94	11.35	11.77	12.13	12.17
FeO	0.88	0.94	1.13	0.91	1.13	1.23	0.96	0.92	0.87	0.95	0.91	1.16	1.16	0.92	1.02	0.87	0.88	1.11	1.24
MgO	0.16	0.13	0.15	0.12	0.10	0.16	0.15	0.13	0.28	0.25	0.14	0.22	0.08	0.14	0.17	0.19	0.14	0.15	0.23
CaO	0.95	1.00	0.93	1.03	1.00	1.15	0.92	0.98	1.04	1.06	0.84	1.05	0.76	0.79	1.05	0.88	0.91	1.12	0.94
Na_2O	4.00	3.52	3.61	3.52	3.37	3.44	3.54	3.53	3.71	3.47	3.47	3.70	3.78	4.14	3.57	3.99	3.69	3.72	3.63
K_2O	3.27	4.10	3.74	4.09	3.96	3.31	3.98	3.94	3.56	3.92	3.92	3.99	4.20	2.92	3.58	3.20	3.80	4.00	3.84
Cl	0.21	0.12	0.10	0.09	0.12	0.12	0.22	0.12	0.06	0.24	0.03	0.16	0.23	0.16	0.13	0.18	0.18	0.16	0.24
Totals	96.32	96.45	97.16	97.42	96.45	94.29	95.67	98.02	96.08	96.51	95.64	94.42	96.89	94.24	96.17	95.96	98.42	98.46	97.08
Analyses normalised to 100% loss free																			
SiO_2	77.58	76.98	78.13	77.27	77.45	77.81	77.14	77.16	77.52	77.15	77.93	77.30	76.82	78.14	77.53	78.35	78.06	77.03	76.83
TiO_2	0.20	0.21	0.28	0.24	0.32	0.34	0.26	0.21	0.18	0.18	0.26	0.18	0.21	0.21	0.16	0.14	0.22	0.23	0.22
Al_2O_3	12.40	12.65	11.65	12.47	12.21	11.85	12.40	12.81	12.39	12.43	12.08	11.63	12.45	12.02	12.42	11.83	11.96	12.32	12.53
FeO	0.92	0.97	1.16	0.94	1.17	1.31	1.01	0.94	0.91	0.98	0.95	1.23	1.19	0.98	1.06	0.90	0.89	1.13	1.27
MgO	0.16	0.14	0.15	0.12	0.10	0.17	0.15	0.14	0.29	0.25	0.14	0.24	0.08	0.15	0.17	0.20	0.14	0.16	0.24
CaO	0.98	1.03	0.96	1.06	1.03	1.22	0.96	1.00	1.09	1.09	0.87	1.11	0.79	0.84	1.09	0.91	0.93	1.14	0.97
Na_2O	4.15	3.65	3.71	3.61	3.50	3.65	3.70	3.60	3.86	3.60	3.63	3.92	3.90	4.40	3.71	4.16	3.75	3.78	3.74
K_2O	3.39	4.25	3.85	4.20	4.11	3.51	4.16	4.02	3.70	4.06	4.10	4.23	4.33	3.10	3.72	3.33	3.86	4.06	3.96
Cl	0.21	0.13	0.10	0.09	0.12	0.13	0.23	0.12	0.07	0.25	0.03	0.17	0.23	0.17	0.14	0.18	0.18	0.16	0.24
Totals	100.00	100.00	100.00	100.00	100.00	100.00	100.00	100.00	100.00	100.00	100.00	100.00	100.00	100.00	100.00	100.00	100.00	100.00	100.00

Poraiti #2: 130cm

	1	2	3	4	5	6	7	8	9	10	11	12	13	14	15	16	17	18	19	20	21
SiO_2	74.42	73.53	74.49	73.10	73.24	76.62	75.45	76.05	77.56	75.14	75.34	75.34	75.54	76.13	76.40	73.73	75.51	74.57	73.76	74.68	73.06
TiO_2	0.17	0.17	0.31	0.10	0.21	0.17	0.27	0.15	0.21	0.23	0.20	0.16	1.64	0.22	0.31	0.26	0.16	0.19	0.13	0.19	0.21
Al_2O_3	11.41	11.60	11.37	10.94	11.75	11.62	12.30	12.00	12.12	11.86	11.70	12.35	11.65	11.97	13.08	11.95	12.44	12.56	11.26	10.95	11.70
FeO	1.01	0.92	0.86	1.06	1.15	0.83	1.05	0.75	1.08	1.01	1.01	1.13	1.02	0.88	1.09	0.96	0.98	0.86	0.99	0.85	1.04
MgO	0.12	0.20	0.00	0.08	0.25	0.18	0.16	0.19	0.20	0.18	0.10	0.13	0.26	0.18	0.19	0.17	0.15	0.17	0.13	0.15	0.10
CaO	1.01	0.98	1.04	0.79	1.03	0.74	0.94	0.85	1.03	0.89	0.94	1.03	0.84	0.83	1.03	0.94	0.98	0.86	0.97	0.84	0.77
Na_2O	3.33	3.53	3.42	3.61	3.69	4.28	3.64	4.16	3.55	4.02	3.62	3.56	4.01	3.57	3.65	4.11	3.74	4.00	3.77	4.24	3.49
K_2O	3.74	3.99	3.83	3.95	3.54	3.00	3.87	3.19	3.99	3.24	3.76	3.71	3.22	4.18	3.81	3.08	3.84	3.36	3.62	3.21	4.18
Cl	0.16	0.14	0.00	0.18	0.20	0.23	0.16	0.15	0.18	0.14	0.19	0.27	0.66	0.18	0.17	0.21	0.15	0.16	0.36	0.16	0.26
Totals	95.37	95.04	95.31	93.79	95.06	97.67	97.84	97.48	99.92	96.70	96.86	97.67	98.84	98.13	99.72	95.41	97.94	96.73	94.99	95.27	94.80
Analyses normalised to 100% loss free																					
SiO_2	78.04	77.36	78.15	77.94	77.05	78.45	77.11	78.02	77.62	77.70	77.79	77.13	76.42	77.58	76.61	77.28	77.10	77.10	77.65	78.39	77.06
TiO_2	0.18	0.17	0.33	0.10	0.22	0.17	0.28	0.15	0.21	0.24	0.20	0.16	1.66	0.22	0.31	0.27	0.17	0.19	0.14	0.20	0.22
Al_2O_3	11.97	12.20	11.93	11.67	12.36	11.90	12.57	12.31	12.13	12.26	12.08	12.64	11.79	12.20	13.12	12.52	12.70	12.98	11.85	11.49	12.34
FeO	1.06	0.96	0.90	1.13	1.20	0.85	1.08	0.77	1.08	1.05	1.04	1.16	1.03	0.90	1.10	1.00	1.00	0.89	1.04	0.89	1.09
MgO	0.13	0.21	0.00	0.08	0.27	0.18	0.16	0.19	0.20	0.19	0.10	0.14	0.26	0.18	0.19	0.18	0.15	0.18	0.13	0.15	0.11
CaO	1.06	1.03	1.09	0.84	1.09	0.76	0.96	0.87	1.03	0.92	0.97	1.05	0.85	0.84	1.03	0.98	1.00	0.88	1.03	0.88	0.81
Na_2O	3.49	3.71	3.59	3.85	3.88	4.38	3.72	4.27	3.55	4.16	3.74	3.65	4.06	3.64	3.66	4.31	3.81	4.14	3.97	4.45	3.68
K_2O	3.92	4.20	4.02	4.21	3.72	3.07	3.96	3.27	3.99	3.35	3.88	3.80	3.26	4.26	3.82	3.23	3.92	3.47	3.81	3.37	4.41
Cl	0.16	0.14	0.00	0.19	0.21	0.24	0.17	0.15	0.18	0.14	0.19	0.28	0.67	0.18	0.17	0.22	0.16	0.16	0.38	0.17	0.27
Totals	100.00	100.00	100.00	100.00	100.00	100.00	100.00	100.00	100.00	100.00	100.00	100.00	100.00	100.00	100.00	100.00	100.00	100.00	100.00	100.00	100.00

Poraiti #2: 150cm

	1	2	3	4	5	6	7	8	9	10	11	12
SiO_2	72.47	72.41	74.32	73.37	74.26	72.03	72.61	71.83	74.01	73.72	75.21	72.16
TiO_2	0.21	0.16	0.19	0.16	0.12	0.11	0.14	0.16	0.12	0.11	0.09	0.18
Al_2O_3	11.87	11.51	11.42	11.50	12.00	11.47	11.68	11.73	11.87	11.96	12.15	11.76
FeO	0.89	1.04	1.12	1.21	0.90	1.00	1.29	1.15	0.95	0.80	1.28	0.77
MgO	0.13	0.17	0.18	0.18	0.14	0.12	0.13	0.14	0.11	0.13	0.21	0.14
CaO	0.88	0.92	0.91	0.89	1.02	0.83	1.03	0.95	0.97	1.12	1.12	0.76
Na_2O	3.81	4.02	3.45	3.01	3.35	3.55	3.57	3.32	3.79	3.90	3.67	4.02
K_2O	3.29	3.40	3.10	3.98	3.79	3.62	3.64	3.57	3.29	3.11	3.90	3.39
Cl	0.19	0.30	0.24	0.19	0.13	0.26	0.15	0.13	0.23	0.14	0.20	0.27
Totals	93.73	93.93	94.92	94.49	95.71	92.98	94.24	92.99	95.33	94.98	97.82	93.45
Analyses normalised to 100% loss free												
SiO_2	77.32	77.08	78.29	77.65	77.59	77.46	77.05	77.25	77.64	77.62	76.89	77.22
TiO_2	0.22	0.17	0.20	0.17	0.12	0.12	0.15	0.18	0.13	0.12	0.09	0.19
Al_2O_3	12.66	12.26	12.03	12.17	12.54	12.33	12.39	12.62	12.45	12.59	12.42	12.59
FeO	0.95	1.11	1.17	1.28	0.94	1.08	1.37	1.24	0.99	0.84	1.31	0.82
MgO	0.14	0.18	0.18	0.19	0.15	0.13	0.14	0.15	0.11	0.13	0.21	0.15
CaO	0.94	0.98	0.96	0.94	1.06	0.89	1.09	1.02	1.02	1.17	1.15	0.82
Na_2O	4.06	4.28	3.63	3.18	3.50	3.81	3.79	3.57	3.97	4.11	3.75	4.30
K_2O	3.51	3.61	3.27	4.21	3.96	3.90	3.86	3.84	3.45	3.27	3.99	3.62
Cl	0.20	0.32	0.25	0.21	0.14	0.28	0.16	0.14	0.24	0.15	0.20	0.29
Totals	100.00	100.00	100.00	100.00	100.00	100.00	100.00	100.00	100.00	100.00	100.00	100.00

Poraiti #2: 160cm

	1	2	3	4	5	6	7	8	9	10	11	12	13	14	15	16	17	18	19
SiO_2	74.30	75.31	76.59	75.27	74.70	73.96	73.36	75.82	76.91	74.30	75.36	74.85	74.83	75.77	76.11	75.75	75.46	76.21	75.80
TiO_2	0.20	0.21	0.13	0.13	0.18	0.19	0.16	0.19	0.22	0.09	0.20	0.24	0.18	0.21	0.15	0.16	0.22	0.20	0.23
Al_2O_3	11.56	11.84	12.79	11.96	12.15	11.75	12.61	11.16	12.32	12.07	13.06	11.28	11.77	11.86	11.92	11.71	12.30	11.98	12.33
FeO	0.96	0.97	0.99	0.80	0.95	0.75	1.05	0.96	0.93	1.15	1.14	0.86	0.79	0.87	1.00	0.93	1.01	0.91	0.98
MgO	0.36	0.19	0.14	0.15	0.07	0.16	0.08	0.18	0.15	0.14	0.18	0.20	0.16	0.17	0.16	0.17	0.12	0.14	0.13
CaO	0.78	0.74	0.83	0.90	1.20	0.84	0.54	0.96	0.77	0.96	1.12	0.71	0.91	0.89	0.97	1.10	0.83	0.78	0.75
Na_2O	3.36	3.92	4.38	4.19	3.97	3.99	3.73	4.34	4.36	4.01	3.58	3.92	4.12	4.19	4.08	3.25	3.93	4.23	4.22
K_2O	3.41	3.16	3.25	3.44	3.33	3.30	3.97	3.28	3.38	2.94	3.72	2.95	3.35	3.13	3.17	3.91	3.28	3.12	3.05
Cl	2.46	0.16	0.29	0.25	0.03	0.15	0.14	0.26	0.12	0.18	0.18	0.21	0.17	0.12	0.14	0.12	0.36	0.13	0.18
Totals	97.39	96.50	99.40	97.08	96.58	95.08	95.63	97.15	99.15	95.84	98.53	95.22	96.28	97.20	97.69	97.10	97.51	97.70	97.65
Analyses normalised to 100% loss free																			
SiO_2	76.29	78.04	77.06	77.53	77.34	77.78	76.72	78.05	77.57	77.53	76.49	78.61	77.72	77.95	77.90	78.01	77.39	78.01	77.62
TiO_2	0.21	0.22	0.13	0.13	0.18	0.20	0.17	0.20	0.22	0.09	0.20	0.25	0.18	0.21	0.15	0.17	0.22	0.20	0.23
Al_2O_3	11.87	12.27	12.87	12.32	12.58	12.35	13.19	11.49	12.43	12.59	13.26	11.85	12.23	12.20	12.20	12.06	12.62	12.26	12.62
FeO	0.98	1.01	1.00	0.82	0.98	0.79	1.10	0.98	0.93	1.20	1.15	0.90	0.82	0.89	1.02	0.96	1.04	0.94	1.01
MgO	0.37	0.20	0.14	0.16	0.07	0.17	0.08	0.18	0.15	0.15	0.18	0.21	0.17	0.18	0.17	0.18	0.12	0.14	0.13
CaO	0.80	0.77	0.83	0.93	1.25	0.88	0.56	0.98	0.77	1.00	1.14	0.75	0.94	0.91	0.99	1.13	0.85	0.80	0.77
Na_2O	3.45	4.06	4.41	4.32	4.11	4.20	3.90	4.46	4.40	4.18	3.63	4.11	4.28	4.31	4.18	3.35	4.03	4.33	4.32
K_2O	3.50	3.28	3.27	3.54	3.45	3.47	4.15	3.38	3.41	3.07	3.77	3.10	3.48	3.22	3.24	4.02	3.36	3.19	3.12
Cl	2.52	0.16	0.29	0.26	0.03	0.16	0.14	0.27	0.12	0.19	0.18	0.22	0.17	0.13	0.15	0.13	0.37	0.13	0.19
Totals	100.00	100.00	100.00	100.00	100.00	100.00	100.00	100.00	100.00	100.00	100.00	100.00	100.00	100.00	100.00	100.00	100.00	100.00	100.00

Poraiti #2: 220cm

	1	2	3	4	5	6	7	8	9	10	11	12	13
SiO_2	71.08	72.10	71.31	72.33	73.31	72.53	71.89	72.70	68.56	72.23	74.06	72.67	74.47
TiO_2	0.18	0.21	0.17	0.14	0.27	0.00	0.15	0.16	0.23	0.11	0.23	0.13	0.18
Al_2O_3	11.39	11.86	11.49	11.92	11.86	11.70	11.69	11.47	11.30	11.87	11.11	11.42	10.99
FeO	1.11	1.22	1.21	1.12	1.11	1.29	1.00	1.07	1.23	1.21	0.96	1.12	0.97
MgO	0.13	0.13	0.18	0.17	0.14	0.13	0.11	0.14	0.24	0.16	0.17	0.18	0.17
CaO	1.09	1.17	1.14	0.88	0.92	0.72	1.10	1.13	0.99	0.94	0.94	1.03	0.93
Na_2O	3.31	3.74	3.67	3.35	3.34	3.83	3.67	3.74	3.60	3.82	3.48	3.68	3.44
K_2O	2.70	2.85	3.12	3.93	3.82	3.44	2.88	2.88	2.60	2.84	3.06	2.86	3.72
Cl	0.23	0.25	0.22	0.32	0.28	0.28	0.19	0.20	0.29	0.20	0.38	0.29	0.09
Totals	91.23	93.54	92.51	94.15	95.05	93.92	92.68	93.48	89.02	93.37	94.39	93.37	94.95
Analyses normalised to 100% loss free													
SiO_2	77.92	77.09	77.08	76.82	77.13	77.22	77.57	77.77	77.01	77.36	78.46	77.83	78.43
TiO_2	0.20	0.22	0.19	0.15	0.29	0.00	0.16	0.17	0.26	0.12	0.24	0.14	0.19
Al_2O_3	12.48	12.68	12.42	12.66	12.48	12.46	12.61	12.27	12.69	12.71	11.77	12.23	11.58
FeO	1.22	1.30	1.31	1.19	1.17	1.37	1.08	1.15	1.38	1.30	1.02	1.20	1.02
MgO	0.15	0.14	0.19	0.18	0.15	0.14	0.12	0.14	0.27	0.17	0.18	0.19	0.18
CaO	1.20	1.25	1.23	0.93	0.96	0.77	1.18	1.21	1.11	1.01	1.00	1.10	0.98
Na_2O	3.62	4.00	3.96	3.56	3.52	4.08	3.96	4.00	4.04	4.09	3.68	3.94	3.62
K_2O	2.96	3.04	3.38	4.17	4.02	3.66	3.11	3.08	2.92	3.04	3.25	3.06	3.92
Cl	0.25	0.27	0.24	0.34	0.30	0.29	0.20	0.22	0.32	0.21	0.40	0.31	0.09
Totals	100.00	100.00	100.00	100.00	100.00	100.00	100.00	100.00	100.00	100.00	100.00	100.00	100.00

Poraiti #2:280cm

	1	2	3	4	5	6	7	8	9	10
SiO_2	74.60	75.12	76.69	74.72	74.38	75.08	75.74	74.66	74.95	76.30
TiO_2	0.18	0.17	0.16	0.18	0.18	0.19	0.14	0.14	0.16	0.67
Al_2O_3	11.26	11.47	11.32	11.62	11.66	11.32	11.55	11.29	12.02	11.38
FeO	1.11	1.14	1.23	1.10	1.06	1.00	1.12	1.07	1.09	0.92
MgO	0.14	0.15	0.29	0.20	0.13	0.25	0.26	0.18	0.24	0.19
CaO	0.88	1.08	0.96	1.18	1.01	1.15	1.17	0.94	1.18	0.90
Na_2O	3.47	3.31	3.57	3.54	3.56	3.47	3.45	3.55	3.58	3.34
K_2O	3.11	3.31	3.26	3.39	3.48	3.26	3.17	3.59	3.51	3.70
Cl	0.19	0.24	0.18	0.21	0.23	0.34	0.19	0.21	0.19	0.33
Totals	94.94	95.99	97.66	96.14	95.69	96.05	96.78	95.62	96.92	97.73
Analyses normalised to 100% loss free										
SiO_2	78.58	78.26	78.53	77.72	77.73	78.16	78.26	78.08	77.33	78.07
TiO_2	0.19	0.18	0.16	0.19	0.19	0.20	0.15	0.15	0.17	0.69
Al_2O_3	11.86	11.95	11.59	12.08	12.18	11.79	11.93	11.80	12.40	11.64
FeO	1.17	1.19	1.26	1.15	1.11	1.04	1.16	1.12	1.13	0.94
MgO	0.15	0.16	0.30	0.21	0.13	0.26	0.26	0.19	0.25	0.19
CaO	0.93	1.13	0.99	1.23	1.05	1.19	1.21	0.98	1.21	0.92
Na_2O	3.65	3.45	3.66	3.68	3.72	3.61	3.56	3.71	3.69	3.42
K_2O	3.28	3.44	3.34	3.52	3.64	3.40	3.28	3.76	3.62	3.79
Cl	0.20	0.25	0.18	0.22	0.24	0.35	0.19	0.22	0.19	0.34
Totals	100.00	100.00	100.00	100.00	100.00	100.00	100.00	100.00	100.00	100.00

Poraiti #2:320cm

	1	2	3	4	5	6	7	8	9	10	11	12	13
SiO_2	71.42	74.62	71.99	72.19	73.24	71.60	74.44	71.85	72.80	72.56	70.77	75.65	72.28
TiO_2	0.15	0.24	0.12	0.16	0.14	0.05	0.22	0.17	0.15	0.14	0.27	0.18	0.08
Al_2O_3	11.21	11.28	11.84	11.64	11.37	11.33	11.43	11.68	11.15	11.60	11.35	11.99	11.16
FeO	0.85	0.96	1.07	1.18	1.01	0.89	1.04	1.22	0.79	1.22	1.20	0.84	1.07
MgO	0.15	0.11	0.15	0.14	0.18	0.14	0.19	0.17	0.13	0.09	0.19	0.16	0.07
CaO	0.91	0.93	0.91	0.97	1.00	1.05	1.05	1.24	0.90	0.87	1.18	0.88	0.73
Na_2O	3.46	3.33	3.58	3.58	3.63	3.69	3.40	3.83	3.53	3.96	3.70	3.80	3.62
K_2O	3.65	3.50	3.86	3.91	3.64	2.76	3.85	2.61	3.80	3.44	2.61	3.26	3.18
Cl	0.21	0.18	0.22	0.25	0.24	0.22	0.20	0.18	0.17	0.27	0.22	0.16	0.28
Totals	92.02	95.14	93.73	94.01	94.43	91.74	95.81	92.93	93.42	94.14	91.48	96.93	92.46
Analyses normalised to 100% loss free													
SiO_2	77.61	78.43	76.81	76.79	77.55	78.05	77.69	77.31	77.93	77.08	77.36	78.05	78.17
TiO_2	0.17	0.25	0.12	0.17	0.15	0.06	0.23	0.18	0.16	0.15	0.29	0.18	0.08
Al_2O_3	12.18	11.85	12.63	12.39	12.04	12.35	11.92	12.57	11.93	12.32	12.41	12.37	12.07
FeO	0.93	1.01	1.14	1.26	1.07	0.97	1.08	1.31	0.84	1.29	1.31	0.87	1.16
MgO	0.17	0.12	0.16	0.14	0.19	0.16	0.20	0.18	0.14	0.09	0.21	0.17	0.08
CaO	0.99	0.97	0.97	1.03	1.05	1.14	1.10	1.34	0.96	0.92	1.28	0.91	0.79
Na_2O	3.76	3.50	3.82	3.81	3.84	4.02	3.55	4.12	3.78	4.21	4.05	3.92	3.91
K_2O	3.97	3.68	4.11	4.16	3.85	3.01	4.02	2.81	4.07	3.65	2.85	3.37	3.44
Cl	0.23	0.18	0.24	0.26	0.25	0.24	0.21	0.19	0.19	0.29	0.24	0.17	0.30
Totals	100.00	100.00	100.00	100.00	100.00	100.00	100.00	100.00	100.00	100.00	100.00	100.00	100.00

Poraiti #2: 340cm

	1	2	3	4	5	6	7	8	9	10	11	12	13
SiO_2	73.70	73.51	74.00	73.27	73.79	73.23	75.08	69.44	70.68	69.88	70.65	70.86	70.88
TiO_2	0.25	0.14	0.23	0.19	0.28	0.17	0.22	0.15	0.24	0.20	0.23	0.15	0.16
Al_2O_3	11.81	11.69	11.81	11.86	12.22	11.48	12.27	10.56	10.53	10.80	10.40	10.83	10.85
FeO	1.10	1.02	1.25	1.09	1.32	1.25	1.20	1.20	1.09	1.21	1.05	1.03	1.40
MgO	0.18	0.05	0.11	0.19	0.20	0.21	0.15	0.17	0.11	0.16	0.10	0.16	0.18
CaO	1.11	0.52	1.04	0.94	1.05	1.20	1.15	1.10	0.86	1.04	1.04	0.86	1.10
Na_2O	3.75	3.66	4.03	4.09	3.90	2.34	3.74	3.60	3.24	2.84	3.52	3.28	2.30
K_2O	2.74	3.08	3.04	3.26	2.83	2.63	4.01	2.64	3.83	2.54	2.86	4.14	2.63
Cl	0.20	0.17	0.11	0.29	0.27	0.22	0.34	0.29	0.28	0.22	0.22	0.27	0.25
Totals	94.84	93.82	95.60	95.17	95.86	92.73	98.15	89.14	90.86	88.88	90.07	91.59	89.74
Analyses normalised to 100% loss free													
SiO_2	77.70	78.35	77.40	76.98	76.98	78.97	76.50	77.89	77.79	78.62	78.44	77.37	78.98
TiO_2	0.26	0.14	0.24	0.20	0.30	0.18	0.22	0.16	0.27	0.23	0.26	0.16	0.18
Al_2O_3	12.46	12.45	12.35	12.46	12.75	12.38	12.50	11.85	11.59	12.15	11.54	11.83	12.09
FeO	1.16	1.09	1.31	1.15	1.37	1.35	1.23	1.35	1.20	1.36	1.17	1.13	1.56
MgO	0.19	0.05	0.12	0.20	0.21	0.23	0.15	0.19	0.12	0.17	0.11	0.18	0.20
CaO	1.17	0.55	1.08	0.98	1.10	1.29	1.17	1.24	0.94	1.17	1.16	0.94	1.23
Na_2O	3.95	3.90	4.21	4.30	4.07	2.52	3.81	4.04	3.57	3.19	3.91	3.58	2.56
K_2O	2.89	3.28	3.17	3.43	2.95	2.84	4.08	2.96	4.21	2.86	3.18	4.51	2.93
Cl	0.21	0.18	0.11	0.31	0.28	0.23	0.34	0.33	0.31	0.25	0.24	0.30	0.28
Totals	100.00	100.00	100.00	100.00	100.00	100.00	100.00	100.00	100.00	100.00	100.00	100.00	100.00

Poraiti #2: 370cm

	1	2	3	4	5	6	7	8	9	10	11	12	13	14
SiO_2	73.36	72.32	73.48	69.30	72.62	73.61	72.32	73.68	71.64	72.97	75.25	77.38	75.41	72.36
TiO_2	0.14	0.29	0.19	0.12	0.15	0.16	0.16	0.24	0.16	0.14	0.23	0.13	0.20	0.20
Al_2O_3	11.66	11.58	11.90	11.60	11.49	11.84	12.01	11.70	12.20	11.82	11.50	11.46	11.44	11.66
FeO	1.08	1.12	0.96	1.83	0.93	0.90	1.12	0.84	1.27	1.41	0.97	1.22	1.06	0.90
MgO	0.14	0.12	0.16	0.18	0.26	0.16	0.12	0.16	0.25	0.14	0.12	0.14	0.17	0.11
CaO	0.91	0.96	1.06	1.03	0.89	0.76	0.89	0.96	1.02	1.01	1.19	0.92	0.92	0.89
Na_2O	3.50	3.25	3.32	3.47	3.99	3.73	3.44	3.46	4.02	3.71	3.76	3.31	3.27	3.80
K_2O	3.87	3.86	3.83	3.47	2.87	3.21	3.84	3.90	2.60	2.57	2.85	3.79	3.67	3.04
Cl	0.24	0.20	0.21	0.54	0.27	0.20	0.17	0.20	0.22	0.25	0.20	0.14	0.21	0.22
Totals	94.90	93.71	95.10	91.55	93.46	94.57	94.07	95.14	93.40	94.03	96.07	98.48	96.36	93.20
Analyses normalised to 100% loss free														
SiO_2	77.30	77.18	77.27	75.70	77.70	77.84	76.88	77.45	76.71	77.61	78.33	78.58	78.26	77.65
TiO_2	0.15	0.31	0.20	0.13	0.16	0.16	0.17	0.25	0.17	0.15	0.24	0.13	0.21	0.22
Al_2O_3	12.29	12.36	12.52	12.67	12.29	12.52	12.77	12.29	13.06	12.58	11.97	11.63	11.87	12.51
FeO	1.14	1.20	1.00	2.00	1.00	0.96	1.19	0.88	1.36	1.50	1.01	1.23	1.10	0.97
MgO	0.15	0.12	0.17	0.19	0.28	0.16	0.13	0.17	0.27	0.15	0.12	0.14	0.18	0.12
CaO	0.96	1.02	1.11	1.12	0.95	0.81	0.95	1.01	1.10	1.08	1.24	0.93	0.96	0.95
Na_2O	3.68	3.47	3.49	3.79	4.26	3.95	3.66	3.64	4.31	3.94	3.91	3.36	3.39	4.08
K_2O	4.07	4.12	4.02	3.79	3.07	3.40	4.09	4.10	2.78	2.73	2.97	3.85	3.81	3.27
Cl	0.25	0.21	0.22	0.59	0.29	0.21	0.18	0.21	0.24	0.26	0.21	0.14	0.22	0.23
Totals	100.00	100.00	100.00	100.00	100.00	100.00	100.00	100.00	100.00	100.00	100.00	100.00	100.00	100.00

Poraiti #2: 420cm

	1	2	3	4	5	6	7	8	9	10	11	12	13	14
SiO_2	73.92	70.85	72.84	71.27	74.98	70.86	71.48	72.04	71.95	70.67	75.86	72.89	72.25	75.58
TiO_2	0.23	0.09	0.18	0.15	0.21	0.13	0.18	0.08	0.14	0.14	0.19	0.12	0.17	0.10
Al_2O_3	11.90	11.21	11.84	11.53	11.88	11.45	11.22	11.37	11.65	11.20	11.47	11.77	11.88	11.40
FeO	1.05	1.04	1.15	1.04	0.99	0.95	1.18	1.21	1.12	1.39	1.11	1.17	0.98	1.18
MgO	0.16	0.18	0.17	0.15	0.13	0.10	0.14	0.12	0.15	0.09	0.17	0.19	0.11	0.14
CaO	0.90	0.99	0.91	0.70	1.05	0.79	0.95	1.10	1.04	1.37	0.99	1.03	0.91	1.03
Na_2O	3.26	3.43	3.70	3.17	3.55	3.07	3.56	3.94	3.80	3.32	2.35	3.76	3.49	3.16
K_2O	3.82	2.72	3.15	3.96	4.02	3.82	2.78	2.82	2.83	2.72	2.68	3.07	3.56	2.82
Cl	0.27	0.31	0.16	0.30	0.24	0.17	0.20	0.25	0.00	0.18	0.26	0.24	0.25	0.28
Totals	95.51	90.82	94.09	92.27	97.06	91.34	91.68	92.92	92.68	91.08	95.08	94.23	93.61	95.66
Analyses normalised to 100% loss free														
SiO_2	77.40	78.01	77.41	77.24	77.25	77.58	77.97	77.53	77.63	77.60	79.79	77.35	77.19	79.00
TiO_2	0.24	0.10	0.19	0.16	0.22	0.14	0.19	0.08	0.15	0.15	0.20	0.13	0.18	0.11
Al_2O_3	12.46	12.34	12.58	12.50	12.24	12.53	12.24	12.23	12.57	12.30	12.07	12.49	12.70	11.91
FeO	1.10	1.15	1.22	1.13	1.02	1.04	1.29	1.30	1.21	1.53	1.17	1.24	1.04	1.23
MgO	0.17	0.19	0.18	0.16	0.13	0.11	0.15	0.12	0.17	0.10	0.18	0.20	0.12	0.14
CaO	0.94	1.09	0.97	0.76	1.08	0.86	1.04	1.18	1.12	1.50	1.04	1.10	0.98	1.07
Na_2O	3.41	3.78	3.93	3.43	3.66	3.36	3.89	4.24	4.10	3.64	2.47	3.98	3.73	3.30
K_2O	4.00	3.00	3.35	4.29	4.15	4.18	3.03	3.03	3.05	2.99	2.82	3.26	3.80	2.94
Cl	0.28	0.34	0.17	0.32	0.25	0.19	0.21	0.27	0.00	0.20	0.27	0.25	0.27	0.29
Totals	100.00	100.00	100.00	100.00	100.00	100.00	100.00	100.00	100.00	100.00	100.00	100.00	100.00	100.00

Poraiti #2: 450cm

	1	2	3	4	6	7
SiO_2	70.46	70.55	70.22	71.24	68.35	68.33
TiO_2	0.23	0.20	0.18	0.14	0.13	0.14
Al_2O_3	10.53	10.63	10.57	10.69	10.56	10.65
FeO	1.07	1.34	1.22	1.42	1.08	0.96
MgO	0.17	0.13	0.13	0.10	0.17	0.13
CaO	2.26	0.96	0.99	0.95	1.00	0.86
Na_2O	3.11	3.18	3.61	2.79	2.81	3.24
K_2O	2.63	3.46	2.67	3.58	3.99	3.76
Cl	0.22	0.25	0.19	0.27	0.28	0.28
Totals	90.66	90.68	89.79	91.18	88.36	88.35
Analyses normalised to 100% loss free						
SiO_2	77.72	77.79	78.21	78.13	77.36	77.34
TiO_2	0.25	0.22	0.20	0.15	0.15	0.16
Al_2O_3	11.62	11.72	11.77	11.72	11.95	12.05
FeO	1.18	1.47	1.36	1.56	1.23	1.09
MgO	0.18	0.14	0.15	0.10	0.19	0.15
CaO	2.49	1.06	1.10	1.04	1.13	0.97
Na_2O	3.42	3.50	4.02	3.06	3.18	3.66
K_2O	2.90	3.82	2.97	3.93	4.52	4.25
Cl	0.24	0.28	0.22	0.30	0.31	0.32
Totals	100.00	100.00	100.00	100.00	100.00	100.00

Poraiti #2: 550cm

	1	2	3
SiO_2	72.16	80.82	61.59
TiO_2	0.07	0.07	0.66
Al_2O_3	11.90	7.65	17.77
FeO	0.27	0.65	0.94
MgO	0.08	0.07	0.37
CaO	0.64	0.24	0.40
Na_2O	3.32	1.69	5.90
K_2O	4.59	3.88	5.85
Cl	0.16	0.04	0.04
Totals	93.19	95.10	93.51
Analyses normalised to 100% loss free			
SiO_2	77.44	84.98	65.87
TiO_2	0.08	0.08	0.71
Al_2O_3	12.76	8.04	19.00
FeO	0.29	0.69	1.00
MgO	0.08	0.07	0.40
CaO	0.68	0.25	0.43
Na_2O	3.56	1.78	6.30
K_2O	4.93	4.07	6.25
Cl	0.17	0.04	0.04
Totals	100.00	100.00	100.00

City Hire section tephra

	1	2	3	4	5	6	7	8	9	10	11	12	13	14	15
SiO_2	73.07	71.97	73.82	71.46	71.44	71.75	71.96	71.99	71.56	72.45	74.98	74.18	72.82	71.59	74.17
TiO_2	0.18	0.13	0.16	0.16	0.13	0.21	0.18	0.10	0.17	0.16	0.24	0.10	0.15	0.22	0.60
Al_2O_3	11.48	11.52	11.77	11.49	11.54	11.53	11.76	11.48	11.28	11.89	11.78	11.81	11.57	11.60	11.89
FeO	1.20	0.90	1.11	1.14	0.99	1.14	1.22	1.05	1.03	1.01	1.04	1.16	1.11	1.03	1.05
MgO	0.18	0.18	0.15	0.12	0.10	0.13	0.18	0.09	0.10	0.10	0.20	0.17	0.20	0.17	0.12
CaO	0.78	0.89	0.79	0.72	0.89	0.73	0.76	0.73	0.82	0.81	0.86	0.80	0.76	0.87	0.81
Na_2O	3.77	3.29	3.42	3.58	3.29	3.50	3.37	4.01	3.34	3.32	3.43	3.16	3.49	3.37	3.57
K_2O	3.95	4.20	4.26	3.94	3.79	4.14	3.91	3.32	4.11	4.62	4.09	4.03	4.00	3.95	4.11
Cl	0.30	0.29	0.30	0.25	0.27	0.25	0.20	0.14	0.22	0.26	0.28	0.20	0.24	0.23	0.22
Totals	94.92	93.37	95.79	92.85	92.45	93.37	93.52	92.89	92.63	94.61	96.89	95.61	94.33	93.02	96.53
Analyses normalised to 100% loss free															
SiO_2	76.99	77.08	77.07	76.97	77.28	76.85	76.95	77.50	77.26	76.58	77.39	77.59	77.19	76.96	76.84
TiO_2	0.19	0.14	0.17	0.17	0.14	0.22	0.19	0.10	0.19	0.17	0.25	0.10	0.16	0.23	0.62
Al_2O_3	12.10	12.34	12.28	12.37	12.48	12.35	12.57	12.35	12.17	12.57	12.15	12.36	12.26	12.47	12.32
FeO	1.26	0.96	1.16	1.23	1.07	1.22	1.30	1.13	1.11	1.07	1.07	1.22	1.18	1.11	1.08
MgO	0.19	0.19	0.16	0.12	0.11	0.14	0.19	0.09	0.11	0.10	0.20	0.17	0.22	0.18	0.12
CaO	0.82	0.95	0.83	0.77	0.97	0.78	0.81	0.79	0.89	0.85	0.89	0.84	0.80	0.93	0.84
Na_2O	3.98	3.52	3.57	3.85	3.56	3.75	3.60	4.31	3.60	3.51	3.54	3.31	3.69	3.62	3.70
K_2O	4.16	4.50	4.45	4.24	4.10	4.43	4.18	3.57	4.43	4.88	4.22	4.21	4.24	4.25	4.26
Cl	0.32	0.31	0.31	0.27	0.30	0.26	0.21	0.15	0.24	0.27	0.29	0.21	0.25	0.25	0.22
Totals	100.00	100.00	100.00	100.00	100.00	100.00	100.00	100.00	100.00	100.00	100.00	100.00	100.00	100.00	100.00

Oruanui Ignimbrite: Tarawera Farm, Mohaka River

	1	2	3	4	5	6	7	8	9	10
SiO_2	75.10	73.06	74.54	75.68	76.46	75.16	76.19	75.00	76.06	75.60
TiO_2	0.20	0.14	0.13	0.07	0.11	0.12	0.10	0.19	0.14	0.11
Al_2O_3	11.92	11.44	11.57	11.92	11.87	11.92	11.81	11.73	12.36	11.95
FeO	1.45	1.33	1.29	1.17	1.19	1.28	1.46	1.30	1.28	1.35
MgO	0.17	0.22	0.10	0.12	0.09	0.11	0.19	0.09	0.18	0.15
CaO	1.08	1.04	1.00	1.10	1.20	0.97	1.03	1.04	1.12	0.99
Na_2O	3.64	3.82	3.93	4.09	3.95	4.08	3.84	3.89	4.32	3.99
K_2O	3.40	3.04	3.16	3.20	3.31	2.97	3.13	3.08	2.83	3.33
Cl	0.22	0.18	0.30	0.18	0.16	0.14	0.18	0.17	0.18	0.15
Totals	97.18	94.24	96.01	97.53	98.35	96.74	97.93	96.49	98.46	97.61
Analyses normalised to 100% loss free										
SiO_2	77.28	77.52	77.64	77.60	77.74	77.69	77.81	77.72	77.25	77.45
TiO_2	0.21	0.14	0.13	0.07	0.11	0.12	0.10	0.19	0.14	0.11
Al_2O_3	12.27	12.14	12.05	12.22	12.07	12.32	12.06	12.15	12.56	12.24
FeO	1.49	1.41	1.35	1.20	1.21	1.32	1.49	1.35	1.30	1.38
MgO	0.17	0.23	0.11	0.13	0.09	0.11	0.20	0.10	0.18	0.15
CaO	1.11	1.11	1.04	1.13	1.22	1.00	1.05	1.08	1.13	1.01
Na_2O	3.75	4.05	4.10	4.19	4.02	4.22	3.92	4.04	4.38	4.08
K_2O	3.50	3.22	3.29	3.28	3.37	3.06	3.20	3.19	2.88	3.41
Cl	0.22	0.19	0.31	0.18	0.16	0.15	0.18	0.18	0.18	0.15
Totals	100.00	100.00	100.00	100.00	100.00	100.00	100.00	100.00	100.00	100.00

Potaka Ignimbrite: Mangaonuku Stream

	1	2	3	4	5	6	7	8	9	10	11
SiO_2	73.70	74.78	75.59	75.07	74.46	74.41	74.37	74.37	73.78	73.86	74.38
TiO_2	0.13	0.10	0.22	0.16	0.17	0.11	0.18	0.14	0.13	0.14	0.03
Al_2O_3	11.88	11.84	12.01	12.06	11.95	11.99	11.95	11.85	12.03	11.87	11.81
FeO	0.90	1.01	1.05	1.06	1.19	1.02	1.25	1.29	1.23	1.01	1.50
MgO	0.10	0.07	0.11	0.14	0.08	0.14	0.12	0.16	0.12	0.09	0.05
CaO	0.79	0.84	0.85	0.74	0.70	0.85	1.02	0.94	0.82	0.75	0.61
Na_2O	4.03	3.62	2.58	3.64	3.78	3.80	3.72	3.59	3.70	3.66	3.71
K_2O	3.64	3.88	3.69	3.92	3.68	3.89	3.39	3.59	3.35	3.90	4.27
Cl	0.18	0.24	0.28	0.23	0.23	0.24	0.22	0.21	0.23	0.25	0.23
Totals	95.33	96.39	96.37	97.02	96.24	96.45	96.23	96.13	95.38	95.52	96.58
Analyses normalised to 100% loss free											
SiO_2	77.31	77.59	78.44	77.38	77.37	77.15	77.28	77.36	77.36	77.32	77.01
TiO_2	0.13	0.10	0.22	0.16	0.17	0.12	0.18	0.15	0.14	0.14	0.03
Al_2O_3	12.46	12.29	12.46	12.42	12.42	12.43	12.42	12.33	12.61	12.43	12.23
FeO	0.94	1.05	1.09	1.10	1.24	1.06	1.30	1.34	1.29	1.06	1.55
MgO	0.10	0.07	0.11	0.15	0.08	0.15	0.13	0.16	0.12	0.09	0.05
CaO	0.82	0.87	0.88	0.76	0.73	0.88	1.06	0.98	0.86	0.79	0.63
Na_2O	4.23	3.76	2.67	3.75	3.93	3.93	3.87	3.73	3.88	3.83	3.84
K_2O	3.82	4.03	3.83	4.04	3.82	4.03	3.52	3.73	3.51	4.08	4.42
Cl	0.19	0.25	0.29	0.24	0.23	0.25	0.23	0.22	0.24	0.26	0.24
Totals	100.00	100.00	100.00	100.00	100.00	100.00	100.00	100.00	100.00	100.00	100.00

Ohakean 1 terrace; Mohaka River

	1	2	3	4	5	6	7	8	9	10	11	12	13	14
SiO_2	70.80	73.74	72.59	74.74	70.70	71.09	72.35	72.26	74.99	74.85	74.89	73.76	75.33	68.04
TiO_2	0.06	0.04	0.12	0.21	0.05	0.18	0.07	0.17	0.17	0.17	0.12	0.23	0.16	0.05
Al_2O_3	12.44	11.86	11.72	12.24	11.37	11.06	11.80	11.37	11.88	12.35	12.01	9.64	12.47	11.09
FeO	0.66	0.60	0.94	1.49	0.94	1.17	0.80	1.33	1.31	1.23	1.06	4.51	1.12	1.12
MgO	0.11	0.02	0.10	0.34	0.09	0.14	0.12	0.13	0.13	0.24	0.12	0.04	0.09	0.38
CaO	0.90	0.59	0.82		0.76	0.85	0.73	1.02	0.95	1.29	0.78	0.17	0.66	0.96
Na_2O	4.14	3.93	3.66	4.06	3.47	3.82	3.34	3.79	3.84	4.21	3.73	5.13	3.68	3.69
K_2O	3.70	3.97	3.70	2.92	3.62	2.92	3.77	2.95	3.33	2.79	4.09	4.42	3.92	2.75
Cl	0.12	0.20	0.12	0.15	0.19	0.17	0.12	0.21	0.14	0.14	0.20	0.29	0.17	n.d.
Totals	92.93	94.94	93.77	97.42	91.19	91.40	93.09	93.21	96.74	97.27	96.99	98.19	97.57	88.06
Normalised data														
SiO_2	76.19	77.67	77.41	76.72	77.52	77.78	77.72	77.52	77.52	76.95	77.21	75.12	77.20	77.26
TiO_2	0.06	0.05	0.13	0.22	0.06	0.19	0.08	0.18	0.17	0.18	0.13	0.23	0.16	0.05
Al_2O_3	13.39	12.49	12.50	12.56	12.47	12.10	12.68	12.20	12.28	12.70	12.38	9.82	12.78	12.59
FeO	0.71	0.63	1.01	1.53	1.03	1.28	0.86	1.42	1.36	1.27	1.09	4.60	1.15	1.27
MgO	0.12	0.02	0.11	0.35	0.10	0.15	0.12	0.14	0.13	0.25	0.12	0.04	0.09	0.43
CaO	0.97	0.62	0.87	1.31	0.83	0.93	0.78	1.09	0.99	1.32	0.81	0.17	0.68	1.09
Na_2O	4.46	4.14	3.90	4.17	3.80	4.18	3.59	4.07	3.96	4.33	3.84	5.23	3.77	4.18
K_2O	3.98	4.18	3.95	2.99	3.97	3.20	4.04	3.16	3.44	2.87	4.21	4.50	4.02	3.12
Cl	0.13	0.21	0.12	0.15	0.21	0.19	0.13	0.22	0.14	0.14	0.20	0.30	0.17	n.d
Totals	100.00	100.00	100.00	100.00	100.00	100.00	100.00	100.00	100.00	100.00	100.00	100.00	100.00	100.00

	15	16	17	18	19	20	21	22
SiO_2	76.59	72.10	75.00	76.78	76.52	76.74	74.27	76.63
TiO_2	0.23	0.06	0.23	0.07	0.08	0.20	0.18	0.10
Al_2O_3	11.76	12.06	11.62	12.24	12.08	11.97	9.24	11.72
FeO	0.85	0.85	1.11	0.78	1.21	0.77	4.49	0.80
MgO	0.21	0.43	0.18	0.08	0.15	0.22	0.00	0.23
CaO	0.88	0.83	1.06	0.81	0.92	0.69	0.25	0.91
Na_2O	3.99	3.83	3.62	4.01	3.62	3.22	5.35	3.66
K_2O	3.26	3.33	3.16	3.82	3.43	4.02	4.26	3.31
Cl	n.d	n.d	n.d	n.d	n.d	n.d	n.d	n.d
Totals	97.75	93.47	95.97	98.58	98.00	97.83	98.04	97.36
Normalised data								
SiO_2	78.35	77.13	78.15	77.88	78.08	78.44	75.76	78.71
TiO_2	0.24	0.06	0.24	0.07	0.08	0.21	0.18	0.10
Al_2O_3	12.03	12.90	12.11	12.41	12.33	12.23	9.42	12.04
FeO	0.86	0.90	1.15	0.79	1.24	0.79	4.58	0.82
MgO	0.21	0.45	0.18	0.08	0.16	0.23	0.00	0.24
CaO	0.90	0.88	1.10	0.82	0.94	0.70	0.25	0.93
Na_2O	4.08	4.10	3.77	4.07	3.69	3.30	5.46	3.76
K_2O	3.34	3.57	3.30	3.88	3.50	4.11	4.35	3.40
Cl	n.d	n.d	n.d	n.d	n.d	n.d	n.d	n.d
Totals	100.00	100.00	100.00	100.00	100.00	100.00	100.00	100.00

Variation Matrix for Ohakean 1 terrace

Numbers above unit diagonal are SIMILARITY COEFFICIENTS, below are COEFFICIENTS OF VARIATION.

	Karapiti	Waiohau	Rotorua	Puketera	unTu	Rerewhak	Okareka	Te Rere	Kawakawa	Oh1/1	Oh1/2	Oh1/3	Oh1/4	Oh1/5	Oh1/6
Karapiti	--	0.81	0.89	0.87	0.56	0.76	0.75	0.91	0.83	0.70	0.59	0.78	0.86	0.71	0.84
Waiohau	13.76	--	0.86	0.80	0.57	0.92	0.89	0.89	0.89	0.82	0.70	0.93	0.76	0.86	0.90
Rotorua	9.20	11.73	--	0.71	0.59	0.80	0.76	0.93	0.86	0.74	0.84	0.82	0.87	0.77	0.91
Puketera	19.63	18.79	20.39	--	0.56	0.86	0.88	0.73	0.76	0.79	0.79	0.83	0.84	0.86	0.72
unTu	25.86	26.30	28.19	25.31	--	0.56	0.56	0.57	0.55	0.54	0.80	0.59	0.59	0.54	0.82
Rerewhak	18.09	10.39	17.22	10.74	25.37	--	0.97	0.84	0.89	0.83	0.72	0.94	0.72	0.92	0.83
Okareka	17.48	9.23	18.49	10.99	25.09	4.12	--	0.81	0.87	0.83	0.74	0.92	0.89	0.90	0.80
Te Rere	12.06	7.52	8.34	18.46	26.26	14.31	13.43	--	0.89	0.77	0.85	0.86	0.82	0.80	0.90
Kawakawa	12.00	7.23	16.45	14.52	24.62	7.74	9.89	11.07	--	0.81	0.86	0.90	0.78	0.83	0.88
Oh1/1	18.79	15.29	19.70	12.62	28.94	12.48	12.07	18.24	15.70	--	0.79	0.85	0.68	0.89	0.78
Oh1/2	25.14	25.71	26.87	22.38	26.48	23.85	23.68	25.56	23.34	24.34	--	0.72	0.81	0.78	0.86
Oh1/3	14.52	7.15	14.77	13.83	27.34	4.82	5.11	12.36	8.89	16.48	26.23	--	0.74	0.91	0.86
Oh1/4	14.30	18.39	13.12	22.29	28.19	20.93	20.57	15.09	20.05	23.41	28.84	20.08	--	0.89	0.84
Oh1/5	19.01	18.34	22.28	10.26	26.80	14.87	14.20	20.35	14.49	10.10	23.91	17.46	23.80	--	0.80
Oh1/8	9.00	9.45	7.70	17.87	29.56	13.52	13.32	5.12	11.40	20.57	27.35	10.80	17.57	19.86	--

	Karapiti	Waiohau	Rotorua	Puketerata	unTu	Rerewhak	Okareka	Te Rere	Kawakawa	Oh1/7	Oh1/8	Oh1/9	Oh1/10	Oh1/11	Oh1/12
Karapiti	--	0.81	0.89	0.87	0.56	0.78	0.75	0.91	0.83	0.73	0.87	0.85	0.89	0.78	0.55
Waiohau	13.76	--	0.86	0.80	0.57	0.92	0.89	0.89	0.89	0.87	0.89	0.91	0.80	0.92	0.57
Rotorua	9.20	11.73	--	0.71	0.59	0.80	0.78	0.93	0.88	0.77	0.91	0.89	0.91	0.82	0.56
Puketera	19.63	18.79	20.39	--	0.56	0.86	0.88	0.73	0.78	0.90	0.71	0.74	0.86	0.83	0.59
unTu	25.86	26.30	28.19	25.31	--	0.56	0.56	0.57	0.55	0.55	0.81	0.81	0.59	0.80	0.85
Rerewhak	18.09	10.39	17.22	10.74	25.37	--	0.97	0.84	0.89	0.90	0.82	0.86	0.75	0.92	0.57
Okareka	17.48	9.23	18.49	10.99	25.09	4.12	--	0.81	0.87	0.93	0.79	0.83	0.73	0.90	0.57
Te Rere	12.06	7.52	8.34	18.46	26.26	14.31	13.43	--	0.89	0.80	0.90	0.90	0.89	0.86	0.55
Kawakawa	12.00	7.23	16.45	14.52	24.62	7.74	9.89	11.07	--	0.85	0.90	0.90	0.82	0.91	0.55
Oh1/7	18.46	12.41	16.39	13.25	28.35	8.46	9.33	15.68	13.15	--	0.78	0.82	0.72	0.90	0.55
Oh1/8	7.49	11.62	9.56	17.46	28.54	12.78	13.41	7.20	11.00	18.50	--	0.95	0.89	0.85	0.80
Oh1/9	10.20	9.96	10.17	16.86	27.95	12.10	12.75	9.08	8.32	16.42	3.33	--	0.86	0.89	0.80
Oh1/10	9.47	13.32	6.89	20.14	29.51	17.11	16.87	9.80	15.40	17.92	13.48	14.55	--	0.78	0.57
Oh1/11	14.21	8.84	14.61	14.80	27.97	8.20	7.08	12.56	9.91	12.78	10.59	8.92	18.08	--	0.80
Oh1/12	21.69	22.32	24.59	22.62	22.82	21.78	21.61	22.18	21.11	23.37	23.29	22.85	25.08	23.80	--

	Karapiti	Waiohau	Rotorua	Puketerata	unTu	Rerewhak	Okareka	Te Rere	Kawakawa	Oh1/13	Oh1/14	Oh1/15	Oh1/16	Oh1/17	Oh1/18
Karapiti	--	0.81	0.89	0.87	0.56	0.76	0.75	0.91	0.83	0.79	0.75	0.80	0.70	0.85	0.88
Waiohau	13.78	--	0.86	0.80	0.57	0.92	0.89	0.89	0.89	0.87	0.75	0.88	0.81	0.86	0.83
Rotorua	9.20	11.73	--	0.71	0.59	0.80	0.78	0.93	0.88	0.82	0.82	0.89	0.78	0.95	0.73
Puketera	19.63	18.79	20.39	--	0.56	0.88	0.88	0.73	0.78	0.85	0.70	0.74	0.78	0.71	0.89
unTu	25.86	26.30	28.19	25.31	--	0.56	0.56	0.57	0.55	0.82	0.51	0.58	0.52	0.58	0.55
Rerewhak	18.09	10.39	17.22	10.74	25.37	--	0.97	0.84	0.89	0.89	0.74	0.82	0.81	0.81	0.88
Okareka	17.48	9.23	18.49	10.99	25.09	4.12	--	0.81	0.87	0.88	0.72	0.81	0.80	0.78	0.89
Te Rere	12.06	7.52	8.34	18.46	26.26	14.31	13.43	--	0.89	0.86	0.79	0.86	0.77	0.92	0.76
Kawakawa	12.00	7.23	16.45	14.52	24.62	7.74	9.89	11.07	--	0.85	0.80	0.81	0.75	0.88	0.79
Oh1/13	19.77	10.93	18.44	14.87	27.41	9.80	9.87	18.21	12.88	--	0.71	0.79	0.74	0.82	0.84
Oh1/14	21.50	23.19	26.30	21.83	26.28	22.97	22.04	23.84	25.88	25.85	--	0.76	0.89	0.79	0.75
Oh1/15	14.50	14.85	8.88	23.11	27.98	19.88	19.91	9.71	18.95	18.04	24.50	--	0.81	0.92	0.79
Oh1/16	20.47	24.76	22.10	23.97	26.99	25.11	24.35	21.54	21.23	25.45	9.78	25.88	--	0.75	0.84
Oh1/17	11.16	13.89	5.80	21.44	26.94	18.34	17.56	10.81	17.70	17.95	26.79	9.31	23.77	--	0.74
Oh1/18	19.29	17.57	21.42	7.45	26.87	11.73	11.49	19.08	13.26	17.33	23.27	25.34	24.88	22.04	--

	Karapiti	Waiohau	Rotorua	Puketerata	unTu	Rerewhak	Okareka	Te Rere	Kawakawa	Oh1/19	Oh1/20	Oh1/21	Oh1/22
Karapiti	--	0.81	0.89	0.87	0.56	0.76	0.75	0.91	0.83	0.81	0.78	0.55	0.78
Waiohau	13.78	--	0.86	0.80	0.57	0.92	0.89	0.89	0.89	0.88	0.83	0.56	0.88
Rotorua	9.20	11.73	--	0.71	0.59	0.80	0.78	0.93	0.88	0.88	0.84	0.56	0.84
Puketera	19.63	18.79	20.39	--	0.56	0.86	0.88	0.73	0.78	0.82	0.80	0.54	0.79
unTu	25.86	26.30	28.19	25.31	--	0.56	0.56	0.57	0.55	0.54	0.80	0.81	0.54
Rerewhak	18.09	10.39	17.22	10.74	25.37	--	0.97	0.84	0.89	0.87	0.80	0.55	0.87
Okareka	17.48	9.23	18.49	10.99	25.09	4.12	--	0.81	0.87	0.85	0.83	0.54	0.87
Te Rere	12.06	7.52	8.34	18.46	26.26	14.31	13.43	--	0.89	0.88	0.81	0.56	0.85
Kawakawa	12.00	7.23	16.45	14.52	24.62	7.74	9.89	11.07	--	0.88	0.78	0.53	0.85
Oh1/19	14.75	13.87	18.27	17.63	25.02	13.44	13.30	15.09	11.21	--	0.77	0.52	0.88
Oh1/20	17.00	12.42	12.76	25.87	29.42	18.45	19.63	10.79	16.19	18.13	--	0.56	0.88
Oh1/21	25.53	25.63	26.54	25.61	30.44	25.04	24.93	25.90	24.22	24.02	26.12	--	0.53
Oh1/22	15.14	14.41	15.61	20.13	25.92	17.63	17.39	12.84	15.62	13.63	16.18	24.74	--

Ohakean 2 terrace: Mohaka River

	1	2	3	4	5	6	7	8	9	10	11	12	13	14	15
SiO_2	73.43	75.18	75.35	74.25	73.30	73.36	74.07	73.37	70.73	74.91	73.04	74.88	74.07	75.75	76.89
TiO_2	0.09	0.12	0.18	0.14	0.21	0.10	0.13	0.13	0.18	0.31	0.09	0.10	0.13	0.14	0.25
Al_2O_3	11.78	12.05	11.91	11.98	11.56	11.90	11.85	11.80	11.33	12.42	11.74	12.02	11.62	11.61	11.68
FeO	1.16	1.11	1.03	0.90	0.95	0.92	1.19	1.03	1.20	1.94	1.45	1.15	1.08	1.15	1.02
MgO	0.17	0.17	0.19	0.13	0.19	0.05	0.14	0.17	0.16	0.29	0.12	0.10	0.17	0.41	0.45
CaO	1.08	0.84	0.91	0.74	0.88	0.58	1.07	0.88	0.94	1.49	1.06	0.77	1.00	1.03	1.06
Na_2O	3.67	3.90	3.42	3.86	3.93	3.44	4.01	3.80	3.46	4.18	3.72	3.91	3.87	3.42	3.54
K_2O	2.93	3.44	3.13	4.11	2.99	3.88	3.11	3.03	2.76	2.90	3.05	3.85	3.29	3.22	3.39
Cl	0.20	0.12	0.13	0.14	0.18	0.12	0.25	0.16	0.21	0.09	0.33	0.16	0.19	n.d.	n.d.
Totals	94.51	96.94	96.19	96.24	94.19	94.35	95.81	94.35	90.97	98.52	94.61	96.92	95.41	96.72	98.28
Normalised data															
SiO_2	77.70	77.55	78.34	77.15	77.83	77.75	77.31	77.76	77.75	76.03	77.20	77.26	77.64	78.32	78.24
TiO_2	0.10	0.13	0.18	0.15	0.22	0.11	0.13	0.14	0.20	0.31	0.10	0.10	0.13	0.14	0.26
Al_2O_3	12.46	12.43	12.38	12.44	12.27	12.61	12.36	12.50	12.46	12.61	12.41	12.40	12.18	12.01	11.88
FeO	1.23	1.14	1.07	0.94	1.01	0.98	1.24	1.09	1.31	1.97	1.53	1.18	1.13	1.19	1.04
MgO	0.18	0.17	0.20	0.13	0.20	0.05	0.15	0.18	0.17	0.29	0.13	0.10	0.18	0.42	0.45
CaO	1.14	0.87	0.95	0.77	0.93	0.61	1.12	0.93	1.04	1.51	1.12	0.79	1.05	1.06	1.08
Na_2O	3.89	4.02	3.56	4.01	4.17	3.65	4.18	4.03	3.80	4.24	3.93	4.03	4.06	3.53	3.60
K_2O	3.10	3.55	3.26	4.27	3.18	4.11	3.25	3.21	3.04	2.95	3.22	3.98	3.45	3.33	3.45
Cl	0.21	0.12	0.13	0.14	0.19	0.13	0.26	0.16	0.23	0.09	0.35	0.16	0.20	n.d.	n.d.
Totals	100.00	100.00	100.00	100.00	100.00	100.00	100.00	100.00	100.00	100.00	100.00	100.00	100.00	100.00	100.00

	16	17	18	19	20	21	22	23	24	25	26	27	28	29	30
SiO_2	75.60	73.10	75.14	75.47	73.17	72.88	70.56	78.11	70.62	72.16	73.37	78.14	77.58	76.17	77.38
TiO_2	0.04	0.08	0.21	0.36	0.11	0.09	0.14	0.08	0.23	0.11	0.16	0.20	0.14	0.13	0.18
Al_2O_3	11.53	11.30	12.01	12.40	12.06	12.08	11.47	11.68	11.69	12.50	11.52	12.35	12.10	12.46	12.87
FeO	1.14	1.05	1.31	1.34	1.01	0.87	1.22	0.97	0.78	1.65	0.99	0.98	0.93	0.91	1.64
MgO	0.09	0.13	0.21	0.33	0.16	0.22	0.29	0.14	0.12	0.16	0.18	0.11	0.01	0.32	0.11
CaO	0.98	1.03	1.14	1.50	1.23	1.50	1.37	0.89	0.63	1.31	1.07	1.00	0.67	0.72	1.41
Na_2O	3.57	3.51	4.04	4.24	4.06	4.84	3.75	2.44	4.03	4.14	3.60	2.60	2.08	1.95	2.77
K_2O	2.95	2.67	3.31	2.56	3.20	1.46	3.15	3.68	3.88	2.90	3.48	2.96	3.73	3.52	2.93
Cl	n.d.	n.d.	n.d.	n.d.	n.d.	n.d.	n.d.	n.d.	n.d.	n.d.	n.d.	0.16	0.14	0.20	0.15
Totals	95.90	92.86	97.36	98.18	94.99	93.93	91.95	97.98	91.98	94.92	94.38	98.50	97.38	96.38	99.43
Normalised data															
SiO_2	78.84	78.72	77.18	76.86	77.03	77.59	76.73	79.72	76.78	76.02	77.74	79.34	79.67	79.03	77.82
TiO_2	0.04	0.09	0.22	0.36	0.11	0.09	0.15	0.08	0.25	0.12	0.17	0.20	0.14	0.14	0.19
Al_2O_3	12.02	12.17	12.33	12.63	12.69	12.86	12.48	11.92	12.71	13.16	12.21	12.54	12.43	12.93	12.94
FeO	1.19	1.13	1.34	1.36	1.06	0.92	1.33	0.99	0.85	1.73	1.05	0.99	0.95	0.95	1.65
MgO	0.09	0.14	0.21	0.33	0.17	0.23	0.32	0.14	0.13	0.17	0.19	0.11	0.01	0.33	0.11
CaO	1.02	1.10	1.17	1.53	1.29	1.60	1.49	0.91	0.68	1.38	1.13	1.01	0.69	0.75	1.42
Na_2O	3.73	3.78	4.15	4.32	4.27	5.15	4.08	2.49	4.38	4.36	3.82	2.64	2.13	2.03	2.78
K_2O	3.07	2.87	3.40	2.60	3.37	1.56	3.42	3.75	4.21	3.05	3.69	3.00	3.83	3.66	2.95
Cl	n.d.	n.d.	n.d.	n.d.	n.d.	n.d.	n.d.	n.d.	n.d.	n.d.	n.d.	0.17	0.14	0.20	0.15
Totals	100.00	100.00	100.00	100.00	100.00	100.00	100.00	100.00	100.00	100.00	100.00	100.00	100.00	100.00	100.00

Variation Matrix for Ohakean 2 terrace

Numbers above unit diagonal are SIMILARITY COEFFICIENTS, below are COEFFICIENTS OF VARIATION.

	Karapiti	Waiohau	Rotorua	Puketerata	unTu	Rerewhak	Okareka	Te Rere	Kawakawa	Oh2/1	Oh2/2	Oh2/3	Oh2/4	Oh2/5	Oh2/6
Karapiti	–	0.81	0.89	0.67	0.56	0.76	0.75	0.91	0.83	0.88	0.83	0.87	0.78	0.83	0.70
Waiohau	13.76	–	0.86	0.80	0.57	0.92	0.89	0.89	0.89	0.88	0.93	0.90	0.93	0.88	0.82
Rotorua	9.20	11.73	–	0.71	0.59	0.80	0.78	0.93	0.88	0.91	0.88	0.94	0.82	0.93	0.74
Puketera	19.83	16.79	20.39	–	0.56	0.86	0.88	0.73	0.78	0.75	0.77	0.75	0.83	0.73	0.89
unTu	25.66	26.30	28.19	25.31	–	0.56	0.56	0.57	0.55	0.54	0.58	0.59	0.62	0.59	0.60
Rerewhak	16.09	10.39	17.22	10.74	25.37	–	0.97	0.84	0.89	0.85	0.89	0.85	0.89	0.83	0.88
Okareka	17.48	9.23	16.49	10.99	25.09	4.12	–	0.81	0.87	0.82	0.86	0.82	0.89	0.80	0.87
Te Rere	12.06	7.52	6.34	18.46	26.26	14.31	13.43	–	0.89	0.91	0.92	0.94	0.86	0.90	0.76
Kawakawa	12.00	7.23	16.45	14.52	24.62	7.74	9.89	11.07	–	0.91	0.89	0.87	0.85	0.84	0.80
Oh2/1	11.63	11.05	16.16	17.62	25.01	13.80	14.26	11.71	10.59	–	0.91	0.88	0.81	0.86	0.78
Oh2/2	11.41	6.63	10.90	16.62	26.70	12.95	12.61	7.14	9.19	9.01	–	0.90	0.90	0.89	0.81
Oh2/3	12.43	10.06	4.89	21.02	28.06	17.11	16.70	3.92	14.18	13.22	8.32	–	0.85	0.94	0.77
Oh2/4	15.99	6.33	12.31	17.53	29.49	9.38	9.48	11.27	9.84	13.21	8.63	10.50	–	0.85	0.84
Oh2/5	12.88	12.65	6.22	21.58	28.33	18.76	17.27	7.48	15.72	16.54	12.31	8.77	12.89	–	0.75
Oh2/6	22.26	19.50	22.95	10.59	24.87	17.17	15.66	21.66	19.13	22.22	20.38	22.75	18.97	23.09	–

	Karapiti	Waiohau R	otorua	Puketerata	unTu	Rerewhak	Okareka	Te Rere	Kawakawa	Oh2/7	Oh2/8	Oh2/9	Oh2/10	Oh2/11	Oh2/12
Karapiti	–	0.81	0.89	0.67	0.56	0.76	0.75	0.91	0.83	0.85	0.86	0.88	0.83	0.85	0.75
Waiohau	13.76	–	0.86	0.80	0.57	0.92	0.89	0.89	0.89	0.91	0.93	0.87	0.71	0.87	0.87
Rotorua	9.20	11.73	–	0.71	0.59	0.80	0.78	0.93	0.88	0.90	0.91	0.96	0.81	0.85	0.80
Puketera	19.83	16.79	20.39	–	0.56	0.86	0.88	0.73	0.78	0.74	0.75	0.71	0.60	0.76	0.85
unTu	25.66	26.30	28.19	25.31	–	0.56	0.56	0.57	0.55	0.57	0.57	0.59	0.57	0.56	0.58
Rerewhak	16.09	10.39	17.22	10.74	25.37	–	0.97	0.84	0.89	0.85	0.87	0.81	0.67	0.86	0.94
Okareka	17.48	9.23	16.49	10.99	25.09	4.12	–	0.81	0.87	0.83	0.84	0.78	0.65	0.83	0.93
Te Rere	12.06	7.52	6.34	18.46	26.26	14.31	13.43	–	0.89	0.90	0.95	0.94	0.78	0.85	0.82
Kawakawa	12.00	7.23	16.45	14.52	24.62	7.74	9.89	11.07	–	0.93	0.89	0.88	0.73	0.92	0.88
Oh2/7	7.69	8.85	12.07	16.10	26.69	10.39	11.64	5.67	8.12	–	0.93	0.91	0.77	0.92	0.88
Oh2/8	11.67	7.24	9.24	17.55	26.50	13.23	12.55	4.53	9.80	6.69	–	0.91	0.76	0.87	0.85
Oh2/9	8.24	11.13	5.21	19.33	27.88	15.88	15.45	6.80	13.68	10.44	9.50	–	0.80	0.87	0.81
Oh2/10	15.27	19.99	14.42	22.65	26.23	21.90	21.65	17.74	20.59	19.98	19.23	15.35	–	0.76	0.68
Oh2/11	12.04	13.43	17.31	15.52	24.87	11.82	13.46	12.63	7.49	8.99	12.68	15.65	21.95	–	0.88
Oh2/12	15.20	10.61	18.81	10.15	26.67	5.77	8.77	15.25	9.35	12.57	14.64	16.75	22.77	11.83	–

	Karapiti	Waiohau	Rotorua	Puketerata	unTu	Rerewhak	Okareka	Te Rere	Kawakawa	Oh2/13	Oh2/14	Oh2/15	Oh2/16	Oh2/17	Oh2/18
Karapiti	–	0.81	0.89	0.67	0.56	0.76	0.75	0.91	0.83	0.85	0.82	0.77	0.74	0.83	0.86
Waiohau	13.78	–	0.88	0.80	0.57	0.92	0.89	0.89	0.89	0.91	0.85	0.81	0.80	0.89	0.83
Rotorua	9.20	11.73	–	0.71	0.59	0.80	0.78	0.93	0.88	0.90	0.87	0.86	0.81	0.87	0.94
Puketera	19.83	16.79	20.39	–	0.56	0.86	0.88	0.73	0.78	0.75	0.72	0.70	0.78	0.79	0.69
unTu	25.66	26.30	28.19	25.31	–	0.56	0.56	0.57	0.55	0.57	0.56	0.56	0.50	0.52	0.60
Rerewhak	16.09	10.39	17.22	10.74	25.37	–	0.97	0.84	0.89	0.88	0.81	0.78	0.84	0.86	0.78
Okareka	17.48	9.23	16.49	10.99	25.09	4.12	–	0.81	0.87	0.83	0.79	0.76	0.81	0.84	0.75
Te Rere	12.06	7.52	6.34	18.46	26.26	14.31	13.43	–	0.89	0.94	0.87	0.83	0.82	0.90	0.87
Kawakawa	12.00	7.23	16.45	14.52	24.62	7.74	9.89	11.07	–	0.91	0.88	0.81	0.87	0.93	0.83
Oh2/13	9.60	8.04	10.27	17.71	27.07	12.96	13.18	6.98	10.06	–	0.89	0.83	0.81	0.90	0.89
Oh2/14	16.13	20.73	17.12	23.37	26.40	22.00	22.18	17.00	22.66	17.94	–	0.91	0.79	0.83	0.84
Oh2/15	17.48	22.51	16.76	26.50	27.13	25.97	24.94	19.02	25.50	21.84	14.72	–	0.75	0.79	0.85
Oh2/16	22.51	21.41	27.75	14.84	24.49	18.70	18.35	25.58	21.63	23.47	29.80	30.94	–	0.86	0.77
Oh2/17	14.26	12.27	18.34	16.26	24.09	10.02	10.58	14.82	8.32	10.96	21.20	25.67	18.85	–	0.82
Oh2/18	7.81	14.50	3.41	21.17	28.69	18.21	18.08	7.63	15.94	12.87	18.34	15.91	25.76	17.81	–

	Karapiti	Waiohau	Rotorua	Puketerata	unTu	Rerewhak	Okareka	Te Rere	Kawakawa	Oh2/19	Oh2/20	Oh2/21	Oh2/22	Oh2/23	Oh2/24
Karapiti	–	0.81	0.89	0.67	0.56	0.76	0.75	0.91	0.83	0.80	0.85	0.75	0.88	0.73	0.72
Waiohau	13.78	–	0.86	0.80	0.57	0.92	0.89	0.89	0.89	0.71	0.88	0.74	0.82	0.87	0.85
Rotorua	9.20	11.73	–	0.71	0.59	0.80	0.78	0.93	0.88	0.81	0.87	0.75	0.85	0.77	0.79
Puketera	19.83	16.79	20.39	–	0.56	0.86	0.88	0.73	0.78	0.60	0.75	0.69	0.88	0.84	0.80
unTu	25.66	26.30	28.19	25.31	–	0.56	0.56	0.57	0.55	0.53	0.56	0.48	0.58	0.51	0.62
Rerewhak	16.09	10.39	17.22	10.74	25.37	–	0.97	0.84	0.89	0.68	0.86	0.73	0.77	0.87	0.82
Okareka	17.48	9.23	16.49	10.99	25.09	4.12	–	0.81	0.87	0.65	0.84	0.72	0.75	0.85	0.84
Te Rere	12.06	7.52	6.34	18.46	26.26	14.31	13.43	–	0.89	0.78	0.89	0.76	0.84	0.80	0.79
Kawakawa	12.00	7.23	16.45	14.52	24.62	7.74	9.89	11.07	–	0.74	0.88	0.73	0.82	0.84	0.78
Oh2/19	17.50	19.79	14.91	23.41	25.97	22.30	21.84	18.01	21.56	–	0.78	0.75	0.88	0.64	0.72
Oh2/20	11.92	10.61	12.96	17.72	27.08	14.51	15.01	10.05	8.00	21.97	–	0.81	0.88	0.82	0.79
Oh2/21	16.40	18.10	17.44	24.69	25.43	20.41	20.70	15.31	14.85	21.77	15.01	–	0.77	0.72	0.66
Oh2/22	11.77	19.59	12.19	22.23	28.42	20.81	20.70	13.83	17.86	18.92	15.11	16.59	–	0.72	0.73
Oh2/23	13.17	15.40	18.10	15.92	24.20	12.71	11.16	14.28	10.83	20.00	12.48	19.36	17.29	–	0.78
Oh2/24	18.08	12.57	12.82	22.46	29.79	15.49	18.41	12.43	15.24	20.92	18.77	23.30	20.10	19.88	–

	Karapiti	Waiohau	Rotorua	Puketerata	unTu	Rerewhak	Okareka	Te Rere	Kawakawa	Oh2/25	Oh2/26	Oh2/27	Oh2/28	Oh2/29	Oh2/30
Karapiti	–	0.81	0.89	0.67	0.56	0.78	0.75	0.91	0.83	0.92	0.88	0.79	0.66	0.74	0.89
Waiohau	13.76	–	0.86	0.80	0.57	0.92	0.89	0.89	0.89	0.82	0.89	0.86	0.79	0.84	0.78
Rotorua	9.20	11.73	–	0.71	0.59	0.80	0.78	0.93	0.88	0.84	0.93	0.87	0.89	0.77	0.83
Puketera	19.83	16.79	20.39	–	0.56	0.86	0.88	0.73	0.78	0.66	0.75	0.78	0.77	0.75	0.70
unTu	25.66	26.30	28.19	25.31	–	0.56	0.56	0.57	0.55	0.57	0.60	0.55	0.66	0.53	0.57
Rerewhak	16.09	10.39	17.22	10.74	25.37	–	0.97	0.84	0.89	0.79	0.85	0.85	0.77	0.81	0.77
Okareka	17.48	9.23	18.49	10.99	25.09	4.12	–	0.81	0.87	0.76	0.82	0.83	0.78	0.81	0.78
Te Rere	12.06	7.52	8.34	18.46	26.26	14.31	13.43	–	0.89	0.85	0.93	0.87	0.72	0.79	0.82
Kawakawa	12.00	7.23	18.45	14.52	24.62	7.74	9.89	11.07	–	0.86	0.87	0.87	0.72	0.76	0.83
Oh2/25	8.82	13.64	12.82	17.00	26.21	15.04	18.15	11.72	11.70	–	0.83	0.78	0.64	0.71	0.85
Oh2/26	11.88	9.95	8.31	20.95	29.29	18.79	18.34	6.45	12.63	11.05	–	0.84	0.73	0.80	0.80
Oh2/27	14.00	11.16	15.35	17.76	26.03	14.27	13.18	13.71	12.75	15.58	13.06	–	0.75	0.79	0.89
Oh2/28	24.47	28.99	24.71	26.03	25.37	27.08	26.82	25.63	24.81	24.48	27.48	25.55	–	0.85	0.87
Oh2/29	18.45	20.89	14.36	23.25	24.97	22.78	22.31	15.51	18.25	18.22	16.72	19.07	30.73	–	0.71
Oh2/30	13.92	13.39	14.69	18.39	26.60	15.14	18.47	13.93	11.89	15.82	13.07	14.22	23.58	19.20	–

Ohakean 3 terrace: Mohaka River

	1	2	3	4	5	6	7	8	9	10	11	12	13	14	15	16	17	18	19	20	21
SiO_2	73.51	73.24	70.53	72.81	74.08	73.98	74.89	75.23	74.86	73.55	77.85	78.54	76.59	78.38	77.18	77.21	75.43	75.81	77.30	75.61	77.20
TiO_2	0.19	0.17	0.07	0.24	0.11	0.10	0.15	0.14	0.16	0.10	0.24	0.20	0.15	0.11	0.21	0.09	0.25	0.11	0.25	0.21	0.05
Al_2O_3	12.04	12.26	11.77	11.44	12.10	12.23	11.98	11.58	11.72	11.36	12.18	11.79	11.93	12.05	11.76	12.56	11.95	12.13	11.48	11.39	11.90
FeO	0.97	1.02	0.93	0.88	1.28	0.90	0.88	1.12	0.97	1.20	1.10	1.03	0.73	0.98	0.87	1.50	1.02	1.03	1.20	1.00	1.04
MgO	0.19	0.18	0.30	0.09	0.21	0.24	0.11	0.13	0.17	0.10	0.26	0.27	0.05	0.26	0.04	0.25	0.11	0.24	0.15	0.26	0.12
CaO	0.86	1.00	0.88	0.57	1.07	0.83	0.74	0.89	0.96	1.15	1.22	0.96	0.86	0.80	1.13	1.30	0.74	0.65	0.74	0.98	0.79
Na_2O	4.11	3.90	3.76	3.11	3.97	4.00	3.74	4.00	3.72	3.43	3.94	3.07	3.92	3.40	4.16	3.95	3.97	3.94	3.73	3.45	3.83
K_2O	3.32	3.00	3.03	5.13	3.15	3.29	4.47	3.38	3.55	3.33	3.13	3.72	3.39	3.53	3.45	3.04	3.32	3.84	3.29	3.47	3.14
Cl	n.d.	n.d.	n.d.	n.d.	n.d.	n.d.	n.d.	n.d.	n.d.	n.d.	n.d.	n.d.	n.d.	n.d.	n.d.	n.d.	n.d.	n.d.	n.d.	n.d.	n.d.
Totals	95.19	94.78	91.25	94.27	95.96	95.56	96.96	96.47	96.11	94.23	99.92	99.56	97.63	99.50	98.79	99.89	96.80	97.74	98.13	96.37	98.07
Normalised data																					
SiO_2	77.23	77.27	77.29	77.24	77.20	77.41	77.24	77.98	77.89	78.06	77.92	78.89	78.45	78.77	78.12	77.30	77.92	77.57	78.77	78.47	78.72
TiO_2	0.20	0.18	0.07	0.25	0.11	0.11	0.15	0.14	0.17	0.11	0.24	0.20	0.15	0.11	0.21	0.09	0.26	0.11	0.25	0.22	0.06
Al_2O_3	12.65	12.93	12.89	12.13	12.61	12.80	12.36	12.00	12.19	12.05	12.19	11.84	12.22	12.11	11.90	12.57	12.35	12.42	11.70	11.82	12.13
FeO	1.01	1.08	1.01	0.94	1.34	0.94	0.91	1.16	1.01	1.28	1.10	1.03	0.75	0.98	0.88	1.50	1.05	1.05	1.22	1.04	1.06
MgO	0.20	0.19	0.33	0.10	0.22	0.25	0.11	0.14	0.17	0.11	0.26	0.27	0.05	0.26	0.04	0.25	0.12	0.24	0.15	0.27	0.12
CaO	0.91	1.06	0.96	0.61	1.11	0.86	0.77	0.92	1.00	1.22	1.22	0.96	0.88	0.80	1.14	1.30	0.77	0.67	0.76	1.01	0.80
Na_2O	4.31	4.11	4.12	3.29	4.14	4.19	3.86	4.15	3.87	3.64	3.94	3.08	4.02	3.42	4.21	3.95	4.11	4.03	3.80	3.58	3.90
K_2O	3.49	3.17	3.32	5.44	3.28	3.44	4.61	3.51	3.69	3.54	3.13	3.73	3.47	3.55	3.49	3.04	3.43	3.93	3.35	3.60	3.21
Cl	n.d.	n.d.	n.d.	n.d.	n.d.	n.d.	n.d.	n.d.	n.d.	n.d.	n.d.	n.d.	n.d.	n.d.	n.d.	n.d.	n.d.	n.d.	n.d.	n.d.	n.d.
Totals	100.00	100.00	100.00	100.00	100.00	100.00	100.00	100.00	100.00	100.00	100.00	100.00	100.00	100.00	100.00	100.00	100.00	100.00	100.00	100.00	100.00

n.d. not determined

Variation Matrix for Ohakean 3 terrace

Numbers above unit diagonal are SIMILARITY COEFFICIENTS, below are COEFFICIENTS OF VARIATION.

	Karapiti	Waiohau	Rotorua	Puketerata	unTu	Rerewhak	Okareka	Te Rere	Kawakawa	Oh3/1	Oh3/2	Oh3/3	Oh3/4	Oh3/5	Oh3/6
Karapiti	–	0.81	0.89	0.67	0.56	0.76	0.75	0.91	0.83	0.83	0.88	0.75	0.89	0.86	0.79
Waiohau	13.78	–	0.86	0.80	0.57	0.92	0.89	0.89	0.89	0.89	0.88	0.83	0.80	0.85	0.90
Rotorua	9.20	11.73	–	0.71	0.59	0.80	0.78	0.93	0.88	0.93	0.95	0.81	0.75	0.90	0.84
Puketera	19.83	16.79	20.39	–	0.56	0.86	0.86	0.73	0.78	0.74	0.72	0.77	0.83	0.73	0.78
unTu	25.66	26.30	28.19	25.31	–	0.56	0.56	0.57	0.55	0.81	0.59	0.52	0.58	0.56	0.56
Rerewhak	16.09	10.39	17.22	10.74	25.37	–	0.97	0.84	0.89	0.84	0.82	0.82	0.83	0.84	0.89
Okareka	17.48	9.23	16.49	10.99	25.09	4.12	–	0.81	0.87	0.81	0.79	0.79	0.84	0.81	0.87
Te Rere	12.06	7.52	6.34	18.46	26.26	14.31	13.43	–	0.89	0.90	0.94	0.83	0.75	0.86	0.85
Kawakawa	12.00	7.23	16.45	14.52	24.62	7.74	9.89	11.07	–	0.82	0.87	0.80	0.77	0.89	0.84
Oh3/1	12.91	11.36	7.43	20.85	30.17	18.29	16.81	6.43	13.17	–	0.94	0.85	0.78	0.87	0.90
Oh3/2	11.55	8.51	3.55	19.04	29.03	15.03	14.18	3.53	13.22	4.39	–	0.84	0.75	0.90	0.87
Oh3/3	17.66	20.67	20.06	21.70	26.15	21.28	19.75	19.22	19.29	22.10	21.26	–	0.89	0.86	0.90
Oh3/4	18.48	15.56	16.56	21.32	24.90	18.48	18.12	18.02	17.89	15.45	15.51	23.36	–	0.89	0.74
Oh3/5	8.96	12.47	13.92	18.40	26.13	17.03	17.55	9.23	13.49	14.32	12.85	14.31	17.90	–	0.91
Oh3/6	13.86	14.63	13.18	20.10	26.71	19.14	18.30	10.29	14.45	14.65	12.81	12.39	20.46	10.94	–

	Karapiti	Waiohau R	otorua	Puketerata	unTu	Rerewhak	Okareka	Te Rere	Kawakawa	Oh3/7	Oh3/8	Oh3/9	Oh3/10	Oh3/11	Oh3/12
Karapiti	–	0.81	0.89	0.67	0.56	0.76	0.75	0.91	0.83	0.78	0.62	0.85	0.83	0.83	0.79
Waiohau	13.76	–	0.86	0.80	0.57	0.92	0.89	0.89	0.89	0.91	0.95	0.92	0.86	0.82	0.84
Rotorua	9.20	11.73	–	0.71	0.59	0.80	0.78	0.93	0.88	0.80	0.87	0.90	0.84	0.92	0.88
Puketera	19.83	16.79	20.39	–	0.56	0.86	0.88	0.73	0.78	0.84	0.77	0.76	0.79	0.89	0.75
unTu	25.66	26.30	28.19	25.31	–	0.56	0.56	0.57	0.55	0.80	0.59	0.60	0.56	0.57	0.59
Rerewhak	16.09	10.39	17.22	10.74	25.37	–	0.97	0.84	0.89	0.90	0.88	0.87	0.91	0.77	0.81
Okareka	17.48	9.23	16.49	10.99	25.09	4.12	–	0.81	0.87	0.91	0.86	0.84	0.89	0.75	0.80
Te Rere	12.06	7.52	6.34	18.46	26.26	14.31	13.43	–	0.89	0.84	0.90	0.94	0.84	0.86	0.86
Kawakawa	12.00	7.23	16.45	14.52	24.62	7.74	9.89	11.07	–	0.85	0.91	0.87	0.94	0.84	0.81
Oh3/7	17.63	9.44	14.88	15.74	28.21	8.81	9.08	14.27	11.24	–	0.87	0.87	0.84	0.77	0.80
Oh3/8	10.10	5.96	10.71	15.32	27.35	9.22	9.65	8.91	6.48	8.62	–	0.91	0.89	0.83	0.84
Oh3/9	12.10	8.96	6.44	19.93	29.15	15.27	14.53	6.83	10.56	11.72	8.48	–	0.85	0.87	0.90
Oh3/10	13.00	11.07	16.80	14.83	25.45	11.24	13.57	12.51	4.81	13.60	9.68	13.40	–	0.82	0.79
Oh3/11	11.63	16.81	7.65	23.23	27.42	20.86	19.91	12.28	20.34	18.50	18.74	12.41	21.53	–	0.89
Oh3/12	10.71	14.53	8.37	24.35	29.01	20.64	20.23	10.09	17.15	15.87	15.60	12.24	18.89	8.10	–

	Karapiti	Waiohau R	otorua	Puketerata	unTu	Rerewhak	Okareka	Te Rere	Kawakawa	Oh3/13	Oh3/14	Oh3/15	Oh3/16	Oh3/17	Oh3/18
Karapiti	–	0.81	0.89	0.67	0.56	0.76	0.75	0.91	0.83	0.74	0.78	0.74	0.87	0.78	0.77
Waiohau	13.78	–	0.86	0.80	0.57	0.92	0.89	0.89	0.89	0.87	0.86	0.81	0.79	0.89	0.86
Rotorua	9.20	11.73	–	0.71	0.59	0.80	0.78	0.93	0.88	0.78	0.82	0.82	0.85	0.84	0.82
Puketera	19.83	18.79	20.39	–	0.56	0.86	0.86	0.73	0.78	0.80	0.81	0.76	0.72	0.77	0.82
unTu	25.66	26.30	28.19	25.31	–	0.56	0.56	0.57	0.55	0.80	0.55	0.62	0.53	0.59	0.58
Rerewhak	16.09	10.39	17.22	10.74	25.37	–	0.97	0.84	0.89	0.85	0.90	0.80	0.78	0.86	0.87
Okareka	17.48	9.23	16.49	10.99	25.09	4.12	–	0.81	0.87	0.85	0.90	0.79	0.78	0.85	0.86
TeRere	12.06	7.52	6.34	18.46	26.26	14.31	13.43	–	0.89	0.81	0.84	0.79	0.84	0.84	0.83
Kawakawa	12.00	7.23	16.45	14.52	24.62	7.74	9.89	11.07	–	0.81	0.85	0.79	0.84	0.85	0.82
Oh3/13	22.54	20.40	21.69	13.66	26.40	15.94	14.97	21.40	17.47	–	0.80	0.86	0.72	0.82	0.78
Oh3/14	14.34	14.43	12.87	21.44	25.30	19.77	19.83	10.34	16.35	23.83	–	0.76	0.84	0.82	0.93
Oh3/15	21.42	21.89	23.89	19.99	26.06	19.77	20.38	21.47	20.77	10.48	25.48	–	0.73	0.82	0.74
Oh3/16	13.29	16.26	16.95	21.15	25.06	18.11	18.32	14.34	15.47	24.12	12.80	25.65	–	0.74	0.84
Oh3/17	14.54	14.23	12.86	20.00	26.52	17.26	17.43	13.08	16.95	20.15	21.50	20.59	21.57	–	0.83
Oh3/18	14.92	12.78	15.07	21.06	27.21	18.30	17.87	12.58	15.97	23.10	5.83	24.94	15.90	21.33	–

	Karapiti	Waiohau	Rotorua	Puketerata	unTu	Rerewhak	Okareka	Te Rere	Kawakawa	Oh3/19	Oh3/20	Oh3/21
Karapiti	–	0.81	0.89	0.67	0.56	0.76	0.75	0.91	0.83	0.80	0.81	0.74
Waiohau	13.78	–	0.86	0.80	0.57	0.92	0.89	0.89	0.89	0.89	0.85	0.86
Rotorua	9.20	11.73	–	0.71	0.59	0.80	0.78	0.93	0.88	0.86	0.90	0.80
Puketera	19.83	16.79	20.39	–	0.56	0.86	0.88	0.73	0.78	0.75	0.73	0.82
unTu	25.66	26.30	28.19	25.31	–	0.56	0.56	0.57	0.55	0.59	0.59	0.52
Rerewhak	16.09	10.39	17.22	10.74	25.37	–	0.97	0.84	0.89	0.83	0.82	0.88
Okareka	17.48	9.23	16.49	10.99	25.09	4.12	–	0.81	0.87	0.82	0.80	0.86
Te Rere	12.06	7.52	6.34	18.46	26.26	14.31	13.43	–	0.89	0.86	0.88	0.82
Kawakawa	12.00	7.23	16.45	14.52	24.62	7.74	9.89	11.07	–	0.85	0.83	0.88
Oh3/19	13.14	14.09	11.13	20.34	26.05	17.18	17.83	11.19	16.65	–	0.86	0.84
Oh3/20	12.14	15.86	7.18	24.08	28.43	22.03	21.27	11.84	19.43	13.86	–	0.78
Oh3/21	18.45	17.50	21.85	12.08	24.78	13.50	13.53	19.17	16.57	23.23	24.29	–

APPENDIX IV

SOIL CHEMISTRY AND ELEMENTAL ANALYSIS

Appendix 4.1: Major oxide data from Pakaututu Road reference section

Depth (cm)	SiO_2 (%)	TiO_2 (%)	Al_2O_3 (%)	Fe_2O_3 (%)	MnO_2 (%)	MgO (%)	CaO (%)	Na_2O (%)	K_2O (%)	P_2O_5 (%)	LOI (%)	Total (%)
0	56.85	0.41	14.11	3.92	0.10	1.09	2.32	3.12	1.88	0.14	16.27	100.21
10	59.14	0.39	14.70	3.74	0.10	0.90	2.18	3.32	1.97	0.11	13.75	100.30
30	65.82	0.46	13.66	3.76	0.10	0.68	1.99	3.66	2.29	0.07	7.68	100.17
40	68.05	0.38	13.85	3.26	0.09	0.43	1.69	3.82	2.47	0.06	5.92	100.02
80	44.32	0.51	17.91	5.28	0.11	1.12	1.44	1.84	1.32	0.16	26.16	100.17
110	41.57	0.70	18.20	8.24	0.12	4.56	5.10	1.66	0.60	0.10	19.42	100.27
120	38.97	0.56	16.77	6.03	0.09	1.55	1.62	1.46	1.00	0.13	32.07	100.25
170	48.94	0.67	17.88	7.01	0.12	3.29	2.43	1.64	1.44	0.12	16.62	100.16
200	58.49	0.64	17.72	5.61	0.11	1.54	0.85	1.77	2.36	0.09	10.83	100.01
230	56.61	0.58	17.05	5.59	0.10	2.29	1.48	1.84	2.15	0.10	12.30	100.09
250	59.23	0.59	17.92	5.17	0.09	1.23	0.81	1.83	2.37	0.07	10.93	100.24
270	60.21	0.55	17.85	4.71	0.08	0.93	0.72	1.88	2.30	0.07	10.84	100.14
290	61.10	0.48	17.51	4.39	0.08	0.92	0.86	2.06	2.21	0.07	10.33	100.01
300	59.73	0.50	18.73	4.47	0.08	0.74	0.71	1.79	1.90	0.05	11.11	99.81
315	63.62	0.37	16.31	3.37	0.07	0.97	1.98	2.93	1.99	0.05	7.94	99.60
335	62.27	0.59	17.10	5.11	0.08	0.91	0.64	1.82	2.25	0.05	8.93	99.75
390	58.77	0.64	18.63	5.36	0.10	0.88	1.00	1.93	1.94	0.10	10.93	100.28
400	58.42	0.65	18.37	5.45	0.10	0.92	1.09	1.97	1.87	0.11	11.02	99.97
450	57.16	0.62	18.21	5.39	0.07	0.88	1.31	2.04	1.59	0.13	12.72	100.12
520	54.24	0.67	18.94	5.82	0.12	1.04	0.98	1.77	1.64	0.15	14.66	100.03
560	65.00	0.52	16.66	4.30	0.13	0.85	0.57	2.08	2.53	0.07	7.57	100.28
570	60.24	0.37	18.94	2.93	0.06	0.55	0.85	2.12	1.96	0.05	12.02	100.09
620	64.07	0.61	16.48	5.12	0.04	1.04	0.56	1.76	2.64	0.05	7.75	100.12
670	69.34	0.52	15.11	3.23	0.03	0.92	0.57	1.75	2.75	0.03	5.83	100.08

NORMALISED ELEMENTAL ANALYSES

Depth (cm)	SiO_2 (%)	TiO_2 (%)	Al_2O_3 (%)	Fe_2O_3 (%)	MnO_2 (%)	MgO (%)	CaO (%)	Na_2O (%)	K_2O (%)	P_2O_5 (%)	Total (%)
0	67.73	0.49	16.81	4.67	0.12	1.30	2.76	3.72	2.24	0.17	100.00
10	68.33	0.45	16.98	4.32	0.12	1.04	2.52	3.84	2.28	0.13	100.00
30	71.16	0.50	14.77	4.07	0.11	0.74	2.15	3.96	2.48	0.08	100.00
40	72.32	0.40	14.72	3.46	0.10	0.46	1.80	4.06	2.62	0.06	100.00
80	59.88	0.69	24.20	7.13	0.15	1.51	1.95	2.49	1.78	0.22	100.00
110	51.42	0.87	22.51	10.19	0.15	5.64	6.31	2.05	0.74	0.12	100.00
120	57.16	0.82	24.60	8.84	0.13	2.27	2.38	2.14	1.47	0.19	100.00
170	58.58	0.80	21.40	8.39	0.14	3.94	2.91	1.96	1.72	0.14	100.00
200	65.59	0.72	19.87	6.29	0.12	1.73	0.95	1.98	2.65	0.10	100.00
230	64.48	0.66	19.42	6.37	0.11	2.61	1.69	2.10	2.45	0.11	100.00
250	66.32	0.66	20.06	5.79	0.10	1.38	0.91	2.05	2.65	0.08	100.00
270	67.42	0.62	19.99	5.27	0.09	1.04	0.81	2.11	2.58	0.08	100.00
290	68.13	0.54	19.52	4.90	0.09	1.03	0.96	2.30	2.46	0.08	100.00
300	67.34	0.56	21.12	5.04	0.09	0.83	0.80	2.02	2.14	0.06	100.00
315	69.41	0.40	17.79	3.68	0.08	1.06	2.16	3.20	2.17	0.05	100.00
335	68.56	0.65	18.83	5.63	0.09	1.00	0.70	2.00	2.48	0.06	100.00
390	65.78	0.72	20.85	6.00	0.11	0.98	1.12	2.16	2.17	0.11	100.00
400	65.68	0.73	20.65	6.13	0.11	1.03	1.23	2.21	2.10	0.12	100.00
450	65.40	0.71	20.84	6.17	0.08	1.01	1.50	2.33	1.82	0.15	100.00
520	63.54	0.78	22.19	6.82	0.14	1.22	1.15	2.07	1.92	0.18	100.00
560	70.11	0.56	17.97	4.64	0.14	0.92	0.61	2.24	2.73	0.08	100.00
570	68.40	0.42	21.51	3.33	0.07	0.62	0.97	2.41	2.23	0.06	100.00
620	69.36	0.66	17.84	5.54	0.04	1.13	0.61	1.91	2.86	0.05	100.00
670	73.57	0.55	16.03	3.43	0.03	0.98	0.60	1.86	2.92	0.03	100.00

Appendix 4.2: Trace element data from Pakaututu Road reference section

Depth (cm)	Ga ppm	Pb ppm	Rb ppm	Sr ppm	Th ppm	U ppm	Y ppm	As ppm	Sc ppm
0	17.7	17.8	75.9	168.1	8.8	2.3	23.8	4.2	11.3
10	18.8	17.2	78.9	155.5	8.3	3.4	27.6	5.4	10.9
30	18.6	19.0	93.0	152.5	9.1	2.9	32.5	5.2	11.9
40	19.5	20.1	94.5	144.7	9.9	2.8	34.2	5.2	11.9
80	21.5	18.8	47.1	98.3	9.8	2.9	35.3	4.7	15.6
110	18.3	12.0	23.7	149.5	4.5	2.4	19.9	2.4	31.9
120	23.8	15.9	43.1	97.4	7.4	2.9	31.3	5.7	22.0
170	23.8	21.1	73.8	138.9	9.3	2.3	25.7	6.9	18.7
200	24.3	29.2	124.0	150.2	12.3	3.9	32.0	10.1	18.5
230	21.9	25.9	105.6	154.9	10.7	3.7	24.3	9.3	16.4
250	23.5	28.7	129.0	154.6	12.6	2.7	36.7	10.9	14.7
270	22.6	28.2	117.4	146.5	13.6	3.3	32.1	10.8	13.6
290	21.7	26.6	100.8	139.3	13.6	3.5	25.9	8.8	12.9
300	22.1	24.9	104.5	124.3	13.3	3.7	31.6	10.5	13.3
315	19.6	19.6	84.9	152.4	11.8	3.1	19.5	9.7	10.9
335	20.7	26.7	126.9	149.2	11.6	4.3	32.1	9.5	14.4
390	22.5	27.6	103.8	171.1	12.6	2.8	25.3	9.7	14.0
400	23.0	27.2	102.2	171.7	12.5	3.9	25.2	9.5	15.1
450	22.7	24.1	78.1	181.1	12.2	2.9	24.2	10.6	16.1
520	25.8	26.3	83.2	169.5	11.2	3.3	25.5	8.7	19.3
560	20.0	29.6	124.7	167.7	11.9	3.6	29.4	10.0	15.9
570	22.7	23.1	81.0	121.6	15.8	3.8	17.1	6.3	7.8
620	21.4	25.8	139.0	144.7	11.5	3.4	30.8	9.7	15.0
670	19.6	22.0	121.3	152.3	11.3	3.2	23.2	3.0	14.0

Depth (cm)	V ppm	Cr ppm	Ba ppm	La ppm	Ce ppm	Ni ppm	Cu ppm	Zn ppm	Zr ppm	Nb ppm
0	36.6	13.6	503.8	29.6	47.5	3.6	8.1	69.8	187.4	7.2
10	28.2	10.5	456.5	26.0	50.4	2.5	6.4	66.1	198.7	7.2
30	31.1	10.0	538.9	31.0	53.0	3.0	4.8	63.6	226.2	9.3
40	20.1	8.2	542.7	36.6	52.3	1.6	3.9	62.9	229.1	8.9
80	95.5	33.7	329.5	64.5	72.1	4.8	19.1	61.8	181.0	7.4
110	236.1	100.3	173.3	28.3	44.5	23.3	34.0	70.3	113.1	3.9
120	144.6	48.4	286.9	44.7	58.0	7.5	18.5	54.4	168.9	7.3
170	151.5	41.0	385.1	27.2	65.5	17.1	32.6	80.5	171.5	7.5
200	122.6	46.9	902.6	30.8	85.7	22.3	30.2	76.3	244.2	11.0
230	119.2	69.9	464.4	28.1	76.1	25.5	34.9	75.6	213.8	8.6
250	111.3	43.2	673.1	32.7	78.7	19.7	23.3	73.0	241.9	11.0
270	87.2	36.5	671.6	25.6	74.8	15.6	20.0	67.4	249.1	11.2
290	76.7	36.0	655.4	23.2	59.7	13.3	19.2	68.6	236.5	11.1
300	81.8	34.1	593.9	29.5	78.4	13.0	18.1	57.7	261.1	10.5
315	41.3	27.7	594.8	21.3	49.9	7.3	12.6	54.1	180.2	7.3
335	110.8	43.8	545.3	34.9	85.9	16.5	22.5	62.6	260.9	9.8
390	109.1	42.4	701.9	25.9	68.6	23.3	29.0	68.7	234.7	11.0
400	111.9	45.9	691.3	26.9	65.4	23.2	27.2	69.7	227.7	10.4
450	102.2	68.2	471.8	28.4	68.0	18.9	27.5	65.8	206.7	8.3
520	127.0	55.9	527.4	27.7	74.1	26.0	33.3	83.5	247.3	10.9
560	108.6	32.1	621.2	38.7	139.3	19.3	28.5	72.8	240.2	11.1
570	41.4	26.7	721.4	22.4	58.1	12.7	12.5	61.8	235.1	11.8
620	122.1	47.8	538.3	39.8	84.1	17.5	19.8	69.6	237.0	9.5
670	80.1	38.8	499.7	31.5	63.7	11.6	13.3	60.0	329.0	8.9

Appendix 4.3: Major oxide data from Poraiti #1 reference section

Depth (cm)	SiO_2 (%)	TiO_2 (%)	Al_2O_3 (%)	Fe_2O_3 (%)	MnO_2 (%)	MgO (%)	CaO (%)	Na_2O (%)	K_2O (%)	P_2O_5 (%)	LOI (%)	Total (%)
10	64.15	0.49	14.09	3.73	0.17	1.06	2.11	2.90	1.69	0.09	9.78	100.26
30	66.11	0.57	14.83	4.57	0.05	1.25	1.73	2.62	1.66	0.03	6.80	100.22
40	65.86	0.58	14.79	4.60	0.04	1.25	1.58	2.49	1.66	0.02	7.04	99.91
60	64.92	0.62	14.90	4.60	0.04	1.17	1.35	2.26	1.65	0.02	8.66	100.19
80	67.97	0.57	14.07	4.33	0.04	1.20	1.45	2.56	1.83	0.03	6.07	100.12
90	68.40	0.52	13.85	3.97	0.05	1.16	1.48	2.71	1.91	0.02	5.60	99.67
120	69.46	0.36	14.02	3.32	0.05	0.80	1.40	2.90	2.28	0.02	5.02	99.63
130	70.37	0.23	13.53	2.48	0.05	0.42	1.26	3.03	2.68	0.02	6.06	100.13
150	67.87	0.28	13.62	2.87	0.06	0.58	1.58	3.18	2.50	0.02	7.46	100.02
190	68.63	0.28	14.47	2.81	0.06	0.87	2.56	3.55	2.20	0.04	4.64	100.11
221	70.32	0.22	13.15	2.37	0.05	0.47	1.35	3.29	2.80	0.03	6.10	100.15

NORMALISED ELEMENTAL ANALYSES

Depth (cm)	SiO_2 (%)	TiO_2 (%)	Al_2O_3 (%)	Fe_2O_3 (%)	MnO_2 (%)	MgO (%)	CaO (%)	Na_2O (%)	K_2O (%)	P_2O_5 (%)	Total (%)
10	70.90	0.54	15.57	4.12	0.19	1.17	2.33	3.21	1.87	0.10	100.00
30	70.77	0.61	15.87	4.89	0.05	1.34	1.85	2.80	1.78	0.03	100.00
40	70.92	0.62	15.93	4.95	0.04	1.35	1.70	2.68	1.79	0.02	100.00
60	70.93	0.68	16.28	5.03	0.04	1.28	1.47	2.47	1.80	0.02	100.00
80	72.27	0.61	14.96	4.60	0.04	1.28	1.54	2.72	1.95	0.03	100.00
90	72.71	0.55	14.72	4.22	0.05	1.23	1.57	2.88	2.03	0.02	100.00
120	73.42	0.38	14.82	3.51	0.05	0.85	1.48	3.07	2.41	0.02	100.00
130	74.81	0.24	14.38	2.64	0.05	0.45	1.34	3.22	2.85	0.02	100.00
150	73.33	0.30	14.71	3.10	0.06	0.63	1.71	3.44	2.70	0.02	100.00
190	71.89	0.29	15.16	2.94	0.06	0.91	2.68	3.72	2.30	0.04	100.00
221	74.77	0.23	13.98	2.52	0.05	0.50	1.44	3.50	2.98	0.03	100.00

Appendix 4.4: Major oxide data from Poraiti #2 reference section

Depth* (cm)	SiO_2 (%)	TiO_2 (%)	Al_2O_3 (%)	Fe_2O_3 (%)	MnO_2 (%)	MgO (%)	CaO (%)	Na_2O (%)	K_2O (%)	P_2O_5 (%)	LOI (%)	Total (%)
60	69.06	0.55	13.35	3.87	0.06	1.16	1.65	2.84	1.97	0.09	5.10	99.70
120	68.78	0.50	13.88	3.56	0.04	0.77	1.71	2.95	1.61	0.02	5.80	99.62
140	66.92	0.50	14.26	3.90	0.05	0.87	1.68	2.70	1.65	0.03	7.01	99.57
160	67.41	0.51	13.70	3.90	0.03	0.93	1.37	2.50	1.44	0.03	7.65	99.47
180	65.71	0.58	14.32	4.51	0.03	1.07	1.21	2.37	1.30	0.03	8.45	99.58
210	67.87	0.60	13.34	4.33	0.04	1.12	1.39	2.53	1.54	0.03	7.01	99.80
230	65.61	0.70	13.96	4.65	0.03	1.15	1.34	2.21	1.37	0.03	8.70	99.75
260	67.55	0.58	13.65	4.53	0.05	1.07	1.52	2.60	1.48	0.04	6.80	99.87
280	66.11	0.64	14.52	5.31	0.06	0.86	1.43	2.52	1.09	0.04	7.47	100.05
300	57.84	0.70	17.57	6.78	0.02	0.76	0.95	1.65	0.72	0.02	13.10	100.11
310	59.53	0.69	17.32	6.30	0.02	0.70	0.94	1.70	0.70	0.02	12.16	100.08
320	65.67	0.60	13.47	5.35	0.05	1.17	1.28	2.00	1.13	0.03	9.40	100.15
360	64.29	0.58	14.95	4.82	0.03	1.08	1.27	2.23	1.32	0.02	9.53	100.12
440	62.38	0.58	14.98	5.11	0.03	1.37	1.45	2.01	1.54	0.03	10.67	100.15
485	65.63	0.51	13.59	4.88	0.03	1.43	1.88	2.27	1.67	0.07	8.07	100.03
550	66.32	0.55	13.48	4.72	0.05	1.36	1.70	2.45	1.93	0.09	7.34	99.99

NORMALISED ELEMENTAL ANALYSES

Depth (cm)	SiO_2 (%)	TiO_2 (%)	Al_2O_3 (%)	Fe_2O_3 (%)	MnO_2 (%)	MgO (%)	CaO (%)	Na_2O (%)	K_2O (%)	P_2O_5 (%)	Total (%)
60	69.28	0.55	13.39	3.88	0.06	1.16	1.66	2.85	1.98	0.09	100.00
120	69.04	0.50	13.93	3.57	0.04	0.77	1.72	2.96	1.62	0.02	100.00
140	67.21	0.50	14.32	3.92	0.05	0.87	1.69	2.71	1.66	0.03	100.00
160	67.78	0.51	13.77	3.92	0.03	0.94	1.38	2.51	1.45	0.03	100.00
180	65.99	0.58	14.38	4.53	0.03	1.07	1.22	2.38	1.31	0.03	100.00
210	68.01	0.60	13.37	4.34	0.04	1.12	1.39	2.54	1.54	0.03	100.00
230	65.77	0.70	13.99	4.66	0.03	1.15	1.34	2.22	1.37	0.03	100.00
260	67.63	0.58	13.67	4.54	0.05	1.07	1.52	2.60	1.48	0.04	100.00
280	66.08	0.64	14.51	5.31	0.06	0.86	1.43	2.52	1.09	0.04	100.00
300	57.77	0.70	17.55	6.77	0.02	0.76	0.95	1.65	0.72	0.02	100.00
310	59.48	0.69	17.31	6.29	0.02	0.70	0.94	1.70	0.70	0.02	100.00
320	65.57	0.65	13.45	5.34	0.05	1.17	1.28	2.00	1.13	0.03	100.00
360	64.22	0.58	14.93	4.81	0.03	1.08	1.27	2.23	1.32	0.02	100.00
440	62.29	0.58	14.96	5.10	0.03	1.37	1.45	2.01	1.54	0.03	100.00
485	65.61	0.51	13.59	4.88	0.03	1.43	1.88	2.27	1.67	0.07	100.00
550	66.33	0.55	13.48	4.72	0.05	1.36	1.70	2.45	1.93	0.09	100.00

* Depth measurements are taken from the base of the Kawakawa Tephra (0cm)

Appendix 4.5: Trace element data from Poraiti #1 reference section

Depth) (cm)	Ga (ppm)	Pb (ppm)	Rb (ppm)	Sr (ppm)	Th (ppm)	U (ppm)	Y (ppm)	As (ppm)	Sc (ppm)	V (ppm)
10	17.0	17.2	93.2	223.6	8.1	2.3	20.8	2.7	12.5	73.4
30	18.1	14.9	84.8	224.6	7.6	3.1	15.8	4.4	12.9	100.5
40	17.1	14.8	82.1	223.6	7.5	2.9	15.0	4.7	11.9	99.9
60	19.1	16.8	78.7	205.1	8.8	2.8	16.1	5.0	15.5	102.0
80	17.1	16.6	82.6	234.5	8.7	3.3	19.6	5.8	12.3	90.6
90	16.5	15.9	85.1	237.5	7.6	2.7	19.2	5.4	10.2	81.4
120	17.4	16.3	95.4	155.0	9.9	2.6	23.0	6.8	9.5	51.3
130	15.6	18.1	103.6	101.5	11.5	3.2	22.9	7.0	9.5	28.0
150	17.0	15.7	99.1	120.6	10.0	3.2	23.6	6.6	8.9	35.7
190	17.5	15.6	86.4	181.4	8.3	2.7	19.8	6.8	9.2	34.4
221	14.9	16.5	108.4	110.0	11.8	3.8	24.0	6.1	9.6	24.0

Depth) (cm)	Cr (ppm)	Ba (ppm)	La (ppm)	Ce (ppm)	Ni (ppm)	Cu (ppm)	Zn (ppm)	Zr (ppm)	Nb (ppm)
10	40.4	522.7	25.7	51.2	10.6	9.8	64.5	257.3	8.1
30	49.8	424.5	19.5	45.3	10.8	10.5	50.6	279.7	9.8
40	54.5	409.7	19.8	43.4	11.0	9.9	48.6	276.4	7.8
60	56.9	399.5	24.7	44.5	13.2	11.7	51.5	257.3	8.1
80	47.9	455.4	23.1	52.3	12.6	9.9	52.0	268.7	8.5
90	44.5	480.2	23.3	56.2	13.2	8.1	49.5	266.1	7.2
120	28.0	515.2	25.0	52.5	10.8	6.9	48.0	197.0	6.9
130	12.6	560.0	22.8	46.7	8.2	6.3	46.4	143.5	7.8
150	17.5	545.4	22.4	46.7	7.1	8.5	48.2	155.1	6.1
190	15.4	518.0	22.6	40.4	5.3	5.8	46.9	137.5	5.2
221	9.1	548.6	24.8	49.4	5.0	6.0	47.1	156.2	7.4

Appendix 4.6: Trace element data from Poraiti #2 reference section

Depth* (cm)	Ga (ppm)	Pb (ppm)	Rb (ppm)	Sr (ppm)	Th (ppm)	U (ppm)	Y (ppm)	As (ppm)	Sc (ppm)	V (ppm)
60	16.1	13.2	83.4	261.0	9.2	2.3	25.5	6.7	9.6	84.8
120	14.0	13.4	72.8	237.6	7.8	1.1	18.3	3.2	9.0	66.6
140	16.6	13.5	75.2	209.9	9.5	2.7	18.6	4.2	9.5	71.2
160	14.9	12.7	69.1	215.7	10.1	2.6	17.7	4.2	8.7	82.2
180	17.2	13.8	64.2	214.8	9.1	2.8	15.3	4.4	9.6	97.2
210	15.2	12.9	65.3	238.1	10.2	3.0	18.4	6.6	9.5	96.2
230	15.6	15.9	62.7	217.5	11.6	2.9	17.7	5.5	11.6	98.3
260	15.3	13.5	66.3	243.4	9.3	1.9	20.1	4.7	11.1	100.9
280	14.8	13.2	56.9	225.7	7.5	2.4	17.1	5.4	11.0	137.8
300	19.7	12.8	37.4	143.1	7.6	2.2	11.9	4.0	13.9	145.2
310	19.4	12.7	34.9	151.9	8.1	2.4	10.4	4.1	14.3	139.7
320	15.5	15.5	51.6	187.2	7.5	1.9	14.9	5.1	11.0	121.5
360	16.5	12.6	60.7	203.4	8.9	3.4	14.0	4.4	14.8	102.8
440	16.0	16.0	75.6	195.6	11.5	2.4	19.4	5.7	15.1	98.5
485	13.9	17.6	74.4	222.9	10.2	1.2	27.7	6.5	12.4	92.5
550	14.9	15.6	83.6	227.0	10.0	2.2	44.8	8.5	9.9	94.7

Depth* (cm)	Cr (ppm)	Ba (ppm)	La (ppm)	Ce (ppm)	Ni (ppm)	Cu (ppm)	Zn (ppm)	Zr (ppm)	Nb (ppm)
60	54.4	479.0	24.6	52.5	21.4	12.8	54.2	312.3	7.2
120	45.3	458.3	21.2	44.5	15.2	10.7	39.9	293.9	9.1
140	43.6	484.5	22.3	46.3	11.8	11.8	44.8	258.5	7.3
160	51.5	449.4	22.8	48.3	11.9	12.3	42.1	291.3	8.5
180	55.9	393.4	17.7	45.5	11.0	11.7	43.7	284.5	8.6
210	58.0	450.9	24.5	57.6	17.1	10.2	44.5	292.9	8.8
230	57.7	423.5	24.1	58.9	14.9	13.1	45.5	269.0	10.6
260	59.9	477.8	24.6	58.0	16.8	11.2	45.3	297.1	9.0
280	64.6	376.9	17.5	43.5	12.0	14.2	40.5	294.9	6.7
300	67.6	300.7	12.6	27.7	18.1	25.4	39.7	229.7	7.9
310	65.1	290.5	13.0	34.9	16.5	25.2	36.9	222.5	6.9
320	57.1	447.7	19.9	46.8	22.6	19.1	41.6	257.2	7.0
360	56.7	426.1	15.3	42.4	16.7	16.3	45.1	238.3	8.9
440	62.1	488.4	23.9	58.9	20.1	15.2	57.5	191.5	8.3
485	56.3	502.4	35.5	75.9	19.8	12.6	57.8	195.6	6.8
550	56.6	527.8	52.9	61.4	24.4	13.0	62.8	217.6	8.6

* Depth measurements are taken from the base of the Kawakawa Tephra (0cm)

Appendix 4.7: Soil chemistry at Pakaututu Road reference section

Depth (cm)	% Feo	% Alo	% Sio	% Fep	% Alp	Al/Si (molar ratio)	% Allophane	% Ferrihydrite
0	0.43	1.2	0.26	0.32	0.76	1.8	1.7	0.7
10	0.38	1.1	0.30	0.25	0.58	1.8	2.0	0.6
20	0.36	1.0	0.36	0.21	0.45	1.6	2.2	0.6
30	0.29	0.49	0.20	0.14	0.27	1.1	1.0	0.5
40	0.44	0.87	0.26	0.19	0.30	2.3	2.3	0.7
50	0.43	0.80	0.41	0.09	0.26	1.4	2.4	0.7
60	1.4	4.6	1.8	0.38	0.60	2.3	16.2	2.4
70	1.5	5.2	2.5	0.25	0.59	1.9	17.0	2.6
80	1.5	5.2	2.4	0.25	0.45	2.1	18.0	2.6
90	1.4	4.6	2.1	0.20	0.47	2.0	14.7	2.4
100	1.3	4.4	1.9	0.15	0.38	2.2	15.2	2.2
110	0.74	4.5	2.5	0.05	0.22	1.8	16.5	1.3
120	1.4	4.5	2.4	0.06	0.33	1.8	15.8	2.4
130	1.6	4.6	2.8	0.04	0.32	1.6	17.4	2.7
140	1.6	4.9	2.9	0.03	0.29	1.6	18.0	2.7
150	1.3	4.3	2.3	0.03	0.23	1.8	15.2	2.2
160	1.4	4.8	2.6	0.02	0.27	1.8	17.2	2.4
170	1.2	3.6	2.4	0.02	0.20	1.5	14.4	2.0
180	1.0	3.0	2.0	0.02	0.21	1.4	11.6	1.7
190	1.1	3.2	1.9	0.02	0.22	1.6	11.8	1.9
200	0.83	0.55	0.29	0.26	0.10	1.6	1.8	1.4
210	0.84	0.46	0.47	0.28	0.12	0.8	1.9	1.4
220	1.0	2.1	1.2	0.07	0.12	1.7	7.7	1.7
230	0.85	2.1	1.6	0.02	0.13	1.3	9.0	1.4
240	0.73	0.96	0.85	0.05	0.09	1.1	4.4	1.2
250	0.61	0.35	0.28	0.13	0.06	1.1	1.5	1.0
260	0.55	0.43	0.15	0.12	0.08	2.4	1.4	0.9
270	0.53	0.28	0.20	0.13	0.07	1.1	1.0	0.9
280	0.53	0.45	0.30	0.08	0.08	1.3	1.7	0.9
290	0.52	0.69	0.50	0.05	0.13	1.2	2.7	0.9
300	0.31	0.30	0.21	0.03	0.03	1.3	1.2	0.5
310	0.27	0.37	0.16	0.03	0.01	2.3	1.4	0.5
320	0.17	1.2	0.58	0.01	0.06	2.0	4.1	0.3
330	0.28	0.51	0.14	0.04	0.03	3.6	2.4	0.5
340	0.35	0.63	0.12	0.04	0.07	4.8	2.4	0.6
350	0.35	0.00	0.10	0.04	0.05	0.0	0.0	0.6
360	0.35	0.10	0.10	0.04	0.02	0.8	0.4	0.6
370	0.43	0.24	0.16	0.03	0.01	1.5	1.0	0.7
380	0.47	0.35	0.31	0.09	0.07	0.9	1.4	0.8
390	0.57	0.46	0.26	0.10	0.06	1.6	1.6	1.0
400	0.61	0.12	0.27	0.10	0.11	0.0	0.0	1.0
410	0.69	0.28	0.17	0.16	0.11	1.0	0.9	1.2
420	0.46	0.29	0.35	0.19	0.15	0.4	0.7	0.8
430	0.65	0.43	0.35	0.20	0.12	0.9	1.6	1.1
440	0.70	0.61	0.44	0.20	0.11	1.2	2.4	1.2
450	0.65	0.44	0.51	0.12	0.10	0.7	1.8	1.1
460	0.98	0.63	0.34	0.05	0.05	1.8	2.2	1.7
470	0.86	0.60	0.30	0.05	0.06	1.9	2.0	1.5
480	0.83	0.57	0.27	0.05	0.06	2.0	1.9	1.4
490	0.55	0.25	0.17	0.07	0.04	1.3	1.0	0.9
500	0.65	0.32	0.19	0.09	0.07	1.4	1.1	1.1
510	0.95	0.69	0.34	0.09	0.08	1.9	2.3	1.6
520	1.1	0.97	0.50	0.05	0.07	1.9	3.4	1.9
530	1.1	1.0	0.51	0.06	0.07	1.9	3.5	1.9
540	1.1	1.0	0.51	0.05	0.06	1.9	3.5	1.9
550	0.73	0.57	0.25	0.04	0.05	2.2	2.1	1.2
560	0.51	0.19	0.16	0.04	0.01	1.2	0.9	0.9
570	0.23	0.62	0.29	0.01	0.03	2.1	2.3	0.4
580	0.43	0.27	0.20	0.03	0.02	1.3	1.1	0.7
590	0.37	0.13	0.14	0.02	0.01	0.9	0.6	0.6
600	0.37	0.12	0.13	0.02	0.02	0.8	0.5	0.6
610	0.39	0.13	0.12	0.02	0.02	1.0	0.6	0.7
620	0.39	0.13	0.12	0.03	0.02	1.0	0.6	0.7
630	0.31	0.11	0.12	0.02	0.01	0.9	0.5	0.5
640	0.21	0.09	0.10	0.01	0.00	0.9	0.5	0.4
650	0.13	0.08	0.10	0.01	0.01	0.7	0.3	0.2
660	0.10	0.06	0.00	0.00	0.00	0.0	0.0	0.2
670	0.22	0.13	0.00	0.01	0.01	0.0	0.0	0.4

Appendix 4.8: Soil chemistry at Manaroa reference section

Depth (cm)	% Fe_o	% Al_o	% Si_o	% Fe_p	% Al_p	Al/Si (molar ratio)	% Allophane	% Ferrihydrite
0	0.83	2.3	0.45	0.18	0.38	4.4	7.2	1.4
10	0.93	2.4	0.55	0.29	0.43	3.7	8.8	1.6
20	0.83	1.8	0.35	0.27	0.42	4.1	5.6	1.4
30	0.85	2.7	0.82	0.16	0.37	2.9	9.8	1.4
40	1.1	3.8	1.2	0.27	0.47	2.9	14.4	1.9
50	1.3	4.4	1.4	0.34	0.55	2.9	16.8	2.2
60	1.6	4.5	1.5	0.32	0.50	2.8	16.5	2.7
70	1.8	4.8	1.6	0.20	0.47	2.8	17.6	3.1
80	2.6	5.2	1.8	0.15	0.41	2.8	19.8	4.4
90	2.7	5.9	1.8	0.07	0.40	3.2	25.2	4.6
95	1.8	5.2	1.8	0.03	0.35	2.8	19.8	3.1
100	2.1	4.9	1.8	0.03	0.31	2.6	18	3.6
110	1.7	4.0	1.7	0.02	0.26	2.3	15.3	2.9
120	1.3	3.3	1.3	0.02	0.24	2.4	11.7	2.2
130	0.54	1.5	0.49	0.03	0.18	2.8	5.4	0.9
140	0.46	0.75	0.09	0.08	0.11	7.4	1.4	0.8
150	0.41	0.60	0.02	0.09	0.10	25.9	0.3	0.7
160	0.40	0.87	0.17	0.04	0.10	4.7	2.7	0.7
170	0.41	1.08	0.33	0.02	0.15	3.0	4.0	0.7
180	0.38	1.14	0.43	0.01	0.16	2.3	3.9	0.7
190	0.27	0.80	0.15	0.01	0.13	4.6	2.4	0.5
200	0.27	0.12	0.00	0.03	0.05	0	0	0.5
210	0.23	0.12	0.00	0.02	0.03	0	0	0.4
220	0.29	0.14	0.00	0.02	0.04	0	0	0.5
230	0.28	0.14	0.00	0.02	0.04	0	0	0.5
240	0.37	0.15	0.00	0.03	0.04	0	0	0.6
250	0.34	0.14	0.00	0.03	0.04	0	0	0.6
260	0.29	0.12	0.00	0.03	0.04	0	0	0.5
270	0.23	0.14	0.00	0.03	0.04	0	0	0.4
280	0.17	0.10	0.00	0.01	0.03	0	0	0.3
290	0.23	0.12	0.00	0.01	0.03	0	0	0.4
295	0.20	0.10	0.00	0.01	0.03	0	0	0.3
300	0.20	0.10	0.00	0.01	0.02	0	0	0.3
310	0.16	0.07	0.00	0.01	0.02	0	0	0.3
320	0.17	0.03	0.00	0.01	0.02	0	0	0.3
330	0.14	0.05	0.00	0.00	0.01	0	0	0.2
340	0.15	0.07	0.00	0.01	0.02	0	0	0.3
350	0.11	0.06	0.00	0.01	0.03	0	0	0.2
360	0.14	0.09	0.00	0.01	0.03	0	0	0.2
365	0.31	1.9	0.93	0.03	0.10	2	6.5	0.5
370	0.13	0.07	0.00	0.02	0.02	0	0	0.2
380	0.16	0.08	0.00	0.02	0.03	0	0	0.3
390	0.14	0.07	0.00	0.02	0.02	0	0	0.2
400	0.12	0.06	0.00	0.01	0.03	0	0	0.2
410	0.14	0.06	0.00	0.01	0.02	0	0	0.2
420	0.13	0.06	0.00	0.01	0.02	0	0	0.2
430	0.14	0.07	0.00	0.01	0.02	0	0	0.2
440	0.11	0.05	0.07	0.01	0.02	0.4	0.1	0.2
450	0.10	0.06	0.04	0.01	0.01	1.3	0.2	0.2
460	0.12	0.05	0.04	0.01	0.01	1.0	0.2	0.2
470	0.10	0.07	0.06	0.01	0.01	1.0	0.3	0.2
480	0.11	0.06	0.03	0.01	0.02	1.4	0.2	0.2
490	0.11	0.05	0.05	0.01	0.02	0.6	0.2	0.2
500	0.10	0.05	0.03	0.01	0.01	1.4	0.2	0.2
510	0.08	0.04	0.02	0.01	0.01	1.6	0.1	0.1
520	0.08	0.05	0.04	0.01	0.01	1.0	0.2	0.1
530	0.06	0.04	0.01	0.01	0.01	3.1	0.1	0.1